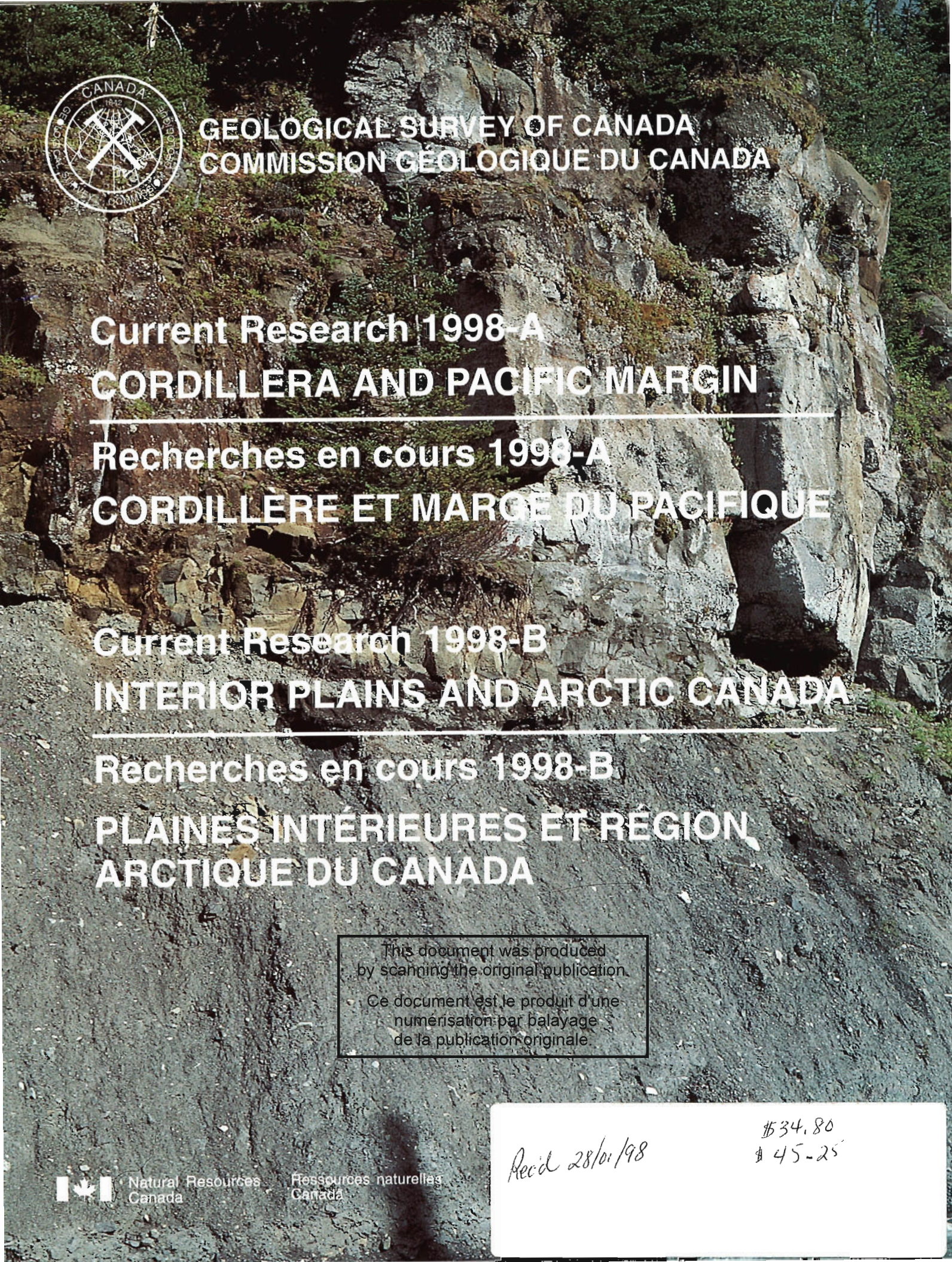

GEOLOGICAL SURVEY OF CANADA
COMMISSION GÉOLOGIQUE DU CANADA

Current Research 1998-A
CORDILLERA AND PACIFIC MARGIN

Recherches en cours 1998-A
CORDILLÈRE ET MARGE DU PACIFIQUE

Current Research 1998-B
INTERIOR PLAINS AND ARCTIC CANADA

Recherches en cours 1998-B
PLAINES INTÉRIEURES ET RÉGION ARCTIQUE DU CANADA

Natural Resources Canada
Ressources naturelles Canada

NOTICE TO LIBRARIANS AND INDEXERS

The Geological Survey's Current Research series contains many reports comparable in scope and subject matter to those appearing in scientific journals and other serials. Most contributions to Current Research include an abstract and bibliographic citation. It is hoped that these will assist you in cataloguing and indexing these reports and that this will result in a still wider dissemination of the results of the Geological Survey's research activities.

AVIS AUX BIBLIOTHÉCAIRES ET PRÉPARATEURS D'INDEX

La série Recherches en cours de la Commission géologique contient plusieurs rapports dont la portée et la nature sont comparables à celles des rapports qui paraissent dans les revues scientifiques et autres périodiques. La plupart des articles publiés dans Recherches en cours sont accompagnés d'un résumé et d'une bibliographie, ce qui vous permettra, on l'espère, de cataloguer et d'indexer ces rapports, d'où une meilleure diffusion des résultats de recherche de la Commission géologique.

GEOLOGICAL SURVEY OF CANADA
COMMISSION GÉOLOGIQUE DU CANADA

CURRENT RESEARCH 1998-A
CORDILLERA AND PACIFIC MARGIN

RECHERCHES EN COURS 1998-A
CORDILLÈRE ET MARGE DU PACIFIQUE

CURRENT RESEARCH 1998-B
INTERIOR PLAINS AND ARCTIC CANADA

RECHERCHES EN COURS 1998-B
PLAINES INTÉRIEURES ET RÉGION ARCTIQUE DU CANADA

1998

Catalogue No. M44-1998/1-2E
ISBN 0-660-17299-2

Available in Canada from
Geological Survey of Canada offices:

601 Booth Street
Ottawa, Ontario K1A 0E8

3303-33rd Street N.W.
Calgary, Alberta T2L 2A7

101-605 Robson Street
Vancouver, B.C. V6B 5J3

or from

Canadian Government Publishing
Public Works and Government Services Canada
Ottawa, Ontario K1A 0S9

A deposit copy of this publication is also available for reference
in selected public libraries across Canada

Price subject to change without notice

Cover illustration

Flat-lying basalt flows overlying Pleistocene, possibly glacial deposits southeast of Mount Hoadley, British Columbia. See paper by Haggart et al., this volume. Photograph by Glenn Woodsworth. GSC 1997-83

Photo en page couverture

Coulées de basalte disposées en couches horizontales sur des dépôts du Pléistocène, probablement d'origine glaciaire, au sud-ouest du mont Hoadley, Colombie-Britannique. Cette photographie se rapporte à l'article de Haggart et al. dans le présent volume. Photo : Glenn Woodsworth, GSC 1997-83

Separates

A limited number of separates of the papers that appear in this volume are available by direct request to the individual authors. The addresses of the Geological Survey of Canada offices follow:

Geological Survey of Canada
601 Booth Street
Ottawa, Ontario
K1A 0E8
(FAX: 613-996-9990)

Geological Survey of Canada (Calgary)
3303-33rd Street N.W.
Calgary, Alberta
T2L 2A7
(FAX: 403-292-5377)

Geological Survey of Canada (Pacific)
101-605 Robson Street
Vancouver, British Columbia
V6B 5J3
(FAX: 604-666-1124)

Geological Survey of Canada (Pacific)
P.O. Box 6000
9860 Saanich Road
Sidney, British Columbia
V8L 4B2
(FAX: 604-363-6565)

Geological Survey of Canada (Atlantic)
Bedford Institute of Oceanography
P.O. Box 1006
Dartmouth, Nova Scotia
B2Y 4A2
(FAX: 902-426-2256)

Quebec Geoscience Centre/INRS
2535, boulevard Laurier
C.P. 7500
Sainte-Foy (Québec)
G1V 4C7
(FAX: 418-654-2615)

Tirés à part

On peut obtenir un nombre limité de «tirés à part» des articles qui paraissent dans cette publication en s'adressant directement à chaque auteur. Les adresses des différents bureaux de la Commission géologique du Canada sont les suivantes :

Commission géologique du Canada
601, rue Booth
Ottawa (Ontario)
K1A 0E8
(facsimilé : 613-996-9990)

Commission géologique du Canada (Calgary)
3303-33rd Street N.W.,
Calgary, Alberta
T2L 2A7
(facsimilé : 403-292-5377)

Commission géologique du Canada (Pacifique)
101-605 Robson Street
Vancouver, British Columbia
V6B 5J3
(facsimilé : 604-666-1124)

Commission géologique du Canada (Pacifique)
P.O. Box 6000
9860 Saanich Road
Sidney, British Columbia
V8L 4B2
(facsimilé : 604-363-6565)

Commission géologique du Canada (Atlantique)
Institut océanographique Bedford
P.O. Box 1006
Dartmouth, Nova Scotia
B2Y 4A2
(facsimilé : 902-426-2256)

Centre géoscientifique de Québec/INRS
2535, boulevard Laurier
C.P. 7500
Sainte-Foy (Québec)
G1V 4C7
(facsimilé : 418-654-2615)

CONTENTS

CORDILLERA AND PACIFIC MARGIN
CORDILLÈRE ET MARGE DU PACIFIQUE

INTERIOR PLAINS AND ARCTIC CANADA
PLAINES INTÉRIEURES ET RÉGION ARCTIQUE DU CANADA

Relationships between chemical composition, physical properties, and geology of the mineralized Emerald Lake Pluton, Yukon Territory

R.A. Duncan[1], J.K. Russell[2], N.L. Hastings, and R.G. Anderson
GSC Pacific, Vancouver

Duncan, R.A., Russell, J.K., Hastings, N.L., and Anderson, R.G., 1998: Relationships between chemical composition, physical properties, and geology of the mineralized Emerald Lake Pluton, Yukon Territory; in Current Research 1998-A; Geological Survey of Canada, p. 1-11.

Abstract: Emerald Lake Pluton is a newly remapped member of the mid-Cretaceous Tombstone plutonic suite in Yukon. It is crudely concentrically-zoned comprising: augite syenite, hornblende quartz syenite, hornblende quartz monzonite, and biotite granite, from west to east and in order of relative age. Density and magnetic susceptibility values of samples from each phase decrease, and Shand Indices increase, from west to east and correlate with mapped intrusive phases. The intrusion is also characterized by the presence of large miarolitic cavities distributed along the southern and eastern margins of the intrusion. They are spatially and temporally associated with a sheeted system of aplite dykes, quartz K-feldspar pegmatites, and molybdenite bismuthinite gold quartz veins. Miarolitic cavity and pegmatite formation are coeval with the main intrusive events, and were followed by continued pegmatite development, fracturing, and injection of aplite dykes and veins.

Résumé : Le pluton d'Emerald Lake est un membre de la suite plutonique du Crétacé moyen de Tombstone, au Yukon; récemment, il a été cartographié de nouveau. Il est zoné grossièrement de manière concentrique et comprend, d'ouest en est et par ordre d'âge relatif (des phases les plus vieilles aux phases les plus jeunes) : des syénites à augite, des syénites quartziques à hornblende, des monzonites quartziques à hornblende et des granites à biotite. D'ouest en est et en corrélation avec les phases intrusives cartographiées, les valeurs de la densité et de la susceptibilité magnétique des échantillons de chaque phase diminuent, tandis celles de l'indice de Shand s'accroissent. L'intrusion se caractérise en outre par la présence de grandes cavités miarolitiques réparties le long de ses marges sud et est. Ces cavités sont associées spatialement et temporellement à un système feuilleté de dykes aplitiques, de pegmatites à quartz et feldspath potassique et de filons quartzeux aurifères à molybdénite et bismuthine. La formation des cavités miarolitiques et des pegmatites est contemporaine des principaux épisodes intrusifs et a été suivie par des processus continus, en l'occurrence la formation de pegmatites, la fracturation ainsi que l'injection de dykes et de filons aplitiques.

[1] Mineral Deposit Research Unit - Igneous Petrology Laboratory, Department of Earth and Ocean Sciences, University of British Columbia, 6339 Stores Road, Vancouver, British Columbia V6T 1Z4
[2] Igneous Petrology Laboratory, Geological Sciences Division, Department of Earth and Ocean Sciences, University of British Columbia, 6339 Stores Road, Vancouver, British Columbia V6T 1Z4

INTRODUCTION

Emerald Lake Pluton is situated within the Rogue Range, in the Arrowhead Lake 1:50 000 map area (105O/11) (Fig. 1). The intrusion occurs in a T-shaped valley at the head of Emerald Lake; it is mainly exposed along the surrounding ridges. A satellitic stock is located on the flank of Horn Peak (the Horn Peak outlier). It occurs in the eastern part of the Tombstone plutonic suite (Fig. 2; J.K. Mortensen, D.C. Murphy, K.H. Poulsen, and T. Bremner, unpub. course notes, Cordilleran Roundup, Vancouver, 1996).

We present preliminary results from new field mapping and sampling of the pluton, and ongoing laboratory studies. A revised geological map for Emerald Lake Pluton, petrographic descriptions, physical properties, and preliminary chemical data for these rocks, and a relative timing sequence for events at Emerald Lake are summarized here. The widespread distribution of miarolitic cavities makes Emerald Lake Pluton an exceptional opportunity to study the evolution and behaviour of magmatic fluid phases and the transition from magmatic to hydrothermal activity. These critical data help to constrain a petrogenetic model for Emerald Lake Pluton and, by analogy, for other intrusions within the Tombstone plutonic suite.

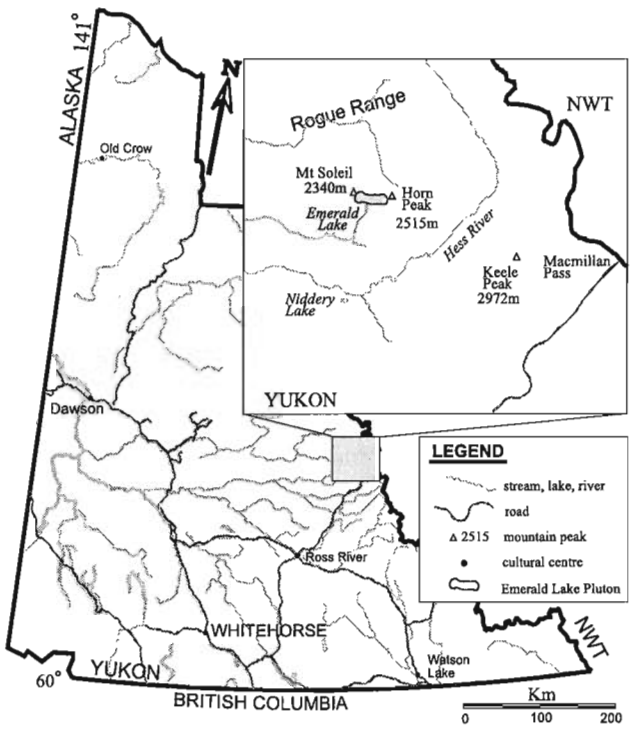

Figure 1. *Location and access to Emerald Lake Pluton and the surrounding area (modified from Gordey and Anderson, 1993).*

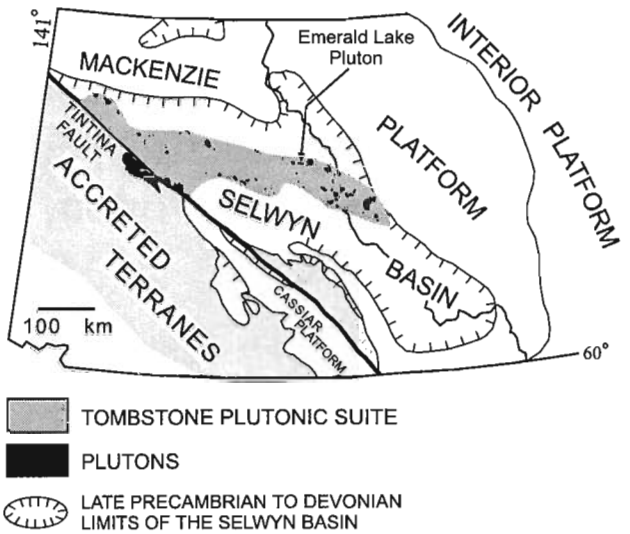

Figure 2. *Location and distribution of mid-Cretaceous plutons of the Tombstone plutonic suite with respect to major late Precambrian to Middle Devonian tectonic and depositional elements of the northern Cordilleran miogeocline (Gabrielse, 1967; modified from Gordey and Anderson, 1993; J.K. Mortensen, D.C. Murphy, K.H. Poulsen, and T. Bremner, unpub. course notes, Cordilleran Roundup, Vancouver, 1996).*

REGIONAL GEOLOGY

Emerald Lake Pluton intrudes deformed Cambrian to Devonian sedimentary rocks of the Selwyn Basin (Fig. 2; Cecile, 1984; Cecile and Abbott, 1992). From east to west these include a 400 m thick sequence of Cambrian argillite interstratified with shale, volcaniclastic rocks, mafic flows, and minor quartzite (Cecile, 1984). Ordovician to Silurian chert and argillite with minor shale and limestone stratigraphically overlie the Cambrian strata, and are estimated to be 100-160 m thick (Cecile, 1984). Devonian shale, chert, and minor argillite, estimated to be 100 to more than 400 m thick form the top of the succession (Cecile, 1984). All sedimentary units in the area were shortened along folds and thrust faults and tectonically thickened up to three times their original thickness (Cecile, 1984).

Intrusive contacts with the country rocks dip steeply outward from the intrusion except in areas along the north contact where dips shallow to as little as 18°. The country rocks show a metamorphic contact aureole that reaches biotite grade. The aureole is up to 3.5 km wide along the southern margin of the intrusion, and is especially pronounced along the northern contact where it merges with aureoles from intrusions located 5.5 km and 9.5 km to the northeast of Emerald Lake Pluton (Cecile, 1984). These large contact metamorphic aureoles are also a feature of several other Tombstone plutonic suite intrusions (Poulsen et al., 1997). Rare fine-grained selvages occur within 5 to 15 m of the margin of the intrusion.

Emerald Lake Pluton is classified as a hornblende-bearing member of the Selwyn Plutonic Suite (Anderson, 1988; Woodsworth et al., 1991; Gordey and Anderson, 1993). More recently, Mortensen and co-workers (J.K. Mortensen, D.C. Murphy, K.H. Poulsen, and T. Bremner, unpub. course notes, Cordilleran Roundup, Vancouver, 1996) suggested that the Emerald Lake Pluton is part of the Tombstone plutonic suite. The suite comprises a 550 km long belt of lithologically diverse, mid-Cretaceous plutons that extends from the eastern Yukon Territory to the Dawson area of western Yukon Territory (Fig. 2). Near Dawson, the belt is offset by the Tintina Fault, where it continues to the west at least to the Fairbanks District (J.K. Mortensen, D.C. Murphy, K.H. Poulsen, and T. Bremner, unpub. course notes, Cordilleran Roundup, Vancouver, 1996). Emerald Lake Pluton is considered a member of the Tombstone plutonic suite because of its location (Fig. 2), its age (92 ± 3 Ma, K-Ar) (Smit et al., 1985), and its similarities in metallogeny to other Tombstone plutonic suite intrusions, such as Fort Knox and Dublin Gulch (Bakke, 1995; J.K. Mortensen, D.C. Murphy, K.H. Poulsen, and T. Bremner, unpub. course notes, Cordilleran Roundup, Vancouver, 1996).

EXPLORATION HISTORY

Emerald Lake Pluton was first mapped by Blusson (1974) as part of a reconnaissance program. In 1979, the northwestern portion of the intrusion was staked by AGIP Canada Ltd. on the basis of a radiometric anomaly in this area; evaluation of the gold, molybdenum, copper, and tungsten mineralization continued until 1983 when AGIP ceased their North American activities. Emerald Lake Pluton was then remapped by Smit (Smit, 1984; Smit et al., 1985) as part of his undergraduate thesis project. The intrusion was staked again in 1995 by Yukon Gold Corporation; exploration in 1995 and 1996 for large tonnage, low-grade porphyry gold potential established several drill targets based on surface chip sampling. One such target at the eastern margin of the pluton was tested during 1996, with negative results. The property is now a joint venture between Alliance Pacific Gold Corp. (formerly Yukon Gold Corporation) and Cyprus/Amax Mineral Co. The mineral specimen collecting rights are held by the Tyson Group who exploit the intrusion for large quartz, tourmaline, apatite, and aquamarine crystals found in the miarolitic cavities directly associated with the volatile evolution of the intrusion.

GEOLOGY OF THE PLUTON

Emerald Lake Pluton is an easterly elongate body about 11 km by 2.5 km (Fig. 3a). The intrusion has a surface area of 27.5 km^2 and a vertical exposure of 700-900 m. The intrusion is crudely concentrically zoned, particularly in the western portion of the main body, marked by augite syenite, hornblende quartz syenite, hornblende quartz monzonite, and biotite granite phases. Intrusive phases are described below in order of their relative sequence of intrusion, from oldest to youngest.

Minor intrusive phases include syenogabbro bodies about a metre to tens of metres across within, and contemporaneous with, the augite syenite. Late aplite, syenite, and granodiorite dyke phases occur within and outside the pluton. Late K-feldspar, quartz, tourmaline ± biotite pegmatite sweats and dykes are also common. The aplite and pegmatite dykes are associated with large miarolitic cavities and mineralized, sheeted quartz veins (Fig. 3b, 4a, b).

Augite syenite (mKas)

The western margin of the pluton and the Horn Peak outlier consist of trachytic augite syenite (Fig. 3a).

The augite syenite is characterized by the alignment of coarse-grained K-feldspar megacrysts, which have an aspect ratio of at least 5:1 (Fig. 5a). K-feldspar generally accounts for 60-75% of the rock; the groundmass consists of medium-grained clinopyroxene, hornblende, biotite, plagioclase, and quartz. Hornblende and plagioclase exhibit pronounced zoning. K-feldspar laths range from 1-3 cm, are simply twinned, and contain apatite, magnetite, and zircon inclusions (see Fig. 6). Clinopyroxene grains are substantially altered to hornblende, contain abundant inclusions of magnetite, titanite, and apatite, and rarer biotite, zircon, and tourmaline inclusions. Titanite, tourmaline, and quartz occur as accessory phases in the groundmass.

The alignment of megacrysts defines a foliation that dips steeply inward from, and is subparallel to the margin of the pluton, and may indicate a possible flow direction. A dominant fracture set, along which aplites, pegmatites, and veins are injected, is approximately perpendicular to trachytic foliation (Fig. 3b).

Variations in the phase are mainly in size and content of K-feldspar megacrysts. The phase also contains abundant country rock inclusions. The contact between augite syenite and hornblende quartz syenite is gradational over 100 m and is defined by a decrease in clinopyroxene abundance and size of K-feldspar megacrysts. Dykes of hornblende quartz syenite locally intrude augite syenite.

Hornblende quartz syenite (mKhqs)

A body of porphyritic to seriate hornblende quartz syenite outcrops directly east of the augite syenite (Fig. 3a). It is characterized by 55-65% stubby (0.5-0.75 cm) K-feldspar megacrysts in a fine- to medium-grained groundmass, which defines a porphyritic to seriate texture (Fig. 5b). Megacrysts are perthitic, zoned, and contain small inclusions of plagioclase, apatite, and zircon (Fig. 6). The inclusions are oriented parallel to growth faces. Hornblende is the primary mafic mineral and is also zoned with apatite inclusions crudely oriented parallel to crystal faces. Magnetite, titanite, and zircon are also included in hornblende, and zircon and apatite are included in biotite. Some hornblende grains contain relict

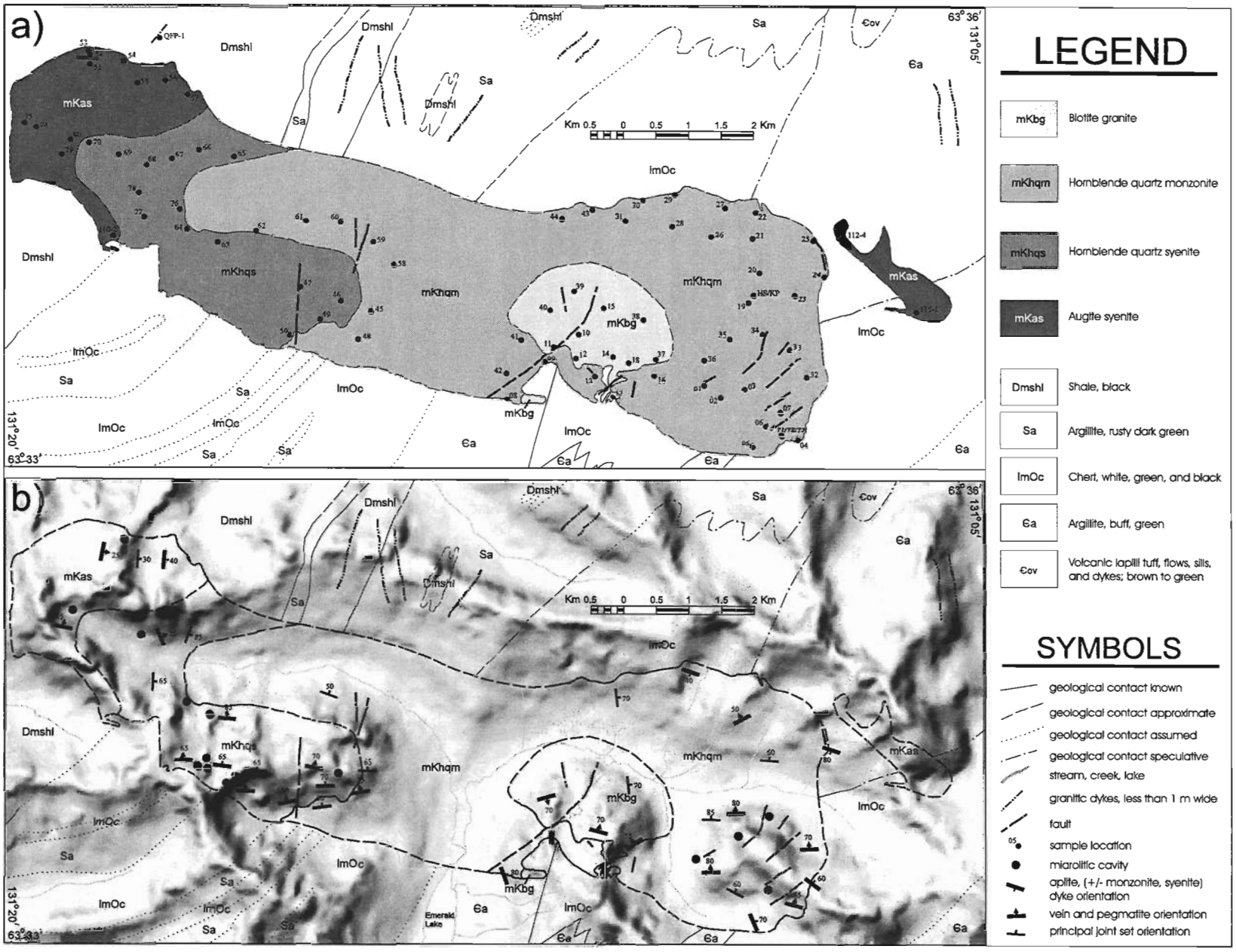

Figure 3. *Geological maps for Emerald Lake Pluton;* ***a)*** *distribution of major phases and sample locations,* ***b)*** *shaded relief map depicting the occurrence and orientation of dykes and pegmatites, veins, primary joint set, faults, and miarolitic cavities.*

cores of clinopyroxene. Groundmass phases consist of zoned plagioclase, quartz, K-feldspar and biotite, which exhibit local granophyric textures.

Variations within the phase are biotite content and the abundance of 3 to 4 cm K-feldspar megacrysts. The contact between the hornblende quartz syenite and the hornblende quartz monzonite is gradational over 100 m, and is defined by an increase in K-feldspar megacryst and groundmass grain size, a decrease in biotite content, and the disappearance of 3 to 4 cm size K-feldspar megacrysts. Small dykes of hornblende quartz monzonite cut hornblende quartz syenite.

Hornblende quartz monzonite (mKhqm)

More than half of Emerald Lake Pluton (by area) consists of crowded porphyritic to seriate hornblende quartz monzonite (Fig. 3a), and is characterized by 60-65% perthite megacrysts

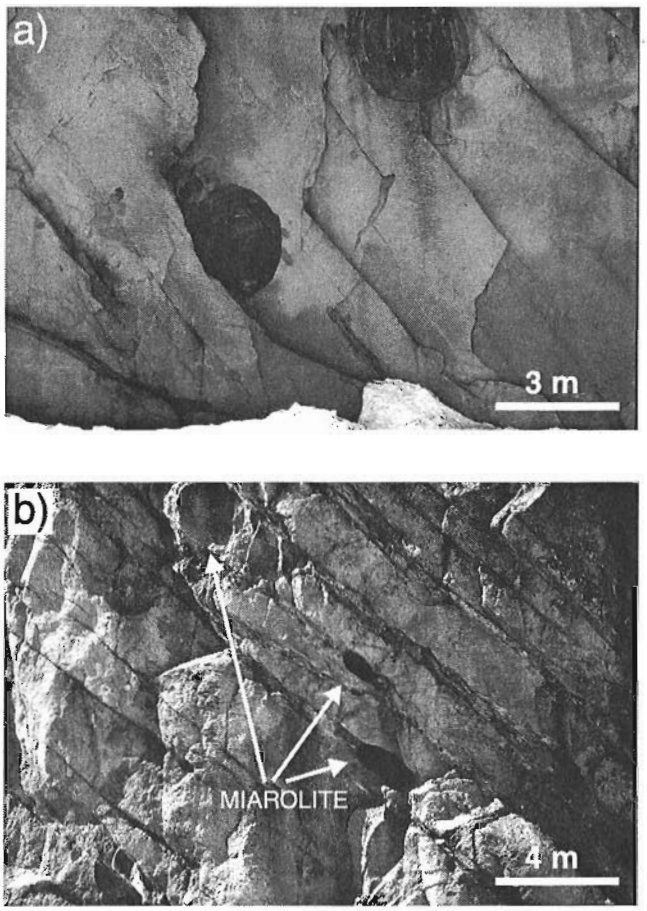

Figure 4. *Photographs of:* ***a)*** *two miarolitic cavities within the hornblende quartz syenite (looking west). The fracture set developed here is the same as that along which veins and pegmatites occur, and* ***b)*** *a cliff face (looking west) along the southern margin of the intrusion within the hornblende quartz syenite depicting 20-50 cm wide quartz K-feldspar pegmatites oriented easterly and intersecting two miarolitic cavities, which are elongated subparallel to the pegmatites.*

(0.5 x 1.0 cm) which display strong zoning (Fig. 6). Megacrysts contain abundant small inclusions of hornblende, plagioclase, and apatite, which are aligned with growth zoning (known as epitaotic overgrowth) (Bard, 1986). Megacrysts usually have an inclusion-rich zone beyond which the grain growth may have been achieved through diffusion. Hornblende phenocrysts (2-4 mm) are crudely zoned and contain inclusions of magnetite, titanite, and apatite (Fig. 5c). Groundmass phases are distinctly coarser-grained than those of the hornblende quartz syenite resulting in a more pronounced seriate texture. Groundmass phases include zoned plagioclase, quartz, minor biotite, titanite, and magnetite. Granophyric and myrmekitic textures occur at the edges of K-feldspar and plagioclase grains. Feldspars are rarely altered to carbonate and sericite.

The hornblende quartz monzonite varies in composition and texture. Compositional variability is imparted by quartz and hornblende content resulting in local gradational changes to granite and monzonite. Monzonite shows higher abundances of hornblende along the southeast and northeast margins of the pluton, and locally shows layering of mafic minerals. Textural variations include local changes in K-feldspar megacryst content to as low as 30%, and a finer-grained groundmass.

The contact between the hornblende quartz monzonite and biotite granite is gradational over 50 m. It is defined by a decrease in K-feldspar megacryst and hornblende content, and an increase in quartz and biotite content.

Biotite granite (mKbg)

A small circular body of porphyritic biotite granite occurs within the hornblende monzonite and along the south-central margin of the pluton (Fig. 3a). The biotite granite is characterized by 20% K-feldspar megacrysts, 0.75 by 1.0 cm in size, which also display prominent growth zoning with inclusions of biotite, hornblende, plagioclase, and apatite aligned on growth surfaces (Fig. 5d, 6). The groundmass consists of fine- to medium-grained quartz, plagioclase, hornblende, biotite, allanite, muscovite, and titanite, creating a pronounced porphyritic texture. Biotite replaces hornblende but also occurs as very fine grains disseminated in the groundmass, and more rarely as sheeted masses accounting for up to 10-15% of the rock. Accessory phases include magnetite, pyrite, zircon, and apatite. Titanite is rare and its scarcity is a significant mineralogical characteristic compared to other phases. Feldspars show a pervasive weak alteration to sericite and carbonate, whereas hornblende and biotite alter to chlorite. Variations in this phase are controlled by abundance of K-feldspar megacrysts and biotite.

Late stage magmatism and fluid events

The record of late stage magmatic and fluid events is preserved as aplite and pegmatite dykes, miarolitic cavities, veins, alteration, and coated joints. Aplite dykes are typically 5 cm to 1 m wide and contain sparse grains of hornblende and biotite. Dykes are abundant along all margins of the intrusion, but the greatest density occurs along the southern and western

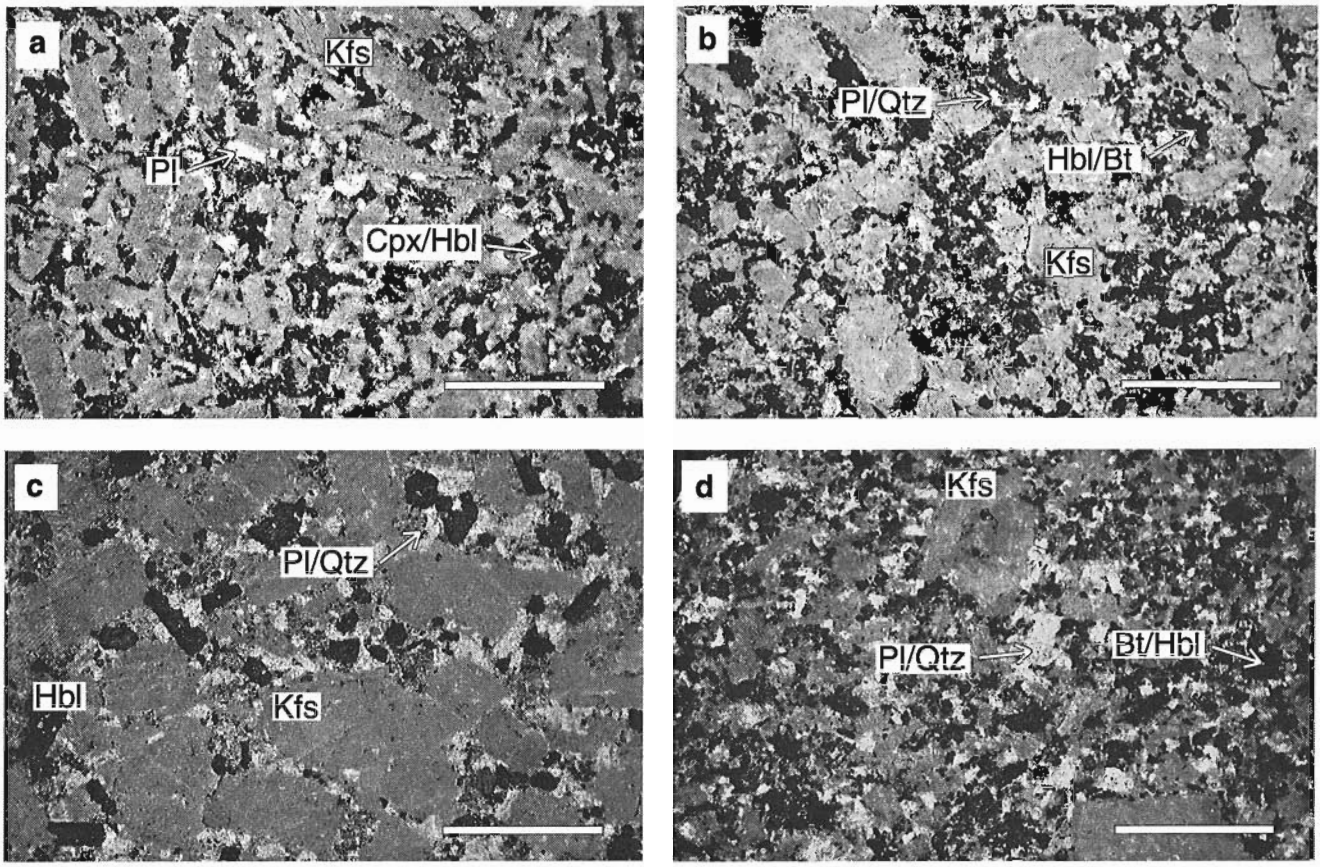

Figure 5. *Slabbed and stained hand samples of the* ***a)*** *augite syenite,* ***b)*** *hornblende quartz syenite,* ***c)*** *hornblende quartz monzonite, and* ***d)*** *biotite granite. Scale bar is 1.0 cm. Kfs=K-feldspar, Pl=plagioclase, Cpx=clinopyroxene, Hbl=hornblende, Qtz=quartz, Bt=biotite.*

contacts where they are closely associated with pegmatites, miarolitic cavities, and mineralized veins (Fig. 3b). Miarolitic cavities represent a macroscopic expression of volatile-rich fluids being emplaced in a predominantly melt system; they indicate that the magma was able to deform in response to bubble growth and coalescence.

Southern contact region

Along the southern contact of the intrusion, aplite, pegmatite, vein, and major joint set orientations are parallel, trend east, and dip north at 50° to 70° (Fig. 3b); a trend that also parallels the long dimension of the intrusion.

A variety of east-trending, north-dipping mainly quartz-K-feldspar pegmatites intrude the southern contact of the intrusion. Pegmatites are commonly spatially associated with large miarolitic cavities; they intersect or connect with miarolitic cavities and commonly the cavities are elongate parallel to the dykes (Fig. 4a, b). These may be similar to porous zones described in the Capitan pluton by Dunbar et al. (1996), along which transport of a magmatic volatile phase has been postulated. Pegmatites comprising massive, coarse biotite up to 3 cm in width, are rare but appear to be associated with bleached surrounding wall rock.

Miarolitic cavities along the southern contact are observed in all phases, but occur mainly within the hornblende quartz syenite (Fig. 3b), and attain sizes up to several metres in diameter (Fig. 4a, b). The spherical cavities commonly contain a outer coating of very coarse grained K-feldspar, with open-space-filling of quartz, tourmaline, muscovite, apatite, pyrrhotite, chalcopyrite, pyrite, bismuthinite, molybdenite, arsenopyrite, and gold. Quartz crystals can be over 60 cm long. Smaller, 1 m scale miarolitic cavities are commonly filled with tourmaline crystals.

Veins along the southern contact are structurally concordant with aplite and pegmatite dykes (Fig. 4b). They are mainly coarse-grained quartz, with subordinate K-feldspar, and variable amounts of tourmaline and biotite. Mineralization usually occurs within veins and consists of molybdenite, pyrrhotite, pyrite, chalcopyrite, arsenopyrite, bismuthinite, and gold (Baker et al., 1997). Molybdenite mineralization dominates the system at deeper levels of the intrusion;

bismuthinite and gold mineralization appears at higher levels. Alteration is sparse around veins and consists of narrow envelopes of sericite. Joints have sericite alteration envelopes and are rarely coated with quartz. Within the biotite granite, joints are coated with massive tourmaline and show no alteration of the wall rock.

Western contact region

Along the western margin of the intrusion, veins and dykes are oriented in a north-trending, shallow east-dipping direction (Fig. 3b). In this area, there are much fewer veins and pegmatites, but many more aplite dykes and coated joints compared to the southern margin. Aplite dykes occur as centimetre-scale bodies. Joint surfaces are coated with chlorite, hornblende, tourmaline, chalcopyrite, pyrite, and pyrrhotite. Chlorite alteration extends into the wall rock for 1-2 cm. Fracture coatings and veinlets parallel aplite dykes and are not observed crosscutting the dykes. Pegmatites and veins also trend north and dip shallowly to the east but are otherwise similar to those along the southern margin. Miarolitic cavities in the western margin are on the decimeter scale and contain quartz and scheelite crystals.

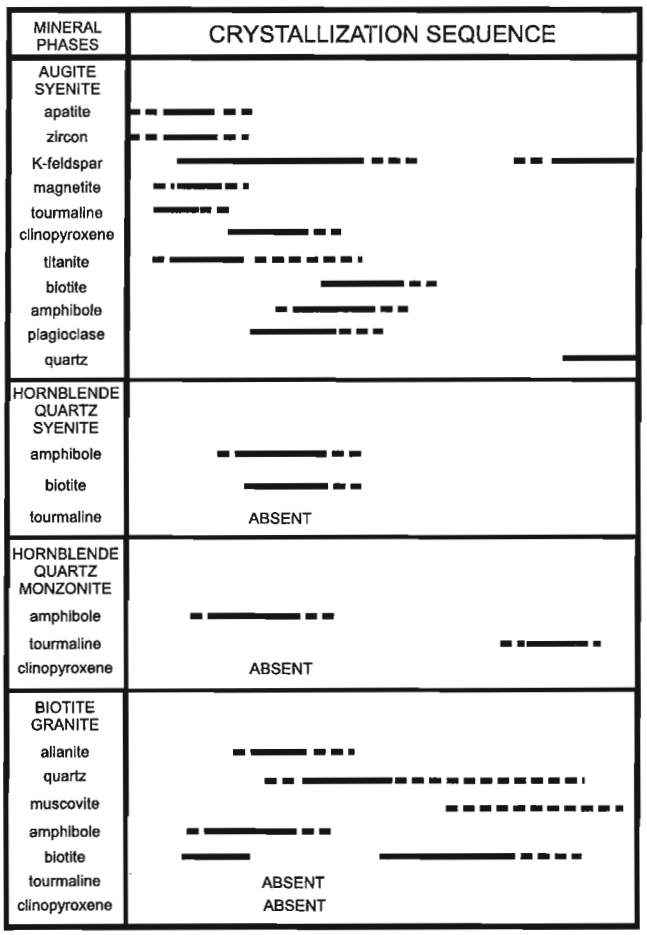

Figure 6. *Crystallization sequences for the four major intrusive phases at Emerald Lake Pluton. Diagrams for the hornblende quartz syenite, hornblende quartz monzonite, and biotite granite only show mineral phases that are not present in the augite syenite, or relative sequences that are significantly different from the augite syenite.*

PHYSICAL PROPERTIES AND CHEMICAL COMPOSITION

Density and magnetic susceptibility and whole-rock chemical compositions of the different phases of Emerald Lake Pluton are summarized in Table 1. Bulk density was determined on large, 500-2000 g hand samples. Samples were dried at 105°C and allowed to cool in a desiccator until equilibrated with room temperature. Density was measured by the hydrostatic weighing technique (Hutchison, 1974; Muller, 1977) using a Mettler PL3000 electronic top-loading balance. The density of water was corrected for temperature variations and an average precision of ± 0.0017 g/cm^3 was achieved. Magnetic susceptibility of the same sample suite was measured with a hand held Exploranium KT-9 Kappameter and values reported in Table 1 are from an average of ten measurements (L'Heureux and Anderson, 1997).

Samples chosen for chemical analysis were approximately 2-2.5 kg and underwent standard rock crushing procedures (Cui and Russell, 1995), but were powdered to about 200 mesh using a chrome steel shatter box. Major and some trace elements were measured by X-ray fluorescence (XRF) at McGill University using a PW2400 XRF spectrometer on fused beads prepared from a 1:5 mixture of rock powder to lithium tetraborate. Iron oxide was determined directly by volumetric analysis. Additional trace elements (e.g. Rb, Sr, Y, Zr) were measured at Activation Laboratories Ltd. using inductively coupled plasma mass spectrometry (ICP-MS) on totally digested samples.

Measured values of density and magnetic susceptibility are presented as contoured data superimposed on the geological map (Fig. 7a, b). Contouring has been implemented as a graphical tool to aid in the visualization of physical properties data. The distribution of data in the western half of the pluton leads contours in this area is highly interpretive. It is recognized that the contouring presented here is nonunique, but represents one valid interpretation of the data. Contour intervals are substantially greater than the precision of the data. A summary of the data used to create contours is provided here (Table 1).

Contour distribution conforms to the following geologically based guidelines: contour lines can be cut by the boundaries of the intrusion, contour lines can be cut by inferred younger phases of the intrusion, and contour lines cannot be cut by older intrusive phases. These rules are justified because the full extent of the pluton is not observed; therefore, density contours can extend beneath the present day pluton-country rock contact. Younger magmatic phases may have disrupted the density configuration of older intrusive phases.

The data reveal that each intrusive phase has a distinct average density value. However, there is significant overlap in the range of values between the different phases (Table 1). Contours show a general decreasing trend in density from west to east commensurate with the relative mafic to felsic emplacement sequence of the augite syenite through to biotite granite phases (Fig. 7a). More detailed examination reveals that the augite syenite is defined by bands of increasing density with a high core value (2.77-2.79 g/cm^3). These contours are cut by the hornblende quartz syenite; contours in this younger phase form an elongate bulls eye pattern with a lower (2.65-2.67 g/cm^3) core increasing outwards to a margin of 2.70-2.75 g/cm^3. The hornblende quartz monzonite displays a general decrease in density from west to east (2.68-2.79 g/cm^3 to 2.60-2.61 g/cm^3) with a relatively denser northern boundary and a core of very low density (2.60-2.61 g/cm^3) in the southeastern portion of the pluton. The biotite granite is defined by a concentric pattern with a low density core (2.60-2.61 g/cm^3) increasing to a maximum of 2.63 g/cm^3 at the phase boundary.

The density contours primarily reflect differences in mineralogy. Thus, the augite syenite, more mafic-rich than other phases, is denser, whereas the biotite granite, dominated by feldspar, quartz, and fewer mafic minerals, is less dense. The correlation with mineralogy is also confirmed within the hornblende quartz monzonite. The high density band along the northeast contact of the pluton (Fig. 7a) corresponds to an increase in modal abundance of hornblende observed as the contact with the country rocks is approached. Likewise, the low density core within the hornblende quartz monzonite corresponds to samples with higher quartz content. Superimposed structural elements such as faulting and fracturing can have a minor effect on the density contour patterns. Two

Figure 7.

*Comparative maps of **a)** contoured density values, **b)** contoured magnetic susceptibility values, and **c)** Shand Index values for the Emerald Lake Pluton.*

Table 1. Average and range of major element, selected trace element, and physical property compositions of major intrusive phases of Emerald Lake Pluton.

	Augite Syenite		Hornblende Quartz Syenite		Hornblende Quartz Monzonite		Biotite Granite	
	Average (N=8)	Range	Average (N=11)	Range	Average (N=10)	Range	Average (N=6)	Range
SiO_2	58.22	54.81 - 62.75	65.11	62.46 - 66.20	66.74	64.00 - 68.99	70.89	69.22 - 72.55
TiO_2	0.763	0.565 - 1.013	0.582	0.464 - 0.768	0.479	0.341 - 0.687	0.239	0.174 - 0314
Al_2O_3	15.60	14.64 - 17.01	14.69	14.31 - 15.05	14.91	14.36 - 15.31	14.71	14.19 - 15.03
FeO	4.12	2.57 - 5.87	3.07	2.58 - 3.82	2.81	2.01 - 4.66	1.69	1.13 - 2.10
Fe_2O_3	2.06	0.87 - 3.49	1.69	1.16 - 2.47	1.09	0.54 - 1.64	0.41	0.25 - 0.55
MnO	0.126	0.094 - 0.146	0.094	0.077 - 0.132	0.086	0.051 - 0.122	0.035	0.029 - 0.041
MgO	2.48	0.87 - 3.72	1.31	0.87 - 1.93	1.01	0.59 - 1.50	0.38	0.21 - 0.59
CaO	5.71	3.69 - 7.09	3.47	2.93 - 4.26	3.00	2.37 - 3.71	1.71	1.45 - 2.31
Na_2O	2.46	1.71 - 3.10	2.41	2.28 - 2.58	2.53	2.28 - 2.98	2.94	2.78 - 3.13
K_2O	7.25	6.13 - 9.14	6.44	6.19 - 6.95	6.35	5.64 - 6.78	5.57	5.07 - 5.81
P_2O_5	0.404	0.155 - 0.561	0.271	0.191 - 0.407	0.208	0.133 - 0.301	0.088	0.058 - 0.124
LOI	0.40	0.29 - 0.58	0.53	0.24 - 0.81	0.53	0.29 - 1.08	1.15	0.50 - 1.49
Total	99.58	99.13 - 99.73	99.67	99.56 - 99.76	99.73	99.53 - 99.84	99.80	99.75 - 99.84
Fe_2O_3 Tot	6.63	4.70 - 8.22	5.10	4.48 - 6.72	4.21	3.07 - 5.84	2.29	1.74 - 2.79
CO_2	0.20	0.05 - 0.57	0.23	0.05 - 0.40	0.23	0.08 - 0.67	0.74	0.65 - 0.82
V	142	81 - 184	87	70 - 125	69	40 - 103	24	16 - 35
Cu	38	18 - 76	28	11 - 55	14	6 - 30	24	13 - 51
Zn	83	57 - 130	66	26 - 87	66	34 - 97	33	12 - 57
Rb	314	241 - 368	369	319 - 430	368	358 - 383	321	293 - 347
Sr	1119	921 - 1670	732	609 - 848	709	673 - 778	391	307 - 479
Y	29	23 - 36	23	21 - 25	21	19 - 22	13	11 - 15
Zr	294	245 - 334	286	277 - 296	230	217 - 243	159	122 - 190
Ba	2027	1632 - 3056	1669	1195 - 2002	1364	965 - 1857	631	447 - 790
DI	66.47	55.26 - 78.74	76.03	72.09 - 80.28	78.71	72.60 - 82.53	86.79	84.12 - 90.21
Shand Index	0.70	0.59 - 0.78	0.85	0.76 - 0.89	0.91	0.85 - 0.98	1.05	0.98 - 1.09
	Average (N=8)	Range	Average (N=16)	Range	Average (N=41)	Range	Average (N=11)	Range
Density (g/cm^3)	2.725	2.668 - 2.77	2.675	2.650 - 2.717	2.649	2.606 - 2.701	2.615	2.603 - 2.626
MS	17.07	0.33 - 48.58	16.05	5.42 - 23.48	10.31	0.19 - 26.27	1.01	0.09 - 5.61

Notes:
MS = magnetic susceptibility, values are x 0.001 S.I. units.
DI = Differentiation Index (sum of normative quartz, orthoclase, albite, nepheline, kaliophilite, and leucite).
Shand Index = Molar $Al_2O_3/(CaO+Na_2O+K_2O)$.

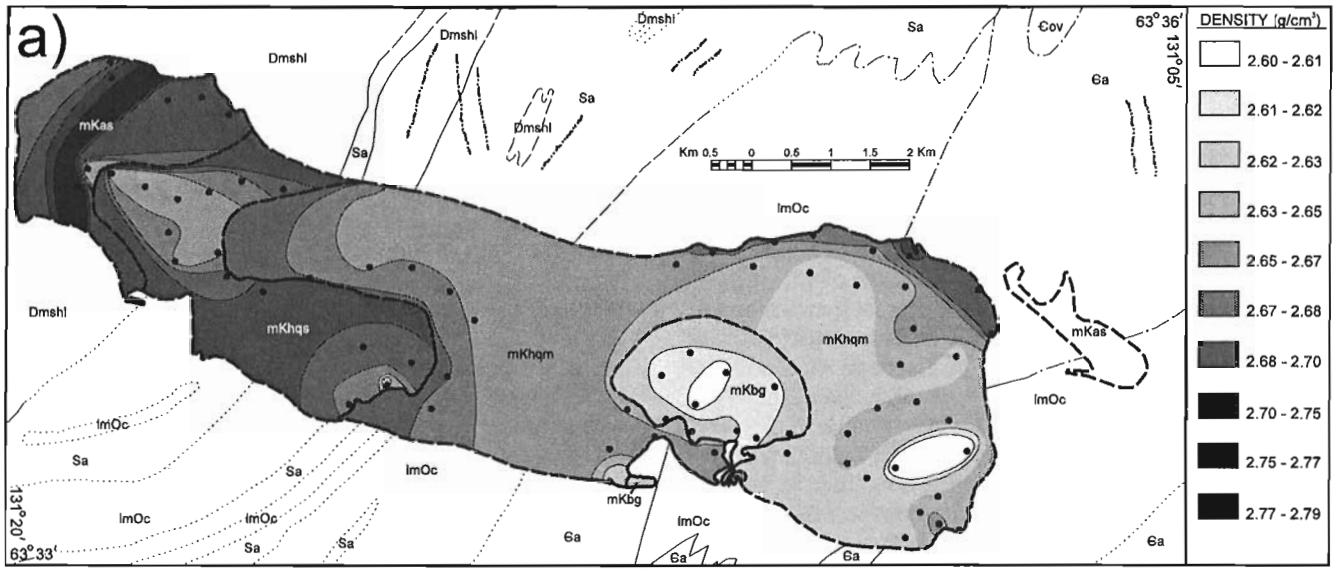
a)
DENSITY (g/cm³)
2.60 - 2.61
2.61 - 2.62
2.62 - 2.63
2.63 - 2.65
2.65 - 2.67
2.67 - 2.68
2.68 - 2.70
2.70 - 2.75
2.75 - 2.77
2.77 - 2.79
63°36'
131°05'
131°20'
63°33'
Km 0.5 0 0.5 1 1.5 2 Km
Dmshl
mKas
mKhqs
mKhqm
mKbg
lmOc
Sa
Ea
Cov

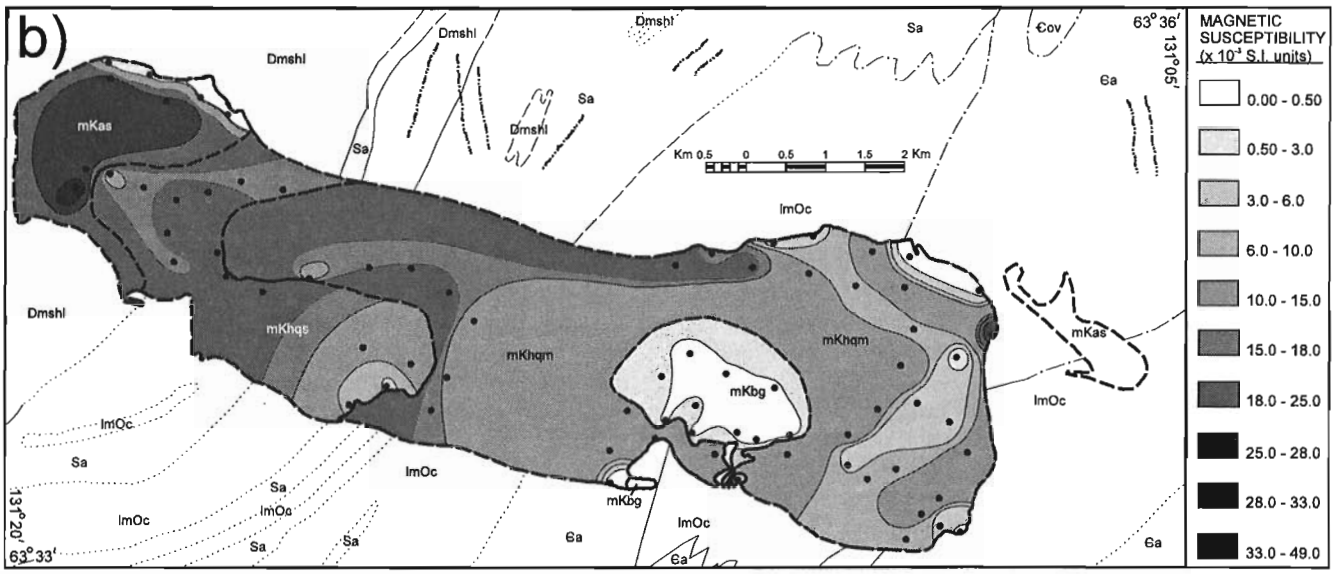
b)
MAGNETIC SUSCEPTIBILITY
(x 10⁻³ S.I. units)
0.00 - 0.50
0.50 - 3.0
3.0 - 6.0
6.0 - 10.0
10.0 - 15.0
15.0 - 18.0
18.0 - 25.0
25.0 - 28.0
28.0 - 33.0
33.0 - 49.0
63°36'
131°05'
131°20'
63°33'
Km 0.5 0 0.5 1 1.5 2 Km
Dmshl
mKas
mKhqs
mKhqm
mKbg
lmOc
Sa
Ea
Cov

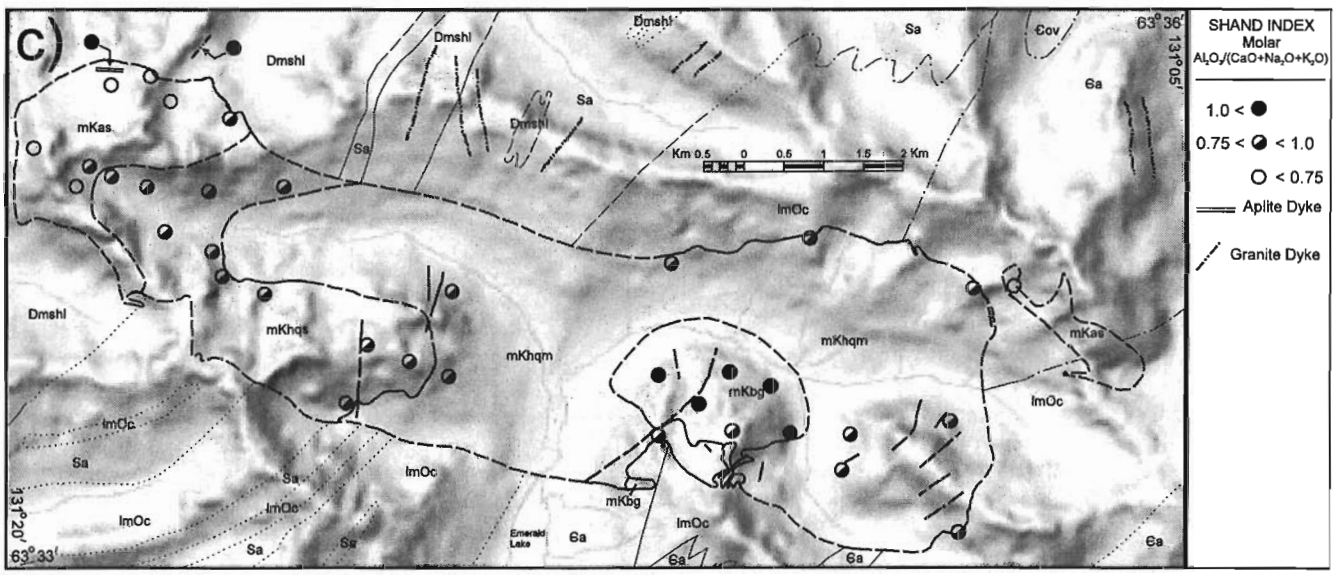
c)
SHAND INDEX
Molar
Al₂O₃/(CaO+Na₂O+K₂O)
1.0 <
0.75 < < 1.0
< 0.75
Aplite Dyke
Granite Dyke
63°36'
131°05'
131°20'
63°33'
Km 0.5 0 0.5 1 1.5 2 Km
Dmshl
mKas
mKhqs
mKhqm
mKbg
lmOc
Sa
Ea
Cov
Emerald Lake

contoured zones of 2.60-2.61 g/cm^3 (Fig. 7a) correspond to areas which have faults, and may result from a decrease in density due to the presence of micro-fractures in the sample, or the partial alteration of K-feldspar, plagioclase, and amphibole to less dense clay, carbonate, and phyllosilicate minerals.

Magnetic susceptibility is contoured according to the same rules as density data (Fig. 7b). Each intrusive phase has a characteristic average magnetic susceptibility value, but again, there is significant overlap in the range of values present in each phase (Table 1). The same general trends found in the density data are observed in the magnetic susceptibility data. There is a general decrease in magnetic susceptibility from west to east from high values (33-49) in the augite syenite to low values (0.0-0.5) in the biotite granite. There are, however important differences between the contour patterns for density and magnetic susceptibility data (Fig. 7a, b). The two most striking differences are located along the northern contact between augite syenite and country rocks, and the northeastern contact between hornblende quartz monzonite and country rocks. Both these areas have high density values, but very low magnetic susceptibility values. If magnetic susceptibility is a measure of magnetite content, then these two areas, which represent a local negative correlation between density and magnetic susceptibility, are unexpected because a positive correlation between magnetic susceptibility and density would be expected due to the high density of magnetite. The nature of these anomalies is under investigation.

The intrusive phases of the Emerald Lake Pluton are also distinct chemically; there is an expected general increase in SiO_2 and decrease in MgO and FeO(T) from augite syenite to biotite granite (Table 1). A similar trend is observed in Shand Index (Molar $Al_2O_3/(CaO+Na_2O+K_2O)$, SI), (Table 1, Fig. 7c). The distribution of Shand Index values shows the general increase in SI from augite syenite samples (SI <0.75, metaluminous) to hornblende quartz syenite and hornblende quartz monzonite (SI: 0.75-1.00, metaluminous), and most biotite granite samples (SI >1, peraluminous). Granitic and aplite dyke samples are also peraluminous. These chemical trends correlate with both variations in mineralogy and the observed trends in the physical property data.

SEQUENCE OF EVENTS

The inferred sequence of magmatic and late stage fluid events associated with the Emerald Lake Pluton (Fig. 8) are established on the basis of crosscutting relationships and inclusion relationships among the four major igneous phases and dykes, pegmatites, miarolitic cavities, and veins.

The history of the pluton began with the emplacement of the augite syenite in a partially crystallized state; the trachytic texture was possibly derived from this event and marks flow direction. Intrusion of augite syenite was followed in quick succession by emplacement of the hornblende quartz syenite and hornblende quartz monzonite. The biotite granite is hypothesized to be the last major intrusive event at Emerald Lake and was emplaced soon after the hornblende quartz monzonite. Closely spaced major intrusive events allowed the entire pluton to behave as one body from the onset of late stage magmatism and production of a magmatic volatile phase through the transition to hydrothermal activity.

Saturation of volatiles and vesiculation of the pluton to form miarolitic cavities occurred over a similar range of relative time as emplacement of intrusive phases (Fig. 8). The extended range of miarolitic cavity occurrence in the timing sequence is known because cavities are present in all intrusive phases, although rarer in the hornblende quartz monzonite and biotite granite. The existence of miarolitic cavities dictates that the intrusive phases were above the solidus. A similar argument applies to pegmatites. Small ameoboid patches of pegmatite are present in the augite syenite and the hornblende quartz monzonite indicating that they existed as part of the melt system. The difference between miarolitic cavities and pegmatites, however, is that pegmatites predominantly occur as dykes indicating brittle-style injection into the pluton and suggesting that pegmatites are a near subsolidus event. Pegmatites that intersect and elongate miarolitic cavities (Fig. 4b) are believed be emplaced while the pluton was significantly above the solidus. For the same reason, aplite dykes, veins, faults, fractures, and fracture coatings are all postulated to have essentially formed over the same interval of time, and are restricted to the subsolidus portion of the pluton's history. Mineral precipitation along open fracture surfaces marked the end of magmatic-hydrothermal activity at Emerald Lake Pluton.

Molybdenite, bismuthinite, chalcopyrite, and gold mineralization coincide with the development of miarolitic cavities, quartz K-feldspar veins, and joint surfaces. This dictates that these minerals of economic interest span both the magmatic and hydrothermal portions of the history of the pluton.

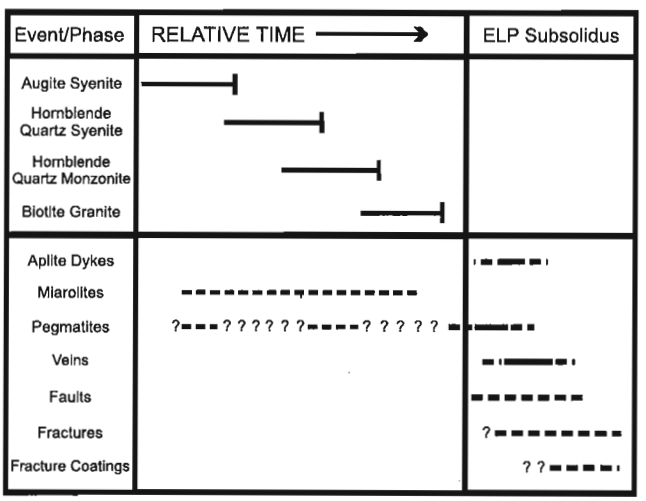

Figure 8. *Relative timing sequence for major intrusive phases, late stage magmatic phases, fluid phases, and structural features at Emerald Lake Pluton.*

ACKNOWLEDGMENTS

The senior author was supported by a Natural Sciences and Engineering Research Council of Canada (NSERC) PGS-A scholarship. Research costs were borne by the Mineral Deposit Research Unit through the NSERC Industrially Oriented Research grant: "Regional and System-Scale Controls on the Formation of Cu and/or Au Magmatic-Hydrothermal Mineralization". All geological maps were produced under the aegis of the Geological Survey of Canada. Logistical support from Brian Lueck and Alliance Pacific Gold Corporation during the 1996 field season is greatly appreciated. Steve Gordey is thanked for providing us with the digital base maps for Figures 1 and 2. We appreciate a review of an earlier version of the manuscript by Glenn Woodsworth, and checking of the final version by Bev Vanlier.

REFERENCES

Anderson, R.G.
1988: An overview of some Mesozoic and Tertiary plutonic suites and their associated mineralization in the northern Cordillera; in Recent Advances in the Geology of Granite-Related Mineral Deposits, (ed.) R.P. Taylor and D.F. Strong; Canadian Institute of Mining and Metallurgy, Special Voume 39, p. 96-113.

Baker, T., Lang, J.R., and Mortensen, J.K.
1997: Au-mineralization associated with the mid-Cretaceous Tombstone-Tungsten Magmatic Belt, Yukon and Alaska; Program with Abstracts, Geological Association of Canada/Mineralogical Association of Canada, v. 22, p. A7.

Bakke, A.
1995: The Fort Knox "porphyry" gold deposit - structurally controlled stockwork and shear quartz vein, sulphide-poor mineralization hosted by a Late Cretaceous pluton, east-central Alaska; in Porphyry Deposits of the Northwestern Cordillera of North America, (ed.) T.G. Schroeter; Canadian Institute of Mining and Metallurgy and Petroleum, Special Volume 46, p. 795-802.

Bard, J.P.
1986: Microtextures of Igneous and Metamorphic Rocks; D. Reidel Publishing Company, 264 p.

Blusson, S.L.
1974: Geology, Operation Stewart (northern Selwyn Basin) Yukon and District of Mackenzie, N.W.T. (106A, B, C; 105N, O); Geological Survey of Canada, Open File 205.

Cecile, M.P.
1984: Geology of southwest and central Niddery Lake (105O-4,5,6,11); Geological Survey of Canada, Open File 1118.

Cecile, M.P. and Abbott, J.G.
1992: Geology of the Niddery Lake map-area (NTS 105O); Geological Survey of Canada, Open File 2465.

Cui, Y. and Russell, J.K.
1995: Magmatic origins of calc-alkaline intrusions from the Coast Plutonic Complex, southwestern British Columbia; Canadian Journal of Earth Sciences, v. 32, p. 1643-1667.

Dunbar, N.W., Campbell, A.R., and Candela, P.A.
1996: Physical, chemical, and mineralogical evidence for magmatic fluid migration within the Capitan pluton, southeastern New Mexico; Geological Society of America Bulletin, v. 108, p. 318-333.

Gabrielse, H.
1967: Tectonic evolution of the northern Canadian Cordillera; Canadian Journal of Earth Sciences, v. 4, p. 271-298.

Gordey, S.P. and Anderson, R.G.
1993: Evolution of the Northern Cordilleran miogeocline, Nahanni map area (105I), Yukon and Northwest Territories; Geological Survey of Canada, Memoir 428, 214 p.

Hutchison, C.S.
1974: Laboratory Handbook of Petrographic Techniques; John Wiley & Sons, New York, 257 p.

L'Heureux, R.L. and Anderson, R.G.
1997: Early Cretaceous plutonic rocks and molybdenite showings in the Nithi Mountain area, central British Columbia; in Current Research 1997-A; Geological Survey of Canada, p. 117-124.

Muller, L.D.
1977: Density determination; in Physical Methods in Determinative Mineralogy, (ed.) J. Zussman; Academic Press, London, p. 663-673.

Poulsen, K.H., Mortensen, J.K., and Murphy, D.C.
1997: Styles of intrusion-related gold mineralization in the Dawson-Mayo area, Yukon; in Current Research 1997-A; Geological Survey of Canada, p. 1-11.

Smit, H.
1984: Petrology, chemistry, age, and isotope study of the high potassium Emerald Lake pluton, eastern Yukon Territory; B.Sc. thesis, University of British Columbia, Vancouver, British Columbia, 42 p.

Smit, H., Armstrong, R.L., and van der Heyden, P.
1985: Petrology, chemistry and radiogenic isotope (K-Ar, Rb-Sr, and U-Pb) study of the Emerald Lake pluton, eastern Yukon Territory; in Current Research, Part B; Geological Survey of Canada, Paper 85-1B, p. 347-359.

Woodsworth, G.J., Anderson, R.G., and Armstrong, R.L.
1991: Plutonic Regimes, Chapter 15; in Geology of the Cordilleran Orogen in Canada, (ed.) H. Gabrielse and C.J. Yorath; Geological Survey of Canada, Geology of Canada, no. 4, p. 491-531. (also Geological Society of America, The Geology of North America, no. G-2).

Geological Survey of Canada Project 840046

Development and application of a three-dimensional surface model for the Emerald Lake Pluton, east-central Yukon Territory

N.L. Hastings, R.A. Duncan[1], S. Williams, and R.G. Anderson
GSC Pacific, Vancouver

Hastings, N.L., Duncan, R.A., Williams, S., and Anderson, R.G., 1998: Development and application of a three-dimensional surface model for the Emerald Lake Pluton, east-central Yukon Territory; in Current Research 1998-A; Geological Survey of Canada, p. 13-17.

Abstract: Development of a three-dimensional surface model is a useful analytical tool for geoscientists. The main benefits are in improvements to visualisation of the topography and geology and the ability to analyze the spatial relationships of multiple data sets. Emerald Lake (NTS 105 O/11) is an ideal site for the development of a surface model due to its mountainous terrain and abundance of geological data. This paper explores the techniques for creation of a surface model and demonstrates the analytical benefits gained. The surface model allows for quick visualization of geological information from Emerald Lake Pluton, which reveals the subhorizontal nature of phase contacts, suggesting that phases may have been intruded as sheets. Information can be gained on the occurrence of miarolitic cavities and veins at various elevations. The model provides capabilities for querying multiple data sets to reveal spatial patterns and allow development of prediction models.

Résumé : Un modèle de surface tridimensionnel constitue un outil analytique utile aux géoscientifiques. Ses principaux avantages sont une amélioration de la visualisation de la topographie et de la géologie ainsi que la possibilité d'analyser les relations spatiales entre plusieurs ensembles de données. La région du lac Emerald (feuillet 105O/11 du SNRC) est idéale pour la conception d'un modèle de surface en raison du caractère montagneux du terrain et de l'abondance des données géologiques. Le présent article décrit les techniques de conception d'un modèle de surface et illustre les avantages analytiques qui en découlent. Le modèle de surface permet une visualisation rapide de l'information géologique relative au pluton d'Emerald Lake; ainsi, la nature subhorizontale des contacts entre les phases est mise en évidence, ce qui laisse supposer que chacune d'elles a pu faire intrusion sous la forme d'un feuillet. Il est aussi possible d'obtenir des indications sur la présence de cavités miarolitiques et de veines à divers intervalles d'élévation. Le modèle offre enfin la possibilité d'interroger plusieurs ensembles de données à la fois et, en conséquence, de mettre en évidence des relations spatiales et d'en arriver à l'élaboration de modèles prédictifs.

[1] Mineral Deposit Research Unit - Igneous Petrology Laboratory, Department of Earth and Ocean Sciences, University of British Columbia, 6339 Stores Road, Vancouver, British Columbia V6T 1Z4

INTRODUCTION

A three-dimensional surface model is an important tool for readily visualizing and interpreting the geology and related terrain of a region. The Emerald Lake area is located approximately 70 km northwest of Macmillan Pass in eastern Yukon Territory (Fig. 1). The area is particularly well suited for the development of a surface model due to the physiography of the area, which consists of deeply cut glacial valleys and over-steepened ridges, that imparts significant relief to the area (Fig. 2). Creation of the surface model for Emerald Lake and the Pluton which underlies it has the potential to reveal important spatial and statistical information which will aid in the development of a rigorous petrogenetic model for the intrusion.

Traditionally, geological maps are presented in a two-dimensional format (Duncan et al., 1998). For those unfamiliar with the region, visualizing the interrelationships between the topographic and geological data can be difficult. The geographic information systems (GIS) based software ARC/INFO™ contains two modules: Triangulated Irregular Networks (TIN) and GRID which create, analyze, and display surfaces onto which any point or areal data set may be projected. These modules are utilized to develop a surface model of the region.

Humans can more readily understand complex spatial representations as opposed to data portrayed in tables (Bonham-Carter, 1994). Typically, geochemical data is portrayed in tables, two-dimensional plots, cross-sections, and long sections. This information can be difficult to visualize in three dimensions. Superimposing the data on a surface model allows one to maintain a spatial and geological context.

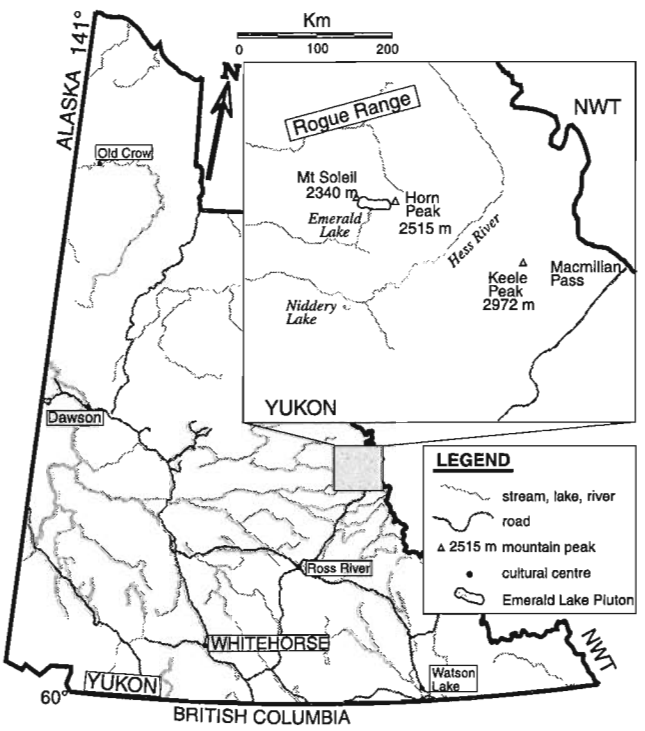

Figure 1. *Location map of the study area, Emerald Lake, Yukon Territory.*

Figure 2. *Emerald Lake area looking east. The pluton extends from the ridge in the foreground to the peak in the background on the left hand side of the photograph.*

A GIS has the capability of overlaying multiple spatial data sets. The display and manipulation of data layers may improve or reveal interpretations of spatial relationships. Spatial patterns which could otherwise go unnoticed become more apparent upon superposition of the geological data. Subsequent queries of the geological data sets can be performed in ARC/INFO™ to reveal the specific details of the geology. The possibilities for visualizing data and combining queries are unlimited. Geochemical data can be analyzed in all the methods familiar to geologists and portrayed with instant spatial and geological context. Petrographic information, for example modal abundances, can be given a spatial context which may reveal more subtle intraphase variations not observable in the field.

The objective of this article is to summarize the techniques involved in the creation of a three-dimensional model for the Emerald Lake area and, using the data sets collected from the Emerald Lake Pluton as an example, to demonstrate the general utility of the tool in order that geoscientists may be encouraged to use this tool.

STUDY AREA

The Emerald Lake Pluton underlies rugged terrain which results in 700-900 m relief elevation gain through the pluton and requires a significant vertical component to the positioning of geological data. The area is characterized by deep valleys and hanging valley glaciers with many cirques. Because of their resistance to erosion, the plutonic rocks underlie more rugged topography and higher elevations. Sedimentary rocks in the area tend to form more subdued terrain, where they consist of shales, resulting in more rounded ridges and gentler valleys. Mountains and ridges are more pronounced where chert-like units dominate and plutonic units form extremely sharp-ridged cliffs.

Emerald Lake Pluton is a composite body consisting of four major intrusive phases; augite syenite, hornblende quartz syenite, hornblende quartz monzonite, and biotite granite (Duncan et al., 1998). Spectacular miarolitic cavities (an indication of magmatic volatiles) occur within the pluton and are associated with sheeted aplite dykes, quartz-alkali feldspar-biotite pegmatite, and mineralized quartz vein systems (Duncan et al., 1998). The pluton is a member of the mid-Cretaceous Tombstone Plutonic Suite, and contains a sheeted pegmatite/vein system which contains bismuthinite, gold, and molybdenite mineralization similar to other deposits (Fort Knox, Dublin Gulch) within the suite (Mortensen et al., 1996; Duncan et al., 1998).

METHODOLOGY

Background and utility of the method

A three-dimensional surface model of a terrain surface can be generated using the ARC/INFO™ software ARC TIN™. A digital elevation model (DEM) is the digital format which represents a surface as a matrix of equally or unequally spaced points. These points form profiles across a surface (ARC/INFO™ software v. 7.0.4 Help, 1994). Canadian data sources for development of a surface model include an existing ARC/INFO™ coverage, a TRIM (Terrain Resource Information Management) positional file (for 1:20 000 coverage of British Columbia), Canadian digital elevation data, digital terrain elevation data (see Geomatics Canada Digital Products and Services page: http://www.ccg.nrcan.gc.ca/ext/html/english/products/products.html., 1997), an ASCII file containing point data, or an image.

The ARC TIN™ module of ARC/INFO™ contains tools which input the DEM data to create a TIN or lattice surface model. ARC TIN™ uses the Delaunay triangulation method ARC/INFO™ software v. 7.0.4 Help, 1994) which bases its model on continuous data, such as elevation. Using this model, a surface can be established by joining irregularly spaced points, lines, or polygons to a create a set of points with x, y, and z values. The points are joined to form triangles which mimic the topographical surface. Where no x, y, z points are located, the Triangulated Irregular Network (TIN) module interpolates to calculate the z value. In this model, the quintic interpolation option was utilized. This method of interpolation is best suited where the set of data points are highly irregular and define steep surfaces. Once the TIN is generated, the surface can be analyzed and altered to create an optimal view or orientation. Some of the analytical capabilities of the software include the creation of contours; the calculation of slope, aspect, surface area, and volume; the generation of cross-section profiles, and the establishment of hill shading. ARC/INFO™ coverages or images can then be draped on top of the model and queried for their associated data. For example, a scanned air photo could be draped on to the TIN to yield a three-dimensional view of the air photo. One of the challenges in creation of a TIN is the depiction of the three-dimensional perspective, because visualizing the ideal perspective usually takes time and requires experience. The latest version of ARC TIN™ (version 7.1.2) has improved the capacity to set up the optimum view and developed a means for creating three-dimensional flybys of an area (ESRI ARC/INFO™ website: http://www.esri.com/base/products/arcinfo/wntin.html, 1997). With the new version of ARC/INFO™, the model can be quickly rotated and manipulated within minutes as compared with the earlier ARC TIN™ version 7.0.4 which can take several hours to set up the optimum view. With the improvements to ARC TIN™ and the development of 3-D tools for the PC and UNIX-based program ArcView™, development of surface models are now more accessible to geoscientists.

Model development

The 1:10 000 scale TIN was generated from contour lines that had been digitized into AutoCAD® from the 1:50 000 scale NTS topographic map, 105 O/11. Contour lines were separated onto different layers according to their elevation value. A Drawing Interchange File (DXF) file was created from the AutoCAD® drawing and converted into ARC/INFO™ format. Using the CREATETIN function, the TIN was developed from a line coverage. The resulting shaded relief map displayed an undesirable 'banded effect' marked by dark bands along the contour lines derived as a result of a large number of vertices along each segment of the line coverage. When the TIN model was created, these vertices were automatically combined to form many small triangles along the edges of the contour lines.

To alleviate the problem, the TIN was resampled and created from a point coverage. An Arc Macro Language (AML) program was written to create a matrix of points, each assigned a label and covering the entire map, based on a 50 m by 50 m grid spacing. An elevation was assigned to each point using the TINSPOT command. This command interpolates the z value from adjacent sample points and assigns the value to the label. The resulting point coverage was utilized as the data source to create a new TIN. To remove some of the ambiguities and reduce the file size, the proximal tolerance of the TIN was set to 75 m, which eliminates those data points that occur within 75 m of other points, giving a final spacing of 100 m.

The SURFACEMENU program is included with the TIN software and allows the user to easily set up the orientation of a perspective or planimetric view. Hill shading can be draped over the TIN model. This applies varying shades of grey which correspond to different slope and aspect values and assist in illustrating the geomorphic and topographical features. The effects of the sun illumination angle and local shadows are calculated by specifying the sun angle and altitude. The optimal sun angle for highlighting the surface without obscuring most of the surface and geological data in dark shade was at an azimuth of 35° and an altitude of 40° relative to the model. There was no vertical exaggeration added; the inherent rugged topography of the area enabled most of the features to be clearly highlighted with a correct choice of sun angle compared with areas of comparatively flat terrain, where increasing the vertical exaggeration helps emphasize topographic variations. A surface resolution of 40 m was

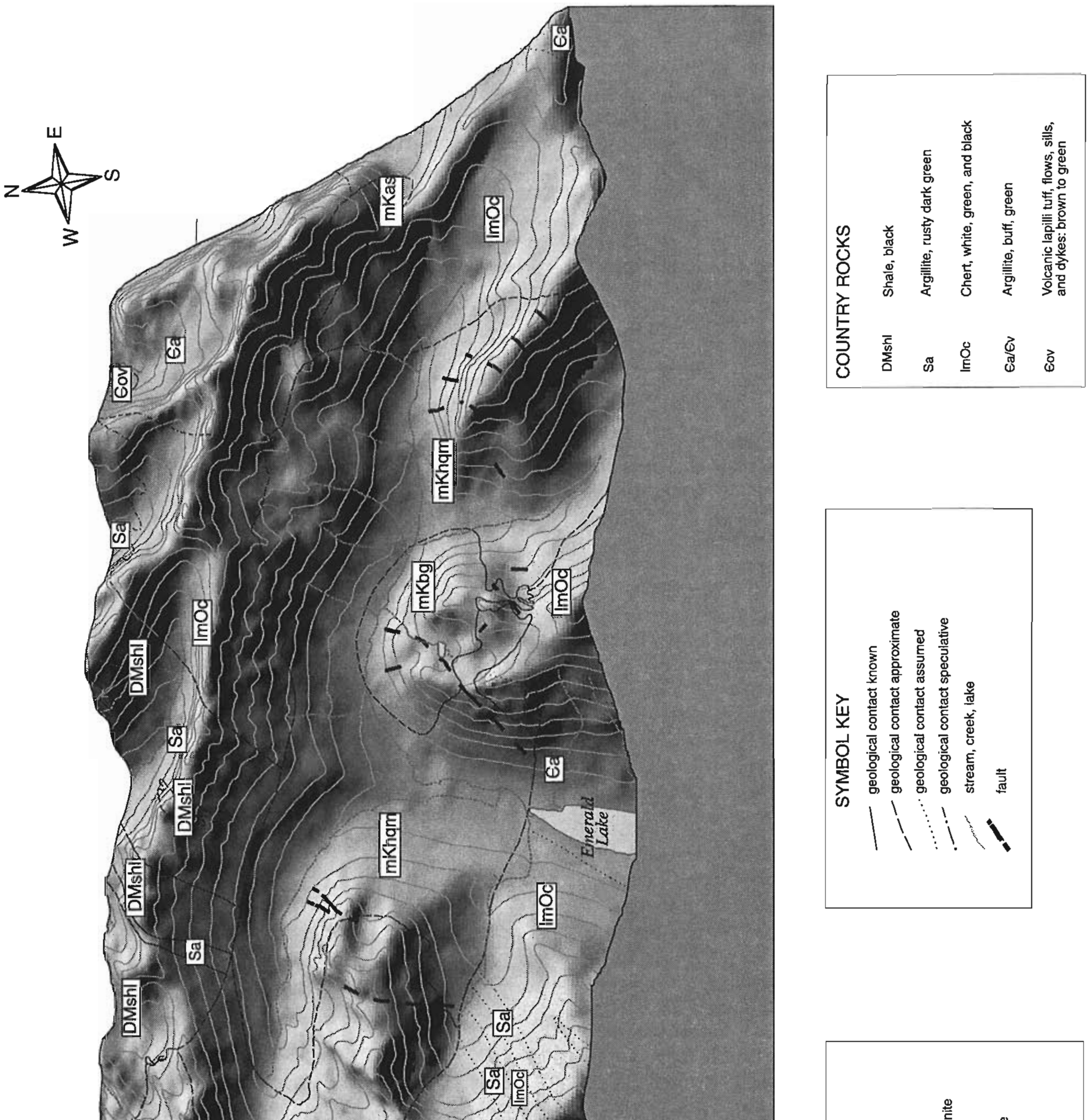

Figure 3. *Three-dimensional surface model of the Emerald Lake Pluton, where the sun illumination angle is located at an azimuth of 35° and an altitude of 40°.*

sufficient to produce a smooth surface and minimum file size. The raster image was exported as a postscript file and further enhanced and manipulated in CorelDRAW™, version 7.0. Using the ARC/INFO™ command SURFACEPROFILE, a cross-section of the surface model was generated along its southern edge and imported into the CorelDRAW™ file, to finish off the diagram and demonstrate the profile creation process (Fig. 3).

Geoscience applications

There are numerous analytical and visual benefits gained from the development of the Emerald Lake surface model, principally in visualization and interpretation of geological data, spatial analysis, and model development and prediction.

The most obvious benefit of the model to the reader is the improved visualization of the topography, as the model approximates the real-world surface. The terrain of the map becomes 'real' and it is immediately apparent to the reader what the area looks like. For a reader unfamiliar with the area, it allows one to rapidly gain a level of understanding of the geological features. The surface model aids in visualizing the nature and orientation of intrusive contacts at Emerald Lake Pluton (Fig. 3). The model reveals with ease that the augite syenite, hornblende quartz syenite, and hornblende quartz monzonite contacts in the western portion of the pluton are subhorizontal and that the phases may be intrusive sheets (Fig. 3). The orientation of faults can be visualized more quickly without resorting to structure contours (Fig. 3).

An obvious application specific to Emerald Lake Pluton is to query overlap of bismuthinite gold veins with the occurrence of miarolitic cavities. This may reveal possible elevation control on the development of volatiles which are spatially, temporally, and genetically associated with gold mineralization (Duncan et al., 1998). If miarolites are found restricted to one elevation range, this may suggest a sensitive pressure and have structural control on their formation and subsequent mineral deposition. Another query could verify whether the gold-associated minerals, molybdenite, tourmaline, and bismuthinite occur at restricted elevations or throughout the intrusive phase. These types of queries will be further developed and displayed in future publications.

There are many other possibilities for visualizing data and combining queries. Geochemical data can be analyzed in all the standard ways, but can now be put into a geological-spatial context. For example, the contoured physical and chemical properties maps presented in Duncan et al. (1998) would gain the benefit of adding elevation control to the interpretation of contours. This may reveal links between physical properties, chemical properties, and field observations that are obscured when viewed in two dimensions. To further test the hypothesis that Emerald Lake Pluton may be a series of intrusive sheets, detailed petrographic observations of modal abundances, grain size, or mineral chemistry could be added to the database, which may reveal more subtle intraphase and interphase gradations and layering.

CONCLUSIONS

The tools of GIS provide a means to utilize spatial data in problem solving and take spatial data beyond the retrieval and display of information (Bonham-Carter, 1994). Improvements to the TIN module and the availability of 'user-friendly' PC based three-dimensional analytical software make the development of surface models more accessible to geoscientists. Applying this model to Emerald Lake Pluton provides easy visualization of geological and structural relationships in three dimensions. As such, the subhorizontal nature of intrusive contacts are revealed, leading to the hypothesis that some portion of the phases may have been intruded as sheets. Insightful information on the topography of intrusive phases and the occurrence of miarolitic cavities and veins can be gained. The model also allows for the detailed querying of petrographic, chemical, physical, and field observations in a three-dimensional geological context. Multiple data sets can be queried and superimposed to reveal spatial patterns and create prediction models. Development of a surface model for the Emerald Lake Pluton has proven to be a very useful technique in gaining additional information and insight into the geology of the region.

ACKNOWLEDGMENTS

Many thanks to A. Makepeace for helpful advice in using the TIN module and critical reading of the report. Critical review of the article by G. Woodsworth is greatly appreciated. Assistance from B. Vanlier in formatting and editing of the manuscript is greatly appreciated. Thanks to R. Cocking for resource information. Support for the project was through the Geological Survey of Canada.

REFERENCES

Bonham-Carter, G.F.
1994: Geographic Information Systems for Geoscientists: Modelling with GIS; Pergamon, New York, 398 p.

Duncan, R.A., Russell, J.K., Hastings, N.L., and Anderson, R.G.
1998: Relationships between chemical composition, physical properties and geology of the mineralized Emerald Lake Pluton, Yukon Territory; in Current Research 1998-A; Geological Survey of Canada.

Mortensen, J.K., Murphy, D.C., Poulsen, K.H., and Bremner, T.
1996: Intrusion-related gold and base metal mineralization associated with the Early Cretaceous Tombstone Plutonic Suite, Yukon and east-central Alaska; in New Mineral Deposit Models of The Cordillera, Cordilleran Roundup Short Course Notes, p. L1-L13.

Geological Survey of Canada Project 840046

Progress report on bedrock geology of Lansing map area, central Yukon Territory

Charlie F. Roots[1]
GSC Pacific, Vancouver

Roots, C.F., 1998: Progress report on bedrock geology of Lansing map area, central Yukon Territory; in Current Research 1998-A; Geological Survey of Canada, p. 19-28.

Abstract: Regional mapping in 1996 and 1997 in western Lansing map area defined an upper Hyland Group succession, Cambrian submarine mafic volcanic accumulations, new exposures of Keno Hill quartzite, and several probable Permian and Triassic localities. The Robert Service Thrust trends southeast across the map area as an overturned contact between Yusezyu Formation sandstone and green Permian argillite. Tombstone Thrust lies within recessive Earn Group shale in the northwest, and is linked to the dextral Macmillan Fault in eastern Lansing map area. Folded Upper Paleozoic units along its south side imply that the fault formed the vertical northeastern boundary of the northwest-directed Tombstone thrust sheet.

Résumé : La cartographie régionale entreprise en 1996 et 1997 dans la partie ouest de la région cartographique de Lansing a permis de définir une succession de la partie supérieure du Groupe de Hyland, des accumulations volcaniques mafiques sous-marines cambriennes, de nouveaux affleurements du quartzite de Keno Hill et plusieurs localités à roches permiennes et triasiques probables. Le chevauchement de Robert Service s'étend en direction sud-est de part et d'autre de la région cartographique sous forme de contact renversé entre le grès de la Formation de Yusezyu et de l'argilite permienne verte. Le chevauchement de Tombstone se rencontre au sein du shale en retrait du Groupe d'Earn au nord-ouest et est associé à la faille dextre de Macmillan dans la partie est de la région cartographique de Lansing. La présence d'unités plissées du Paléozoïque supérieur le long de son côté sud porte à croire que la faille formait la limite nord-est verticale de la nappe de charriage de Tombstone, de direction nord-ouest.

[1] Yukon Geology Program, Canada-Yukon Geoscience Office, 2099 - 2nd Avenue, Whitehorse, Yukon Territory Y1A 2C6

INTRODUCTION

The field season of 1997 was the fourth in the revision mapping of Lansing map area, centred 140 km east of Mayo in central Yukon Territory (Fig. 1). Previously the area was a "knowledge gap" between regional mapping around Macmillan Pass to the east (Abbott, 1982; Cecile and Abbott, 1992; Gordey and Anderson, 1993) and the same rock units in McQuesten (e.g. Murphy and Héon, 1995) and Mayo (Roots and Murphy, 1992; Roots, 1997b) map areas to the west. The major structures extend into Lansing map area from both east and west, but do not "line up"; furthermore most stratigraphic and structural contacts were not resolved during preliminary mapping there (Blusson, 1974). This report builds upon previous findings (Roots and Brent, 1994a, b; Roots et al., 1995a, b; Roots, 1997a) and presents a summary of new mapping results from southwestern Lansing map area (Fig. 2, Table 1). Geochronological and biochronological dating and structural analyses continue as part of the contribution toward compilation of the regional bedrock map.

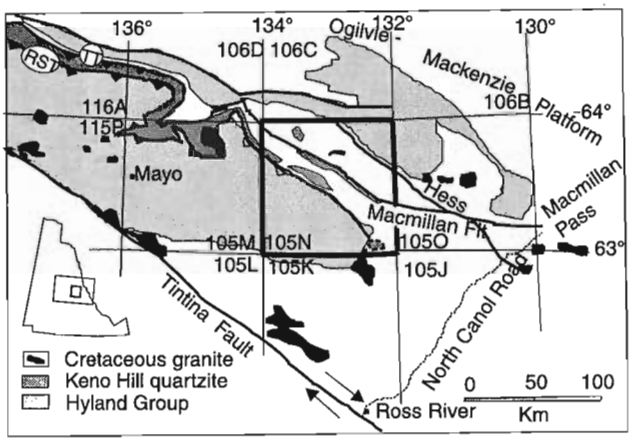

Figure 1. *Lansing map area (105N; outlined) in central Yukon. The Hyland Group pattern outlines the northern extent of the Selwyn Basin; the regional faults: Robert Service Thrust (RST), Tombstone Thrust (TT), and Hess and Macmillan faults are shown.*

REGIONAL STRATIGRAPHY AND STRUCTURE

Lansing map area lies near the northern edge of the Selwyn Basin, which was the outer part of the Lower Paleozoic miogeocline of ancestral North America (Gordey and Anderson, 1993). In the Lansing area, sedimentary rocks range in age from probable Late Proterozoic to Triassic or younger (Table 1). The oldest exposed rocks – grit and sandstone of the Hyland Group – were probably deposited upon a Proterozoic continental shelf that subsided as a result of extension during the Late Proterozoic. Selwyn Basin stratigraphy is dominated by dark shale, siltstone, and chert (Gull Lake Formation and Road River Group). The starved basin was disrupted in Middle Devonian time by block faulting (a probable extension event) and over-run by turbidites and fanglomerate as well as widespread black shale and chert (Earn Group). A clastic shelf regime was established in Early Carboniferous time with sandstone (now Keno Hill quartzite) succeeded by chert, laminated green argillite, calcareous

Table 1. Rock stratigraphic units in Lansing map area.

Map unit	Period or Epoch	Formation (if established)	Lithology	Reference
(crosses) Kg	Late Early Cretaceous	Tombstone Intrusions	Biotite-hornblende granodiorite	
Clastic shelf (Middle Carboniferous to Jurassic)				
TJ	Triassic, poss. Jurassic	Jones Lake Formation	Calcareous black shale, micaceous crossbedded sandstone; grey, noncalcareous shale	Roots et al., 1995a
(stripes)	Mid.Triassic	Mafic intrusions	Metadiorite, gabbro	Mortensen and Thompson, 1990
P	Permian	Mt. Christie Formation	Green-grey siltstone, buff green phyllite, brown chert	Roots et al., 1995a
C	Permian-Carboniferous		Dark grey slate interbedded with laminated quartz sandstone, quartzite and black / white chert	Roots et al., 1995a
(stippie)	Carboniferous	Keno Hill quartzite	Quartzite, carbonaceous schist, chloritic phyllite	Abbott and Turner, 1990; Roots, 1997a
Turbidite basin (Middle Devonian to Middle Carboniferous)				
DCE	Devonian to Carboniferous	Earn Group	Black shale, sandstone, chert grit, chert pebble conglomerate, minor limestone (Kalzas Fm.)	Gordey, 1990a; Gordey and Anderson, 1993
Selwyn Basin (Late Proterozoic to Middle Devonian)				
ЄSR	Cambrian to Early Devonian	Road River Group	Dark coloured argillite, siltstone, varicoloured chert	Roots et al., 1995a;
		Rabbitkettle Formation	Silty limestone	Roots, 1997b
		Gull Lake Formation	Olive and brown siltstone and shale, white limestone	Roots et al., 1995a
v v v	Cambrian	Plateau Mtn. volcanics	Mafic flows; locally pillows and hyaloclastite, diorite	
PЄH	Late Prot. to	Hyland Group		
(dashes)	Middle Cambrian	Narchilla Formation	Maroon argillite, green slate with minor quartzite	Roots et al., 1995a
		Senoah Member	Green to brown silicious phyllitic siltstone	M.P. Cecile pers. comm., 1994
		Algae Lake Formation	Light weathering, massive limestone	M.P. Cecile pers. comm., 1994
		Yusezyu Formation	Sandstone, grit, metasiltstone; quartzite top	Gordey and Anderson, 1993

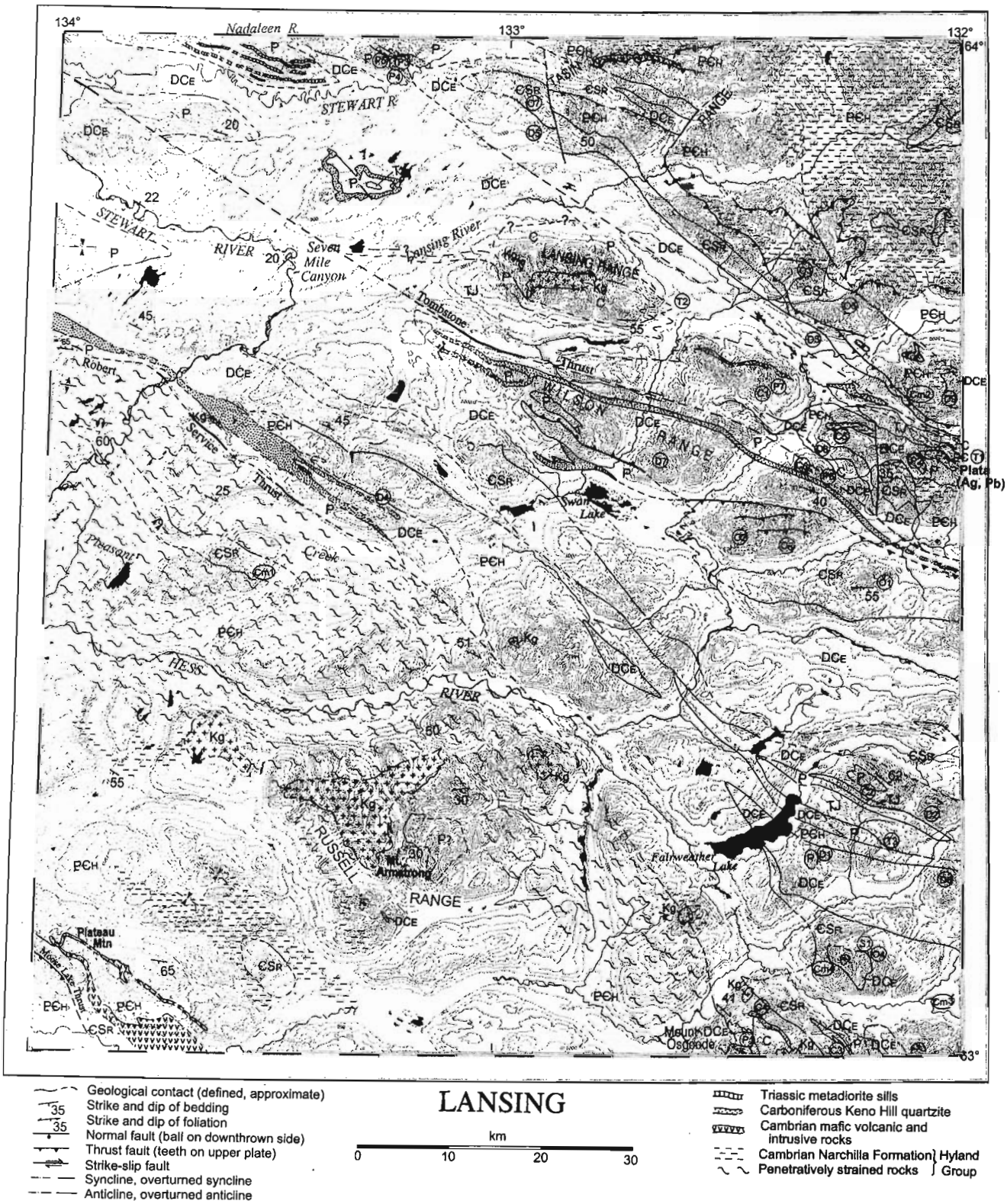

Figure 2. *Generalized geological map of Lansing map area. See Table 1 for explanation of units.*

sandstone, and noncalcareous shale of Carboniferous, Permian (Mount Christie Formation), and Triassic (Jones Lake Formation) age.

Collision of the miogeocline with exotic and pericratonic terranes to the southwest (e.g., Tempelman-Kluit, 1979) began in Middle Jurassic time. Incompetent strata of the Selwyn Basin were telescoped into thrust-imbricated folds; in the Early Cretaceous, large thrust panels moved north- and northwestward. Postorogenic plutons of the Tombstone Suite (J.K. Mortensen, pers. comm., 1994) core the highest ranges of the Lansing map area.

STRATIGRAPHY

In this section are highlights from new mapping in the western half of the Lansing map area. They include excellent exposures of a four-part Hyland Group and previously unrecognized Cambrian volcanics near Plateau Mountain. All major valleys in the northwestern part of the map area are underlain by Earn Group; some higher ground exposes erosional outliers and infolds of Carboniferous, Permian, and Triassic strata. New microfossils identified in limestones collected from the eastern and northern areas (Table 2) have shown a wider distribution of Upper Paleozoic and Triassic rocks than previously reported (e.g. Roots et al., 1995a). Collections in 1997 are expected to confirm the existence of younger strata in northwestern Lansing map area.

Proterozoic to Middle Devonian rocks

Yusezyu Formation

Chiefly exposed in both northeastern and southwestern parts of the map area, rocks of the Hyland Group (Gordey and Anderson, 1993) constitute four formations previously defined for adjacent Niddery Lake map area (M.P. Cecile, pers. comm., 1994). In southwestern Lansing map area, the Yusezyu Formation is the dominant unit in the hanging wall of the Robert Service Thrust. It is a coarse- to fine-grained sandstone succession containing minor grit intervals and dark green or grey siltstone layers; the succession appears to be at least several hundred metres thick, and is probably repeated by thrusts and folds at least 60 km across strike. Graded beds are common and clasts are not recrystallized. At the top of the Yusezyu Formation is a quartzite layer 5-15 m thick.

Upper Hyland Group

The three units of the upper Hyland Group are Algae Lake Formation, and Senoah and Arrowhead Lake members of the Narchilla Formation. They are well exposed on Plateau Mountain and in the highlands 10 km east of Plateau Mountain. The Yusezyu Formation is overlain by 10-30 m of light grey-weathering, coarsely recrystallized limestone which correlates with the Algae Lake Formation (M.P. Cecile, pers. comm., 1994). Above the limestone are two members of the Narchilla Formation. Lowermost is a resistant, medium-bedded, brown and greenish siliceous phyllitic siltstone. This indurated rock forms cliffs and talus of large slabs. Rare light-coloured limy layers which contain small authigenic pyrite crystals are the only break in the monotonous silicious phyllitic siltstone. This unit is lithologically and stratigraphically equivalent to the Senoah Member (M.P. Cecile, pers. comm., 1994). Conformably overlying the Senoah Member is maroon and brick-red argillite, siltstone, and purple slate that clearly correlates with the Arrowhead Lake Member (M.P. Cecile, pers. comm., 1994) of the Narchilla Formation.

Plateau Mountain volcanics

Several observations suggest that Plateau Mountain was the locus of igneous activity in the Early Cambrian. An accumulation of mafic volcanic flows and breccias is exposed on the south side of the mountain and discontinuously to the southeast. The volcanic rocks directly overlie the maroon argillite, limestone, and quartzite of the Hyland Group. Most exposures consist of well preserved amygdaloidal mafic flows, pillows, and interstitial hyaloclastite (Fig. 3). Terraces on the north and west sides of Plateau Mountain are formed by felsenmeer of chloritized diorite and gabbroic sills within the Yusezyu Formation sandstone. Seven kilometres southeast of Plateau Mountain, a continuously exposed diorite dyke intrudes maroon argillite and possibly fed the overlying pillow lavas. Another centre is indicated by prominent brown-weathering, south-facing cliffs up to 200 m high overlooking the Macmillan River, where an accumulation of pillowed and massive flows is inflated by comagmatic mafic intrusions.

Gull Lake Formation

In a few places in southwestern Lansing map area the Gull Lake Formation is recognized. This unit consists of olive and brown, silty argillite with thin sandstone beds and rounded cobbles of dark brown mudstone (possibly mafic volcanic mudstone) in a dark greenish-brown shale. In both southwest and northeast Lansing map area, the Gull Lake sediments appear to have a volcanic derivation as noted elsewhere (Cecile and Abbott, 1992; Gordey and Anderson, 1993).

Duo Lake Formation

The next overlying unit is dark grey, thin bedded mudstone and grey chert with wispy white laminae. This succession has an apparent thickness of 350 m south of Plateau Mountain. It is correlated with the Duo Lake Formation of the Road River Group but the overlying Steel Formation is missing. Instead the chert is succeeded by several tens of metres of thin bedded black chert and pisolitic limestone. Barite nodules in the dark grey mudstone could be Devonian, Carboniferous, or Permian. The succession is truncated by the Moose Lake Thrust which extends from adjacent Mayo map area (Roots, 1993).

Table 2. Fossil determinations and age assignments from internal GSC paleontology reports, identified by M.J. Orchard (MJO), B.S. Norford (BSN), F. Cordey (FC), and A.W.H. Pedder (AWHP).

No.	GSC Loc.	Age	Ident. by	Faunal List	Location	UTM coordinates
T1	C-108166	Late Carnian, Late Triassic	MJO 1994-27	*Metapolygnathus* ex. gr. *nodosus*	63°36'10"N;131°59'20"W	9 351580E 7056145N
T2	C-302203	Early? Triassic	MJO 95-35	*Neogondolilela* sp. cf. *N. sweeti*, *Neospathodus* sp . cf. *N. abruptus*, *Neospathodus* sp. cf. *N. crassatus*	63°44'42"N;132°37'00"W	8 617610E 7070600N
T3	C-302233	Triassic	MJO 95-35	*Neogondolella* sp.	63°12'24"N;132°09'50"W	8 642610E 7011585N
P1	C-302160	Late Permian?	FC 1994-1	*Entactina* sp., ?*Follicucullis* sp., *Pseudoalbaillella* sp.	63°00'12"N;132°25'54"W	8 630045E 6988372N
P2	C-300480	Early Permian	MJO 94-25	*Neogondolella* sp. cf. *N. idahoensis*	63°35'03"N;132°04'52"W	8 644850E 7053800N
P3	C-303087	Early Permian	MJO 97-15	*Neogondolella* sp., ramiform elements	63°59'31"N;133°17'21"W	8 583700E 7097050N
P4	C-303088	Early Permian, Artinskian	MJO 97-15	*Sweetognathus* sp., *Neogondolella* sp., *Neostreptognathus* sp. cf. *N. pequopensis*	63°59'06"N;133°43'12"W	8 584180E 7096300N
P5	C-303102	Early Permian	MJO 97-15	*Neogondolella*, sp., *Polygnathus* sp.	63°59'13"N;133°16'31"W	8 584390E 7096520N
P6	C-301303	Early Permian, ?Artinskian	MJO 94-25	*Neogondolella* sp. cf. *N. intermedia* *Sweetognathus* sp.	63°33'31"N;132°16'23"W	8 635450E 7050550N
P7	C-302219	Permian?	FC-1994-1	?*Latentifistula* sp., ?*Quadricaulis* sp.,?*Quinqueremis* sp.	63°39'46"N;132°23'45"W	8 628840E 7061760N
C1	C-301307	Early Carbonif. Visean-Serp.	MJO 94-25	*Vogelgnathus* sp. cf. *V. campbelli*, *Rhachistognathus*? sp.	63°39'10"N;132°25'32"W	8 627450E 7060700N
C2	C-302234	Early Carbonif. Tournaisian	MJO 95-35	*Bispathodus* ex gr. *stabilus*, *Pseudopolygnathus* spp. *Polygnathus communis*, *Siphonodella* spp.	63°16'07"N;132°12'44"W	8 639875E 7018380N
C3	C-303103	Early Carbonif. Tournaisian	MJO 97-15	*Bispathodus* sp., *Mehlina*? sp, *Polygnathus* spp. *Palmatolepis* sp., *Pseudopolygnathus* spp., *Siphonodella* spp.	63°01'04"N;132°15'27"W	8 638800E 6990345N
C4	C-303105	Tournasian Early Carboniferous	MJO 97-15	*Bispathodus*? sp., *Hindeodus*? sp., *Siphonodella* sp.	63°03'51"N;132°24'08"W	8 630200E 6992710N
C5	C-302367	Tournasian, Early Carb.	MJO 97-6 FC96-GSC1	*Siphonodella* sp., *Entactina* sp., *Entactinosphaera* sp.	63°36'54"N;132°16'36"W	8 635000E 7056800N
C6	C-302239	Late Dev. - Early? Carb.	MJO 95-35	*Rhachistognathus*? sp.	63°34'05"N;132°20'01"W	8 632400E 7051460N
D1	C-302214	Late Dev.?	FC-1995	*Astroentactina* sp., *Entactina* sp., *Tetraentactina barisphaera*	63°11'29"N;132°18'41"W	8 635260E 7009560N
D2	C-302204	Late Devonian, mid-Famennian.	MJO 95-35	*Palmatolepis glabra pectinata*, *Palmatolepis perlobata*,. *Palmatolepis* sp.	63°14'22"N;132°03'34"W	8 647682E 7015483N
D3	C-301309	Late Devonian, Middle Fam.	MJO 94-25	*Palmatolepis glabra pectinata*, *Palmatolepis marginifera* *Palmatolepis tenuipunctata*	63°42'57"N;132°17'43"W	8 633600E 7068000N
D4	C-203022	Late Devonian Frasnian	CR-183-AEHP-96	*Amphipora* sp., *Alveolites* sp., *Chuanbeiphyllum* sp.nov.	63°32'40"N;133°16'10"W	8 585760E 7047650N
D5	C-302241	late Emsian-Early Eifelian	MJO 95-35	*Polygnathus serotinus*	63°55'45"N;132°55'57"W	8 601360E 7090590N
D6	C-302366	Devonian	FC96-GSC1	Entactinids, one pylentonemid	63°36'29"N;132°17'33"W	8 634250E 7056000N
D7	C-302202	Middle Dev.,	MJO 95-35	*Polygnathus dobrogensis*, *Bellodella* sp.	63°35'30"N;132°39'35"W	8 616120E 7053460N
D8	C-302246	E. Dev., Emsian	MJO 95-35	*Icriodus* sp., *Polygnathus* sp. cf. *P. inversus* *Pseudoneotodus* *Pandorinella* sp.	63°10'25"N;132°01'53"W	8 649435E 7008199N
D9	C-203018	E.Dev. Pragian	D-3 BSN 94	*Monograptus yukonensis*	63°39'35"N;132°01'30"W	8 647247E 7062326N
S1	C-302163	Sil.-Devonian	FC	Spumellarians, no *Latentifistula*	63°05'55"N;132°10'55"W	8 642230E 6999510N
O1	C-203020	Ashgill?, prob. Late Ordovician	O-8 BSN 94	*Arachniograptus* sp., ?*Climacograptus* sp., *Dicellograptus* sp., *Orthograptus* sp.	63°28'10"N;132°11'30"W	8 639932E 7040766N
O2	C-302235 (Also C -300496-498)	Ordovician	MJO 95-35	*Periodon* sp., *Ansella*? sp., *Drepanistodus* sp. *Walliserodus* sp.	63°30'52"N;132°28'24"W	8 625705E 7045200N
O3	C-300599	Ordovician	FC	?*Futobari* sp., sp.	63°47'08"N;132°19'51"W	8 631525E 7075686N
O4	C-302162	Ordovician	FC	*Futobari* sp., *Inangutta* sp.	63°05'57"N;132°12'00"W	8 641452E 6999535N
O5	C-302368	Ordovician?	MJO 97-6 FC96-GSC-1	*Protopanderodus*? sp., *Inanigutta* spp.	63°44'53"N;132°14'22"W	8 636200E 7071710N
O6	C-300494	Arenig, Early Ordovician	MJO 94-25	*Drepanoistodus* sp., *Oepikodus*? sp., *Walliserodus* sp.	63°30'17"N;132°23'05"W	8 630150E 7044300N O7.
	C-302240	Tremadocian, Early Ord.	MJO 95-35	*Cordylodus*? sp., *Hirsutodontus*? sp., *Protopanderodus*? sp.	63°56'49"N;132°58'15"W	8 599425E 7092505N
Cm1	C-300466	L.Cam.E. Ord.	MJO 94-25	coniform element	63°28'12"N;133°32'57"W	8 572300E 7038600N
Cm2	C-300473	Camb.-Ord.	MJO 94-25	Protoconodont?	63°38'35"N;132°02'45"W	8 646300E 7060450N
Cm3	C-302237	L. Camb.-Ord.	MJO 95-35	coniform elements	63°02'49"N;132°02'35"W	8 649501E 6994070N
Cm4	C-302210?	Late Camb .	MJO 95-35	coniform element, protoconodonts	63°05'52"N;132°17'23"W	8 636795E 6999195N

Newly recognized Paleozoic strata

Another belt of Lower Paleozoic rocks was recently recognized about 40 km northeast of Plateau Mountain. The beds were described by Roots and Brent (1994b; their Fig. 3) and a Late Cambrian-Early Ordovician coniform element (C-300466 on Table 2) has since been recovered from the silty limestone horizon. The succession consists of a 5 m thick, chloritic volcaniclastic sandstone; thin-bedded, dark brown shale and siltstone (Gull Lake Formation); light grey-weathering, silty limestone (possibly Rabbitkettle Formation); and soft black mudstone (Duo Lake Formation). The inlier is interpreted as a south-verging, overturned infold of lower Paleozoic rocks that unconformably overlies Yusezyu Formation sandstone.

Upper Paleozoic and Mesozoic strata

Younger sedimentary rocks are mostly confined to a 40 km wide belt trending southeast across the centre of the map area; they are difficult to differentiate from older strata in the field. Permian and Carboniferous units are lithologically varied and contain strata which resemble those in the Yusezyu, Gull

Figure 3. Cambrian-Ordovician mafic volcanics include amygdaloidal pillowed flows (draping down to left), separated by darker hyaloclastite. Pillow cross-section left of centre is 50 cm. From the south flank of Plateau Mountain.

Figure 4. Folded black mudstone with light-weathering siltstone rhythmite, interpreted as Earn Group; from Seven Mile Canyon. Notebook at lower left is 20 cm high.

Lake, and Steel formations. Accordingly the recognition of the Upper Paleozoic units is tentative until calcareous rocks have been checked for microfossils.

Earn Group

In northern Selwyn Basin the Earn Group comprises carbonaceous siltstone, thin bedded chert and shale, minor conglomerate, and black or white carbonate. Monotonous, generally north-dipping, dark grey siltstone and shale underlie a broad area (40 km from northeast to southwest); they are best exposed at Seven Mile Canyon (Fig. 4) and along southwestward flowing tributaries of the Stewart and Lansing rivers. Strata dip steeply, forming tight upright folds. Resistant, strongly flattened, chert-cobble conglomerate cores a lone peak 14 km south of the mouth of Lansing River; other conglomerate exposures are west of Seven Mile Canyon. Blue-grey-weathering, black, siliceous siltstone, the other distinctive lithology of the Earn Group, is only exposed north of the conglomerate occurrences, and in small patches in the Russell Range. The other lithology of note is a continuous band of white-weathering limestone 5-50 m thick, trending northwest from Pleasant Creek to the edge of the map area. In one place Frasnian (Late Devonian) corals were discovered, and indicate that this is the Kalzas Formation of the Earn Group (Campbell, 1967), which is also found along strike south of Mount Selous in northern Tay River map area (S. Gordey, pers. comm., 1996).

Keno Hill quartzite

The Keno Hill quartzite map unit consist of black or dark grey, vitreous quartzite with black slaty interbeds. A newly discovered exposure extends for 50 km northwest from Pleasant Creek (Roots, 1997a). Outcrops are typically massive quartzite lacking recognizable detrital grains; a network of white quartz veins comprise 10% of rock volume and commonly reveal Reidel shear fabrics.

Unnamed map units of Permian age

Within Lansing map area three lithologically different successions have yielded Permian microfossils. Green argillite and silicious shale are the most abundant: they correlate with almost all the "green-grey phyllite" occurrences in northwestern Lansing map area (Roots, 1997a). South and east of Fairweather Lake a rust-brown-weathering, jet-black, siliceous shale which contains barite is present. The third succession, located in the Wilson Range comprises grey, brown, and purple locally laminated siltstone, limy black siltstone, and interbedded green and grey chert. A second area, north of the Stewart River east of the mouth of the Nadaleen River, is intruded by numerous 10-20 m thick, hornblende diorite sills of probable Triassic age.

Mount Christie Formation

The quartzite is in most places overlain by a thin brown shale and a considerable thickness of green- and brown-weathering phyllite (Fig. 5) which is readily recognized as Mount Christie Formation. In the Wilson Range, however, the Keno Hill quartzite is absent and Carboniferous conodonts have been recovered from a brown- and grey-weathering succession of mudstone and siltstone with white-grey chert beds. The presence of Carboniferous rocks in western Lansing map area is as yet unknown.

Jones Lake Formation

Triassic strata are preserved in three localities in the map area. The brown-weathering, ripple cross-laminated, fine sandstone and shale is correlated with the Jones Lake Formation (Gordey and Anderson, 1993). The sandstone is overlain by several tens of metres of medium- to dark-grey, poorly lithified shale with minor orange-weathering sandstone beds (Fig. 6), and rare dark grey limestone in Murray Creek. The shale may be Jurassic; Gordey (1990b) and Abbott (1990b) included these rocks in their unit TJps.

Figure 5. Green and beige fine-laminated phyllite of the Mount Christie Formation. Bedding dips steeply southwest and the closely spaced vertical fractures trend northeast. Outcrop 20 km west of Seven Mile Canyon and 1 km north of the buried trace of Robert Service Thrust.

Figure 6. North-plunging fold of orange-weathering fine grained sandstone beds within dark grey silty shale, of Triassic or Jurassic age. From a cutbank in Murray Creek.

Enigmatic strata

The eastern half of the Russell Range consists of the Yusezyu Formation sandstone (Fig. 7), dark grey phyllitic mudstone, and brown and green phyllitic siltstone. The last lithology strongly resembles the Permian Mount Christie Formation, and units below are sufficiently different from typical Yusezyu Formation as to arouse doubts about its uniform Late Proterozoic age. No angular unconformity is evident. The succession may instead be Carboniferous and younger and will require further study.

Cretaceous granite

The map area contains two plutons which core the Lansing and Russell ranges (Fig. 8), and four stocks which trend northwest, collinear with the Robert Service Thrust. All consist of granodiorite, with abundant quartz (up to 25% and 4 mm diameter grains); biotite is more prevalent than

Figure 7. Crossbedded limy sandstone bed within dark grey mudstone, 6 km northeast of Mount Armstrong.

hornblende. Mineralogically distinct phases were not observed, although no traverses penetrated the centre of the plutons. Uranium-lead zircon dates from two samples from the Lansing Pluton are 92.7 Ma (J.K. Mortensen, pers. comm., 1996).

The contact metamorphic aureole around the pluton is typically 1 km wide; within it fine clastic rocks contain square-ended needles (likely andalusite) and spotted chlorite, sandy rocks develop a purplish hornfels, and limy rocks form light-coloured calc-silicate. Magnetite is abundant in the Lansing Range aureole. In a cirque north of Mount Armstrong, the upper part of the pluton is exposed (Fig. 9), and the diopside skarn above it contains scheelite and chalcopyrite (Yukon Minfile 105N #014). Russell Creek, which drains the west side of the pluton, was intermittently placer mined between 1901 and 1925 (Bostock, 1970) and in the mid-1980s. Boulders of galena, scheelite, and cassiterite were recovered during placer mining.

Figure 8. *South-dipping succession of sandstone, quartzite, and silty argillite in the eastern Russell Range. The succession overlies Yusezyu sandstone, but is believed to be Upper Paleozoic to Triassic. Figure 7 is of ridge outcrop above shadowed buttress at right.*

Figure 9. *View westward to Mount Armstrong, showing the top of granite pluton and baked sandstone containing light-coloured calcareous horizons.*

JURASSIC-CRETACEOUS STRUCTURES

In Lansing map area competent rocks form tight, upright-to-overturned folds; fine grained, clastic strata are typically telescoped and thickened by minor stratabound thrust faults. All rocks are subgreenschist metamorphic grade, except in kilometre-wide zones around the postorogenic plutons, where andalusite and biotite porphyroblasts and chloritic spotting are common. The regional structures suggest early, thin-skinned contraction on broad underlying detachments; these thrust panels were later split by steeper dipping, northwest-trending (dominantly dextral) faults. Older units typically reveal more complex fabrics than younger ones, as a result of greater depth of burial as well as the likelihood of previous deformation events. Nevertheless the strata in the Lansing map area are not as highly strained as they are along strike in northern Mayo map area; thus the presence of large overlapping thrust sheets at structurally high levels is unlikely.

Unlike the eastern part of the map area where south-dipping strata predominate (Roots et al., 1995a), the west half of Lansing map area is composed of southeast-trending structural domains. The domains are in most cases bounded by major faults, chiefly the Moose Lake, Robert Service, and Tombstone thrusts. Discussion of the geometry of the last two thrusts is the main focus of this section, but the structural domains are summarized first.

Between the Moose Lake and Robert Service thrusts are large upright to south-verging folds of Hyland Group strata. North of the Hess River, the Yusezyu Formation sandstone exhibits an increased strain fabric, with steep south-plunging fold axes and a predominantly northeastward dip of both bedding and foliation. North of the Robert Service Thrust, Paleozoic and Mesozoic rocks compose open folds along the central axis of the domain, flanked to northeast (Wilson Range) and southwest (between Stewart River and Pleasant Creek) by 5 km wide, tight, northward-overturned synclinoria. The eastern extension of the Tombstone Thrust separates this structural domain from one to the north characterized by flat to gently undulating Upper Paleozoic units, with structurally controlled pockets of Mesozoic strata. Another structural domain consists of north-dipping Upper Paleozoic strata east of the mouth of the Nadaleen River into the Stewart River. There the southwest-verging folds could be related to a fault (possibly a south-directed thrust) in the valley of the Stewart River.

Both the Robert Service and Tombstone thrusts were originally identified in the southern Ogilvie Mountains and traced eastward. Similarly the Macmillan and Hess faults were elucidated in the Macmillan Pass area and traced westward into Lansing map area. The nature, and possible linkage between these faults is discussed below.

Along the Robert Service Thrust generally, Yusezyu Formation is thrust over Keno Hill quartzite and younger strata (Roots and Murphy, 1992); however in northeastern Mayo map area both the Yusezyu Formation and adjacent unit (Dmp, Gordey, 1990a, b; equivalent to Earn Group and Keno Hill quartzite) dip northeast. Gordey (1990b) suggested that the Robert Service Thrust remained a buried detachment beneath the entire region, however no other area along trend reveals Keno Hill quartzite in the hanging wall (Robert Service thrust panel). Alternatively Roots and Murphy (1992) suggested the Robert Service thrust panel became overturned around southwest-verging folds associated with later motion along the Tombstone Thrust.

The Robert Service Thrust extends into Lansing map area 20 km west of Seven Mile Canyon. Folded Yusezyu Formation is in contact with generally south-dipping Permian strata above the Keno Hill quartzite. The fault is considered to be steeply dipping because the surface trace is straight, trending east-southeast at least as far as the Stewart River. The Yusezyu Formation sandstone near Pleasant Creek near the trace of the Robert Service Thrust dips moderately northeast, and where bedding tops can be determined the strata are overturned to the southwest. Thus the possibility of a north-dipping unconformity (instead of a thrust) may be discarded, and the idea that Robert Service Thrust has been folded southward is strengthened. The southeast trend of the Robert Service Thrust intersects the strain gradient described in Roots et al. (1995a); its probable location near Fairweather Lake awaits further analysis.

The Tombstone Thrust was the locus of significant northwestward translation (Abbott, 1990a; Gordey, 1990a; Roots and Murphy, 1992; D.C. Murphy and J.G. Abbott, abstract, Canadian Cordilleran Tectonic Workshop, Victoria, British Columbia, 1994). Immediately northeast of Mayo map area it is defined as the abrupt northward decrease in strain within Abbott's (1990a, DMpq unit) unit; he suggested the thrust continued southeast along the Beaver River into Lansing map area. At the corner of the map area Triassic strata are present in the footwall, but a clear distinction between strongly deformed rock to the south, and less strain to the north is not evident in the poorly exposed, incompetent rocks. On the north side of the Stewart River, 2 km below the mouth of Beaver River, a thin mylonite, separating grey-green phyllite from underlying, less deformed black mudstone, may mark a splay of Tombstone Thrust (Roots, 1997a: locality 2).

There are no other indications of a fault in the broad expanse of Earn Group southeastward until Murray Creek, where Triassic strata are fault-bounded on the south by overturned Keno Hill quartzite and other units. A complex fold belt in which steeply dipping resistant layers can be traced 50 km, almost to the east edge of the map area, is considered to be on the leading edge or hanging wall of a major fault. It is likely continuous with the Macmillan Fault, a Devonian syndepositional fault (Abbott, 1982) re-activated in Jurassic-Cretaceous time with 30 km of inferred dextral displacement (Abbott and Turner, 1990). The working hypothesis is that northwest translation of the Tombstone thrust sheet employed the reactivated Macmillan Fault as part of its northeast boundary; subsequent northward translation of the Tombstone thrust sheet created the tight fold belts south of Murray Creek and north of Pleasant Creek.

PRE-JURASSIC STRUCTURES

Full comprehension of the distribution and thickness of Paleozoic units warrants assessment of the facies and paleogeography; furthermore early faults and extension zones probably focused later contraction structures. In particular, the extended basement inferred beneath Selwyn Basin may have "closed-up" during Jurassic and Cretaceous contraction, resulting in thrust ramps (Gordey, 1981).

Cambrian mafic volcanic and intrusive rocks inflate the stratigraphic succession in the Tasin Range, north of the Plata property and at Plateau Mountain. These areas probably contain deep crustal breaks; both areas are bounded to the south by Yusezyu Formation sandstone where thrusting may have reactivated old faults. The absence of Narchilla Formation beneath the infold of Cambrian strata in the Pleasant Creek area indicates probable uplift and erosion.

In the Macmillan Pass area, Middle and Upper Devonian syndepositional faults are inferred by the presence or absence, and contrasting facies of Earn Group units. In Lansing map area the Earn Group cannot be separated to formation level with confidence; however over most of the central and southwestern parts of the map area this unit rests unconformably atop the Hyland Group or Gull Lake Formation. Absence of the thick Road River Group chert implies erosion that could have occurred on an uplifted block, and therefore the presence of extension faults. Such a fault is inferred parallel to (and possibly reactivated by) the Robert Service Fault near Fairweather Lake, and along the trend of the Hess Fault northeast of the Lansing Range.

ACKNOWLEDGMENTS

The professional assistance of Angelique Justason and Bruce Mitford, as well as the capable flying of Will Thompson and Ernie Onafreychuk contributed to an excellent 1997 field season. The relative abundance of fossil and microfossil localities in Lansing map area are the key to identifying the enigmatic younger units. Microfossils were identified by M.J. Orchard (GSC Vancouver) and F. Cordey. Graptolite collections were examined by B.S. Norford, Upper Devonian corals by A.E.H. Pedder (both of GSC Calgary), and the paleontology database was checked by S.E.B. Irwin of GSC Vancouver. Earlier versions of the text provoked comments by Don Murphy and Bob Thompson for which I am grateful, but flaws in the interpretation are my own. The final text was greatly improved by Glenn Woodsworth, Steve Gordey, and Bev Vanlier.

REFERENCES

Abbott, J.G.
1982: Structure and stratigraphy of the Macmillan Fold Belt: evidence for Devonian faulting; in Yukon and Exploration and Geology, 1981, Exploration and Geological Services Division, Yukon, Indian and Northern Affairs Canada, p. 22-33.
1990a: Preliminary results of the stratigraphy and structure of the Mount Westman map area (106D/1), central Yukon; in Current Research, Part E; Geological Survey of Canada, Paper 90-1E, p. 15-22.
1990b: Geological map of Mount Westman map area (106 D/1); Exploration and Geological Services Division, Mineral Resources Directorate, Whitehorse, Yukon, Indian and Northern Affairs Canada, Open File 1990-1 (scale 1:50 000).

Abbott, J.G. and Turner, R.J.
1990: Character and paleotectonic setting of Devonian stratiform sediment-hosted Zn, Pb, Ba deposits, Macmillan Fold Belt, Yukon; in Fieldtrip Guidebook 14, (ed.) J.G. Abbott and R.J.W. Turner; 8th International Association on the Genesis of Ore Deposits symposium, 1990, Geological Survey of Canada, Open File 2169, p. 99-136.

Blusson, S.L.
1974: Geology of Nadaleen River, Lansing, Niddery Lake, Bonnet Plume Lake and Mount Eduni map areas, Yukon Territory; Geological Survey of Canada, Open File 205, scale 1:250 000.

Bostock, H.S.
1970: Prospecting on Russell Creek; North (Indian Affairs and Northern Development), Nov.-Dec./70, p. 30-43.

Campbell, R.B.
1967: Geology, Glenlyon map area, Yukon Territory; Geological Survey of Canada, Map 1221A, scale 1:253 440.

Cecile, M.P. and Abbott, J.G.
1992: Geology of Niddery Lake map area (105O), Yukon; Geological Survey of Canada, Open File 2465, scale 1:125 000.

Gordey, S.P.
1981: Structure section across south-central Mackenzie Mountains, Yukon and Northwest territories; Geological Survey of Canada, Open File 809.
1990a: Geology and mineral potential, Tiny Island Lake map area, Yukon; in Current Research, Part E; Geological Survey of Canada, Paper 90-1E, p. 23-29.
1990b: Geology of Tiny Island Lake map area (105M/16); Exploration and Geological Services Division, Yukon Region, Indian and Northern Affairs Canada, Open File 1990-2, scale 1:50 000.

Gordey, S.P. and Anderson, R.G.
1993: Evolution of the northern Cordilleran miogeocline, Nahanni map area (105I), Yukon Territory and District of Mackenzie; Geological Survey of Canada, Memoir 428.

Mortensen, J.K. and Thompson, R.I.
1990: An U-Pb zircon-baddeleyite age for a differentiated mafic sill in the Ogilvie Mountains, west-central Yukon Territory; in Radiogenic Age and Isotopic Studies: Report 3; Geological Survey of Canada, Paper 89-2, p. 23-28.

Murphy, D.C. and Héon D.
1995: Geology and Mineral Occurrences of Seattle Creek map area (115P/16), western Selwyn Basin, Yukon; in Yukon Exploration and Geology 1994; Exploration and Geological Services, Indian and Northern Affairs Canada, p. 58-72.

Roots, C.F.
1997a: Upper Paleozoic strata with potential for massive sulphide mineralization, northwestern Lansing map area (105N), Yukon; in Yukon Exploration and Geology, 1996; Exploration and Geological Services Division, Yukon, Indian and Northern Affairs Canada, p. 138-146.
1997b: Geology of the Mayo map area, Yukon; Exploration and Geological Services Division, Yukon, Indian and Northern Affairs Canada, Bulletin 7, 110 p.
1993: Geological map of southern Mayo map area; Geological Survey of Canada, Open File 3022, and Exploration and Geological Services Division, Yukon, Indian and Northern Affairs Canada Open File 1993-11 (G), scale 1:100 000.

Roots, C.F. and Brent, D.
1994a: Geological framework of West Lake map area (NTS 105N/9), Hess Mountains, east-central Yukon; in Yukon Exploration and Geology, 1993; Exploration and Geological Services Division, Yukon, Indian and Northern Affairs Canada, p. 111-121.
1994b: Preliminary stratigraphy from Lansing map area, central Yukon Territory; in Current Research 1994-A; Geological Survey of Canada, p. 1-9.

Roots, C.F. and Murphy, D.C.
1992: New developments in the geology of Mayo map area, Yukon Territory; in Current Research, Part A; Geological Survey of Canada, Paper 92-1A, p. 163-171.

Roots, C.F., Abbott, J.G., Cecile, M.P., Gordey, S.P., and Orchard, M.J.
1995a: New stratigraphy and structures in eastern Lansing map area, central Yukon Territory; in Current Research 1995-A, Geological Survey of Canada, p. 141-147.
1995b: Bedrock geology of Lansing map area (105N) east half, Hess Mountains, Yukon; Exploration and Geological Services Division, Yukon, Indian and Northern Affairs, Open File 1995-7 and Geological Survey of Canada, Open File 3171, scale 1:125 000.

Tempelman-Kluit, D.J.
1979: Transported cataclasite, ophiolite and granodiorite in Yukon: Evidence of arc-continent collision; Geological Survey of Canada, Paper 79-14, 27 p.

Geological Survey of Canada Project 900035

Ravens Throat project – geology of Mount Kraft and part of Dal Lake map areas, Mackenzie Mountains, Northwest Territories

Maurice Colpron[1] and Carole Augereau[2]
Mineral Resources Division, Ottawa

Colpron, M. and Augereau, C., 1998: Ravens Throat project – geology of Mount Kraft and part of Dal Lake map areas, Mackenzie Mountains, Northwest Territories; in Current Research 1998-A; Geological Survey of Canada, p. 29-38.

Abstract: The Ravens Throat project area is underlain by strata of the Neoproterozoic Mackenzie Mountains and Windermere supergroups, and by Lower Cambrian to Upper Devonian siliciclastic and carbonate rocks of the Mackenzie Platform. The basal Windermere strata were deposited during Neoproterozoic rifting, and numerous extension faults associated with this tectonic event cut older Neoproterozoic strata of the Mackenzie Mountains Supergroup. Mesozoic contractional deformation resulted in the development of broad folds and thrust faults, which were transected by younger right-lateral strike-slip faults. The development of both thrust faults and strike-slip faults was influenced by pre-existing, basin-bounding extension faults. Copper is concentrated as stratabound disseminated sulphides in the Coates Lake Group and as vein systems along fracture zones in the Little Dal Group. Zinc occurrences are associated with hydrothermal dolomite near the base of the Middle Devonian Landry Formation, and with a regolith at the sub-Whittaker (Late Ordovician) unconformity.

Résumé: Le sous-sol de la région de Ravens Throat comporte des strates néoprotérozoïques des supergroupes de Mackenzie Mountains et de Windermere et des roches silicoclastiques et carbonatées du Cambrien inférieur au Dévonien supérieur de la plate-forme de Mackenzie. Les strates de la base du Supergroupe de Windermere se sont déposées lors de rifting au Néoprotérozoïque, et de nombreuses failles de distension associées à cet événement tectonique recoupent les strates néoprotérozoïques plus anciennes du supergroupe de Mackenzie Mountains. Une déformation au Mésozoïque a produit de vastes plis et des failles de chevauchement qu'ont recoupés par la suite des failles de décrochement dextres. La présence de failles de distension en bordure de bassins sédimentaires a influencé la formation des failles de chevauchement et des décrochements. Du cuivre se présente à la fois en concentrations stratiformes de sulfures disséminés dans le Groupe de Coates Lake et en veines le long de zones de fractures dans le Groupe de Little Dal. Du zinc se retrouve en association avec des dolomites hydrothermales à la base de la Formation de Landry (Dévonien moyen), et dans un régolithe le long de la discondance sous-jacente à la Formation de Whittaker (Ordovicien tardif).

[1] Resources, Wildlife, and Economic Development, Government of the Northwest Territories, P.O. Box 1320, Yellowknife, Northwest Territories X1A 2L9
[2] Department of Geology and Geophysics, University of Calgary, Calgary, Alberta T2N 1N4

INTRODUCTION

The Ravens Throat project involves 1:50 000 scale bedrock mapping with the primary objective being to delineate the stratigraphy that hosts Cu and Zn-Pb mineralization. Numerous Cu and Zn-Pb showings are located within the map area, which lies immediately north of the Redstone Copper deposit at Coates Lake (Fig. 1). The study area was mapped at a reconnaissance scale of 1:250 000 in the mid 1960s (Gabrielse et al., 1973). Since then, the Neoproterozoic to Paleozoic rocks of the Mackenzie Mountains have been the subject of numerous detailed stratigraphic studies (e.g., Aitken, 1981; Fritz et al., 1991; Narbonne and Aitken, 1993; and references therein), which have resulted in the introduction of several new formations that are not shown on existing geological maps (Table 1).

This paper presents the preliminary results of bedrock mapping during the 1997 field season (Fig. 2, 3). Mapping of the Neoproterozoic geology in the Mount Kraft (95L/15) area was initiated by C.W. Jefferson in 1976, 1977, and 1984. Our primary objective for 1997, in the Mount Kraft area, was to complete the mapping of the Neoproterozoic and Paleozoic sequences and to re-evaluate the nature of the faults. Detailed mapping of the Dal Lake (95M/2) area was initiated during the second half of the 1997 field season and has resulted in

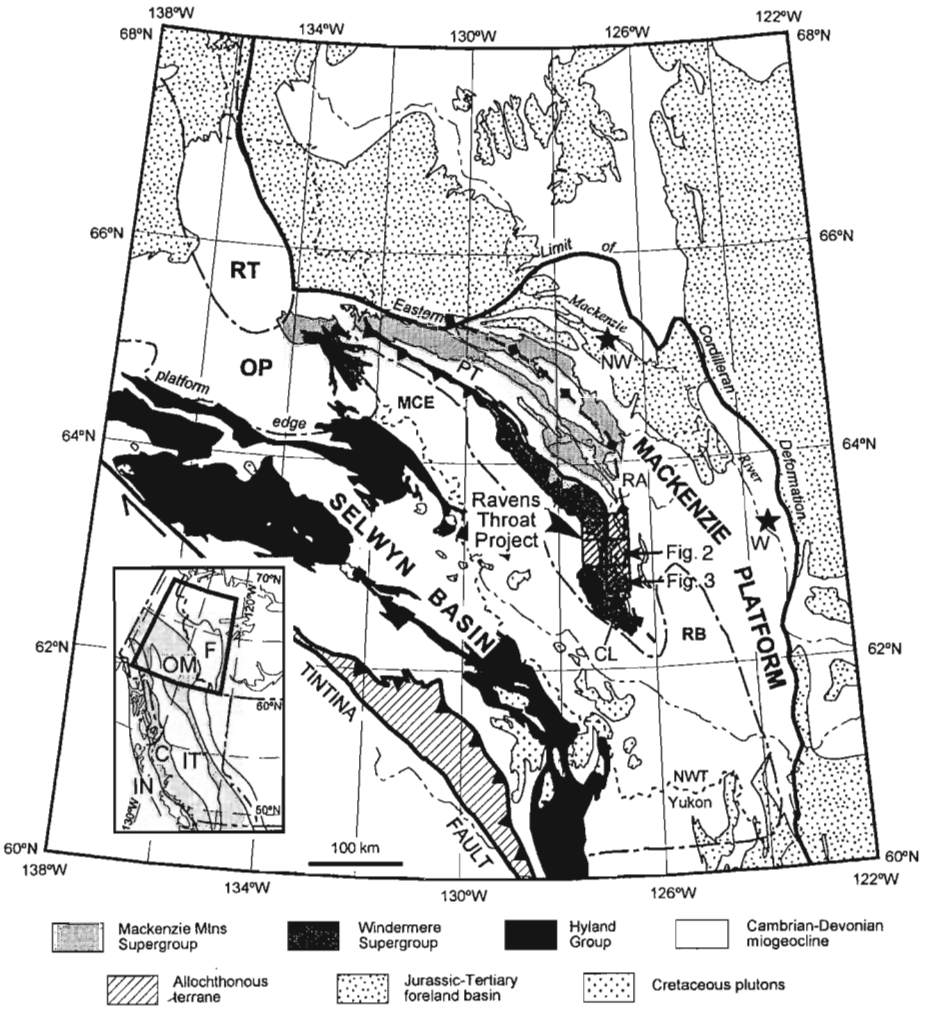

Figure 1. *Simplified geological map of the northern Canadian Cordillera showing distribution of Neoproterozoic assemblages (after Wheeler and McFeely, 1991). The location of the Ravens Throat mapping project, in the Mackenzie Mountains, is indicated. This report presents the results of regional mapping in the Dal Lake (95M/2; Fig. 2) and Mount Kraft (95L/15; Fig. 3) map areas. Inset shows morphogeological belts of the Canadian Cordillera: F = Foreland Belt, OM = Omineca Belt, IT = Intermontane Belt, C = Coast Belt, and IN = Insular Belt. Stars indicate geographic locations: CL = Coates Lake, NW = Norman Wells, and W = Wrigley. Other abbreviations: RA = Redstone Arch, PT = Plateau Thrust, RT = Richardson Trough, OP = Ogilvie Platform, MCE = Misty Creek Embayment, and RB = Root Basin.*

significant improvement to the reconnaissance mapping of Gabrielse et al. (1973); the mapping of new units introduced since publication of these reconnaissance maps is one obvious contribution.

Regional geology

The Ravens Throat area lies within the Foreland Belt of the northern Canadian Cordillera (Fig. 1). It is underlain by Neoproterozoic strata of the Mackenzie Mountains and Windermere supergroups, and by Cambrian to Devonian strata of the lower to middle Paleozoic Mackenzie Platform (Table 1). The area lies along the west flank of the Redstone Arch (Fig. 1), a late Proterozoic–early Paleozoic culmination where terminal Neoproterozoic (Windermere) to Devonian strata overlie the Neoproterozoic Mackenzie Mountains Supergroup along a series of overstepping unconformities. The study area is located in the footwall of the Plateau Fault, a major east-verging thrust fault that extends some 350 km along strike to the northwest.

STRATIGRAPHY

Table 1 summarizes the lithostratigraphic units present in the Dal Lake and Mount Kraft map areas (Fig. 2 and 3, respectively). The lithostratigraphy of the area is best described in terms of three assemblages that reflect distinct tectonic/depositional settings. The oldest assemblage, the Mackenzie Mountains Supergroup (Sequence B of Young et al., 1979; 1.08-0.78 Ga), records stable platformal deposition, possibly in an intracratonic basin (Aitken and McMechan, 1991; Narbonne and Aitken, 1993; Rainbird et al., 1996). The overlying Windermere Supergroup (Sequence C of Young et al., 1979; 0.78-0.54 Ga) records the Neoproterozoic rifting of northwestern Laurentia and the subsequent development of a passive margin (Ross, 1991). The basal part of the Windermere Supergroup was deposited (in part) in restricted, fault-bounded basins developed upon a "basement" of Mackenzie Mountains Supergroup strata. The youngest assemblage comprises the Paleozoic rocks that define the Mackenzie Platform. Lower Cambrian to Devonian siliciclastic and carbonate rocks of the Mackenzie Platform overlie the Neoproterozoic sequences along a series of overstepping unconformities.

Table 1. Stratigraphic units present in the Mount Kraft (95L/15) and Dal Lake (95M/2) map areas.

Era	Period	Super-group	GROUPS	FORMATIONS	*LITHOLOGICAL UNITS*	*MAP UNIT*
Paleozoic	*Miss.*			Besa River (?)	*black shale, limestone, chert*	DMs
	Devonian			Nahanni	*fossiliferous limestone*	DN
				Headless	*very fossilliferous argillaceous limestone*	DH
				Landry	*limestone*	DL
				Arnica	*thinly bedded dolostone*	DA
				Sombre	*dolostone*	Ds
	Sil.			Delorme	*tan-weathering dolostone*	SDD
	Ord.		*unconformity*	Whittaker	*dark grey, cherty dolostone*	OSW
	Cambrian		*unconformity*	Backbone Ranges	*sandstone*	€BR
Neoproterozoic		Windermere		Keele	*sandstone, minor dolostone*	PKe
				Twitya	*sandstone/shale*	PTw
			Rapitan	Shezal	*green diamictite*	PSh
				Sayunei	*maroon mudstone, rhythmites (dropstones)*	PSa
				Mt. Berg	*diamictite/conglomerate*	PMB
			Coates Lake	Coppercap	*limestone*	PCp
				Redstone River	*red mudstone/evaporites*	PRr
			unconformity	Thundercloud	*sandstone/mudstone*	PTh
		Mackenzie Mtns.	**Little Dal PLD**	Little Dal volc.	*basalt*	PLDv
				"upper" Upper carb. / Rusty shale / Gypsum	*dolostone / red-weathering argillaceous limestone / evaporites*	PLDu
				"lower" Grainstone / Platform / Mudcracked	*oolitic limestone, packstone* PLDg / *micritic limestone, stromatolite bioherms* PLDp / *shale/sandstone*	PLDl
			Katherine PK	"upper" *(K7)*	*sandstone*	PKu
				"middle" *(K6)*	*black shale, brown-weath. cherty dolostone*	PKm
				"lower" *(K1-K5)*	*sandstone*	PKl
				Tsezotene	*black shale, siltstone, sandstone (±dolostone)*	PTz

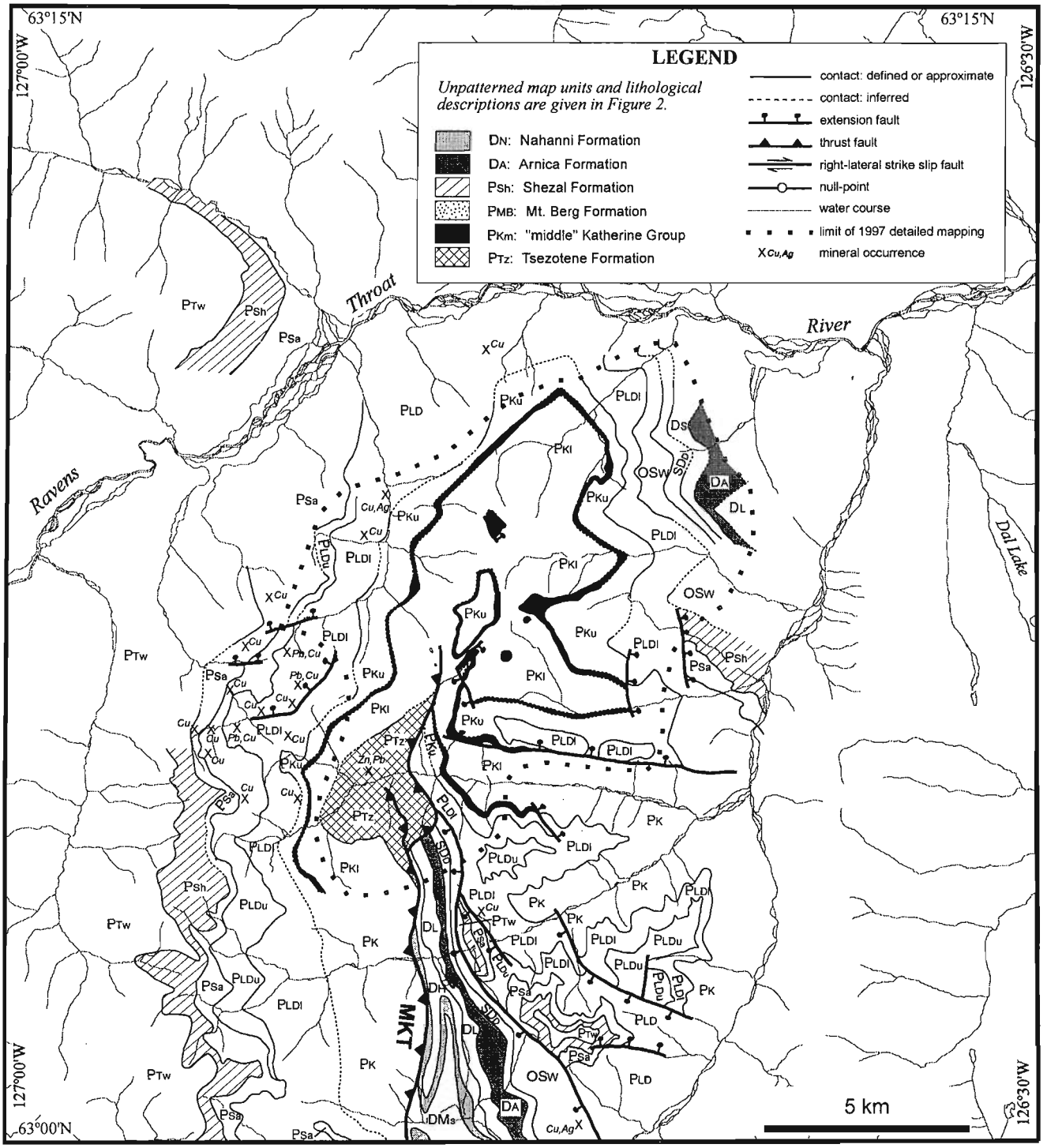

Figure 2. *Preliminary geology of part of the Dal Lake (95M/2) map area. Compiled from mapping by M. Colpron and C. Augereau (1997), Jory (1962), and Gabrielse et al. (1973). See Table 1 for description of all map units. Abbreviation: MKT = Mount Kraft Thrust.*

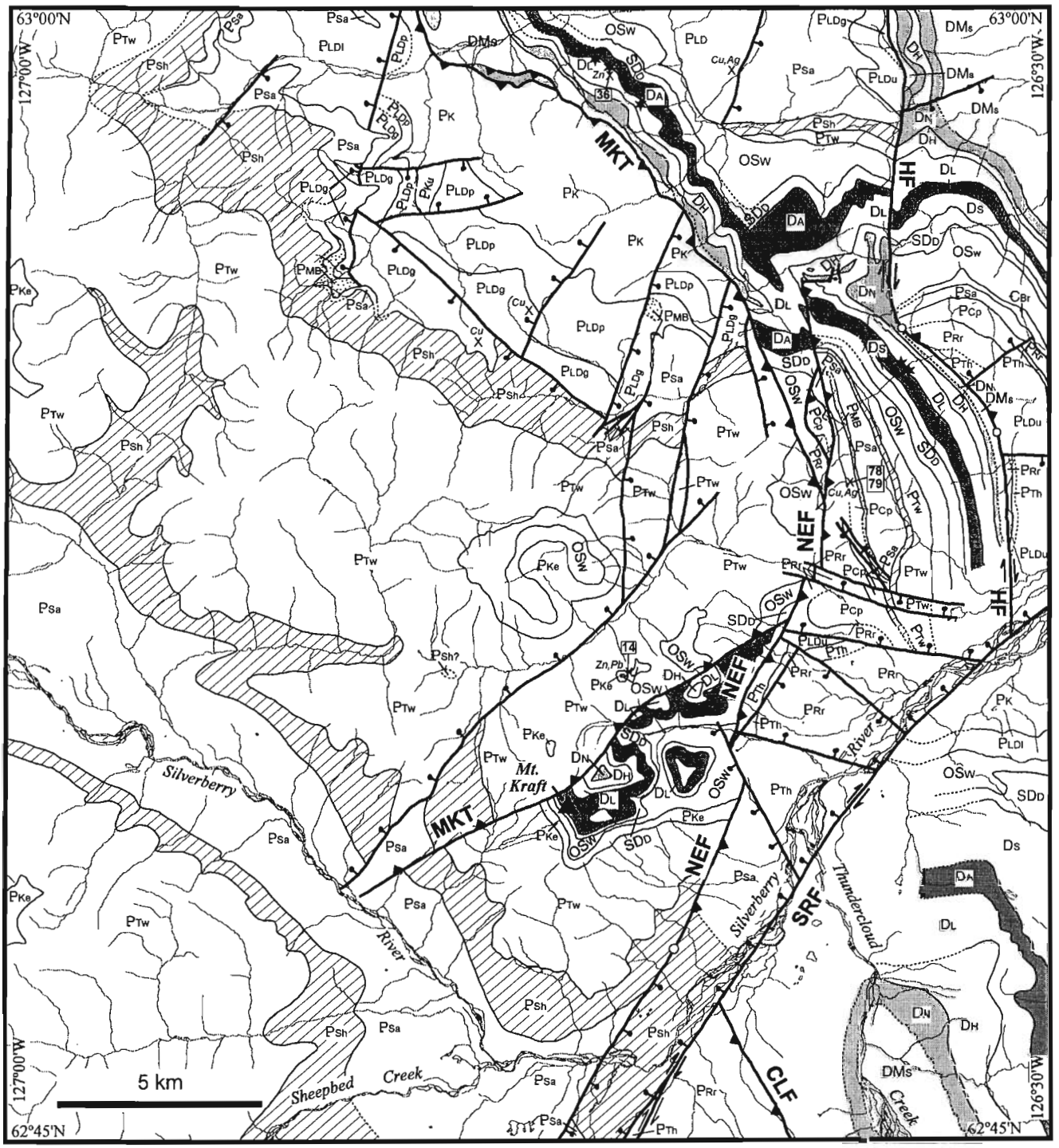

Figure 3. *Simplified geology of the Mount Kraft (95L/15) map area. Compiled from mapping by C.W. Jefferson (1976, 1977, 1984), M. Colpron and C. Augereau (1997), Gabrielse et al. (1973), and Eisbacher (1981). Legend is given in Table 1 and Figure 2. Numbers in rectangles refer to assay samples listed in Table 2. The prefix "97MC0" has been omitted for clarity. Stars (*) indicate occurrences of Manetoe dolomite facies at the base of the Landry Formation. Abbreviations: MKT = Mount Kraft Thrust; NEF = North Extension Fault; HF = Hayhook Fault; SRF = South Redstone Fault; CLF = Coates Lake Fault.*

It is not the purpose of this report to present a complete description of each lithostratigraphic unit mapped in the Mount Kraft and Dal Lake areas. Instead, our discussion of the stratigraphy will focus on the new contributions made by our mapping of the area. The reader is referred to Narbonne and Aitken (1993; and references therein) for a concise summary of the Neoproterozoic stratigraphy of the Mackenzie Mountains (Mackenzie Mountains and Windermere supergroups). The Paleozoic rocks of the Mackenzie Platform are described by Gabrielse et al. (1973), Fritz et al. (1991), and Morrow (1991).

Mackenzie Mountains Supergroup

The informally defined Mackenzie Mountains Supergroup comprises four main units: unit H_1, Tsezotene Formation, Katherine Group, and Little Dal Group. Only the uppermost three units of the Mackenzie Mountains Supergroup are exposed in the Ravens Throat area (Table 1; Fig. 2, 3).

Tsezotene Formation

The sequence of pyritic dark grey and black shale, grey and green siltstone and sandstone, and minor orange-weathering cherty dolostone that is exposed in stream sections in the south-central part of the Dal Lake area (Fig. 2) is herein assigned to the Tsezotene Formation of Gabrielse et al. (1973). The dolostone contains fine microbial or stromatolitic laminae and is locally mudcracked. The sandstone is commonly crossbedded and becomes more prominent near the upper contact with Katherine Group. These exposures of the Tsezotene Formation were previously unrecognized by Gabrielse et al. (1973) who mapped them as part of the Katherine Group (Tigonankweine Formation). The Tsezotene Formation is restricted to the hanging wall of the Mount Kraft Thrust (Fig. 2).

Katherine Group

Orthoquartzites of the Katherine Group (Aitken et al., 1978) gradationally overlie the Tsezotene Formation. Aitken et al. (1978) subdivided the Katherine Group (the Tigonankweine Formation of Gabrielse et al., 1973) into three units of formational rank, which are readily mapped in the Dal Lake area (Fig. 2). The middle Katherine (unit K_6 of Aitken et al., 1978) is a particularly useful stratigraphic marker. It is composed of dark grey to black shale and orange-to brown-weathering cherty dolostone. The dolostone locally contains poorly developed stromatolite bioherms. This shale/dolostone unit stands in sharp contrast with the orthoquartzite that makes up the bulk of the Katherine Group.

Little Dal Group

Aitken (1981) subdivided the Little Dal Group into six informal units of formational rank (Table 1). Although all units are recognized in the Ravens Throat area, only a twofold subdivision of the Little Dal Group (following the criteria defined by Aitken, 1981; Table 1) can be mapped at a regional scale (Fig. 2, 3) even though detailed stratigraphic study shows that the informal units are recognizable along the length of the Mackenzie Mountains. Red and green shale and siltstone of the "Mudcracked" formation are locally well exposed, but never exceed 15 m in thickness and, therefore, are not mappable at the scale of 1:50 000. The distinction between the "Platform" and the "Grainstone" formations is difficult to assess from a distance, and as exposures of the Little Dal Group commonly occur in rugged terrain, both units are generally mapped together as part of the lower Little Dal Group. The red-weathering "Rusty Shale" formation is quite distinct and is readily traced near the base of the upper subdivision of the Little Dal Group (Fig. 2). The underlying "Gypsum" formation is very recessive and, as a result, is typically poorly exposed. Consequently, the base of the upper Little Dal Group is drawn at the base of the "Rusty Shale" formation on the map in Figure 2. Strata of the upper Little Dal Group are only preserved in the west-central part of the Dal Lake map area (Fig. 2) and in the east-central part of the Mount Kraft map area (Fig. 3). The upper Little Dal Group is apparently bevelled beneath the sub-Rapitan unconformity in the southwest part of the Dal Lake area (Fig. 2). Throughout much of the area, only the lower Little Dal Group is preserved beneath the sub-Rapitan or sub-Whittaker unconformities (Fig. 2, 3).

Windermere Supergroup

The Windermere Supergroup of the Mackenzie Mountains, as defined by Narbonne and Aitken (1993), includes the Coates Lake Group (Jefferson, 1983; Jefferson and Ruelle, 1986), the glaciogenic Rapitan Group (Gabrielse et al., 1973; Eisbacher, 1978, 1981; Yeo, 1981) and six post-Rapitan formations (Narbonne and Aitken, 1993; see Table 1).

Coates Lake Group

The Coates Lake Group was originally included within the Mackenzie Mountains Supergroup (Young et al., 1979; Jefferson, 1983) because of the lithological similarities between the two rock assemblages. However, Aitken (1981, 1991) proposed that the Coates Lake Group be considered as the basal part of the Windermere Supergroup because of its obvious relation to rift tectonism and the presence of a major unconformity at its base.

The Coates Lake Group includes three formations: the Thundercloud, Redstone River, and Coppercap (Jefferson, 1983; Jefferson and Ruelle, 1986; Table 1). Strata of the Coates Lake Group are only exposed in the east-central part of the Mount Kraft map area (Fig. 3) in the northern extension of the Coates Lake embayment (Jefferson and Ruelle, 1986). The transition between the Redstone River and Coppercap formations is locally host to significant copper mineralization.

Rapitan Group

Previous mapping of the Ravens Throat area by Gabrielse et al. (1973) only locally subdivided the Rapitan Group (which also included the shale and sandstone now attributed to the Twitya Formation). In the Mount Kraft area, the

Table 2. Selected assay results from the Mount Kraft (95L/15) map area.

Specimen	Easting	Northing	Lithology	Au ppb	Ag ppm	Cu ppm	Pb ppm	Zn ppm	Cd ppm	As ppm
97MC014	617155	6971136	regolith sub-OSw	<5	0.2	93	482	2528	2.4	1932
97MC036-1	616158	6985679	Manetoe dolomite (DL)	<5	0.2	4	3	8784	15.3	9
97MC036-2	616158	6985679	Manetoe dolomite (DL)	<5	0.3	2	<2	40	<0.2	<5
97MC078-1	622292	6975967	calcareous siltstone (Pcp)	<5	<0.2	56	19	49	<0.2	11
97MC078-2	622292	6975967	dolomitic mudstone (Pcp)	<5	0.3	243	42	123	<0.2	42
97MC079	622186	6975963	dolomitic mudstone (Pcp)	32	0.5	3827	<2	29	<0.2	6

Note: All analyses performed by ITS-Bondar Clegg (North Vancouver); Au by fire assay, all other elements by ICP. Specimen locations (easting and northing) are given for Universal Transverse Mercator 1000 m grid, zone 9, North American Datum 1927 (NAD27), and are shown on Figure 3.

Rapitan Group locally includes a basal conglomerate/diamictite facies, in addition to the regionally extensive Sayunei and Shezal formations (Table 1; Fig. 3). This conglomerate/diamictite unit is tentatively correlated with the Mount Berg Formation of Yeo (1981). Eisbacher (1981), Jefferson (1983), and Jefferson and Parrish (1989) have described carbonate orthoconglomerate and breccia deposited adjacent to paleofault scarps cutting the lower part of Little Dal Group (see Fig. 5 in Jefferson and Parrish, 1989, p. 1792). In most cases, the basal conglomerate unit overlies rocks of the Little Dal Group, with no intervening strata identified as Coates Lake Group (Jefferson, 1983; Jefferson and Parrish, 1989), and grades upward into the Sayunei Formation. In the hanging wall of the North Extension Fault (Fig. 3), the base of the Rapitan Group is marked by a 100 m thick section of sharpstone diamictite (also described by Eisbacher, 1981, p. 31). The first diamictite bed overlies highly weathered cherty dolostone of the Coppercap Formation with apparent disconformity. But, higher in the section, the diamictite is interbedded with black cherty dolostone and pale green calcareous mudstone, similar to rocks of the underlying Coppercap Formation, and, therefore, at this locality the contact between the Coates Lake and Rapitan groups appears to be conformable. The diamictite contains clasts of black chert, laminated dolostone, oolitic dolostone, red mudstone, carbonate conglomerate, and quartz grit. Locally, the abundance of clasts is such that the rock is best described as an orthoconglomerate. This diamictite unit is gradationally overlain by red mudstone of the Sayunei Formation.

Formations that postdate the Rapitan Group

The Twitya and Keele formations are the only two Windermere Supergroup units postdating the Rapitan Group that are exposed in the study area (Table 1; Fig. 2, 3). The Twitya Formation consists of a coarsening-upward sequence of turbiditic shale and sandstone. At one locality, 4.2 km northwest of Mount Kraft, an outcrop of green diamictite similar to typical diamictite of the Shezal Formation occurs within the Twitya Formation (Fig. 3). This single occurrence of diamictite is interpreted as a mass-flow deposit of recycled Shezal diamictite. Debris-flow deposits of orange-weathering, stromatolitic dolostone are also present near the top of the Twitya Formation in the southwest corner of Mount Kraft map area (Fig. 3).

The Keele Formation is exposed on high mountain peaks in the central part and along the western edge of the Mount Kraft map area (Fig. 3). It consists predominantly of clean, cross-stratified orthoquartzite with only minor buff-weathering oolitic dolostone at the base of the formation. The orthoquartzite commonly has a dolomitic cement, and locally contains ovoid, brown-weathering dolomitic concretions. North of Mount Kraft, the Keele Formation locally contains a few thin (<1 m) horizons of coarse, graded arkosic grit and conglomerate that contain rounded pebbles of orthoquartzite. This suggests episodic deposition and erosion in a shallow marine to fluvial environment.

Paleozoic sequence of the Mackenzie Platform

Throughout much of the Mount Kraft and Dal Lake area, dolostone of the Upper Ordovician-Silurian Whittaker Formation overlies Neoproterozoic strata of the Mackenzie Mountains and Windermere supergroups with angular unconformity. The Whittaker Formation marks the base of the conformable sequence of Upper Ordovician to Upper Devonian carbonate rocks that defines the Mackenzie Platform (Table 1; Fig. 2, 3). The basal Whittaker Formation typically is a dark-grey-weathering, fossiliferous dolostone with abundant chert nodules. It is a bioclastic dolostone in the northern part of the Dal Lake map area (Fig. 2), where it has characteristic light grey and dark grey banding. In the central part of Mount Kraft map area (Fig. 3), the sub-Whittaker unconformity is marked by a gossaneous regolith that has anomalous concentrations of Zn, Pb, and Cu (Table 2).

A white orthoquartzite unconformably overlies the Coates Lake and Rapitan groups along the east side of the Hayhook Fault, in the Mount Kraft map area (Fig. 3). This orthoquartzite was interpreted by Eisbacher (1981, p. 11) as part of the Keele Formation, although he noted that its stratigraphic position is uncertain (Eisbacher, 1981, p. 31). We propose that this orthoquartzite be reassigned to the Lower Cambrian Backbone Ranges Formation, because its

hematitic cement and its onlapping relationship above a Windermere-age fault are uncharacteristic of the Keele Formation in the area (Fig. 3). The orthoquartzite of the Backbone Ranges Formation is unconformably overlain by the Whittaker Formation.

STRUCTURAL RELATIONSHIPS

The structural style of the Ravens Throat area is the result of the interplay between Neoproterozoic-Early Paleozoic extension faulting and Mesozoic folding and thrust faulting. Neoproterozoic transtension faults developed during rift tectonism, accompanied by deposition of the Coates Lake and Rapitan groups (Eisbacher, 1981; Park and Jefferson, 1991). The majority of extension faults in the study area cut older Neoproterozoic units of the Mackenzie Mountains Supergroup but are onlapped by the basal units of the Rapitan Group (Sayunei and Shezal formations; Fig. 3). Fanglomerate assigned to the Mount Berg Formation are deposited locally adjacent to extension faults in the Mount Kraft area. A few extension faults offset the Twitya Formation and this may indicate that rifting continued during deposition of the Twitya Formation. Alternatively, these faults may have been reactivated during later Paleozoic and/or Mesozoic deformation.

The Mount Kraft Thrust is the most significant Mesozoic compressional structure in the study area (Fig. 2, 3). The southern segment of this fault was previously interpreted by Eisbacher (1981, p. 11) as a southeast-dipping extension fault. Our mapping of the Mount Kraft area indicates that this fault is a shallowly to moderately westerly dipping thrust fault, which juxtaposes Neoproterozoic rocks, in its hanging wall, over Paleozoic strata, in its footwall (Fig. 2, 3). The Mount Kraft Thrust is arcuate and broadly follows the trend of Neoproterozoic extension faults preserved in its hanging wall, to the west (Fig. 3). It dies out to the north in the core of a broad anticline that exposes strata of the Tsezotene Formation and Katherine Group (Fig. 2). To the south, the Mount Kraft Thrust and an extension fault preserved in its hanging wall both terminate abruptly in the Silverberry Valley (Fig. 3). This may indicate that the Plateau Thrust extends along Silverberry River from the west, where it was mapped by Gabrielse et al. (1973).

The Mount Kraft Thrust is truncated by the North Extension Fault in the east-central part of Mount Kraft map area (Fig. 3). The North Extension Fault is a moderately east-dipping, west-verging thrust fault that marks the western limit of exposure of the Coates Lake Group in the area. It is interpreted to follow the trace of an older southeast-dipping extension fault, which delimited the western margin of the north extension of the Coates Lake Embayment (Jefferson, 1983).

Gabrielse et al. (1973) speculated that about 15 km of right-lateral transcurrent displacement occurred along the Hayhook Fault. Our examination of the fault in the eastern part of the Mount Kraft map area (Fig. 3) supports the notion of strike-slip displacement along Hayhook Fault. The fault is steeply dipping and, in the northeast part of Mount Kraft map area, it juxtaposes a south-dipping sequence of Paleozoic rocks, on the west, and a north-dipping panel comprising the same stratigraphic interval, on the east (Fig. 3). Paleozoic rocks along the fault are locally silicified and commonly have a cataclastic structure. The fold pattern west of Hayhook Fault shows a complex interplay between folding associated with thrusting (along Mount Kraft and North Extension faults) and strike-slip displacement along Hayhook Fault. In the north-central part of Mount Kraft area (Fig. 3), Paleozoic strata are exposed along the lower limb of a northeast-verging syncline developed in the footwall of the Mount Kraft Thrust. The axis of this syncline and a congruent anticline-syncline pair are rotated counterclockwise by as much as 90° near the northern termination of the North Extension Fault. In the immediate vicinity of Hayhook Fault, the folds are tight, upright, and congruent with the trend of the fault. This pattern of folding suggests that transcurrent displacement along Hayhook Fault occurred, at least in part, during the Mesozoic. Hayhook Fault probably follows the locus of an older extension fault as suggested by distinct facies in the Neoproterozoic rocks on either side of the fault (Eisbacher, 1981).

The South Redstone Fault is another structure that is interpreted to follow an older basement discontinuity (Aitken and Pugh, 1984; Cecile et al., 1997). In the Mount Kraft map area, the South Redstone Fault has a net down-to-the-northwest displacement (Fig. 3). However, on a regional scale, the South Redstone Fault shows as much as 10-12 km of right-lateral strike-slip displacement (Jefferson, 1983). The South Redstone Fault truncates Mesozoic thrust structures (e.g. Coates Lake Fault; Fig. 3) and, therefore, part of its displacement postdates the development of compressional structures in the area.

Our preliminary assessment of the Ravens Throat project area suggests the following sequence for the evolution of structures:

1. Development of transtension faults during Neoproterozoic rifting (some of these faults may have been reactivated during later Paleozoic and/or Mesozoic deformation).
2. Folding and east-verging thrust faulting (Mount Kraft Thrust).
3. West-verging thrust faulting along North Extension Fault.
4. Out-of-sequence thrust faulting along the east-verging Plateau Thrust (Gabrielse et al., 1973).
5. Right-lateral strike-slip faulting along Hayhook and South Redstone faults.

Absolute timing of the compressional structures cannot be determined directly in the study area. Folding and thrust faulting in the Selwyn Fold Belt, to the southwest, postdates deposition of Middle Jurassic rocks, but predates emplacement of Late Cretaceous (104-80 Ma) granitoid plutons (Gordey and Anderson, 1993). At the Mackenzie Mountain front, to the northeast, strata as young as Tertiary are

deformed (Aitken and Cook, 1974). Therefore, structures in the Ravens Throat project area are broadly of Late Cretaceous–Tertiary age.

MINERAL OCCURRENCES

Significant copper mineralization occurs within the transition zone between the Redstone River and Coppercap formations (e.g. Jefferson and Ruelle, 1986). At Coates Lake, immediately south of the Mount Kraft map area (Fig. 1), reserves are estimated at 37 million tonnes averaging 3.9% Cu and 11.3 g/t Ag (Kirkham, 1996). In the study area, the favourable stratigraphy is limited to the hanging wall of the North Extension Fault and to the east side of Hayhook Fault (Fig. 3); the latter occurrence of Coates Lake strata was previously unrecognized. Copper sulphides are disseminated within a 2 m thick carbonate bed near the base of the transition zone at the North Extension showing (specimens 97MC078 and 97MC079, Table 2; Fig. 3); this unit extends approximately 300 m along strike. There is a rapid decrease in Cu content between the base (specimen 97MC079) and the top (specimen 97MC078-1) of the transition zone, as indicated by Jefferson (1983) and Jefferson and Ruelle (1986).

Additional Cu sulphides are disseminated along fracture zones closely associated with Neoproterozoic extension faults. These occurrences are typically hosted within strata of the Little Dal Group (Fig. 2, 3). Examination of such occurrences in the Mount Kraft area revealed that the mineralization is restricted to a veneer of malachite/bornite along fractures, with rare disseminated pyrite and chalcopyrite. The numerous occurrences reported by Jory (1962) in the Dal Lake area (Fig. 2) were not visited during the 1997 field season. Ruelle and Bond (1976) assigned no economic interest to these fracture-hosted Cu occurrences.

Zinc mineralization in the Ravens Throat area is spatially associated with occurrences of the Manetoe dolomite facies. The Manetoe facies is a hydrothermal sparry dolomite facies (Morrow and Cook, 1987), which in the study area locally replaces the basal Landry Formation. Development of the Manetoe dolomite is restricted in the Mount Kraft area (Fig. 3) and no visible mineralization was detected. Assay results from two samples of Manetoe dolomite collected a few metres apart are presented in Table 2 (specimens 97MC036-1 and 97MC036-2); they show the highly variable zinc concentrations within the Manetoe facies.

Finally, anomalous Zn, Pb, and Cu values were obtained from a gossany regolith at the sub-Whittaker unconformity, in the central part of Mount Kraft map area (Table 2, specimen 97MC014; Fig. 3). The regolith is developed in the Twitya Formation and its thickness varies from 1 to 5 m. This is the only occurrence noted of a well developed regolith beneath the sub-Whittaker unconformity in the area.

ACKNOWLEDGMENTS

We thank Tim Simmons (Canadian Helicopters, Norman Wells) and the staff at Mary's Store for logistical support while in the field. Andrea Mills provided invaluable assistance in the preparation of the figures for this paper. The manuscript has benefited from critical reviews by Don Cook, Charlie Jefferson, Doug Irwin, and Carolyn Relf.

REFERENCES

Aitken, J.D.
1981: Stratigraphy and sedimentology of the Upper Proterozoic Little Dal Group, Mackenzie Mountains, Northwest Territories; in Proterozoic basins of Canada (ed.) F.H.A. Campbell; Geological Survey of Canada, Paper 81-10, p. 47-71.
1991: The Ice Brook Formation and post-Rapitan, Late Proterozoic glaciation, Mackenzie Mountains, Northwest Territories; Geological Survey of Canada, Bulletin 404, 43 pages.

Aitken, J.D. and Cook, D.G.
1974: Carcajou Canyon map area (96D), District of Mackenzie; Geological Survey of Canada, Paper 74-13, 28 pages.

Aitken, J.D. and McMechan, M.E.
1991: Middle Proterozoic assemblages; in Chapter 5 of Geology of the Cordilleran Orogen in Canada, (ed.) H. Gabrielse and C.J. Yorath; Geological Survey of Canada, Geology of Canada, no. 4, p. 97-124 (also Geological Society of America, The Geology of North America, v. G-2, p. 97-124).

Aitken, J.D. and Pugh, D.C.
1984: The Fort Norman and Leith Ridge structures: major, buried, Precambrian features underlying Franklin Mountains and Great Bear and Mackenzie plains; Bulletin of Canadian Petroleum Geology, v. 32, p. 139-146.

Aitken, J.D., Long, D.G.F., and Semikhatov, M.A.
1978: Progress in Helikian stratigraphy, Mackenzie Mountains; in Current Research, Part A, Geological Survey of Canada, Paper 78-1A, p. 481-484.

Cecile, M.P., Morrow, D.W., and Williams, G.K.
1997: Early Paleozoic (Cambrian to Early Devonian) tectonic framework, Canadian Cordillera; Bulletin of Canadian Petroleum Geology, v. 45, p. 54-74.

Eisbacher, G. H.
1978: Re-definition and subdivision of the Rapitan Group, Mackenzie Mountains; Geological Survey of Canada, Paper 77-35, 21 pages.
1981: Sedimentary tectonics and glacial record in the Windermere Supergroup, Mackenzie Mountains, northwestern Canada; Geological Survey of Canada, Paper 80-27, 40 pages.

Fritz, W.H., Cecile, M.P., Norford, B.S., Morrow, D., and Geldsetzer, H.H.J.
1991: Cambrian to Middle Devonian assemblages; in Chapter 7 of Geology of the Cordilleran Orogen in Canada, (ed.) H. Gabrielse and C.J. Yorath; Geological Survey of Canada, Geology of Canada, no. 4, p. 151-218 (also Geological Society of America, The Geology of North America, v. G-2, p. 151-218).

Gabrielse, H., Blusson, S.L., and Roddick, J.A.
1973: Geology of Flat River, Glacier Lake, and Wrigley Lake map-areas, District of Mackenzie and Yukon Territory; Geological Survey of Canada, Memoir 366 (parts I and II), 421 pages.

Gordey, S.P. and Anderson, R.G.
1993: Evolution of the northern Cordilleran miogeocline, Nahanni map area (105I), Yukon and Northwest Territories; Geological Survey of Canada, Memoir 428, 214 pages.

Jefferson, C.W.
1983: The Upper Proterozoic Redstone Copper Belt, Mackenzie Mountains, N.W.T.; Ph.D. thesis, University of Western Ontario, 445 pages.

Jefferson, C.W. and Parrish, R.R.
1989: Late Proterozoic stratigraphy, U-Pb zircon ages, and rift tectonics, Mackenzie Mountains, northwestern Canada; Canadian Journal of Earth Sciences, v. 26, p. 1784-1801.

Jefferson, C.W. and Ruelle, J.C.L.
1986: Late Proterozoic Redstone Copper Belt, Mackenzie Mountains, N.W.T.; in Mineral deposits of the northern Cordillera, (ed.) J.A. Morin; Canadian Institute of Mining and Metallurgy, Special Volume 37, p. 154-168.

Jory, L.T.
1962: Geological mapping and trenching, North Redstone claim group, Dal Lake, N.W.T.; Department of Indian Affairs and Northern Development, Assessment Report 017596.

Kirkham, R.V.
1996: Sediment-hosted stratiform copper; in Geology of Canadian Mineral Deposit Types, (ed.) O.R. Eckstrand, W.D. Sinclair, and R.I. Thorpe; Geological Survey of Canada, Geology of Canada, no. 8, p. 223-240 (also Geological Society of America, The Geology of North America, v. P-1, p.223-240).

Morrow, D.W.
1991: The Silurian-Devonian sequence in the northern part of the Mackenzie shelf, Northwest Territories; Geological Survey of Canada, Bulletin 413, 121 pages.

Morrow, D.W. and Cook, D.G.
1987: The Prairie Creek embayment and Lower Paleozoic strata of the southern Mackenzie Mountains; Geological Survey of Canada, Memoir 412, 195 pages.

Narbonne, G.M. and Aitken, J.D.
1993: Neoproterozoic of the Mackenzie Mountains, northwestern Canada; Precambrian Research, v. 73, p. 101-121.

Park, J.K. and Jefferson, C.W.
1991: Magnetic and tectonic history of the Late Proterozoic upper Little Dal and Coates Lake groups of northwestern Canada; Precambrian Research, v. 52, p. 1-35.

Rainbird, R.H., Jefferson, C.W., and Young, G.M.
1996: The early Neoproterozoic sedimentary Succession B of northwestern Laurentia: Correlations and paleogeographic significance; Geological Society of America Bulletin, v. 108, p. 454-470.

Ross, G.M.
1991: Tectonic setting of the Windermere Supergroup revisited; Geology, v. 19, p. 1125-1128.

Ruelle, J.C. and Bond, I.J.
1976: Geological assessment report on the Backbone project claims south and west of permit 361 and extending from Keele River to Coates Lake, N.W.T.; Department of Indian Affairs and Northern Development, Assessment Report 080570, 21 p.

Wheeler, J.O. and McFeely, P.
1991: Tectonic assemblage map of the Canadian Cordillera and adjacent parts of the United States of America; Geological Survey of Canada, Map 1712A (scale 1:2 000 000).

Yeo, G. M.
1981: The Late Proterozoic Rapitan glaciation in the northern Cordillera; in Proterozoic basins of Canada, (ed.) F.H.A. Campbell; Geological Survey of Canada, Paper 81-10, p. 25-46.

Young, G.M., Jefferson, C.W., Delaney, G.D., and Yeo, G.M.
1979: Middle and late Proterozoic evolution of the northern Canadian Cordillera and Shield; Geology, v. 7, p. 125-128.

Geology of the Babiche Mountain and Chinkeh Creek map areas, southeastern Yukon Territory and southwestern Northwest Territories

Lisel D. Currie, Thomas E. Kubli[1], Michael R. McDonough[2], and Denise N. Hodder[3]

GSC Calgary, Calgary

Currie, L.D., Kubli, T.E., McDonough, M.R., and Hodder, D.N., 1998: Geology of the Babiche Mountain and Chinkeh Creek map areas, southeastern Yukon Territory and southwestern Northwest Territories; in Current Research 1998-A; Geological Survey of Canada, p. 39-48.

Abstract: Regional geological mapping at a scale of 1:50 000 in the Babiche Mountain and Chinkeh Creek map areas during 1997 marked the beginning of the multiyear Central Foreland Project. The stratigraphy and structural style of these and surrounding areas in the Fort Liard-La Biche map areas (NTS 95B, C) will be compared with those of Trutch map area (NTS 94G).

The map pattern is controlled by broad, west-verging, detachment box folds of the Kotaneelee and La Biche anticline-syncline pairs. Their sinuous traces are associated with shortening transferred via southeastward-stepping, en echelon folds. Many previously inferred faults do not exist.

Anticlines are cored by the Devonian to Lower Carboniferous Besa River and Lower Carboniferous Mattson formations, and flanked by Permian rocks of the informal Tika map unit (previously considered Mattson Formation) and Fantasque Formation. Synclines are filled with Cretaceous Fort St. John Group strata.

Résumé : La cartographie géologique régionale à l'échelle de 1:50 000 réalisée en 1997 dans les régions cartographiques du mont Babiche et du ruisseau Chinkeh marque le début d'un projet pluriannuel, le Projet de l'avant-pays central. La topographie et le style structural de ces régions et des territoires environnants dans les régions cartographiques de Fort Liard-La Biche (SNRC 95B, C) sont comparées à celles de la région cartographique de Trutch (SNRC 94G).

La configuration cartographique est contrôlée par de larges plis coffrés à décollement à vergence ouest des paires anticlinal-synclinal de Kotaneelee et La Biche. Leurs tracés sinueux sont associés à un raccourcissement matérialisé par des plis en échelon décalés vers le sud-est. De nombreuses failles dont l'existence avait été déduite n'existent pas.

Le coeur des anticlinaux se compose des formation de Besa River (Dévonien-Carbonifère inférieur) et de Mattson (Carbonifère inférieur). Ces anticlinaux sont flanqués par des roches permiennes de l'unité cartographique informelle de Tika (considérée auparavant comme faisant partie de la Formation de Mattson) et de la Formation de Fantasque. Les synclinaux comportent des strates du groupe crétacé de Fort St. John.

[1] TEK Consulting Ltd., 1315-6th Street N.W., Calgary, Alberta T2M 3E5

[2] Apu Consulting Ltd.

[3] Department of Geology and Geophysics, University of Calgary, 2500 University Drive N.W., Calgary, Alberta T2N 1N4

INTRODUCTION

The Kotaneelee and La Biche ranges lie within the southern Franklin Mountains (in part also referred to as the Liard Plateau), in a geographic position comparable to that of the Rocky Mountain Front Ranges. Like the Front Ranges, this foreland fold and thrust belt is underlain by Paleozoic and Mesozoic strata, and contains economically viable gas fields, including the Beaver River, Kotaneelee, Pointed Mountain, and La Biche fields. However, in contrast to the stacked thrusts of the Front Ranges, the Kotaneelee and La Biche ranges are characterized by broad folds at the surface.

To provide a regional context for more detailed mapping, parts of the the Kotaneelee and La Biche ranges were mapped at a scale of 1:50 000 during the summer of 1997. This work builds on mapping by M.R. McDonough (in 1995 and 1996), generously donated by Husky Oil Operations Ltd; mapping by T. Kubli (in 1996) that was kindly made available by Norcen Resources Ltd.; and a 1:250 000 scale compilation map by Douglas (1974; see Douglas and Norris; 1959; Fig. 1). This research is the first part of the Central Foreland Project, a multidisciplinary, multipartner geological study of parts of northeastern British Columbia, southeastern Yukon Territory, and southwestern Northwest Territories. Fieldwork in map areas NTS 95B and C is expected to continue as part of the Central Foreland Project during the years 2000, 2001, and 2002.

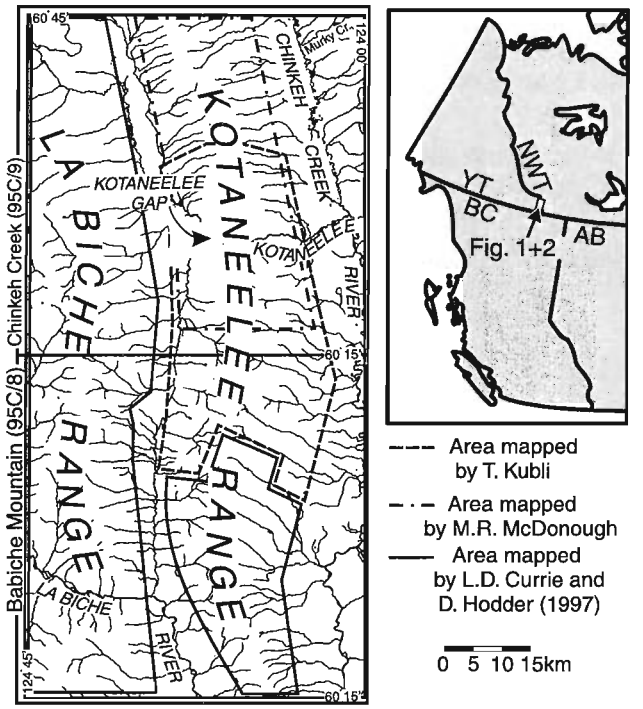

Figure 1. *Map of NTS 95C/8 and 9 showing the locations of the Kotaneelee and La Biche ranges, and their sinuous traces. Areas mapped by T. Kubli, M.R. McDonough, L.D. Currie, and D. Hodder are outlined. Geology shown in Figure 2 for the intervening and adjacent areas is based on the compilation by Douglas (1974). AB, Alberta; BC, British Columbia; NWT, Northwest Territories; YT, Yukon Territory.*

REGIONAL GEOLOGY

The map area lies on the east side of the Liard Basin, where topography is structurally controlled. The La Biche and Kotaneelee anticlines have 1 to 3 km amplitudes, 10 to 15 km wavelengths, and form the cores of the La Biche and Kotaneelee ranges, respectively (Fig. 2). The heavily forested valley that separates these ranges is underlain by the broad, open La Biche Syncline, and east of the Kotaneelee Range, the Kotaneelee Syncline forms the Chinkeh Creek-Kotaneelee River valley (Fig. 2).

The nomenclature used herein is based on and modified from that of Douglas (1974), and the sedimentary classification is that of Folk (1974). The mountain ranges are primarily cored by shale and minor siltstone and sandstone of the Besa River Formation; shale, quartz arenite, and limestone of the Mississippian Mattson Formation; and limestone of the herein informally named "Tika map unit". Chert belonging to the Permian Fantasque Formation overlies the Tika map unit and forms the flanks of the mountain ranges. The Fantasque Formation is unconformably overlain by the Cretaceous shale and minor sandstone preserved in the cores of the La Biche and Kotaneelee synclines. Shales are generally poorly exposed, whereas quartz arenite, limestone, dolostone, and chert layers commonly outcrop as resistant bands on cliffs and ridges, or as flat irons.

STRATIGRAPHY

Besa River Formation (DMBR)

The Devonian to Carboniferous Besa River Formation comprises variably calcareous, and locally dolomitic dark grey to black shale with minor interbedded siltstone and lesser, orange-weathering, fine grained sandstone layers.

Because just the top 150 to 250 m of the Besa River Formation are exposed in the study area, only minimum thicknesses can be determined. Total thickness in the study area was estimated at 1500 to 1750 m by Douglas and Norris (1959) and Douglas (1974) and, on the basis of the Pan-Am Kotaneelee O-67 well records, at 1271 m by Richards (1989).

The Besa River Formation exposed in map areas NTS 94C/8 and 9 is considered part of the "shale and sandstone lithofacies" of Richards (1989), who interpreted this lithofacies as a prodelta deposit because it is "transitional between the delta slope deposits in the overlying Mattson Formation and underlying lithofacies deposited basinward of carbonate buildups" (Richards, 1989, p. 13).

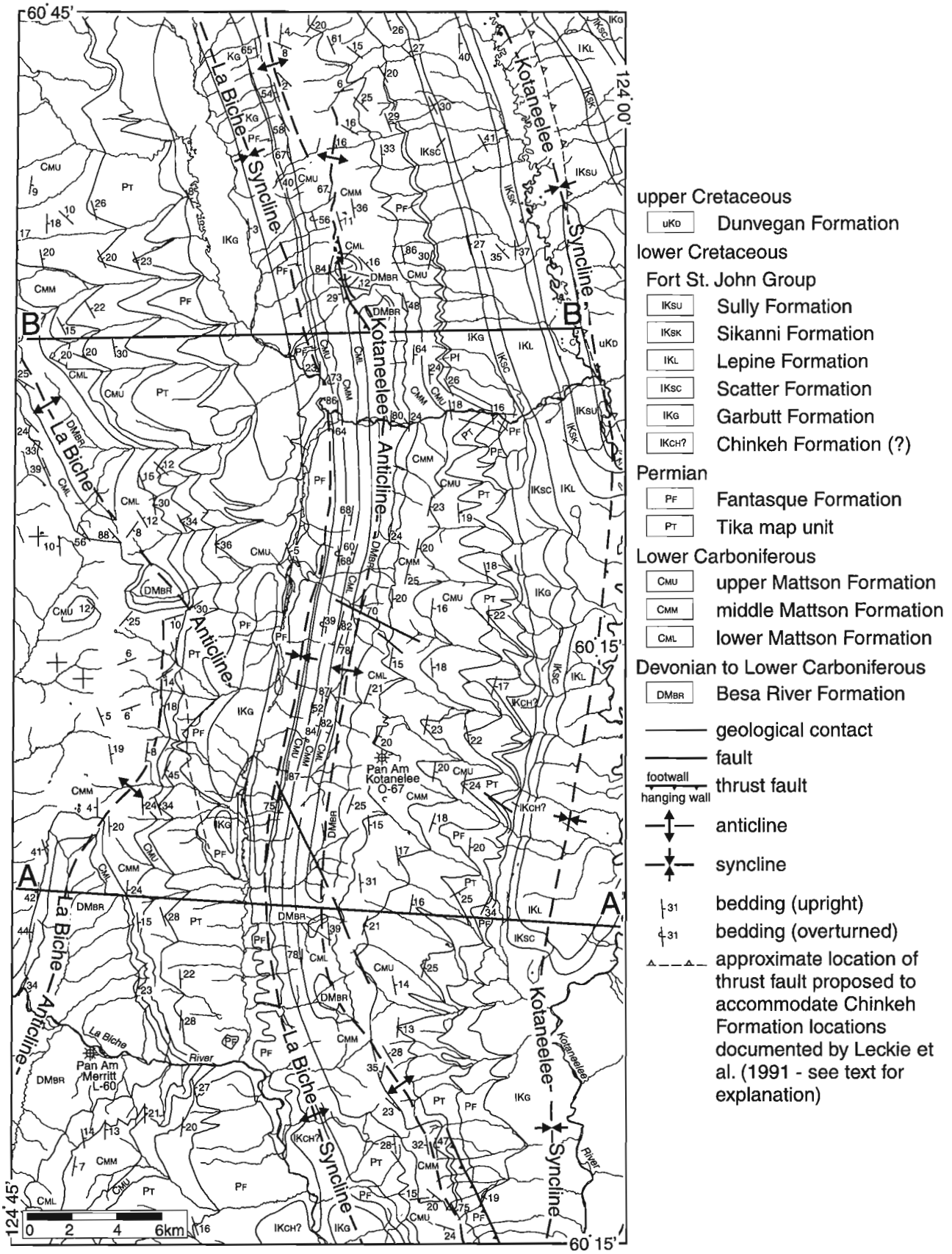

Figure 2. *Geological map of NTS 95C/8 and 9.*

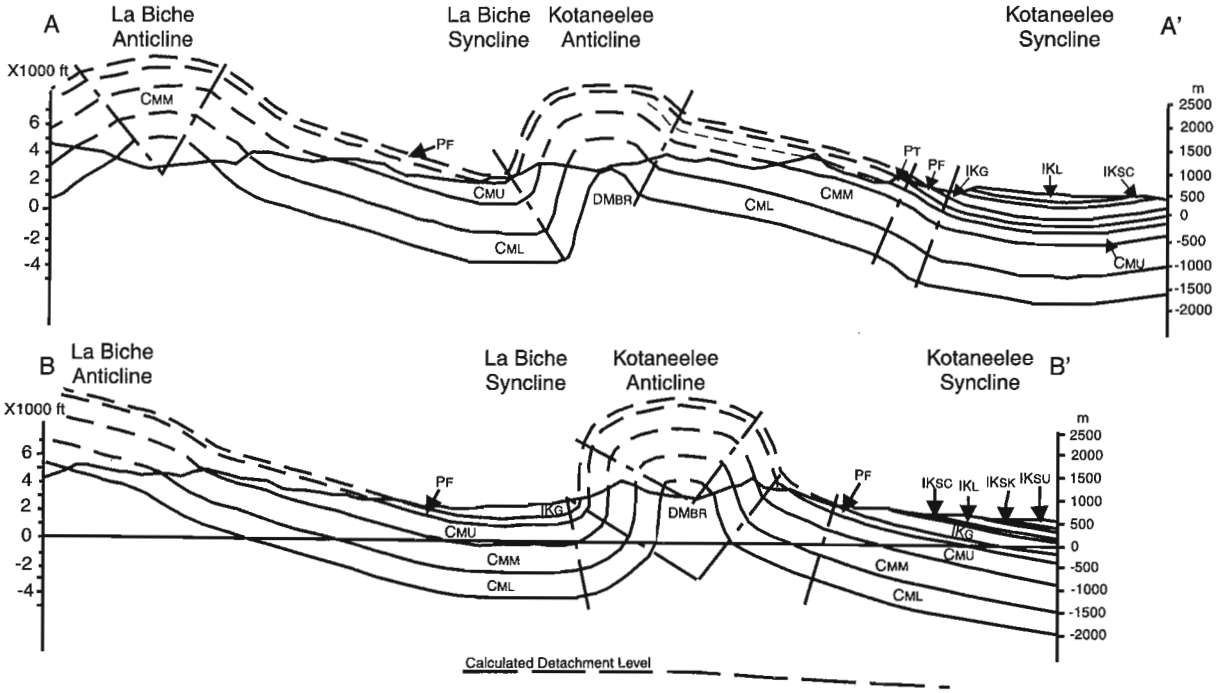

Figure 3. Cross-sections through the Kotaneelee and La Biche ranges. See Figure 2 for locations.

Mattson Formation

Douglas and Norris (1959) and Douglas (1974) divided the Viséan to Surpukovian (Lower Carboniferous; Patton, 1958) Mattson Formation into informal lower, middle and upper "parts".

Richards et al. (1993, and references therein) interpreted the Mattson Formation as "fluvially dominated, wave- and tide-influenced deltas" (p. 244).

The thickness of the Mattson Formation, estimated from cross-sections (Fig. 3), ranges from 1440 to 1700 m. This is considerably thicker than the 1250 m shown in cross-sections of the Kotaneelee Range by Douglas (1974) and the 1130 m measured at Mattson Gap in the Liard Range (Douglas and Norris, 1959). Although some of this discrepancy may result from uncertainty in placing the contacts between the Besa River-lower Mattson Formation and the upper Mattson Formation-Tika map unit contacts, some westward stratigraphic thickening has to be inferred.

Lower Mattson Formation (CML)

The lower Mattson Formation comprises fine- to medium-grained quartz arenite interbedded with medium grey to dark grey shale layers. Shale-dominated sections are 1 to 20 m thick and quartz arenite-dominated sections are from 0.5 to 35 m thick.

Quartz arenite beds are generally platy, and 0.1 to 50 cm thick. They are commonly rusty-weathering, and characterized by coarsening-upward sequences with gradational bases and sharp tops. However, locally, the basal quartz arenite unit is in sharp contact with the underlying Besa River Formation. Quartz arenite layers contain small scale (~2-5 cm amplitude by 15-25 cm wavelength) wave- and current-formed ripples and crossbeds, with subordinate, medium scale, planar-tabular crossbeds. Evidence of bioturbation is common in both quartz arenite and shale layers, but fossils are rare.

Because of the platy nature of the quartz arenite layers, the lower Mattson Formation is more recessive than the overlying middle Mattson Formation, and tends to form cliffs below the "cap rocks" of the more resistant, thick quartz arenite bands of the middle Mattson Formation (Fig. 4). This is true even in the La Biche Range, where thick (1-2 m), but discontinuous (less than 30 m wide) quartz arenite layers occur near the top of the lower Mattson Formation (Fig. 4).

The thickness of the lower Mattson Formation, estimated from cross-sections, ranges from 550 m in the north of the study area to 650 m in the south.

Richards (1989) interpreted the lower Mattson Formation as a delta front succession. The rock types and sedimentary structures described above are consistent with this interpretation. The thick but discontinuous quartz arenite layers that occur near the top of the lower Mattson Formation in the La Biche Range (Fig. 4) are interpreted as submarine channels. Note that these channels have not been observed in the Kotaneelee Range.

Middle Mattson Formation (CMM)

Poor- to well-indurated, medium grained, buff-weathering quartz arenite and medium grey to dark grey shale, with minor dark orange-weathering limestone and sandy

Figure 4. *The lower Mattson Formation exposed on the western limb of the La Biche Range, near the north end of NTS 95C/9. Note the isolated channel near the centre left of the photo (viewed from the southeast). GSCC 4637-7*

limestone form the middle Mattson Formation. The thickness of this map unit, estimated from cross-sections, ranges from 440 to 640 m.

The middle Mattson Formation can be distinguished from the lower Mattson Formation by its fining-, rather than coarsening-upward sequences, and because its quartz arenite layers are, in general, more coarse grained, lighter in colour, and thicker (commonly 5-10 m thick) than lower Mattson Formation quartz arenite layers. In addition, evidence for bioturbation in the middle Mattson Formation quartz arenite layers is rare. The base of the middle Mattson Formation is placed at the lowest thick, laterally continuous, resistant quartz arenite sheet. The lowest channel cannot be considered the base of the middle Mattson Formation, because channels occur in the lower Mattson Formation of the La Biche Range.

Near the base of the middle Mattson Formation, quartz arenite sheets are 1 to 20 m thick, and exhibit planar bedding and wave-form ripples, with subordinate trough crossbeds. Quartz arenite layers vary in thickness from 0.01 to 2 m, have sharp erosive bases (as evidenced by scour marks and grooves), and locally developed, matrix-supported conglomerate that has mudstone pebbles and cobbles.

Overlying the lower 20 to 30 m of this unit are 1 to 3 m thick, discontinuous, orange-weathering limestone and calcareous quartz arenite layers and lenses that locally contain pelmatozoan fragments, gastropods, and spiriferid brachiopods. These layers are overlain by an 100 to 150 m thick, shale-dominated sequence.

Above the shale-dominated sequence, quartz arenite sequences are from 0.3 to 30 m thick, and are commonly poorly indurated. Trough crossbeds are common throughout, with lesser planar-tabular crossbeds and planar bedding. Locally, crossbeds are as high as 3 m, and thicken upward, suggesting that the sand was deposited in an eolian environment (Fig. 5).

The lower part of the middle Mattson Formation is interpreted as transitional between delta front and fluvial lithofacies because channels are not well developed – they are considered distributary mouth and overbank deposits. The overlying dark orange-weathering and locally fossiliferous calcareous layers and shale-dominated section may record a minor transgression. The upper part of the middle Mattson contains channel fills that are commonly amalgamated. The channels are interpreted as fluvial deposits, and together with the eolian deposits, they appear to reflect the hiatus of a regression.

Upper Mattson Formation (CMU)

The base of the upper Mattson Formation is defined as the base of the lowest thick carbonate layer. Like the middle Mattson Formation, it includes quartz arenite and shale, but the upper Mattson Formation also contains significant quantities of limestone and dolostone, minor chert arenite, and poorly cemented, dolomitic quartz arenite. The carbonate layers commonly contain brachiopod (mostly productid and minor spiriferid), pelecypod, pelmatozoan, and bryozoan (both branching and fenestral) debris. Vugs are locally developed (Fig. 6). The quartz arenite layers are dominated by fining-upward sequences, medium- to large-scale trough crossbedding, with lesser planar-tabular crossbedding, planar-laminar bedding, and small symmetrical and asymmetrical crossbeds. Thin (less than 10 cm thick) chert arenite layers were observed near the top of the upper Mattson Formation.

The thickness of the upper Mattson Formation (as defined herein), estimated from cross-sections, ranges from 300 to 575 m.

Both fluvial and tidal environments appear to be recorded by the upper Mattson Formation. The sharp-based channel fills with fining-upward sequences are considered indicative

Figure 5. *Crossbedding in poorly indurated sandstone of the middle Mattson Formation. On the basis of upward-thickening within individual crossbeds, they are thought to have formed in an eolian environment. This bed is 3 m thick. GSCC 4637-8*

of a shoreline facies. Because the carbonate layers are generally less than 10 m thick, and overlie deltaic deposits and delta-related siliclastics, they are thought to record numerous transgressions (Richards et al., 1993).

Tika map unit (PT)

A monotonous sequence of medium brown to dark brown (fresh surface), fine grained silty limestone, silty dolostone, and calcareous quartz arenite previously included in the upper Mattson Formation is herein informally referred to as the "Tika map unit". The base of the Tika map unit is marked by a 10 to 50 cm thick breccia (Fig. 7). Overlying fine grained silty limestone and silty dolostone beds 1 to 20 cm thick have planar or wavy bedding. Beds greater than 20 cm thick have a characteristic, irregular and/or concoidal fracture pattern (Fig. 8). Near the top of this unit, beds with abundant, unbroken brachiopod shells are common. The Tika map unit is from 50 to 120 m thick. Note that the Tika map unit has not been mapped in the Kotaneelee Range north of Kotaneelee Gap, or on the west limb of the Kotaneelee Anticline, south of Kotaneelee Gap.

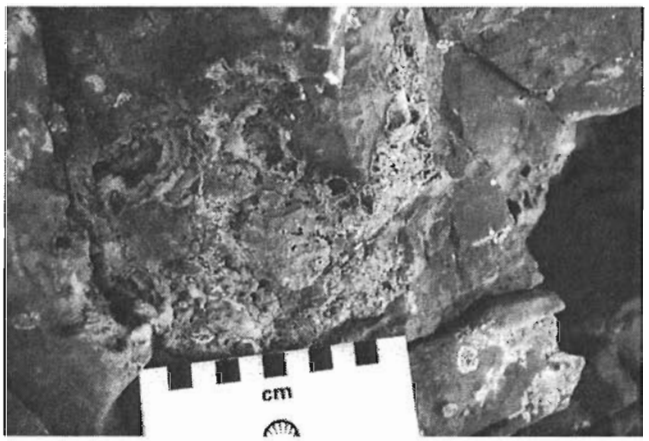

Figure 6. *Vugs in upper Mattson Formation limestone. GSCC 4637-11*

Figure 7. *Calcareous breccia at the base of the Tika map unit overlying limestones of the upper Mattson Formation. GSCC 4637-10*

Figure 8. *Irregular, conchoidal fracture characteristic of sandy carbonate beds in the Tika map unit. GSCC 4637-5*

Rocks considered part of the Tika map unit were previously included in the upper Mattson Formation by Harker (1963), and considered Carboniferous to Permian, but are now known to be Permian (B.C. Richards, pers. comm., 1997). Previously, fine grained Permian siliclastic rocks that are in part calcareous, and underlie the Fantasque Formation, have been included in the Kindle Formation (e.g. Bamber et al., 1968; Henderson, 1989, and references therein). However, we have chosen not to refer to the Tika map unit as Kindle Formation because conodont biostratigraphy has demonstrated that the type section of the Kindle Formation, and one additional Kindle Formation location, comprise Serpukhovian to Bashkirian (Carboniferous) and possibly Moscovian (upper Carboniferous) strata (Chung, 1993).

The depositional setting of the Tika map unit is not known.

Fantasque Formation (PF)

The Fantasque Formation primarily comprises rhythmically bedded chert and associated minor shale and siliceous siltstone. The chert bands vary in width from 5 to 15 cm, and weather white, alternating dark grey and white, or, rarely, red. Fresh surfaces are generally light to medium grey.

The base of the Fantasque Formation is commonly marked by chert breccia. In the southern La Biche Range, near the base of the Fantasque Formation, there is a 3 m thick, matrix-supported conglomerate with shale clasts from 1 to 5 cm in diameter (Fig. 9). Elsewhere, the lower 30 m of the Fantasque Formation consists of medium- to thick-bedded

Figure 9. *Matrix-supported conglomerate with shale clasts at base of Fantasque Formation and overlying the Tika map unit. GSCC 4637-1*

siliceous siltstone with interbeds of thick-bedded chert. It is overlain by a horizon with abundant iron concretions, which is in turn overlain by massive bedded chert with local accumulations of sponge spicules and minor interbedded siltstone and shale.

In the central and southern Kotaneelee and La Biche ranges, the Fantasque Formation has a thickness of approximately 112 m. However, the Fantasque Formation thins toward the north, in the Kotaneelee Range, and disappears approximately 10 km north of "Kotaneelee Gap". Presumably its absence reflects downcutting due to erosion.

Fort St. John Group and Dunvegan Formation (Cretaceous)

Formations of the Lower Cretaceous Fort St. John Group and Upper Cretaceous Dunvegan Formation represent repeated transgressive-regressive sequences composed of sediments derived primarily from the deformed belt that was advancing from the west (Stott, 1982). The Fort St. John Group and Dunvegan Formation were not mapped in detail during this study, with the exception of the possible Lower Cretaceous strata mapped on the east flank of the Kotaneelee Range, described below.

*Chinkeh Formation (*lKCH?)

The Fantasque Formation is locally overlain by a 8 to10 cm thick silicified breccia with very angular clasts of white chert in a matrix of dark grey silicified siltstone. On the east side of the Kotaneelee Range, interbedded shales, bioturbated siltstones, and fine grained sandstones with abundant *Zoophycos* overlie this basal unit.

Douglas (1974) inferred that these strata, and their continuation in the core of the La Biche Syncline, were Triassic, because he considered them contiguous with Triassic strata that occupy the same stratigraphic position farther south (Fig. 2). However, Leckie et al. (1991) documented the presence of lower Cretaceous Chinkeh Formation rocks in the "Kotaneelee Gap", in the northeast corner of the map area (near Murky Creek; Fig. 1), just south of the Kotaneelee River-Chinkeh Creek confluence, and in adjacent and nearby map areas. The Chinkeh Formation consists of the basal chert breccia overlying the Fantasque Formation, conglomerate, fine- to medium-grained, well-sorted marine sandstone, and bioturbated shale. Despite its lack of conglomerate, the map unit on the east side of the Kotaneelee Range is tentatively included in the Chinkeh Formation. However, further biostratigraphic work is needed to make a definite age assignment.

More problematic are the sections that Leckie et al. (1991) measured near Murky Creek and just south of the Kotaneelee River-Chinkeh Creek confluence. If they are indeed Lower Cretaceous Chinkeh Formation rocks, then the map pattern shown in Figure 2 for the Cretaceous rocks in the northeast part of the map area is incorrect. Instead, there may be a west-verging thrust fault near the trace of the Kotaneelee Syncline that places Paleozoic rocks over Mesozoic rocks.

STRUCTURE

Folds

The Kotaneelee and La Biche anticline-syncline pairs are large-scale detachment box folds with sinuous axial traces that dominate the map pattern of NTS 95C/8 and 95C/9 (Fig. 2). Field observations and systematic measurement of bedding attitudes document the existence of distinct domains of constant dip, separated by sharp kinks (Fig. 2).

Kotaneelee Anticline

The 90 km long Kotaneelee Anticline extends from south of the La Biche River (about 60°00'N) northward to Etanda Lakes (60°50'N; Douglas, 1974). It is the northern extension of the gas-bearing Beaver River Anticline. The Kotaneelee Anticline verges to the west, except in the south, and has a box-fold geometry with a near-vertical to overturned west limb and shallow-dipping east limb (Fig. 2, 3, 10). Parasitic folds are rare, but they do exist on the overturned west limb of the Kotaneelee Anticline, at "Kotaneelee Gap".

Two structural styles contribute to the sinuous nature of the axial trace of the Kotaneelee Anticline. First, the axial plane is curved (see strike and dip symbols in Fig. 2), and second, shortening is transferred from southeast to northwest by left-handed en echelon steps (Fig. 2, 11). The east limb of a northern segment of the anticline flattens at the same latitude as the west limb of the adjacent southern segment, creating an area with relatively flat dips at point "C" (Fig. 11). Presumably, the shortening lost by flattening these limbs is taken up by the west limb of the northern segment, the east limb of the southern segment, and/or adjacent structures.

Large-scale folds are considered detachment folds, rather than fault propagation folds, on the basis of their box-fold geometries, and the lack of significant thrust faults exposed

Figure 10. Kotaneelee Anticline, viewed from the south, showing its steep west limb and shallow east limb. The Liard Range forms the horizon to the east. GSCC 4637-2

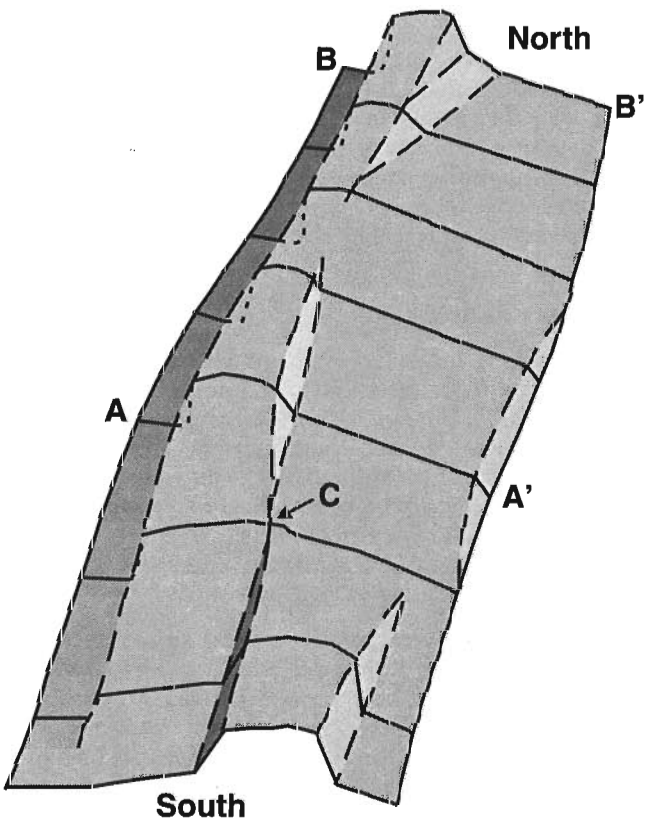

Figure 11. Block diagram showing the geometry of structures that contribute to the sinuous axial trace of the Kotaneelee Anticline. The east limb of a northern segment of the anticline flattens at the same latitude as the west limb of the adjacent southern segment, creating an area with relatively flat dips (point "C").

on the west limbs of the anticlines at surface. Room restrictions in the core of the Kotaneelee Anticline and seismic data strongly suggest it was detached at the base of the Besa River Formation, above the Horn River Formation. A depth to detachment calculation for cross-section A-A', using the method of Epard and Groshong (1993) indicates the detachment is 1660 m below the top of the Besa River Formation. A comparison of this depth with the estimated total thickness of the formation (1500 to 1750 m), leads to the conclusion that in this area a major detachment exists at the base of the Basa River Formation. However, this does not exclude the possibility that older strata may be involved in folding as well; it only limits the depth to which surface structures can be projected downward to obtain accurate fold geometries. Although this structure forms the detachment for the large-scale folds in the map area, seismic data indicate that a deeper detachment controls regional deformation patterns.

La Biche Anticline

The La Biche Anticline extends from approximately 60°N to 61°N, and is separated from the Kotaneelee Anticline to the east by the broad, open La Biche Syncline. Like the Kotaneelee Anticline, it has a box-fold geometry with a series of en echelon anticlinal structures (Fig. 2, 3). Its moderately dipping east limb steepens locally, and has the same kink fold structural style characteristic of all other folds seen in this map area (Fig. 12). Near its axial trace, the west limb of the La Biche Anticline is steep, but it flattens toward the west, before dipping moderately near the axial trace of the Fantasque Syncline (Douglas, 1974).

Faults

Steep, west-directed reverse faults of great lateral extent, and some minor, east-directed thrust faults are shown on Douglas's (1974) reconnaissance maps, but in most cases their existence could not be confirmed by this study, implying that faulting is much less common than previously thought.

Figure 12. La Biche Anticline. Note the box-fold geometry of the steep portion of its east limb. Immediately to the east, the dip of this limb becomes more shallow (view from the south). GSCC 4637-3

North of Kotaneelee Gap, there is a small, near-vertical, west-side-up (possibly reverse) fault near the core of the Kotaneelee Anticline, where Douglas (1974) mapped the Kotaneelee Fault (Fig. 2). It coincides with a monoclinal hinge, separating the near-horizontal top from the steep, overturned west limb of the box fold. The fault has an offset of some 20 m and places Besa River strata onto lower Mattson sandstones. To the south, the Kotaneelee Fault was shown to offset the Besa River Formation-lower Mattson Formation contact (Douglas, 1974), but this could not be confirmed because of a lack of outcrop.

Several west- to west-northwest- striking, near-vertical faults occur locally in the Kotaneelee Anticline. They have very small offsets and are of limited lateral extent. Most of them are either confined to a specific stratigraphic interval or a small portion of the anticline (Fig. 2). It is not possible to determine whether normal or strike-slip movement is predominant on these faults, and there is no systematic pattern of offset sense. The largest vertical offset is estimated at 40 m. These faults are interpreted as adjustment features, which responded to differential movement during the formation of the Kotaneelee Anticline.

One transverse fault was mapped over a distance of 10 km (Fig. 2). It has a northwesterly strike and cuts the core of the Kotaneelee Anticline obliquely. Offsets in the near-vertical west limb of the fold indicate a minor component of strike-slip displacement. This fault has the same orientation as normal faults mapped west of the map area, in the Fantasque Syncline (Douglas, 1974). Southeast of this fault, at the south end of the map area, there is a northeast-verging thrust fault that places Fantasque Formation over Chinkeh and Fantasque formations, and truncates the footwall strata (Fig. 2). Both the thrust fault and the transverse fault line up with a northwesterly striking segment of the La Biche Anticline (Fig. 2). These faults could be associated with a pre-existing pattern of wrench faulting (see below).

DISCUSSION

The alternation of shale and sandstone intervals in the Kotaneelee Anticline facilitated flexural slip-folding and the development of parallel folds. A relatively low amount of shortening in the area has led to generally broad, open-fold geometries.

Numerous possible explanations of the sinuous trace of the Kotaneelee and La Biche anticline and syncline traces have been proposed. Interpretations of surface structures in the northern Franklin Mountains and the Colville Hills suggest a shallow response to deep-seated wrench faults (Cook, 1983). A similar interpretation could be applied to the southern Franklin Mountains. Gabrielse (1966) suggested that in the Mackenzie Mountains, a pre-existing pattern of northeast- and possibly northwest-trending strike-slip faults, overprinted by one prolonged phase of shortening, could have been sufficient to cause the warping of axial planes. Richards (1989) proposed that the sinuous fold geometries could be the result of two phases of deformation, the latter under a transpressional tectonic regime. Alternatively, the folds could have nucleated as separate fold structures with overlapping axial traces that grew into larger amalgamated structures. None of these interpretations can be confirmed or refuted in this study. The question of what caused the warping of axial planes has to be investigated on a more regional scale.

CONCLUSIONS

The 1:50 000-scale geological map of the Babiche Mountain and Chinkeh Creek map areas is in general agreement with Douglas's (1974) 1:250 000-scale map of the La Biche River map area (NTS 95C), with some notable exceptions. Stratigraphic units used by Douglas are reasonable, but do not reflect the observed facies changes, especially in the lower Mattson Formation. We propose that the strata dominated by silty limestones and dolostones at the top of the upper Mattson Formation of Douglas (1974), and herein referred to as the "Tika map unit", be considered an informal mappable unit, until a type-section is found and documented.

The Kotaneelee and La Biche anticline-syncline pairs are detachment box folds that appear to have detached at the base of the Besa River Formation. The structural style that has resulted in their sinuous traces has been documented, but the primary cause of the sinuous axial traces must be investigated on a larger scale. Faulting is less common than previously thought. North-northwest to northwest-striking transverse faults generally have little displacement, but may be genetically linked to the sinuous traces of the Kotaneelee and La Biche anticlines and synclines.

ACKNOWLEDGMENTS

We are grateful to Vaughan Allan and Carol Laws of Husky Oil Operations Ltd. and Allan Bishop of Norcen Resources Ltd. for generously donating the maps and reports prepared by M.R. McDonough and T. Kubli, respectively. L. Currie and D. Hodder would like to thank Barry Richards, of the Geological Survey of Canada, Calgary, for an informative introduction to the stratigraphy of the map area during the field season, and George Fawcett of Deh Cho Helicopters for safe and efficient service. Daniel Lebel and Steve Hinds gave generously of their time to introduce L. Currie to the world of digital cartography. Larry Lane and Barry Richards are thanked for reviewing earlier versions of this paper.

REFERENCES

Bamber, E.W., Taylor, G.C., and Proctor, R.M.
1968: Carboniferous and Permian stratigraphy of northeastern British Columbia; Geological Survey of Canada, Paper 68-15, 25 p.

Chung, P.
1993: Conodont biostratigraphy of the Carboniferous to Permian Kindle, Fantasque, an unnamed, and Beloy formations, western Canada; M.Sc. thesis, University of Calgary, Calgary, Alberta, 189 p.

Cook, D.G.
1983: The northern Franklin Mountains, Northwest Territories, Canada – a scale model of the Wyoming province; in Rocky Mountain Foreland Basins and Uplifts (ed.) J.D. Lowell; Field Conference, Rocky Mountain Association of Geologists, p. 314-338.

Douglas, R.J.W. (comp.)
1974: La Biche River; Geological Survey of Canada, Map 1380A; scale 1:250 000.

Douglas, R.J.W. and Norris, D.K.
1959: Fort Liard and La Biche map-areas, Northwest Territories and Yukon; Geological Survey of Canada Paper 59-6, 23 p.

Epard, J.L. and Groshong, R.H., Jr.
1993: Excess area and depth to detachment; American Association of Petroleum Geologists, Bulletin, v. 77, p. 1291-1302.

Folk, R.L.
1974: Petrology of Sedimentary Rocks; Hemphill Publishing Co., Austin, Texas, 182 p.

Gabrielse, H.
1966: Tectonic evolution of the northern Canadian Cordillera; Canadian Journal of Earth Sciences, v. 4, p. 271-298.

Harker, P.
1963: Carboniferous and Permian Rocks, southern District of Mackenzie; Geological Survey of Canada, Bulletin 95, 91 p.

Henderson, C.M.
1989: Absaroka Sequence – the Lower Absaroka Sequence: Upper Carboniferous and Permian; in Western Canada Sedimentary Basin – a Case History, (ed.) B.D. Ricketts; Canadian Society of Petroleum Geologists, Special Publication No. 30, Calgary, Alberta, p. 203-217.

Leckie, D.A., Potocki, D.J., and Visser, K.
1991: The lower Cretaceous Chinkeh Formation: a frontier-type play in the Liard Basin of Western Canada; American Association of Petroleum Geologists, Bulletin, v. 75, p. 1324-1352.

Patton, W.J.H.
1958: Mississippian succession in South Nahanni River area, Northwest Territories; in Jurassic and Carboniferous of Western Canada (ed.), A.J. Goodman; American Association of Petroleum Geologists, John Andrew Allan Memorial Volume, p. 309-326.

Richards, B.C.
1989: Uppermost Devonian and lower Carboniferous stratigraphy, sedimentation, and diagenesis, southwestern District of Mackenzie and southeastern Yukon Territory; Geological Survey of Canada, Bulletin 390, 135 p.

Richards, B.C., Bamber, E.W., Higgins, A.C., and Utting, J.
1993: Carboniferous; Subchapter 4E in Sedimentary Cover of the Craton in Canada, (ed.) D.F. Stott and J.D. Aitken; Geological Survey of Canda, v. 5, p. 202-271.

Stott, D.F.
1982: Lower Cretaceous Fort St. John Group and upper Cretaceous Dunvegan Formation of the Foothills and plains of Alberta, British Columbia, District of Mackenzie and Yukon Territory; Geological Survey of Canada, Bulletin 328, 124 p.

Geological Survey of Canada Project 850032

The Hoodoo '97 Expedition: probing the ice cap of Hoodoo Mountain volcano, Iskut River region, British Columbia[1]

J.K. Russell[2], M.V. Stasiuk[3], C.J. Hickson, M. Maxwell[4] and B.R. Edwards[2]

GSC Pacific, Vancouver

Russell, J.K., Stasiuk, M.V., Hickson, C.J., Maxwell, M., and Edwards, B.R., 1998: The Hoodoo '97 Expedition: probing the ice cap of Hoodoo Mountain volcano, Iskut River region, British Columbia; in Current Research 1998-A; Geological Survey of Canada, p. 49-54.

Abstract: Hoodoo Mountain volcano is a Quaternary volcano located on the north side of the Iskut River, in the Coast Mountains of northwestern British Columbia. An ice cap, 3-4 km in diameter, covers the summit region of the volcano and obscures the youngest volcanic stratigraphy. In 1995, an Industrial Partners Program project involving the Geological Survey of Canada, Golder Associates Ltd., and several universities, was initiated. The aim of this field-based project was to map the thickness and shape of the ice cap with radar to produce an image of the sub-ice topography of the summit to the volcano. The survey comprised Global Positioning System-controlled traverses across the ice sheet using both ice radar and ground-penetrating radar. The radargrams give clues to the evolution of Hoodoo Mountain volcano and are critical for assessing the nature and magnitude of hazards that would arise from renewed volcanism.

Résumé : Le volcan quaternaire du mont Hoodoo est situé sur la rive nord de la rivière Iskut dans la chaîne Côtière, dans le nord-ouest de la Colombie-Britannique. Une calotte glaciaire de 3-4 km de diamètre recouvre la région sommitale du volcan et masque la stratigraphie volcanique la plus récente. En 1995 a été mis sur pied un projet dans le cadre du Programme des partenaires industriels regroupant la Commission géologique du Canada, la Golder Associates Ltd. et plusieurs universités. L'objectif de ce projet axé sur les travaux de terrain est de cartographier au radar l'épaisseur et la forme de la calotte glaciaire afin d'obtenir une image de la topographie sous-glaciaire du sommet du volcan. Le levé comprend des traverses contrôlées par le Système de positionnement global d'un côté à l'autre de la nappe glaciaire au moyen du glacioradar et du géoradar. Les radargrammes fournissent des indices sur l'évolution du volcan du mont Hoodoo et sont d'importance critique pour l'évaluation de la nature et de la magnitude des dangers qui seraient engendrés par un renouveau du volcanisme.

[1] Research completed under the Industrial Partners Program (IPP) of the Geological Survey of Canada in collaboration with Golder Associates Ltd. and University of British Columbia

[2] Igneous Petrology Laboratory, Geological Sciences Division, Department of Earth and Ocean Sciences, University of British Columbia, 6339 Stores Road, Vancouver, British Columbia V6T 1Z4

[3] Environmental Sciences Division, Lancaster University, United Kingdom

[4] Golder Associates Ltd., #500 - 4260 Still Creek Drive, Burnaby, British Columbia V5C 6C6

INTRODUCTION

Hoodoo Mountain is a phonolitic volcano (Edwards and Russell, 1994; Edwards et al., 1995, 1997; Edwards, 1997) rising to 1850 m elevation on the north side of the Iskut River, in the Coast Mountains of northwestern British Columbia (Fig. 1; Kerr, 1948; Grove, 1986; Souther, 1991a). It has been an active volcano during the last 100 000 years and may have erupted as recently as 9000 years ago (Edwards et al., 1997; Edwards, 1997). Throughout its history, much of the volcanic activity has been subglacial (e.g. Mathews, 1947) and this accounts for its distinctive shape in plan and cross-section views (Fig. 2; Edwards and Russell, 1997a).

At present, the summit region of Hoodoo Mountain is covered by a 3-4 km diameter ice cap that obscures much of the volcanic stratigraphy above 1700 m elevation. Indeed, some of the youngest lava flows found on the slopes of Hoodoo volcano derive from sources that clearly lie beneath the ice (Edwards et al., 1997; Edwards, 1997). There may also be other younger volcanic deposits that are completely covered by the ice sheet (e.g., Gilbert et al., 1996). Another consequence of the ice cap is that the topography of the volcanic

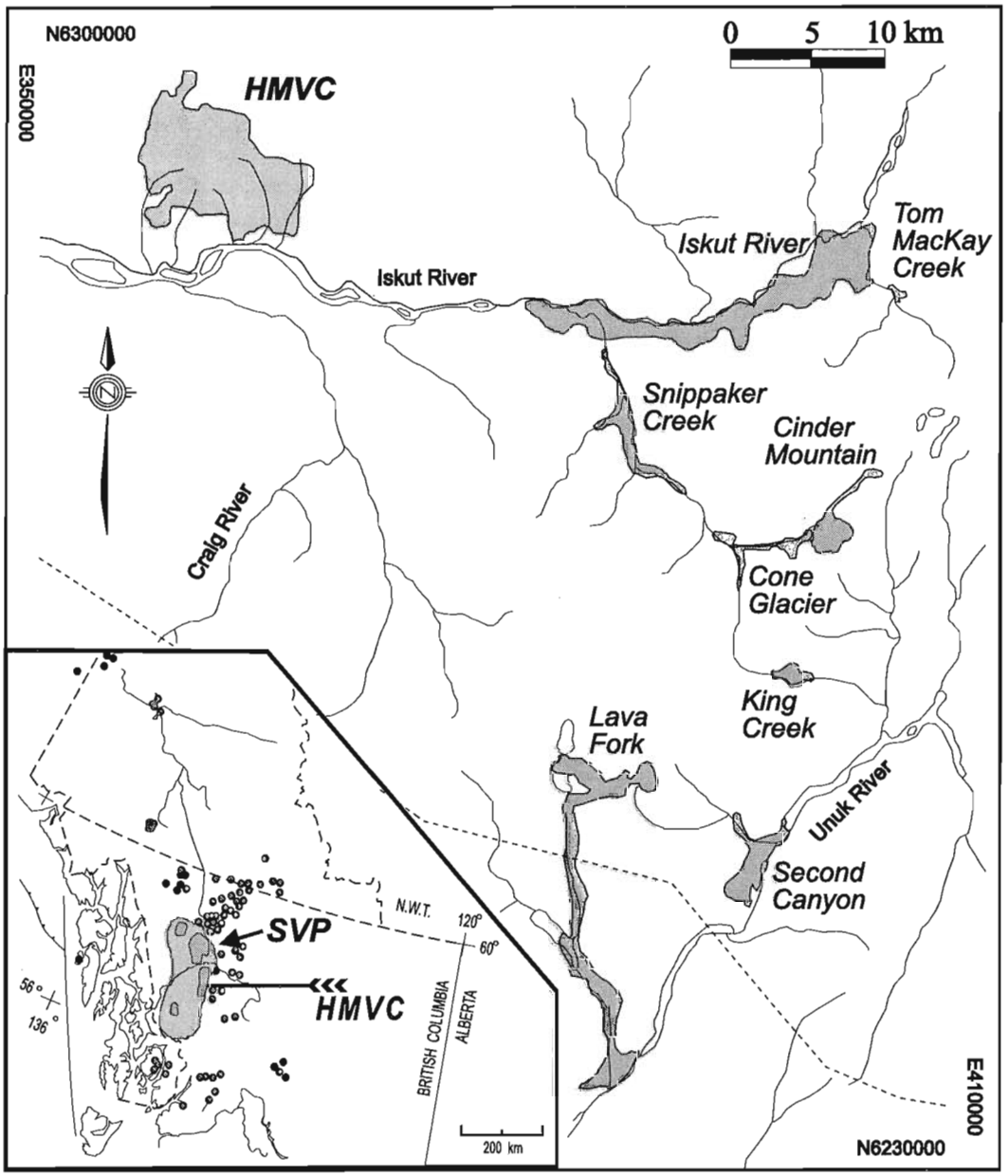

Figure 1. *Location of Hoodoo Mountain volcanic complex (HMVC) and other Quaternary volcanic centres (stippled) along the Iskut and Unuk rivers (modified from Souther, 1991b; Hickson, 1991; Hauksdóttir et al., 1994). Inset shows volcanic centres of the Northern Cordilleran Volcanic Province (Edwards and Russell, 1996; Edwards, 1997). SVP indicates Stikine Volcanic Province.*

summit is unknown. Does the volcano comprise a central caldera, a number of fissure vents, or another structure? These uncertainties represent a lack of scientific information and, perhaps more importantly, they drastically limit our ability to assess the nature and magnitude of the hazard presented by Hoodoo Mountain volcano.

The Hoodoo '97 expedition was aimed at addressing these uncertainties. Specifically, the main objective of the 1997 field season was to map the shape of the ice sheet using radar, and to produce a preliminary hazard assessment for the Iskut River region. The research program involved ten scientists from five different institutions and was funded by an Industrial Partners Program grant. This introductory paper discusses the

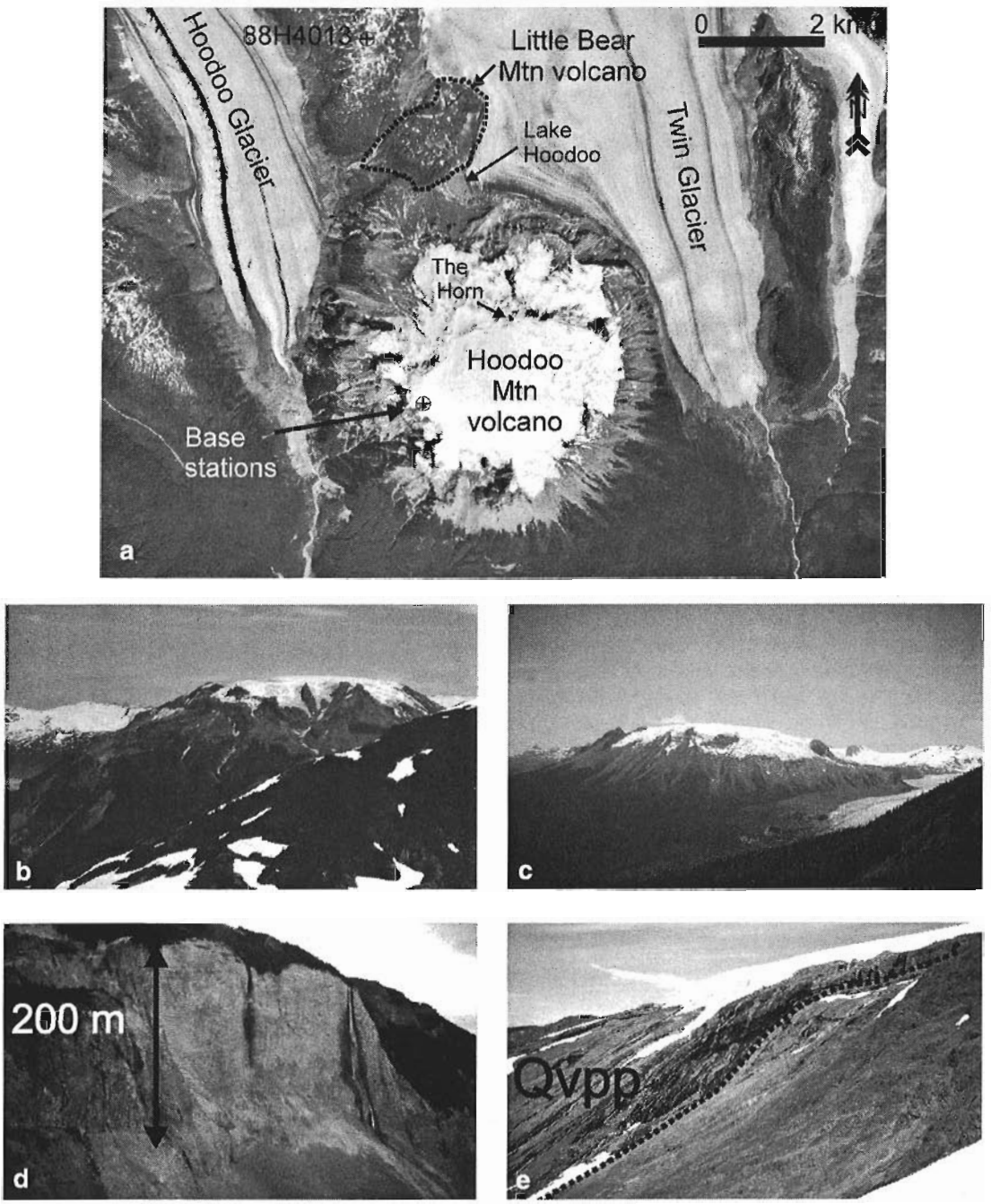

Figure 2. ***a)*** *Aerial photograph of Hoodoo Mountain volcano and surrounding features, including smaller basaltic volcano at Little Bear Mountain, the Hoodoo and Twin valley glaciers, and Lake Hoodoo (airphoto BC82022). Other points include the location of the base camp and GPS base stations, and 'The Horn': a nunatak used for navigation.* ***b, c)*** *The flat topped, steep sided form of Hoodoo Mountain volcano is clearly seen in these photographs.* ***d)*** *The stratigraphy of the volcano is dominated by thick lava flows, such as that shown here.* ***e)*** *The youngest lavas form a thin veneer over the steep slopes of Hoodoo Mountain and appear to derive from vents that are beneath the current ice cap.*

nature and benefits of the IPP partnership, summarizes the physiography and geology of Hoodoo Mountain volcano, and defines the scope of the research program. Preliminary scientific results are presented in detail in two papers in this volume which report on the GPS (Nicholls et al., 1998) and radar surveys (Russell et al., 1998), respectively.

STRUCTURE AND BENEFITS OF THE IPP PROJECT

The Industrial Partners Program (IPP) was initiated by the Geological Survey of Canada in 1992. The intent was to foster cost-shared projects with industry. IPP projects were intended to focus on problems important to the industry partner and to the GSC (e.g. within the GSC mandate). Ideally, these partnerships take advantage of unique skills offered by GSC staff and directly involve the skills and staff of the industry partner in order to break new ground for both partners. The IPP program has now evolved into Co-operative Agreements, though the name has changed, the goals are the same.

The Hoodoo '97 expedition was supported as an IPP between the GSC, the industry partner Golder Associates Ltd., and staff and students from three universities: the University of British Columbia, Lancaster University (England), and the University of Calgary. The project touched a number of scientific or geotechnical subdisciplines of interest to each of the partners. These sub-disciplines included volcanology, glaciology, geophysics, and environmental hazards.

To date, there have been a number of significant benefits to each group of participants. The GSC and Golder Associates Ltd. benefitted from the expertise provided by the university participants. Edwards recently published a detailed geological map for Hoodoo Mountain volcano (Edwards et al., 1997; Edwards, 1997) and provided detailed geology, stratigraphy, and the knowledge of the terrain. Russell and Stasiuk have pioneered the application of ground-penetrating radar to young volcanic deposits (Stasiuk and Russell, 1994; Russell and Stasiuk, 1997, unpub. data; Rust and Russell, unpub. data) and thus provided expertise in volcanology and field-based geophysics. J. Nicholls (University of Calgary) and T. Page (Lancaster University) set up local base stations, processed the GPS data, and produced the final traverse maps which allowed us to tie all radar data by time to GPS-controlled locations. A. Rust (University of British Columbia) provided geophysical expertise.

Monitoring and assessing volcanic hazards is part of the GSC mandate and the project served to advance skills in this area. Radar has not been used previously by the GSC as a tool for exploring volcanic deposits in general and, specifically, for assessing the hazards associated with volcanoes. The effectiveness of radar in this study suggests that it is a useful tool for mapping modern volcanoes and assessing associated hazards. Many of the Quaternary volcanoes distributed throughout the Canadian Cordillera are capped with ice and radar techniques could and should be applied to these other volcanic edifices.

Golder Associates Ltd. is a geophysically oriented geotechnical-environmental-mining engineering company. Much of their consulting success has been due to the diverse techniques they are capable of employing to solve geological and geotechnical problems. The Hoodoo '97 project provided Golder Associates Ltd. with an opportunity to use their expertise in geophysics and radar methodology in a new and complex setting while also learning about the structure of volcanoes and volcanic deposits. Within British Columbia, the need to assess volcanic hazards will continue to grow as resource extraction and population pressures force development of the hinterland.

HOODOO MOUNTAIN VOLCANO

Hoodoo Mountain volcano is situated immediately north of the Iskut River between two prominent valley glaciers, Hoodoo and Twin glaciers (Fig. 2a), and is centred at latitude 56°46'N and longitude 131°17'W (UTM centre 360000E/6295000N). It is located 120 km northwest of Stewart, British Columbia, 30 km east of the confluence of the Stikine and Iskut rivers, and is only accessible by helicopter. Hoodoo Mountain volcano is the most southerly of three large volcanic complexes that constitute the Stikine Subprovince of the Northern Cordilleran Volcanic Province (Edwards and Russell, 1997b; Fig. 1). The maximum total volume of volcanic material at Hoodoo Mountain volcano is 17.3 km^3.

Prior to the recent work by Edwards and Russell (1994, 1997a), Edwards et al. (1995, 1997), and Edwards (1997), only brief, general descriptions of Hoodoo Mountain volcano existed (Kerr, 1948; Souther and Yorath, 1991; Souther, 1991a,b,c). Kerr (1948) first described the units and the stratigraphy of Hoodoo Mountain and recognized three major episodes of volcanic activity: 1) an early episode of subaerial eruption of aphanitic lava flows that were dammed by surrounding glaciers and formed steep cliffs, 2) a subsequent episode of subaerial eruption of porphyritic lava flows, found mainly on the south and east sides of the volcano, and 3) a late-stage subaerial eruption characterized by aa flows that form the top of the volcano. Kerr also recognized a basal grey till underlying the oldest lava series, and interflow pyroclastic deposits. However, the work of Edwards and Russell (1994), Edwards et al. (1995, 1997) provided the first detailed geological map and description of the stratigraphy of the volcano and showed that Kerr's second phase of activity was actually younger than his third phase.

The following is a summary of the volcanology of Hoodoo Mountain volcano based on the detailed 1:20 000 scale geological mapping of Edwards et al. (1997) and the detailed petrographic, geochemical, and stratigraphic descriptions in Edwards (1997). The geology and stratigraphy of Hoodoo Mountain volcano is dominated by thick lava flows (e.g. Fig. 2d), domes, and volcanic breccia. The lavas at Hoodoo Mountain are dominantly pyroxene-bearing phonolites and trachytes. Non-fragmental volcanic deposits are volumetrically more important and predominantly comprise fine- to medium-grained subglacial and subaerial lava flows, domes, spines, and dykes. Aphanitic trachyte and phonolite

constitute more than 75% of the rocks exposed at Hoodoo Mountain. Fragmental units are less abundant and comprise minor pyroclastic and mass flow deposits formed in both subglacial and intraglacial environments (Kerr, 1948; Edwards and Russell, 1994; Edwards et al., 1995, 1997). Pyroclastic flows and falls form a minor portion of the edifice; they occur in the middle of the stratigraphic sequence and are best exposed on the northern side of the volcano (Edwards et al., 1995; Edwards, 1997).

The youngest volcanic deposits found at Hoodoo Mountain are a series of highly porphyritic lava flows, which although volumetrically minor (<10%), cover much of the northwest, south, and east sides of Hoodoo Mountain (Fig. 2e) (Edwards et al., 1997). These lavas form a thin veneer over the steep slopes of Hoodoo Mountain and appear to derive from vents that are beneath the current ice cap (Fig. 2e).

Perhaps the most remarkable feature of Hoodoo Mountain volcano is its geomorphological form (Fig. 2a,b,c); the geology and stratigraphy of the volcano have been dominated for the last 100 ka by processes that reflect that close spatial and temporal association between volcanism and glaciation (Edwards and Russell, 1997a). For example, at least two sets of cliffs (Fig. 2d) between 100 and 200 m in height discontinuously circumscribe the volcano. The cliffs, and an abundance of subglacial volcanic deposits (e.g., hyaloclastite), indicate that Hoodoo Mountain volcano erupted subglacially and that its morphology was controlled by the presence of bounding glacial ice during many of its eruptive episodes.

AGE OF VOLCANISM

Isotopic age constraints for Hoodoo Mountain volcano include conventional whole-rock K-Ar age determinations on five samples collected by J.G. Souther and R.L. Armstrong in 1976 (University of British Columbia Geochron Files) and high precision $^{40}Ar/^{39}Ar$ measurements on ten samples discussed by Edwards (1997) (Villeneuve et al., unpub. data; Edwards et al., unpub. data). The K-Ar ages range from 110 ± 30 ka to 20 ± 13 ka. The utility of the K-Ar ages is difficult to evaluate because the samples are located only at a scale of 1:250 000 and are not well correlated to the present stratigraphy.

In contrast, the $^{40}Ar/^{39}Ar$ age determinations relate directly to the stratigraphy established by Edwards et al. (1997). Finally, minimum ages for the youngest volcanic deposits are constrained by a single ^{14}C date on wood within lacustrine sediments overlying lavas (670 ± 50 BP; Geological Survey of Canada radiocarbon age determination GSC 5868) and by tree ring counts on living trees covering the surface of a young lava flow on the southwest side of Hoodoo Mountain (>180 years; BC Hydro, 1985).

The $^{40}Ar/^{39}Ar$ data establish several key points concerning the age of volcanism at Hoodoo Mountain. Firstly, the oldest volcanic rocks that can be related to Hoodoo Mountain volcano are dykes found cutting the surrounding bedrock; they are 1800 ka in age. The oldest volcanic rocks from Hoodoo Mountain volcano itself are 85 ka; during the last 100 ka there have been at least five episodes of volcanism producing lava flows and pyroclastic deposits (Edwards, 1997). The stratigraphically youngest volcanic deposits are a set of highly porphyritic lavas which derive from the summit region and cover the slopes of the volcano; these lavas erupted over a period of at least 18 000 years, from 9-10 ka to 28 ka. Because the youngest age for the most recent of the porphyritic lavas (Qvpp) is 9 ka, the volcanic edifice must be considered dormant, but potentially active.

OBJECTIVES

Our intent was to use ground-penetrating radar and ice radar to map the shape of the ice sheet covering the summit of Hoodoo Mountain volcano, establish its maximum thickness, and estimate its volume. The mapping was performed with an ice radar unit using an antenna centre frequency of 3 or 8 MHz and a pulse voltage of 1000 V (Russell et al., 1998). Results from these surveys define the sub-ice topography of the volcano and can be used directly to

1. infer the nature of the volcanic edifice and its vents (caldera, fissure, etc.);
2. search for young volcanic deposits beneath the ice cap;
3. determine the hydrogeology of the summit region of the volcano, and;
4. constrain the origin and age of the ice cap.

We also mapped the internal stratigraphy of the ice sheet using a pulseEKKO 100 ground-penetrating radar device. This device employed a 50 MHz antennae and a 1000 V source (Russell et al., 1998). For example, in addition to layering in the firn, there was the distinct possibility of defining layers attributable to accumulations of volcanic ash (e.g. debris or material from past volcanic eruptions) or volcanic-derived aerosols (e.g. Clarke and Cross, 1989). Regardless of their origins, we planned to map some of the layering within the ice sheet with the intent of showing continuities and/or discontinuities in the internal stratigraphy. Results of this survey could be used to identify areas of old and young ice, or identify stratigraphic disruptions that might derive from young thermal events, or define draping structures over young subglacial volcanic deposits.

A Global Positioning System (GPS) was used for two purposes: a) to provide control on the locations of both ice radar and ground-penetrating radar survey lines, and b) to map more precisely the upper surface of the ice cap (Nicholls et al., 1998). GPS data were collected along all radar traverse lines (1 position/second) and serve the dual purposes of fixing the locations of each radar trace and locating the surface of the ice cap. We also implemented several traverses with the sole objective of obtaining precise GPS data across the ice sheet. All GPS data were integrated with data from the relevant digital terrain map to provide a more precise map for the upper surface of the ice sheet (Nicholls et al., 1998). These data could potentially be used to monitor longer term losses and accumulations of ice on the Hoodoo ice cap.

CONCLUSION

The Hoodoo '97 expedition successfully deployed a number of geophysical tools to probe the Hoodoo volcano ice cap. The multidisciplinary approach benefitted all partners in the project. The project proved the effectiveness of radar for penetrating the ice cap and assessing the subglacial topography (Russell et al., 1998). Additionally, GPS provided details of the upper surface of the ice sheet (Nicholls et al., 1998). In completion of this project, new tools and insights into hazard assessment at glacier-covered volcanoes were obtained. This new knowledge will be instrumental for studying other ice-covered volcanoes in the Cordillera and around the world, helping assess the hazard associated with these types of volcanoes.

ACKNOWLEDGMENTS

The original objectives for this field project derived from interactions between J.K. Russell, M.V. Stasiuk and B.R . Edwards while mapping Hoodoo Mountain. Costs of the research were borne mainly by an IPP grant to the Geological Survey of Canada (C.J. Hickson), Golder Associates Ltd. (M. Maxwell), and The University of British Columbia (J.K. Russell). Ancillary costs were covered by NSERC grants (J.K. Russell and J. Nicholls) and a grant from the National Geographic Society. We are indebted to Golder Associates Ltd. and the Geological Survey of Canada for logistical and other in-kind support. We are also grateful to B. Jaworski and Whitegold Resources for helicopter and other logistical support. Our manuscript benefitted from critical review by C. Roots and editorial work by B. Vanlier.

REFERENCES

BC Hydro
1985: Stikine-Iskut development, Iskut Canyon and More Creek Projects, 1982-1984; Geotechnical Investigations, Main Report, Volume 1, Report No. H1614, BC Hydro Information Centre.

Clarke, K.C. and Cross, G.M.
1989: Radar imaging of glaciovolcanic stratigraphy, Mount Wrangell caldera, Alaska: interpretation, model and results; Journal of Geophysical Research, v. 94, p. 7237-7249.

Edwards, B.R.
1997: Field, kinetic and thermodynamic studies of magmatic assimilation in the Northern Cordilleran Volcanic Province, northwestern British Columbia; Ph.D. thesis, University of British Columbia, Vancouver, British Columbia, 316 p.

Edwards, B.R. and Russell, J.K.
1994: Preliminary stratigraphy of Hoodoo Mountain volcano, northwestern British Columbia; in Current Research 1994-A; Geological Survey of Canada, p. 69-76.
1996: An overview of the nature, distribution and tectonic significance of xenoliths from the Stikine Volcanic Belt, northern Cordillera; in 1996 Slave-Northern Cordillera Lithospheric Evolution (SNORCLE) Transect and Cordilleran Tectonics Workshop Meeting (March 1-3), (ed.) F. Cook and P. Erdmer; Lithoprobe Report No. 50, p. 96-107.
1997a: Terrestrial subglacial volcanism: glacial influences on volcanic morphology and eruption products at the Hoodoo Mountain Volcanic Complex, northwestern British Columbia; Geological Society of America, Program with Abstracts 1997, v. 29, p. 6.

Edwards, B.R. and Russell, J.K. (cont.)
1997b: Definition of a new volcanic province in northwestern Canada: the Northern Cordilleran Volcanic Province; Geological Association of Canada - Mineralogical Association of Canada, 1997 Annual Meeting, Program with Abstracts.

Edwards, B.R., Anderson, R.G., and Russell, J.K.
1997: Geology of the Quaternary Hoodoo Mountain Volcanic Complex and adjacent Paleozoic and Mesozoic basement rocks - parts of Hoodoo Mountain (NTS 104 B/14) and Craig River (NTS 104 B/11) map areas, northwestern British Columbia; Geological Survey of Canada, Open File 3321, scale 1:20 000.

Edwards, B.R., Edwards, G., and Russell, J.K.
1995: Revised stratigraphy for the Hoodoo Mountain volcanic centre, northwestern British Columbia; in Current Research 1995-A; Geological Survey of Canada, p. 105-115.

Gilbert, J.S., Stasiuk, M.V., Lane, S.J., Adam, C.R., Murphy, M.D., Sparks, R.S.J., and Naranjo, J.A.
1996: Non-explosive, constructional evolution of the ice-filled caldera at Volcan Sollipulli, Chile; Bulletin of Volcanology, v. 58, p. 67-83.

Grove, E.W.
1986: Geology and mineral deposits of the Unuk River - Salmon River - Anyox Area; British Columbia Ministry of Energy, Mines and Petroleum Resources, Bulletin 63, 152 p.

Hauksdóttir, S., Enegren, E.G., and Russell, J.K.
1994: Recent basaltic volcanism in the Iskut-Unuk rivers area, northwestern British Columbia; in Current Research 1994-A; Geological Survey of Canada, p. 57-68.

Hickson, C.J.
1991: Volcano vent map and table; in Volcanoes of North America, (ed.) C.A. Wood and J. Kienle; Cambridge University Press, New York, p. 116-118.

Kerr, F.A.
1948: Lower Stikine and western Iskut river areas, British Columbia; Geological Survey of Canada, Memoir 246, 94 p.

Mathews, W.H.
1947: Tuyas, flat-topped volcanoes in northern British Columbia; American Journal of Science, v. 245, p. 560-570.

Nicholls, J., Page, T., Schmok, J., Russell, J.K., and Stasiuk, M.V.
1998: Global Positioning System survey of ground-penetrating radar traverses of the ice cap, Hoodoo Mountain, British Columbia; in Current Research 1998-A; Geological Survey of Canada.

Russell, J.K. and Stasiuk, M.V.
1997: Characterization of volcanic deposits with ground penetrating radar; Bulletin of Volcanology, v. 58, p. 515-527.

Russell, J.K., Stasiuk, M.V., Schmok, J., Nicholls, J., Page, T., Rust, A., Cross, G., Edwards, B.R., Hickson, C.J., and Maxwell, M.
1998: The ice cap of Hoodoo Mountain Volcano: Radar estimates of shape and thickness; in Current Research 1998-A, Geological Survey of Canada.

Souther, J.G.
1991a: Volcanic Regimes, in Geology of the Cordilleran Orogen in Canada, (ed.) Gabrielse, H. and Yorath, C.J.; Canada Geological Survey, Geology of Canada, no. 4., p. 457-490 (also Geological Society of America, The Geology of North America, no. G-2).
1991b: Hoodoo; in Volcanoes of North America, (ed.) C.A. Wood and J. Kienle; Cambridge University Press, New York, p. 127-128.
1991c: Iskut-Unuk River cones; in Volcanoes of North America, (ed.) C.A. Wood and J. Kienle; Cambridge University Press, New York, p. 128-129.

Souther, J.G. and Yorath, C.J.
1991: Neogene assemblages; in Geology of the Cordilleran Orogen in Canada, (ed.) H. Gabrielse and C.J. Yorath; Geological Survey of Canada, Geology of Canada, no. 4, p. 373-401. (also Geological Society of America, The Geology of North America, no. G-2).

Stasiuk, M.V. and Russell, J.K.
1994: Preliminary studies of Recent volcanic deposits in southwestern British Columbia using ground penetrating radar; in Current Research 1994-A; Geological Survey of Canada, p. 151-157.

Geological Survey of Canada Project 920008

The ice cap of Hoodoo Mountain volcano, northwestern British Columbia: estimates of shape and thickness from surface radar surveys[1]

J.K. Russell[2], M.V. Stasiuk[3], J. Schmok[4], J. Nicholls[5], T. Page[3], A. Rust[2], G. Cross[4], B.R. Edwards[2], C.J. Hickson, and M. Maxwell[4]
GSC Pacific, Vancouver

Russell, J.K., Stasiuk, M.V., Schmok, J., Nicholls, J., Page, T., Rust, A., Cross, G., Edwards, B.R., Hickson, C.J., and Maxwell, M., 1998: The ice cap of Hoodoo Mountain volcano, northwestern British Columbia: estimates of shape and thickness from surface radar surveys; in Current Research 1998-A; Geological Survey of Canada, p. 55-63.

Abstract: Preliminary results from a multiple-traverse radar survey across an ice cap situated on top of Hoodoo Mountain, a Quaternary subglacial stratovolcano in northwestern British Columbia are presented. The project defined the shape of the ice sheet and mapped the subglacial summit region of the volcano. Four traverses, using low-frequency ice radar and higher frequency ground-penetrating radar units, provided traces of the ice base as well as shallow, finer scale, internal reflectors. GPS was used to locate survey lines and individual radar traces were time tagged to position.

The ice cap has a relatively even thickness (120-150 m) across the summit region, with no evidence of a deep crater or caldera beneath. The minimum volume of ice is estimated at 3.2 km^3. To more accurately gauge the potential for significant jökulhlaups at Hoodoo Mountain, additional work is necessary to define the nature and size of subglacial catchments basins.

Résumé : Sont présentés les résultats préliminaires d'un levé au radar à traverses multiples d'un côté à l'autre d'une calotte glaciaire située au sommet du mont Hoodoo, stratovolcan sous-glaciaire quaternaire dans le nord-ouest de la Colombie-Britannique. Ce projet a permis de définir la forme de la calotte glaciaire et de cartographier la région du sommet sous-glaciaire du volcan. Quatre traverses au moyen d'un glacioradar à basse fréquence et d'un géoradar à fréquence plus élevée ont fourni des indications sur la base de la glace ainsi que sur des réflecteurs internes peu profonds de plus petite échelle. On a utilisé le GPS pour localiser les lignes de levé; les tracés radar individuels ont été localisés au moyen de descripteurs temporels.

La calotte glaciaire est d'épaisseur relativement uniforme (120-150 m) de part et d'autre de la région sommitale, rien n'indiquant la présence dessous d'un cratère ou d'une caldera de grande profondeur. Le volume minimal de glace est estimé à 3,2 km^3. Afin d'évaluer avec plus de précision le potentiel de jokulhlaups importants au mont Hoodoo, il faudra entreprendre des travaux additionnels pour définir la nature et la taille des bassins hydrologiques sous-glaciaires.

[1] Research completed under the Industrial Partners Program (IPP) of the Geological Survey of Canada in collaboration with Golder Associates Ltd., University of British Columbia, and Lancaster University
[2] Igneous Petrology Laboratory, Geological Sciences Division, Department of Earth and Ocean Sciences, University of British Columbia, 6339 Stores Road, Vancouver, British Columbia V6T 1Z4
[3] Environmental Sciences Division, Lancaster University, United Kingdom
[4] Golder Associates Ltd., #500 - 4260 Still Creek Drive, Burnaby, British Columbia V5C 6C6
[5] Department of Geology and Geophysics, University of Calgary, 2500 University Drive N.W., Calgary, Alberta T2N 1N4

INTRODUCTION

Hoodoo Mountain volcano is the largest of ten Quaternary volcanic centres distributed along the Iskut and Unuk rivers in the Coast Mountains of northwestern British Columbia, Canada (cf. Fig. 1 in Russell et al., 1998). It is a long-lived, Quaternary, phonolitic stratovolcano comprising dominantly subglacial lavas and pyroclastic deposits (Kerr, 1948; Grove, 1974, 1986; Souther, 1991a; Edwards and Russell, 1994, 1997; Edwards et al., 1995, 1997; Edwards, 1997). The nine other volcanoes in the region are small-volume centres comprising basaltic lava flows, cinder, and pillowed lavas (Stasiuk and Russell, 1990; Souther, 1991b; Hickson, 1991; Hauksdóttir, 1994; Hauksdóttir et al., 1994).

Hoodoo Mountain volcano has been active during the last 100 ka and may have erupted as recently as 9000 BP (Edwards, 1997; Souther and Armstrong, unpub. University of British Columbia geochronology files). The volcano has a gently rounded summit with a maximum elevation of 1850 m a.s.l. In plan view, the volcano is symmetrical and circular and has a basal diameter of 6 km (Fig. 1). The summit is covered by a 3-4 km diameter ice cap which obscures all volcanic stratigraphy at elevations above 1730 m a.s.l (Fig. 2).

During the 1997 field season we mapped the shape of the ice sheet that caps Hoodoo Mountain volcano with radar in order to deduce the topography of the underlying volcanic summit (e.g. Watts and England, 1976; Clarke and Cross, 1989). This paper reports and interprets radar data for several traverses across the ice cap. Our results define the maximum thickness of ice, the volume of ice, and the sub-ice topography of the volcano.

Our characterization of the ice sheet has two applications. Firstly, the shape of the summit region beneath the ice cap relates directly to the style of the most recent volcanism. For example, these data allow us to look for craters, fissures, or a caldera beneath the ice. Secondly, we can arrive at a quantitative assessment of the hazard posed by melting of the ice sheet during a volcanic eruption (e.g. Bjornsson, 1974; Bjornsson and Einarsson, 1991; Einarsson et al., 1997). Conventional calculations of ice volumes as performed on Cascade volcanoes (e.g. Dreidger and Fountain, 1989; Walder and Dreidger, 1993) are inappropriate because of the cross-sectional shape of the volcano. The radar results clearly delineate the sub-ice topography and can be used to estimate the total volume of the ice sheet. The nature and magnitude of floods induced by renewed volcanism are sensitive to both of these parameters.

RADAR SURVEY

Our program comprised a series of traverses using a low-frequency monopulse radar unit in conjunction with a higher frequency ground-penetrating radar instrument. The scope of our survey, in general, and the locations of all (>20) radar traverses are described in Nicholls et al. (1998). Survey

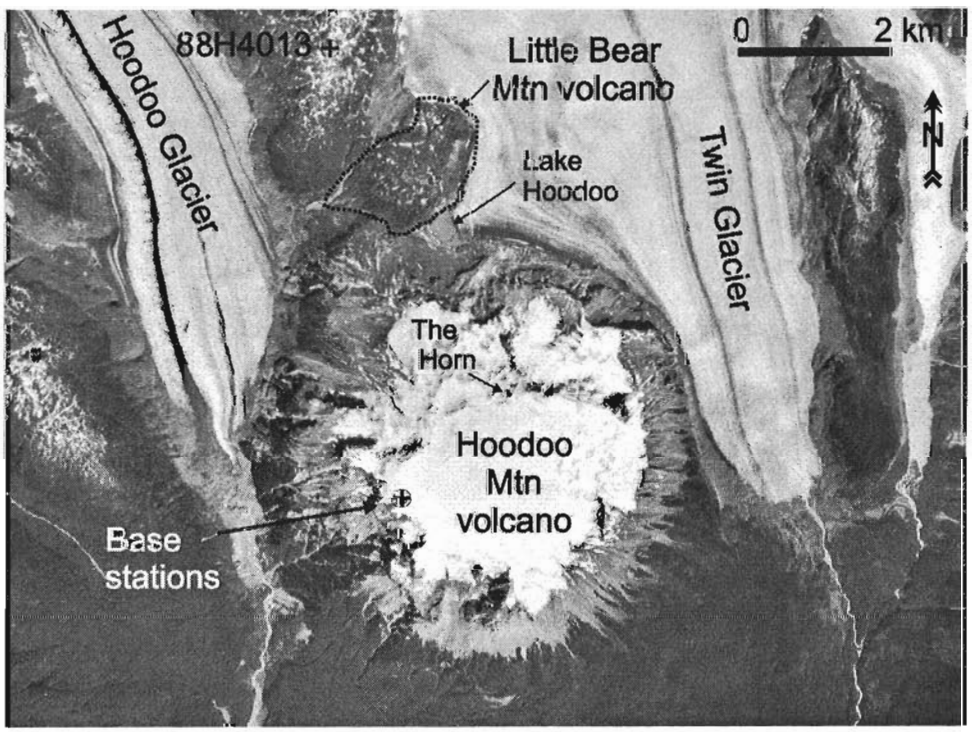

Figure 1. *Aerial photograph of Hoodoo Mountain showing summit ice cap and surrounding ice fields (airphoto BC82022). Also marked are locations of British Columbia horizontal control point, local GPS control point (base stations), and the nunatak which is informally named 'The Horn'.*

parameters pertinent to the 4 traverses described here (Fig. 2) are summarized in Table 1. Both radar devices employed a 1000 V transmitter. Higher frequency (50 MHZ) radar data were collected using a pulseEkko 100A (Sensors & Software Inc.) ground-penetrating radar (GPR) instrument. The majority of radar data were collected using a low-frequency monopulse radar unit that was originally designed and built at the University of British Columbia by researchers in glaciology. Lower frequency (3 or 8 MHz) monopulse radar data were collected in step and free mode.

Both radar surveys were located using a Global Positioning System tied in to two local control points established on Hoodoo Mountain (Fig. 1; Nicholls et al., 1998). Specifically, we controlled the differential position of each radar unit during the traverse by dragging a rover unit on each sled. Post-processing the radar data for position involved matching time tags between the radar trace of interest and the position recorded by the GPS unit (1 position/second). Our preliminary results use a mean radar velocity in ice of 0.16 m/ns to convert 2-way travel-times to depth.

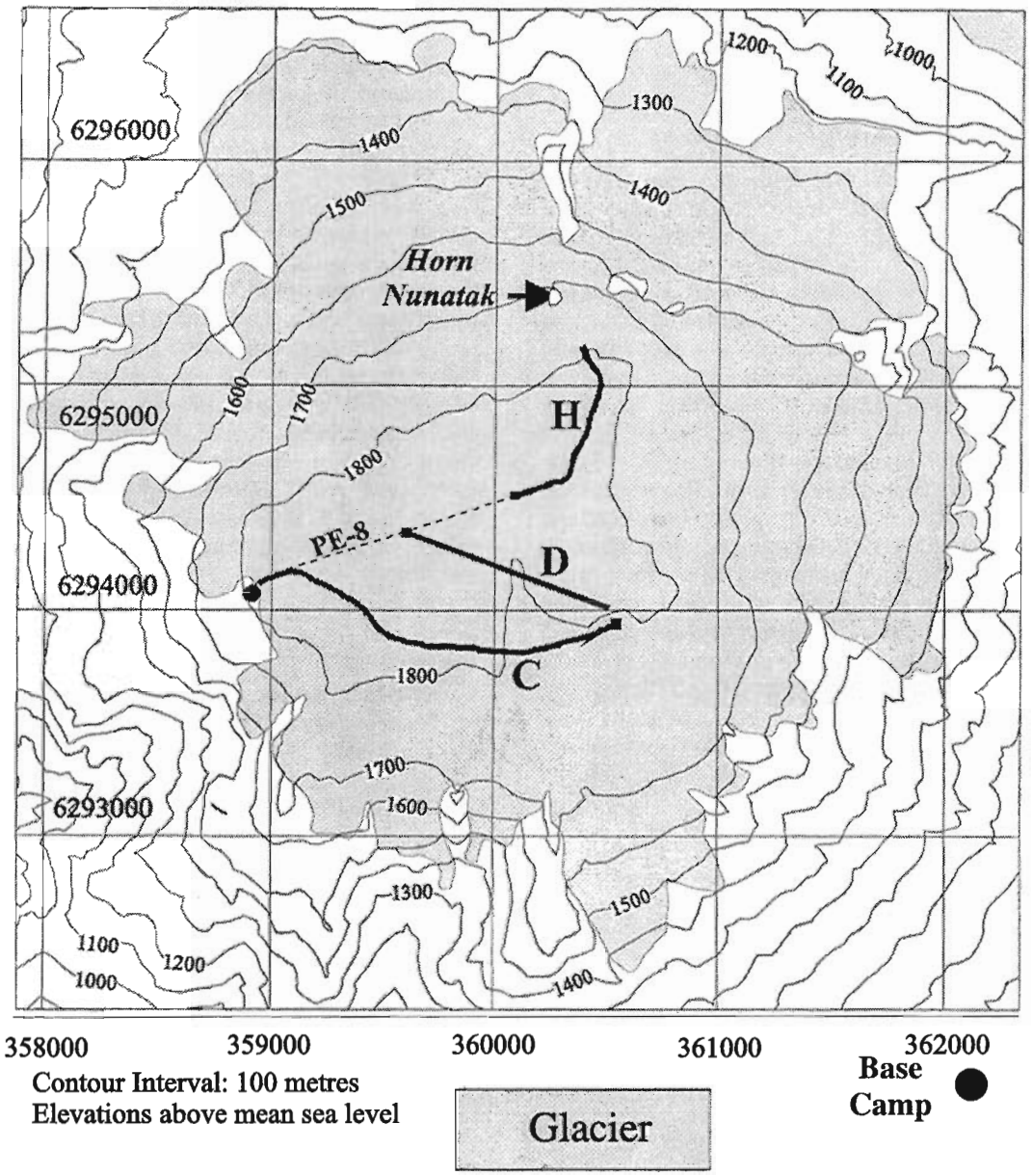

Figure 2. *Geographic positions of radar traverses (Table 1) as located by GPS (Nicholls et al., 1998). PulseEkko traverse (PE-8) went from the base camp to the 'Horn' nunatak. Monopulse radar surveys include traverses C, D, and H; the H traverse is coincident with the eastern end of PE-8.*

Table 1. List of survey parameters pertinent to radar traverses, including time window (TW), total traces collected (N), sampling interval (SI) and total length of traverse (L).

Line	Radar Device	TW (ns)	Stacks	Mode	N	SI (m)	L (m)	Description
PE-8	pulseEkko 100A	2000	128	Step	737	2-4	904	W-E; from base camp to the Horn
C	monopulse*	4096	8	Free	198	8-10	1870	E-W; across southern edge of ice cap
D	monopulse*	4096	8	Step	46	20-27	1106	NW-SE; across centre of ice cap
H	monopulse*	4096	8	Step	59	25-30	1574	W-E; from centre of ice cap to the Horn
* 1000 V transmitter designed by B. Narod and G.K. Clarke at University of British Columbia.								

RESULTS

Traverse PE-8: ground-penetrating radar

We present here a radargram for a single traverse completed with the pulseEkko radar device using 50 MHz antennas. The traverse ran from the eastern edge of the ice cap near the base camp to the northeast portion of the ice cap and ended several hundred metres south of the 'Horn' (Fig. 2), a prominent nunatak. Results from the traverse are shown as a series of radargrams in Figure 3. The radar data are topographically corrected; thus, the first amplitude (direct wave) on each trace also maps the shape of the surface of the ice sheet. The highest elevation on the traverse was 1838 m and the lowest point was 1770 m, where the traverse was descending to the Horn. The deepest reflectors found in this data set, using a conservative gain, are discontinuous and are located at between 40 and 50 m. Most of the continuous reflectors seen are subparallel to the surface and are situated in the upper 25 m of ice. In the westernmost part of the survey these reflectors intersect the ice cap surface. The continuous reflectors probably represent snow and firn stratigraphy, possibly corresponding to layers of dirt separating annual accumulations (e.g. Paren and Robin, 1975). Because of the limited depths of penetration, the pulseEkko device with 50 MHz antennas is most useful for exploring the margins of the ice sheet and elucidating shallow internal ice structures.

Traverse C: southern flank of the dome

Traverse C crossed the southern edge of the ice cap (Fig. 2) and ended about 100 m from the western edge of the ice cap. The traverse was more than 1.8 km long and the data were collected in free mode (Table 1); a trace was collected approximately every 8-10 m. The topographically corrected radargram for Traverse C is shown in Figure 4i. The two most prominent features seen in the radar section are the surface of the ice, which shows a slight rise to the east, and a flat, continuous reflector between depths of 100 and 150 m. We interpret this reflector as the base of the ice sheet. The reflector could represent either an ice-rock interface or a contact between the overlying ice and water pooled in topographic lows in the underlying volcanic rocks. Both geometries can be expected to generate consistently strong reflectors and further work is required to determine which is the best explanation. Regardless, the radar data establishes the thickness of the ice and puts constraints on the shape of the volcanic summit. The results show the ice cap to be a maximum of 125 m thick at this location. Over the majority of the section, the ice is of uniform thickness and there are no obvious discontinuities in the contact between the base of the ice and the underlying volcanic rock. The ice sheet thins slightly to the west to approximately 100 m (position 1500 m), before the reflector is lost. Two parts of the radargram are characterized by an unexpected series of short, discontinuous, strong reflections that mask the base of the ice. These occur between 800 and 1100 m along the traverse and in the last 250 m (west end) of the radargram. We interpret these as real, albeit enigmatic, reflectors whose origin and exact nature are yet to be determined. These reflections may derive from out-of-plane features or irregular geometries of reflectors and may turn out to be a characteristic feature of the Hoodoo Mountain volcano ice sheet.

Traverse D: centre of the dome

Traverse D crossed the summit of the ice cap from northwest to southeast (Fig. 2). The traverse was oriented to transect the topographically highest part of the dome (1855+ m), which was predicted to correspond with the thickest part of the ice cap. The traverse was just over 1 km in length and the data were collected in step mode; the traverse comprised a total of 46 traces collected every 20-27 m (Table 1). The corresponding radargram (Fig. 4ii) reveals the same features as described for Traverse C. The radargram shows the topographically corrected surface and a set of deeper reflectors that define a discontinuous horizon that approximates the base of the ice sheet. This horizon is extremely planar at this scale and has a maximum depth of 145 m beneath the peak of the dome (position 450 m). The ice thickness thins slightly toward each end of the traverse (≈120 m).

Traverse H: dome centre to the Horn

Traverse H extended northward 1.5 km from the centre of the dome and ended 218 m southeast of the Horn (Fig. 2); it exactly followed the eastern portion of the 50 MHz survey (PE-8). The radar data were collected in step mode using a

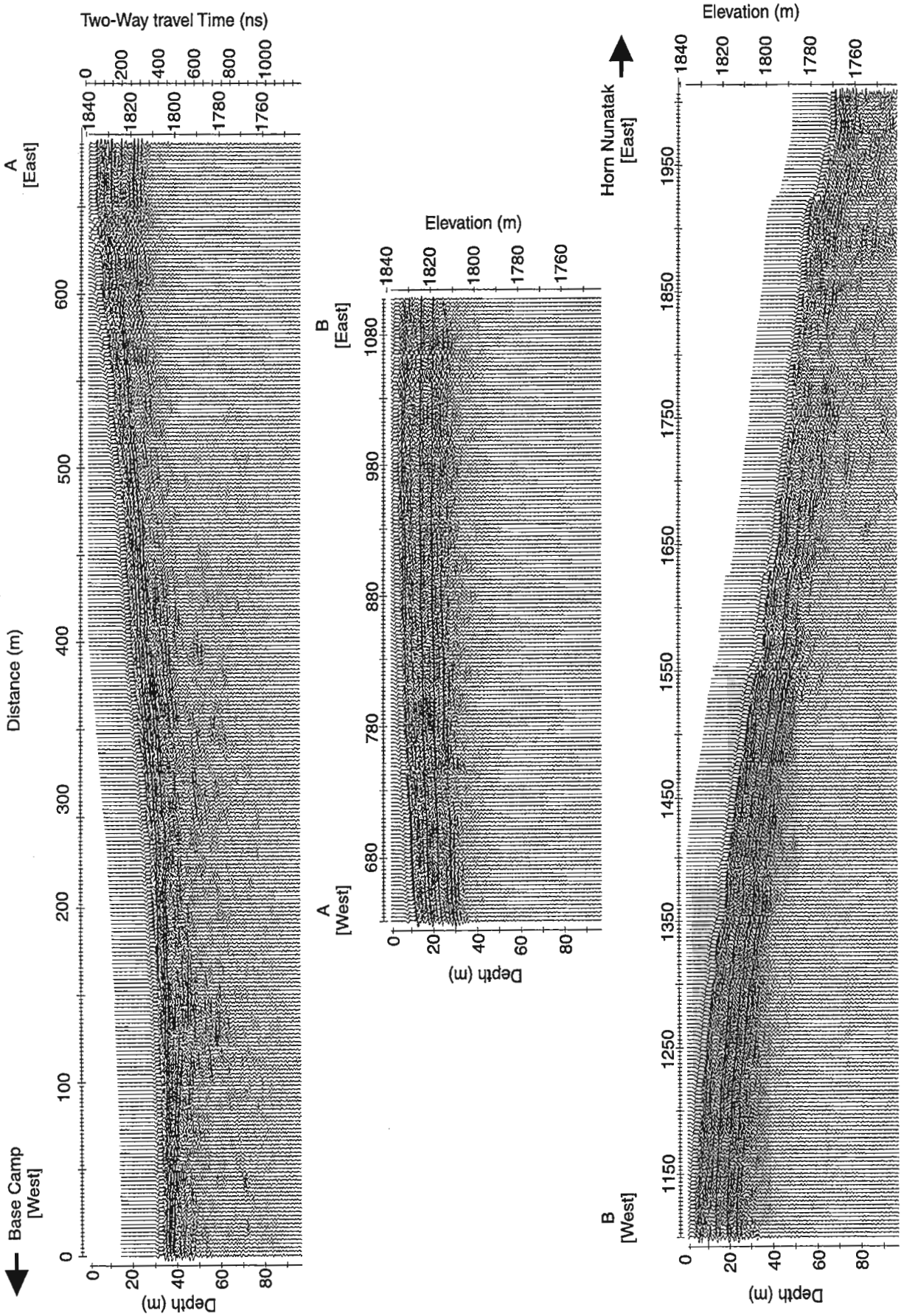

Figure 3. *Results of pulseEkko survey (Table 1) shown as topographically corrected radargrams. Three panels constitute one continuous (west to east) traverse from Base Camp to the 'Horn' nunatak (Fig. 2). The 50 MHz antennas did not image the ice-bedrock interface but results show the character of shallow (20-40 m) reflectors within the ice sheet.*

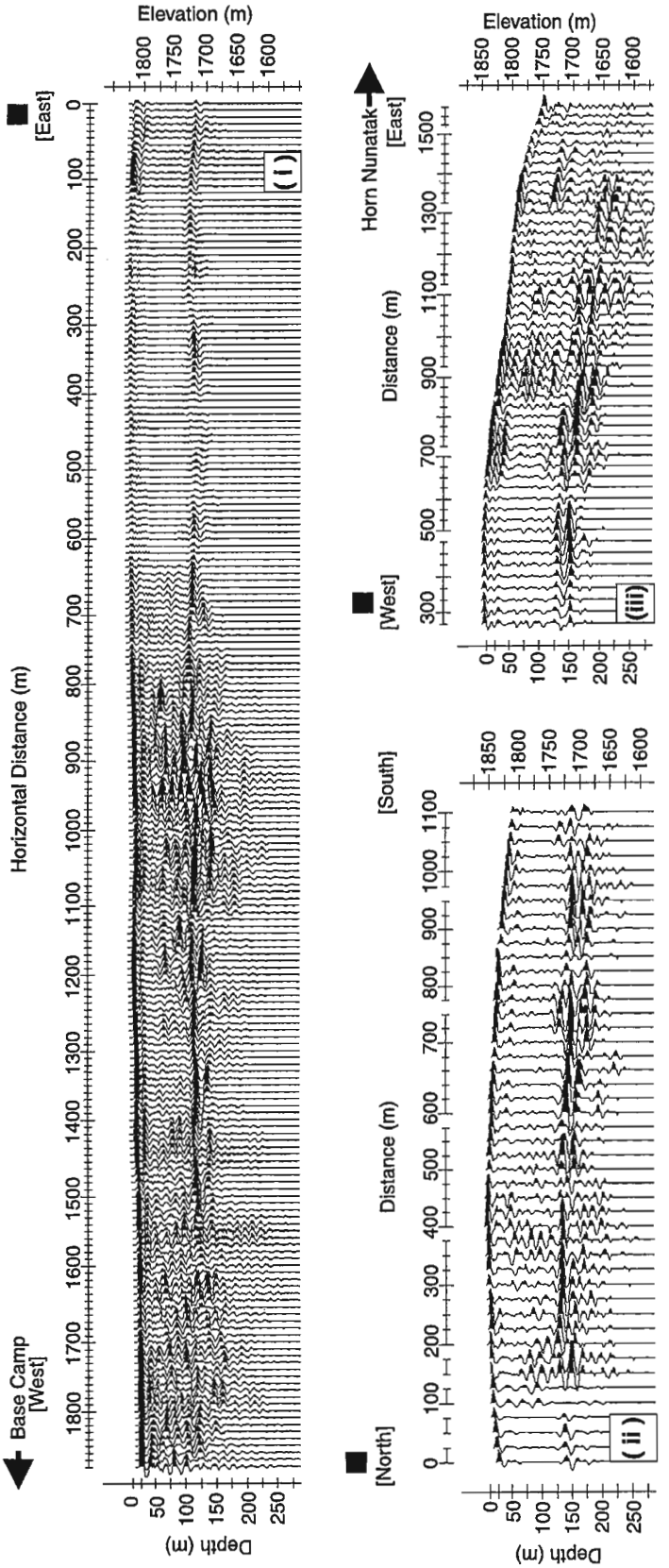

Figure 4. *Results of monopulse radar traverses (Fig. 2) shown as topographically corrected radargrams: **i)** results of traverse C showing depth of ice (100-125 m) in middle southern portion of ice cap, **ii)** traverse D shows north-south profile of ice sheet with depths of ice between 125-150 m, and **iii)** traverse H which overlaps pulseEkko traverse (PE-8) and shows ice thicknesses of 125-150 m. All two-way travel-times for radar data have been converted to depth using a velocity of 0.16 m/ns. See Table 1 for other parameters.*

sample interval of 25-30 m (Table 1) and are shown in Figure 4iii. The ice surface slopes to the east. We interpret a set of strong reflections at depths of 125-150 m (Positions 0-300 m) as the base of the ice. This interface appears to be fairly continuous across the radargram, although it shows two discontinuities across the radargram. The reflector is parallel to the ice surface, implying that the ice has a uniform thickness. The deep reflector representing the base of the ice disappears from position 1400 m onwards. As discussed briefly above, the shallow (50-100 m), discontinuous reflections between positions 850 and 1050 m are interpreted as real but are, as yet, unexplained.

Analysis of data

Prior to this survey, there was no reliable estimate of ice thickness for the Hoodoo Mountain ice cap. The volcano has a distinctive and somewhat anomalous shape (cf. Fig. 2a, b, c, in Russell et al., 1998) that precludes using the methods used to estimate ice accumulations on Cascade volcanoes (e.g. Walder and Dreidger, 1993). Based on these preliminary data, we are able to make several key observations on the ice cap that relate to the volcanic history and evolution of Hoodoo Mountain and its potential as a volcanic hazard. Clearly, as we process data from other radar traverses (cf. Nicholls et al., 1998), there will be refinements to this analysis.

Firstly, the ice cap appears to be no more than about 150 m in thickness. Across the summit of the ice sheet, the ice appears to have a constant thickness, varying from 125-150 m. Furthermore, excluding the marginal areas of the ice cap, the thickness of the ice sheet remains fairly constant and varies only from 100-150 m.

These results delineate the shape of the volcano. The summit region of Hoodoo Mountain is remarkably flat; there is no evidence of a caldera or any substantial craters and, at best, the summit region shows the topography of an inverted and very shallow saucer. Finally, based on an average ice thickness of 125 m distributed conservatively over a circular area with a 900 m radius, we calculate a minimum volume of ice of 3.2 km^3.

DISCUSSION: HAZARD FROM RENEWED VOLCANISM AT HOODOO MOUNTAIN

There are a number of hazards associated with volcanic eruptions. These include the effects of volcanic ash on aircraft (e.g. Mount Redoubt), the filling, damming, and flooding of drainages by volcanic material (e.g. Mount Meager volcanic complex), or the loss of life and local habitat due to pyroclastic flows (e.g. Mount St. Helens) and lahars (e.g. Nevado del Ruiz), to name but a few. Below, we present preliminary ideas on what is perhaps the greatest hazard posed by renewed volcanism at Hoodoo Mountain volcano: large-scale, rapid melting of the ice cap and subsequent flooding of the Iskut drainage.

Assessing the nature and magnitude of hazards posed by this volcanic edifice to the Iskut River region is important because of recent and future economic developments in the area. The region has been evaluated by BC Hydro for its hydroelectric potential and is viewed very favourably. In this region of high relief, relatively small dams can generate bodies of water with substantial head. There are currently several producing gold mines along the south side of the Iskut River, and an air-strip used continuously to ship concentrate. There is also a prospective industrial minerals (wollastonite) operation centred on Zippa Mountain. Lastly, the region is rich in timber and there is a large salmon fishery associated with the Iskut River and tributary streams in the vicinity of Hoodoo Mountain volcano.

Catastrophic floods associated with subglacial volcanic eruptions are relatively common events in Iceland; Grimsvotn is a subglacial volcano entirely covered by Vanajokull glacier (400-600 m thick). A subglacial eruption in late 1996 lasted only a few weeks, but produced 0.6-0.7 km^3 of hyaloclastite (0.4 km^3 of solid rock), melted enough of the ice cap to fill Grimsvotn caldera with water and culminated in a glacial outburst flood (jökulhlaup). The jökulhlaup discharged approximately 3 km^3 of ash-laden water from beneath Vatnajokull Glacier. The flood travelled several kilometres downstream to the coast, then streamed 35 km out into the ocean (Einarsson et al., 1997). Estimated flow rates for the jökulhlaup started at 6000 m^3/s, peaked at 45 000 m^3/s and declined to about 15 000 m^3/s (H. Torfason, Report to Global Volcanism Network, posted in VOLCANO ListServ, November 6, 1996.).

The youngest volcanic activity at Hoodoo Mountain is represented by numerous highly porphyritic lava flows. These flows form a thin veneer over the steep slopes of Hoodoo Mountain and probably originated at one or more vents beneath the current ice cap (Edwards, 1997; Russell et al., 1998). Volumetrically, the exposed portions of the lava flows constitute between 1 and 2 km^3 of material and a substantial volume is likely buried. A repeat of this kind of volcanism in the summit area may melt significant portions of the ice cap, releasing substantial volumes of water into the Iskut drainage. Furthermore, the proximity and positions of two valley glaciers (Fig. 1) increases the volume of water that would be produced in such an eruption. For example, lavas could easily flow down slope to pond against or burrow under Twin and Hoodoo glaciers (e.g., Edwards, 1997; Edwards et al., 1997).

Our work shows the potential for a jökulhlaup event is diminished. Unlike the caldera at Grimsvotn, there appears to be no large-scale depression at Hoodoo Mountain volcano to fill with meltwater before producing substantial volumes of water. At Grimsvotn, the caldera serves as a catchment to allow the melted glacier water to pond to a critical volume. At this point, portions of the ice cap that blocked local drainages are floated and there is a rapid, near-instantaneous release of large volumes of ponded meltwater and sediment. Our preliminary results at Hoodoo Mountain reveal a relatively uniform thickness of ice and little sub-ice topography. There are no obvious large-scale depressions to serve as a catchment. Renewed volcanism, leading to rapid melting of the ice cap

could cause substantial flooding. However, in order to generate catastrophic flooding (e.g. Grimsvotn eruption in 1996), Hoodoo Mountain volcano must have a sufficiently large volcanic eruption to melt most of the ice cap in a period of days.

CONCLUSIONS

During the 1997 field season, we collected radar data with which to map the shape of the Hoodoo Mountain volcano ice cap as part of an Industrial Partners Program project between the Geological Survey of Canada, Golder Associates Ltd., and several universities. Our preliminary results show the ice sheet is up to 150 m thick and more or less uniform in thickness across the summit region. The volcano appears to be flat topped or tuya shaped (Mathews, 1947) and our preliminary results show no evidence for a caldera or large craters beneath the ice. These data represent a small portion of the total data collected, and when we have processed all traverse data (Nicholls et al., 1998), we will more accurately define the nature and size of subglacial basins or catchments at Hoodoo Mountain volcano.

Radar surveys have been useful for exploring modern volcanic deposits (Stasiuk and Russell, 1994; Russell and Stasiuk, 1997, unpub. data) and volcanic landforms (e.g. Clarke and Cross, 1989; Gilbert et al., 1996; Russell and Stasiuk, 1997), in general. They will become an important component of studies of past, present, and future volcanic hazards. It seems only prudent to consider similar studies of ice caps on other major Quaternary Cordilleran volcanoes (e.g. Edziza, Silverthrone, Garibaldi area) in order to fully document their potential hazards.

ACKNOWLEDGMENTS

This field program was funded through an Industrial Partnership Program grant between the Geological Survey of Canada (C.J. Hickson) and Golder Associates Ltd. (J. Schmok, M. Maxwell, and G.Cross). Ancillary costs were covered by NSERC Research grants to J.K. Russell and J. Nicholls and a grant from the National Geographic Society held by J. Nicholls. We are indebted to Golder Associates Ltd. and the Geological Survey of Canada for logistical and other in-kind support. B. Jaworski and Whitegold Resources also contributed helicopter and other logistical support. Data acquisition and processing were greatly facilitated by access to programs of G.K. Clarke of the University of British Columbia. We appreciate greatly the work of C. Roots in critically reading and editing an earlier version of the manuscript. Any further inconsistencies in presentation and interpretation remain the responsibility of the authors.

REFERENCES

Bjornsson, H.
1974: Explanation of jokulhlaups from Grimsvotn, Vatnajokull, Iceland; Jokull, v. 24, p. 1-24.

Bjornsson, H. and Einarsson, P.
1991: Volcanoes beneath Vatnajokull, Iceland: Evidence from radio echo-sounding, earthquakes and jokulhlaups; Jokull, v. 40, p. 147-168.

Clarke, G.K. and Cross, G.M.
1989: Radar imaging of glaciovolcanic stratigraphy, Mount Wrangell caldera, Alaska: Interpretation, model and results; Journal of Geophysical Research, v. 94, p. 7237-7249.

Dreidger, C. and Fountain, A.G.
1989: Glacier outburst floods at Mount Rainier, Washington State, U.S.A; Annals of Glaciology, v. 13, p. 51-55.

Edwards, B.R.
1997: Field, kinetic and thermodynamic studies of magmatic assimilation in the Northern Cordilleran Volcanic Province, northwestern British Columbia; Ph.D. thesis, University of British Columbia, Vancouver, British Columbia, 316 p.

Edwards, B.R. and Russell, J.K.
1994: Preliminary stratigraphy of Hoodoo Mountain volcano, northwestern B.C.; in Current Research 1994-A; Geological Survey of Canada, p. 69-76.
1997: Terrestrial subglacial volcanism: glacial influences on volcanic morphology and eruption products at the Hoodoo Mountain Volcanic Complex, northwestern British Columbia; Geological Society of America, Program with Abstracts 1997, v. 29, No. 6.

Edwards, B.R., Anderson, R.G., and Russell, J.K.
1997: Geology of the Quaternary Hoodoo Mountain Volcanic Complex and adjacent Paleozoic and Mesozoic basement rocks – parts of Hoodoo Mountain (NTS 104B/14) and Craig River (NTS 104B/11) map areas; northwestern British Columbia; Geological Survey of Canada, Open File 3321.

Edwards, B.R., Edwards, G., and Russell, J.K.
1995: Revised stratigraphy for the Hoodoo Mountain volcanic centre, northwestern British Columbia; in Current Research 1995-A; Geological Survey of Canada, p. 105-115.

Einarsson, P., Brandsdottir, B., Gudmundsson, M., Bjornsson, H., and Grinvold, K.
1997: Center of the Iceland hotspot experiences volcanic unrest; EOS, Transactions, American Geophysical Union, v. 78, 369-375.

Gilbert, J.S., Stasiuk, M.V., Lane, S.J., Adam, C.R., Murphy, M.D., Sparks, R.S.J., and Naranjo, J.A.
1996: Non-explosive, constructional evolution of the ice-filled caldera at Volcan Sollipulli, Chile; Bulletin of Volcanology, v. 58, p. 67-83.

Grove, E.W.
1974: Deglaciation – a possible triggering mechanism for Recent volcanism; in International Association of Volcanology and Chemistry of the Earth's Interior, Proceedings of the Symposium on Andean and Antarctic Volcanology Problems, Santiago, Chile, September 1974, p. 88-97.
1986: Geology and mineral deposits of the Unuk River – Salmon River – Anyox Area; British Columbia Ministry of Energy, Mines and Petroleum Resources, Bulletin 63, 152 p.

Hauksdóttir, S.
1994: Petrography, geochemistry and petrogenesis of the Iskut-Unuk rivers volcanic centres, northwestern British Columbia; M.Sc. thesis, University of British Columbia, Vancouver, British Columbia, 253 p.

Hauksdóttir, S., Enegren, E.G., and Russell, J.K.
1994: Recent basaltic volcanism in the Iskut-Unuk rivers area, northwestern British Columbia; in Current Research 1994-A; Geological Survey of Canada, p. 57-67.

Hickson, C.J.
1991: Volcano vent map and table; in Volcanoes of North America, (ed.) C.A. Wood and J. Kienle; Cambridge University Press, New York, p. 116-118.

Kerr, F.A.
1948: Lower Stikine and western Iskut river areas, British Columbia; Geological Survey of Canada, Memoir 246, 94 p.

Mathews, W.H.
1947: Tuyas, flat-topped volcanoes in northern British Columbia; American Journal of Science, v. 245, p. 560-570.

Nicholls, J., Page, T., Schmok, J., Russell, J.K., and Stasiuk, M.V.
1998: Global Positioning System survey of ground-penetrating radar traverses of the ice cap, Hoodoo Mountain, British Columbia; in Current Research 1998-A; Geological Survey of Canada.

Paren, J.G. and Robin, G. de Q.
1975: Internal reflections in polar ice sheets; Journal of Glaciology, v. 14, p. 251-259.

Russell, J.K. and Stasiuk, M.V.
1997: Characterization of volcanic deposits with ground penetrating radar; Bulletin of Volcanology, v. 58, p. 515-527.

Russell, J.K., Stasiuk, M.V., Hickson, C.J., Maxwell, M., and Edwards, B.R.
1998: The Hoodoo '97 Expedition: Probing the ice cap of Hoodoo Mountain volcano, Iskut River region, British Columbia; in Current Research 1998-A; Geological Survey of Canada.

Souther, J.G.
1991a: Hoodoo; in Volcanoes of North America, (ed.) C.A. Wood and J. Kienle; Cambridge University Press, New York, p. 127-128.
1991b: Iskut-Unuk River cones; in Volcanoes of North America, (ed.) C.A. Wood and J. Kienle; Cambridge University Press, New York, p. 128-129.

Stasiuk, M.V. and Russell, J.K.
1990: Quaternary volcanic rocks of the Iskut River region, northwestern British Columbia; in Current Research, Part E; Geological Survey of Canada, Paper 90-1E, p. 153-157.
1994: Preliminary studies of Recent volcanic deposits in southwestern British Columbia using ground penetrating radar; in Current Research 1994-A; Geological Survey of Canada, p. 151-157.

Walder, J. and Dreidger, C.
1993: Glacier-generated debris flows at Mount Rainier; United States Geological Survey, Open File Report 93-124.

Watts, R.D. and England, A.E.
1976: Radio-echo sounding of temperate glaciers: ice properties and sounder design criteria; Journal of Glaciology, v. 17, p. 39-48.

Geological Survey of Canada Project 920008

Global Positioning System survey of ground-penetrating radar traverses of the ice cap, Hoodoo Mountain, British Columbia[1]

J. Nicholls[2], T. Page[3], J. Schmok[4], J.K. Russell[5], and M.V. Stasiuk[3]
GSC Pacific, Vancouver

Nicholls, J., Page, T., Schmok, J., Russell, J.K., and Stasiuk, M.V., 1998: Global Positioning System survey of ground-penetrating radar traverses of the ice cap, Hoodoo Mountain, British Columbia; in Current Research 1998-A; Geological Survey of Canada, p. 65-68.

Abstract: Three single-frequency GPS instruments were used to provide horizontal and vertical control for radar surveys of the ice cap on Hoodoo Mountain, British Columbia. Survey control was established by locating two survey control markers on a moraine at the edge of the ice cap. The survey control markers were located relative to a B.C. Government horizontal control point approximately 6 km from the new survey control markers on Hoodoo Mountain. Vertical adjustment to height above the ellipsoid was accomplished by comparing survey control-marker data on Hoodoo Mountain with GPS data collected by the British Columbia Active Control System (BC ACS) station at Dease Lake.

Résumé : Trois instruments GPS à fréquence unique ont été utilisés afin d'obtenir un contrôle altimétrique et planimétrique pour des levés radar de la calotte glaciaire sur le mont Hoodoo, en Colombie-Britannique. L'établissement de levés a été assuré par l'implantation de deux marqueurs repères sur une moraine en bordure de la calotte glaciaire. Ces marqueurs ont été localisés relativement à un point géodésique du gouvernement de la Colombie-Britannique situé à quelque 6 km des nouveaux marqueurs repères sur le mont Hoodoo. L'ajustement vertical par rapport à la hauteur au-dessus de l'ellipsoïde a été obtenu en comparant les données fournies par les marqueurs repères sur le mont Hoodoo aux données GPS recueillies par la station du British Columbia Active Control System à Dease Lake.

[1] Research completed under the Industrial Partners Program (IPP) of the Geological Survey of Canada in collaboration with Golder Associates Ltd., and University of British Columbia.
[2] Department of Geology and Geophysics, University of Calgary, 2500 University Drive N.W., Calgary, Alberta T2N 1N4
[3] Environmental Sciences Division, Lancaster University, United Kingdom
[4] Golder Associates Ltd., #500 - 4260 Still Creek Drive, Burnaby, British Columbia V5C 6C6
[5] Igneous Petrology Laboratory, Geological Sciences Division, Department of Earth and Ocean Sciences, University of British Columbia, 6339 Stores Rd., Vancouver, British Columbia V6T 1Z4

INTRODUCTION

Global Positioning System (GPS) surveys are capable of providing accurate geographic locations. GPS instruments are an advantage for surveys in remote areas where precise locations for instrumental surveys are needed. Three single-frequency GPS instruments, ProXL models manufactured by Trimble Navigation, Ltd., provided locations for the radar surveys of the Hoodoo '97 Expedition. One instrument was used as a base station and the other two instruments accompanied the radar equipment. Differential corrections were made with Pathfinder Office™ software provided by Trimble Navigation, Ltd. The objectives of the GPS surveys were to provide locations for the radar surveys and to provide elevations of the ice cap.

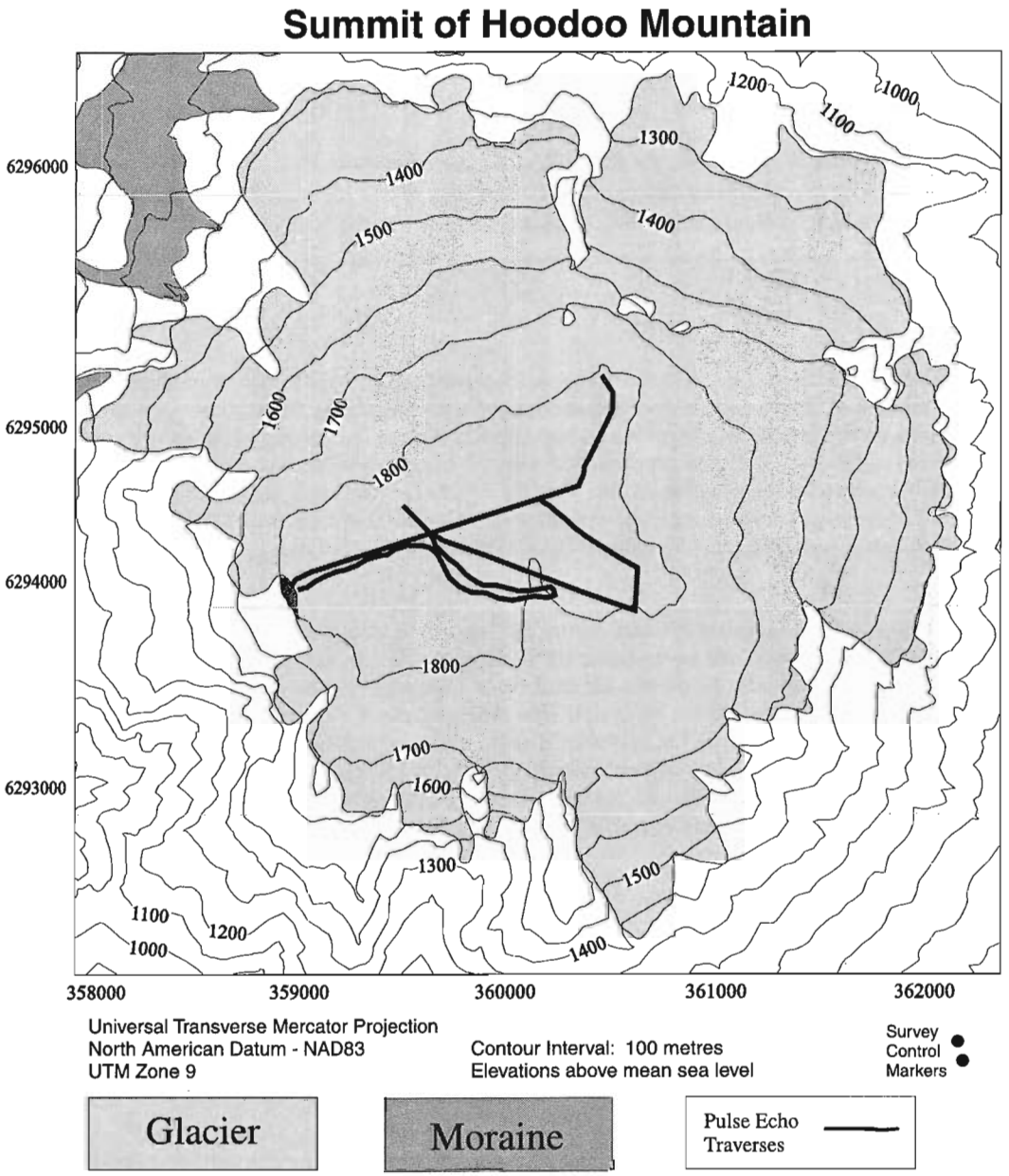

Figure 1. *Location of traverses of Pulse Echo ground-penetrating radar surveys.*

HOODOO MOUNTAIN SURVEY CONTROL POINTS

Two survey control markers (Fig. 1, 2) were established on a moraine on the west side of the ice cap. The three instruments were run in carrier-phase mode and were then capable of providing decimetre accuracy in horizontal position. One instrument was set on a B.C. Government control point (88H4013, 5961.91 m north of the southernmost survey control marker established on Hoodoo Mountain) and the other two instruments were set on the locations of the new survey control markers on the moraine. The three instruments were simultaneously operated for more than 30 minutes. After postcollection processing and differential correction, the 1 sigma RMS errors in the horizontal positions of the survey control markers were less than 10 cm. The B.C. Government control marker is located at 56°49'19.09686"N, 131°19'38.88255"W, relative to NAD83 and has an elevation of 1333.195 m, relative to Canadian Vertical Datum 1928 (CVD28). The coordinates of the survey control markers on the moraine at Hoodoo are: 6294089.642 N, 358911.609 E (56°46'09.6633"N, 131°18'30.6431"W), height above ellipsoid (HAE) 1805.790 m and 6294120.411 N, 358903.617 E

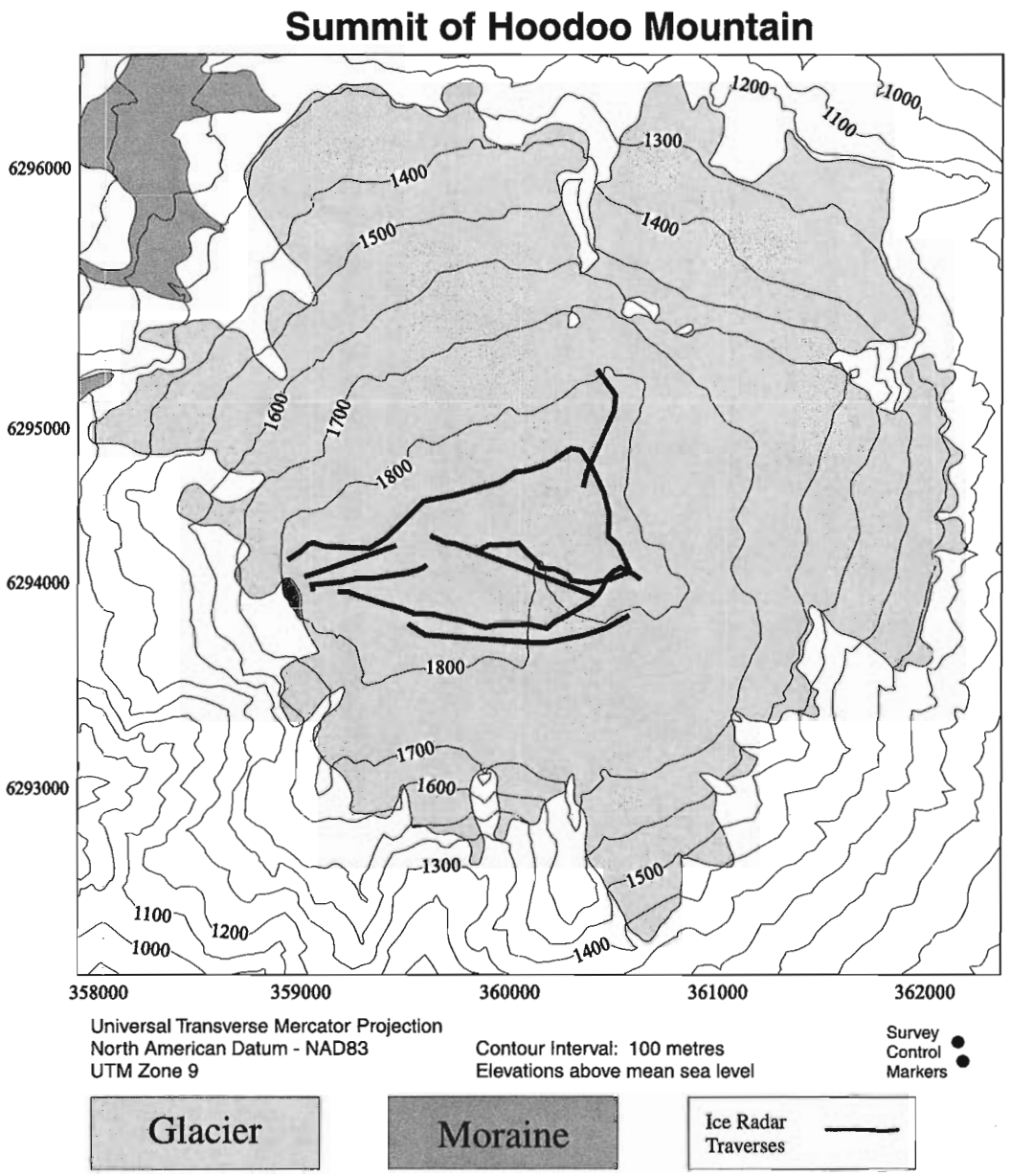

Figure 2. *Location of traverses of ice-radar surveys.*

(56°46'10.6489"N, 131°18'31.1745"W) HAE 1807.029 m. To refer elevations to WGS84 ellipsoid, a correction of -5.56 m, supplied by Geographic Data British Columbia, was made to the elevations. Comparison of elevations corrected with reference to the Dease Lake Station and elevations corrected with reference to the survey control markers on the moraine at Hoodoo showed differences of less than 1 m.

RADAR SURVEYS

The roving instruments were operated in continuous acquisition, code phase (C/A) mode when accompanying a radar unit. With differential correction, the position data, relative to the control markers on the moraine, are accurate to approximately 1 m. The accuracy was estimated by examining how close points along a linear traverse approached a straight line. The total length of the radar traverses was approximately 20 km (Fig. 1 and 2).

TOPOGRAPHY OF THE ICE CAP

Part of one day was spent collecting carrier-phase data with one single-frequency rover. Approximately 50 stations were occupied on the summit of the ice cap. The data are accurate, with respect to the locations of the control markers on the moraine, to better than 1 dm horizontally. Vertical elevations are accurate to 2 to 5 times the horizontal precision (i.e. <20 to 50 cm). The data are currently being compared to DEM elevations associated with the digital terrain map (TRIM) for Hoodoo Mountain.

ACKNOWLEDGMENTS

This project was supported by an IPP grant between the Geological Survey of Canada, Golder Associates Ltd., and The University of British Columbia. Ancillary costs were costs were covered by NSERC grants to J.K. Russell and J. Nicholls and by a National Geographic Grant to J. Nicholls.

Geological Survey of Canada Project 920008

Update on geological mapping, southeast Nass River map area, British Columbia

James W. Haggart, G.J. Woodsworth, and Angelique Justason[1]
GSC Pacific, Vancouver

Haggart, J.W., Woodsworth, G.J., and Justason, A., 1998: Update on geological mapping, southeast Nass River map area, British Columbia; in Current Research 1998-A; Geological Survey of Canada, p. 69-77.

Abstract: Paleontological data indicate that Lower Jurassic strata are present in the Hazelton Mountains, southeastern Nass River map area. Upper Jurassic strata of the Bowser Lake Group underlie most parts of the Kiteen River map area, British Columbia, although (?)Eocene plutonic rocks and Pleistocene volcanic and sedimentary strata are noted locally. Within the Bowser Lake Group, a fossiliferous, massive, fine-grained facies and a poorly fossiliferous turbidite facies are recognized; the former may predate the latter within the group. Bowser Lake Group strata are deformed into east-verging fold and thrust structures, cut by undeformed (?)Tertiary dykes. Available evidence suggests that no gradational relationship exists between the Bowser Lake Group and the Lower Cretaceous Skeena Group.

Résumé : Les données paléontologiques indiquent que des strates du Jurassique inférieur sont présentes dans les monts Hazelton, dans le sud-est de la région cartographique de la rivière Nass. Des strates du Jurassique supérieur du Groupe de Bowser Lake se retrouvent dans la plus grande partie de la région cartographique de la rivière Kiteen, en Colombie-Britannique, bien qu'on note localement la présence de roches plutoniques (?)éocènes et de strates volcaniques et sédimentaires pléistocènes. Au sein du Groupe de Bowser Lake, on reconnaît la présence d'un faciès massif fossilifère à grain fin et d'un faciès de turbidites pauvre en fossiles; le premier faciès est peut-être antérieur au second au sein du groupe. Les strates du Groupe de Bowser Lake sont déformées en structures de plissement et de chevauchement à vergence est et sont recoupées par des dykes (?)tertiaires non déformés. Les données disponibles laissent supposer qu'il n'existe pas de contact progressif entre le Groupe de Skeena, du Crétacé inférieur, et le Groupe de Bowser Lake.

[1] 4020 A Grange Road, Victoria, British Columbia V8Z 4V3

INTRODUCTION

The east half of the Nass River map area (103P), particularly the southeast quarter, contains a widespread assemblage of Mesozoic clastic strata, exposed in the uplift of the Hazelton Mountains. These rocks have traditionally been correlated with the upper Middle Jurassic to Upper Jurassic Bowser Lake Group (Carter and Grove, 1972; Evenchick and Mustard, 1996; Evenchick et al., 1997), although little detailed geological mapping had been undertaken in the region. Tertiary volcanic and plutonic rocks are also found in localized exposures.

A brief reconnaissance of the Hazelton Mountains area was undertaken in 1996 and resulted in an initial overview (see Evenchick et al., 1997), although no details of paleontology or geochronology were available at that time. Detailed geological mapping was initiated in 1997 by JWH in the southeastern Nass River map area (Fig. 1) as a component of the Nass River multidisciplinary geoscience project (see Evenchick et al., 1997). In addition, some paleontological data were available from areas in the southeastern Nass River map area visited by JWH during the 1996 survey. In 1995, GJW spent several days examining the Pleistocene volcanic rocks. This contribution is a progress report on geological mapping and paleontological studies in this region.

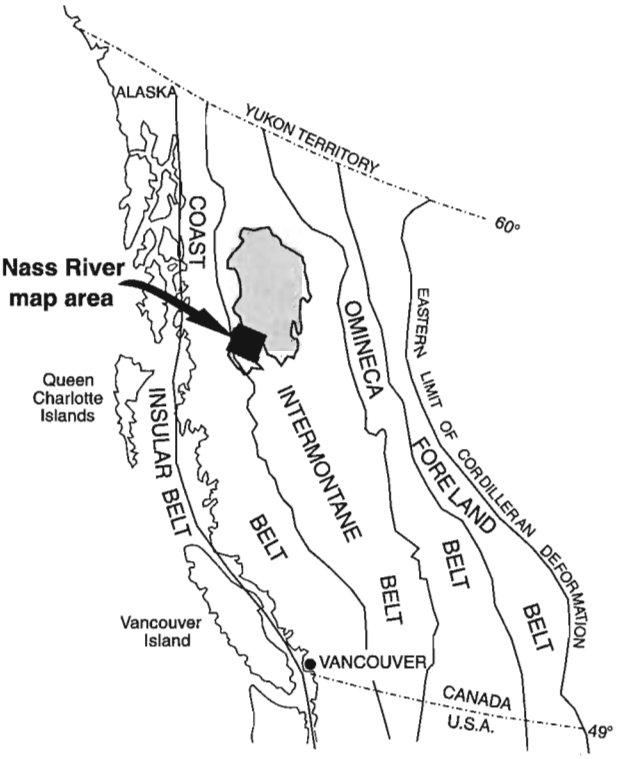

Figure 1. *Location map of the Nass River map area, British Columbia.*

GEOLOGY OF THE KITEEN RIVER MAP AREA

The Kiteen River map area (103P/7) embraces a portion of the Nass River valley on its west side, but most of the map area covers the high country of the Nass Ranges east of the Nass River valley (Fig. 2). The Kiteen River transects the map area from south to north. Mapping in 1997 concentrated on the east margin of the Nass River valley and the high country to the east; the larger part of the area of the Nass River valley was not examined. The Nass Ranges in the Kiteen River map area are apparently composed almost wholly of upper Mesozoic clastic strata. Minor Tertiary plutonic and Pleistocene volcanic rocks occur locally.

Upper Jurassic Bowser Lake Group

Upper Mesozoic strata are widely distributed across the Kiteen River map area; outcrops are found along the Kiteen River and at the highest points of the region, in the Mount Priestly area. Strata of this unit also outcrop along the east margin of the Nass River valley. The preliminary examination of roadcuts in the central part of the valley and of exposures along the Nass River suggests that such strata also occur within the valley itself (C. Evenchick, pers. comm., 1997). Although thick soil and forest cover obscure the bedrock geology across much of the Kiteen River map area, the aerial examination of slide and slump scars and isolated cliff exposures indicates that upper Mesozoic strata underlie almost all of the map area.

Fossils are relatively uncommon in the Bowser Lake Group of the Kiteen River map area. Buchiid and pectinid bivalves are the most common types. Several buchiid faunas were recognized in the field, including Upper Oxfordian to Kimmeridgian *Buchia concentrica*, upper Kimmeridgian *Buchia mosquensis*, and Tithonian *Buchia piochii*. No younger buchiids were identified in the field.

On the basis of age and lithological similarity, these rocks are correlated with the Bowser Lake Group, widely distributed across the Cranberry River and Brown Bear Lake map areas to the north (Evenchick, 1996a, b; Evenchick and Mustard, 1996). Two distinct lithofacies are found in the Bowser Lake Group strata of the Kiteen River map area: turbidite deposits and massive fine-grained clastic deposits. They may represent different stratigraphic levels within the Bowser Lake Group.

Turbidite facies

This facies is lithologically diverse and includes thin-bedded siltstone turbidite deposits within thick shale sequences, as well as thin- to thick-bedded sandstone turbidites within thinner shale sequences. Siltstone turbidites in fine-grained strata typically show Bouma T_{CDE} or T_{CD} units and grading is generally indeterminate, although truncated ripple stratifications and basal scour are often present, allowing determination of stratigraphic-up direction. In contrast, sandstone turbidites typically include Bouma T_{ACDE} units. Conglomerate forms a very minor component of several sandstone turbidite flows;

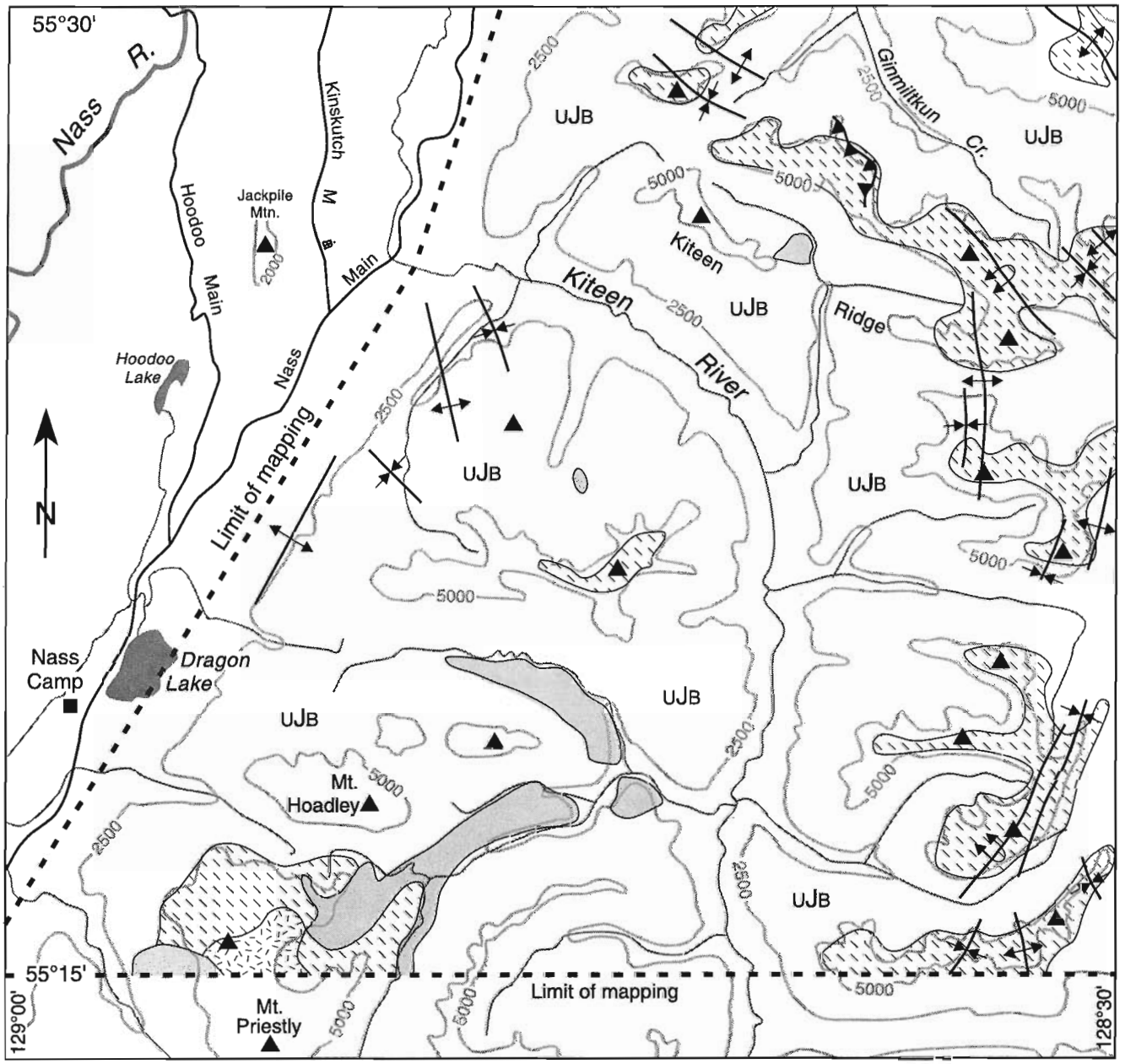

Pleistocene

Basalt flows, breccia

Eocene (?)

Mt. Priestly stock

Mainly granodiorite, tonalite

Upper Jurassic

Bowser Lake Group

Turbidite facies

UJB — Undifferentiated sedimentary rocks

5 km

5000 — Contour line (in feet)

▲ Peak, summit of ridge

Antiform, synform, overturned antiform

Figure 2. Generalized geological map of the Kiteen River map area (103P/7).

beds reach 40 cm in thickness and about 12 m in lateral extent. Clast types within the conglomerate include pebbles to small cobbles of argillite, metavolcanic rock, and chert; granitic clasts were not noted. In some sections, some of the coarser grained turbidite beds show preferential calcareous cementation, forming spherical concretions or concretionary horizons, none of which contained fossils. Ripple marks exposed on the bedding-plane surfaces of these coarser units allowed measurement of paleocurrent direction at several localities; the limited data suggest a westerly source.

In both fine- and coarse-grained turbidite facies, individual flow deposits are interstratified with shale interbeds, which range in thickness from several centimetres to several metres. Finer grained turbidites are generally associated with thicker shale interbeds whereas coarser grained ones are associated with thinner interbeds. The shale interbeds are typically massive or show parallel laminations. Organic debris, sometimes forming coalified mats several centimetres thick and up to 75 cm in lateral extent, are often associated with these interbeds. With the exception of plant detritus, fossils are extremely rare in all turbidite facies. The only material found consists of buchiid and other rare bivalves from the shale interbeds.

Most of the coarser grained clastic turbidite facies are oriented in successive fining-upward cycles (Fig. 3), each up to approximately 80 m in thickness. The upper parts of the cycles consist of fine-grained siltstone turbidites within thick shale successions. A maximum of four of these fining-upward cycles, stacked in stratigraphic succession, were noted in the northeastern Kiteen River map area.

Massive fine-grained clastic facies

Turbidite deposits are distinctly lacking in this facies, which comprises massive to rare parallel-laminated mudstone, silty mudstone, and siltstone. Siltstone is generally found as lenticular deposits within the shale, but distinct beds were sometimes noted. Fossils are moderately common and consist predominantly of buchiid and other bivalves, and rare gastropods. Burrows are common; they are mostly horizontal and are generally oxidized to orange. Plant debris, principally branches and coalified mats up to 5 mm thick and 75 cm in lateral extent, is also common. Pyrite is present locally, either disseminated in the sedimentary rocks or as spherical nodules to 3 cm across; some fossils and burrows also exhibit pyritization.

Rocks of this facies are widespread in the north-central part of the Kiteen River map area. They apparently include a succession of massive fine-grained clastic facies, probably over 350 m thick.

Depositional environments

The turbidite sequences observed in the Bowser Lake Group suggest distal submarine fan and fan-channel environments. Macrofauna are sparse and coarser grained clastic rocks such as conglomerate are relatively rare. The interpretation of the depositional environment of the massive fine-grained facies of the Bowser Lake Group is more problematic. Marine macrofauna are more widely distributed in this facies and the geometric relationship of the coarser grained and finer grained clastic fractions is more lenticular than interbedded. Strata of this facies may represent deep-water shelf environments, significantly shallower than the submarine fan environments represented by the turbidite facies.

In general, outcrops of the massive fine-grained clastic facies occupy topographically lower areas in the Kiteen River map area while turbidite facies outcrops are widespread at higher elevations. All the high peaks in the map area east of the Kiteen River are capped by sandstone, siltstone, and shale of the turbidite facies while low-elevation regions, such as along the Kiteen River and the east margin of the Nass River valley, consist mostly of the massive fine-grained facies. The reasons for this segregation are not clear. One possibility is that the fine-grained massive facies may represent a lower stratigraphic level of the Bowser Lake Group succession in

Figure 3.

View looking northeast showing successive fining-upward cycles in turbidite facies, northeast Kiteen River map area.

the Kiteen River map area, while the turbidite facies may represent a higher and younger stratigraphic level. Analysis of fossil ages may provide additional information.

No tuffaceous strata were noted in the Bowser Lake Group in the Kiteen River map area, indicating that this part of the basin was spatially or temporally removed from the influence of Late Jurassic magmatic activity.

Carter and Grove (1972) reported the presence of "minor limestone and coal" in Bowser Lake Group rocks in a much larger area, encompassing the Nass River and Terrace map areas. While it is possible that deposits of limestone and coal may eventually be found locally in the Bowser Lake Group in other areas, no such deposits were noted in the Kiteen River map area except for minor amounts of coalified wood and other plant debris, as well as calcareous-cemented mudstone and sandstone beds. Alternatively, limestone and coal facies identified in Bowser Lake Group strata by Carter and Grove (1972) may reflect misidentification of older strata as Bowser Lake Group deposits (see below).

Given that rocks of the Bowser Lake Group in the Kiteen River map area represent primarily deep-water environments in a basin of rapid clastic sedimentation, it is unlikely that significant biogenic limestone and coal will be found. Use of the term "limestone" suggests biogenic deposits, with a genetically distinct mode of origin; to avoid confusion in interpretation, we prefer to refer to these lithological units as calcareous-cemented mudstone, siltstone, and sandstone.

(?)Eocene Mount Priestly stock

Plutonic rocks are known only from the southwestern corner of the Kiteen River map area, where they form a circular body about 5 km in diameter in the glaciated topographically high region south of Mount Hoadley and north of Mount Priestly (Fig. 2). The intrusion was called the Mount Priestly stock by Carter (1981), who noted the presence of minor fracture-controlled molybdenite. We investigated the stock only briefly, with emphasis on delineating the contact zone of the plutonic body with the older Bowser Lake Group country rocks. Lithological units observed include equigranular unfoliated granodiorite, tonalite, and quartz diorite. Hornblende is generally more abundant than biotite, and minor titanite is present locally. The contact with the country rocks is typically sharp and discordant, although in some areas an extensive stockwork of dykes cuts sedimentary strata near the pluton margin. Country rocks are locally pyritized and are highly disrupted at and adjacent to the contact with the pluton.

Carter (1981) obtained a K-Ar age of 49 Ma on biotite from the Mount Priestly stock. Because the stock is high level and undeformed, we regard the age as a reliable indicator of age of emplacement, but we plan to test it with a U-Pb zircon age from a sample collected in 1997. The stock is the northernmost in a chain of high-level plutons extending south about 50 km from Mount Priestly into the Terrace map area. Most plutons in the chain are topographically high, suggesting a structural control on pluton emplacement and/or uplift. One stock in the Terrace map area gave a U-Pb age of 86 Ma (R. Friedman, pers. comm., 1987), indicating (accepting the 49 Ma age from the Mount Priestly stock) that plutons of more than one age are present in the chain.

A stock mapped by Carter and Grove (1972) north of the Mount Priestly stock on the ridge and south slopes of Mount Hoadley was not found. Although felsic dykes intruding Bowser Lake Group strata are common in this area and extend some distance north across the slopes north of Mount Hoadley, no mappable plutonic body was seen in the area.

Pleistocene glacial gravels

Small deposits of glacially derived gravel and conglomerate are found locally, underlying Quaternary volcanic deposits, and are briefly described below. In addition, the larger valleys, especially those of the Kiteen River and its lower tributaries, contain localized deposits of poorly sorted alluvial gravel and conglomerate that locally reach 120 m in thickness.

Pleistocene volcanic strata

Volcanic strata are found locally in the Kiteen River map area. The largest exposures were noted in valleys east and south of Mount Hoadley and on the north and west sides of the high massif north of Mount Priestly. Other smaller outcrops are found farther north in the map area. We recognize two distinct facies within the volcanic rocks, a vent facies and a flow facies.

Vent facies

Outcrops of this facies in the Kiteen River map area are found on the east and west sides of the Mount Priestly pluton, in a small cone in the centre of the map area, and in a larger cone on Kiteen Ridge north of the Kiteen River (Fig. 2). The volcanic vent facies rests on older rocks of the Mount Priestly pluton and the Bowser Lake Group northeast of Mount Priestly (Fig. 4), and on Bowser Lake Group rocks at Kiteen Ridge. It consists predominantly of heterogenous basalt breccia, flow breccia, scoria, and cinder deposits. Inclusions of country rock are abundant in breccia on Mount Priestly. The vent facies on Mount Priestly apparently includes abundant flow-breccia deposits that traversed the underlying topography, sometimes forming steep cascades (Fig. 4). At the two deposits in the north half of the map area, vent-facies deposits closely approximate cinder-cone morphologies, showing depositional dips of up to 44° (Fig. 5), and including basalt breccia, scoria, and cinder lithologies and textures.

Flow facies

Columnar basalt forms thick sequences in the two valleys northeast and southeast of Mount Hoadley and west of the Kiteen River, as well as in the large isolated body at the junction of these two valleys (Fig. 2). No additional exposures of volcanic strata were noted in the valley downstream from the junction to the Kiteen River and beyond. The rocks southeast

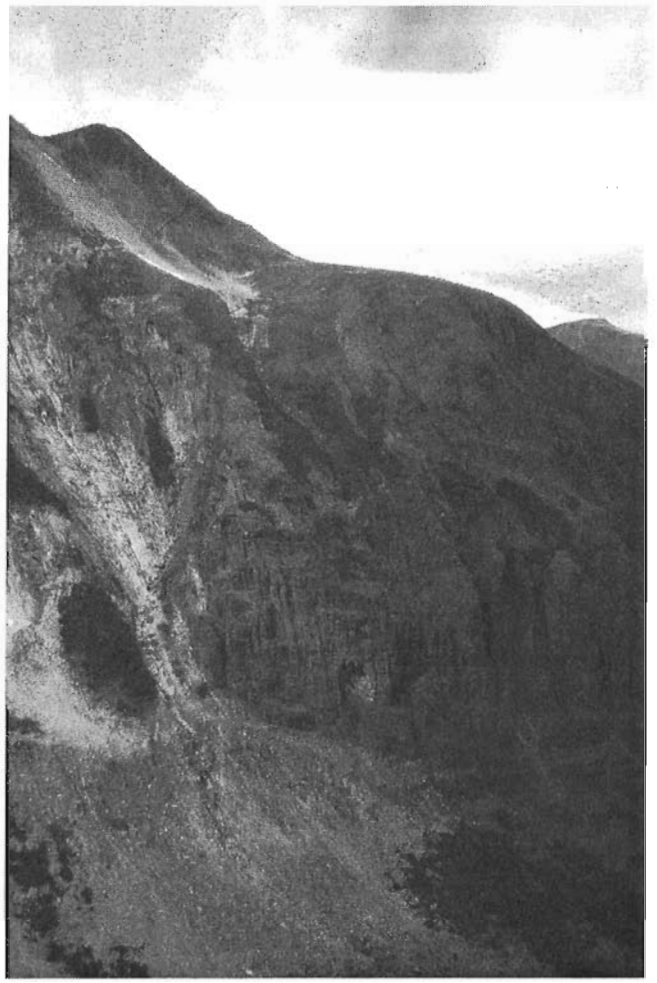

Figure 4. *Pleistocene volcanic vent facies (centre and right of photo) resting on (?)Eocene Mount Priestly stock (far left-centre) and Upper Jurassic Bowser Lake Group strata (ridge line at left) southeast of Mount Hoadley.*

of Mount Hoadley were examined in some detail; the other exposures were studied only by aerial reconnaissance and several brief spot landings.

The flows southeast of Mount Hoadley have a total thickness of about 60 m, are slightly vesicular, and have conspicuous columnar jointing. The rocks are fine-grained basalts, commonly with large, conspicuous plagioclase phenocrysts and small olivine and titanaugite phenocrysts. No ultramafic nodules were found. The upper surface is locally glacially grooved, striated, and covered with a thin veneer of glacial deposits. It lies at an elevation of about 1000 m and between 30 and 250 m above the current valley bottom. The basal surface slopes gently east, suggesting that the source of the flows was farther up the valley and that the valley was extensively deepened after volcanic activity (Fig. 6).

The Mount Hoadley flows rest on about 30 m of unconsolidated sediments (Fig. 7) consisting of a mixture of grey clay containing rounded pebbles to boulders of sedimentary and granitic rock. The sediments show no sorting or stratification and are interpreted to be glacial till. If such is the case, then the Mount Hoadley flows are interglacial and may have acted as a caprock that preserved the earlier till from erosion. The upper surface has a well developed forest and grassland cover, with extensive lakes and marshland. Valley drainage has resumed along the margins of the flow surface and streams there have incised the underlying Bowser Lake Group strata to a depth of at least several tens of metres.

Age and correlation

The basalt flows are lithologically very similar to many young volcanic rocks elsewhere in the Nass River map area, especially those at Hoan Creek, dated at 175 000 ± 50 000 years by the ^{40}Ar-^{39}Ar method, and those near Cranberry Junction (Evenchick et al., 1997). The heavy forest cover over the flows, the glacial cover, and the depth of stream incision along the flow margins indicate that the flows are substantially older than the well known Aiyansh flow that

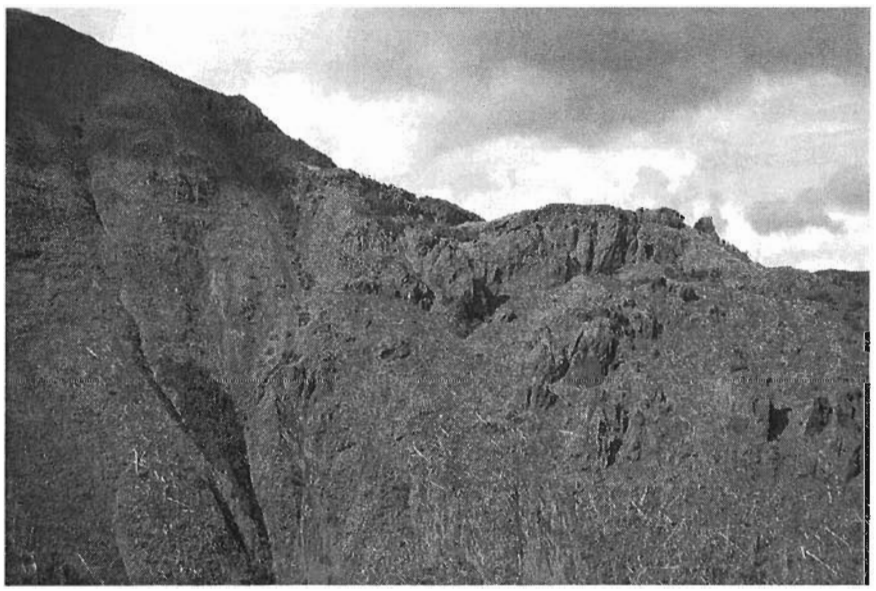

Figure 5.

Pleistocene cinder cone formed at the east end of Kiteen Ridge, north of the Kiteen River. Vent-facies strata of the cone comprise the dissected strata on right (north) side of photo and unconformably overlie Upper Jurassic Bowser Lake Group strata, seen on left.

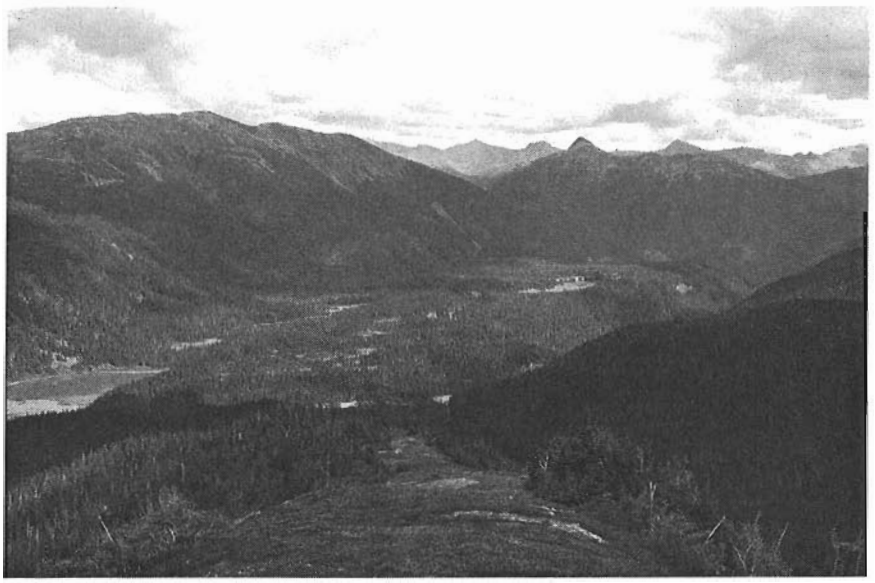

Figure 6.

View looking northeast to the terrace formed on the upper surface of the Pleistocene volcanic flow (valley in centre of photo) east of Mount Hoadley. The light area on the right of the centre of the photo is an outcrop of cliff-forming columnar basalt. The location of Figure 7 is just south of the lake on the left side of the photo.

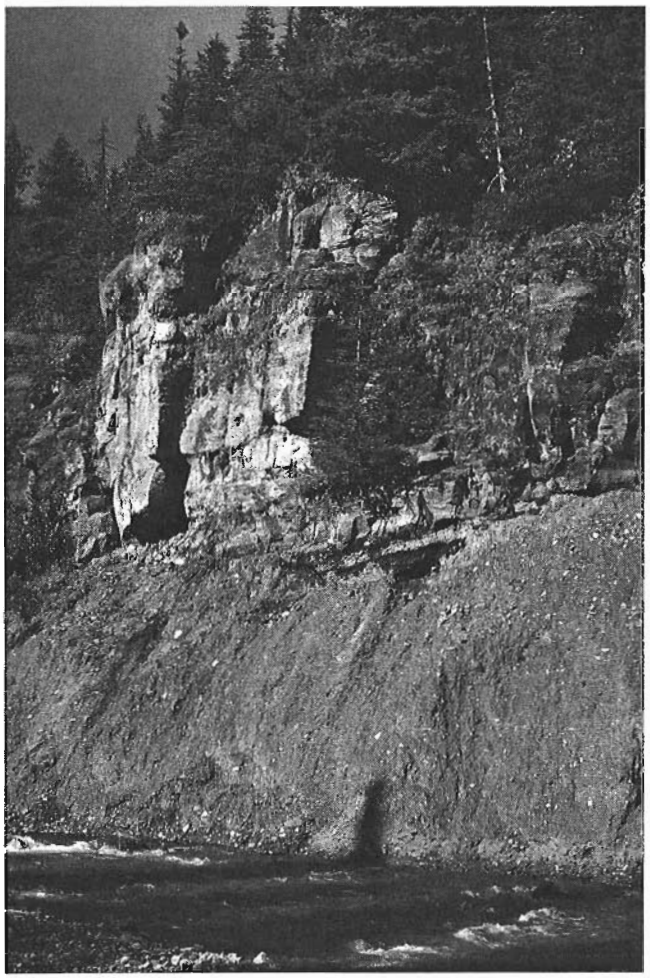

Figure 7. *Flat-lying volcanic basalt overlying Pleistocene glacial deposits, southeast of Mount Hoadley. Photo by C. Evenchick.*

is about 12 km to the south and roughly 220 years old (Sutherland Brown, 1969; S. McCuaig, pers. comm., 1997). A Pleistocene age seems probable and, until radiometric dates are available, the age of 175 000 ± 50 000 from the Hoan Creek flow is the best guess for the age of the basalts in the Kiteen River map area.

Volcanic rocks in the Kiteen River map area are interpreted as representing several dissected, areally restricted, monogenetic lava flows and related deposits. Together with the Aiyansh lava flow, they mark the southern known limit of the Northern Cordilleran Volcanic Province of Edwards (1997). Geochemical work is underway to further characterize these rocks.

Late (?)Mesozoic and younger dykes

Dykes of rhyolitic to basaltic compositions cut the Bowser Lake Group in most areas of the Kiteen River map area, although they are most abundant in areas of exposure of the massive fine-grained facies of the Bowser Lake Group, and adjacent to the Mount Priestly stock. The dykes are generally oriented parallel to the local structural grain. Dykes of basaltic composition are sparsely but widely distributed and are considered likely to be related to the young Pleistocene volcanic activity that occurred across the central part of the map area; several basalt dykes contain ultramafic xenoliths. Dykes of more felsic composition are probably related to magmatic activity associated with emplacement of the older Mount Priestly pluton. Felsic dykes cutting Bowser Lake Group strata north of Mount Priestly are apparently overlain by Pleistocene basaltic volcanic vent-facies strata; their age cannot be constrained beyond post-early Late Jurassic to Pleistocene.

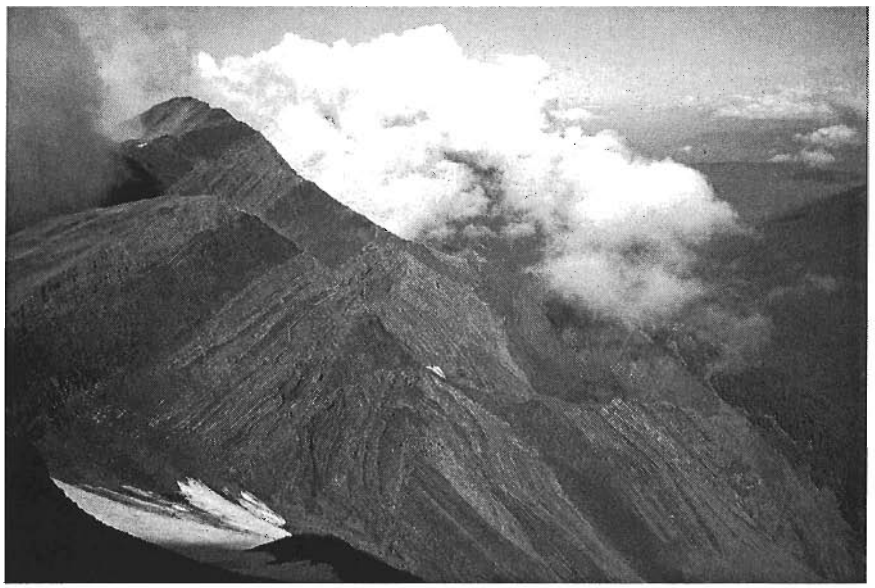

Figure 8.

Northeast-vergent folds in Bowser Lake Group strata, northeast Kiteen River map area, showing continuity of structure across several ridges. North is to the right. Three successive fining-upward cycles in turbidite facies can be seen.

Structural geology

Throughout the Kiteen River map area, strain is preferentially accommodated in fine-grained facies (shale and siltstone); coarser grained strata are more competent and resist deformation. The most common deformation fabric seen in fine-grained strata is a ubiquitous foliation pattern; in many cases, the strongest foliation is parallel to bedding and attributed to the original depositional fabric. In other instances, foliation is oriented oblique to bedding and is attributed to local variations in the stress regime. Strata of the massive fine-grained facies are typically strongly foliated, and fossils collected from the facies often show strain-related elongation or compression.

Evidence for large-scale compressional stress is readily seen in areas underlain by turbidite facies of the Upper Jurassic Bowser Lake Group. The central and east-central portions of the Kiteen River map area are characterized by north-oriented, eastward-vergent structures developed in Bowser Lake Group rocks, principally large-scale folds but also localized thrusts. Similar structures in the northeast part of the map area have a more northwesterly trend (Fig. 8) while those in the southeast part of the map area trend NE. Similar structural styles have been documented previously in the Skeena Fold Belt to the northwest (Evenchick, 1991). The age of deformation in the Kiteen River map area is poorly constrained although a vertical dyke cutting deformed Bowser Lake Group strata in the southeast part of the map area is relatively undeformed. We assume the dyke is Tertiary and collected samples for U-Pb age determination.

NEW PALEONTOLOGICAL DATA

The preliminary study of marine fossils collected from the Kitwanga 1:50 000 map area (103P/1) in 1996 has identified the marine bivalve *Weyla* sp. (possibly *Weyla acutiplicata*; H.W. Tipper, pers. comm., 1997), indicating an Early Jurassic age for these rocks. Strata at this locality (GSC Loc. C-302908) are thus temporally equivalent with the Lower Jurassic Hazelton Group, which is well developed to the east in the Hazelton 1:250 000 map area (Richards, 1991), and are not related to the Bowser Lake Group.

DISCUSSION

The preliminary study of fossil collections from the Kiteen River map area suggests that all buchiid bivalve assemblages indicate a Late Jurassic age; Cretaceous faunas have not been found. The Mesozoic strata of the Kiteen River map area are thus correlative with the Bowser Lake Group, particularly with strata exposed in the Brown Bear Lake and Cranberry River map areas to the north (Evenchick and Mustard, 1996). Bowser Lake Group strata in those areas apparently represent distal turbidite facies in deep-water submarine-fan environments. The depositional environments of most Bowser Lake Group strata of the Kiteen River map area are interpreted similarly.

Field observations suggest that the massive fine-grained facies of the Bowser Lake Group may represent shallower water depositional environments than the turbidite facies. If so, this may be evidence of possible shallowing of the environment of deposition of Bowser Lake Group strata across the Kiteen River map area, and suggestive of a possible gradational relationship between Bowser Lake Group strata and the Lower Cretaceous Skeena Group exposed to the east and south (Bassett and Kleinspehn, in press). Field observations also suggest, however, that the massive fine-grained facies of the Bowser Lake Group may represent an older stratigraphic level within the group in the Kiteen River map area than the deeper water turbidite facies (see above). In addition, all fossils collected to date from Bowser Lake Group strata exposed farther south in the Hazelton Mountains, in the northeast Terrace map area (103I), are also Late Jurassic; no Cretaceous fossils have been identified. The available

evidence suggests that a significant stratigraphic gap may exist between Upper Jurassic Bowser Lake Group strata and Lower Cretaceous Skeena Group strata in the Hazelton Mountains.

In their reconnaissance assessment of the sedimentary strata of the Hazelton Mountains, Evenchick et al. (1997) identified several distinct sedimentary facies from various localities in the Hazelton Mountains, all of which they considered to be Late Jurassic and possibly Early Cretaceous and thus correlative, at least in part, with the Bowser Lake Group. They proposed a model for the deposition of Upper Jurassic strata in the southeastern Nass River map area that features a southeastward-shallowing basin. The identification of specimens of *Weyla* sp. in the Kitwanga map area (103P/1) indicates that a greater range in ages is represented in strata of the southeast Nass River map area than was previously recognized. The simplified interpretation of the genetic relationships of the various facies advanced in Evenchick et al. (1997) must be revised, although additional detailed geological field mapping will be required to do so.

ACKNOWLEDGMENTS

We thank Wally Zec and Ian Swan for expert helicopter piloting, and Carol Evenchick for stimulating discussion of the Nass River geology. M. Futakami made several important fossil collections in 1997 and Paul Adam and Nikki Tatum provided cheerful assistance during the bleak 1995 field season. Lionel Jackson reviewed the manuscript.

REFERENCES

Bassett, K. and Kleinspehn, K.
in press: Early to mid-Cretaceous paleogeography of north-central British Columbia: stratigraphy and basin analysis of the Skeena Group; Canadian Journal of Earth Sciences.

Carter, N.C.
1981: Porphyry copper and molybdenum deposits, west-central British Columbia; British Columbia Ministry of Energy, Mines and Petroleum Resources, Bulletin 64, 150 p.

Carter, N.C. and Grove, E.W. (comp.)
1972: Geological compilation map of the Stewart, Anyox, Alice Arm, and Terrace areas; British Columbia Department of Mines and Petroleum Resources, Preliminary Map No. 8 (scale 1:250 000).

Edwards, B.R.
1997: Field, kinetic, and thermodynamic studies of magmatic assimilation in the Northern Cordilleran Volcanic Province, northwestern British Columbia; Ph.D. thesis, University of British Columbia, Vancouver, British Columbia.

Evenchick, C.A.
1991: Geometry, evolution, and tectonic framework of the Skeena Fold Belt, north-central British Columbia; Tectonics, v. 10, p. 527-546.
1996a: Geology, Cranberry River, British Columbia (103 P/10); Geological Survey of Canada, Open File 3224 (scale 1:50 000).
1996b: Geology, Brown Bear Lake, British Columbia (103 P/15); Geological Survey of Canada, Open File 3225 (scale 1:50 000).

Evenchick, C.A. and Mustard, P.S.
1996: Bedrock geology of north-central and west-central Nass River map area, British Columbia; in Current Research 1996-A; Geological Survey of Canada, p. 45-55.

Evenchick, C.A., Alldrick, D.J., Currie, L.D., Haggart, J.W., McCuaig, S., McNicoll, V., and Woodsworth, G.J.
1997: Status of research in the Nass River multidisciplinary geoscience project, British Columbia; in Current Research 1997-A; Geological Survey of Canada, p. 21-30.

Richards, T.A.
1991: Geology and mineral deposits of Hazelton (93M) map area, British Columbia; Geological Survey of Canada, Open File 2322, 2 maps (scale 1:250 000).

Sutherland Brown, A.
1969: Aiyansh lava flow, British Columbia; Canadian Journal of Earth Sciences, v. 6, p. 1460-1468.

Geological Survey of Canada Project 950037

Nechako NATMAP Project overview, central British Columbia, year three[1]

L.C. Struik and D.G. MacIntyre[2]
GSC Pacific, Vancouver

Struik, L.C. and MacIntyre, D.G., 1998: Nechako NATMAP Project overview, central British Columbia, year three; in Current Research 1998-A; Geological Survey of Canada, p. 79-87.

Abstract: More than 25 government, university, and industry researchers were active during the 1997 field season of the joint Geological Survey of Canada and British Columbia Geological Survey Branch Nechako project. In addition, university students assisted in the mapping programs. Bedrock geology was mapped in eleven 1:50 000 scale areas and surficial geology in five 1:50 000 scale areas. Researchers sampled till, silt, lodgepole pine, and rocks in various geochemical studies. Others measured paleomagnetic signatures, studied biostratigraphy, sampled for isotopic age determination, and conducted detailed sedimentological and stratigraphic studies. New geoscience contributions include 1) defining the distribution of Jura-Cretaceous volcanic stratigraphy in northern Nechako River map area, 2) more clearly defining Eocene felsic and mafic volcanic stratigraphy and crustal structures, 3) detailed differentiation of Cretaceous and Eocene felsic igneous suites of the Babine Belt, 4) improved constraints on Pleistocene ice-flow and lacustrine deposits, and 5) characterizing Cache Creek and Sitlika groups biostratigraphy and tectonostratigraphy.

Résumé : Plus de 25 chercheurs des gouvernements, des universités et de l'industrie ont participé activement à la saison de terrain de 1997 du Projet du plateau de Nechako, géré conjointement par la Commission géologique du Canada et la British Columbia Geological Survey Branch. Des étudiants universitaires ont en outre collaboré aux programmes de cartographie. La géologie du substratum rocheux a été cartographiée dans onze régions à l'échelle de 1/50 000 et la géologie de surface, dans cinq régions à la même échelle. Des chercheurs ont échantillonné du till, du silt, des pins de Murray et des roches dans le cadre de diverses études géochimiques. D'autres chercheurs ont mesuré des signatures paléomagnétiques, étudié la biostratigraphie, prélevés des échantillons pour déterminer les âges radiométriques et mené des études sédimentologiques et stratigraphiques détaillées. Parmi diverses contributions géoscientifiques nouvelles figurent : 1) la détermination de la distribution des successions volcaniques jurassiques-crétacées dans le nord de la région cartographique de la rivière Nechako; 2) une détermination plus précise de la stratigraphie des successions volcaniques felsiques et mafiques et des structures crustales de l'Éocène; 3) une différenciation détaillée des suites ignées felsiques crétacées et éocènes de la ceinture de Babine; 4) une meilleure compréhension des contraintes naturelles régissant le mouvement des glaces et les dépôts lacustres au Pléistocène; et 5) une caractérisation de la biostratigraphie et de la tectonostratigraphie des groupes de Cache Creek et de Sitlika.

[1] Contribution to the Nechako NATMAP Project

[2] Geological Survey Branch, British Columbia Ministry of Employment and Investment, 1810 Blanshard Street, Victoria, British Columbia V8V 1X4

INTRODUCTION

The Nechako NATMAP project is a joint mapping venture between the GSC, British Columbia Geological Survey Branch, universities and industry (Struik and McMillan, 1996; McMillan and Struik, 1996; Struik and MacIntyre, 1997; MacIntyre and Struik, in press). The project encompasses more than 30 000 km^2 in central British Columbia (Fig. 1, 2). Its focus is to improve the quality and detail of bedrock and surficial maps to help resolve several geological problems. In particular, it addresses the following questions: 1) the extent and nature of Tertiary crustal extension, 2) Mesozoic compression and the manner of accretion of exotic terranes, 3) the geological and geophysical definition of the terranes, 4) the sequence of changing Pleistocene glacial ice-flow directions, and 5) the character and dispersion of glacial deposits.

In this third field season of the Nechako NATMAP project, a total of 16 new 1:50 000 scale areas have been mapped for their bedrock (11) and surficial (5) geology (Fig. 3). In addition, detailed sampling and stratigraphic studies have been undertaken. Samples were collected for till, silt, lake, biological, and lithological chemistry, paleomagnetic studies, and paleontological and radio-isotopic geochronology. Stratigraphic studies concentrated on sections within the Cache

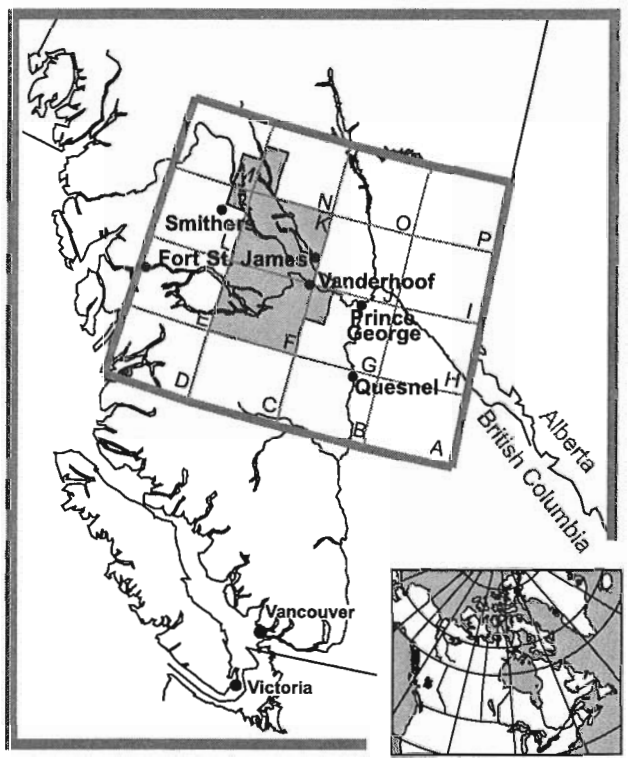

Figure 1. *Location of the Nechako NATMAP project area within British Columbia. The Parsnip River (NTS 93) 1:1 000 000 scale map area is shown for reference.*

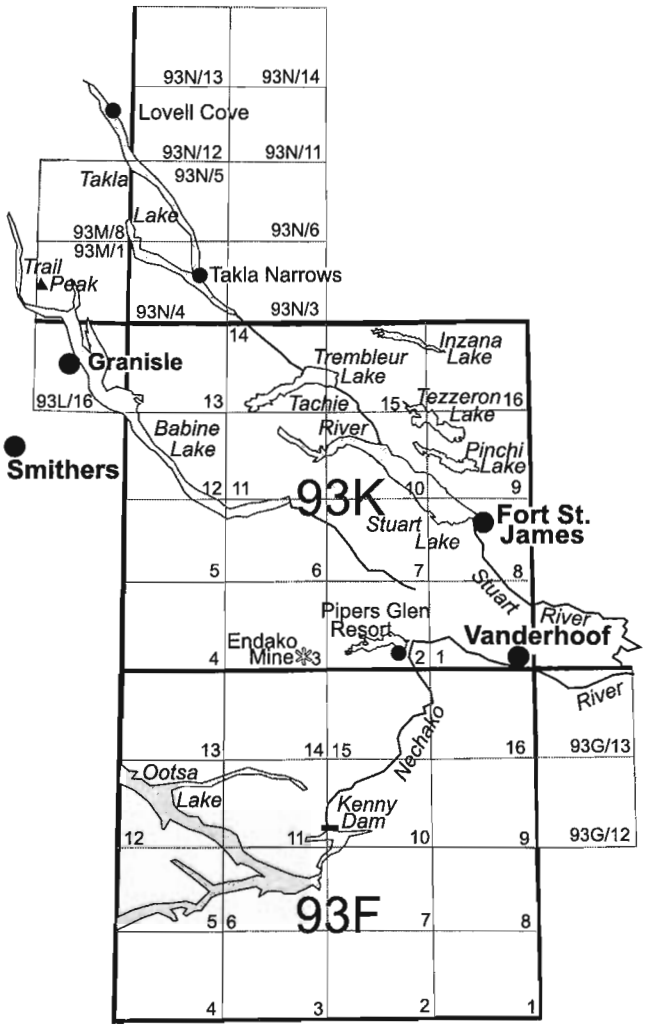

Figure 2. *Reference map of geographic and NTS map locations mentioned in the text. See Figure 1 for the location of the Nechako NATMAP project area within central British Columbia.*

Creek Group near Fort St. James and mainly volcanic sequences of the Ootsa Lake and Endako groups. Digital GIS projects included compilation of mapping data from Placer Dome Incorporated, construction and addition to the digital field mapping databases, cartography of geological maps, and the initiation of internet GIS data sharing (Fig. 3).

This paper outlines research that is in many cases preliminary. References are given to more in-depth summaries in this volume and *Geological Fieldwork 1998* of the British Columbia Ministry of Employment and Investment. For others the continuing research will lead to more comprehensive government and journal reports and maps. Analytical data is not reported in this paper.

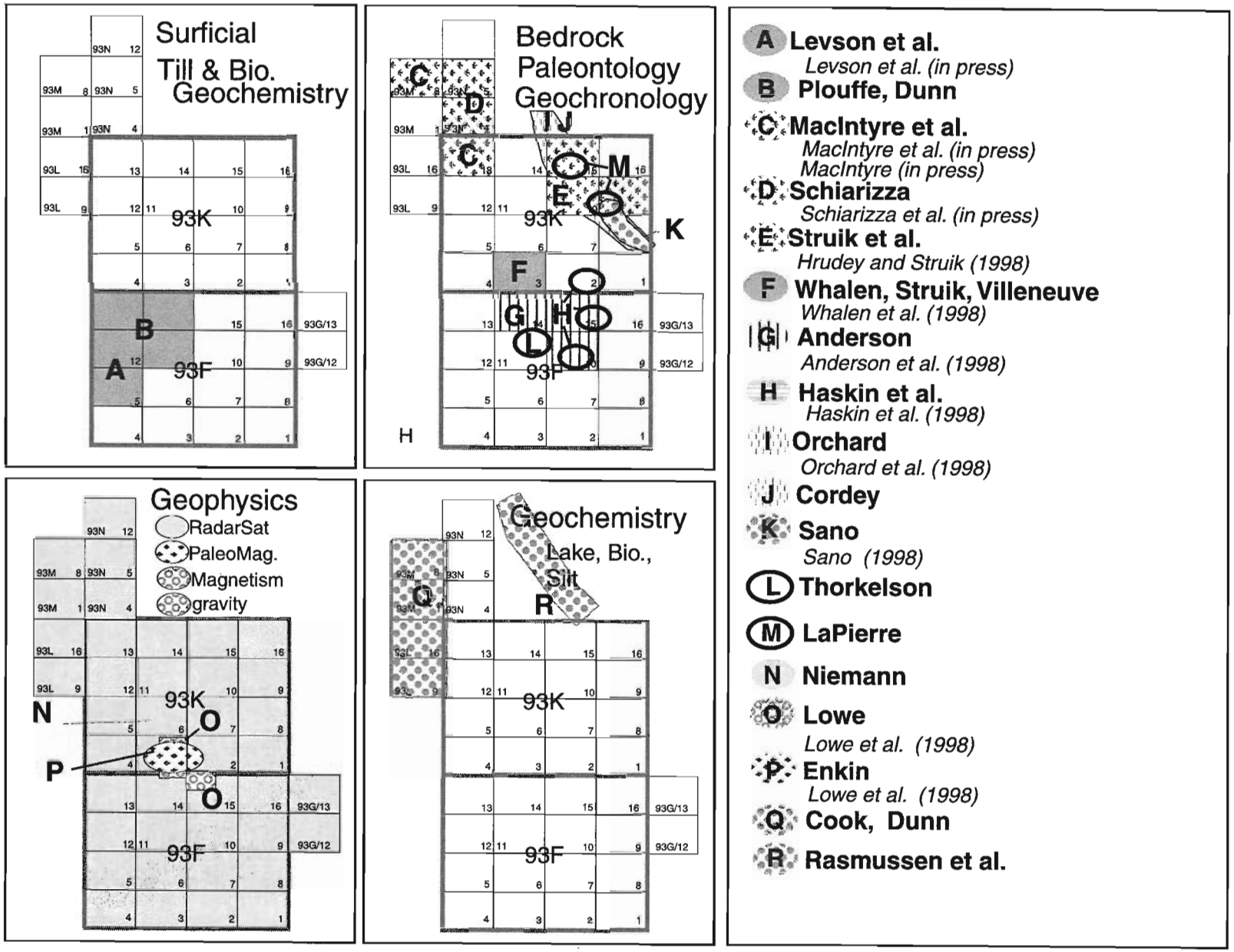

Figure 3. *Location of various Nechako subprojects active in 1997. Associated researchers are listed and their affiliations are described in the text.*

OVERVIEW OF 1997 NECHAKO PROJECT RESULTS

Babine and Sitlika studies

Bedrock mapping in the Babine-Takla lakes area built on previous mapping by D. MacIntyre in the Babine Porphyry belt (93L/16, 93M/1) and P. Schiarizza in the Sitlika belt east of Takla Lake (93N/12, 93N/13) (Fig. 2). The 1997 bedrock mapping crew comprised D.G. MacIntyre, P. Schiarizza, and N.W.D. Massey of the British Columbia Geological Survey Branch. Excellent geological field assistance was provided by summer students M. Lepitre (University of British Columbia), R. Metcalf (University of British Columbia), S. Modeland (University of Victoria), S. Munzar (University of British Columbia) and D. Tackaberry (University of Victoria). From late June until the end of August, this crew completed bedrock mapping of areas covered by NTS map sheets 93M/8, 93N/5 and 93K/13, plus most of 93N/4 and parts of 93M/7, 93N/6, 93N/12 and 93N/3.

Helicopter set-outs and pickups were used to cover poorly accessible areas. Other areas were mapped using logging road access, inflatable boat, and the B.C. Rail line along the east shore of Takla Lake.

Accomplishments

Bedrock mapping was done at 1:50 000 scale in 93M/8 and 93N/5 and at a more regional 1:100 000 scale in 93N/4 and 93K/13 (MacIntyre, in press; MacIntyre et al., in press; Schiarizza et al., in press). Samples were collected for micro- and macro-paleontology, isotopic age determination, paleomagnetic determinations, whole-rock and trace-element geochemistry. All mineralized outcrops were sampled to determine base and precious metal content.

Following are the main highlights of the Babine and Sitlika mapping of 1997:

1. Trail Peak and Nak porphyry copper deposits are associated with northwest-trending biotite-feldspar porphyry dykes of the Eocene Babine Intrusions. The dykes cut an earlier granodiorite to quartz diorite phase and hornfelsed Hazelton Group volcanics and sediments. High-angle normal faults, Eocene or younger, cut the intrusions and surrounding rocks (MacIntyre, in press).
2. The belt of Lower to Middle Jurassic bimodal volcanics first recognized in the area west of Granisle in 1995 was traced into the 93M/8 map area. The unit appears to be thinning and contains less felsic volcanics going northward toward the Bowser Basin. This coincides with a general change in the nature of Lower to Middle Jurassic sedimentary rocks from shallow to deep-water facies.
3. An area of hornblende-biotite-feldspar porphyry flows was mapped northwest of Trail Peak. These rocks are tentatively correlated with the Late Cretaceous Kasalka Group. Previous mapping suggested these flows were part of the Tertiary Babine Intrusive suite.
4. A large stock of porphyritic quartz monzonite with a border phase of hornblende diorite was mapped east of Tochcha Lake in the 93K/13 map area. This stock, which does not appear on previous maps, is considered part of the Topley suite and intrudes volcanics of the Takla Lake Group. Other large plutons north and south of the northwest arm of Takla lake in the 93N/4 map area also intrude Takla rocks and have similar lithologies to the Topley suite with which they are tentatively correlated.
5. The three lithologic divisions of the Sitlika assemblage were traced southward from 93N/12, through 93N/5 and into the northern part of 93N/4. The western clastic unit was traced into rocks previously included in the Upper Triassic Takla Group. As lithologically similar sedimentary rocks are intercalated with typical Takla Group volcanics, it is suspected that the western clastic unit might be a fault-bounded sliver of Takla rocks. The Sitlika volcanic unit and overlying eastern clastic unit were traced southwards into volcanic and sedimentary rocks that had previously been mapped as Cache Creek Group.
6. The ultramafic unit that marks the boundary between the Sitlika assemblage and Cache Creek Group in 93N/12 and 13 continues southward through 93N/5 and into 93N/4. This unit is a serpentinite melange in the north, but to the south includes relatively coherent intervals of tectonized harzburgite and dunite, confirming an ophiolitic origin for the ultramafic belt.
7. The contact between Cache Creek Group and Sitlika assemblage was observed east of Tsayta Lake (93N/5) where it is a low-angle fault that places the Cache Creek ultramafic unit above Sitlika eastern clastic unit. This fault contact is truncated by monzogranite of the Mitchell pluton.
8. The Sitlika assemblage in 93N/4 and 5 is separated from the Upper Triassic Takla Group of Stikine Terrane by a system of north- to northwest-striking faults of uncertain sense of displacement. This fault system is truncated by the north-striking Takla Fault, which marks the western boundary of the Sitlika assemblage in 93N/12 and 13.

Cache Creek Group tectonostratigraphic studies in northeastern Fort Fraser map area

Studies in the Cache Creek Group of eastern Fort Fraser map area consisted of bedrock mapping, biostratigraphy, lithogeochemistry, and geochronological sampling. This work was conducted by L.C. Struik (Geological Survey of Canada), H. Sano (Kyushu University, Japan), M.J. Orchard (Geological Survey of Canada), F. Cordey (Université Claude Bernard à Lyon, France), W. Bamber (Geological Survey of Canada), Henriette LaPierre (Université Joseph Fourier, France) and M. Tardy (Université de Savoie, France). Excellent geological mapping assistance was provided by students M.G. Hrudey (University of Alberta), C. Huscroft (University of British Columbia), A. Blair (Okanagan College), A. Justason (Comasun College), and S. Lewis (University of Melbourne). Primary access was by forest service roads branching from Fort St. James, and the extensive lake system.

Accomplishments

Bedrock mapping of map areas 93K/9, 10, and 15 was completed at 1:100 000 scale (Fig. 2, 3). That mapping built on recent mapping by Ash et al. (1993, 93K/9, 10) and Nelson et al. (1991, 93K/16). H. Sano spent 3.5 weeks doing detailed biostratigraphic mapping of the Cache Creek Group's Mount Pope formation near Fort St. James. M.J. Orchard, F. Cordey, and W. Bamber joined H. Sano to map and sample Cache Creek Group limestones and cherts for conodont, radiolarian, and coral assemblages in the context of the sedimentological environments interpreted from depositional textures (Orchard et al., 1998; Sano, 1998). Lithogeochemical sampling of basalts of the Cache Creek and Takla Group was done by H. LaPierre and M. Tardy to constrain the basalt petrogenesis.

Following are the main highlights of the 1997 Cache Creek Group tectonostratigraphic studies in northeastern Fort Fraser map area:

1. Upper Triassic and possibly Lower Jurassic basalt tuff, greywacke, siltstone, conglomerate, and minor limestone straddle the Pinchi Fault zone along Pinchi and Tezzeron lakes (93K/9,15). These rocks, formerly mapped as Takla Group, are tentatively differentiated, called Tezzeron assemblage, and are interpreted to have been an overlap assemblage onto oceanic assemblages of the Cache Creek Group.
2. Pinchi Fault probably cuts the former suture between the oceanic Cache Creek Group and the island arc Takla Group. The suture itself is exposed along Pinchi Lake as the blueschist terrane documented by Paterson (1973). Cache Creek Group ultramafic rocks overthrust Tezzeron assemblage tuff and greywacke on either side of the Pinchi Fault.
3. All of the contacts of the Mount Pope formation limestone, chert, and minor basalt are probably thrust faults. Where Mount Pope limestone and its underlying units have been dated, the underlying rocks are younger.
4. Limestone of the Cache Creek Group has been constrained to three time intervals: earliest Upper Carboniferous to Early Permian, Late Permian, and Early Triassic.
5. Upper Carboniferous to Early Permian Cache Creek Group limestone is generally clastic, shallow- to moderately shallow-water facies and thought to have developed on basaltic ocean islands.
6. Quartz diorite plutons of the McElvey and Tachie plutons are generally unfoliated and crosscut all structures in the Cache Creek Group metasediments of the Middle and Upper Triassic Sowchea assemblage near Tachie River, north of Stuart Lake (Hrudey and Struik, 1998).
7. From new lithogeochemistry, basalts of Cache Creek Group are mainly ocean-island type.

Endako plutonism and tectonics

Bedrock of Endako map area (93K/3, 1:50 000 scale, Fig. 2, 3) was mapped in detail using previous Endako Mines mapping (Kimura et al., 1980; G. Johnson, pers. comm., 1997) as a guide and template. J. Whalen and L.C. Struik (both from Geological Survey of Canada) were ably assisted by N. Grainger (University of Alberta) and the student assistants of the Cache Creek Group-east study (Whalen et al., 1998). R. Enkin and J. Baker (both of Geological Survey of Canada) continued Tertiary paleomagnetic tilt studies in the Endako area (Lowe et al., 1998). C. Lowe (Geological Survey of Canada) interpreted the magnetic signature of the Endako molybdenum camp (Lowe et al., 1998). The area was accessed through forest roads and highways.

Accomplishments

A detailed bedrock map of the Endako map area (93K/3) was completed (Whalen et al., 1998). Stratigraphic sequences in the Ootsa Lake and Endako groups were constrained within the limits of the poor exposure. N. Grainger and M. Villeneuve (Geological Survey of Canada) sampled igneous suites for U-Pb and Ar-Ar isotopic dating throughout the area, concentrating on the Tertiary volcanic units to constrain their stratigraphy and the tectonic events that generated them. Representative samples of each of the Tertiary volcanic units and the Jura-Cretaceous plutonic phases were taken for detailed lithogeochemistry to constrain interpretations of the genetic history of those rocks. Samples were taken by backpack diamond drilling from within the Endako Mine, and from Tertiary dykes and flows of the surrounding area, for paleomagnetic measurements to quantitatively constrain Tertiary block rotations about horizontal and vertical axes.

The following are the main highlights of the Endako study of 1997:

1. Endako Group basalt occurs in small areas mainly in the southern and central Endako map area. In the central part of the sheet, the basalt forms a thick hyaloclastite breccia overlying andesite and biotite-hornblende-plagioclase dacite of the Ootsa Lake Group (Whalen et al., 1998).
2. The Eocene-age Ootsa Lake Group in the Endako area contains transitions from andesite through rhyolite to dacite crystal tuffs, conglomerates, and basalts. Contacts between mafic to intermediate ash flow and lahar, and rhyodacitic crystal tuffs were observed, and these units were in turn intruded by Eocene quartz-feldspar rhyolite dykes. A chert-, andesite-, and dacite-clast conglomerate to sandstone unit was found interlayered with Eocene rhyolite and rhyodacite to the west. Ootsa Lake Group disconformably overlies plutons of the Francois Lake and Stern Creek suites.
3. Regional tilting of the Endako and Ootsa Lake Groups, as determined from bedding attitudes, has been confirmed by paleomagnetic measurements of Eocene dykes within the Endako Mine. The tilting is controlled by closely spaced extensional faults across which block rotation vary from 10 to 40° (Enkin et al., 1997; Lowe et al., 1998).

4. The Francois Lake and Endako phases of the Late Jurassic Francois Lake plutonic suite appear to be the same age and may be regionally indistinct variations of each other (Whalen et al., 1998). The Endako phase hosts the molybdenum of the Endako Mine.
5. The Francois Lake and Glenannon granodiorite phases each appear to have finely crystalline subphases (Whalen et al., 1998). Miarolitic subvolcanic granodiorite east of Endako Mine may be the carapace of the Francois Lake phase.

Nechako River map area bedrock mapping

Bedrock mapping at 1:100 000 and 1:50 000 scales continued in the Nechako River (NTS 93F) map area by R.G. Anderson (Geological Survey of Canada) and crew concentrated on the Hallett Lake (NTS 93F/15; Anderson and Snyder, 1998), Big Bend Creek (NTS 93F/10; Anderson et al., 1998), and Knapp Lake (93F/14; Anderson et al., unpub. data) map areas. It linked with previous mapping in the south (NTS 93F/07) by Diakow et al. (1997), to the east (NTS 93F/09, 16) by Wetherup (1997), and to the north by Struik et al. (1997, 93K/02) and Whalen et al. (1998, 93K/03). Anderson's core crew of senior mapper L.D. Snyder (University of Wisconsin, Eau Claire, USA), and junior mappers J. Resnick (University of British Columbia) and S. Wearmouth (Upper Caledonia College, Kamloops) was reinforced by volunteers E. Barnes (University of Glasgow), M. Haskin (University of Wisconsin, Eau Claire, USA), and S. Lewis and S.Y. Siew (both from University of Melbourne).

Accomplishments

Stratigraphic sections of Endako Group basalt were measured in detail at Mount Greer (93F/15), Nautley (93K/02), and Kenney Dam (93F/10, Haskin et al., 1998). These units were also extensively sampled for lithogeochemistry and Ar-Ar age determination. N. Grainger, M. Villeneuve, and R. Anderson re-examined some of these contacts as well as the nature and relationships between Ootsa Lake Group and Eocene (?) Copley Lake as reconnaissance for Grainger's 1998 M.Sc. thesis research. D. Thorkelson (Simon Fraser University) completed a two-week reconnaissance of Tertiary volcanic rocks in the Cheslatta Lake (93F/10) map area which will be one focus of 1998 mapping.

1. Moderately to steeply dipping and deformed volcanic and sedimentary rocks of the undivided Hazelton Group, Naglico Formation, and Bowser Lake Group were traced north from NTS 93F/07 (Diakow et al., 1995a, b, 1997) in the Big Bend Creek map area (Anderson et al., 1998). A system of Tertiary block faults deformed Mesozoic and Tertiary basement rocks as a north-trending graben developed synchronously with eruption of the Endako Group.
2. In Hallett Lake area (Anderson and Snyder, 1998), Tertiary faults have protracted down-to-the-southeast motion predating and synchronous with Ootsa Lake and Endako Group volcanism. These faults apparently localized the distribution of the Tertiary volcanic units and may be an upper-plate manifestation of northwesterly-directed ductile extension recorded in the western part of the structurally lower, Eocene Vanderhoof Metamorphic Complex as described by Wetherup (1997).
3. Preliminary mapping in the Knapp Lake area (Anderson et al., unpub. data) revealed significant variations in Ootsa Lake Group stratigraphy noted in the Endako map area (93K/03) to the north. The group rests unconformably on Lower and Middle Hazelton Group rocks. Chilcotin Group olivine-phyric and nodule-bearing glassy basalt is widespread in the southern part of Knapp Lake map area and is mineralogically distinct from Eocene Endako Group clinopyroxene-plagioclase-phyric basalt.
4. Detailed studies of Eocene Endako Group basalts in the Nechako River and southern Fort Fraser areas (Haskin et al., 1998) established the rocks as aphyric to plagioclase-, pyroxene-, and rarely olivine-phyric and commonly amygdaloidal. The Kenney Dam (NTS 93F/10) locality provides the thickest section of Endako Group basalt.

Nechako River and environs Quaternary surficial mapping

Surficial mapping concentrated on the northwest quadrant of Nechako River map area and the north half of 93F/05, and provided ground verification of aerial photograph interpretations. That work was done by A. Plouffe (Geological Survey of Canada) and student assistant J. Bjornson (University of Ottawa) and in the southwest by A. Stumpf (University of New Brunswick) and V. Levson (British Columbia Geological Survey Branch) (Levson et al., in press).

During the 1997 field season, A. Plouffe and J. Bjornson completed the surficial geology mapping of the northwestern sector of Nechako River map area (93F), ie. 93F/11, F/13, and F/14. More than 180 till samples were collected and the extent of glacial lake sediments was mapped in the lowest valleys of this region, including the Francois Lake valley. This summer's findings corroborate the observations by Plouffe (1997) that the maximum elevation of continuous glacial lake sediment cover decreases to the west. Sites interpreted to be susceptible to instability when disturbed were investigated in conjunction with the British Columbia Ministry of Forests.

Abundant striated outcrops in this region reveal a general ice movement to the east and northeast with minor local fluctuations. Very little Quaternary stratigraphy is exposed and no pre-Fraser sediments (pre-late-Wisconsinan) were found.

Geochemical studies

S. Cook (British Columbia Geological Survey Branch) conducted various geochemical studies as follow up to previous surveys done in the Nechako NATMAP Project area.

Accomplishments

RGS interpretation studies

To assess the usefulness of element sum ranking in the search for volcanogenic massive sulphide deposits in Carboniferous-Jurassic Cache Creek Group and Upper Triassic Kutcho Formation rocks, two Takla Lake-area watersheds identified as being in the top five percentiles of the combined Cu-Zn-Pb-Ag data ranking for the western half of the Manson River (NTS 93N) map area were investigated and resampled.

Till dispersal studies

Till dispersal studies were continued in the vicinity of Babine Porphyry Belt copper prospects near the Dorothy and Hearne Hill prospects (93M/1) with V. Levson. Till and profile sampling was conducted at these sites to document glacial dispersal, and copper concentrations in various soil horizons.

Lake sediment studies

An Open File is currently being prepared documenting wide variations in sediment metal concentrations between three distinct sub-basins of Hill-Tout Lake, near the Dual porphyry copper prospect, and their implications for regional geochemical exploration. Fieldwork was conducted to obtain additional surface and bottom-water samples to be analyzed by ICP-MS methods, superior for trace elements such as copper.

Biogeochemical surveys

C.E. Dunn (Geological Survey of Canada) and R. Scagel (Pacific Phytometric Consultants, Surrey) conducted a reconnaissance-level, lodgepole pine sampling program (late July). The sampling extends 1996 northeastern coverage throughout the northwest quadrant of Nechako River. Samples were taken from the outer bark of lodgepole pine. Samples were collected from 282 sites; 265 at 2 km intervals along all driveable roads and trails, and 17 from sites remote from trails (by A. Plouffe).

Biogeochemical work with R. Anderson is testing the possibility of 'fingerprinting' pluton compositions. Vegetation was collected from sites on plutons where samples for lithogeochemical analysis were previously obtained. In particular they will look at rare earth elements (REE) and high field strength elements (HFSE) to determine their patterns. If this technique works, it will provide a quick and economical means to help differentiate underlying rock types (where overburden is thin).

Follow-up sampling was done of last year's reconnaissance biogeochemical survey along the Kluskus forest service road in northeast Nechako River map area (NTS 93F/9, 16). This was to establish the source of Co and Cr enrichment in samples from this area. Enquiries at local forestry offices found that prior to about 1990, parts of the Kluskus road were paved with oxidized volcanic rocks (basaltic) from borrow pits at km 35 and km 36. Samples of the oxidized material and road dust were collected to test for enrichment in Co and Cr. Vegetation was sampled at several sites eastward from the road for a distance of 1 km to ascertain the potential maximum extent of contamination by road dust.

Metals in the environment (MITE)

As part of the Geological Survey of Canada Metals in the Environment (MITE) Initiative, reconnaissance field work was conducted in August 1997 by C. Dunn, P. Rasmussen (Geological Survey of Canada), and A. Plouffe in the area of the old Takla Bralorne mercury mine, located approximately 4 km northwest of the confluence of Silver and Kwanika creeks, in the 93N/11 NTS map area.

The main purpose of the work undertaken by A. Plouffe was to 1) determine if there is any anthropogenic mercury in the humus horizon; 2) identify the different phases of mercury in soil profiles developed on till and glaciofluvial sediments; 3) establish the mobility of these phases; 4) develop criteria to distinguish between natural and anthropogenic mercury; and 5) provide a framework to measurement of mercury flux to the atmosphere (by P. Rasmussen). This summer, humus, B-horizon, and, till and/or glaciofluvial sediments were sampled at a total of 13 sites in the Silver Creek and Kwanika Creek valleys, and detailed sampling of soil profiles was done at two sites.

P. Rasmussen, C. Dunn and G. Edwards (University of Guelph) collected biogeochemical samples at the same sites as A. Plouffe and at additional sites along the Pinchi fault zone as part of a nation-wide survey of natural mercury emissions to the atmosphere. Results will be used to evaluate the Takla Bralorne site and other areas as potential mercury flux monitoring sites.

Industrial minerals investigations

D. Hora and G. Simandl (British Columbia Geological Survey Branch) continued follow up on industrial mineral and precious stone sites previously known and newly reported during mapping of the Nechako project. Dimension stone, decomposed lapilli tuffs (for clays), ornamental and landscaping rock (basalts mainly), perlite, vermiculite, opal, and agate were investigated.

Geographic Information System development

S. Williams and N. Hastings (both from Geological Survey of Canada) continued development of the Nechako Project digital point, line, and areal database and query system. Work focused on digital integration of the bedrock mapping data donated by Placer Dome Ltd., the digitization and cartography of geological maps, and the initiation of an internet GIS data-sharing system. D. MacIntyre initiated the use of ARC/INFO™ at the British Columbia Geological Survey Branch for digital cartography and for GIS database development.

Accomplishments

1. Creation of a GIS database of the Placer Dome bedrock geology maps for the Endako Mine and surrounding region has been completed. This database includes half of the field notes gathered during that project. All of this information will be combined with Nechako Project mapping.
2. Several new geological maps are in the process of production as coloured 1:100 000 and 1:50 000 scale bedrock maps.
3. This summer the Nechako Project supported and initiated the acquisition and installation of Autodesk MapGuide™ and its appropriate server hardware and software at the Vancouver Office. MapGuide™ is a collection of software packages (Server, Author and Reader) that provides real-time WEB browser access to maps and their associated databases. MapGuide has been used extensively by the British Columbia Geological Survey Branch to make the Mineral Potential of British Columbia project data accessible over the World Wide Web. We hope to use MapGuide first to distribute the digital data for the Nechako Project to its participants to facilitate research. Later we hope to be able to use it for broader distribution of the data.

For monthly updates in Nechako NATMAP Project developments, see the Nechako Newsletters posted on the Nechako Project website (http://www.ei.gov.bc.ca/~NATMAP/) during the life of the project.

ACKNOWLEDGMENTS

All project participants contributed to the success of this years research and to this overview. Project funding comes directly through continuing Geological Survey of Canada and British Columbia Geological Survey Branch programs and the Geological Survey of Canada NATMAP program. In addition, in-kind funding comes from the many universities and industry listed throughout the text.

REFERENCES

Anderson, R.G. and Snyder, L.D.
1998: Jurassic to Tertiary volcanic, sedimentary, and intrusive rocks in the Hallett Lake area, central British Columbia; in Current Research 1998-A; Geological Survey of Canada.

Anderson, R.G., Snyder, L.D., Resnick, J., and Barnes, E.
1998: Geology of the Big Bend Creek map area, central British Columbia; in Current Research 1998-A; Geological Survey of Canada.

Ash, C.H., MacDonald, R.W.J., and Paterson, I.A.
1993: Geology of the Stuart - Pinchi Lakes area, central British Columbia; British Columbia Ministry of Energy, Mines and Petroleum Resources, Open File 1993-9, 1:100 0000.

Diakow, L.J., Webster, I.C.L., Richards, T.A., and Tipper, H.W.
1997: Geology of the Fawnie and Nechako Ranges, southern Nechako Plateau, central British Columbia (93F/2,3,6,7); in Interior Plateau Geoscience Project: Summary of Geological, Geochemical and Geophysical Studies, (ed.) L.J. Diakow and J.M. Newell; British Columbia Geological Survey Branch, Open File 1996-2 and Geological Survey of Canada, Open File 3448, p. 7-30.

Diakow, L.J., Webster, I.C.L., Whittles, J.A., and Richards, T.A.
1995a: Stratigraphic highlights of bedrock mapping in the Southern Nechako Plateau, Northern Interior Plateau Region; in Geological Fieldwork 1994, B. Grant and J.M. Newell (ed.); British Columbia Ministry of Energy, Mines and Petroleum Resources, Paper 1995-1, p. 171-176.

Diakow, L.J., Webster, I.C.L., Whittles, J.A., Richards, T.A., Giles, T.R., Levson, V.M., and Weary, G.F.
1995b: Bedrock and surficial geology of the Chedakuz Creek map area (NTS 93F/7); British Columbia Ministry of Energy, Mines and Petroleum Resources, Open File 1995-17, 1:50 000.

Enkin, R.J., Baker, J., Struik, L.C., Wetherup, S., and Selby, D.
1997: Paleomagnetic determination of post-Eocene tilts in the Nechako Region; Geological Association of Canada/Mineralogical Association of Canada, Abstracts , p. A46.

Haskin, M.L., Snyder, L.D., and Anderson, R.G.
1998: Tertiary Endako Group volcanic and sedimentary rocks at four sites in the Nechako River and Fort Fraser map areas, central British Columbia; in Current Research 1998-A; Geological Survey of Canada.

Hrudey, M.G. and Struik, L.C.
1998: Field observations of the Tachie Pluton near Fort St. James, central British Columbia; in Current Research 1998-A; Geological Survey of Canada.

Kimura, E.T., Bysouth, G.D., Cyr, J., Buckley, P., Peters, J., Boyce, R., and Nilsson, J.
1980: Geology of parts of southeast Fort Fraser and northern Nechako River map areas, central British Columbia; Placer Dome Incorporated, Internal Report and Maps, Vancouver, British Columbia.

Levson, V., Stumpf, A., and Stuart, A.
in press: Quaternary geology studies in the Smithers and Hazelton map areas (93L and M): Implications for exploration; in Geological Fieldwork 1997; British Columbia Ministry of Employment and Investment, Paper 1998-1.

Lowe, C., Enkin, R.J., and Dubois, J.
1998: Magnetic and paleomagnetic constraints on Tertiary deformation in the Endako region, central British Columbia; in Current Research 1998-A; Geological Survey of Canada.

MacIntyre, D.G.
in press: Babine Porphyry Belt Project: Bedrock geology of the Nakinilerak Lake map sheet (93M/8), British Columbia; in Geological Fieldwork 1997; British Columbia Ministry of Employment and Investment, Paper 1998-1.

MacIntyre, D.G. and Struik, L.C.
in press: Nechako Natmap Project: 1997 Overview; in Geological Fieldwork 1997; British Columbia Ministry of Employment and Investment, Paper 1998-1.

MacIntyre, D.G., Struik, L.C., and Schiarizza, P.
in press: Preliminary bedrock geology of the Tochcha Lake map sheet (93K/13), British Columbia; in Geological Fieldwork 1997; British Columbia Ministry of Employment and Investment, Paper 1998-1.

McMillan, W.M. and Struik, L.C.
1996: NATMAP: Nechako Project, central British Columbia; in Geological Fieldwork 1995, (ed.) B. Grant and J.M. Newell; British Columbia Ministry of Energy, Mines and Petroleum Resources, Paper 1996-1, p. 3-9.

Nelson, J.L., Bellefontaine, K.A., Green, K.C., and Maclean, M.E.
1991: Geology and mineral potential of Wittsichica Creek and Tezzeron Creek map areas; British Columbia Ministry of Energy, Mines and Petroleum Resources, Open File 1991-3, 1:50 000.

Orchard, M.J., Struik, L.C., and Taylor, H.
1998: New conodont data from the Cache Creek Group, central British Columbia; in Current Research 1998-A; Geological Survey of Canada.

Paterson, I.A.
1973: The geology of the Pinchi Lake area, central British Columbia; Ph.D. thesis, University of British Columbia, Vancouver, British Columbia, 263 p.

Plouffe, A.
1997: Ice flow and late glacial lakes of the Fraser Glaciation, central British Columbia; in Current Research 1997-A; Geological Survey of Canada, p. 133-144.

Sano, H.
1998: Preliminary report on resedimented carbonates associated with basaltic rocks of Cache Creek Group near Spad Lake, east of Fort St. James, central British Columbia; in Current Research 1998-A; Geological Survey of Canada.

Schiarizza, P., Massey, N.W.D., and MacIntyre, D.G.
in press: Geology of the Sitlika assemblage in the Takla Lake area (93N/3,4,5,6,12); in Geological Fieldwork 1997; British Columbia Ministry of Employment and Investment, Paper 1998-1.

Struik, L.C. and McMillan, W.J.
1996: Nechako Project Overview, central British Columbia; in Current Research 1996-A; Geological Survey of Canada, p. 57-62.

Struik, L.C. and MacIntyre, D.G.
1997: Nechako Plateau NATMAP Project Overview, central British Columbia, year two; in Current Research 1997-A; Geological Survey of Canada, p. 57-64.

Struik, L.C., Whalen, J.B., Letwin, J.M., and L'Heureux, R.
1997: General geology of southeast Fort Fraser map area, central British Columbia; in Current Research 1997-A; Geological Survey of Canada, p. 65-75.

Wetherup, S.
1997: Geology of the Nulki Hills and surrounding area (NTS 93F/9 and F/16), central British Columbia; in Current Research 1997-A; Geological Survey of Canada, p. 125-132.

Whalen, J.B., Struik, L.C., and Hrudey, M.G.
1998: Bedrock geology of the Endako map area, central British Columbia; in Current Research 1998-A; Geological Survey of Canada.

Geological Survey of Canada Project 950036-02

Preliminary report on resedimented carbonates associated with basaltic rocks of Cache Creek Group near Spad Lake, east of Fort St. James, central British Columbia[1]

H. Sano[2]
GSC Pacific, Vancouver

Sano, H., 1998: Preliminary report on resedimented carbonates associated with basaltic rocks of Cache Creek Group near Spad Lake, east of Fort St. James, central British Columbia; in Current Research 1998-A; Geological Survey of Canada, p. 89-97.

Abstract: A 220 m thick sequence of resedimented limestone and basaltic volcaniclastic rocks of the Pope formation is exposed in a quarry east of Fort St. James. The rocks are informally designated the Spad Lake member. Fragmented and abraded fusuline debris from the limestone is preliminarily assessed an upper Asselian age. The base of the Spad Lake member is basalt breccia. The lower to middle part has disorganized, completely unsorted limestone breccia (debris flows) and crudely graded granule-pebble limestone conglomerate (basal Bouma sequence) of shallow-marine affinity. The bedded, thick upper part has graded, densely packed granule-pebble limestone conglomerate, crudely laminated limestone sandstone, and stylonodular-bedded siliceous lime-mudstone with chert nodules, and is interpreted as turbidites resedimented by high-density turbidity currents. The Spad Lake member was probably formed on an upper flank of a shallow-marine buildup resting upon a basaltic substratum probably of a plateau, or seamount. The Pope formation limestone may be from the platform top.

Résumé : Une séquence de 220 m d'épaisseur de calcaire resédimenté et de roches volcanoclastiques basaltiques de la formation de Pope, à laquelle on a donné le nom informel de «membre de Spad Lake», affleure dans une carrière à l'est de Fort St. James. Des débris fragmentés et abrasés de fusilines provenant du calcaire sont datés provisoirement de l'Asselien supérieur. La base du membre de Spad Lake est une brèche basaltique. La partie inférieure à moyenne du membre comporte une brèche calcaire (coulées de débris) désorganisée et complètement non triée et un conglomérat à granules-cailloux de calcaire (base de la séquence de Bouma) grossièrement granoclassé de milieu marin peu profond. La partie supérieure épaisse et litée du membre comprend un conglomérat à granules-cailloux de calcaire granoclassé, d'un grès calcaire imparfaitement laminé et d'un calcaire micritique siliceux à nodules de chert; il s'agirait de turbidites resédimentées par des courants de turbidité de forte densité. Le membre de Spad Lake s'est probablement accumulé sur le flanc supérieur d'un monticule épicontinental reposant sur un substratum basaltique, probablement d'un plateau ou d'un mont sous-marin. Le calcaire de la formation de Pope pourrait provenir du sommet de la plate-forme.

[1] Contribution to the Nechako NATMAP Project
[2] Department of Earth & Planetary Sciences, Kyushu University, Fukuoka, 812-81 Japan

INTRODUCTION

During 1997 fieldwork, as a part of the Nechako NATMAP project, a variety of clastic limestones of the Pope formation were found with basaltic volcaniclastic rocks in a quarry near the Spad Lake, east of Fort St. James. The clastic limestones and basaltic rocks are intimately associated with each other and form a distinct lithologic association. The succession, herein named the Spad Lake member, reaches 220 m or more in thickness. The sedimentary fabric of the clastic limestones implies their redeposition by sediment-gravity flows including debris flows and turbidity currents. The clast association indicates their origin in a shallow-marine buildup. Fragmented and abraded fusuline debris of the upper Asselian was identified from the upper part of the clastic limestone succession. The clastic limestones are thought to have been displaced by sediment-gravity flows from a shallow-marine buildup and redeposited most probably on an upper slope of an oceanic plateau or a basaltic seamount.

This preliminary report focuses upon the lithostratigraphy of the Spad Lake member characterized by resedimented shallow-marine limestones closely associated with basaltic volcaniclastic rocks. The field properties of the redeposited limestones, the variety of clastic natures, and the basaltic rocks are also described. Although thin and sporadic beds of clastic limestones in a bedded chert succession of the Pope formation have been reported by Sano and Struik (1997), no such thick sequence of the redeposited limestones in a close association with basaltic volcaniclastic rocks has been previously documented in the area of Fort St. James. Along with several limestone types of the Pope formation recognized by Sano and Struik (1997), the resedimented limestones of the Spad Lake member play an important role for the facies interpretation of shallow-marine carbonates of the Pope formation.

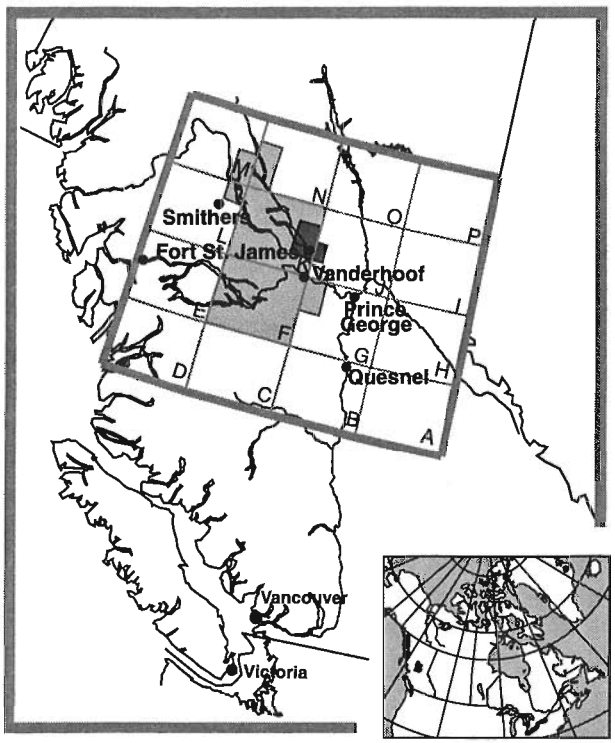

Figure 1. Location of the study area. The grid represents 1:1 000 000 scale map of Parsnip River (NTS 93).

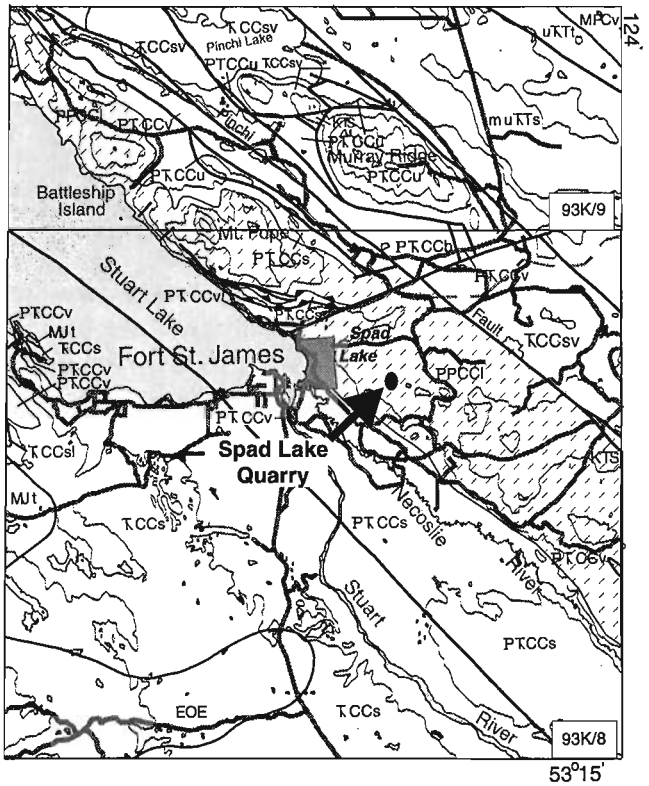

Miocene and Pliocene
- MPCv — Chilcotin Group: olivine basalt

Eocene
- EOE — Endako Group: basalt, andesite

Cretaceous and Tertiary
- KTS — Sifton Formation: conglomerate

Jurassic
- MJt — tonalite, diorite

Triassic
Takla Group (uTRt, muTRTs)
- uTRt — tuff, cherty tuff, siliceous argillite
- uTRv — basalt
- muTRTs — argillite, greywacke, siltstone, shale, minor limestone, tuff, basalt

upper Carboniferous to Triassic
Cache Creek Group (TRCCsv - PTRCCb)
- TRCCsv — Pinchi sequence: greywacke, silstone, slate, basalt tuff, minor limestone, siliceous argillite
- Sowchea sequence (TRCCs - PTRCCsl)
- TRCCs — argillite, chert, siltstone, phyllite, phyllite, sandstone, limestone, basalt
- TRCCsl — limestone, greenstone,chert
- PTRCCs — ribbon chert, siltstone, slate, minor basalt tuff
- PPCCl — Pope formation: limestone, greenstone, chert
- PTRCCv — basalt, minor limestone, argillite, chert
- PTRCCu — Trembleur Ultramafics: serpentinite, harzburgite, dunite, peridotite, carbonatized equivalents
- PTRCCb — blueschist (chert, schist, greywacke, metabasalt, limestone

Figure 2. Geological map of Fort St. James area, central British Columbia. Arrow indicates location of the quarry, south of Spad Lake, east of Fort St. James. The base map is modified from Bellefontaine et al. (1995).

GEOLOGICAL SUMMARY

The area of Fort St. James, central British Columbia (Fig. 1) is known as one of the excellent outcrop areas of the Paleozoic and Mesozoic rocks of the Cache Creek Group. The Cache Creek rocks of this area are distributed in a general northwest-southeast trending belt, up to 7 km wide (Fig. 2).

The Cache Creek Group comprises a lithologically and structurally complicated aggregate of sedimentary, volcanic, and metamorphic rocks. These rocks are informally divided into five units in the Fort St. James area (Struik et al., 1996). They are the Trembleur ultramafics, composed mainly of the serpentinite and harzburgite; the Railway gabbro, composed chiefly of gabbro and basalt; the Pope formation, characterized by shallow-marine limestone, and undifferentiated basaltic rocks; the Sowchea sequence, dominated by ribbon-bedded chert, argillite, and greywacke with minor basalt and limestone; and the Pinchi sequence, chiefly consisting of argillite, greywacke, and basalt (Fig. 2). The sedimentary rocks of the Cache Creek Group in this region range in age from the Late Carboniferous to the Late Triassic.

The Pope formation is a conspicuous rock unit that characterizes the Cache Creek Group of the Fort St. James area. The major component of the formation is a thick pile of massive, shallow-marine limestone with subordinate basaltic rocks and ribbon-bedded chert (Cordey and Struik, 1996; Struik et al., 1996). The limestones yield shallow-marine organic debris, including crinoids, fusulines and smaller foraminifers, mollusks, *Komia*, chaetetids, corals, calcareous algae, and cyanobacteria (Sano and Struik, 1997). Much of the limestone of the Pope formation is bioclastic. In addition to the predominant bioclastic limestone, Sano and Struik (1997) recognized a small amount of cyanobacterial boundstone, as well as thin and sporadic beds of clastic limestone in a ribbon-bedded chert succession.

The limestone of the Pope formation of the Fort St. James area has been dated by fusulines and conodonts (Thompson et al., 1953; Thompson, 1965; Orchard and Struik, 1996; Orchard et al., 1997, 1998). According to these authors, the limestone is considered to be mostly referable to as Bashkirian to Moscovian, and much less commonly Gzhelian to Asselian.

SPAD LAKE MEMBER

Various types of clastic limestone of the Pope formation extensively outcrop with basaltic rocks and tuffaceous-siliceous shale in and around a quarry, about 1 km south of the Spad Lake, east of Fort St. James (Fig. 2). The rocks have a general northwest-southeast strike and are steeply inclined to the northeast (Fig. 3). Sedimentary structures seen in the clastic limestone indicate the normal stratigraphy, the beds younging to the northeast.

Though the stratal continuity has been disrupted in places, careful observation and mapping revealed that the clastic limestone and associated rocks form a distinct stratigraphic unit, informally designated the Spad Lake member. Despite

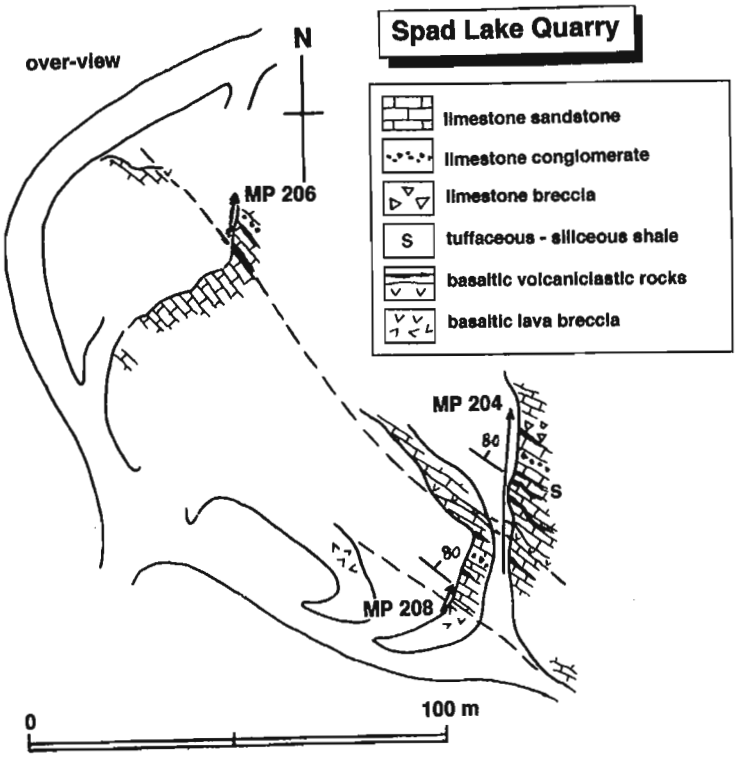

Figure 3.

Map showing distribution of northwest-southeast trending and steeply north-dipping basaltic rocks and clastic limestones of Spad Lake member in the quarry south of Spad Lake. Localities of measured sections MP 204, 206, and 208 are shown.

its distinctive lithologic association, no correlative rocks have been described in the Pope formation in the area of Fort St. James.

The Pope formation around the Spad Lake has been insufficiently dated. Thompson et al. (1953) and Thompson (1965) described the Moscovian fusuline fauna including *Akiyoshiella toriyamai*, *Fusulinella jamesensis*, *Millerella* sp., and several species of *Nankinella* and *Staffella* from a locality near the quarry. Orchard et al. (1997) recently reported upper Bashkirian to Moscovian conodont faunas from two localities southwest of the quarry (K8-16, 17) and Bashkirian faunas from several localities southeast of the quarry (K8-11, 12, 13, 14).

The preliminary examination revealed that the upper part of the Spad Lake member contains fragmented and abraded fusuline debris indicative of the upper Asselian. The fusuline debris includes a few species of the genus *Pseudofusulina*.

Lithostratigraphy

The rocks of the Spad Lake member most typically outcrop in the quarry (Fig. 3) and along the roadcut exposure immediately north of the quarry. The Spad Lake member predominantly consists of three types of clastic limestone in close association with basaltic volcaniclastic rocks and minor tuffaceous-siliceous shale (Fig. 4). The clastic limestone of the Spad Lake member is often dolomitized and contains nodular chert.

The Spad Lake member is lithologically subdivided into the lower, middle, and upper units (Fig. 4). The total thickness that the member attains is 220 m, so far as it is exposed in and around the quarry. The stratigraphic relationship of the member to the other rock units of the Cache Creek Group remains uncertain.

The lower unit begins with basaltic lava breccia that is directly covered by alternating beds of dolomitic limestone and basaltic volcaniclastic rocks; which, in turn, are

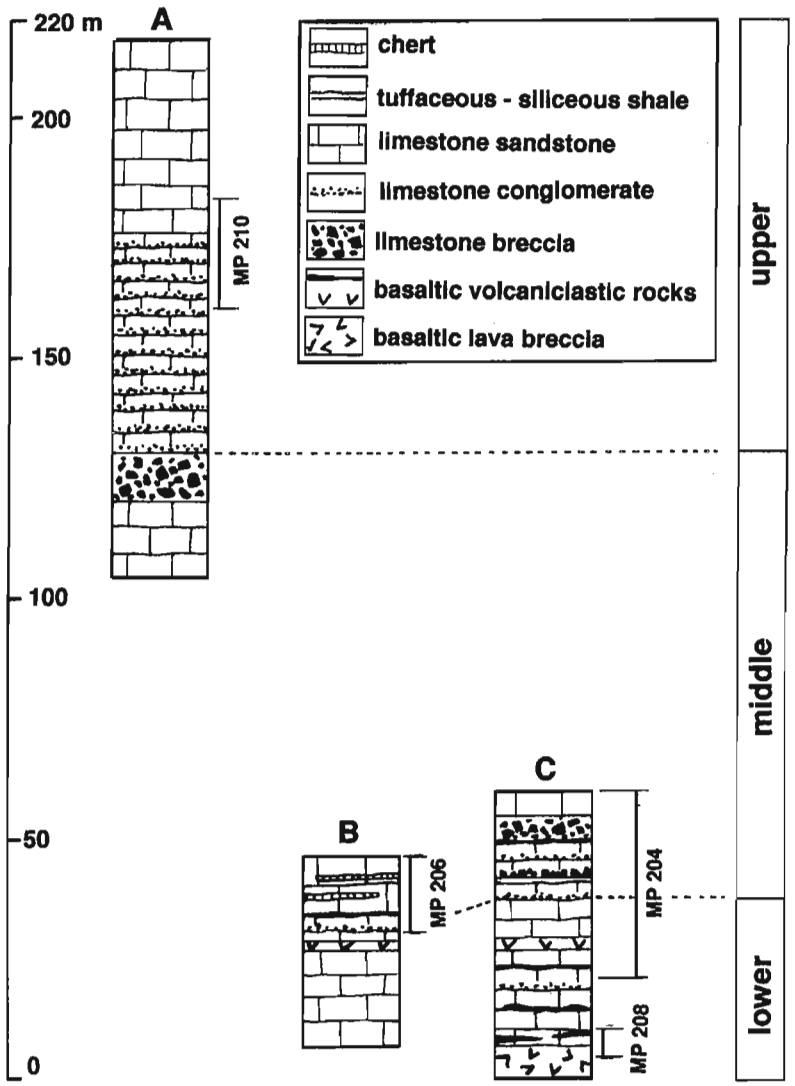

Figure 4.

Lithostratigraphy of basaltic rocks and clastic limestones of the Spad Lake member. Column A was measured along roadcut exposures outside the quarry, about 50 m north of the locality MP 206, and columns B and C were measured in the southeastern and northwestern parts of the quarry. Approximate stratigraphic positions of localities MP 204 in Figure 6 and MP 206 and 208 in Figure 5 are shown.

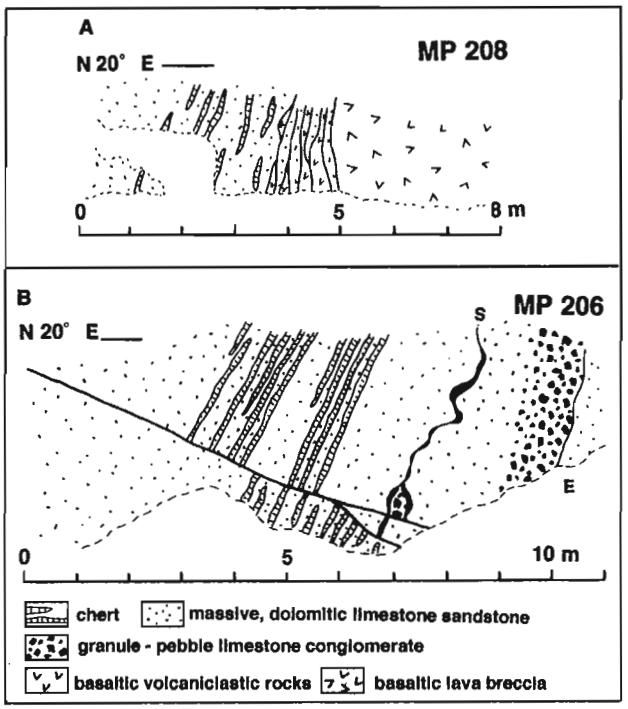

Figure 5.

Field-sketches showing stratigraphic relationship between basaltic rocks and clastic limestones of Pope formation. See Figure 3 for localities and Figure 4 for approximate stratigraphic levels.

A. Basaltic lava breccia and associated volcaniclastic rocks having lenticular limestone beds overlain by thick and massive, dolomitic limestone sandstone containing chert nodules. MP 208 section at the basal part of the Spad Lake member.

B. Stylolitized, thin intercalation of basaltic volcaniclastic rocks in massive, dolomitic limestone sandstone containing nodular chert and crudely graded limestone conglomerate of which bottom surface is well defined and erosional. Lower part of the middle Spad Lake member.

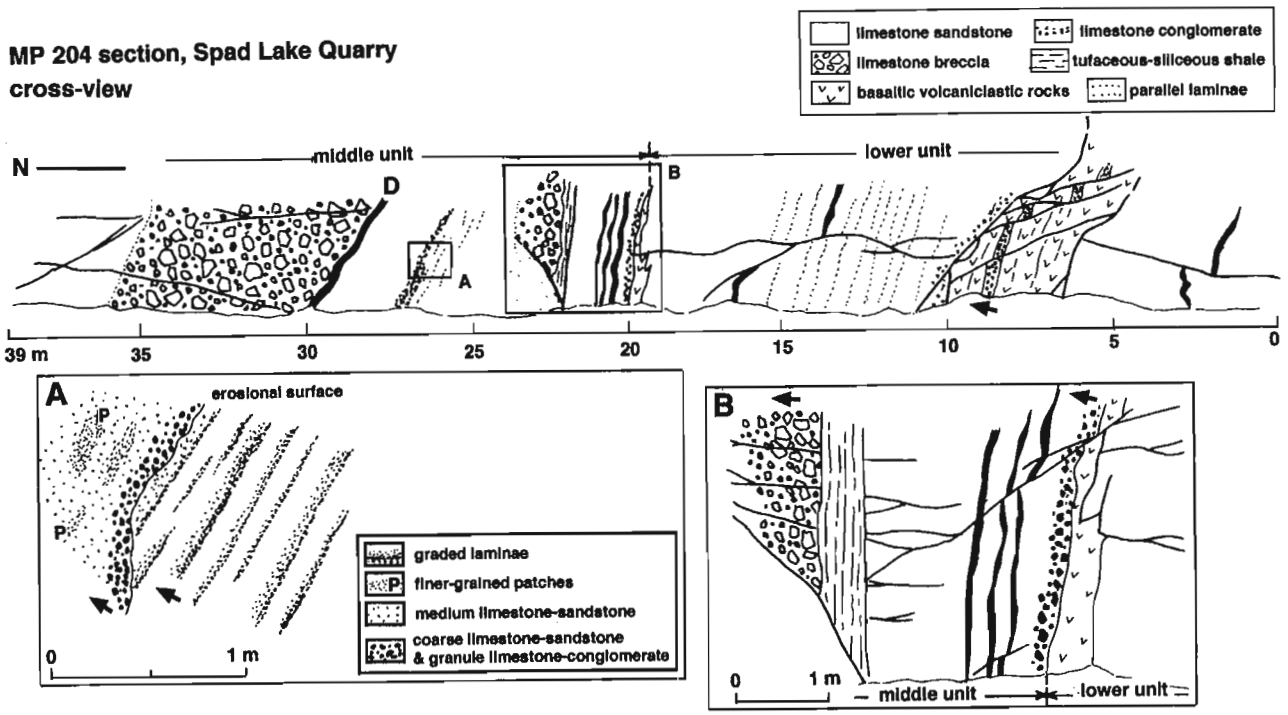

Figure 6. Stratigraphic succession of basaltic volcaniclastic rocks, tuffaceous-siliceous shale, and clastic limestones of the lower and middle units of the Pope formation, measured at MP 204. See locality for Figure 3. Short arrows indicate the face of beds. D denotes coarse sand-grained basaltic volcaniclastic rock having abundant dolomitic limestone debris. Close-up view in inset A shows erosional bottom surface of granule limestone conglomerate clearly truncating graded laminae of underlying medium-grained limestone sandstone. Abrupt lithologic change between tuffaceous-siliceous shale below and limestone breccia above is shown in inset B.

succeeded by a thick dolomitic limestone, in places containing lenticular nodules of chert (Fig. 5A). The top of the lower unit is occupied by basaltic volcaniclastic rocks, which are overlain by granule-pebble limestone conglomerate of the middle unit with an irregularly undulated and knobby, erosional surface (Fig. 6B). The middle unit is characterized by thick, crudely graded beds of limestone breccia and dolomitic limestone, and contains minor basaltic volcaniclastic rocks and tuffaceous siliceous shale (Fig. 4, 7). The basaltic rocks are intercalated in the middle unit (Fig. 5B, 7), but are much less abundant than in the lower unit. The upper unit consists chiefly of graded limestone beds of a turbidite origin, which are overlain by massive dolomitic limestone containing some chert nodules.

Basaltic rocks

The basaltic lava breccia at the base of the member (Fig. 5A) is dark greenish and consists of cobble- to boulder-sized, poorly sorted, angular clasts of basalt lava randomly set in a matrix of coarse-grained hyaloclastic materials. The lava clasts are, in places, highly vesiculated. The basaltic volcaniclastic rocks are intercalated at several stratigraphic levels of the lower and middle units of the Spad Lake member (Fig. 4). It is noted that the basaltic rocks decrease in amount up-section through the entire succession of the Spad Lake member. The rocks are mainly greenish, but in places dark reddish, and often calcareous. Most of the volcaniclastic rocks seem to have been altered so that constituent grains are invisible in the field. Poorly defined siliceous laminae occur sporadically. The thickness of the basaltic volcaniclastic rocks ranges from a few centimetres (Fig. 5B) to a few metres (Fig. 6, 7). Bed thickness changes abruptly laterally, chiefly due to stylolitization (Fig. 5B). The graded limestone bed and crowded, subangular and pebble-sized limestone debris are locally contained in the basaltic volcaniclastic rocks (Fig. 6).

Tuffaceous – siliceous shale

Though thin and rare, an intercalation of tuffaceous and siliceous shale occurs in the lower part of the middle unit (Fig. 6B). The limestone breccia directly overlies the shale, and the contact is gently undulated and erosional. The shale is greenish-grey, crudely laminated, extremely fine grained and fissile, and seems to have been contaminated with basaltic volcaniclastic material.

Clastic limestone

Three types of clastic limestone and related rocks, differing in the grain size and fabric as well as components, were seen in the Spad Lake member. They were described as limestone

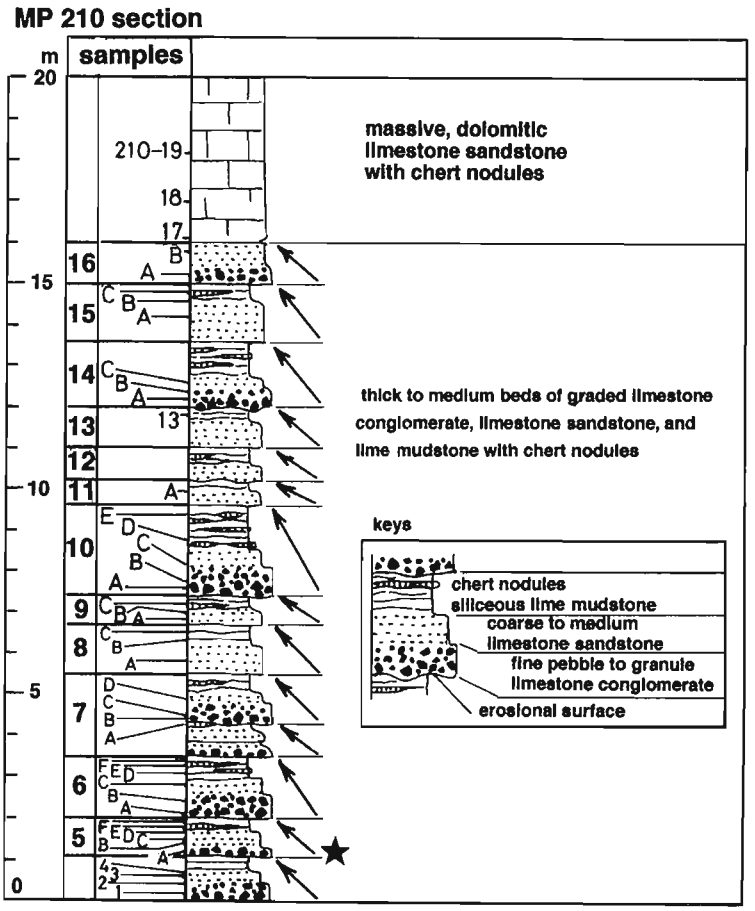

Figure 7.

Lithostratigraphy of the turbiditic succession comprising graded limestone conglomerate, limestone sandstone, and siliceous lime-mudstone in the lower part of the upper Spad Lake member. A star indicated the stratigraphic position of the limestone conglomerate containing fragments of upper Asselian fusulines. Measured along the roadcut exposure approximately 50 m north of loc. MP 206 in Figure 3.

breccia, limestone conglomerate, and limestone sandstone in the field. Their field-scale properties are briefly described below.

The limestone breccia occurs at a few levels of the middle unit (Fig. 4) and is most typically seen in the lower part exposed in the quarry (Fig. 6). The thickness ranges from less than 1 m (Fig. 6B) to 15 m (Fig. 4).

The limestone breccia is composed predominantly of limestone and dolomitic limestone clasts and has minor basaltic debris and fragmented skeletal debris, all embedded in a dolomitic matrix. The carbonate clasts are almost disorganized and poorly sorted, but crudely graded (Fig. 6). The size of the clasts ranges from a few millimetres to several tens of centimetres or more. The clasts are invariably angular and irregularly shaped. The clast association is polymictic, comprising various types of limestones having a shallow-marine affinity. The skeletal debris mainly comprises crinoids and fusulines. The basaltic detritus is dark greenish and usually less than the sand size. The matrix is weathered yellowish-brown and in place greenish where a large amount of the fine-grained basaltic detritus is included. The matrix is dolomitic and heavily crystalline. Large-sized clasts are usually clast supported, but smaller ones of basaltic and skeletal debris are supported by the matrix.

The limestone conglomerate is intercalated at several levels of the lower and middle units (Fig. 5B, 6), and also occurs forming a lower division of a limestone turbidite sheet of the upper unit (Fig. 7). The bottom of the limestone conglomerate beds are well defined and often erosional (Fig. 6A). The thickness of the beds rarely exceed 1 m, and is most commonly a few to several tens of centimetres.

The limestone conglomerate is characterized by a densely packed fabric of granule- to pebble-sized limestone gravels, coarse sandy crinoid and fusuline debris, and sandy basaltic debris with a generally sparse carbonate matrix. Beds of limestone conglomerate grade up into the overlying massive dolomitic limestone sandstone (Fig. 6B). The limestone gravels and skeletal debris are subrounded to subangular. The skeletal debris is almost invariably fragmented. The granule-sized limestone gravels and crinoidal debris are crudely oriented in many cases. The clast association is polymictic, consisting of various types of the shallow-marine limestone and dolomite. The basaltic debris is sand-sized, and much less abundant than the limestone clasts and skeletal debris. All these carbonate and basaltic particles are supported by one another to form a coarse-grained packstone fabric. Stylolites commonly formed along the clast boundaries. The matrix seems to consist of poorly sorted lime-silt to sand and has often been dolomitized.

Two types of these gravely limestones are contaminated with sand-sized basaltic debris. They are generally inconspicuous, but often occur condensed in basal parts of the gravely limestones, which are directly underlain by the basaltic rocks (Fig. 6).

The limestone sandstone constitutes the most predominant component of the Spad Lake member (Fig. 4). It most commonly outcrops as thick beds, attaining several metres in thickness or more, with the limestone breccia and limestone conglomerate. The limestone sandstone also occurs in the bedded limestone succession of the lower part of the upper unit, forming a middle division of a turbiditic sheet with an incomplete Bouma sequence (Fig. 7). Although many of the primary fabrics have been obliterated by dolomitization, the limestone sandstone appears to have an arenitic texture with some limy matrix. Skeletal fragments recognizable in the limestone sandstone include crinoids and fusulines. The skeletal fragments are mainly coarse to medium sand-sized, and in many cases are sorted and densely packed. Crudely graded laminae, usually a few centimetres thick and laterally discrete, are seen in thick beds of the limestone sandstone (Fig. 6A). Parallel laminae are locally present (Fig. 6). The limestone sandstone often contains layer-shaped to elongated nodules of chert at many stratigraphic levels (Fig. 5B).

The sedimentary features indicate that the limestone breccia of the Spad Lake member was deposited by debris flows. The absence of preferred clast orientation, very poor sorting of clasts, and massive to unstratified bedding style of the Spad Lake limestone breccia are characteristic of a limestone debride. The Spad Lake limestone breccia in many cases has a clast-supported fabric. A debris-flow deposit is generally known to have a matrix-supported fabric, but the clast-supported debris-flow deposits are also reported to occur along with matrix-supported ones off the Bahamas (Mullins et al., 1984).

The limestone conglomerate and limestone sandstone of the middle Spad Lake member are thought to be graded and horizontally laminated divisions (Ta-b) of an incomplete Bouma sequence that lacks upper fine-grained divisions. Thus, thick beds of the middle Spad Lake limestone conglomerate and limestone sandstone are considered to result from amalgamation of two or more flows.

Bedded limestones

A conspicuous succession of bedded limestones of the lower part of the upper unit (Fig. 4) have more distinct characteristics of turbiditic sedimentation than the amalgamated thick beds of the limestone conglomerate and limestone sandstone of the middle unit. The bedded limestone succession characterizes the Spad Lake member.

The upper Spad Lake bedded limestone rests upon the limestone breccia of the middle unit and underlies a thick section of massive dolomitized limestone that in places contains chert nodules (Fig. 4). The entire bedded limestone succession is approximately 50 m thick (Fig. 4). Detailed measurement of the upper part revealed 13 turbiditic sheets, each of which averages approximately 1.2 m in thickness (Fig. 7).

The turbidite sheets in many cases comprise a graded bed of limestone conglomerate like the lower division, limestone sandstone like the middle division, and lime-mudstone with greenish shale partings, chert nodules, and marly interlayers characteristic of the upper division (Fig. 7). A few of the turbiditic sheets begin with the limestone sandstone, without a lower division of the limestone conglomerate (e.g. MP 210-13, 15 in Fig. 7). Lower, middle, and upper divisions are in many cases several tens of centimetres to 1 m, a few to several tens of centimetres, and several tens of centimetres to 1 m thick, respectively.

The limestone conglomerate of the lower division most commonly consists of granule- to pebble-sized limestone clasts, sand-sized skeletal fragments, and a very sparse limy matrix. The limestone clasts are polymictic, poorly sorted, subrounded to subangular, and crudely laminated and oriented. Crinoids occur as the most abundant skeletal fragments. Fusulines are almost always fragmented and their outer shells have been exfoliated in many cases. A few species of the genus *Pseudofusulina*, indicative of the upper Asselian, were identified during preliminary examination (Fig. 7). All these limestone clasts and skeletal fragments are densely packed within the sparse limy matrix. The bottom surface of the lower division is always sharp and well defined and occasionally gently undulated and erosional. The size of the clasts and skeletal fragments gradually decreases upward, grading up-section into the limestone sandstone of a middle division.

The limestone sandstone of a middle division is coarse to medium grained, often siliceous and dolomitic, and crudely laminated. Discernible in the field are sand-sized crinoidal debris and foraminifers, exhibiting an arenitic texture.

The upper division consists of lime mudstone having abundant chert nodules and rare greenish shale partings. The lime mudstone is very fine grained, highly siliceous, dolomitic, and wavy- to stylonodular-bedded. Greenish shaly partings are seen in places along the wavy bedding surfaces. The chert nodules are grey to black, a few to several centimetres thick, and aligned nearly parallel to the bedding surface. Wavy- to nodular-bedded interlayers of light grey and siliceous marlstone are occasionally seen in the lime mudstone. They are less than 4 cm thick and have gently undulated top and bottom surfaces.

No complete Bouma sequence has been recognized in the bedded limestone succession of the upper Spad Lake member. However, according to the criteria for the identification of resedimented limestones (Flügel, 1982; Tucker and Wright, 1990), the upper Spad Lake member is best described as a succession predominantly of incomplete limestone turbidites. The lower, middle, and upper divisions are most likely to be compared to Ta, Ta-b, and Te, but the horizontal laminae are in many cases indistinct and crossbedding is totally absent. The internal sedimentary structure, as well as the grain-size distribution, implies that the upper Spad Lake limestone turbidites were resedimented by high-density turbidity currents.

In summary, the entire succession of the Spad Lake member is characterized by the basaltic volcaniclastic rocks in the lower unit, carbonate debrides in the middle, and calciturbidites in the upper. Turbidity currents and debris flows responsible for the redeposition of the Spad Lake limestone are closely related and combined with each other.

DISCUSSION

A thick succession of resedimented limestone in close association with basaltic rocks was first described in the Pope formation in the area of Fort St. James. Although the areal extent as well as the stratigraphic distribution remains uncertain, a variety of the resedimented limestones offers a significant clue to the facies interpretation of shallow-marine carbonates of the Pope formation.

Sano and Struik (1997) reported intermittent beds of graded and densely packed granule-cobble limestone conglomerate and crudely laminated, medium-grained, arenitic limestone sandstone in a chert-micrite succession at the southeastern foot of Mt. Pope. The limestone clasts invariably have a shallow-marine affinity and these clastic limestones contain an appreciable amount of basaltic detritus. The sedimentary features of this clastic limestone show their redeposition was chiefly due to high-density turbidity currents that transported shallow-marine carbonate debris together with basaltic detritus from a shallow-marine buildup into a deep-water basin where the chert and micrite accumulated. An admixture of the basaltic detritus in these clastic limestones implies the existence of a basaltic substratum underlying the shallow-marine buildup. The clastic limestones exposed at the foot of Mt. Pope and in the Spad Lake quarry are similar in fabric and components. Both clastic limestones are comparable to a variety of gravitationally displaced shallow-marine carbonate.

The clastic limestones at the two localities, however, differ markedly in thickness as well as lithologic association. The clastic limestone beds at the foot of Mt. Pope are less than 1 m thick and occur intercalated in a radiolaria- and sponge spicule-bearing, ribbon-bedded, chert-micrite, deep-water facies succession (Sano and Struik, 1997). The Spad Lake member exceeds 200 m in thickness and is characterized by an intimate association of redeposited limestones and basaltic rocks. No ribbon-bedded chert succession is present in the Spad Lake member, which, in turn, contains nodular cherts composed of the diagenetically replaced silica.

Sano and Struik (1997) interpreted the chert-micrite succession at the foot of Mt. Pope to have accumulated on the lower flank of a basaltic seamount to surrounding ocean floor, where shallow-marine carbonates were gravitationally displaced down and resedimented. According to this facies interpretation, with an emphasis upon the comparison of the lithologic association, the Spad Lake member is best interpreted to have been deposited on an upper flank of a basaltic seamount, or a basaltic plateau. In comparison with the clastic limestones in the chert-micrite succession, the Spad Lake clastic limestones represent more proximal facies with respect to the shallow-marine buildup resting upon a basaltic substratum.

ACKNOWLEDGMENTS

Special thanks are due to L.C. Struik for his support and suggestion for the fieldwork. The author much appreciates the fruitful discussion on the Pope formation with W. Bamber, L.C. Struik, M.J. Orchard, and F. Cordey and the identification of the fusulines by K. Kanmera (Professor Emeritus of Kyushu University, Japan). A. Blair and A.S.-L. Justason provided excellent assistance during the fieldwork. M.J. Orchard reviewed and helped improve an early version of the manuscript.

REFERENCES

Bellefontaine, K.A., Legun, A., Massey, N., and Desjardins, P.
1995: Digital computer compilation of northeast B.C. – Southern half (NTS 83D, E, 93F, G, H, I, J, K, N, O, P); British Columbia Ministry of Energy, Mines and Petroleum Resources, Open File 1995-24.

Cordey, F. and Struik, L.C.
1996: Radiolarian biostratigraphy and implications, Cache Creek Group of Fort Fraser and Prince George map areas, central British Columbia; in Current Research 1996-E; Geological Survey of Canada, p. 7-18.

Flügel, E.
1982: Microfacies Analysis; Springer-Verlag, Berlin, Germany, 633 p.

Mullins, H.T., Heath, K.C., Van Buren, H.M., and Newton, C.R.
1984: Anatomy of modern open-ocean carbonate slope: Northern Little Bahama Bank; Sedimentology, v. 31, p. 141-168.

Orchard, M.J. and Struik, L.C.
1996: Conodont biostratigraphy, lithostratigraphy, and correlation of the Cache Creek Group near Fort St. James, British Columbia; in Current Research 1996-A; Geological Survey of Canada, p. 77-82.

Orchard, M.J., Struik, L.C., and Taylor, H.
1997: Conodont biostratigraphy and correlation, Cache Creek Group, Fort St. James, central British Columbia; in Current Research 1997-A; Geological Survey of Canada, p. 95-102.
1998: New conodont data from the Cache Creek Group, central British Columbia; in Current Research 1998-A; Geological Survey of Canada.

Sano, H. and Struik, L.C.
1997: Field properties of Pennsylvanian - Lower Permian limestones of Cache Creek Group, northwest of Fort St. James, central British Columbia; in Current Research 1997-A; Geological Survey of Canada, p. 85-93.

Struik, L.C., Floriet, C., and Cordey, F.
1996: Geology near Fort St. James, central British Columbia; in Current Research 1996-A; Geological Survey of Canada, p. 71-76.

Thompson, M.L.
1965: Pennsylvanian and Early Permian fusulinids from Fort St. James, British Columbia, Canada; Journal of Paleontology, v. 39, p. 224-234.

Thompson, M.L., Pitrat, C.W., and Sanderson, G.A.
1953: Primitive Cache Creek fusulinids from central British Columbia; Journal of Paleontology, v. 27, p. 545-552.

Tucker, M.E. and Wright, V.P.
1990: Carbonate Sedimentology; Blackwell, Oxford, England, 482 p.

Geological Survey of Canada Project 950036

New conodont data from the Cache Creek Group, central British Columbia[1]

M.J. Orchard, L.C. Struik, and H. Taylor
GSC Pacific, Vancouver

Orchard, M.J., Struik, L.C., and Taylor, H., 1998: New conodont data from the Cache Creek Group, central British Columbia; in Current Research 1998-A; Geological Survey of Canada, p. 99-105.

Abstract: Forty-seven new collections of conodonts recovered from the Cache Creek Group in central British Columbia are reported and preliminary taxonomic and age determinations presented. The data confirms that most of the limestones of the Mt. Pope sequence near Fort St. James are of Late Carboniferous age and only locally extend into the Lower Permian. A distinctive basalt unit within the limestone is constrained as Bashkirian to Moscovian in age. Upper Carboniferous limestones extend northward to Kloch Lake in Manson River sheet where much younger Permian limestones predominate. In the latter area, Late Permian limestones are overlain by an Early Triassic sedimentary and volcanic sequence. Some limestones of the Mt. Pope sequence were evidently subject to weathering and erosion during or after the Middle Triassic because Permian and Triassic conodonts are only known as cavity fill in Upper Carboniferous strata.

Résumé : Quarante-sept nouvelles collections de conodontes prélevés dans le Groupe de Cache Creek en Colombie-Britannique centrale sont décrites et des déterminations taxonomiques et chronologiques préliminaires sont présentées. Les données obtenues confirment que la plupart des calcaires de la séquence de Mt. Pope près de Fort St. James datent du Carbonifère tardif; ils ne relèvent du Permien inférieur que localement. Une unité basaltique distinctive au sein du calcaire s'inscrit dans l'intervalle bashkirien-moscovien. Les calcaires du Carbonifère supérieur se prolongent vers le nord jusqu'au lac Kloch sur la feuille de la rivière Manson, où prédominent des calcaires permiens beaucoup plus jeunes. Dans cette dernière région, une séquence sédimentaire et volcanique du Trias précoce recouvre les calcaires du Permien tardif. Certains calcaires de la séquence de Mt. Pope ont manifestement été soumis à l'altération et à l'érosion pendant ou après le Trias moyen, car les conodontes permiens et triasiques ne sont connus que comme remplissage de cavités dans les strates du Carbonifère supérieur.

[1] Contribution to the Nechako NATMAP Project

INTRODUCTION

In an earlier paper (Orchard et al., 1997) we summarized available conodont data from the Cache Creek Group in the area around Fort St. James, central British Columbia (Fig. 1). Herein, new conodont data is reported from samples collected during the summer of 1996. This comprises 47 new collections, many of them from the Cache Creek belt north of Fort St. James, the age of which has been poorly constrained up to now. In addition, some further details are presented for previously reported localities that have been resampled (Fig. 2, 3, Table 1). A total of 93 conodont collections are now known from the region.

GEOLOGY

The Cache Creek Group of central British Columbia has been interpreted to consist of an oceanic assemblage of mainly siltstone, ribbon chert, limestone, ultramafite, basalt, and gabbro. Details on the correlatives of these rocks in the North American Cordillera can be found in Gabrielse and Yorath (1991) and Silberling et al. (1992). The Cache Creek Group, and the terrane to which it lends its name, represents minor fragments of an oceanic assemblage built off the western North American margin during the Early Carboniferous through Early Jurassic, and destroyed during subduction under North America from Early Triassic to Early Jurassic.

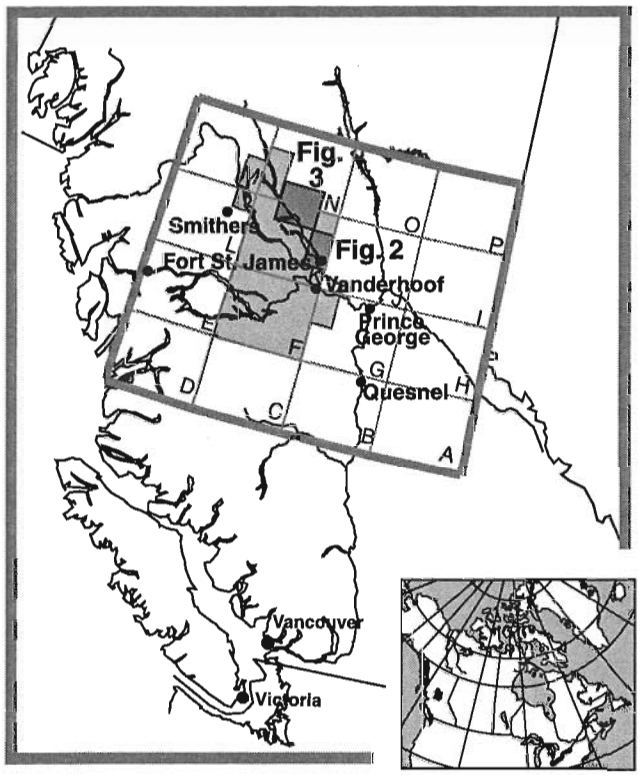

Figure 1. Location of the study areas shown in Figures 2 and 3. The NTS 1:250 000 scale map areas of the Parsnip River (NTS 93) 1:1 000 000 scale map area are shown for reference.

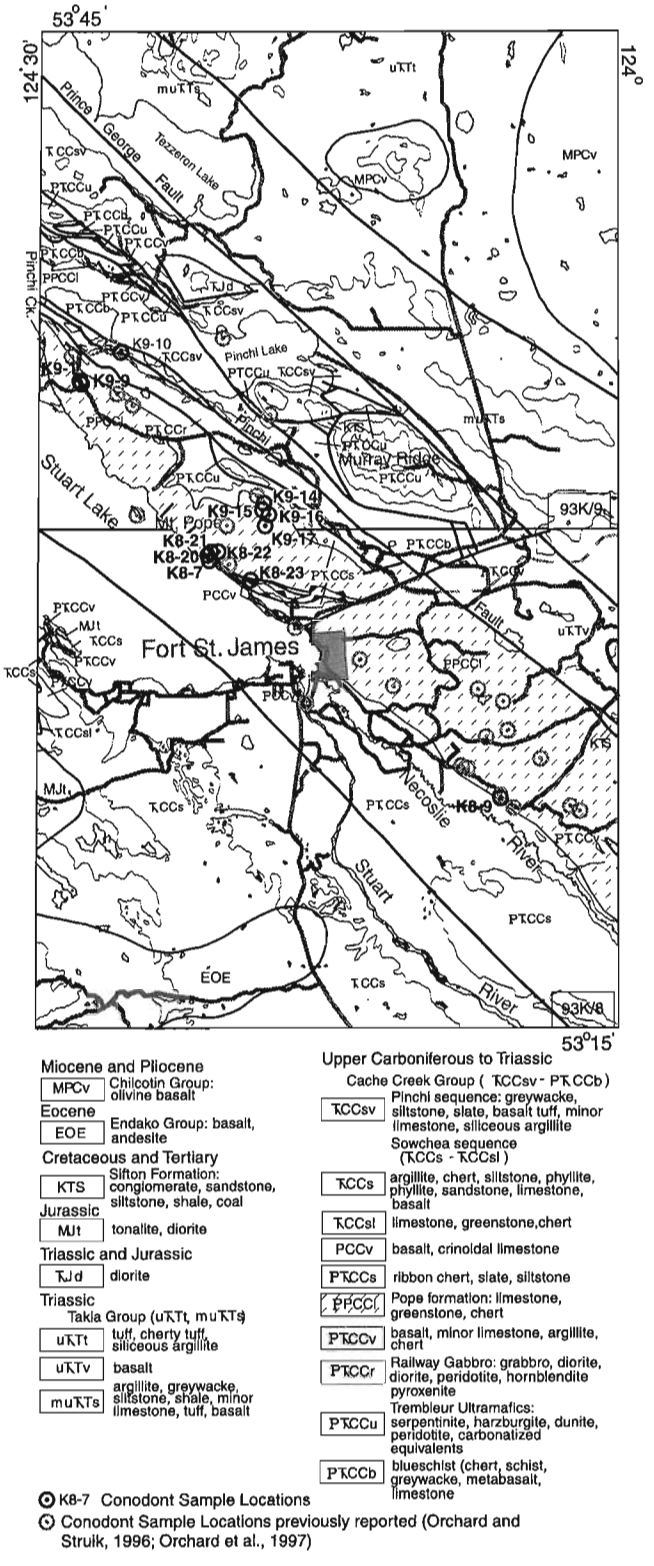

Figure 2. Geology of Fort St. James area of Fort Fraser map area (NTS 93K) with location of 1996 conodont sample sites.

In central British Columbia, the largest volume of Cache Creek Group rocks are siliciclastics, followed by carbonate, and then ultramafite. The carbonate has yielded the conodont fossils reported in this paper. The largest masses of carbonate are contained in or completely define detached thrust sheets and fault blocks. The thrust sheets everywhere overlie siliciclastic sequences ranging in age from Permian to Late Triassic. The siliciclastic sequences contain thin beds of limestone that locally have yielded Late Triassic fossils.

The carbonate can be divided into three sequences: Mt. Pope, Kloch Lake, and Whitefish Bay. The Mt. Pope sequence described in part by Struik et al. (1996), Orchard and Struik (1996), Orchard et al. (1997), Sano and Struik (1997), and Sano (1998) consists predominately of limestone of Upper Carboniferous age, and minor dolostone, ribbon chert, and basalt. From the work of Sano (Sano and Struik, 1997; Sano, 1998), the Mt. Pope sequence has been determined mainly as a shallow water mud and clastic succession locally redeposited within deeper water settings peripheral to an oceanic plateau or seamount. The Kloch Lake sequence

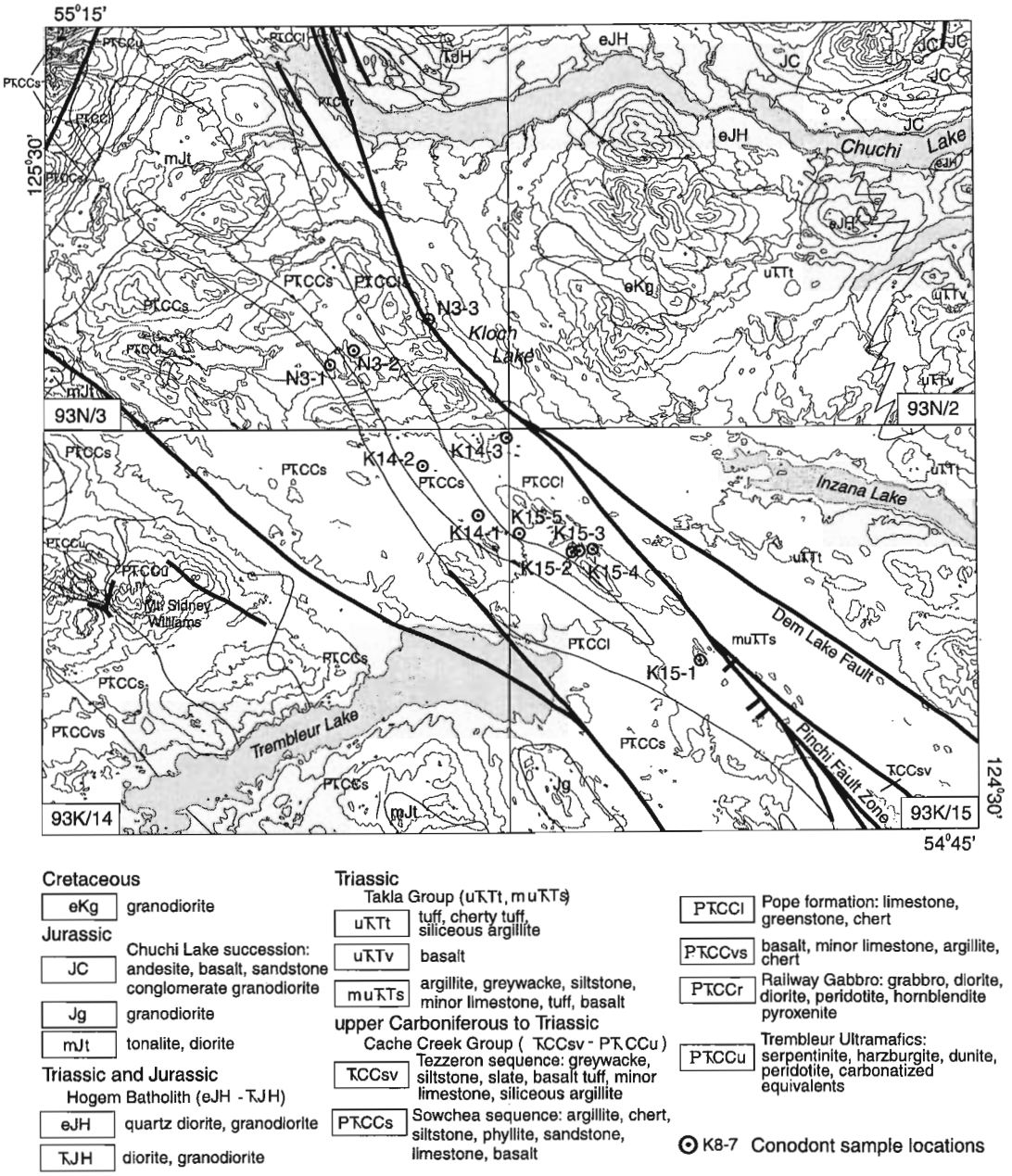

Figure 3. *Geology of northern part of Fort Fraser map area (NTS 93K) and southern part of Manson River map area (NTS 93N) with location of 1996 conodont sample sites. Geological compilation is simplified from Bellefontaine et al. (1995).*

consists of limestone, siltstone, and basalt tuff mostly of Permian and Lower Triassic age. Monger and Ross (1971) described fusulinid fauna from the Kloch Lake area and used the provincial character of that fauna to argue for transport of the Cache Creek Group rocks from Permian Tethyan realms.

The Whitefish Bay sequence consists of limestone, limestone conglomerate, and calcareous siliciclastic rocks. Whitefish Bay sequence is a subunit of the Sowchea siliciclastic sequence as described by Struik et al. (1996, 1997) and Cordey and Struik (1996). The Sowchea sequence includes the majority of the siliciclastic rocks of the Cache Creek Group near Fort St. James and north to Trembleur Lake, and is considered to be predominately of Middle and Late Triassic age.

Table 1. Faunal composition and provisional age assignments of 1996 conodont collections from the Cache Creek Group, central British Columbia.

Map no. Field no. GSC loc. no.	Conodont Taxa	Age
93K/8 - Fort St. James		
K8-20 96OF-FF-B2 C-302953	*Adetognathus* sp., ramiform elements	Late Carboniferous- Early Permian
K8-21 96OF-FF-B4 C-302954	*Adetognathus*? sp., *Declinognathodus* sp., *Hindeodus* sp., *Idiognathoides* sp., *Neognathodus* sp., ramiform elements	Late Carboniferous, Bashkirian-Moscovian
K8-9 (1995) 96OF-FF-C5 C-302955	*Hindeodus* sp., *Idiognathodus* sp., *Neogondolella* spp., *Neospathodus* spp., ramiform elements	Permian, Early Triassic
K8-9 (1995) 96OF-FF-C5B C-303451	*Idiognathodus* sp., *Idiognathoides*? sp., *Neogondolella* sp., *Neospathodus* sp., ramiform elements	Late Carboniferous, Early Permian, Early Triassic
K8-9 (1995) 96OF-FF-C6 C-302956	*Hindeodus* sp., *Idiognathodus* sp., ramiform elements	Late Carboniferous- Early Permian
K8-9 (1995) 96OF-FF-C8 C-302957	*Hindeodus* sp., *Idiognathodus* sp., ramiform elements	Late Carboniferous- Early Permian
K8-9 (1995) 96OF-FF-C9 C-302958	*Hindeodus*? sp., *Idiognathodus*? sp., *Idiognathoides* sp., ramiform elements	Late Carboniferous, Bashkirian-Moscovian
K8-9 (1995) 96OF-FF-C10 C-302959	*Diplognathodus* sp., *Hindeodus*? sp., *Idiognathodus* sp., *Idiognathoides* sp., *Neognathodus* spp., *Neogondolella clarki,* *Neogondolella* cf. *constricta,* *Neospathodus*? sp., ramiform elements	Late Carboniferous, Early and Middle Triassic
K8-7 (1995) 96OF-FF-G26 C-302971	*Adetognathus* sp., *Diplognathodus*? sp., *Hindeodus* sp., *Idiognathodus* sp., ramiform elements	Late Carboniferous- Early Permian
K8-22 96OF-FF-B27 C-302972	*Idiognathodus* sp., ramiform elements	Late Carboniferous- Early Permian
K8-22 96OF-FF-B28 C-302973	*Idiognathodus* sp., ramiform elements	Late Carboniferous- Early Permian
K8-22 96OF-FF-B30 C-302975	ramiform elements	Ordovician-Triassic
K8-23 96SCB-C-MP5-1 C-303325	*Neognathodus* sp., ramiform elements	Late Carboniferous
K8-23 96SCB-C-MP5-6 C-303326	*Diplognathodus*? sp., *Idiognathodus* sp., *Idiognathoides* spp., *Neognathodus* spp., ramiform elements	Late Carboniferous, Bashkirian-Moscovian
K8-23 96SCB-C-MP5-8 C-303327	*Idiognathodus* sp., *Idiognathoides* sp., *Neognathodus* spp., ramiform elements	Late Carboniferous, Bashkirian-Moscovian
K8-23 96SCB-C-MP5-15 C-303328	*Declinognathodus* sp., *Idiognathodus* sp., *Idiognathoides* sp., *Neognathodus* sp., ramiform elements	Late Carboniferous, Bashkirian-Moscovian
93K/9 - Pinchi Lake		
K9-17 96SCB-L-4002A C-209051	*Hindeodus* sp., *Idiognathodus*? sp., ramiform elements	Late Carboniferous- Early Permian
K9-16 96SCB-L-4003A C-209052	*Streptognathodus* sp., *Neogondolella*? sp., ramiform elements	Late Carboniferous- Early Permian
K9-15 96SCB-L-4004A C-209053	*Streptognathodus* sp.	Late Carboniferous- Early Permian
K9-14 96SCB-L-4005A C-209054	*Adetognathus*? sp., *Idiognathodus* sp., *Neognathodus* sp., ramiform elements	Late Carboniferous
K9-1 (1995) 96SCB-1901A C-209055	*Hindeodus* sp., *Neognathodus* sp., ramiform elements	Late Carboniferous
K9-1 (1995) 96SCB-1901B C-209056	*Diplognathodus* sp., *Hindeodus* sp., ramiform elements	Late Carboniferous- Permian
K9-18 96SCB-4501D C-209062	*Declinognathodus*? sp., *Gondolella* sp., *Idiognathoides* sp., *Neognathodus* sp., *Neogondolella* sp., ramiform elements	Late Carboniferous, Bashkirian-Moscovian

New conodont faunas reported in this paper come from the Mt. Pope and Kloch Lake. They are listed in Table 1, and some key localities are discussed below.

MT. POPE

The Bashkirian conodonts identified as the Mt. Pope fauna (Fauna A) by Orchard et al. (1997, Fig. 2, map site K8-7) occur near the base of the thick carbonates underlying Mt. Pope. Topographically higher samples collected on a traverse on the southwest flank of the mountain produced few additional conodonts, none of which are well preserved, and all of which have elevated colour alteration indices (CAI) of about 6, implying postdepositional temperatures in excess of 350°C. The most notable collection (site K8-21, GSC loc. C-302954) was recovered 12-15 m below a basalt marker. It differs from Fauna A in including *Declinognathodus* sp. and *Neognathodus* sp., and in being dominated by *Idiognathoides* sp. rather than *Idiognathodus*. In these respects, the fauna is

Table 1 (cont.)

Map no. Field no. GSC loc. no.	Conodont Taxa	Age
K9-9 (1995) 96OF-FF-E13 C-302961	*Idiognathodus* sp., *Idiognathoides* sp., *Neognathodus* sp., ramiform elements	Late Carboniferous, Bashkirian-Moscovian
K9-9 (1995) 96OF-FF-E14 C-302962	*Adetognathus*? sp., *Neognathodus* sp., ramiform elements	Late Carboniferous
K9-9 (1995) 96OF-FF-E15 C-302963	*Declinognathodus* sp., *Diplognathodus*? sp., *Hindeodus*? sp.	Late Carboniferous, Bashkirian-Moscovian
K9-9 (1995) 96OF-FF-E16 C-302964	*Neognathodus* sp.	Late Carboniferous
K9-9 (1995) 96OF-FF-E17 C-302965	*Adetognathus*? sp., *Declinognathodus* sp., ramiform elements	Late Carboniferous, Bashkirian-Moscovian
K9-9 (1995) 96OF-FF-E18 C-302966	*Declinognathodus* sp., *Diplognathodus* sp., *Hindeodus* sp., *Idiognathoides* sp., *Neognathodus* sp., ramiform elements	Late Carboniferous, Bashkirian-Moscovian
K9-9 (1995) 96OF-FF-E19 C-302967	*Declinognathodus* sp., *Diplognathodus* sp., *Idiognathoides* sp., *Neognathodus* sp., ramiform elements	Late Carboniferous, Bashkirian-Moscovian
K9-9 (1995) 96OF-FF-E24 C-302969	*Declinognathodus* sp., *Hindeodus* sp., *Idiognathodus* sp., *Idiognathoides* sp., *Neognathodus* sp., ramiform elements	Late Carboniferous, Bashkirian-Moscovian
K9-9 (1995) 96OF-FF-E20 C-302999	*Declinognathodus* sp., *Idiognathoides*? sp., *Neognathodus* sp., ramiform elements	Late Carboniferous, Bashkirian-Moscovian
K9-9 (1995) 96OF-FF-E21 C-303076	*Diplognathodus* sp., *Hindeodus* sp., *Idiognathoides* sp., ramiform elements	Late Carboniferous, Bashkirian-Moscovian
93K/14 - Trembleur Lake		
K14-1 96OF-FF-O39 C-302983	*Hindeodus* sp., *Idiognathoides* sp.,	Late Carboniferous, Bashkirian-Moscovian
K14-3 96OF-FF-R42 C-302986	*Declinognathodus* sp., *Idiognathodus* sp., *Idiognathoides* sp., ramiform elements	Late Carboniferous, Bashkirian-Moscovian
K14-2 96OF-FF-T44 C-302988	ramiform elements	Ordovician-Triassic
93K/15 - Inzana Lake		
K15-1 96OF-FF-J34 C-302978	*Diplognathodus*? sp., *Hindeodus* sp., *Neogondolella* sp., ramiform elements	Permian
K15-1 96-OF-FF-J52 C-303079	*Diplognathodus*? sp., *Hindeodus* sp., *Neogondolella* sp., ramiform elements	Permian
K15-4 96OF-FF-K35 C-302979	*Adetognathus* sp., *Idiognathoides* sp., ramiform elements	Late Carboniferous, Bashkirian-Moscovian
K15-3 96OF-FF-L36 C-302980	*Adetognathus*? sp., *Hindeodus* sp., *Idiognathodus*? sp., ramiform elements	Late Carboniferous-Early Permian
K15-2 96OF-FF-M37 C-302981	ramiform elements	Ordovician-Triassic
K15-5 96OF-FF-N38 C-302982	*Idiognathodus* sp., *Idiognathoides* sp., *Neognathodus* sp., ramiform elements	Late Carboniferous, Bashkirian-Moscovian
Manson River		
93N/3 - Takatoot Lake		
N3-3 96OF-FF-U46 C-302990	*Adetognathus* sp., *Hindeodus*? sp., *Streptognathodus* sp., ramiform elements	Late Carboniferous-Early Permian
N3-2 96OF-FF-W48 C-302992	*'Ellisonia'* sp., *'Neospathodus'* ex gr. *conservativus*, *Neospathodus* spp., ramiform elements	Early Triassic, Dienerian-Smithian
N3-2 96OF-FF-W49 C-302993	*Hindeodus typicalis*, *Iranognathus* ex gr. *nudus*, *Neogondolella* sp., ramiform elements	Late Permian
N3-2 96OF-FF-W50 C-302994	ramiform elements	Late Permian-Early Triassic
N3-1 96OF-FF-X51 C-302995	*Hindeodus*? sp., *Neogondolella* sp., ramiform elements	Late Permian

similar to Fauna B of Orchard et al. (1997), although *Declinognathodus* was not previously known from the Cache Creek Group and does not occur in any of the conodont faunas to the southeast, grouped as the Necoslie fauna B. Nevertheless, the age of the subbasalt conodonts are also regarded as Bashkirian, or possibly early Moscovian. Only *Idiognathodus* is known from samples above the basalt, the age of which can therefore be no older than Bashkirian, but is probably no younger than Moscovian.

A new suite of samples have also been recovered from close to the Mt. Pope trail (Fig. 2, site K8-23), a locality described in detail by Sano and Struik (1997, loc. MP-5). These are regarded as approximately coeval with the fauna discussed above and yet, in contrast, they are abundant, relatively well preserved, and have a lesser CAI of about 5. They occur in dark, well bedded, sometimes lenticular micrites interbedded with chert and some clastic limestones, a stark contrast with the massive, often fusulinid-bearing carbonates typical of the Mt. Pope formation. These rocks are interpreted to have accumulated in a relatively deep water setting which received detritus through downslope movement of debris flows and turbidity currents (Sano and Struik, 1997). There is a notable absence of the 'shallow-water' conodont *Adetognathus*, a common element in Fauna A (Orchard et al., 1997). As in the subbasalt collection, *Declinognathodus* is a notable component in one collection, and in all collections *Idiognathoides*, *Idiognathodus*, and *Neognathodus* (in decreasing order of abundance) occur. The Mt. Pope trail collections lack gondolellids which might be expected in a deeper water facies such as this and therefore may predate the Necoslie collections of Fauna B wherein both *Gondolella* and *Neogondolella* occur.

PINCHI CREEK

North of Mt. Pope, a roadside outcrop between Stuart and Pinchi lakes (Fig. 2, site K9-1) exposes well bedded limestones of the Mt. Pope sequence containing solitary corals. These strata also contain red calcareous argillite intimately but irregularly associated with some limestones beds, which are locally extensively silicified. As at Mt. Pope, the limestones appear to be overlain by basalt although no contact is evident here. Samples taken throughout this outcrop yield a similar conodont fauna to that from the Mt. Pope trail, although they are more diverse and less abundant; preservation and CAI are similar. In these collections, *Adetognathus*, *Diplognathodus*, and *Hindeodus* are represented although *Idiognathoides*, *Neognathodus*, and *Declinognathodus* are more common; *Idiognathodus* is rare.

Again, the collections are regarded as Bashkirian-early Moscovian but resolution of their age relative to the other collections previously described as Faunas A and B requires additional study. Unfortunately, superimposition of conodont faunas is generally lacking in the Cache Creek Group and it is difficult to determine whether observed variations reflect environmental rather than age differences.

NECOSLIE BRECCIA

The mixed conodont fauna from a single sample of massive limestone breccia of Mt. Pope sequence collected north of the Necoslie River (Orchard et al., 1997, Fauna F; Fig. 2, site K8-9) has now been reproduced in several further collections. Examination of the discontinuous section reveals that a variety of carbonate lithotypes are represented, and conglomeratic or brecciated lithofacies occur irregularly in a relatively homogenous, fusulinid-bearing carbonate mudstone. However, it has proved impossible to segregate clasts from matrix in these recrystallized limestones and it is still unclear exactly how the late Paleozoic and Triassic conodonts are mixed, and indeed how many different ages are represented.

However, samples taken from apparently nonbrecciated carbonates have thus far produced only *Hindeodus* and *Idiognathodus*, and less commonly *Idiognathoides*. Fusulinids from the same lithofacies have been dated as Moscovian (L. Rui, pers. comm., 1997), which is consistent with the conodonts. These Late Carboniferous limestones appear to represent the bulk of the outcrop. Two additional collections extracted from samples that included clasts contain both Late Carboniferous and Triassic species, the latter including Early and Middle Triassic species. One of these samples (GSC loc. C-303451) also contains common specimens of *Neogondolella*, some of which appear to be of Permian age. Hence, the 'host' or 'wall' rock and possibly some or all of the clasts are interpreted to be Late Carboniferous in age, as are virtually all the limestones in the area. The Permian and Triassic components may be partly in clasts, or wholly or partly in a secondary carbonate matrix that surrounds the clasts and infills cracks or voids within the Late Carboniferous limestones.

The genesis of these deposits is intriguing and as yet unresolved. One scenario is that several generations of carbonates are represented as clasts or carbonate residuum that has been eroded and possibly partly dissolved during or even after the Triassic and are now preserved as infilling of crevasses, or possibly solution cavities, within the Carboniferous limestone.

KLOCH LAKE

Cache Creek Group rocks exposed north of Kloch Lake, some 80 km north of Mt. Pope, include sedimentary strata and fauna that has not been found to the south (Fig. 3). Upper Permian limestones of this Kloch Lake sequence outcrop over a broad area and contrast with the predominant Upper Carboniferous limestones around Fort St. James. Only a single Upper Carboniferous fauna is known from the area (site N3-3) and it is exceptional in containing a rich macrofauna of sponges (*Chaetetes*), solitary corals, and fewer brachiopods. Fusulinids include *Millerella marblensis* of Bashkirian to early Moscovian age (L. Rui, pers. comm., 1997). Conodonts from this locality comprise a low diversity association of *Adetognathus* with fewer *?Streptognathodus*.

Dated limestone outcrops to the west are all younger. These include richly fossiliferous fusulinid limestones in which *Colania* and *Parafusulina* of Late Permian, Wordian age are identified (L. Rui, pers. comm., 1997). Nearby, other outcrops have yielded corals and the Upper Permian bivalve *Shikamaia* (H. Sano, pers. comm., 1997). To date, these limestones have yielded only rare conodonts (site N3-1).

The fossiliferous Upper Permian limestones are not seen in stratigraphic contact with overlying strata but a glimpse of the younger history of the Cache Creek Group can be observed in a largely recessive section on the Kloch Creek forest service road. Strata there comprise interbedded argillite, limestones, laminated chert, volcaniclastics, and vesicular basalt. Structural complexity and poor exposure obscure stratigraphic relationships, but both Upper Permian and Lower Triassic strata are identified. A large, albeit poorly preserved Lower Triassic, Dienerian-Smithian fauna occurs in limestone at the east end of the section (site N3-2) - these strata and fauna are very similar to that reported from Marble Canyon near Cache Creek by Orchard (1981). The limestone also contains poorly preserved, indeterminate ammonoids. Downdip to the west, several other limestones occur but it is unclear whether they are in situ or are olistoliths within the clastics; certainly several horizons of small limestone clasts are interbedded. Some of the larger limestones contain Late Permian conodonts, including forms assigned to *Iranognathus* ex gr. *nudus* by Beyers and Orchard (1991). These elements, previously reported from the Marble Range in the type Cache Creek Group of southern British Columbia, are the youngest Permian conodonts on the continent. They are probably no older than Dzhulfian but may be Changshingian in age.

Two stratigraphic interpretations are possible for the Kloch Creek road section based on currently available data. One is that these very young Permian limestones are olistoliths derived from the underlying Permian carbonates during the Early Triassic, and the volcanism is Early Triassic in age. Alternatively, they are in situ beds lying beneath the Triassic and the section embraces a Permian-Triassic boundary, with the volcanism dating from around that interval. In either case, this stratigraphic record is exceptional and apparently unique to the Cache Creek Group in North America.

ACKNOWLEDGMENTS

Steve Irwin reviewed the manuscript and provided useful and constructive suggestions for improvement. Bev Vanlier assisted in the preparation of the manuscript.

REFERENCES

Bellefontaine, K.A., Legun, A., Massey, N., and Desjardins, P.
1995: Digital geological compilation of northeast B.C. - southern half (NTS 83D, E, 93F, G, H, I, J, K, N, O, P); British Columbia Ministry of Energy, Mines and Petroleum Resources, Open File 1995-24.

Beyers, J.M. and Orchard, M.J.
1991: Upper Permian and Triassic conodont faunas from the type area of the Cache Creek Complex, south-central British Columbia; in Ordovician to Triassic Conodont Paleontology of the Canadian Cordillera, (ed.) M.J. Orchard and A.D. McCracken; Geological Survey of Canada, Bulletin 417, p. 269-298.

Cordey, F. and Struik, L.C.
1996: Radiolarian biostratigraphy and implications, Cache Creek Group of Fort Fraser and Prince George map areas, central British Columbia; in Current Research 1996-E; Geological Survey of Canada, p. 7-18.

Gabrielse, H. and Yorath, C.J.
1991: Tectonic synthesis, Chapter 18; in Cordilleran Orogen in Canada, (ed.) H. Gabrielse and C.J. Yorath; Geological Survey of Canada, Geology of Canada, no. 4, p. 677-705.

Monger, J.W.H. and Ross, C.
1971: Distribution of fusulinaceans in the Western Canadian Cordillera; Canadian Journal of Earth Sciences, v. 8, p. 259-278.

Orchard, M.J.
1981: Triassic conodonts from the Cache Creek Group, Marble Canyon, southern British Columbia; in Current Research, Part A; Geological Survey of Canada, Paper 81-1A, p. 357-359.

Orchard, M.J. and Struik, L.C.
1996: Conodont biostratigraphy, lithostratigraphy, and correlation of the Cache Creek Group near Fort St. James, British Columbia; in Current Research 1996-A; Geological Survey of Canada, p. 77-82.

Orchard, M.J., Struik, L.C., and Taylor, H.
1997: Conodont biostratigraphy and correlation, Cache Creek Group, Fort St. James, central British Columbia; in Current Research 1997-A; Geological Survey of Canada, p. 95-102.

Sano, H.
1998: Preliminary report on resedimented carbonates associated with basaltic rocks of Cache Creek Group near Spad Lake, east of Fort St. James, central British Columbia; in Current Research 1998-A; Geological Survey of Canada.

Sano, H. and Struik, L.C.
1997: Field properties of Pennsylvanian-Lower Permian limestones of Cache Creek Group, northwest of Fort St. James, central British Columbia; in Current Research 1997-A; Geological Survey of Canada, p. 85-93.

Silberling, N.J., Jones, D.L., Monger, J.W.H., Coney, P.J., Berg, H.C., and Plafker, G.
1992: Lithotectonic terrane map of the North American Cordillera; United States Geological Survey, Miscellaneous Investigations Series, I-2176, 2 maps.

Struik, L.C., Floriet, C., and Cordey, F.
1996: Geology near Fort St. James, central British Columbia; in Current Research 1996-A; Geological Survey of Canada, p. 71-76.

Struik, L.C., Whalen, J.B., Letwin, J.M., and L'Heureux, R.
1997: General geology of southeast Fort Fraser map area, central British Columbia; in Current Research 1997-A; Geological Survey of Canada, p. 65-76.

Geological Survey of Canada Project 950036

Field observations of the Tachie Pluton near Fort St. James, central British Columbia[1]

M.G. Hrudey[2] and L.C. Struik
GSC Pacific, Vancouver

Hrudey, M.G. and Struik, L.C., 1998: Field observations of the Tachie Pluton near Fort St. James, central British Columbia; in Current Research 1998-A; Geological Survey of Canada, p. 107-111.

Abstract. The Tachie Pluton, found northwest of Fort St. James, consists of biotite diorite to tonalite. It is equigranular, medium grained, and composed of abundant plagioclase, quartz and biotite. Schlieren textures and enclaves occur with biotite pegmatite and mafic concentrations in discrete bands. Aplite and pegmatite dykes, along with hornblende-rich dykes are late syn- to post-intrusion features found throughout the pluton. The pluton resembles diorite and quartz diorite of the McKnab Pluton south of Stuart Lake.

Résumé : Le pluton de Tachie, une entité géologique qui s'observe au nord-ouest de Fort St. James, varie en composition de la diorite à biotite à la tonalite à biotite. Il est équigranulaire et à grain moyen et se compose de plagioclase (abondant), de quartz et de biotite. Des textures de schlieren et des enclaves s'observent là où il y a de la pegmatite à biotite et des concentrations de minéraux mafiques en bandes distinctes. La mise en place de dykes aplitiques et pegmatitiques ainsi que de dykes riches en hornblende correspond à la fin de l'intrusion du pluton de Tachie ou en est postérieure; ces dykes apparaissent dans l'ensemble du pluton. Les roches du pluton sont semblables aux diorites et aux diorites quartziques du pluton de McKnab, au sud du lac Stuart.

[1] Contribution to the Nechako NATMAP Project
[2] Department of Earth and Atmospheric Sciences, University of Alberta, Edmonton, Alberta T6G 2E3

INTRODUCTION

The previously unnamed Tachie Pluton is located approximately 30 km northwest of Fort St. James, and south of Trembleur Lake (93K/15, Fig. 1, 2). The intrusion is exposed over an area of approximately 5 by 8 km, and lies east of the McElvey Lake pluton (Ash et al., 1993). The area underlain by Tachie Pluton was first regionally mapped by Armstrong (1949). More recent work in the nearby areas of

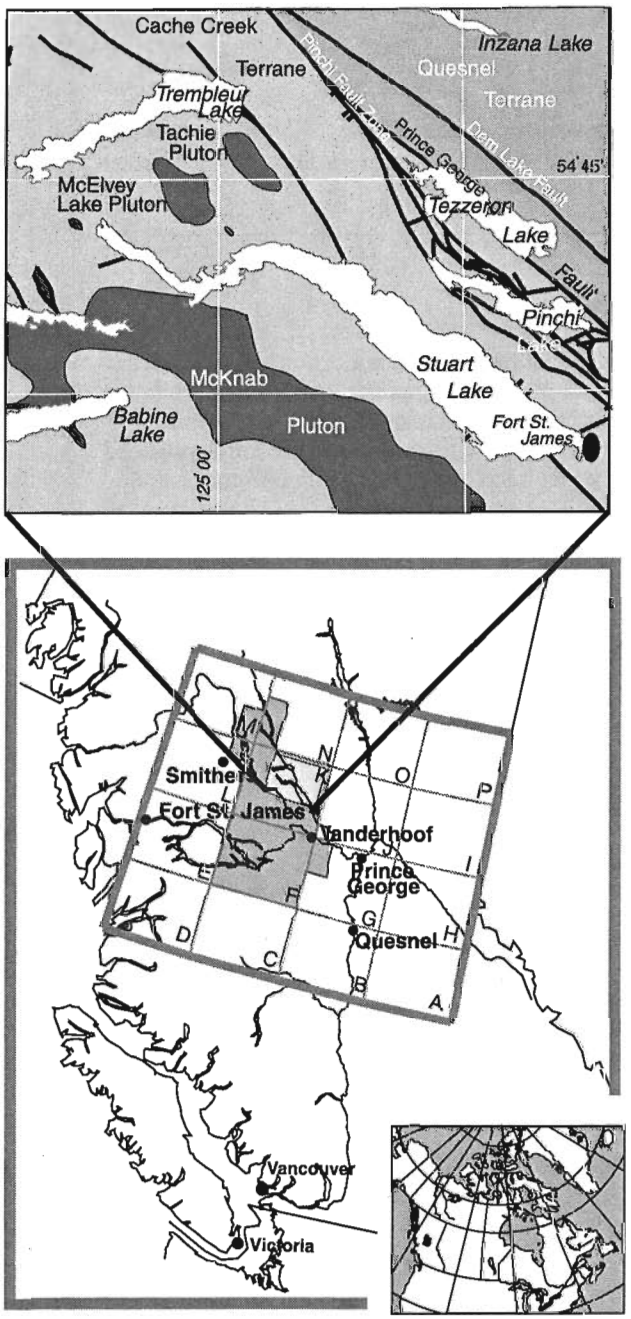

Figure 1. Location of the study area within central British Columbia and the Nechako NATMAP Project. The Parsnip River (NTS 93) 1:250 000 scale map areas are shown for reference.

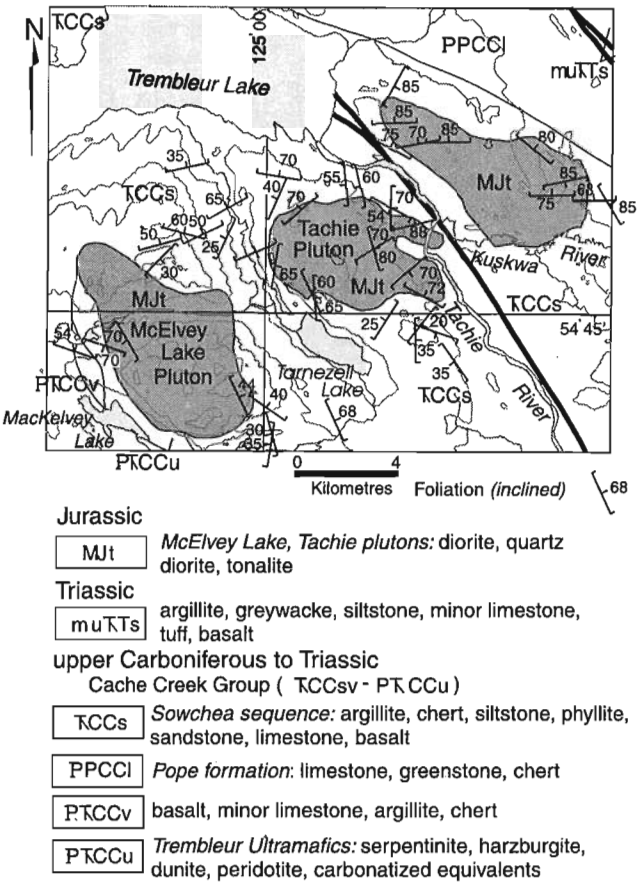

Figure 2. Local geology surrounding the Tachie Pluton.

Stuart Lake and Pinchi Lake area was done by Paterson (1973) and Ash et al. (1993). This report contains field observations of the Tachie Pluton gathered in the summer of 1997 in preparation for a B.Sc. thesis study of the pluton's petrography and textural genesis by M.G. Hrudey.

The Tachie Pluton is surrounded by rocks of the Cache Creek Terrane, a Carboniferous to Lower Jurassic (Struik et al., 1996) exotic oceanic assemblage, obducted on to the North American margin during Mesozoic time. Post-obduction, the terrane was intruded by several Mesozoic granitoid bodies, and disrupted by Tertiary extension and volcanism. Mapping, petrological, geochronological, and geochemical aspects of the Tachie Pluton are currently under study as part of the Nechako Plateau NATMAP project (Struik and MacIntyre, 1998): a project designed to better understand the intricate geological and tectonic history of the central Canadian Cordillera.

GEOLOGY

Regional setting

The Tachie Pluton intrudes the Middle to Upper Triassic Sowchea sequence sedimentary rocks of the Cache Creek Group (Struik et al., 1996). The Sowchea sequence argillite,

metasiltstone, slate, ribbon chert, limestone, and quartzite are both regionally and contact metamorphosed near the pluton. Blocks of marble and metasiltstone are locally found within the pluton. They range from centimetres to several metres long and are ductilely strained. Most sedimentary inclusions are found near the pluton margins, and in places internally as possible roof pendants (see also Armstrong, 1949). Fine-grained microdiorite plagioclase porphyry dykes cut the country rock near the pluton contact.

Contact relationships

The contact of the Tachie Pluton is exposed in several areas. The geometries and textures are different in each case, probably reflecting the bounding rock types. To the southeast near Tachie River, the pluton intrudes marble and phyllite of the Cache Creek Group. Along that contact, various calc-silicate assemblages have been formed along with fine- to medium-grained crystalline marble and interlayered phyllite. The metasediments are tightly folded, and in places those folds are cut by thin aplitic dykes. The pluton adjacent to the contact is rich in hornblende, has partially saussuritized plagioclase, and has fine-grained pyrrhotite.

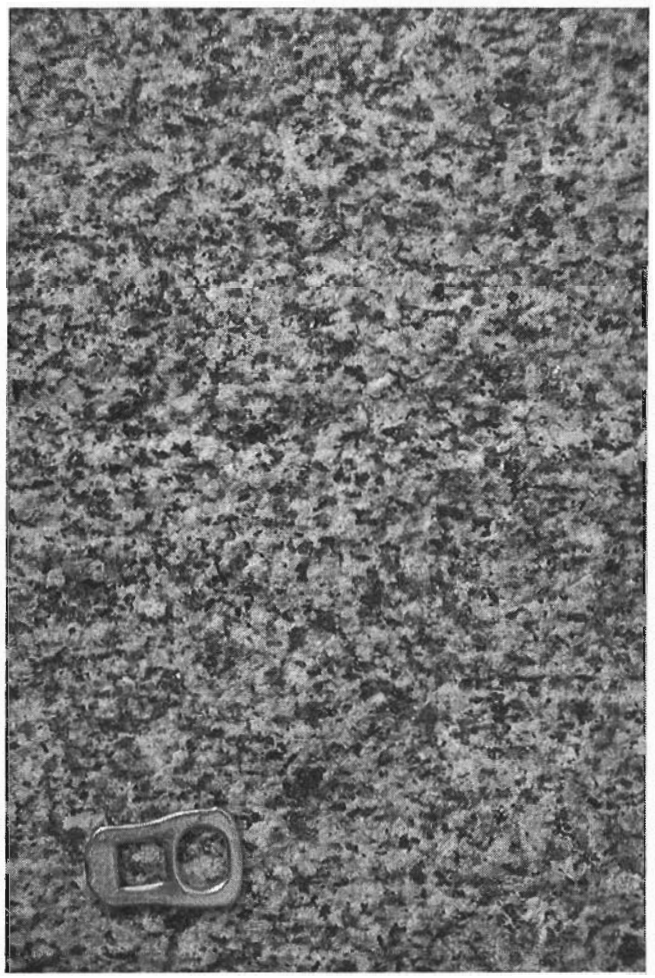

Figure 3. *Texture of the Tachie Pluton diorite.*

To the north, the pluton intrudes siltstone, chert, and mudstone of the Cache Creek Group. The sediments are weakly hornfelsed and strongly deformed with a well developed cleavage, and tight folds parallel to the contact. The pluton has a foliation defined by aligned biotite, hornblende, and flattened and elongate quartz crystals, is cut by numerous aplitic dykes, and has partially chloritized plagioclase.

Petrography and textures

The Tachie Pluton is a homogeneous biotite diorite to biotite tonalite (Fig. 3). It is medium grained and equigranular, with abundant chalky weathering, anhedral to euhedral plagioclase laths (1-5 mm), anhedral quartz (0.5-1 mm), mainly subhedral biotite (0.5-2 mm), local sphene, and minor secondary epidote. Biotite is altered slightly to chlorite, but otherwise the intrusion is relatively pristine. From field observation, plagioclase ranges from approximately 40 to 60%, biotite from 10 to 20%, and quartz from 5 to 20%. The rock is white to light grey, peppered with dark biotite on fresh exposure, and weathers light grey to grey.

Hornblende- and biotite-rich inclusions ranging in size from 1 to 5 cm are found throughout the pluton. Hornblende-rich dykes 30 cm to 3 m thick are also common. These dykes show 2 to 3 cm amplitude undulating contacts with the host diorite, and are therefore likely late syn- or early post-intrusion features.

At many exposures biotite defines a weak foliation mainly striking east-northeast and dipping between 70 and 80° to the south or north. Bands defined by biotite foliation and variations in feldspar and quartz crystal size are found in various parts of the intrusion, often in areas rich in aplite and pegmatite dykes (Fig. 4), schlieren (Fig. 5) and enclaves, and along the outer portions of the pluton. The schlieren textures/enclaves are commonly cut by aplite and pegmatite dykes. In places the biotite appears to define discreet flow lineations.

The bands can be consistent in width and texture greater than 5 m in length. They can also be truncated by other bands at highly oblique to tangential angles as if marking areas of pluton flow. Locally, the banding is confined to 30 to 60 cm wide pockets with cross-sections like high-sided bowls. The bounding rock to these areas of banding and schlieren is generally massive homogeneous and medium crystalline and in sharp contact.

In one place the diorite has spherules 3 to 5 cm in diameter defined by chlorite and possibly epidote alteration. The spherules are evenly spaced, generally a half-diameter apart, and are concentrated in bands 1 to 2 m wide.

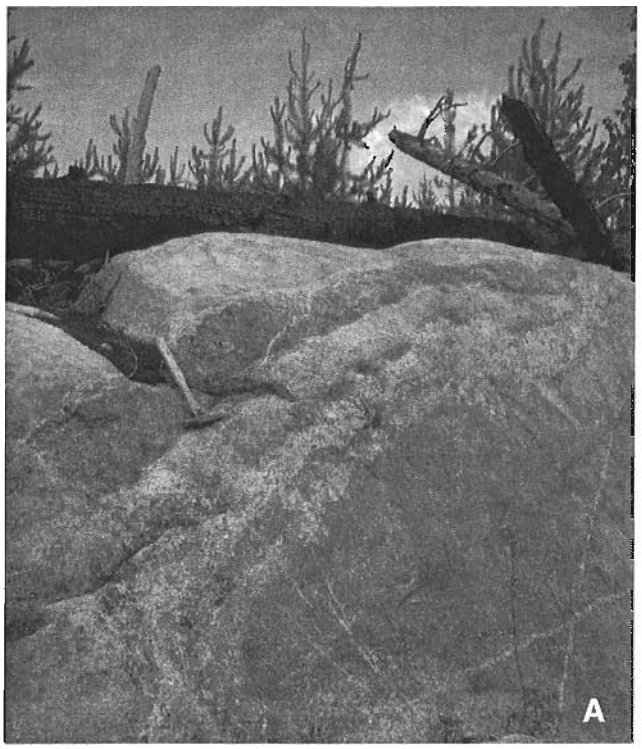

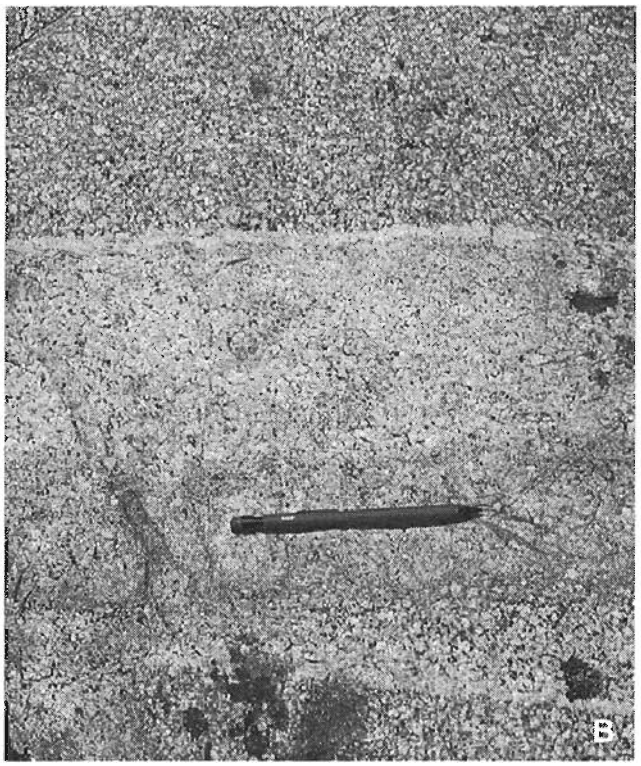

Figure 4. *Character of the banded and vein- and dyke-rich portions of the Tachie Pluton.* ***A****) outcrop-scale banding.* ***B****) detail of one of the bands.*

Figure 5. *Schlieren texture within the southeastern part of the Tachie Pluton.*

Aplite and pegmatite

Light pink, 3-10 cm aplite and pegmatite dykes cut the Tachie Pluton in at least two sets, occurring as semiplanar to planar or slightly anastomosing features. The two sets of crosscutting dykes generally strike east-west and dip steeply. Locally, these dykes change orientation sharply, or pinch out in the host diorite matrix. Their morphology indicates early post-intrusion, and they are likely related to the schlieren enclaves, as late intrusion volatile-rich magma.

DISCUSSION

Armstrong (1949) placed both the Tachie Pluton and the McElvey Lake Pluton (Ash et al., 1993), which underlies the adjacent area to the southwest, in what he termed the 'Upper Jurassic or Lower Cretaceous Omineca Group' intrusions, as best represented by the Hogem Batholith (Armstrong, 1949). Lithological and textural similarity, as well as spatial proximity, would indicate rather that the Tachie pluton, as well as the McElvey Lake pluton, are members of the 165 +2/-1 Ma (Ash et al., 1993; M. Villeneuve, pers. comm., 1997) McKnab Lake Pluton suite. McKnab Lake Pluton underlies a large area to the south of Tachie Pluton, south of Stuart Lake (Ash et al., 1993). McKnab Pluton is quartz diorite with abundant biotite, hornblende and mafic inclusions. It is more fully described by Letwin and Struik (1997) and Ash and Macdonald (1993) as Shass Mountain Pluton.

Precise U-Pb geochronology and petrologic studies on the Tachie Pluton is currently in progress at the University of Alberta, and may place it more accurately within the Cordilleran framework, as well as constraining the timing of Mesozoic Cache Creek Terrane obduction.

CONCLUSIONS

The Tachie Pluton consists of diorite to tonalite. It intrudes mainly Middle to Upper Triassic Sowchea sequence sedimentary rocks, and metasedimentary blocks are found locally within the intrusion, as are hornblende- or biotite-rich inclusions. Hornblende-rich dykes cut the pluton, as do pegmatite and aplite dykes throughout. Enclaves of biotite pegmatite and pegmatite schlieren are found at several exposures, with biotite-defined discrete lineations (flow lines). The intrusion is generally massive, but shows biotite foliation at several exposures.

ACKNOWLEDGMENTS

R.G. Anderson kindly helped us with the digital images for Figures 3 and 4. G. Woodsworth and J. Roddick gave gracious constructive criticism in suggesting a rebirth to the manuscript. B. Vanlier assisted in the delivery.

REFERENCES

Armstrong, J.E.
1949: Fort St. James map-area, Cassiar and Coast districts, British Columbia; Geological Survey of Canada, Memoir 252, 210 p.

Ash, C. and Macdonald, R.J.W.
1993: Mineralization and lithogeochemistry of the Stuart Lake area, central British Columbia (parts of 93K/7, 8, 10 and 11); in Geological Fieldwork 1992; British Columbia Ministry of Energy, Mines and Petroleum Resources, p. 69-86.

Ash, C., Macdonald, R.J.W., and Paterson, I.A.
1993: Geology of the Stuart and Pinchi Lakes area, central British Columbia (93K); British Columbia Ministry of Energy, Mines and Petroleum Resources, Open File 1993-9.

Letwin, J. and Struik, L.C.
1997: Geology of the Shass Mountain area, central British Columbia; in Current Research 1997-A; Geological Survey of Canada, p. 103-106.

Paterson, I.A.
1973: The geology of the Pinchi Lake area, central British Columbia; Ph.D. thesis, University of British Columbia, Vancouver, British Columbia, 263 p.

Struik, L.C. and MacIntyre, D.G.
1998: Nechako NATMAP Project overview, central British Columbia, year three; in Current Research 1998-A; Geological Survey of Canada.

Struik, L.C., Floriet, C., and Cordey, F.
1996: Geology near Fort St. James, central British Columbia; in Current Research 1996-A; Geological Survey of Canada, p. 71-76.

Geological Survey of Canada Project 950036

Bedrock geology of the Endako map area, central British Columbia[1]

J.B. Whalen[2], L.C. Struik, and M.G. Hrudey[3]
GSC Pacific, Vancouver

Whalen, J.B., Struik, L.C., and Hrudey, M.G., 1998: Bedrock geology of the Endako map area, central British Columbia; in Current Research 1998-A; Geological Survey of Canada, p. 113-123.

Abstract: The Endako map area (93K/3) is underlain by two main bedrock assemblages translated and tilted by Tertiary strike-slip and extension faulting. A Mesozoic complex, consisting of various Cretaceous and Jurassic granitic to dioritic phases, has been subdivided, from oldest to youngest, into the Boer, Stag Lake, and Francois Lake suites. The youngest suite, which hosts the Endako molybdenum mine, consists of granodioritic to granitic units that grade into aplitic phases containing miarolitic cavities. A Tertiary complex consists of Eocene Ootsa Lake Group dacite, rhyolite, andesite, and basalt, and Eocene and Oligocene Endako Group basalt. The Ootsa Lake Group is dominated by intermediate crystal tuffs and includes interlayered mafic and felsic volcanic rocks.

Résumé : La région cartographique d'Endako (93K/3) comporte deux assemblages principaux du substratum rocheux qui ont été déplacés et basculés au Tertiaire par le jeu de décrochements et de failles de distension. Un complexe mésozoïque, comprenant diverses phases granitiques à dioritiques crétacées et jurassiques, a été subdivisé, par ordre d'âge décroissant, en suites de Boer, de Stag Lake et du Lac Francois. La suite la plus récente, qui contient la mine de molybdène Endako, comporte des unités granodioritiques à granitiques qui passent à des phases aplitiques contenant des cavités miarolitiques. Un complexe tertiaire comprend des dacites, des rhyolites, des andésites et des basaltes éocènes du Groupe d'Ootsa Lake, et des basaltes éocènes et oligocènes du Groupe d'Endako. Le Groupe d'Ootsa Lake est dominé par des tufs cristallins intermédiaires et comprend des roches volcaniques mafiques et felsiques interstratifiées.

[1] Contribution to the Nechako NATMAP Project
[2] Continental Geoscience Division, Ottawa
[3] Department of Earth and Atmospheric Sciences, University of Alberta, #1 – 26 Earth Sciences Building, Edmonton, Alberta T6G 2E3

SETTING

The Endako map area (NTS 93K/3; Fig. 1) was mapped during the 1997 field season in year three of the five-year Nechako NATMAP project (Struik and MacIntyre, 1997, 1998). This report summarizes observations and preliminary interpretations of the bedrock geology.

Physio-economic components of the map area include an active molybdenum mine, a small town, a major transportation corridor, an active forest service road network, ranches, and nature recreation sites (Fig. 2). The Endako molybdenum mine and the town of Endako are in the southeast corner of the area. The southern and western parts of the map area are transected by the Endako River valley, now a busy transportation corridor that includes Highway 16 (Yellowhead Highway), the Canadian National Railway, two high-voltage long-distance electrical rights-of-way, and a natural gas pipeline. Much of the area is accessible by forest service roads, some of which supported active haulage in 1997 by Babine Forest Products of Burns Lake. Ranching is primarily confined to the Endako River valley and grazing lands along Savory Ridge north of François Lake. Tourist and cottage recreational activities are concentrated along the north shore of François Lake.

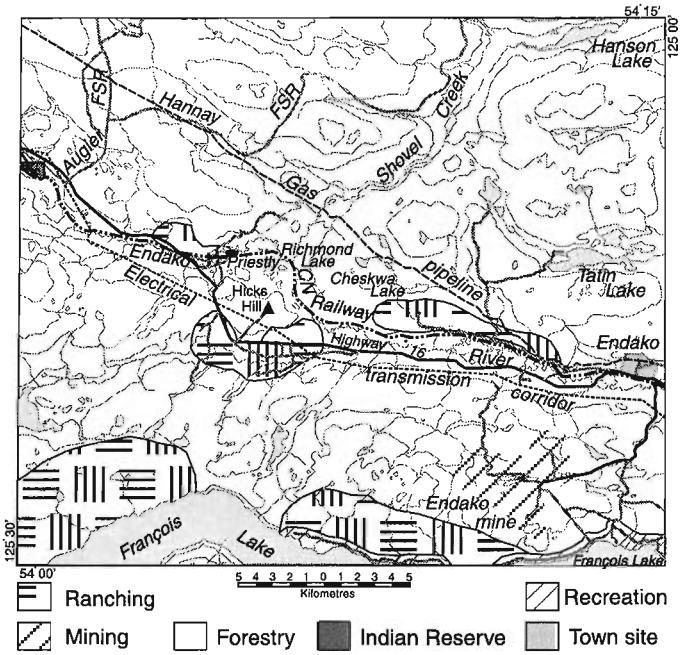

Figure 2. Location of physio-economic components in the Endako map area, from field observations and from Energy, Mines, and Resources (1977).

GEOLOGICAL FRAMEWORK

Bedrock in the Endako map area consists of two mainly igneous assemblages: Mesozoic plutonic rocks and Tertiary volcanic and minor intrusive rocks (Fig. 3).

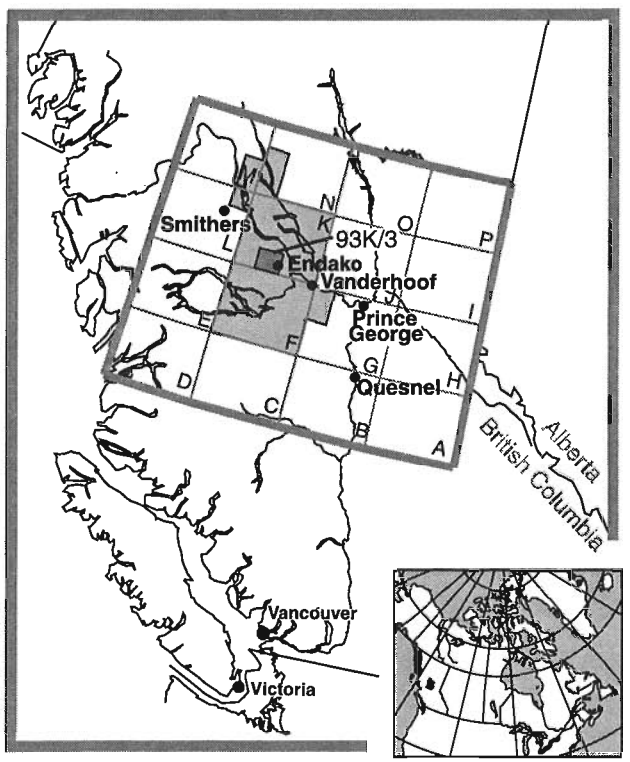

Figure 1. Location of the Endako map area (93K/3) in British Columbia. The Parsnip River (NTS 93) map area is shown for reference.

The Mesozoic assemblage consists of an upper Triassic to Cretaceous plutonic complex divided into three plutonic suites (from oldest to youngest): (1) Boer, (2) Stage Lake, and (3) Francois Lake (Anderson et al., 1997; Whalen and Struik, 1997); it is composed mainly of granodiorite to granite and lesser diorite with minor monzonite and gabbro. There are no remnants of the country rocks that these plutons intruded. The Endako molybdenum mine is hosted by the Late Jurassic to possibly Early Cretaceous Francois Lake plutonic suite (Kimura et al., 1976; Bysouth and Wong, 1995; Villeneuve et al., 1997). Jurassic Hazelton Group andesite, not part of the following discussion, outcrops in a small area bordering François Lake.

The Tertiary assemblage nonconformably overlies the plutonic assemblage and consists of the voluminous Lower Eocene Ootsa Lake Group and less abundant Upper Eocene and possibly Lower Oligocene Endako Group. The Ootsa Lake Group consists mostly of rhyodacite to dacite, rhyolite, and lesser amounts of andesite and basalt. The Endako Group consists of texturally varied basalt flows and minor fragmental units.

The Mesozoic and Tertiary assemblages are cut by Tertiary transcurrent and extensional faults that divide the area into numerous blocks. Some faults offset and rotate Upper Eocene basalt of the Endako Group (Struik and Wetherup, 1997; Enkin et al., 1997). The faults are part of a regional dextral strike-slip and extensional system that extends north and south through the Nechako and Chilcotin plateaus (Struik, 1993; Struik and Wetherup, 1997).

UNIT DESCRIPTIONS

Mesozoic plutonic complex

Late Triassic to Early Jurassic (Boer plutonic suite)

Boer phase (LTJB)

The Boer phase, exposed mainly northwest of the Endako River valley (Fig. 3), is generally weakly foliated and consists of coarse- to medium-grained dark grey hornblende (±biotite) diorite to quartz diorite. Hornblende has a distinctive stubby euhedral habit. The phase is cut by epidote-lined fractures with cm wide selvages in which feldspars are pink and mafic minerals, especially biotite, are altered to chlorite.

Stern Creek phase (LTS)

The Stern Creek phase underlies a narrow band in the northeastern corner of the map area (Fig. 3) and is best exposed to the east and north. It consists of foliated biotite and hornblende diorite and granodiorite. Locally, it has a gneissic texture, contains K-feldspar phenocrysts, and varies significantly in texture and composition at outcrop scale (Whalen and Struik, 1997).

A new U-Pb age from the Stern Creek phase within the Fraser Lake sheet (cf. Whalen and Struik, 1997) indicates that the phase is Late Triassic (M. Villeneuve, pers. comm., 1997).

Middle and Late Jurassic (Stag Lake plutonic suite)

Stellako phase (LJSS)

The Stellako phase outcrops adjacent to both sides of the Endako River valley on the west side of the map sheet (Fig. 3). It consists of an equigranular variety of grey, fine- to medium-grained, biotite-hornblende quartz diorite to granodiorite and a brown to greenish, medium-grained, plagioclase-phyric hornblende-biotite quartz monzonite with plagioclase grains 0.2–0.6 cm in size. Associated with the subporphyritic quartz monzonite is a grey to black equigranular diabase characterized by fractures containing epidote and chlorite. The granodiorite contains small fine-grained ovoid mafic inclusions and is cut by chlorite-lined fractures bordered by selvages of mafic minerals altered to chlorite.

New U-Pb and Ar-Ar ages from this phase indicate that the Stag Lake suite crystallized between 171 and 163 Ma (Villeneuve et al., 1997).

Tintagel phase (LJSTi)

The Tintagel phase, which occupies a relatively small area north of Hicks Hill, in the west-central portion of the map area (Fig. 3), consists of pink, medium-grained, equigranular, leucocratic granite. Its minor mafic minerals (biotite?) are pervasively altered to chlorite and it is crosscut by abundant fractures filled with epidote and quartz. It and the Taltapin phase are closely spatially associated, exhibit similar fracture-related alteration, and may be contemporaneous.

Taltapin phase (LJSTa)

The Taltapin phase underlies a restricted area adjacent to and east of the Tintagel phase, in the centre of the map area (Fig. 3). It consists of grey to black, fine- to medium-grained, equigranular hornblende-biotite diorite to quartz diorite. It is commonly slightly foliated and contains areas with abundant fine-grained mafic inclusions. Some inclusions are angular and most have ovoid and cuspate margins, suggestive of disaggregation of one magma by another coexisting magma. The unit is cut by common epidote-lined fractures.

Sheraton phase (LJSSh)

The Sheraton phase, which is exposed in the northwest corner of the map area (Fig. 3), consists of medium- to coarse-grained grey K-feldspar-subporphyritic biotite-hornblende granodiorite to quartz diorite. It is locally weakly foliated and cut by common epidote-lined fractures bordered by pink alteration selvages.

Late Jurassic (Francois Lake plutonic suite)

New U-Pb and Ar-Ar ages indicate that the Francois Lake plutonic suite crystallized in two pulses, at 157-154 Ma and 148-145 Ma; the Glenannan phase and its subphases were emplaced during the first pulse, while the Endako phase, its subphases, and the Casey phase were emplaced during the second pulse (M. Villeneuve, pers. comm., 1997).

Glenannan phase (LJFG)

The Glenannan phase occupies a large proportion of the eastern half of the map area (Fig. 3). It consists of coarse-grained to very coarse-grained white and pink biotite (±hornblende) granite to granodiorite that is feldspar subporphyritic to porphyritic (crystal sizes reach 0.5-4 cm but are usually 0.5-2.5 cm) (Fig. 4). It is generally massive, unaltered, and compositionally uniform over large areas. Northwest of Cheskwa Lake, it changes to medium grained, seriate, and miarolitic, and grades to drusy (highly miarolitic), patchy pegmatitic biotite aplite of the Tatin Lake subphase; both units contain disseminations and miarolitic fillings of sulphides (Py ± Cpy).

Tatin Lake subphase (LJFGt). The Tatin Lake subphase of the Glenannan phase outcrops over a large area north of the Endako River valley, in the central to eastern portion of the map area (Fig. 3). It consists mostly of beige to pink, fine- to medium-grained, equigranular to K-feldspar-subporphyritic biotite granite, which is more texturally and compositionally varied south of Tatin Lake. It also consists beige to grey, fine- to medium-grained, equigranular hornblende-biotite and biotite-hornblende granodiorite. South of Tatin Lake, internal contacts were observed between texturally different plutonic lithologies, for example, between fine- and

medium-grained variants and equigranular and feldspar-subporphyritic variants. Some contacts were outlined by fringes of unidirectional pegmatite-aplite growths.

The Tatin Lake subphase was mapped by Kimura et al. (1980) as part of the Casey phase. However, south of Tatin Lake, observed contacts of the Tatin Lake subphase and Glenannan phase include both sharp intrusive contacts, the finer grained Tatin Lake subphase being younger, and gradational contacts, the Glenannan phase becoming less coarse grained, less porphyritic, and more felsic over less than 0.25 km. North of Tatin Lake, a sharp intrusive contact was observed between the younger Tatin Lake subphase and the Glenannan phase. Along a logging road northeast of Cheskwa Lake, a gradational contact was observed between these units.

Hanson Lake subphase (LJFGh). The Hanson Lake subphase, which forms an ovoid body in the northeast corner of the map sheet (Fig. 3), consists of grey to white, coarse- to medium-grained, feldspar-porphyritic hornblende-biotite granodiorite to quartz monzonite. In places, it has a fine-grained matrix in which hornblende and quartz are also

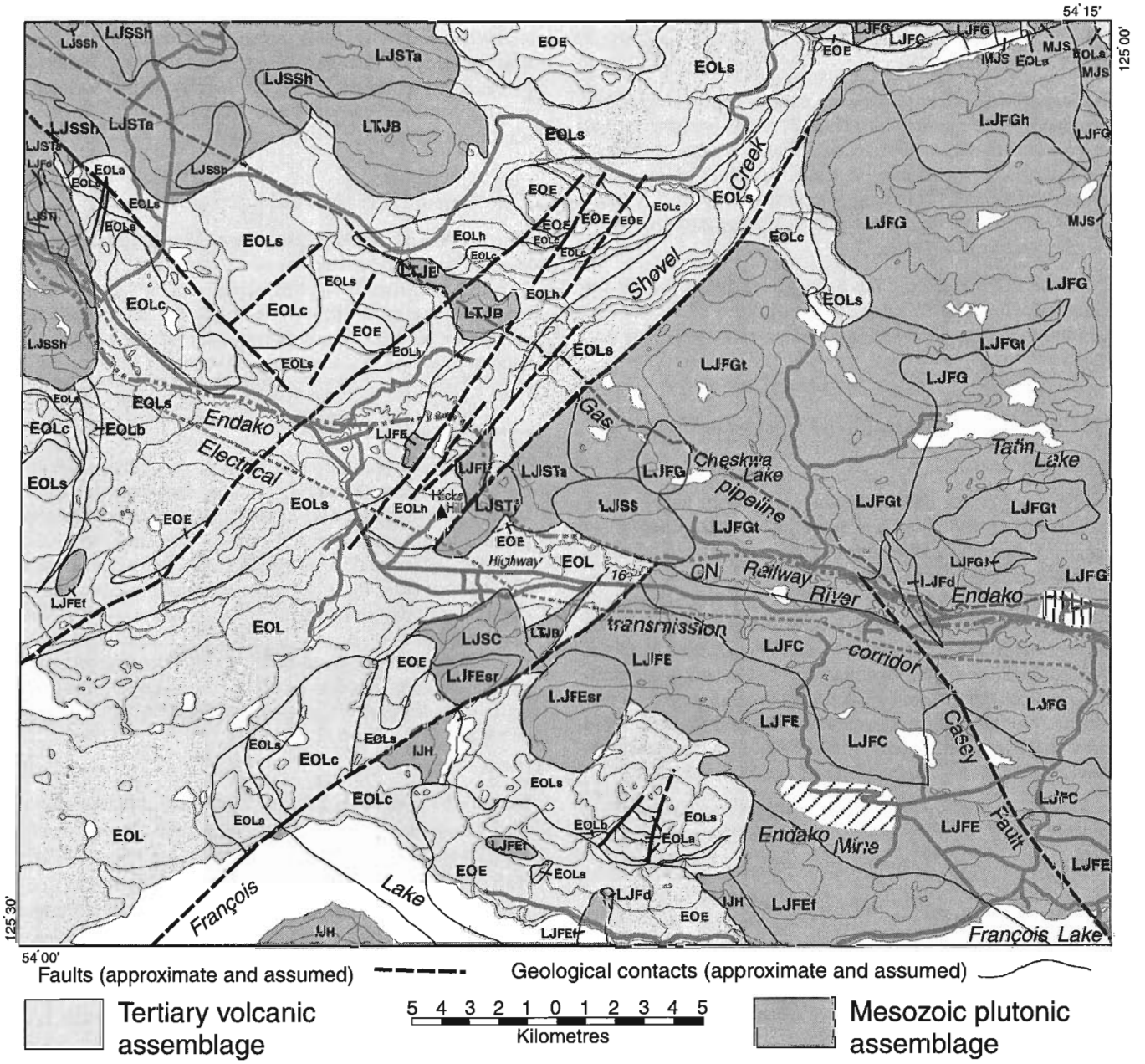

Figure 3. *Geology of the Endako map area and distribution of Tertiary volcanic and Mesozoic plutonic assemblages.*

Tertiary

Eocene - Oligocene

EOE — *Endako Group*: andesite, basalt; flows, breccia, vesicular, amygdaloidal tuff, hyaloclastite, lahar

Eocene

Ootsa Lake Group (**EOL - EOLh**)

EOL — undifferentiated **EOLa - EOLh**

EOLa — rhyodacite, rhyolite; flows, breccia, tuff, locally flow banded; includes some felsic subvolcanic intrusive rocks

EOLb — conglomerate, sandstone, siltstone

EOLc — andesite, basalt, dacite; includes some undifferentiated Ootsa Lake Group units

EOLs — *Savory*: dacite, rhyodacite, and minor andesite and rhyolite

EOLh — *Hicks Hill:* dacite with phenocrystic biotite, hornblende, plagioclase

Mesozoic

Late Jurassic

Francois Lake suite (**LJFC - lJFd**)

LJFC — *Casey phase*: granite, granodiorite

LJFE — *Endako phase*: biotite+/-hornblende granite to granodiorite

LJFEf — *Francois subphase*: biotite granite to granodiorite

LJFEsr — *Sam Ross Creek subphase*: miarolitic granite

LJFG — *Glenannan phase:* biotite granite and granodiorite, porphyritic

LJFGt — *Tatin Lake subphase:* biotite granite, hornblende granodiorite

LJFGh — *Hanson Lake subphase:* biotite granodiorite to quartz monzonite

LJFd — *leucocratic porphyritic granite dykes*

Middle - Late Jurassic

Stag Lake suite (**LJSC - LJSS**)

LJSC — *Caledonia phase*: biotite granodiorite to quartz monzonite, megacrystic

LJSSh — *Sheraton phase*: biotite-hornblende granodiorite to quartz diorite, subporphyritic

LJSTa — *Taltapin phase*: hornblende-biotite diorite to quartz diorite

LJSTl — *Tintagel phase*: granite, chloritized

LJSS — *Stellako phase:* biotite-hornblende quartz diorite to granodiorite

Late Triassic - Middle Jurassic

lJH — *Hazelton Group:* feldspar porphyry andesite, greywacke (S. of François Lake)

Boer plutonic suite (**LTJB - MJS**)

MJS — *Stern Creek phase*: diorite, granodiorite gneiss

LTJB — *Boer phase*: hornblende diorite to quartz diorite

phenocrysts. It was previously mapped by Kimura et al. (1980) as Cretaceous and distinct from the Glenannan phase, but its intrusive relationships with the Glenannan phase suggest that it is a subunit.

The contact between the Hanson Lake subphase and Glenannan phase seems to be gradational, with K-feldspar and plagioclase becoming prominent phenocryst phases, quartz becoming less abundant, and mafic minerals becoming more abundant.

Endako phase (LJFE)

The Endako phase forms an northwest-southeast elongate body in the south-central portion of the map sheet (Fig. 3). It consists of coarse-grained, dark pink to orange, biotite-hornblende granodiorite to granite, subporphyritic with K-feldspar (0.1-1 cm) (Fig. 5). Except within the open pit, where it hosts the Endako molybdenum deposit, it is remarkably fresh with unaltered mafic minerals and a paucity of veining.

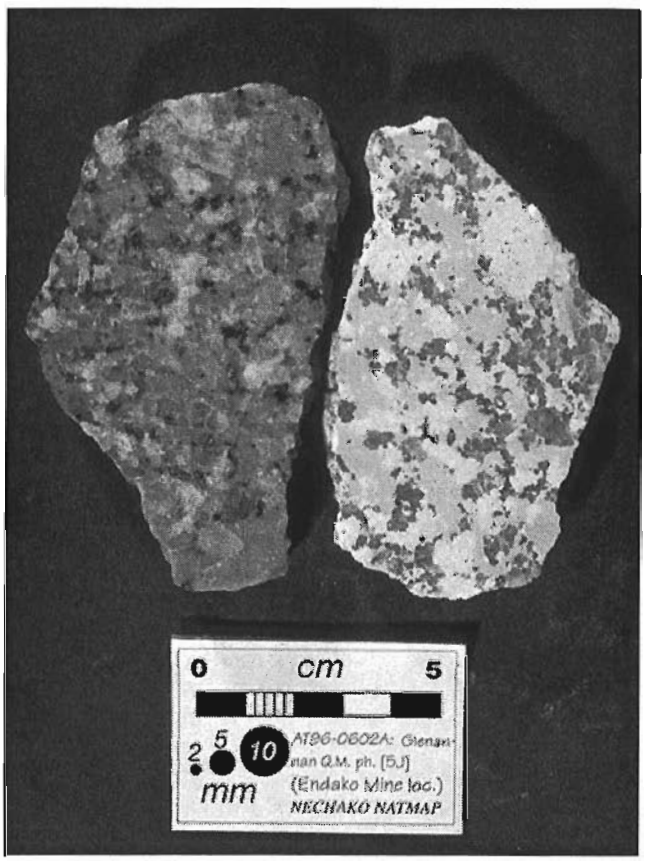

Figure 4. *Polished (left) and stained (right) slabs from the Glenannan phase (a coarse-grained feldspar-porphyritic biotite granodiorite) of the Francois Lake plutonic suite. In the stained slab, quartz is dark grey, K-feldspar is medium grey, and plagioclase is light grey. Photograph by R.G. Anderson.*

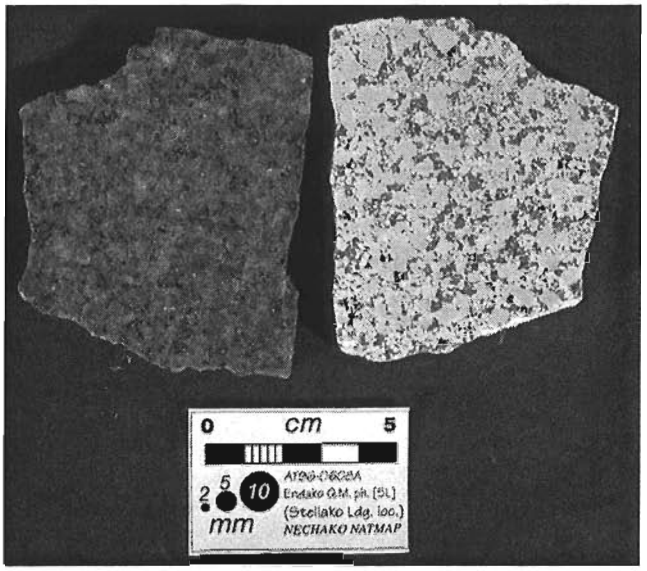

Figure 5. *Polished (left) and stained (right) slabs from the Endako phase (a coarse-grained K-feldspar-subporphyritic biotite-hornblende granodiorite) of the Francois Lake plutonic suite. In the stained slab, quartz is dark grey, K-feldspar is medium grey, and plagioclase is light grey. Photograph by R.G. Anderson.*

Francois subphase (LJFEf). The Francois subphase of the Endako phase is exposed adjacent to the Endako phase, north of François Lake (Fig. 3). It consists of purple to red, medium-grained, equigranular biotite (±hornblende) granodiorite to granite. Although it is relatively equigranular compared to the Endako phase, where fresh, it contains the same distinctive orange K-feldspar. Exposures of this subunit adjacent to and northwest of François Lake are moderately to strongly altered; alteration has imparted a pervasive brick-red to red-brown colour to most of the feldspar and caused the complete replacement of mafic silicates by chlorite. In the most strongly altered portions, chalky white euhedral plagioclase grains stand out on weathered surfaces. The subunit is interpreted to be a 'marginal' or higher-level equivalent of the Endako phase.

Relationships between the Francois subphase and Endako phase are well exposed within a kilometre of the eastern and southern sides of the Endako mine settling pond. There, the contact is marked by a gradational textural change over a short distance (.25 km), but there is no obvious change in bulk composition or in alteration of feldspars or mafic minerals, i.e. in this area, the Francois subphase resembles a medium-grained Endako phase. Furthermore, alteration of the Francois subphase is not associated with the inferred contact between it and the Endako phase, but is developed 0.5 km or more from that contact.

Sam Ross Creek subphase (LJFEsr). The Sam Ross Creek subphase is found on the northern slopes of Savory Ridge, east of Sam Ross Creek. It consists of dark red to purple, medium- to coarse-grained, strongly miarolitic granite with cavities 1–3 cm in size. It exhibits pervasive alteration similar to that of the Francois subphase and, like that subphase, contains chalky white plagioclase grains. The abundant miarolitic cavities are lined with euhedral quartz and feldspar. The subunit is bordered to the west by dark red-brown, white-plagioclase-phyric (0.1–0.3 cm), rhyolitic rocks, which, as they lack obvious flow banding or bedding, could represent high-level intrusive rather than extrusive rocks. These fine-grained felsic rocks are cut by common pyrite-bearing fractures.

On the basis of its appearance and distribution, the Sam Ross Creek subphase is interpreted to be a higher level and/or water-oversaturated equivalent of the Francois subphase, which itself is thought to bear a similar relationship to the Endako phase. The rhyolitic rocks bordering the Sam Ross Creek subphase to the west may also be comagmatic. If so, then their distribution is suggestive of a higher level of exposure within the Endako phase and its subphases from southeast to northwest, away from the Endako mine.

Casey phase (LJFC)

The Casey phase is exposed only south of the Endako River valley, along the northeast side of the Endako phase (Fig. 3). Plutonic rocks of similar texture and composition north of this valley, which were previously included in this phase by Kimura et al. (1980), are now interpreted to be a subunit of the Glenannan phase. The Casey phase consists of dark pink, fine- to medium-grained, granophyric biotite granite or aplitic granite (Fig. 6). Small miarolitic cavities are relatively common. Portions of the unit contain dark pink potassium feldspar and ovoid quartz-eye phenocrysts. Biotite is commonly oxidized or chloritized.

An intrusive contact between the younger Casey phase and Endako phase country rocks was observed northeast of Savory Ridge.

The Casey phase has been dated at 145.0 ± 0.5 Ma using U-Pb zircon (M. Villeneuve, pers. comm., 1997).

Tertiary volcanic complex

Ootsa Lake Group (EOL)

The Ootsa Lake Group consists of dacite, rhyodacite, andesite, rhyolite, and minor conglomerate and sandstone, here subdivided into five named and unnamed informal units: Hicks Hill dacite, Savory dacite, an andesitic sequence, a sedimentary sequence, and a rhyodacite/rhyolite-rich sequence. The stratigraphic order of the rock types varies from place to place, and it is unclear whether there is a consistent pattern of mafic to felsic transition upsection as seen elsewhere (e.g., Diakow and Koyanagi, 1988). It is clear that the composition of the Ootsa Lake Group ranges from mafic to felsic here, to the south (R.G. Anderson and L. Snyder, pers. comm., 1997; Anderson and Snyder, 1998), and elsewhere

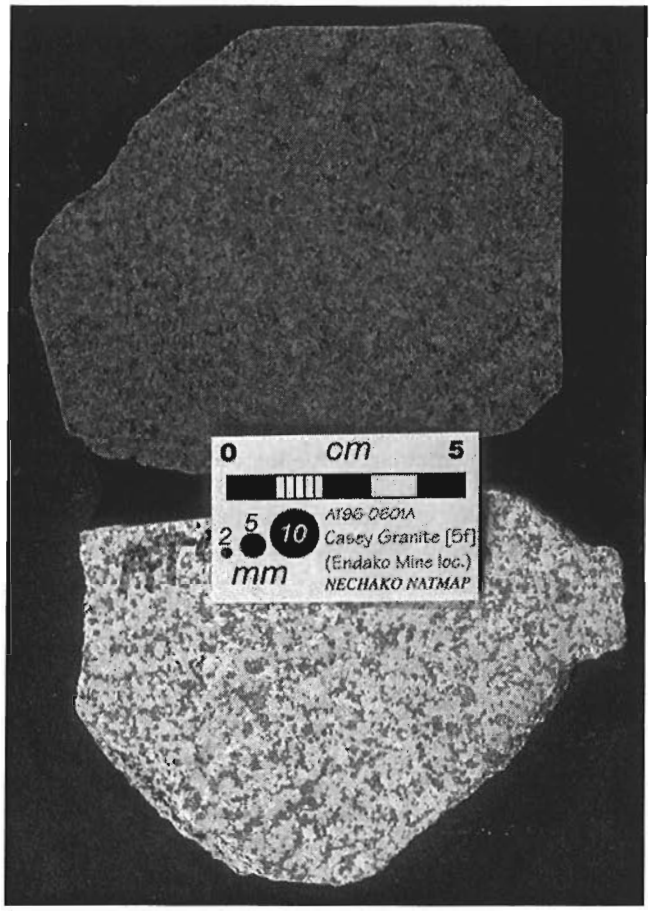

Figure 6. *Polished (top) and stained (bottom) slabs from the Casey phase (a fine- to medium-grained granophyric biotite granite) of the Francois Lake plutonic suite. In the stained slab, quartz is dark grey, K-feldspar is medium grey, and plagioclase is light grey. Photograph by R.G. Anderson*

(Drobe, 1991; Wheeler and McFeely, 1991). Biotite Ar-Ar dating of the Ootsa Lake Group from nearby localities gives an age of 50 ± 0.5 Ma (M. Villeneuve, pers. comm., 1997).

Hicks Hill dacite (EOLh)

The Hicks Hill dacite (Fig. 7) occurs in various parts of the map area and is particularly well exposed on Hicks Hill, near Richmond Lake east of Priestly, and along the Hannay Forest Service Road between kilometres 16 and 18. Similar rocks can be found directly to the south in the Nechako River map area (R.G. Anderson, pers. comm., 1997).

The rock consists of plagioclase, hornblende, and biotite phenocrysts in an olive aphanitic matrix. Phenocrysts constitute approximately 30% of the rock. Plagioclase (2-9 mm, 15%) is euhedral and generally partially altered to epidote, chlorite, and clays. Hornblende (1-5 mm, 6-9%) is acicular and commonly aligned along variably oriented surfaces. In many places, the hornblende cores are preferentially altered, leaving elliptical hollows on weathered surfaces. The biotite (0.5-1.5 mm, 1-5%) is euhedral and varies from fresh to partly chloritized. At Hicks Hill and some other localities, the dacite is layered, as defined by 2-5 cm thick recessive layers separated by 25-40 cm thick more resistant layers. Hornblende is aligned parallel to the layering and locally outlines outcrop-scale undulatory surfaces.

The Hicks Hill dacite is interpreted to be a crystal tuff and flow sequence that may be locally intrusive. In places, it seems to grade into andesite porphyries with coarser crystalline plagioclase and more or less hornblende and biotite.

Savory dacite (EOLs)

Along Savory Ridge and to the west, north of the Tchesinkut River, an extensive plagioclase-phyric dacite unit dominates the Ootsa Lake Group (Fig. 8). The dacite weathers tan and is light olive, mauve-green, or grey on fresh surfaces. Plagioclase phenocrysts are euhedral to subhedral and range in size from 2 to 15 mm and constitute 5 to 20% of the rock. Biotite ranges in size from 2 to 8 mm and constitutes up to 8% of the rock.

Locally, the dacite is interlayered with dacite lapilli tuff. It generally has a closely spaced fracture cleavage. The Savory dacite contains interbeds of rhyolite and rhyolite breccia and conglomerate. The conglomerate exposed in the lower part of the section on the south flank of Savory Ridge contains subangular clasts of dacite, rhyolite, and basalt.

Figure 7. *Hicks Hill dacite of the Ootsa Lake Group.*

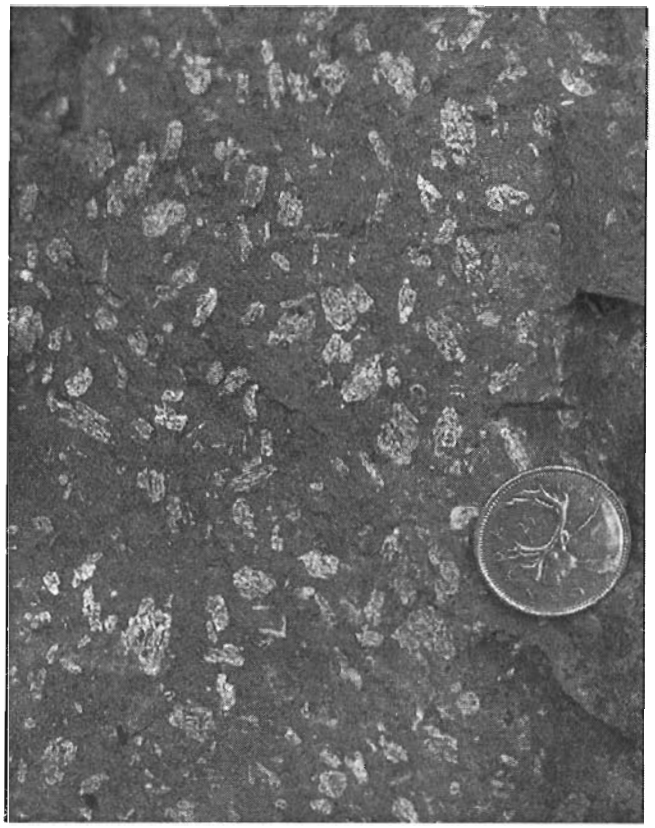

Figure 8. *Savory dacite of the Ootsa Lake Group.*

Andesitic sequence (EOLc)

Mafic volcanic sequences of the Ootsa Lake Group are exposed throughout the map area, and are most abundant to the west. The sequences consist mainly of andesite and basalt, and include some interlayered dacite and rhyodacite. Massive aphanitic to finely crystalline plagioclase-phyric andesite and basalt weather grey to dark grey and are olive-grey, locally mixed with purple, on fresh surfaces. An easily accessible example of the basalt is exposed along the north side of Highway 16, east of Fort Fraser in the Vanderhoof map area (93K/1); it has a whole-rock K-Ar age of 49.6 Ma (Mathews, 1988). Andesite forms the basal part of the Ootsa Lake Group near Priestly and is part of the dacite-rich sequences north of the Tchesinkut River, in the southwestern part of the map area.

South of the Hannay Forest Service Road, fracture-cleaved andesite weathers grey to dark grey and is olive-grey on fresh surfaces. It contains 2-4% euhedral feldspar phenocrysts that could be potassium feldspar. The well preserved crystals are translucent and free of alteration; chlorite or epidote are common in other andesite porphyry units. The rock also contains minor amounts of biotite (0.5-1.5 mm).

A section along Sheraton Creek exposes the contact between the andesite unit and an overlying feldspar-porphyry dacite crystal tuff. The top of the andesite unit consists of several metres of ash, breccia, tuff, and lahar with cobble and smaller sized fragments floating in the ash and tuff matrix. These volcaniclastic rocks grade upwards over 1 m into the dacite tuff sequence.

Conglomerate and sandstone unit (EOLb)

Conglomerate and sandstone of the Ootsa Lake Group are found on the north- and south-facing slopes of the hill south of the electrical transmission corridor at the west end of the map area. They are well exposed along the access road to the communications towers at the top of the hill. They are interbedded in 1-2 m thick units and may form in total a 20-40 m thick sequence.

The conglomerate is purple-grey and contains 0.2-5 cm subrounded and oblate clasts (Fig. 9) of basalt, chert, jasper, granite, and rhyolite. The matrix consists of silt- to sand-sized grains derived from basalt and chert. In most places, the

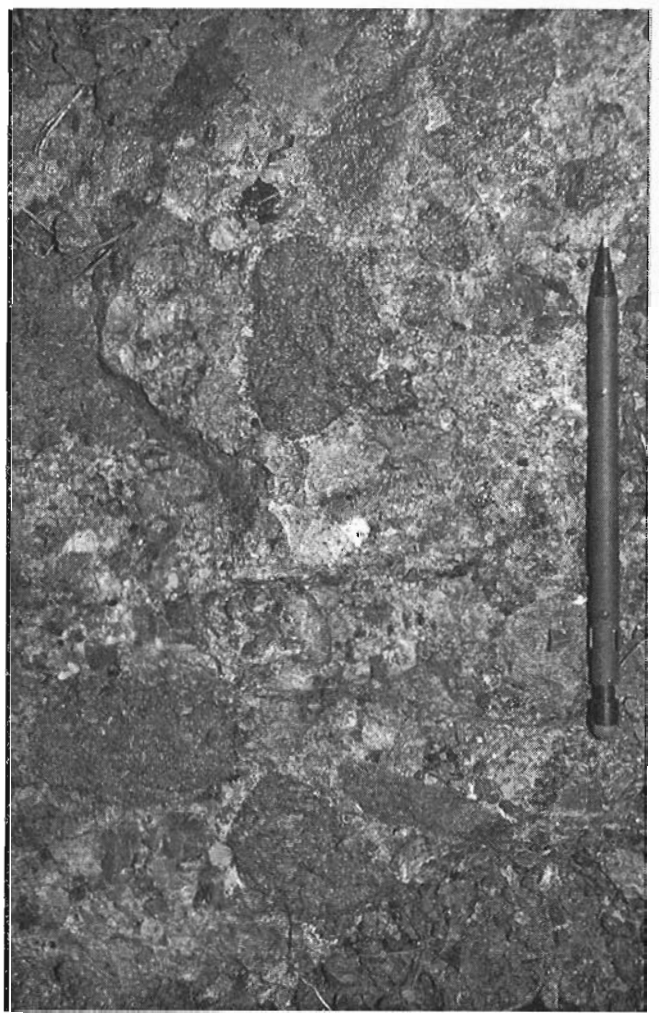

Figure 9. *Conglomerate from the sedimentary unit of the Ootsa Lake Group (EOLb), containing clasts of cherty tuff, rhyodacite, andesite, and quartz.*

sandy matrix of the conglomerate and the sandstone are apparently derived from a basalt or andesitic lapilli tuff. The conglomerate is overlain by Savory dacite and rhyolite and underlain by dacite and andesite.

Rhyodacite/rhyolite sequence (EOLa)

Rhyodacite and rhyolite of the Ootsa Lake Group occur throughout the Endako map area, generally as members in volcanic sequences of more intermediate composition. Local dykes of quartz-feldspar-porphyry rhyolite are included in this unit. The rhyodacite and rhyolite weather tan or cream and are mostly light grey to white on fresh surfaces. They commonly host euhedral to subhedral phenocrysts of plagioclase, K-feldspar, quartz (1-4 mm, 3-25%), and locally biotite.

The textures vary from the commonly massive to local flow-bands, breccias, welded tuffs, and columnar jointing. Breccia fragments range from 1-15 cm long, are randomly dispersed and matrix supported, and have felsic to intermediate compositions. Columnar joints perpendicular to the contacts were found in each of the dykes.

Endako Group (EOE)

The unit outcrops north of the Endako River on a few hills, along the north shore of François Lake, and as scattered basalt dykes cutting older units. In the Endako map area it consists primarily of basalt flows and minor fragmental deposits. The flows are generally 6-12 m thick and are defined by breccias at their base and top and by vesicle-rich zones. Locally, they show columnar jointing.

North of the Endako River, the unit consists mainly of hyaloclastic basalt (Fig. 10) and overlies a possible trachyandesite and a dacite assigned to the Ootsa Lake Group. The unit is over 200 m thick; its lower contact with the andesite was not observed. The hyaloclastite consists of fragments of dark grey basalt with a resinous lustre in a recessive brown- and grey-weathering matrix of similar composition. It weathers to rounded forms. The fragments are 1-80 cm across, subrounded to subangular, and constitue 30% to 70% of the rock. Locally, the unit contains white and apple-green, agate-filled, irregularly shaped interstices. Parallel, slightly more recessive, 5-10 cm thick zones seem to follow depositional layering. A similar hyaloclastic unit outcrops to the southeast in the Fraser Lake map area (93K/2), on the north side of Fraser Lake.

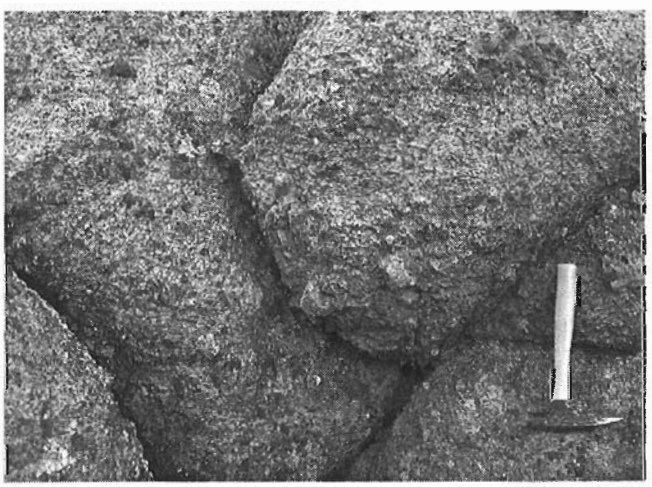

Figure 10. *Endako Group hyaloclastic basalt from north of Shovel Creek.*

Flows of the Endako Group, exposed along the north shore of François Lake, consist of more or less vesicular, dark grey, aphanitic to plagioclase- and pyroxene-phyric basalt. They are presumed to be in angular unconformity with dacites and rhyolite flows of the Ootsa Lake Group and nonconformable with granodiorite of the Francois Lake plutonic suite.

FAULT PATTERNS

Strike-slip and extensional faults have been mapped and interpreted throughout the Endako map area. The best exposed and most studied of the faults are found in the area of the Endako mine (Kimura et al., 1976; Bysouth and Wong, 1995).

The Casey Fault (Fig. 3) flanks the eastern part of the Endako molybdenum mine and extends north-northwesterly to the Endako River. Dextral strike-slip kinematic indicators are seen where it is exposed adjacent to François Lake and offsets latest Jurassic plutons of the Francois Lake plutonic suite.

In the central part of the map area, northeasterly trending extensional faults have been mapped adjacent and parallel to the Shovel Creek valley. They offset the Tertiary Ootsa Lake and Endako groups as well as the Jurassic plutonic suites. Northwest of Shovel Creek, extensional faults downdrop Endako Group basalt and older units to the southeast.

DISCUSSION

Mesozoic assemblage

Some notable changes or revisions have been made to the interpretation of the plutonic units by Kimura et al. (1980). Some of these new ideas have implications for mineral exploration in the Endako molybdenum camp.

It has been recognized that the Francois Lake plutonic suite consists of various phases that have some genetic linkages. Our current understanding has the Glenannan and Endako phases of the Francois Lake plutonic suite as prominent plutonic pulses separated by about 8 to 10 Ma, each of which includes several subphases (M. Villeneuve, pers. comm., 1997).

Our reinterpretation suggests that on the map of Kimura et al. (1980), the Casey phase included not only the 'type' Casey phase, but also compositionally and texturally similar older phases. The type Casey phase underlies an area proximal to the Endako mine and is a relatively late phase of the Francois Lake plutonic suite. The other Casey-like phases are spatially and temporally linked with the Glenannan phase, a relatively early phase of the Francois Lake suite. These older Casey look-alikes have been grouped into a new unit, the Tatin Lake subphase. This may have significance for exploration should there be a genetic link between the Casey phase and molybdenum mineralization, in which case it would be important to distinguish this phase from older compositionally and texturally similar phases.

The Francois granite of Kimura et al. (1976) is here reinterpreted to be a subphase of the Endako phase, as is a newly recognized highly miarolitic granite unit, the Sam Ross Creek subphase. Both subphases are interpreted to be higher level and/or vapour-oversaturated equivalents of the Endako phase. It is also possible that the unstratified (probably high-level intrusive) rhyolitic rocks bordering the Sam Ross Creek subphase on the northwestern slopes of Savory Ridge may be of Jurassic age.

The currently understood outcrop geometry of the Endako phase and its probable subphases would have the Endako pluton tilting west to northwest. Both the Endako phase and Francois subphase are elongated northwest-southeast and, to the northwest, the Francois subphase is bordered by or possibly grades into the Sam Ross Creek subphase, which in turn is bordered to the west by rhyolitic possibly intrusive rocks. These features can be interpreted as reflecting a higher level of exposure within the suite to the west and northwest away from the Endako mine, and the possible presence of a proximal Jurassic extrusive cap, now obscured by unconformable Tertiary volcanic sequences.

Tertiary assemblage

The sedimentary units of the Ootsa Lake Group contain material derived from volcanic rocks of the same group, which implies the existence of local topographic relief established during the deposition of the Ootsa Lake Group. Such relief is consistent with the interpretation of syndepositional extensional faulting concurrent with the crustal extension associated with the formation of the Eocene Vanderhoof Metamorphic Complex east of the Endako map area (Struik and Wetherup, 1977).

The extension faults that offset the rocks of the Ootsa Lake and Endako groups in the Shovel Creek area are at least as young as Middle to Late Eocene. Their northeasterly orientation is consistent with the west-northwesterly direction of extension determined for the Vanderhoof Complex. The extension that started in the Early Eocene could have continued through to the Late Eocene. It may also have occurred in two distinct pulses in slightly different orientations (Struik, 1993).

ACKNOWLEDGMENTS

Crystal Huscroft, Andrew Blair, Angelique Justason, and Nancy Grainger each contributed to the mapping. We thank the Thompson Creek Mining Company who, through Glenn Johnson, provided access for mapping purposes to the company property (formerly Endako Mines). Mary Lou Bevier kindly showed us some of the suites of Tertiary basalts that she has studied in the region. Bob Anderson constructively reviewed an early version of the manuscript and assisted in preparation of the manuscript. Ken and Laurie Lindenberger provided warm hospitality at the Pipers Glen Resort.

REFERENCES

Anderson, R.G. and Snyder, L.D.
1998: Jurassic to Tertiary volcanic, sedimentary, and intrusive rocks in the Hallett Lake area, central British Columbia; in Current Research 1998-A; Geological Survey of Canada.

Anderson, R.G., L'Heureux, R., Wetherup. S., and Letwin, L.
1997: Geology of the Hallett Lake map area, central British Columbia: Triassic, Jurassic, Cretaceous, and Eocene? plutonic rocks; in Current Research 1997-A; Geological Survey of Canada, p. 107-116.

Bysouth, G.D. and Wong, G.Y.
1995: The Endako molybdenum mine, central British Columbia: An update; in Porphyry Deposits of the Northwestern Cordillera of North America, (ed.) T.G. Schroeter; Canadian Institute for Mining, Metallurgy and Petroleum, Special Volume 46, p. 697-703.

Diakow, L.J. and Koyanagi, V.
1988: Stratigraphy and mineral occurrences of Chikamin Mountain and Whitesail Reach map areas; in Geological Fieldwork 1987; British Columbia Ministry of Energy, Mines, and Petroleum Resources, Paper 1988-1, p. 115-168.

Drobe, J.R.
1991: Petrology and petrogenesis of the Ootsa Lake Group in the Whitesail Range, west-central British Columbia; MSc thesis, Queens University, Kingston, Ontario, 220 p.

Energy, Mines, and Resources
1977: Endako (93K/3), British Columbia; Surveys and Mapping Branch, Energy, Mines, and Resources (scale: 1/50 000).

Enkin, R.J, Baker, J., Struik, L.C., Wetherup, S., and Selby, D.
1997: Paleomagnetic determination of post-Eocene tilts in the Nechako Region; Geological Association of Canada, Annual Meeting, Abstract, v. 22, p. A46.

Kimura, E.T., Bysouth, G.D., Cyr, J., Buckley, P., Peters, J., Boyce, R., and Nilsson, J.
1980: Geology of parts of southeast Fort Fraser and northern Nechako River map areas, central British Columbia; Placer Dome Incorporated, Internal Report and Maps, Vancouver, British Columbia.

Kimura, E.T., Bysouth, G.D., and Drummond, A.D.
1976: Endako; in Porphyry Deposits of the Canadian Cordillera, (ed.) A. Sutherland Brown; Canadian Institute of Mining and Metallurgy, Special Volume 15, p. 444-454.

Mathews, W.
1988: Neogene geology of the Okanagan Highland, British Columbia; Canadian Journal of Earth Sciences, v. 25, p. 725-731.

Struik, L.C.
1993: Intersecting intracontinental Tertiary transform fault systems in the North American Cordillera; Canadian Journal of Earth Sciences, v. 30, p. 1262-1274.

Struik, L.C. and MacIntyre, D.G.
1997: Nechako Plateau NATMAP Project overview, central British Columbia, year two; in Current Research 1997-A; Geological Survey of Canada, p. 57-64.
1998: Nechako NATMAP Project overview, central British Columbia, year three; in Current Research 1998-A; Geological Survey of Canada, p. XX-XX.

Struik, L.C. and Wetherup, S.
1997: Features of Tertiary crustal extension in central British Columbia; Geological Association of Canada, Annual Meeting, Abstract, v. 22, p. A144.

Villeneuve, M.E., Struik, L.C., MacIntyre, D.G., Anderson, R.G., and Whalen, J.B.
1997: Timing of Eocene and Jurassic magmatism in Nechako Plateau, Central B.C., and relationships to porphyry deposits; Geological Association of Canada, Annual Meeting, Abstract, v. 22, p. A154.

Whalen, J.B. and Struik, L.C.
1997: Plutonic rocks of southeast Fort Fraser map area, central British Columbia; in Current Research 1997-A; Geological Survey of Canada, p. 77-84.

Wheeler, J.O. and McFeely, P.
1991: Tectonic assemblage map of the Canadian Cordillera and adjacent parts of the United States of America; Geological Survey of Canada, Map 1712A (scale 1:2 000 000).

Geological Survey of Canada Project 950036

Magnetic and paleomagnetic constraints on Tertiary deformation in the Endako region, central British Columbia[1]

C. Lowe, R.J. Enkin, and J. Dubois
GSC Pacific, Sidney

Lowe, C., Enkin, R.J., and Dubois, J., 1998: Magnetic and paleomagnetic constraints on Tertiary deformation in the Endako region, central British Columbia; in Current Research 1998-A; Geological Survey of Canada, p. 125-134.

Abstract: It has been proposed that the Nechako NATMAP Project area in central British Columbia records a significant history of Tertiary transtensional deformation. For evidence of this deformation, the magnetic response and record of rocks were examined in a 1300 km² area encompassing the Endako molybdenite deposit. Magnetic anomaly and rock property data distinguish subtle age and mineralogical differences within lithologically similar rock units. Mapped faults trend predominantly NE and NW and typically correspond to linear zones of steep magnetic gradient. Other prominent northeast- and northwest-trending magnetic lineaments are also interpreted to be shallow faults, which divide the region into fault-bounded blocks. In the Endako mine, paleomagnetically determined tilts on Eocene dykes are aligned with ore-bearing veins, indicating that deformation was Tertiary. A kilometre-scale anticline is recognized within the pit. Tilts tend to be ~20° eastward in map area 93K/2 and more random in map area 93K/3.

Résumé : La région visée par le Projet de Nechako du CARTNAT, dans le centre de la Colombie-Britannique, témoignerait d'une histoire de déformation par transtension au Tertiaire. Nous avons cherché des indices de cette déformation dans la réponse magnétique des roches dans une région de 1 300 km² qui comprend le gisement de molybdénite d'Endako. Les anomalies et propriétés magnétiques des roches font reconnaître de subtiles différences dans l'âge et la minéralogie d'unités rocheuses lithologiquement semblables. Les failles cartographiées ont des directions nord-est et nord-ouest prédominantes et correspondent typiquement à des zones linéaires de gradient magnétique raide. D'autres grands linéaments magnétiques à direction nord-est ou nord-ouest seraient aussi des failles peu profondes, qui divisent la région en blocs. Dans la mine Endako, le basculement de dykes éocènes, déterminé par des données paléomagnétiques, est parallèle aux filons minéralisés, ce qui indique que la déformation remonte au Tertiaire. Un anticlinal d'échelle kilométrique est reconnu dans la mine. Le basculement est d'environ 20° est dans la région cartographique 93K/2 et plus aléatoire dans la région cartographique 93K/3.

[1] Contribution to the Nechako NATMAP Project

INTRODUCTION

One of the primary objectives of the Nechako NATMAP Project in central British Columbia (Fig. 1) is to test the hypothesis that the current distribution of rock units and structures is, in part, due to a Tertiary transtensional tectonic regime (Struik, 1994; MacMillan and Struik, 1996). This hypothesis has direct implications for the location and geometry of economic deposits in the region, and more generally elucidates the geodynamic history and paleogeography of the Cordillera. Extension of the crust during Eocene to Miocene times is evidenced by the continental lava flows of the Endako and Chilcotin groups that now cover large parts of the Nechako Plateau. The portion of the Nechako Plateau investigated here (Fig. 2) is underlain primarily by granitic rocks of the Late Jurassic to Early Cretaceous Francois Lake Plutonic Suite. Field recognition of deformation in massive and lithologically similar rocks is often difficult and is particularly challenging in this area where exposure is very limited. The record of Tertiary deformation in these rocks is evaluated through analysis of their magnetic properties. Aeromagnetic anomaly data, magnetic susceptibility data, and the record of remanent magnetization contained in the rocks were used to interpret the bedrock geology beneath the glacial cover, to locate faults, and to determine the magnitude, timing, and orientation of displacements.

The Endako porphyry molybdenum deposit is 160 km west of Prince George in central British Columbia (Fig. 2). It was discovered in 1927 and officially opened as a mine by Placer Dome Limited in 1965. The mine was sold in the spring of 1997 to Thompson Creek Mining Co. of Denver, Colorado. Ore reserves as of January 1, 1993, were estimated at 120.4 million tonnes averaging 0.136% MoS_2. The low concentration and disseminated nature of sulphides in the ore generally results in weak electromagnetic anomalies, and geophysical delineation of the orebody by other means has not been very successful (Bysouth and Wong, 1995). However, structural control on the mineralized veins and on the host rock is well documented (Bysouth and Wong, 1995), and the displacement structures delineated in this study may be used to guide future molybdenum exploration.

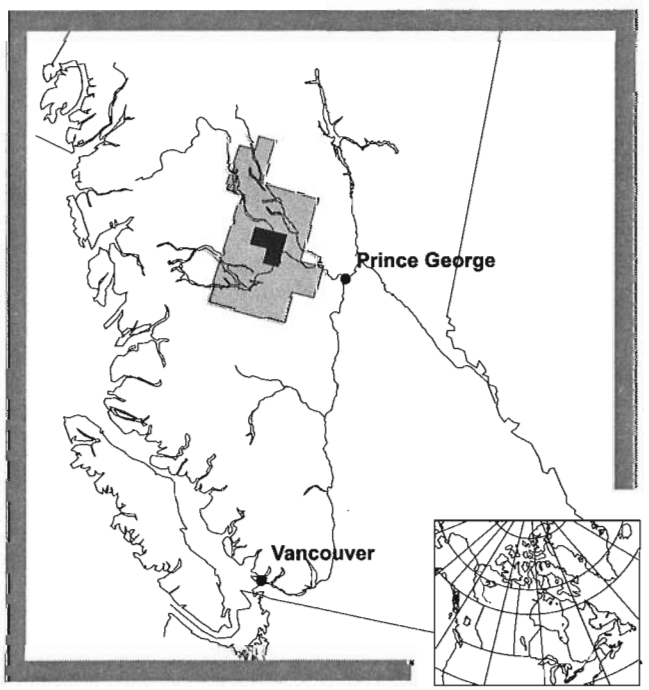

Figure 1. *Map of British Columbia showing the locations of the Nechako NATMAP Project area (grey) and this study (black).*

GEOLOGICAL SETTING

The survey area has a generally subdued topography characterized by broad glaciated valleys separated by gentle flat-topped hills. Overall exposure is limited to approximately 5%.

Upper Triassic volcanic and volcaniclastic rocks of the Takla Group exposed along the north shore of François Lake are the oldest rocks in the study area (Fig. 2). They were intruded by Triassic to Eocene plutons and subsequently overlain by the possibly extension-generated Eocene Ootsa Lake and Eocene and Oligocene Endako groups and the possible mantle-plume generated Miocene Chilcotin Group (Struik et al., 1997). Locally Tertiary sedimentary rocks are included in the Tertiary volcanic sequences. Late Jurassic to Early Cretaceous intrusive rocks (White et al., 1968, 1970; Bysouth and Wong, 1995, and references therein) of the Francois Lake Plutonic Suite dominate much of the central study area. Aerially, the most significant units of this suite are the Casey (an aplitic biotite granite), Nithi, Glenannan, and Endako phases (K-feldspar megacrystic biotite granodiorite to granite; Whalen et al., 1998). The Endako phase hosts the Endako molybdenite orebody.

Regionally, the Nechako has been dissected by northwesterly, northeasterly, and easterly trending fault systems (MacIntyre et al., 1996; Struik and Wetherup, 1997) that are well documented in the Endako mine (Fig. 2). Most faults are poorly exposed and little is known about their geometry or sense of motion. However, at least 4 km of horizontal displacement has occurred across the northwest-trending Casey Fault, as evidenced by the mapped offset of the Endako phase. To date, mapping of the plutonic units has concentrated on resolving intrusive relationships and relatively little work has been undertaken on the extent and/or nature of brittle deformation within the bodies. However, a northwest-trending mineral foliation is observed in several phases of the Francois Lake Plutonic Suite.

Endako molybdenite deposit

The Endako molybdenite deposit is hosted by the Endako phase of the Francois Lake Plutonic Suite (Fig. 2). In the mine area, this phase is intruded by quartz-feldspar porphyry and porphyritic granite dykes that predate the ore and by basalt dykes that postdate it. In plan view, the orebody is 3.4 km

long by 0.4 km wide (Kimura and Drummond, 1969) and consists of four distinct fault-bounded zones (Bysouth and Wong, 1995): Endako East, Endako West, Denak East, and Denak West (see Fig. 5). The sulphides and associated minerals are hosted mainly in structurally controlled, south-dipping quartz vein systems that strike 110° in the Endako zones, 110°-130° in Denak East, and 170° in Denak West (Bysouth and Wong, 1995). Domal uplift accompanying the rise of latest stage magma is considered to have caused intense dilational deformation along older west-northwest-trending shear zones, producing a structural host that is elongated to the northwest.

MAGNETIC SUSCEPTIBILITY DATA

Magnetic susceptibility measurements were conducted on approximately 400 outcrop, hand, and drill core rock samples from the region. Although not all of the exposed map units were sampled and sampling was biased and/or insufficient in some units, the results (Table 1) indicate a strong correlation between silica content and magnetic susceptibility. Diorite and monzodiorite of the Boer and Stag Lake (Limit Lake and Twenty-six Mile Lake phases) plutonic suites yield some of the highest measured magnetic susceptibility values (up to 117 x 10^{-3} SI), basalts in the Chilcotin and Endako groups

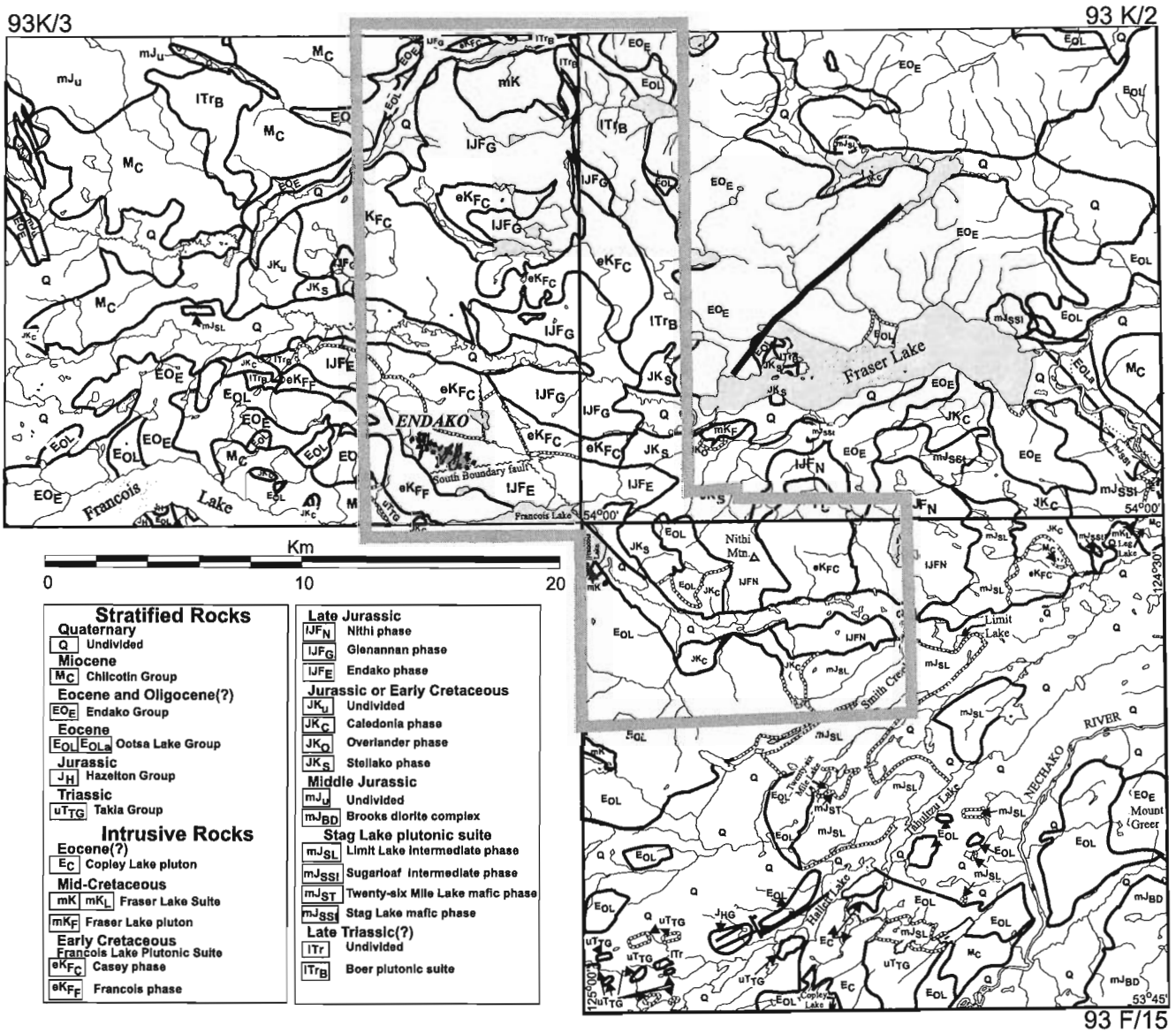

Figure 2. Unpublished regional geological compilation map of the study area by Anderson et al. (1997b), based on work by Kimura et al. (1980), Anderson et al. (1997a), Struik et al. (1997), and Whalen and Struik (1997). The extent of the high-resolution aeromagnetic survey is outlined.

also yield high values (up to 51 x 10^{-3} SI), whereas rhyolites in the Endako and Ootsa Lake groups yield lower values (typically <6 x 10^{-3} SI).

Weathered and/or altered samples from most units yield lower magnetic susceptibility values than fresh and/or unaltered samples. This is well documented by L'Heureux and Anderson (1997) for the Francois Lake Plutonic Suite in the Nithi Mountain area. There, unaltered samples of the Nithi and Casey phases yield values of 5–24 x 10^{-3} SI and 5–10 x 10^{-3} SI, respectively, whereas destruction of magnetite in areas of clay and propylitic alteration results in values that are consistently below 1 x 10^{-3} SI. The Casey phase has a lower mean magnetic susceptibility than the more mafic Glenannan or Endako phases. The mean susceptibilities reported for the Nithi and Francois phases reflect, to some extent, biased sampling of altered rocks. Similarly, as predominantly felsic rocks were measured in the Ootsa Lake Group, the mean susceptibility reported (13 x 10^{-3} SI) is likely lower than the true mean.

AEROMAGNETIC DATA

In 1995, as part of the Nechako NATMAP Project, high-resolution total-field magnetic data were acquired in a 700 km² survey area incorporating the Endako deposit in central British Columbia (Fig. 3). Flight lines were oriented at an azimuth of 90°, with an average line spacing of 500 m, and a mean aircraft-terrain clearance of 100 m. Residual magnetic anomaly data were computed using the 1995 International Geomagnetic Reference Field. These data were analyzed together with older aeromagnetic data acquired by the Geological Survey of Canada as part of the National Aeromagnetic Program, which were collected on north-trending flight lines flown 800 m apart at a mean terrain clearance of 300 m and are consequently of lower resolution.

A variety of processed magnetic images (including first- and second-order derivatives, shaded images and the analytical signal) as well as the results of Euler deconvolution (Reid et al., 1980; Thompson, 1982) were analyzed to extract

Table 1. Measured magnetic susceptibility of rock units in the Endako survey area.

Unit	Description	Susceptibility x 10^{-3} SI		No.
		Mean	Range	
Chilcotin Group	basalt	25.45	13.2 - 35.8	4
Endako Group	basalt, andesite, and volcaniclastic rocks	15.48	1.00 - 51.4	71
Ootsa Lake Group	rhyolite, dacite, andesite, and volcaniclastic rocks	*12.82	0.00 - 26.1	17
Takla Group	basalt, breccia, argillite, and volcaniclastic rocks	80.90		1
Copley Lake pluton	biotite monzogranite	14.53	10.50 - 19.4	3
Leg Lake pluton	biotite monzogranite	17.38	2.40 - 43.4	4
Francois Lake Plutonic Suite				
Casey phase	aplitic biotite granite	9.34	0.00 - 52.30	51
Francois phase	biotite monzogranite	6.48	0.00 - 22.80	17
Nithi phase	K-feldspar biotite granodiorite	6.32	0.13 - 23.80	26
Glenannan phase	granodiorite to granite	13.03	0.29 - 22.30	67
Endako phase	K-feldspar biotite granodiorite	19.52	0.50 - 59.30	28
Tintagel phase	quartz monzonite	33.6	17.20 - 50.0	2
Caledonia phase	K-feldspar biotite monzogranite	27.21	1.09 - 54.7	7
Stellako phase	quartz monzonite	31.89	1.76 - 68.7	19
Undivided mid-Jurassic including Sheraton and Talapin phases		50.43	32.7 - 62.2	3
Stag Lake Suite				
Limit Lake phase	biotite quartz monzodiorite	26.78	2.93 - 70.3	42
Twenty-six Mile	hornblende diorite	62.25	37.8 - 86.7	2
Boer pluton	biotite hornblende diorite	37.15	1.96 - 117.0	57

* The mean magnetic susceptibility of the Ootsa Lake Group is likely higher than listed as measurements were conducted on only the most felsic units (i.e. rhyolites).

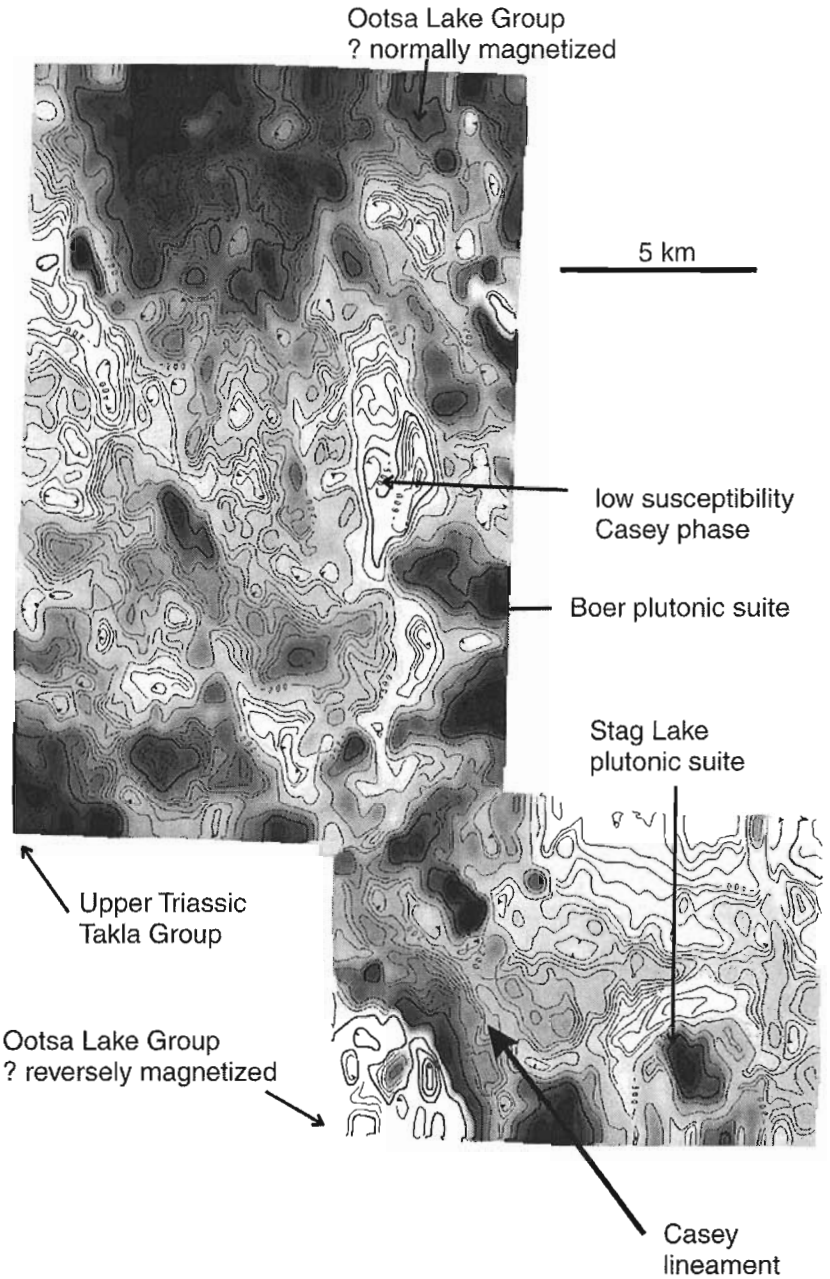

Figure 3. *High-resolution aeromagnetic anomaly data for the area outlined in Figure 2. Low values are shown in light shades and high values, in dark shades. Annotated features are discussed in text.*

geologically and structurally significant information. Published 1:50 000 scale Open File images of the regional magnetic data should be referred to for higher resolution than can be shown here (Geological Survey of Canada, 1961a, 1961b, 1967).

Although some notable exceptions occur, generally a good correlation exists between magnetic data, measured magnetic susceptibilities, and mapped geology. In the area of high-resolution data (Fig. 3), elevated magnetic values correlate with granodiorite of the Stellako phase, basalt of the Upper Triassic Takla Group, and diorite of the Stag Lake plutonic suite. Elsewhere in the study area, elevated magnetic values occur in areas underlain by the Middle Jurassic Brooks diorite complex and by the Boer plutonic suite (Fig. 2, 3).

Strong positive (up to 2200 nT) magnetic anomalies correspond to outcrops of the Endako Group in the northeast and west. Outcrops of the Ootsa Lake Group to the east and of the Chilcotin Group to the west also give high magnetic values (typically >1000 nT). In contrast, these same groups have strong negative anomalies (as low as -800 nT) where they outcrop elsewhere in the study area (for example, anomalies over the Ootsa Lake Group identified in Figure 3). The Chilcotin, Endako, and Ootsa Lake groups have moderate to high mean magnetic susceptibility values. Their mean Koenigsberger ratios are 2.1, 1.51, and 1.78, respectively, indicating that their remanent magnetization is stronger than their induced magnetization. These observations suggest that volcanic units that correlate with strongly positive anomalies were erupted during periods of normal geomagnetic polarity while those that correlate with strongly negative anomalies erupted during periods of reverse geomagnetic polarity; thus the magnetic data provide evidence for age differences within units that cannot be distinguisehd by field mapping.

The Francois Lake Plutonic Suite generally corresponds to moderate magnetic values, although low values (typically <-300 nT) are associated with the felsic Casey phase (Fig. 3). Interestingly, magnetic values are approximately 400 nT higher over exposures of the Glenannan phase in the northern part of the study area compared to those over the same phase farther south. As the magnetic susceptibility of the Glenannan phase shows little spatial variation, this suggests that either the Glenannan phase exposure in the south is quite thin and underlain by low-susceptibility material, possibly the Casey phase, or that the exposure in the north is thin and underlain by high-susceptibility material, possibly the Boer Lake pluton.

Although of bulk composition similar to that of the Endako phase, the Nithi phase provides lower magnetic values, perhaps indicating that it contains less accessory magnetic minerals. This possibility is supported by the lower mean magnetic susceptibility value of the Nithi phase, although altered samples were preferentially measured in this phase. Consequently, magnetic data provide a useful means of distinguishing these two phases where field mapping cannot.

Detailed mapping near the Endako molybdenum deposit delineates northeast-, northwest-, and east-trending faults (Fig. 2). The few mapped faults outside the region trend either NW or NE. In most instances, mapped and inferred faults correspond with linear magnetic features and zones of high magnetic gradient (Fig. 3). Vertical derivative images of magnetic data (Fig. 4, 5), which enhance near-surface features and sharpen edges of anomalies, are particularly useful for delineating anomalies associated with these mapped faults. Given that the faults have a magnetic expression even where they cut a single rock unit and that the estimated depth-to-source using Euler deconvolution is invariably shallow (i.e. a few hundred metres), the most likely source of magnetism is magnetic minerals precipitated in and adjacent to the fault planes.

Several prominent northwest and northeast-trending linear features are recognized in the magnetic data where no faults have been mapped (Fig. 3, 4). These linear features are interpreted to be unmapped faults that cut the region into panels, as suggested by Struik and Wetherup (1997). Detailed examination indicates that the northwest-trending magnetic linear feature coincident with the trace of the Casey fault (Fig. 2, 3, 4) extends approximately 10 km farther northwest and approximately 25 km farther southeast than surface geological mapping indicates. In the southeast and the northwest, the Casey linear feature is underlain by rocks of the Endako and Ootsa Lake groups, respectively, indicating that motion along the fault must be Eocene or younger

PALEOMAGNETICALLY DETERMINED TILTS

Confirmation of the Eocene transtensional event requires measurements of tectonic tilts. In a region of well exposed layered rocks, such measurements are not difficult to make. Unfortunately, in the Nechako Plateau region, outcrops of Eocene and older units are isolated and dominated by massive intrusive and volcanic rocks that make it impossible to measure tilts using standard methods.

Mafic dykes, flows, and intrusions, however, are excellent recorders of the paleomagnetic field. Just as bedding is used to estimate paleohorizontals, the direction of paleomagnetic remanence can be used to estimate the direction of the paleogeomagnetic field. The difference between the two provides a measure of tectonic tilt. Since the Cordillera had largely reached its present configuration by the Eocene (Bardoux and Irving, 1989; Symons and Welling, 1989; Irving and Brandon, 1990), the reference paleopole of North America at 50 Ma can be used to determine the pre-tilting direction expected in Eocene rocks in the study region. In this study, rotations are assumed to be about horizontal axes, analogous to layered beds tilting about their strike line.

Our study focused on the Endako mine open pit, a large area of complete exposure that provides a laboratory to establish the tectonic style of the larger area. Detailed study of the post-mineralization structure of the pit can help in the exploration of additional resources around the mine. We collected samples from 16 Eocene basalt dykes located along the strike length of the pit (Fig. 5), mostly along the southwest wall of the pit.

In an attempt to delineate regional tectonic tilts and to constrain magnetic anomaly interpretation, 13 additional samples were collected from regional sites in map sheets 93K/2 and 93K/3 (Fig. 4). Sites consisted of Eocene mafic dykes, flows, and granites.

Six 2.5 cm diameter cores 5 to 13 cm long were collected from each site. Several sites were highly magnetic (up to 6.7 A/m), so orientations were always confirmed from a distance when a solar compass could not be used. In the laboratory, cores were cut into 2.2 cm long cylinders. Magnetic remanence was measured using a Geofyzika JR5A spinner magnetometer, and susceptibility using a Sapphire SI2B meter. Thermal demagnetization was done using an ASC TD48 furnace, and alternating field demagnetization, using a Schonstedt GSD-1 tumbling AF demagnetizer. Five to ten demagnetization steps were applied to each specimen in order to isolate stable magnetic components.

Most sites provided high-quality data. Single-domain magnetite was the dominant carrier, but hematite was observed in some mine dykes. Both magnetic polarities were observed, providing evidence of the stability of magnetic remanence and of the averaging of secular variations. So far, only one third of our collection has been demagnetized, so only preliminary interpretations can be offered.

In the mine, each fault-bounded pit is roughly a rigid body (Fig. 5), with the Endako East pit dipping east, the Endako West and Denak East pits dipping southeast, and the Denak West pit dipping north. This rotation of the dips follows the orientation of the ore-bearing veins (Bysouth and Wong,

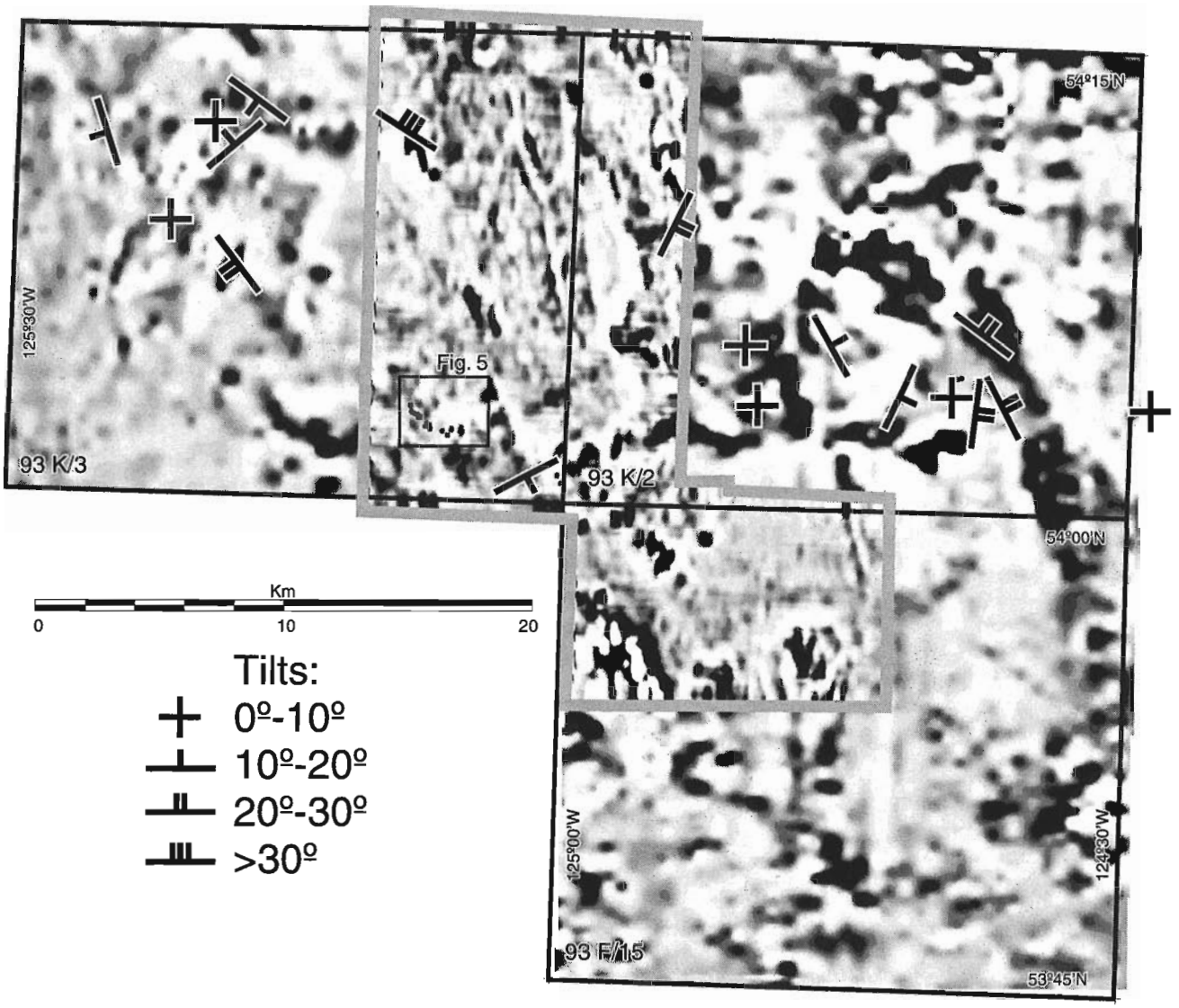

Figure 4. *Vertical derivative of magnetic anomaly data for the study area. High values are shown in dark shades and low values, in light shades. The extent of the high-resolution aeromagnetic data set that includes the Endako mine is outlined (heavy grey line), as is the extent of the area shown in Figure 5. Preliminary tilt directions, determined paleomagnetically on Eocene rocks, are indicated.*

1995), suggesting that the Jurassic veins were initially parallel and were rotated during or after the Eocene. An anticlinal structure is recognized in the northwest quarter of the mine site, with its axis on the boundary between the West Denak and East Denak pits.

A vertical derivative profile for a NW-SE transect through the Endako mine is shown in Figure 6. The locations of mapped faults are indicated and the orientation of paleomagnetically determined tilts are shown schematically. Changes in gradient and in the orientation and magnitude of the paleomagnetically determined tilts are observed across the West Basalt, F1, and F2 faults. The Denak West fault is not imaged in the gradient data and paleomagnetically determined tilts are less than 10° here, suggesting that vertical motion along the fault was not significant. In fact, the fault marks the axis of the paleomagnetically observed anticline and, interestingly, the vertical axis of rotation of the Denak West pit.

In the region east of the mine (mostly map sheet 93K/2), dips are dominantly eastward (Fig. 4). Panel faulting in an extensional regime is expected to have this pattern. Elsewhere tilt directions vary substantially, especially in map sheet 93K/3. This is not surprising, given the separation between neighbouring sites. Note that the anticline within the mine has a sub-kilometre wavelength, so such structures should be expected in the rest of the region. We suggest that panel dips are more coherent east of the Casey fault. Further analysis of this data set must await the measurement of the entire paleomagnetic collection and quantitative modeling of the aeromagnetic data.

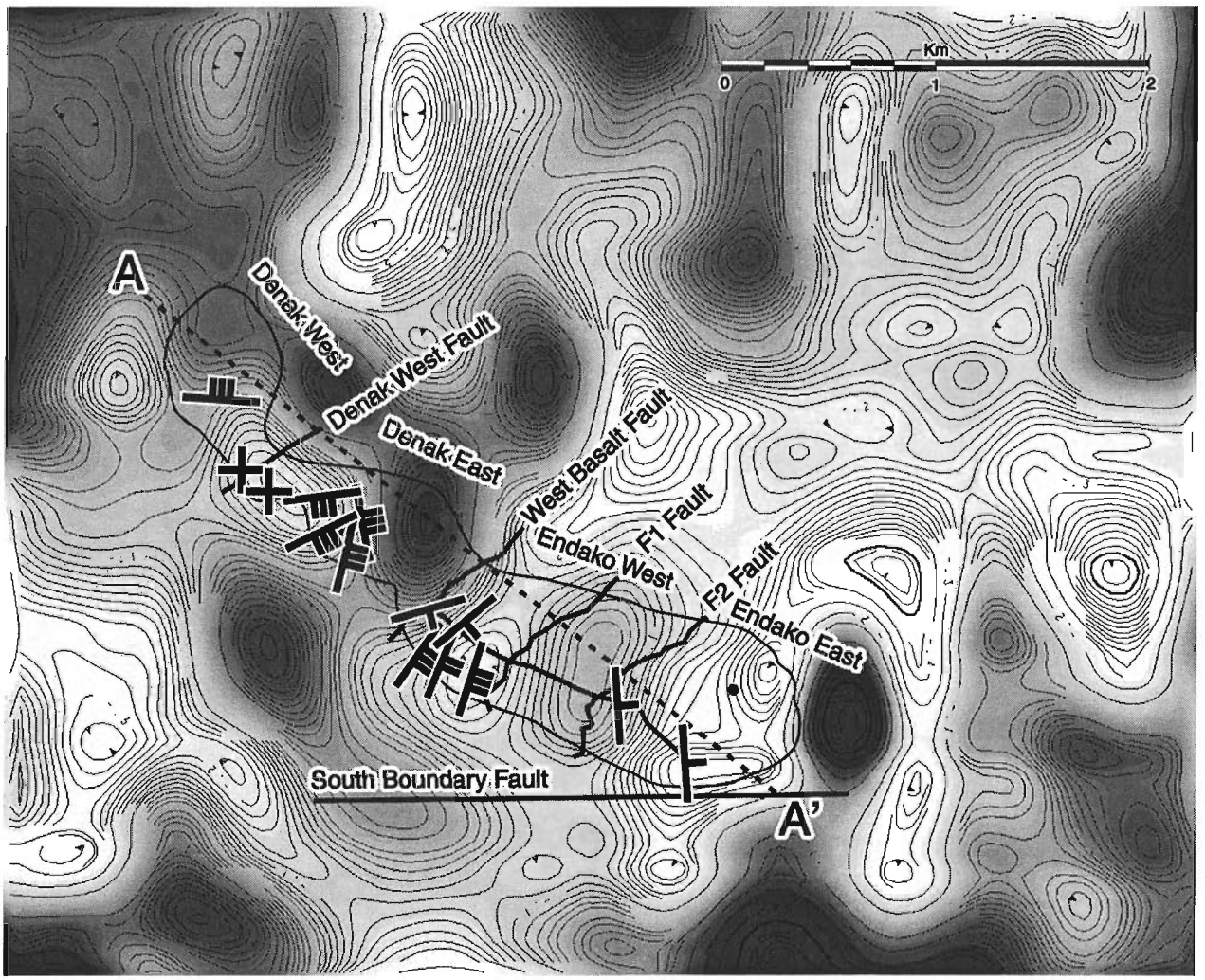

Figure 5. *Vertical derivative of magnetic anomaly data for the mine area (see Figure 4 for location). High values are shown in dark shades and low values, in light shades. The extent of the open-pit mine (dashed line), the surface trace of significant mapped faults (solid lines), and the location of profile A-A' (grey line; see Figure 6) are indicated. Preliminary tilt directions, determined paleomagnetically on Eocene dykes, are indicated with symbols defined in Figure 4.*

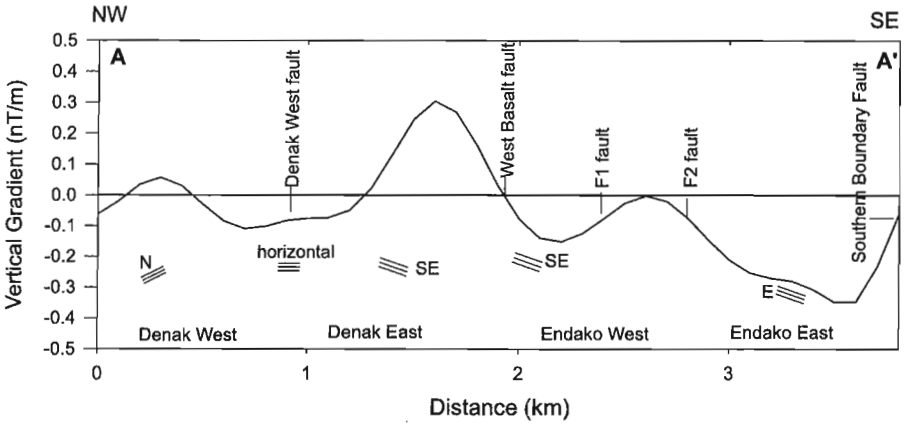

Figure 6. *Vertical derivative of magnetic anomaly data for a NW-SE transect through the Endako mine (see Figure 5 for transect location). Note that the surface locations of the West Basalt, FI, and F2 mapped faults correspond to significant gradients. The paleomagnetically determined tilts are indicated schematically.*

SUMMARY

Although preliminary, this study illustrates that magnetic studies can significantly enhance our understanding of Eocene deformation in the Endako region. Most mapped faults are restricted to the vicinity of the Endako molybdenum deposit and trend predominantly NW and NE. The faults frequently correspond to linear zones of high magnetic gradient and to near-surface magnetic sources. Several other northwest- and northeast-trending linear features are recognized from the magnetic anomaly data. Euler deconvolution solutions indicate that these linear features are also associated with shallow magnetic sources. Consequently, the linear features are interpreted to be unmapped faults that cut the region into a series of fault-bounded blocks.

Variations in the orientation of paleomagnetically determined tilts indicate that the four fault-bounded blocks that constitute the Denak West, Denak East, Endako West, and Endako East pits of the Endako molybdenum mine were rigidly deformed during the Eocene into an anticlinal structure. At a more regional scale, paleomagnetic data indicate that easterly tilts predominate east of the Casey magnetic lineament and that there is significant variation in the orientation and magnitude of tilts west of the lineament. Resolution of the geometry and orientation of the faults requires quantitative modeling of magnetic anomaly data constrained by the paleomagnetic results.

Our study has also shown that magnetic anomaly and magnetic susceptibility data may help distinguish subtle mineralogical differences between the Nithi and Endako phases of the Francois Lake Plutonic Suite and resolve age differences within lithologically similar outcrops of the Eocene Ootsa Lake Group, the Eocene to Oligocene Endako Group, and the Miocene Chilcotin Group.

ACKNOWLEDGMENTS

L. Struik conceived the project and facilitated the fieldwork. We thank R.G. Anderson, R. L'Heureux, L. Struik, S. Wetherup, and J. Whalen for magnetic susceptibility data and many useful discussions on the geology of this region. R.B.K. Shives kindly provided a digital copy of the high-resolution aeromagnetic data collected under his supervision. J. Baker assisted in the field and supervised laboratory work. Thanks to G. Johnson, C. Lee, and G. Ayres of Thompson Creek Mining Company for access to and assistance at the mine site. Reviews by L. Struik and R. Currie helped improve the manuscript.

REFERENCES

Anderson, R.G., L'Heureux, R., Wetherup, S., and Letwin, L.
1997a: Geology of the Hallett Lake map area, central British Columbia: Triassic, Jurassic, Cretaceous and Eocene? plutonic rocks; in Current Research 1997-A; Geological Survey of Canada, p. 107-116.

Anderson, R.G., Whalen, J.B., Villeneuve, M.E., Struik, L.C., and L'Heureux, R.
1997b: Jura-Cretaceous plutonic rocks near the Endako molybdenite mine, central B.C.; Geological Association of Canada-Mineralogical Association of Canada, Program with Abstracts, v. 22, p. A-3.

Bardoux, M. and Irving, E.
1989: Paleomagnetism of Eocene rocks of the Kelowna and Castlegar areas, British Columbia: Studies in determining paleohorizontal; Canadian Journal of Earth Sciences, v. 26, p. 829-844.

Bysouth, G.D. and Wong, G.Y.
1995: The Endako molybdenum mine, central British Columbia: an update; in Porphyry deposits of the northwestern Cordillera of North America, (ed.) T.G. Schroeter; Canadian Institute for Mining, Metallurgy, and Petroleum, v. 46, p. 697-703.

Geological Survey of Canada
1961a: 1:50 000 aeromagnetic map of the Hallett Lake map sheet, Open File 1589G.
1961b: 1:50 000 aeromagnetic map of the Fraser Lake map sheet, Open File 1590G.
1967: 1:50 000 aeromagnetic map of the Endako map sheet, Open File 5304G.

Irving, E. and Brandon, M.T.
1990: Paleomagnetism of the Flores Volcanics, Vancouver Island in place by Eocene time; Canadian Journal of Earth Sciences, v. 27, p. 811-817.

Kimura, E.T. and Drummond, A.D.
1969: Geology of the Endako molybdenum deposit; Bulletin of the Canadian Institute of Mining, v. 62, p. 699-708.

Kimura, E.T., Bysouth, G.D., and Drummond, A.D.
1976: Endako; in Porphyry Deposits of the Canadian Cordillera, Canadian Institute of Mining and Metallurgy, Special Volume 15, p. 444-454.

Kimura, E.T., Bysouth, G.D., Cyr, J., Buckley, P., Peters, J., Boyce, R., and Nilsson, J.
1980: Geology of parts of southeast Fort Fraser and northern Nechako River map areas, central British Columbia; Placer Dome Incorporated, Internal Report and Maps, Vancouver, British Columbia.

L'Heureux, R.L., and Anderson, R.G.
1997: Early Cretaceous plutonic rocks and molybdenite showings in the Nithi Mountain area, central British Columbia; in Current Research 1997-A; Geological Survey of Canada, p. 117-124.

MacIntyre, D.G., Webster, I.C.L., and Bellefontaine, K.A.
1996: Babine porphyry belt project: Bedrock geology of the Fulton Lake map area (93L/16), British Columbia; in Geological Fieldwork 1995, (ed.) B. Grant and J.M. Newell; British Columbia Ministry of Energy, Mines, and Petroleum Resources, Paper 1996-1, p. 11-35.

McMillan, W.J. and Struik, L.C.
1996: Natmap: Nechako project, central British Columbia; in Geological Fieldwork 1995; British Columbia Ministry of Energy, Mines, and Petroleum Resources, Paper 1996-1, p. 3-10.

Reid, A.B., Allsop, J.M., Granser, H., Millett, A.J., and Somerton, I.W.
1990: Magnetic interpretation in three dimensions using Euler deconvolution; Geophysics, v. 55, p. 80-91.

Struik, L.C.
1994: Intersecting intercratonal Tertiary transform fault systems in the North American Cordillera; Canadian Journal of Earth Sciences, v. 30, p. 1262-1274.

Struik, L.C. and Wetherup, S.
1997: Features of Tertiary crustal extension in central British Columbia; in Abstract Volume, Geological Association of Canada/Mineralogical Association of Canada Annual Meeting, May, 1997, p. A144-A145.

Struik, L.C., Whalen, J.B., Letwin, J., and L'Heureux, R.
1997: General geology of southeast Fort Fraser map area, British Columbia; in Current Research 1997-A; Geological Survey of Canada, p. 65-76.

Symons, D.T.A. and Welling, M.R.
1989: Paleomagnetism of the Eocene Kamloops Group and the cratonization of Terrane I of the Canadian Cordillera; Canadian Journal of Earth Sciences, v. 26, p. 821-828.

Thompson, D.T.
1982: EULDPH: A new technique for making computer-assisted depth estimates from magnetic data; Geophysics, v. 47, p. 31-37.

Whalen, J.B. and Struik, L.C.
1997: Plutonic rocks of southeast Fort Fraser map area, central British Columbia; in Current Research 1997-A; Geological Survey of Canada, p. 77-84.

Whalen, J., Struik, L.C., and Hrudey, M.G.
1998: Geology of the Endako map area, central British Columbia; in Current Research 1998-A; Geological Survey of Canada, p. 00.

White, W.H., Harakal, J.E., and Carter, N.C.
1968: Potassium-argon ages dates of some ore deposits in British Columbia; Canadian Institute of Mining and Metallurgy, Bulletin 61, no. 679, p. 1326-1334.

White, W.H., Sinclair, A.J., Harakal, J.E., and Dawson, K.M.
1970: Potassium-argon ages of Topley Intrusions near Endako, British Columbia; Canadian Journal of Earth Sciences, v. 7, p. 1172-1178.

Geological Survey of Canada Projects 910027, 860094

Jurassic to Tertiary volcanic, sedimentary, and intrusive rocks in the Hallett Lake area, central British Columbia[1]

R.G. Anderson and L.D. Snyder[2]
GSC Pacific, Vancouver

Anderson, R.G. and Snyder, L.D., 1998: Jurassic to Tertiary volcanic, sedimentary, and intrusive rocks in the Hallett Lake area, central British Columbia; in Current Research 1998-A; Geological Survey of Canada, p. 135-144.

Abstract: Distribution of and geological relationships amongst Middle Jurassic, Middle and Upper Jurassic, Mid- to Late Cretaceous, and Tertiary volcanic, sedimentary, and plutonic units are better known from bedrock mapping in the Hallett Lake (NTS 93F/15) area in 1997. Undivided Hazelton Group rocks include maroon-grey heterolithic and monolithic laharic boulder breccia, volcanic grit, and mudstone that are localized in northeast-trending fault blocks. Middle Jurassic Naglico Formation (?) clinopyroxene-phyric volcaniclastic rocks, laharic breccia and siliceous siltstone occur within one of these fault blocks.

Eocene Ootsa Lake Group dacitic and rhyolitic crystal tuff, pyroclastic rocks, breccia, flow-layered lavas, vitrophyre, glassy domes, and rare, amygdaloidal, plagioclase-porphyritic basalt overlie various Mesozoic basement units. Eocene Endako Group clinopyroxene-plagioclase porphyry basaltic flow and flow breccia rocks conformably overlie the Ootsa Lake Group and with it, are gently tilted. Small- and large-scale, northeast-trending, down-to-the-southeast, synvolcanic faults apparently localized the distribution of Ootsa Lake Group and Endako Group.

Résumé : Les associations géologiques entre les unités volcaniques, sédimentaires et plutoniques du Jurassique moyen, du Jurassique moyen et supérieur, du Crétacé moyen à tardif et du Tertiaire ainsi que la distribution de ces unités sont mieux connues depuis les travaux de cartographie du substratum rocheux menés en 1997 dans la région du lac Hallett (feuillet 93F/15 du SNRC). Les roches non subdivisées du Groupe de Hazelton comprennent des brèches à gros blocs de lahars hétérolithiques et monolithiques de couleur gris marron, des grès grossiers d'origine volcanique et des mudstones, localisés dans des blocs faillés d'orientation nord-est. Les roches de la Formation de Naglico (?) du Jurassique moyen (volcanoclastites à phénocristaux de clinopyroxène, brèches de lahars et siltstones siliceux) s'observent dans l'un de ces blocs faillés.

Diverses unités mésozoïques du substratum sont recouvertes par les lithologies éocènes du Groupe d'Ootsa Lake, en l'occurrence des tufs cristallins dacitiques et rhyolitiques, des roches pyroclastiques, des brèches, des laves à litage de flux, des vitrophyres, des dômes de roches vitreuses et de rares basaltes porphyriques (plagioclases) et amygdaloïdaux. Le Groupe d'Ootsa Lake est à son tour surmonté (contact concordant) des basaltes porphyriques à clinopyroxène-plagioclase et des brèches fluidales du Groupe d'Endako et, tout comme ce dernier, est légèrement incliné. Des failles synvolcaniques de petite et grande échelle, d'orientation nord-est et plongeant vers le sud-est, sont apparemment venues limiter la superficie que couvrent les roches du Groupe d'Ootsa Lake et du Groupe d'Endako.

[1] Contribution to the Nechako NATMAP Project

[2] Department of Geology, University of Wisconsin-Eau Claire, Eau Claire, Wisconsin 54702-4004

INTRODUCTION

Geological mapping of the Hallett Lake map area (NTS 93F/15) is part of the ongoing revision of the Nechako River 1:250 000 scale geological map (Tipper, 1963) as part of the Nechako NATMAP Project (Fig. 1; Struik and McMillan, 1996; Struik and MacIntyre, 1997, 1998). Mapping in 1996 focused on the distribution of plutonic suites in the area (e.g., Anderson et al., 1997a; L'Heureux and Anderson, 1997) as part of a regional study of plutonic suites (see Struik et al., 1997; Whalen and Struik, 1997; Anderson et al., 1997b; Whalen et al., 1998). In 1997, bedrock mapping concentrated on the Mesozoic and Tertiary volcanic and sedimentary rocks which flank the central plutonic massif. As in 1996, this work builds on the excellent mapping and age-determination contributions by mineral exploration and provincial geological survey geologists in the area over the past 30 years (e.g. Kimura et al., 1980; Lane, 1995; Lane and Schroeter, 1997) which have helped focus this work.

This report summarizes descriptions of the newly discovered Eocene intrusions and phases within the Copley Lake pluton and main stratigraphic units in the area. Observed and inferred geological relationships between stratified and plutonic units suggest that small-scale as well as regional-scale block faults, for example, the Bungalow Lake fault (Fig. 2), were important prevolcanic to synvolcanic Eocene structures.

PHYSIOGRAPHY, ACCESS AND FIELD METHODS

The area's Interior Plateau physiography provides a challenge to mapping the continuity of stratigraphic units, and was briefly described in Anderson et al. (1997a). The discontinuous rock exposure typical of the region lead to the authors having to infer contacts amongst units, except at Mount Greer where the rocks are better exposed (Fig. 2; see also Haskin et al., 1998).

New data reported here were based upon 3 weeks of work (about 32 traverses) in June and early July, 1997. Standard geological mapping techniques were supplemented by global positioning system measurements taken at each station, providing a lateral precision of 50-100 m (depending on number and orientation of satellites). Representative samples were collected for petrographic, mineralogical, $^{40}Ar/^{39}Ar$ age-determination, and geochemical studies in progress. As well, magnetic susceptibility at most outcrops and specific gravity measurements for most samples (see L'Heureux and Anderson, 1997 for details) will aid in the interpretation of potential field geophysical data (Struik and McMillan, 1996).

GEOLOGY

Volcanic and sedimentary rocks flank the north-trending central plutonic massif to the west and southeast (Fig. 2). Below is a brief summary of results of mapping of the plutonic rocks in 1996 (from Anderson et al., 1997a) supplemented by the 1997 results; descriptions of the stratified units, their bounding structures, and metallogeny follow.

Plutonic rocks

New mapping, geochronology, and chemical and isotopic analyses have defined at least five plutonic suites represented in the Hallett Lake area (see details in Anderson et al., 1997a; L'Heureux and Anderson, 1997; Villeneuve et al., 1997): a) the poorly mineralized Middle Jurassic (171-163 Ma) Stag Lake suite (units mJST, mJSSl, mJSL and mJBD; Fig. 2); b) the well mineralized Late Jurassic (158-155 Ma) Francois Lake Plutonic Suite that hosts the Endako-style, low-fluorine, porphyry molybdenum deposits at Nithi Mountain and the Endako Mine (unit lJFN; Fig. 2); c) Early Cretaceous

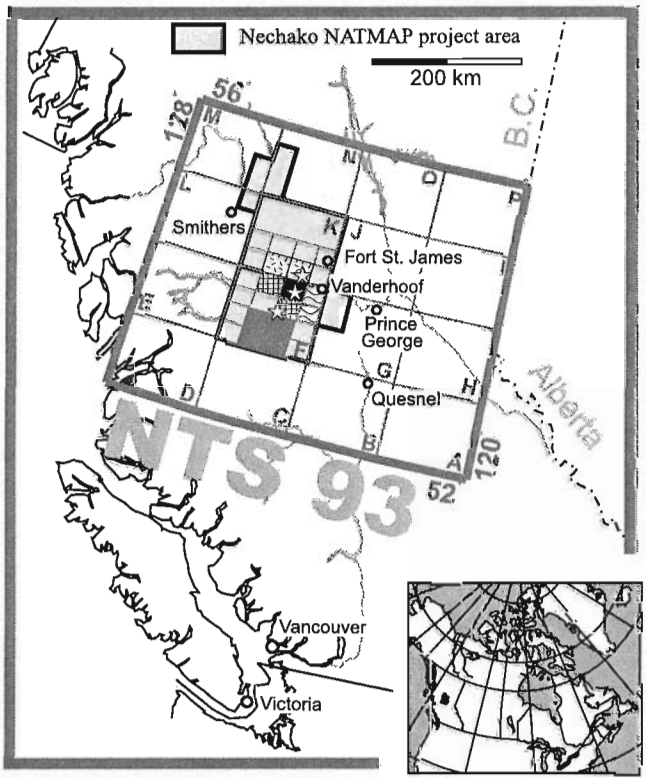

Figure 1. *Location of the Hallett Lake (NTS 93F/15) map area and other recently mapped areas within the Nechako NATMAP Project area.*

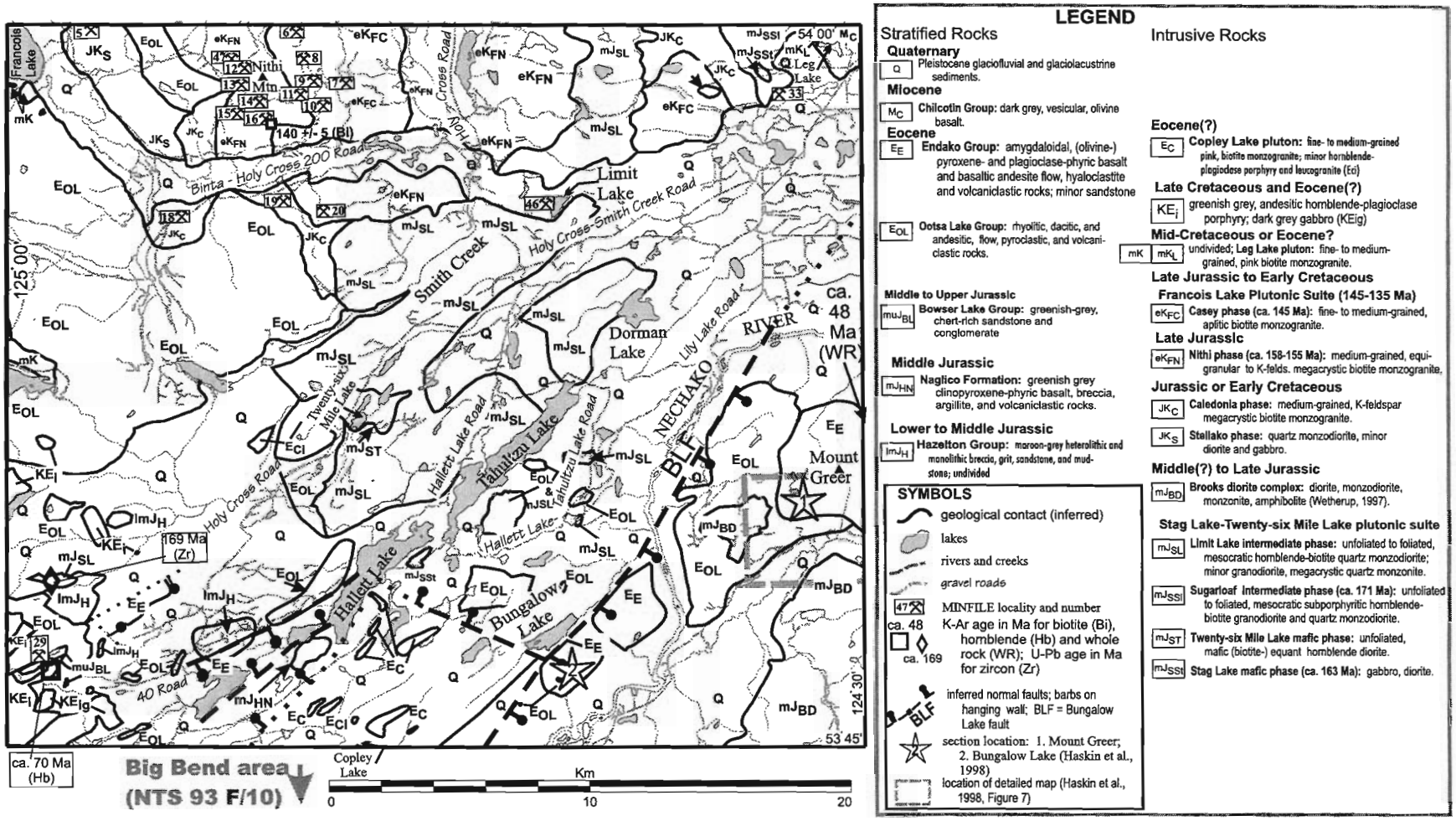

Figure 2. *Geological map of the Hallett Lake map area compiled from mapping reported herein and in Haskin et al. (1998) as well as earlier mapping, age determinations, and compilations (e.g. Tipper, 1963; Kimura et al., 1980; Bellefontaine et al., 1995; Lane, 1995; Lane and Schroeter, 1997; and Williams, 1997).*

(147-145 Ma) intrusions which are coeval with the mineralization (unit eKFC; Fig. 2); d) unmineralized, satellitic Leg Lake pluton of the Mid- to Late Cretaceous Fraser Lake suite, (unit mKFL; Fig. 2; and, the Eocene (?) Copley Lake pluton (unit EC; Fig. 2) and miscellaneous intrusions (unit Ei). Coarse-grained, crowded plagioclase-porphyry basalt included in a Late Triassic suite in previous mapping (Anderson et al., 1997a) is now considered part of the basal member of the Eocene Ootsa Lake Group.

Jurassic plutonic rocks

The distribution of the hornblende-biotite quartz monzodiorite Limit Lake phase of the Stag Lake suite (unit mJSL; Fig. 2) was traced southeast of Hallett and Tahultzu lakes to the Bungalow Lake fault. In this area, it is commonly nonconformably overlain by porphyritic rhyolite and dacite flows, breccia, and pyroclastic rocks of the Eocene Ootsa Lake Group. Its contact with the Middle Jurassic Brooks Diorite Complex of Wetherup (1997) was not observed.

Heterogeneous diorite of the Brooks Diorite Complex (unit mJBD) extends west from the Nulki and Tatuk lakes area (Wetherup, 1997) into Hallett Lake and southwest to Mount Hobson in the Big Bend Creek map area (Anderson et al., 1998). In the Hallett Lake area, on Mount Greer, volcanic rocks of the Eocene Ootsa Lake and Endako groups nonconformably overlie it (see Haskin et al., 1998).

West of Holy Cross Road, a small biotite quartz monzonite pluton (unit eMJgpm of Lane, 1995; unit mJSL, Fig. 2) intruded and altered Hazelton Group rocks. It is included in the Stag Lake plutonic suite because of its similarity to intermediate members of the suite and Middle Jurassic U-Pb age of ca. 169 Ma (cf. Lane (1995) and Lane and Schroeter (1997)). This suggests that Middle Jurassic plutonism extended at least that far west.

Jurassic-Cretaceous plutonic rocks

The age and affinity of Jura-Cretaceous Caledonia and Stellako phases (units JKC and JKS; Fig. 2) are poorly known. New mapping along the western flank of Nithi Mountain of the Stellako phase from previous work. The Stellako phase consists of mainly fine- to medium-grained, unfoliated biotite-hornblende (quartz) monzodiorite; in the south, the unit includes older hornblende diorite and gabbro which resemble mafic phases of the Middle Jurassic Stag Lake plutonic suite. It is likely part of the Middle Jurassic suite rather than the felsic, mineralized Jura-Cretaceous plutons of the Francois Lake Suite. The Stellako phase in Hallett Lake area is dissimilar to felsic granitic rocks included in that phase directly north in the Fort Fraser map area (Whalen and Struik, 1997).

Late Cretaceous plutonic rocks

A distinctive greenish-grey, unfoliated, andesitic hornblende-plagioclase porphyry was first mapped by Lane (1995) in southwestern Hallett Lake area as an Upper Cretaceous volcanic unit (his unit Kv). New mapping has traced the unit west and south of his map area into the Knapp Lake (R.G. Anderson, unpub. data) and Big Bend Creek (Anderson et al., 1998) areas (unit lKi, Fig. 2). Euhedral plagioclase and less common prismatic hornblende phenocrysts, the greenish-grey aphanitic groundmass, and common rusty alteration of the hornblende are distinctive features of the otherwise featureless homogeneous porphyry. A K-Ar date of 70.3 ± 3.0 Ma (R. Friedman in Lane and Schroeter, 1997) was determined for the unit.

Contacts between the porphyry and siltstone of the Middle and Upper Jurassic Bowser Lake Group were re-examined because the homogeneity of the porphyry unit and lack of volcanic flow textures seemed unusual in such a widespread volcanic unit. Three features of the porphyry's contact relationships suggest it is an intrusive rather than volcanic unit. Along the northern contact of the porphyry with Bowser Lake Group (south of north 40 Road, about 1 km east of the Hallett Lake map area boundary, about N5960500, E369250), spotted slates containing altered andalusite (?) occur within 50 m of the well bracketed but unexposed contact. Secondly, the contact zone of the porphyry was finer grained than areas farther from the contact. Thirdly, the distribution of this lobe of Lane's unit Kv is topographically high, and flanked by upright sedimentary rocks which dip radially away from the Late Cretaceous porphyry suggesting that if it is a stratigraphic unit, the sedimentary rocks must be no older than Late Cretaceous. None of that age are known in the region, and the sedimentary unit was correlated with the Mid-Cretaceous Skeena Group by Lane (1995) and with the Middle and Upper Jurassic Bowser Lake Group in this work. An alternative explanation for the structural orientation of the sedimentary rocks is that they were domed up (and metamorphosed) during intrusion of the porphyry.

Eocene (?) intrusive rocks (units Ec and Ei)

Eocene (?) plutons and less common porphyry intrusions occur in the southern Hallett Lake map area where they are associated with the greatest abundance of the Eocene Ootsa Lake Group, or intrude the volcanic rocks. Minor gabbro and miarolitic leucogranite stocks in the southwest, and the more extensive monzogranite of the Copley Lake pluton in the south, are the main representatives.

The distribution and nature of the composite, undated Copley Lake pluton (unit Ec; Fig. 2) is better known than was described in Anderson et al. (1997a). The pluton extends about 5 km south into the Big Bend Creek map area (Anderson et al., 1998). The composite pluton comprises an extensive, mottled pink and white, hornblende-biotite quartz monzonite (Anderson et al., 1997a), subordinate grey hornblende-plagioclase porphyry dykes and stocks, minor pink and white felsic porphyry, and rare leucocratic phases. The porphyry and leucocratic phases mainly occur to the south and southwest. The weathering colour, and composition and abundance of phenocrysts in the quartz-alkali feldspar-plagioclase porphyry phases strongly resemble those of the porphyritic volcanic rocks of the Eocene Ootsa Lake Group which flank the pluton. At one locality southeast of Copley Lake, Ootsa Lake Group volcanic breccia is intruded by aplitic phases of the pluton.

Minor andesitic (hornblende-) plagioclase porphyry south of Cabin Lake is significant because it crosscuts dacitic lapilli breccia of the Ootsa Lake Group as a dyke-and-sill complex and is apparently the youngest intrusive phase in the map area. It is greenish grey and sparsely to moderately hornblende- and plagioclase-phyric, and exhibits local columnar jointing, but has no other volcanic flow-related textures. Its intrusion apparently imparted a local, centimetre-spaced, penetrative, gently dipping fracture cleavage in the volcanic country rocks (Fig. 3), structurally below the sill complex.

Stratified rocks

Almost half of the Hallett Lake map area is underlain by Jurassic to Tertiary volcanic and sedimentary rocks (Fig. 2). Tertiary volcanic rocks of the Ootsa Lake and Endako groups dominate the western and southeastern part of the map area; Lower and Middle Jurassic Hazelton Group volcanic rocks and Middle and Upper Jurassic Bowser Lake Group sedimentary rocks are areally less important but significant in the southwestern part of the map area. Miocene Chilcotin Group rocks have a minor extent in the northeastern part in the Hallett Lake map area and are not described in this report.

Lower and Middle Jurassic Hazelton Group (units lmJH and mJHN)

Unfossiliferous, maroon and green, fine- to coarse-grained volcaniclastic and epiclastic volcanic rocks typical of the Lower to Middle Jurassic Hazelton Group are recognized in fault blocks south and southwest of Hallett Lake and between Holy Cross, 31, and 40 roads (e.g. Lane, 1995) in the southwestern part of the map area (Fig. 2, 4 and 5). Southwest of Hallett Lake, a steeply east-dipping panel of maroon-grey heterolithic and monolithic, laharic boulder breccia, volcanic grit, crystal-lithic tuff, and tuffaceous mudstone is faulted against rocks of the Eocene Ootsa Lake and Endako groups to the north and east, respectively. Although the volcaniclastic and epiclastic rocks are unfossiliferous, they strongly resemble well dated Hazelton Group rocks in the Fawnie and Nechako ranges to the south (L. Diakow, pers. comm., 1997; Diakow et al., 1997).

South of Hallett Lake, a subvertical and overturned panel of greenish-grey, thin-bedded, siliceous siltstone and featureless coarse-grained clinopyroxene-phyric volcaniclastic rocks and laharic breccia is more than 200 m thick and occurs as an isolated block, in possible fault contact with Tertiary rocks to the west and the Eocene (?) Copley Lake pluton to the east. This unit is also unfossiliferous, but strongly resembles strata underlying Cutoff Butte and the Nechako Range in the Big Bend Creek area (see Anderson et al., 1998), which themselves are correlated with the well dated Middle Jurassic Naglico Formation defined by Diakow et al. (1997) in the southern Nechako River map area.

Figure 4. *Heterolithic volcanic breccia of the Lower to Middle Jurassic Hazelton Group southwest of Hallett Lake.*

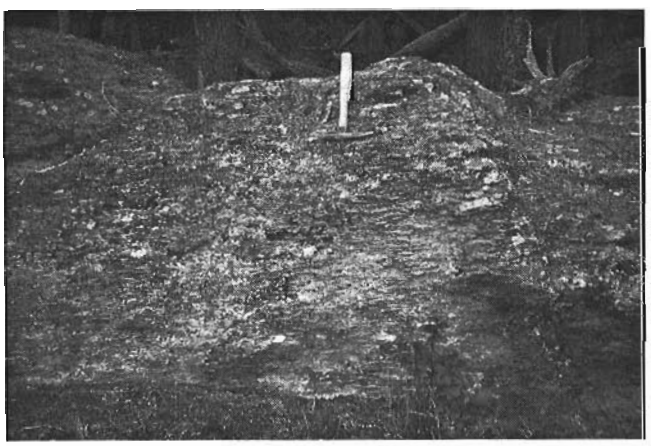

Figure 3. *View west to penetrative centimetre-scale fracture cleavage in heterolithic lapilli breccia of the Ootsa Lake Group which dips moderately beneath andesite porphyry sill.*

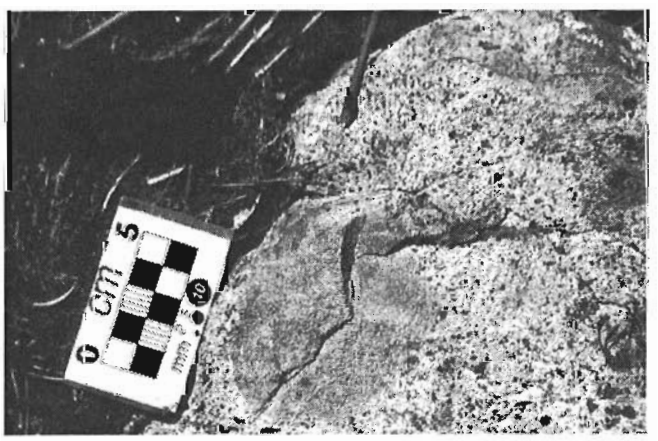

Figure 5. *Clinopyroxene-phyric volcanic breccia in Naglico Formation of Hazelton Group directly southeast of Hallett Lake.*

Hazelton Group rocks between Holy Cross, 31, and 40 roads comprise featureless maroon and green, heterolithic volcanic breccia, crystal lithic tuff, andesitic flow, and weakly graded, epiclastic crystal tuff (Lane, 1995; and this study). The unit is crosscut by a Middle Jurassic (ca. 169 Ma) biotite quartz monzonite pluton and overlain by Eocene Ootsa Lake Group rocks (Lane, 1995). Potassic alteration of country and plutonic rocks is localized near the contact.

Middle and Upper Jurassic Bowser Lake Group (unit muJBL)

In southwestern part of the area, an unfossiliferous, east-northeast-trending and moderately dipping sequence of siliciclastic rocks occurs (Lane, 1995; and this study). Decimetre- to metre-scale (0.25-3 m thick) planar beds of medium to coarse, heterolithic pebble conglomerate and coarse- to medium-grained sandstone make up equal parts of the sequence (Fig. 6). The conglomerate ranges from clast to matrix supported, is poorly sorted, and poorly bedded including local normal graded bedding. Clasts in the conglomerate are dominantly tan and light to dark grey chert with minor aphanitic felsic volcanic rock fragments and rare gneiss. The matrix and the sandstone layers are light grey, poorly sorted and bedded, quartz-, feldspar- and biotite-rich greywacke and grit which contain up to 5% chert fragments.

The sequence is overlain by Eocene Ootsa Lake Group and intruded by a Late Cretaceous (70 Ma) hornblende porphyry as described above. It was correlated with the Mid-Cretaceous Skeena Group by Lane (1995) but its geological and structural relationships with the porphyry described above, and its strong resemblance to the siliciclastic unit mapped to the south in the Big Bend Creek area (Anderson et al., 1998) where it is better dated (Callovian; Diakow et al., 1997) suggest it is part of the Bowser Lake Group.

Eocene Ootsa Lake Group (unit Eol)

The Ootsa Lake Group includes minor, basal mafic volcanic rocks and dominant felsic crystal tuff, pyroclastic rocks, breccia, flows with local moderately dipping flow-layering, and siliceous and glassy domes. The rocks are closely associated with subvolcanic intrusion of the Copley Lake pluton. The basal member is represented by the bladed-plagioclase porphyry basalt (incorrectly grouped with Triassic intrusions by Anderson et al., 1997a) and by amygdaloidal basalt and andesite found at the north end of Targe Lake, east of Bungalow Lake, and northwest of Mount Greer. Near Targe Lake, the basalt was distinguished from older and younger mafic volcanic rocks by its high degree of alteration and chlorite, calcite, and chalcedony amygdule fillings. At Bungalow Lake, a 4-5 m thick, sparingly plagioclase-phyric, amygdaloidal basalt member occurs at the base of the Tertiary section (see Haskin et al., 1998 for more detail). As at Targe Lake, it contains amygdules filled with abundant chalcedony and smaller amounts of fine-grained chlorite, and is intensely altered to clay, with some zones altered to a white-weathering rock.

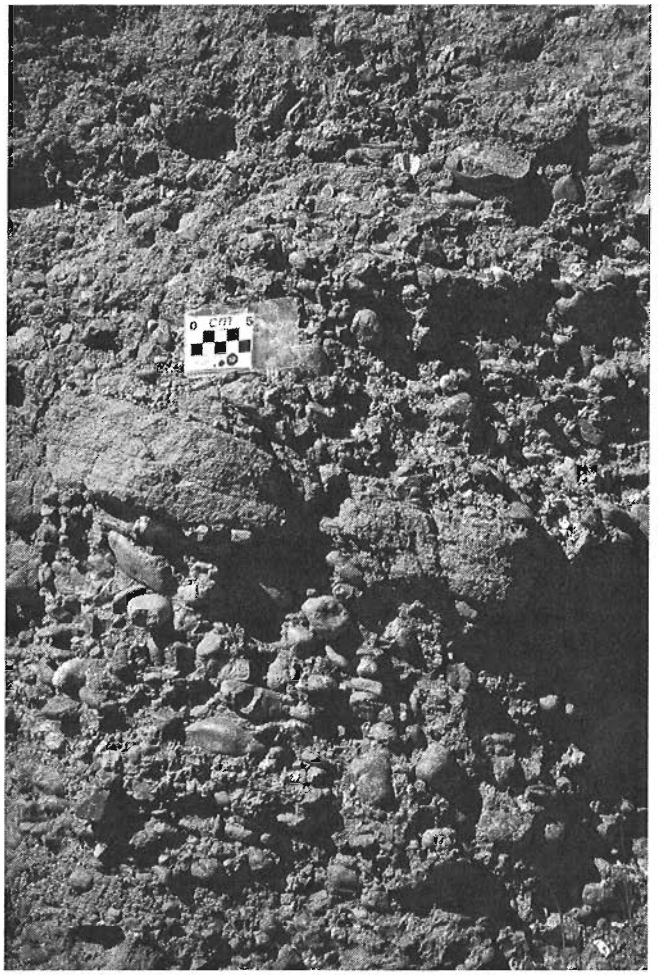

Figure 6. *View west to interbedded greywacke and conglomerate of Middle and Upper Jurassic Bowser Lake Group on northern spur of 40 road.*

The upper Ootsa Lake Group is dominated by white, rhyolitic to dacitic aphyric to porphyritic flow, and pyroclastic and volcaniclastic rocks and domes. The dominant rock type is a dacitic, white- to light-grey-weathering, generally punky, crystal to lapilli tuff. The volcaniclastic tuff contains lapilli- to pebble-sized, monolithic to heterolithic, subround to subangular fragments comprising aphanitic felsic volcanic rocks, flow-banded rhyolite, and dacitic feldspar porphyries (Fig. 7a, 7b). The tuff is locally weakly to moderately welded, as indicated by discontinuous eutaxitic textures (Fig. 7c). At Mount Greer, thin-bedded tuff underlies the Eocene Endako Group (Fig. 7d). The unit is otherwise featureless except where in contact with the andesitic porphyritic dykes and sills described above, or where silicified; at those localities it is characterized by a penetrative cleavage (Fig. 3).

A distinctive and extensive dacitic tuff and flow-layered flow member, which occurs in an area bounded by Hallett, True Triangle and Bungalow lakes, is characterized by

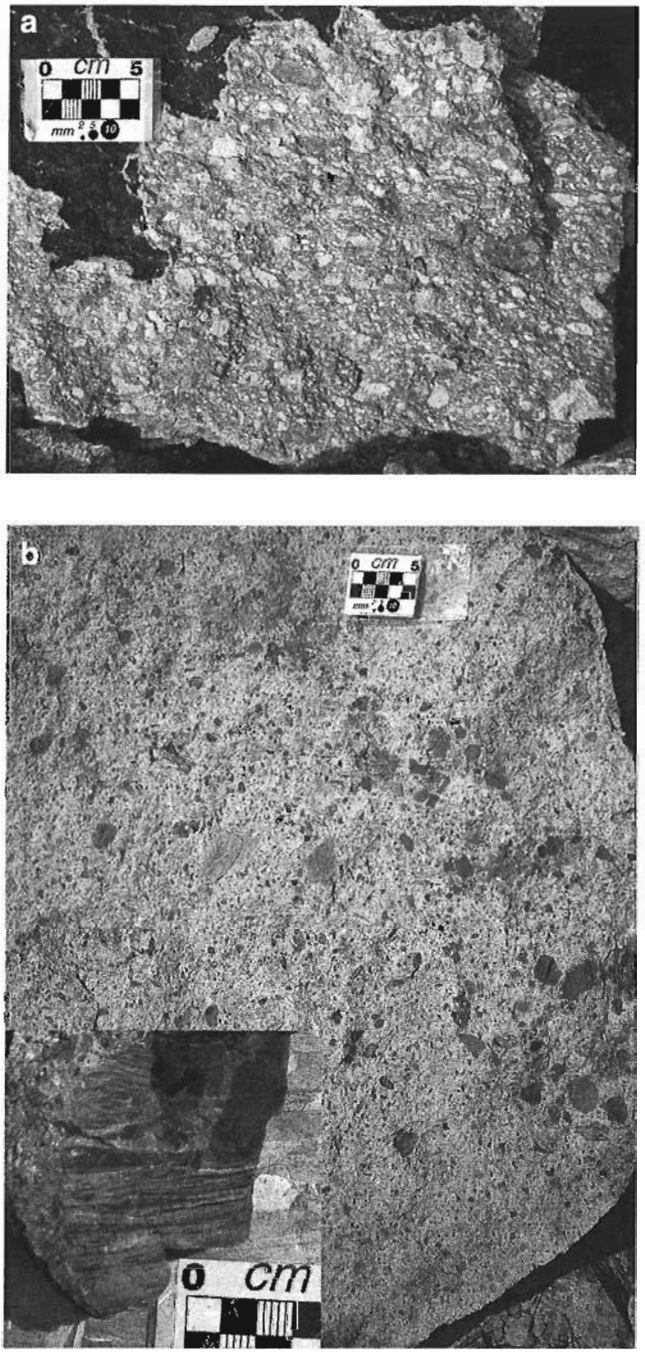

Figure 7. *Typical rock types in the Eocene Ootsa Lake Group:* ***a)*** *monolithic, pumiceous lapilli tuff south of Cabin Lake;* ***b)*** *heterolithic lapilli tuff (inset shows flow-laminated rhyolite fragment common in this variety) on spur off 31 road, southeast of Cabin Lake;* ***c)*** *eutaxitic texture in welded dacitic lapilli tuff;* ***d)*** *view northeast to thin-bedded felsic lapilli tuff at Mount Greer;* ***e)*** *amphibole mineral lineation in porphyritic dacite east of Hallett Lake.*

widespread but variable abundance of amphibole and alkali feldspar phenocrysts, fewer quartz, biotite, and plagioclase

phenocrysts, and amphibole mineral alignment (Fig. 7e). Pumice clasts and vugs are locally characteristic. The tuff is unwelded to moderately welded. Weakly developed flow layering dips 40-70° and local mineral alignment plunges gently, but varies in trend.

White to pink, flow-layered and glassy rhyolite domes are most common north of 40 road and south of Hallett Lake. Along 40 road, they comprise aphanitic to sparsely alkali feldspar phyric, flow-banded rhyolite and rhyolite breccia, spatially associated with basal, amygdaloidal coarse-grained bladed-plagioclase porphyry basalt. The rhyolite domes are commonly silicified.

South of Hallett Lake, a glassy rhyolite dome is localized along synvolcanic normal faults; Mesozoic volcanic rocks in the hanging wall are overturned. Distinctively pinkish-brown, aphyric rhyolite underlies a physiographic dome and contains moderately to steeply inward-dipping cooling fractures. Vitrophyric pyroclastic rocks are preserved elsewhere between Cabin and Francois lakes.

Ootsa Lake Group rocks exhibit a range of alteration types from fresh to weakly argillically altered to highly silicified varieties. Silicification is spatially associated with domes or the Copley Lake pluton. Where most silicified, the Ootsa Lake Group records a subvertical fracture cleavage and is locally pyritic.

Eocene Endako Group (unit Ee)

Brown-to grey-weathering basalt to basaltic andesite flow and volcaniclastic rocks are best recognized east of Bungalow Lake and near Mount Greer (see details in Haskin et al., 1998) in the southeastern part of the map area; scattered outcrops occur in the northeast, west of Holy Cross Road, and south of Hallett Lake.

At Bungalow Lake and Mount Greer, the Endako Group includes sequences at least 100 m thick comprising 4-6 m thick mafic and intermediate flow rocks and interbedded vesicular, flow breccia cut by mafic dykes (Haskin et al., 1998). Plagioclase microphenocrysts, generally not larger than 1-4 mm are ubiquitous; one flow contains zoned anhedral to subhedral seriate plagioclase up to 8 mm in size. Uncommon pyroxene and rare olivine microphenocrysts are locally observed. The rocks range from massive to vesicular, with common vesicle flattening parallel to flow contacts. At Mount Greer, flows with curviplanar bases are common on its western flank, and crude columnar jointing and gas-escape structures occur in flows on its east flank.

Flow breccia is highly vesicular (and amygdaloidal) and is as thick or locally thicker than the associated flow, particularly in the eastern flank of Mount Greer. Breccia units up to 5 m thick are well exposed near the top of the Bungalow Lake section; their intense oxidation lead to an appearance as fairly continuous red zones.

STRUCTURE

A series of Eocene and younger northeast-trending normal faults define the structural style and are subparallel to a Quaternary physiographic grain to the Hallett-Tahultzu-Dorman lakes corridor (Fig. 2). Locally, east of the Holy Cross Road and south of Hallett Lake, outcrops are numerous and units distinctive enough to closely bracket the distribution of the faults.

To the east and west of the northeast-trending Hallett-Tahultzu-Dorman lakes corridor, the land has higher relief and/or is underlain by Jurassic to Tertiary sedimentary and volcanic rocks compared to the Middle Jurassic mafic and intermediate phases of the Stag Lake suite in a medial position. East of Hallett and Tahultzu lakes, Eocene Ootsa Lake Group rocks nonconformably overlie the composite pluton of that suite or, east of Bungalow Lake at Mount Greer, diorite of the Middle Jurassic Brooks Diorite Complex (Wetherup, 1997). West of the Holy Cross Road, Ootsa Lake Group rocks overlie the Jurassic Hazelton or Bowser Lake groups. These stratigraphic relationships indicate a post-Middle Jurassic, pre-Early Eocene uplift and unroofing of the Stag Lake suite in the area, prior to eruption of the Ootsa Lake Group rocks.

Important changes in the nature, thickness, and geological relationships involving the Eocene Ootsa Lake and Endako groups and their basement rocks, occur east of Bungalow Lake (Fig. 2) and help to delineate the Bungalow Lake fault. The Bungalow Lake fault marks the western limit of thick successions of Endako Group rocks and the easternmost limit of the flow-lineated hornblende-phyric dacite flows of the Ootsa Lake Group. The facies variation in the Ootsa Lake Group and localized accumulation of the Endako Group across the Bungalow Lake fault are indicative of period(s) of synvolcanic movement along the fault. Both units are tilted about 20° to the northeast, suggesting additional postdepositional movement along it.

Smaller scale faults south and west of Hallett Lake involve moderately dipping to overturned panels of Mesozoic basement rock which are juxtaposed against Tertiary volcanic rocks along northeasterly or northwesterly trending structures (Fig. 2).

The set of northeast-trending faults occurs in an upper crustal plate to the northwest of the northeast-trending Nulki shear zone (in NTS 93F/09 and 16) which itself marks the western margin of the Vanderhoof Metamorphic Complex (Wetherup and Struik, 1996; Wetherup, 1997). Wetherup (1997) indicated extension to the northwest and southeast based on a number of structural elements in the Vanderhoof Metamorphic Complex and Eocene rocks flanking it. The series of northeast-trending, brittle normal faults inferred in the Hallett Lake area is at least as old as, and likely coeval and kinematically linked with, extensional shear in the lower plate recorded in rocks of the Vanderhoof Metamorphic Complex.

ALTERATION AND MINERAL SHOWINGS

Mineral showings in the Hallett Lake area are dominated by low fluorine, porphyry molybdenum showings in the Late Jurassic and Early Cretaceous plutonic rocks (Anderson et al., 1997a). As reported in the MINFILE compilation for the area (Bailey et al., 1995; Lefebure and Höy, 1996), thirteen showings occur in the Casey or Nithi phases (see L'Heureux and Anderson, 1997) and two occur in the Caledonia alkali-feldspar megacrystic biotite monzogranite phase.

Only one showing occurs in stratified rocks, the Holy Cross epithermal gold prospect (MINFILE number 93F 029; Bailey et al., 1995; Lane and Schroeter, 1997; Fig. 2). The gold mineralization within the Eocene Ootsa Lake Group rhyolite occurs in zones of brecciated and intensely silicified rhyolite and banded hematitic quartz veins, and clear drusy quartz stockwork (Lane and Schroeter, 1997).

CONCLUSIONS

Mesozoic and Tertiary volcanic and sedimentary rocks underlie more than half of the Hallett Lake area and occur along the northwestern and southeastern flanks of the medial Mesozoic composite batholith. Lower to Middle Jurassic Hazelton Group volcaniclastic and volcanogenic sedimentary rocks, Middle and Upper Jurassic Bowser Lake Group siliciclastic rocks, and Eocene felsic and mafic volcanic rocks of the Ootsa Lake and Endako groups make up the main stratified units. Faults or Eocene intrusions mark the contacts between most units except for the Tertiary units. The composition, facies, and localization of the Tertiary volcanic units and their relationships with underlying Mesozoic basement help delineate small- and large-scale, partly synvolcanic, normal faults. The northeast-trending, down-to-the-southeast series of faults may be an upper plate manifestation of northwesterly-directed ductile extension recorded in the western part of the structurally lower, Eocene Vanderhoof Metamorphic Complex.

ACKNOWLEDGMENTS

L.C. Struik provided outstanding support and leadership in providing the logistical and scientific framework for the fieldwork. Our work was focused by discussions with G Johnson of Endako Mines Division, Placer Dome Canada Ltd., and the excellent unpublished maps and data of E.T. Kimura, S. Gardiner and other exploration geologists of Placer Dome Canada Inc. Reconnaissance mapping in 1996 by S. Wetherup, L.C. Struik, R. L'Heureux and J. Letwin contributed to the map and focused the present work. Discussions with and field trips led by L.J. Diakow and M.L. Bevier (Mount Greer locality and elsewhere) were very helpful. Access to R.L. Armstrong's unpublished database by J. Mortensen and to unpublished K-Ar data by M.L. Bevier, both of the Department of Earth and Ocean Sciences, University of British Columbia, is appreciated. Fellow 1997 'GNAT'-mappers J. Resnick, S. Wearmouth, and volunteers E. Barnes and S.Y. Siew provided excellent assistance and contributions during the fieldwork and data compilation. K-H. Reitz, N. Hastings, E. Barnes, J. Ferreria, and B. Vanlier helped in the digital preparation of the photographs, maps, and manuscript. L. and K. Lindenberger of Pipers Glen RV Park provided generous support to the GSC crew throughout the summer. H. Tipper's review helped improve the paper and is appreciated.

REFERENCES

Anderson, R.G., L'Heureux, R., Wetherup. S., and Letwin, L.
1997a: Geology of the Hallett Lake map area, central British Columbia: Triassic, Jurassic, Cretaceous, and Eocene? plutonic rocks; in Current Research 1997-A; Geological Survey of Canada, p. 107-116.

Anderson, R.G., Snyder, L.D., Resnick, J., and Barnes, E.
1998: Geology of the Big Bend Creek map area, central British Columbia; in Current Research 1998-A; Geological Survey of Canada.

Anderson, R.G., Whalen, J.B., Villeneuve, M.E., Struik, L.C., and L'Heureux, R.
1997b: Jura-Cretaceous plutonic rocks near the Endako molybdenite mine, central B.C.; (abstract), Geological Association of Canada/ Mineralogical Association of Canada, Program with Abstracts, v. 22, p. A3.

Bailey, D.G., Jakobsen, D.E., and Lane, R.
1995: MINFILE 093F Nechako River mineral occurrence map; British Columbia Ministry of Energy, Mines and Petroleum Resources, MINFILE, revised March 1995, scale 1:250 000.

Bellefontaine, K.A., Legun, A., Massey, N., and Desjardins, P.
1995: Digital Geological Compilation of Northeast B.C. - Southern Half (NTS 83D, E, 93F, G, H, I, J, K, N, O, P); British Columbia Ministry of Energy, Mines and Petroleum Resources, Open File 1995-24.

Diakow, L.J., Webster, I.C.L., Richards, T.A., and Tipper, H.W.
1997: Geology of the Fawnie and Nechako Ranges, southern Nechako Plateau, central British Columbia (93F/2,3,6,7); in Interior Plateau Geoscience Project: Summary of Geological, Geochemical and Geophysical Studies, (ed.) L.J. Diakow and J.M. Newell ; British Columbia Geological Survey Branch, Open File 1996-2 and Geological Survey of Canada, Open File 3448, p. 7-30.

Haskin, M., Snyder, L.D., and Anderson, R.G.
1998: Tertiary Endako Group volcanic and sedimentary rocks at four sites in the Nechako River and Fort Fraser map areas, central British Columbia; in Current Research 1998-A; Geological Survey of Canada.

Kimura, E.T., Bysouth, G.D., Cyr, J., Buckley, P., Peters, J., Boyce, R., and Nilsson, J.
1980: Geology of parts of southeast Fort Fraser and northern Nechako River map areas, central British Columbia; Placer Dome Incorporated, Internal Report and Maps, Vancouver, British Columbia.

Lane, R.A.
1995: Preliminary bedrock geology, Holy Cross Mountain to Bentzi Lake, central British Columbia (parts of NTS 93F/14E and 15W); British Columbia Geological Survey Branch, Open File 1995-22, scale 1:15 000.

Lane, R.A. and Schroeter, T.G.
1997: A review of metallic mineralization in the Interior Plateau, central British Columbia (Parts of 93B, C and F); in Interior Plateau Geoscience Project: Summary of Geological, Geochemical and Geophysical Studies, (ed.) L.J. Diakow and J.M. Newell; British Columbia Geological Survey Branch Open File 1996-2 and Geological Survey of Canada, Open File 3448, p. 237-256.

Lefebure, D.V. and Höy, T. (editors)
1996: Selected British Columbia mineral deposit profiles, Volume 2—Metallic Deposits; British Columbia Geological Survey Branch, Open File 1996-13, Appendix 1.

L'Heureux. R. and Anderson, R.G.
1997: Early Cretaceous plutonic rocks and molybdenite showings in the Nithi Mountain area, central British Columbia; in Current Research 1997-A; Geological Survey of Canada, p. 117-124.

Struik, L.C. and MacIntyre, D.
1997: Nechako Plateau NATMAP Project overview, central British Columbia, year two; in Current Research 1997-A; Geological Survey of Canada, p. 57-64.
1998: Nechako Plateau NATMAP Project overview, central British Columbia, year three; in Current Research 1998-A; Geological Survey of Canada.

Struik, L.C. and McMillan, W.J.
1996: Nechako NATMAP Project overview, central British Columbia; in Current Research 1996-A; Geological Survey of Canada, p. 57-62.

Struik, L.C., Whalen, J.B., Letwin, J., and L'Heureux, R.
1997: General geology of southeast Fort Fraser map area, British Columbia; in Current Research 1997-A; Geological Survey of Canada, p. 65-76.

Tipper, H.W.
1963: Nechako River map-area, British Columbia; Geological Survey of Canada, Memoir 324, 59 p.

Villeneuve, M.E., Struik, L.C., MacIntyre, D.G., Anderson, R.G., and Whalen, J.B.
1997: Timing of Eocene and Jurassic magmatism in Nechako Plateau, central B.C., and relationship to porphyry deposits; Geological Association of Canada/Mineralogical Association of Canada, Program with Abstracts, v. 22, p. A154.

Wetherup, S.
1997: Geology of the Nulki Hills and surrounding area (NTS 93F/9 and F/16), central British Columbia; in Current Research 1997-A; Geological Survey of Canada, p. 125-132.

Wetherup, S. and Struik, L.C.
1996: Vanderhoof Metamorphic Complex and surrounding rocks, central British Columbia; in Current Research 1996-A; Geological Survey of Canada, p. 63-70.

Whalen, J.B. and Struik, L.C.
1997: Plutonic rocks of southeast Fort Fraser map area, central British Columbia; in Current Research 1997-A; Geological Survey of Canada, p. 77-84.

Whalen, J.B., Struik, L.C., and Hrudey, M.G.
1998: Bedrock geology of the Endako map area, central British Columbia; in Current Research 1998-A; Geological Survey of Canada.

Williams, S.P.
1997: Geological compilation of the Nechako River (93F) map area, British Columbia; Geological Survey of Canada, Open File 3429, scale 1:250 000.

Geological Survey of Canada Project 950036-04

Geology of the Big Bend Creek map area, central British Columbia[1]

R.G. Anderson, L.D. Snyder[2], J. Resnick, and E. Barnes[4]
GSC Pacific, Vancouver

Anderson, R.G., Snyder, L.D., Resnick, J., and Barnes, E., 1998: Geology of the Big Bend Creek map area, central British Columbia; in Current Research 1998-A; Geological Survey of Canada, p. 145-154.

Abstract: The Big Bend Creek map area (NTS 93F/10) encompasses the southern extent and thickest accumulation of fault-bounded Middle and Upper Eocene (48-37 Ma) Endako Group basaltic flow and volcaniclastic rocks and the northern extent of well dated, extensive Jurassic Hazelton and Bowser Lake groups volcanic and sedimentary rocks mapped so far in NTS 93F. Jurassic and Eocene plutons are important in the northern part of the map area.

Moderately to steeply dipping, deformed rocks of the undivided Hazelton Group, Naglico Formation, Bowser Lake Group and Eocene Ootsa Lake Group and (?)Cretaceous porphyry intrusion make up the basement for Endako Group basalt flows. An older deformation recorded in deformed pebble conglomerate of Bowser Lake Group is likely post-Jurassic and pre-Late Cretaceous.

Brittle deformation of Mesozoic and Tertiary basement rocks accompanied initiation of the latest structures such as a north-trending graben developed synchronously with eruption of the Endako Group basalt flows.

Résumé : La région cartographique de Big Bend Creek (coupure 93F/10 du SNRC) comprend deux grands secteurs : un secteur sud où s'observent les coulées basaltiques et les roches volcanoclastiques limitées par des failles (Éocène moyen-supérieur, 48-37 Ma) du Groupe d'Endako et qui constitue l'accumulation la plus épaisse de ce groupe; un secteur nord où s'observent des roches volcaniques et sédimentaires des groupes de Hazelton et de Bowser Lake (Jurassique); ces dernières lithologies, dont l'âge est bien établi, sont présentes sur de grandes étendues et ont toujours été cartographiées à l'échelle du feuillet cartographique 93F du SNRC. Des plutons jurassiques et éocènes occupent une superficie importante dans le secteur nord de la région cartographique.

Des roches déformées montrant un pendage modéré à fort et associées au groupe non subdivisé de Hazelton, à la Formation de Naglico, au Groupe de Bowser Lake et au Groupe d'Ootsa Lake (Éocène) de même qu'une intrusion porphyrique crétacée (?) constituent le substratum rocheux sur lequel se sont déposées les coulées basaltiques du Groupe d'Endako. Une déformation plus ancienne, dont témoigne un conglomérat à cailloux déformé du Groupe de Bowser Lake, est vraisemblablement postérieure au Jurassique et antérieure au Crétacé tardif.

Une déformation cassante des roches mésozoïques et tertiaires du substratum a accompagné la formation initiale des structures les plus tardives, notamment d'un graben d'orientation nord contemporain de l'éruption des coulées basaltiques du Groupe d'Endako.

[1] Contribution to the Nechako NATMAP Project
[2] Department of Geology, University of Wisconsin-Eau Claire, Eau Claire, Wisconsin 54702-4004
[3] Department of Earth and Ocean Sciences, University of British Columbia, 6339 Stores Road, Vancouver, British Columbia V6T 1Z4
[4] Department of Geology and Applied Geology, University of Glasgow, Glasgow, United Kingdom G12 8QQ

INTRODUCTION

Geological mapping of the Big Bend Creek map area (NTS 93F/10) helps revise the Nechako River 1:250 000 scale geological map (Tipper, 1963) as part of the Nechako NATMAP Project (Fig. 1; Struik and McMillan, 1996; Struik and MacIntyre, 1997, 1998). Mapping in 1996 focused on the distribution of plutonic suites to the north in the Hallett Lake area (Fig. 1; e.g., Anderson et al., 1997a; L'Heureux and Anderson, 1997) as part of a regional study of plutonic suites (see Struik et al., 1997; Whalen and Struik, 1997; Anderson, et al., 1997b; Whalen et al., 1998; Anderson and Snyder, 1998). During 1997, bedrock mapping extended south to the Big Bend Creek area to link with detailed mapping in the Nechako Ranges (Diakow et al., 1995a, 1997), to trace Eocene volcanic and plutonic units and structures to the south from Hallett Lake, and to provide a regional context for a detailed study of the Eocene Endako Group (Haskin et al., 1998). As in 1996, the present work builds on the excellent mapping and age-dating contributions by mineral exploration and provincial geological survey geologists in the area over the past 30 years (e.g., Lane, 1995; Diakow et al., 1997; Lane and Schroeter, 1997 and references therein).

This report provides descriptions of Tertiary and newly subdivided Mesozoic basement units and their known or inferred geological relationships to Eocene strata and plutons. The relationships suggest that the small- and regional-scale block faults, recognized to the south and north, extend into the Big Bend Creek area where they are part of a set of normal faults that localized deposition of the Middle and Upper Eocene Endako Group volcanic flow and volcaniclastic rocks (Fig. 2).

PHYSIOGRAPHY, ACCESS, AND FIELD METHODS

The Nechako River map area's Interior Plateau physiography is generally of low relief and entirely below treeline. It is particularly subdued in the Big Bend Creek area, leading to discontinuous outcrops, separated by broad areas of glaciofluvial and glaciolacustrine sediments. This provides a challenge to mapping the continuity of stratigraphic units and bounding structures and leads to inferred contacts amongst units except in the Nechako Ranges where exposure is better (Fig. 2). Continued, extensive logging in the area is continually improving access to outcrop.

New data reported here were based upon five weeks' work (about 55 traverses) in late June and July 1997. The mapping, station location, sampling, and bulk rock geophysical measurement techniques used are the same as summarized in Anderson et al. (1997a).

GEOLOGY

Stratified rocks

Lower and Middle Jurassic Hazelton Group (units lmJH and mJHN)

Unfossiliferous Hazelton Group rocks in the Big Bend Creek area (Fig. 2) occur near Cutoff Butte, where they are well exposed, and along the northern flank of the Nechako Range where they are more accurately correlated with better dated successions to the south described by Diakow et al. (1995a, 1997). Two units are distinguished: green and maroon, plagioclase-rich volcaniclastic rocks of the undivided Lower

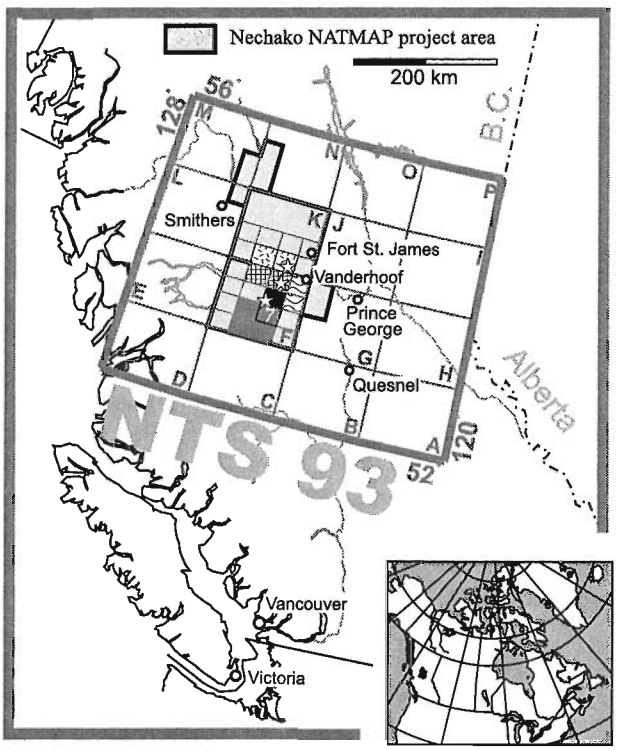

Figure 1. *Location of the Big Bend Creek (NTS 93F/10) map area and other recently mapped areas within the Nechako NATMAP project area.*

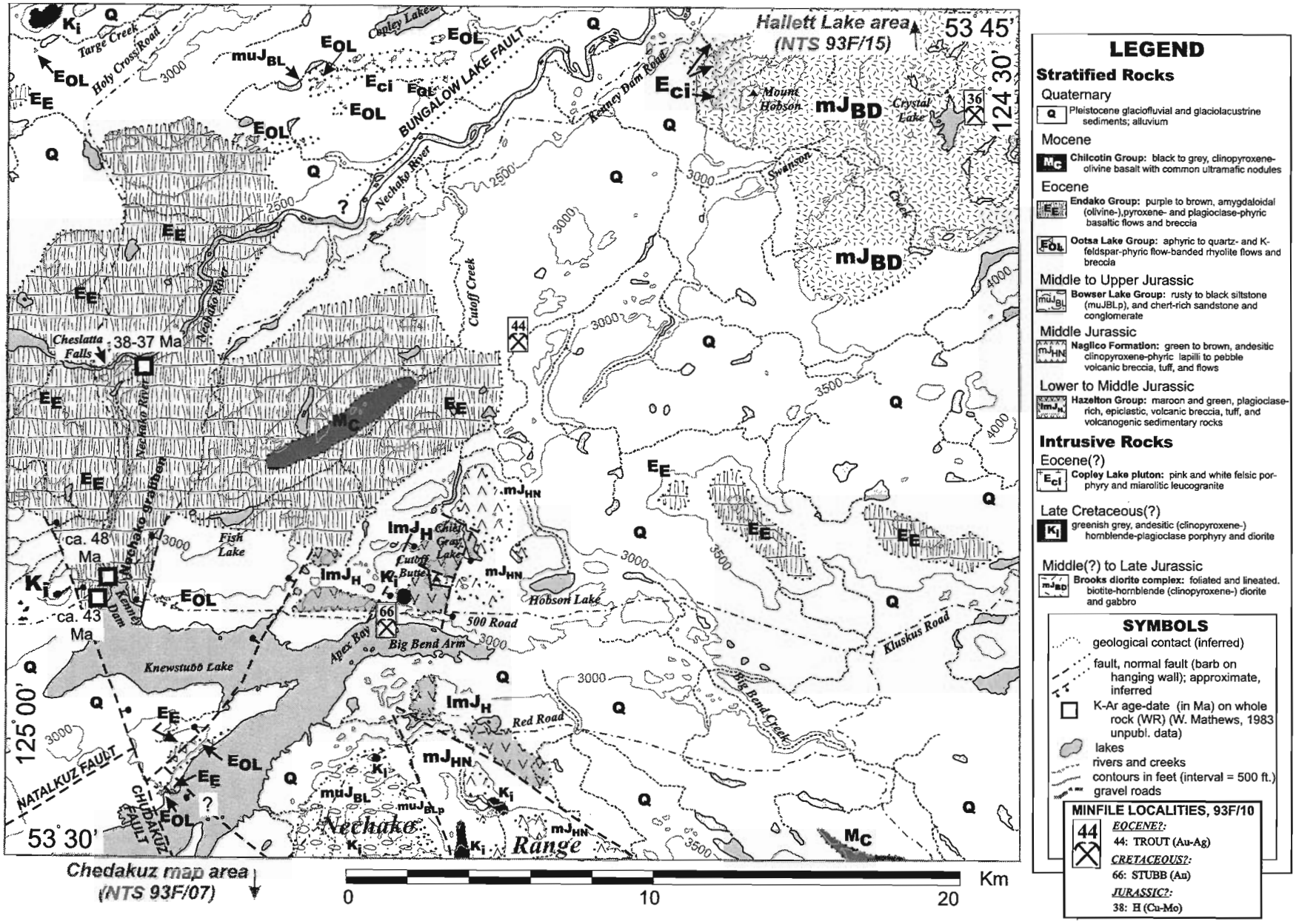

Figure 2. *Geological map of the Big Bend Creek map area compiled from mapping reported herein and in Haskin et al. (1998) as well as earlier mapping, age dating, and compilations (e.g., Tipper, 1963; Bellefontaine et al., 1995; M.L. Bevier, unpub. data, 1981; and Williams, 1997).*

and Middle Jurassic Hazelton Group, and structurally overlying clinopyroxene- and plagioclase-rich volcaniclastic and flow units correlated with the Middle Jurassic Naglico Formation of Diakow et al. (1995a, 1997).

Undivided Hazelton Group

Undivided rocks of the lower Hazelton Group are typically maroon and green, heterogeneous, plagioclase-rich epiclastic volcaniclastic rocks which underlie the west and southern flanks of Cutoff Butte and the area south of Fish Lake (Fig. 2). Layered rocks include thick, massive, heterolithic, lapilli to pebble volcanic breccia and tuff, distinguished by abundant (10-40%) white plagioclase and rare amphibole phenocrysts, that alternate with finely laminated maroon and grey grit and feldspathic greywacke in beds 5-30 cm thick (Fig. 3). Fragments are highly variable in abundance, angularity, sorting, and size: 10-20%, subangular, unsorted, (hornblende-) plagioclase porphyritic andesite fragments are typical. Groundmass for the volcaniclastic rocks is typically an unsorted and immature, feldspar-rich tuffaceous sandstone to grit which resembles the fragments. Planar crossbeds, flame structures, and cut-and-fill structures provide tops indicators and also suggest most of the unit is epiclastic. At Cutoff Butte, strata are steeply northeasterly-dipping and upright to subvertical and overturned. Alteration of the rocks to epidote is common and varies from selective, complete alteration of fragments to nearly complete alteration of the entire rock.

Naglico Formation

Rocks correlated with the Naglico Formation of Diakow et al. (1997) include green-, grey-, or brown-weathering, unbedded and unfossiliferous, heterogeneous clinopyroxene-phyric lahar deposits which underlie Cutoff Butte, ridges near Chief Gray Lake, and the north flank of the Nechako Range (Fig. 2). Abundant lapilli to pebble volcanic breccia and crystal lithic tuff, and rare grit layers and minor andesite flows make up the unit. Fragments make up 10-80% of the rock, vary from lapilli to boulder size (5-40 cm), are commonly subround to subangular, and comprise varieties of clinopyroxene-plagioclase porphyritic andesite to basaltic andesite (Fig. 4). Locally they have a "puzzle-fit" texture and apparently have not been highly disaggregated. Matrix support of the fragments is provided by fine to medium grained, poorly sorted, equigranular to bimodal, clinopyroxene- and plagioclase-bearing sandstone or grit which is compositionally similar to the enclosed fragments. In the matrix, subhedral plagioclase grains (1-3 mm in size, 10-80%) dominate over ubiquitous but less common clinopyroxene (1-4 mm in size, 2-30%). Epidote alteration of fragments (and less commonly of the matrix) and epidote-calcite veinlets are common.

At Cutoff Butte, the unit occurs structurally above the steeply northeasterly dipping panel of undivided Hazelton Group rocks but is separated from it by a minor, east-trending, brittle shear zone. In the Nechako Range, the unit is contiguous with the more fossiliferous Middle Jurassic (Bajocian) Naglico Formation of the Hazelton Group in the Chedakuz Creek area (Diakow et al., 1997).

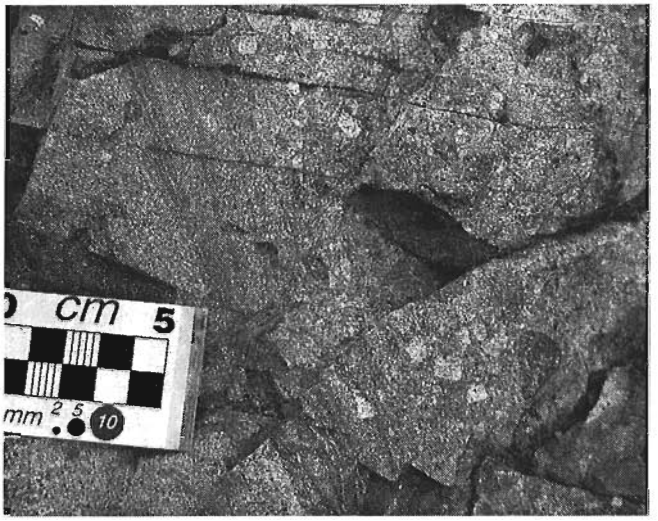

Figure 3. *Thinly laminated, plagioclase-rich, tuffaceous grit intercalated with epiclastic lapilli breccia of the undivided Lower to Middle Jurassic Hazelton Group on the south flank of Cutoff Butte.*

Middle and Upper Jurassic Bowser Lake Group (unit muJBL)

Bowser Lake Group rocks in south-central part of the area underlie the western half of the Nechako Range (Fig. 2). They include rusty to black, unfossiliferous, sedimentary rocks in a north-northwest-trending faulted panel. The sequence comprises: basal well bedded, siltstone and shale; medial siltstone and fine grained, chert-rich sandstone; and, upper sandstone and chert-rich conglomerate. In the east, fine grained shale and siltstone define a unit about 500 m thick but are commonly cleaved due to their proximity to the northwesterly faulted contact against the Naglico Formation (Fig. 5). Farther west is a sequence of siltstone and fine-grained, poorly sorted greywacke 200-300 m thick. Chert pebble conglomerate makes up the upper 2-3 km of the structural panel. It is commonly intruded by (?) Late Cretaceous porphyry and diorite; conglomerate outcrops closest to the Nechako resevoir are commonly deformed.

The upper conglomerate unit is the most distinctive rock type. Fragments vary from grit to granule (1-2 mm in size) to pebble (1-10 cm in size), are round to subround, and are poorly sorted. Locally, they make up 90% of the unit (Fig. 6a). Where the clasts are this abundant, the conglomerate is fragment supported. At one locality, most to least common fragments included: black chert (16-42%), grey chert (15-33%), white aphanitic volcanic rocks (13-19%), white chert (2-11%), and miscellaneous rock types (shale, pink chert or grey siliceous porphyry making up 7-15%); groundmass accounts for 15-26%. The abundance of felsic volcanic fragments is characteristic of the unit in the Big Bend Creek and Hallett Lake areas (e.g., Anderson and Snyder, 1998) but not farther south (Diakow et al., 1997).

The composite sedimentary unit is traceable to the south into similar rocks underlying the southern Nechako Range where they are more fossiliferous, mostly Callovian in age, and correlated with the Ashman Formation of the Bowser Lake Group (Diakow et al., 1997). In the Big Bend Creek area, the unit is included with the Bowser Lake Group because of the dearth of fossils and the dissimilarity of the units with the Ashman Formation on Ashman Ridge type area (Tipper and Richards, 1976) precludes direct correlation.

The conglomeratic unit is thick-bedded (0.3-3 m thick beds); tops indicators provided by cut-and-fill sedimentary structures indicate the unit is upright and west-facing. Bedding varies from subvertical in the shale-siltstone unit adjacent the faulted contact with the Naglico Formation, to moderately southwesterly dipping on the western flank of the Nechako Range. The unit is little deformed except along the fault and along the westernmost flank of the Nechako Range.

In the westernmost Nechako Range, chert pebble conglomerate is deformed into an L-S tectonite featuring prolate chert fragments (Fig. 6b) which define a moderately plunging, down-dip lineation in a moderately southwesterly dipping schistosity. Foliated and cleaved sedimentary rocks extend from these localities to the south (Diakow et al., 1997).

Figure 4. *Clinopyroxene-plagioclase phyric basaltic andesite fragments in lahar deposit appear only slightly disaggregated; Naglico Formation, south flank of the Nechako Range.*

Figure 5. *View to northeast of pencil cleavage in siltstone of basal Bowser Lake Group on south flank of Nechako Range.*

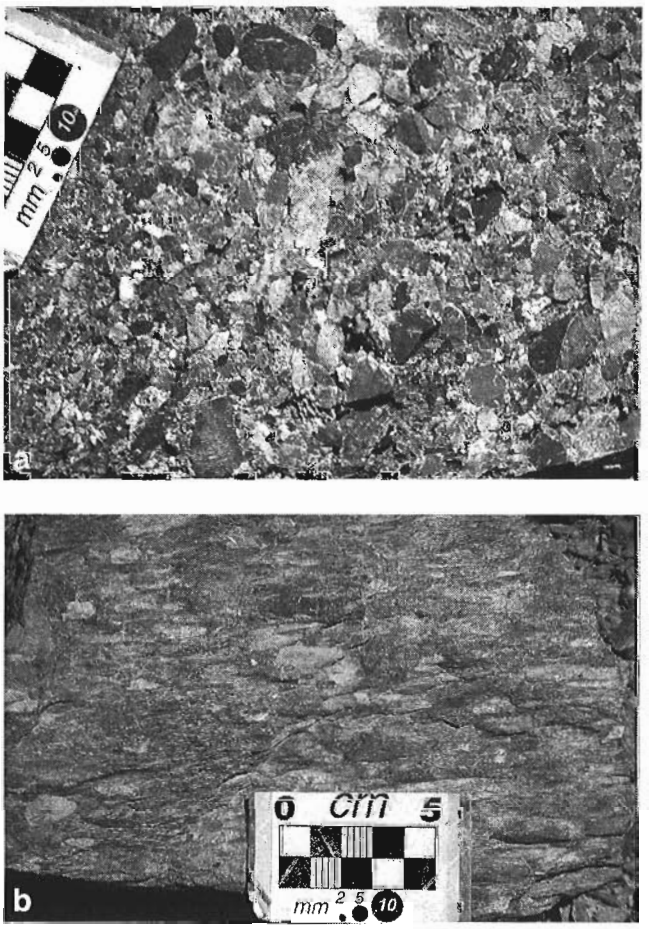

Figure 6. *Conglomerate facies of Bowser Lake Group:* ***a)*** *undeformed granule to pebble conglomerate with variegated chert and minor felsic volcanic rock fragments;* ***b)*** *lineated chert and shale fragments in deformed conglomerate on Red road in southern Big Bend Creek map area.*

The deformed conglomerate and interbedded slate are crosscut by an equigranular hornblende diorite to hornblende-phyric andesite. Similar intrusive rocks directly to the south in the Nechako Range were included with Late Cretaceous intrusions by Diakow et al. (1997).

Eocene Ootsa Lake Group (unit Eol)

Heterogeneous, pale pink to rusty tan felsic porphyry, tuff, breccia, and dacite and rhyolite flows of the Ootsa Lake Group occur mainly south and southeast of Copley Lake (Fig. 2). Porphyry and rhyolite and dacite flows commonly contain phenocrysts of subhedral plagioclase and/or potassium feldspar (5-20%, 1-5 mm in size) and less common biotite (2-5%, 1-2 mm in size) and subhedral to rounded quartz (1-2%, 0.5-4 mm in size), and scattered amphibole (locally as much as 5-15%, 0.5-3 mm in size) in an aphanitic groundmass. The flows are rarely spherulitic (Fig. 7a) or contain elongate vugs. Uncommon flow layering and lamination (Fig. 7b) are moderately easterly or southerly dipping. The rocks commonly exhibit weak but widespread clay alteration, rare disseminated pyrite, and pyrolusite fracture coatings.

Lapilli to pebble breccia commonly contains angular fragments (typically 0.1-5 cm in size but rarely much larger, Fig. 7c) of aphanitic, flow-laminated, pumiceous or sparingly plagioclase-phyric dacite or rhyolite. Breccia occurrence as thin discontinuous zones of highly variable width, particularly near the southern flank of the Copley Lake pluton, might indicate an intrusive origin.

Eocene Endako Group (unit Ee)

The Endako Group is the most widespread and comparatively homogeneous unit in the area with its principal exposures north of Kenney Dam and between Big Bend and Swanson creeks (Fig. 2). At Kenney Dam, where the unit is thickest (at least 150 m thick) and best described (see Haskin et al., 1998 for details), and to the north, it comprises brown to dark grey to rusty red weathering, amygdaloidal, clinopyroxene- and plagioclase-phyric basalt and basaltic andesite. The volcanic rocks occur as thin (0.5-5 m thick), massive to vesicular to columnar-jointed flows (Fig. 8a), hyaloclastite (Fig. 8b), and rare pillowed basalt facies (Fig. 8c). Rusty red sandstone intercalations with the basaltic flows are rare.

North of Kenney Dam, near Cheslatta Falls, a distinctive, black and white succession of felsic ash and thin beds of lignite 5-10 m thick, locally subdivide the Endako Group, a subdivision corroborated by unpublished K-Ar age dates and flora determinations (see below). The sequence closely resembles a unit which defines the base of the Endako Group near the Nautley River (Struik et al., 1997; Haskin et al., 1998) but is significantly younger.

Endako Group flows are commonly equigranular at hand sample scale, but characteristically contains subhedral to euhedral plagioclase microlites (3-30%, 0.5-8 mm in size), less common clinopyroxene (5-20%, 0.5-2 mm) and rare and scattered olivine (<<1%, 0.5 mm in size). Vesicles may account for as much as 40% of the rock, particularly at flow

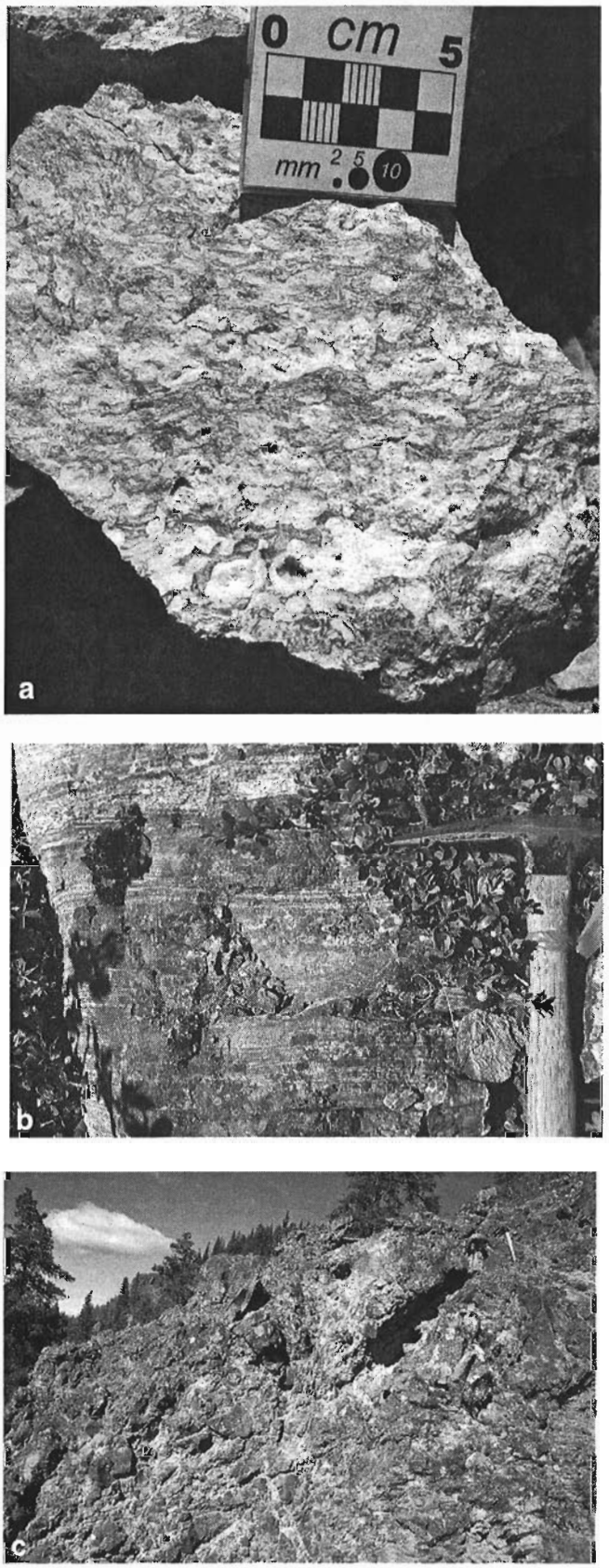

Figure 7. *Eocene Ootsa Lake Group rocks:* ***a)*** *spherulitic rhyolite;* ***b)*** *thinly flow-laminated rhyolite;* ***c)*** *coarse dacite breccia.*

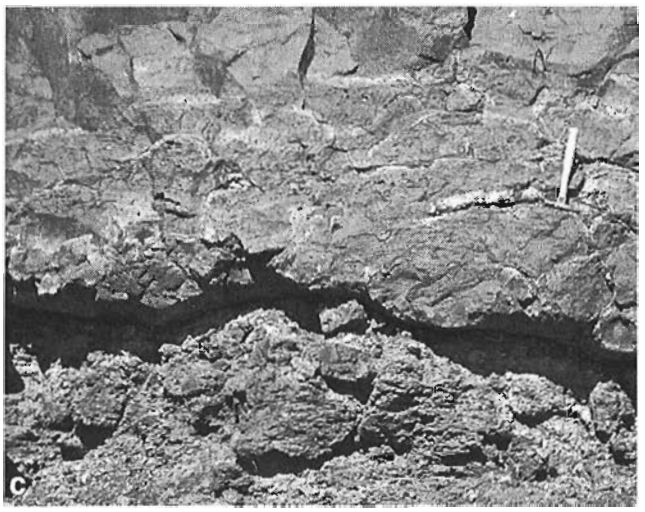

Figure 8. *Endako Group rocks:* ***a)*** *thin flows (0.5-2 m thick) at the Kenney Dam locality (see Haskin et al., 1998). Abandoned log loading apparatus is about 2.5 m tall and cliff attains height of 35 m;* ***b)*** *palagonitized basaltic hyaloclastite deposit;* ***c)*** *local basaltic pillowed lava occurrence near Kenney Dam; white interstitial material near 30 cm long hammer is chalcedony.*

Figure 9. *View west to conformable contact between flow-layered rhyolite of the Ootsa Lake Group and columnar jointed basalt of the Endako Group in southwestern Big Bend Creek map area. Person is 2 m tall.*

tops; chalcedony, chlorite, epidote, hematite, calcite, and a variety of unidentified, variegated zeolites(?) are common fillings.

Flat-lying andesite flows between Big Bend Arm and Swanson creeks cap the ridges above 3500 feet (1067 m) elevation. The flows resemble typical Endako Group in abundance of vesicles and clinopyroxene and plagioclase microphenocrysts, but are distinctly lighter grey and less amygdaloidal.

In the southwestern part of Big Bend Creek area, columnar-jointed basalt flows of the Endako Group rest conformably on Ootsa Lake Group flow-layered rhyolite tuff and flows weakly altered to clay; the sequence dips about 20 degrees northeast (Fig. 9). In the main outcrop area, north and south of Kenny Dam (Fig. 2), the Endako Group rocks are in inferred fault contact with Mesozoic and Tertiary rocks which have sustained brittle fracture and/or exhibit fracture cleavage (see Fig. 10). The distribution of the Endako Group and extent of deformation in the country rocks in this area defines the extent of the synvolcanic, Nechako graben. North of Fish Lake, where the distribution of the Endako Group is most widespread, the trace of the bounding normal faults disappears, presumably beneath the cover of younger flows which overtopped the graben and/or were preserved due to subsequent northward tilting.

Distinctive rusty red oxidized and oblate, vesicle-rich flow tops, sequences of intercalated hyaloclastite, pillowed lava breccia and isolated pillows, or rare stratigraphic contacts help define flow-layering which dips about 15-20° north. The dip magnitude and trend are remarkably similar in Big Bend Creek and Hallett Lake areas and indicative of regional post-Eocene tilting.

Unpublished K-Ar dates for whole rock samples of Endako Group in the area range between 48-37 Ma (M.L. Bevier, unpub. data, 1981) and include samples from Kenney Dam (42.7 ± 1.5 Ma), the floor of the Nechako River valley (47.6 ± 1.7 Ma), and significantly younger dates from basalt flows at Cheslatta Falls (36.5 ± 1.6 and 37.7 ± 1.3 Ma; W.H. Mathews, unpub. data, 1983). The stratigraphically higher and younger flows locally contain olivine and overlie the ash and lignite horizon, described above, which is Late Eocene or Early Oligocene in age based on flora collections (G. Rouse, unpub. data, 1983). The stratigraphic, fossil, and isotopic age data suggest that at least two pulses of Endako basaltic volcanism, in the Middle (48-43 Ma) and Late (38-37 Ma) Eocene, closely followed cessation of the Ootsa Lake Group felsic volcanism in the Middle Eocene (see Haskin et al., 1998).

Miocene Chilcotin Group (unit Mc)

Black to dark grey, columnar-jointed, clinopyroxene-olivine basalt of the Chilcotin Group occurs north of Fish Lake and directly west of Cutoff Creek where it is generally topographically lower than hills surrounding it underlain by Endako Group rocks (Fig. 2). Chilcotin Group basalt strongly resembles Endako Group flows but is thinner (30-40 m thick) and contains glomeroporphyritic olivine phenocrysts (5-10%, 4-40 mm in size) and rare olivine-rich ultramafic nodules with chrome diopside and spinel, and less common amygdules. In addition to olivine, euhedral plagioclase (10-20%, 1-10 mm in size) and clinopyroxene (1-3%, 1-2 mm) are important phenocrysts or microphenocrysts.

The unit is undated in the map area, but to the west (NTS 93F/11) and northeast (NTS 93F/16), similar rocks yielded mid-Miocene whole rock Ar-Ar dates (M. Villeneuve, pers. comm., 1997). The dates are significantly older than the Pliocene age range conventionally assigned to the Chilcotin Group by Bevier (1983) and Souther and Yorath (1991) but are consistent in age and distribution with basalt accumulations along the periphery of the Interior Plateau considered part of the Chilcotin Group in Mathews' (1989) more expanded definition.

Plutonic rocks

Jurassic Brooks Diorite Complex (unit mJBD)

The southwestern part of the Jurassic Brooks Diorite Complex described by Wetherup (1997) is well exposed near Mount Hobson and likely extends east of Crystal Lake, based on the mapping of the subcircular pluton by Tipper (1963; Fig. 2). Near Mount Hobson, well-foliated and lineated, equigranular to seriate, biotite-, clinopyroxene- and hornblende-bearing diorite and gabbro make up the very heterogeneous pluton. Mafic minerals make up 30-60% of the rock and are aligned in a moderately to steeply northeasterly dipping foliation and a steeply plunging mineral lineation oriented in a variety of trends. Epidote and chlorite alterations of the mafic minerals are common. The foliated mafic phase is intruded by a series of northeasterly elongate and subvertical stocks of miarolitic, flow-layered, and locally spherulitic, biotite-potassium feldspar porphyry granite. The younger, likely Tertiary age, felsic phase may be related to the magmatism which gave rise to Ootsa Lake Group and Copley Lake plutonic rocks to the west and north.

Late Cretaceous plutonic rocks (unit Ki)

Distinctive dykes and stocks of greenish-grey, unfoliated, andesitic (clinopyroxene-) hornblende-plagioclase porphyry and diorite are widespread in the western part of the area (Fig. 2). Subhedral clinopyroxene and plagioclase phenocrysts in the seriate diorite account for 20% of the rock; tabular to acicular hornblende makes up 1-5% of the porphyry.

North of Knewstubb Lake, the porphyry forms the western footwall of the Nechako graben; subvertical, centimetre-spaced fracture cleavage is developed within 2 km of the fault contact with the Endako Group (Fig. 10). To the south, in the western Nechako Range, porphyry and diorite intrude schistose and lineated Bowser Lake Group rocks. In the northwest, the porphyry pluton centred around Holy Cross Mountain in

Figure 10. *View to northwest of centimetre-spaced fracture cleavage in Late Cretaceous? hornblende-plagioclase porphyry intrusion west of Knewstubb Lake.*

the Knapp Lake area, extends southeast to Targe Creek (R.G. Anderson, unpub. data, 1997; Anderson and Snyder, 1998).

The porphyry and plutonic rocks are undated in the area; in the Chedakuz Creek map area (NTS 93F/07) to the south, similar rocks are considered Late Cretaceous (Diakow et al., 1997). Late Cretaceous (ca. 60-70 Ma) Ar-Ar dates for hornblende are known from hornblende porphyry units to the west (L. Diakow, pers. comm., 1997) and north (Lane and Schroeter, 1997).

(?)Eocene intrusive rocks (units Ec and Ei)

The composite, undated Copley Lake pluton (unit Ec, Fig. 2) extends south from the Hallett Lake map area (Anderson et al., 1997a; Anderson and Snyder, 1998) and, similarly, is associated with the most widespread distribution of the Eocene Ootsa Lake Group or intruded the volcanic rocks. South of Copley Lake, subvolcanic intrusive rocks (unit Ei) underlie resistant knobs and include pink and white dacite porphyry, which strongly resembles porphyritic flows of the Ootsa Lake Group, as well as rare miarolitic leucogranite stocks as the main constituents of the pluton rather than the phaneritic rocks seen farther north (Anderson et al., 1997a). Thin discontinuous zones of breccia, included with the Ootsa Lake Group, may be intrusive and related to the Copley Lake pluton. South of Copley Lake, heterolithic lapilli breccia of the Ootsa Lake Group is intruded by aplitic phases related to the pluton. Areas of intense silicification are associated with the fine-grained intrusive rocks.

STRUCTURE

Regional scale faults recognized to the south by Diakow et al. (1995b, 1997), such as the Chedakuz and Natalkuz faults, extend north into the Big Bend Creek area where they are part of a newly recognized set of normal faults that localized deposition of the Middle and Upper Eocene Endako Group volcanic flow and volcaniclastic rocks (Fig. 2). The faults are inferred from the extent of Endako Group rocks north and south of Kenny Dam and from features in the footwall rocks such as: a) disrupted stratigraphy involving the undivided Hazelton Group and Naglico Formation rocks near Cutoff Butte; b) brittle deformation, alteration, and development of fault breccia in Ootsa Lake Group rocks along 500 road; c) development of centimetre-spaced fracture cleavage in undivided Tertiary volcanic rocks along the peninsula southwest of the mouth of Big Bend Arm; and, d) development of centimetre-spaced fracture cleavage in Cretaceous porphyry west of Knewstubb Lake (Fig. 10). The set of northeast-trending faults near Cutoff Butte appear to have successively dropped units down to the southeast.

To the north, where the Tertiary Ootsa Lake Group and phases of the Copley Lake pluton are exposed, they are in assumed fault contact with the Jurassic Brooks Diorite Complex. The trace of that northeasterly trending fault, which is the southwestern extension of the Bungalow Lake fault in the Hallett Lake area (Anderson and Snyder, 1998), trends southwestwards along the Nechako River into the Nechako graben and may be another member of this set of faults.

ALTERATION AND MINERAL SHOWINGS

Three mineral showings are known in the area (Bailey et al., 1995; Fig. 2): the H (MINFILE number 93F 038) Cu-Mo showing in the Brooks Diorite Complex west of Crystal Lake; the STUBB Au showing (number 93F 066) possibly related to one of the Cretaceous porphyry intrusions near the eastern headland of Apex Bay near mouth of Big Bend Arm; and, the TROUT Au-Ag showing (MINFILE number 93F 044) north of Chief Gray Lake between Cutoff and Swanson creeks. The TROUT property is the mostly recently explored and is considered to be a low-sulphidation, epithermal deposit (Bailey et al., 1995; Lefebure and Höy, 1996) occurring in rhythmically banded quartz-adularia veins and silica-flooded zones of presumed Eocene age in polymictic conglomerate and andesitic breccia assumed by Lane and Schroeter (1997) to be part of the Cretaceous Kasalka Formation, not recognized elsewhere in the area.

CONCLUSIONS

The Big Bend Creek area is underlain by Mesozoic to Tertiary volcanic, plutonic and sedimentary rocks which record the Jurassic to Miocene magmatism and tectonics. Lower and Upper Jurassic volcanic (Hazelton Group) and sedimentary (Bowser Lake Group) units, and faults which bound them, extend from the northern flanks of the Nechako Range to areas in the south where they were previously mapped and dated (Diakow et al., 1997). Locally, the rocks sustained a somewhat cryptic Jurassic-Cretaceous deformation. The Natalkuz and Chedakuz faults extend north from the Chedakuz Creek map area (Diakow et al., 1995b) and are part of an important system of northeast- and northwest-trending block faults delineated by brittle deformation in Jurassic-Cretaceous stratified and plutonic basement rocks and by the localization and thickest accumulation of Endako Group basalt in the vicinity of Kenney Dam. The Eocene extension-related structures and envisioned tectonic history are similar in trend and nature to those recognized to the north in the Hallett Lake area.

ACKNOWLEDGMENTS

Bert Struik provided outstanding support and leadership in providing the logistical and scientific framework for the fieldwork. Discussions and field trips with Larry Diakow and Mary Lou Bevier were particularly helpful as was their generous sharing of unpublished information and maps. Fellow 1997 "GNAT"-mapper Shireen Wearmouth provided excellent assistance and "nap-mappers" Zulu and Kalo entertaining

companionship during the fieldwork. Nicki Hastings, Juliano Ferreria, and Bev Vanlier helped in the digital preparation of the maps and manuscript. Lori and Ken Lindenberger of Pipers Glen RV Park provided generous support to the GSC crew throughout the summer. Hugh Gabrielse's review helped improve the paper and is appreciated.

REFERENCES

Anderson, R.G. and Snyder, L.D.
1998: Jurassic to Tertiary volcanic, sedimentary and intrusive rocks in the Hallett Lake area, central British Columbia; in Current Research 1998-A; Geological Survey of Canada.

Anderson, R.G., L'Heureux, R., Wetherup. S., and Letwin, L.
1997a: Geology of the Hallett Lake map area, central British Columbia: Triassic, Jurassic, Cretaceous and Eocene? plutonic rocks; in Current Research 1997-A; Geological Survey of Canada, p. 107-116.

Anderson, R.G., Whalen, J.B., Villeneuve, M.E., Struik, L.C., and L'Heureux, R.
1997b: Jura-Cretaceous plutonic rocks near the Endako molybdenite mine, central B.C.; (abstract), Geological Association of Canada-Mineralogical Association of Canada, Program with Abstracts, v. 22, p. A-3.

Bailey, D.G., Jakobsen, D.E., and Lane, R.
1995: MINFILE 093F Nechako River mineral occurrence map; British Columbia Ministry of Energy, Mines and Petroleum Resources, MINFILE, revised March 1995.

Bellefontaine, K.A., Legun, A., Massey, N., and Desjardins, P.
1995: Digital Geological Compilation of Northeast B.C. - Southern Half (NTS 83D, E, 93F, G, H, I, J, K, N, O, P); British Columbia Ministry of Energy, Mines and Petroleum Resources, Open File 1995-24.

Bevier, M.L.
1983: Regional stratigraphy and age of Chilcotin Group basalts, south-central British Columbia; Canadian Journal of Earth Sciences, v. 20, p. 515-524.

Diakow, L.J., Webster, I.C.L., Richards, T.A., and Tipper, H.W.
1997: Geology of the Fawnie and Nechako Ranges, southern Nechako Plateau, central British Columbia (93F/2,3,6,7); in Interior Plateau Geoscience Project: Summary of Geological, Geochemical and Geophysical Studies, (ed.) L.J. Diakow and J.M. Newell; British Columbia Geological Survey Branch Open File 1996-2 and Geological Survey of Canada, Open File 3448, p. 7-30.

Diakow, L.J., Webster, I.C.L., Whittles, J.A., and Richards, T.A.
1995a: Stratigraphic highlights of bedrock mapping in the Southern Nechako Plateau, Northern Interior Plateau Region; in Geological Fieldwork 1994, (ed.) B. Grant and J.M. Newell; British Columbia Ministry of Energy, Mines and Petroleum Resources, Paper 1995-1, p. 171-176.

Diakow, L.J., Webster, I.C.L., Whittles, J.A., Richards, T.A., Giles, T.R., Levson, V.M., and Weary, G.F.
1995b: Bedrock and surficial geology of the Chedakuz Creek map area (NTS 93F/7); British Columbia Ministry of Energy, Mines and Petroleum Resources, Open File 1995-17.

Haskin, M., Snyder, L.D., and Anderson, R.G.
1998: Tertiary Endako Group volcanic and sedimentary rocks at four sites in the Nechako River and Fort Fraser map areas, central British Columbia; in Current Research 1998-A; Geological Survey of Canada.

Lane, R.A.
1995: Preliminary bedrock geology, Holy Cross Mountain to Bentzi Lake, central British Columbia (parts of NTS 93F/14E and 15W); British Columbia Geological Survey Branch, Open File 1995-22.

Lane, R.A. and Schroeter, T.G.
1997: A review of metallic mineralization in the Interior Plateau, central British Columbia (parts of 93B, C and F); in Interior Plateau Geoscience Project: Summary of Geological, Geochemical and Geophysical Studies, (ed.) L.J. Diakow and J.M. Newell; British Columbia Geological Survey Branch Open File 1996-2 and Geological Survey of Canada, Open File 3448, p. 237-256.

Lefebure, D.V. and Höy, T. (ed.)
1996: Selected British Columbia mineral deposit profiles, volume 2—metallic deposits; British Columbia Geological Survey Branch, Open File 1996-13, Appendix 1.

L'Heureux, R. and Anderson, R.G.
1997: Early Cretaceous plutonic rocks and molybdenite showings in the Nithi Mountain area, central British Columbia; in Current Research 1997-A; Geological Survey of Canada, p. 117-124.

Mathews, W.H.
1989: Neogene Chilcotin basalts in south-central British Columbia: geology, ages, and geomorphic history; Canadian Journal of Earth Sciences, v. 26, p. 969-982.

Souther, J.G. and Yorath, C.J.
1991: Neogene assemblages, Chapter 10; in Geology of the Cordilleran Orogen in Canada, (ed.) H. Gabrielse and C.J. Yorath; Geological Survey of Canada, Geology of Canada, no. 4, p. 373-401 (also Geological Society of America, The Geology of North America, v. G-2).

Struik, L.C. and MacIntyre, D.
1997: Nechako Plateau NATMAP Project overview, central British Columbia, year two; in Current Research 1997-A; Geological Survey of Canada, p. 57-64.

1998: Nechako NATMAP Project overview, central British Columbia, year three; in Current Research 1998-A; Geological Survey of Canada.

Struik, L.C. and McMillan, W.J.
1996: Nechako NATMAP project overview, central British Columbia; in Current Research 1996-A; Geological Survey of Canada, p. 57-62.

Struik, L.C., Whalen, J.B., Letwin, J., and L'Heureux, R.
1997: General geology of southeast Fort Fraser map area, British Columbia; in Current Research 1997-A; Geological Survey of Canada, p. 65-76.

Tipper, H.W.
1963: Nechako River map-area, British Columbia; Geological Survey of Canada, Memoir 324, 59 p.

Tipper, H.W. and Richards, T.A.
1976: Jurassic stratigraphy and history of north-central British Columbia; Geological Survey of Canada, Bulletin 270, 73 p.

Wetherup, S.
1997: Geology of the Nulki Hills and surrounding area (NTS 93F/9 and F/16), central British Columbia; in Current Research 1997-A; Geological Survey of Canada, p. 125-132.

Whalen, J.B. and Struik, L.C.
1997: Plutonic rocks of southeast Fort Fraser map area, central British Columbia; in Current Research 1997-A; Geological Survey of Canada, p. 77-84.

Whalen, J.B., Struik, L.C., and Hrudey, M.
1998: Bedrock geology of the Endako map area, central British Columbia; in Current Research 1998-A; Geological Survey of Canada.

Williams, S.P.
1997: Geological compilation of the Nechako River (93F) map area, British Columbia; Geological Survey of Canada, Open File 3429, scale 1:250 000.

Geological Survey of Canada Project 950036-04

Tertiary Endako Group volcanic and sedimentary rocks at four sites in the Nechako River and Fort Fraser map areas, central British Columbia[1]

M.L. Haskin[2], L.D. Snyder[2], and R.G. Anderson
GSC Pacific, Vancouver

Haskin, M.L., Snyder, L.D., and Anderson, R.G., 1998: Tertiary Endako Group volcanic and sedimentary rocks at four sites in the Nechako River and Fort Fraser map areas, central British Columbia; in Current Research 1998-A; Geological Survey of Canada, p. 155-164.

Abstract: Four well-exposed sections of Eocene Endako Group basalt flows with minor associated hyaloclastite and tuffaceous sedimentary rocks in the Nechako NATMAP area were studied and systematically sampled for geochemical and petrographic analysis and for Ar-Ar age dating. The rocks are aphyric to plagioclase- and pyroxene-, and rarely olivine-phyric and are commonly amygdaloidal. At the Nautley River (NTS 93K/02) and Bungalow Lake/Mount Greer (NTS 93F/9 and 93F/15) localities, the basal contact between the Endako Group and underlying Ootsa Lake Group felsic volcanic rocks is exposed; the Kenney Dam (NTS 93F/10) locality provides the thickest section of Endako Group mafic volcanic rocks. Previously determined K-Ar isotopic dates for whole rocks near the Mount Greer and Kenney Dam localities indicate at least two Middle and Late Eocene volcanic episodes that postdate Ootsa Lake Group volcanism and predate the Miocene-Pliocene Chilcotin Group basalt eruptions.

Résumé : De forts tremblements de terre ont laissé des traces de changements du niveau du sol, de tsunamis et de forts ébranlements dans les sédiments côtiers de la partie sud-ouest de la Colombie-Britannique. Les abaissements soudains du terrain lors des tremblements de terre sont à l'origine de l'enfouissement de marais littoraux et de sols forestiers sur l'île de Vancouver et près de Vancouver. Dans la partie ouest de l'île de Vancouver, certaines couches de sable dans des sédiments de marécages tourbeux et boueux sont des dépôts de tsunamis déclenchés par des tremblements de terre dans le Pacifique. Des formes dues à la liquéfaction, notamment des dykes et des cratères de sédiments essentiellement sableux, fournissent des témoignages directs d'ébranlements du sol, mais n'ont jusqu'ici été décrites que dans le delta du Fraser, au sud de Vancouver. Les formes observées découlant de phénomènes de subsidence, de tsunamis et d'ébranlements sont pour la plupart imputables à de forts tremblements de terre dont l'épicentre se trouve à la limite entre la plaque nord-américaine et la plaque Juan de Fuca; cependant, certaines d'entre elles résultent probablement d'un ou plusieurs tremblements de terre au sein de la croûte de l'Amérique du Nord. Par ailleurs, certains dépôts de tsunamis sur l'île de Vancouver sont le produit de forts tremblements de terre en Alaska.

[1] Contribution to the Nechako NATMAP Project
[2] Department of Geology, University of Wisconsin-Eau Claire, Eau Claire, Wisconsin 54702-4004

INTRODUCTION

The extent and age range of various sequences of Tertiary basaltic rocks in the Fort Fraser and Nechako River areas is comparatively better known than the Mesozoic basement (e.g. Armstrong, 1941, 1949; Tipper, 1963; Kimura et al., 1980; Armstrong, 1988; Bellefontaine et al., 1995; Struik et al., 1997; Williams, 1997; M.L. Bevier, L.C. Struik, and M. Villeneuve, pers. comm., 1997) (Fig. 1, 2, and 3). One of these, the Endako Group mafic rocks, is widely exposed in the south-central part of the Fort Fraser and the north-central part of the Nechako River map areas. The rocks display a variety of volcanological features and textures and the distinction of the mafic volcanic rocks of the Endako Group from those in the underlying Eocene Ootsa Lake Group (e.g. Diakow et al., 1997; Whalen et al., 1998) and overlying Miocene Chilcotin Group (e.g. Bevier, 1982, 1983a, b) (Fig. 2) is difficult, partly due to inadequate descriptions of reference areas for the Endako Group.

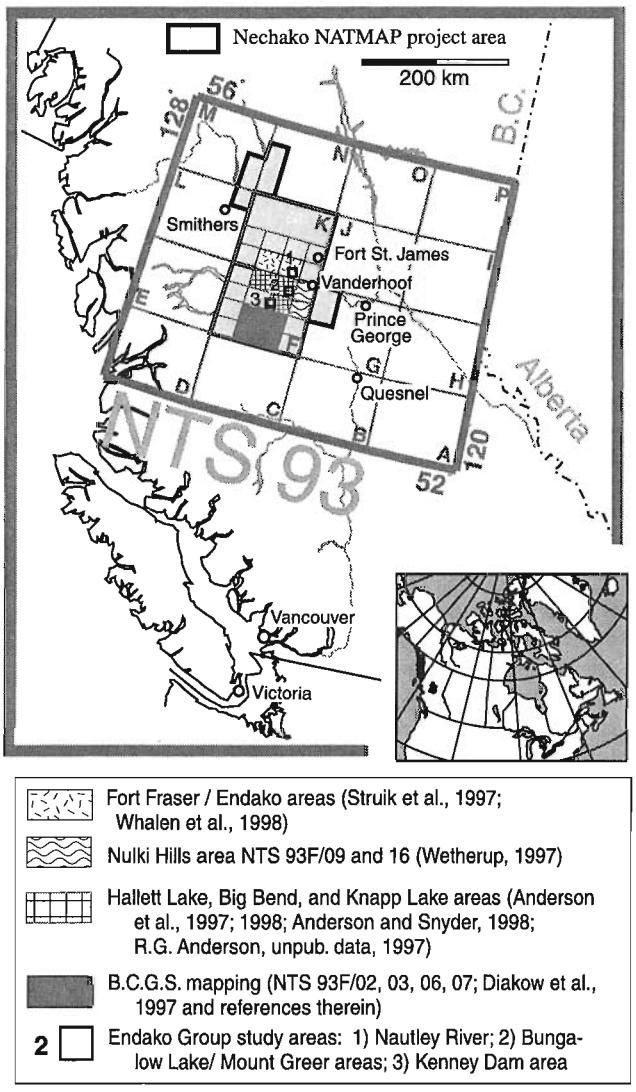

Figure 1. *Location of the sample sites in the Hallett Lake (NTS 93F/15), Fraser Lake (NTS 93K/02), and Big Bend (NTS 93F/10) map areas within the Nechako NATMAP project area.*

Stratigraphic and petrological relationships with the mainly felsic rocks of the underlying but nearly coeval Eocene Ootsa Lake Group, as well as chemical composition and precise isotopic age(s) for the Endako Group are poorly known. In addition, the relationship of Endako Group volcanism with coeval trans-tensional tectonics recognized in the Nechako NATMAP area and elsewhere (Fig. 1; e.g. Struik, 1993; Struik and McMillan, 1996; Struik and MacIntyre, 1997; MacIntyre and Webster, 1997; Struik et al., 1997) is critical in the understanding of their tectonic setting and eruption dynamics.

This baccalaureate study is designed to provide a better understanding of the Endako Group and comprises an investigation of four well-exposed stratigraphic sections of Endako Group rocks. The sections near the Nautley River (see Struik et al., 1997), northeast of Bungalow Lake, and at Mount Greer span the contact between the Endako Group and the underlying Ootsa Lake Group. The study area near Kenney Dam includes the thickest and most extensive section of Endako Group volcanic rocks preserved in the area.

The lithology, stratigraphy, and physical volcanology of the Endako Group rocks observed at these localities and described below by the senior author is supplemented by regional observations and compilations by R.G. Anderson and L.D. Snyder (e.g. Fig. 2 and 3). Geochemical and petrographic characterization of samples collected from the sections is underway as well as a collaborative $^{40}Ar/^{39}Ar$ study by M. Villeneuve (GSC). These new results will help refine the nature and distribution of the Endako Group in ongoing regional mapping of the Nechako River area (e.g. Anderson and Snyder, 1998; Anderson et al., 1998).

PHYSIOGRAPHY, ACCESS, AND FIELD METHODS

The study areas are characterized by low-relief Interior Plateau physiography and are located entirely below tree line, although extensive logging is continually improving access to outcrop. The four locations described in this report were chosen for their stratigraphic significance, nearly continuous exposure, and accessibility.

New data reported here were based upon two weeks' fieldwork in July 1997. Standard geological mapping techniques were supplemented by global positioning system measurements taken at each station, providing a geographic precision of 50-100 m in station location (depending on number and orientation of satellites). Representative samples of Endako Group and directly underlying Ootsa Lake Group rocks were collected for petrographic, mineralogical, $^{40}Ar/^{39}Ar$ dating, and geochemical studies. Magnetic susceptibility (m.s.) measurements were routinely obtained at each outcrop over a 5 minute period using a hand-held Exploranium KT-9 Kappameter and are an average of at least 5 measurements and specific gravity determinations were obtained

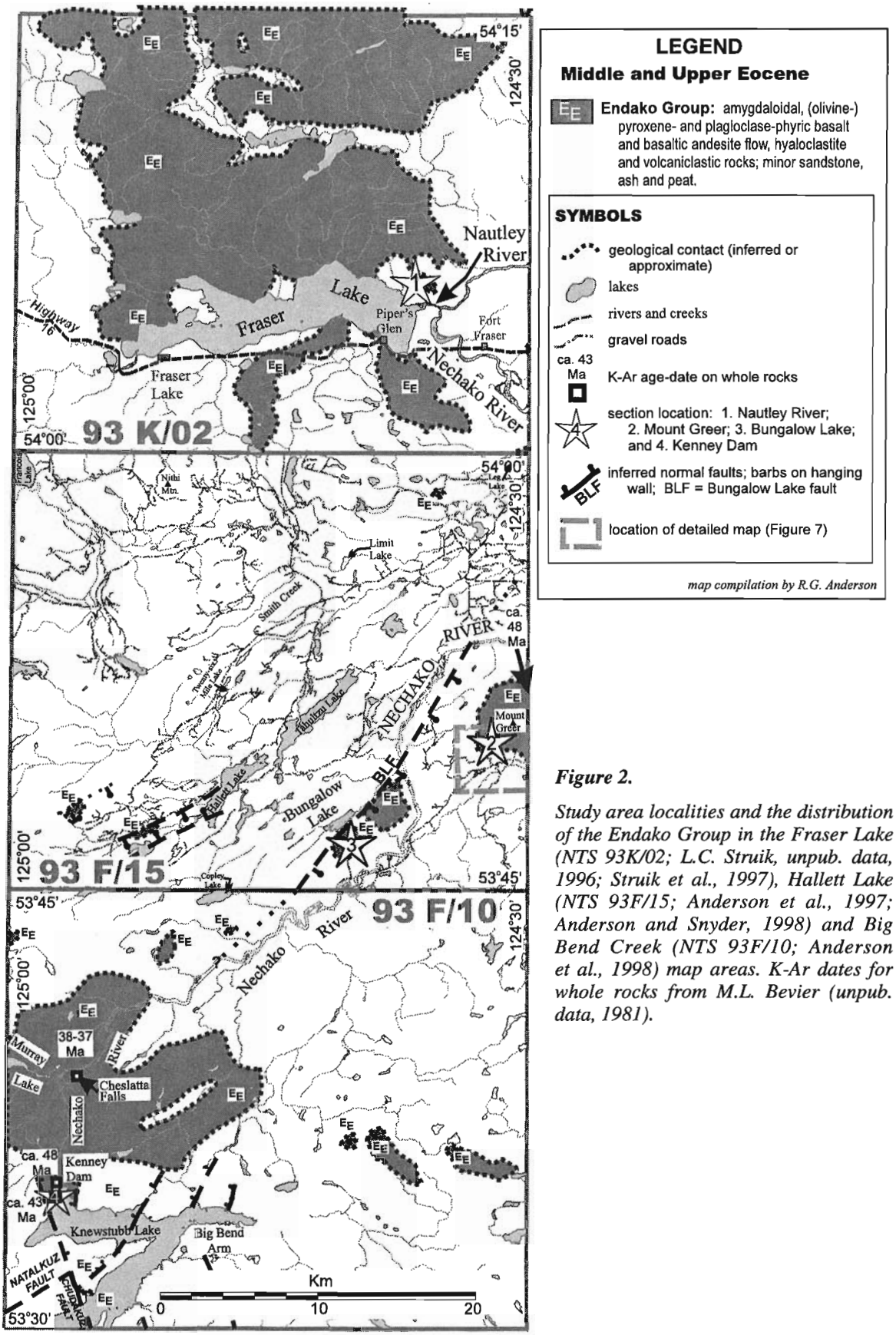

Figure 2.

Study area localities and the distribution of the Endako Group in the Fraser Lake (NTS 93K/02; L.C. Struik, unpub. data, 1996; Struik et al., 1997), Hallett Lake (NTS 93F/15; Anderson et al., 1997; Anderson and Snyder, 1998) and Big Bend Creek (NTS 93F/10; Anderson et al., 1998) map areas. K-Ar dates for whole rocks from M.L. Bevier (unpub. data, 1981).

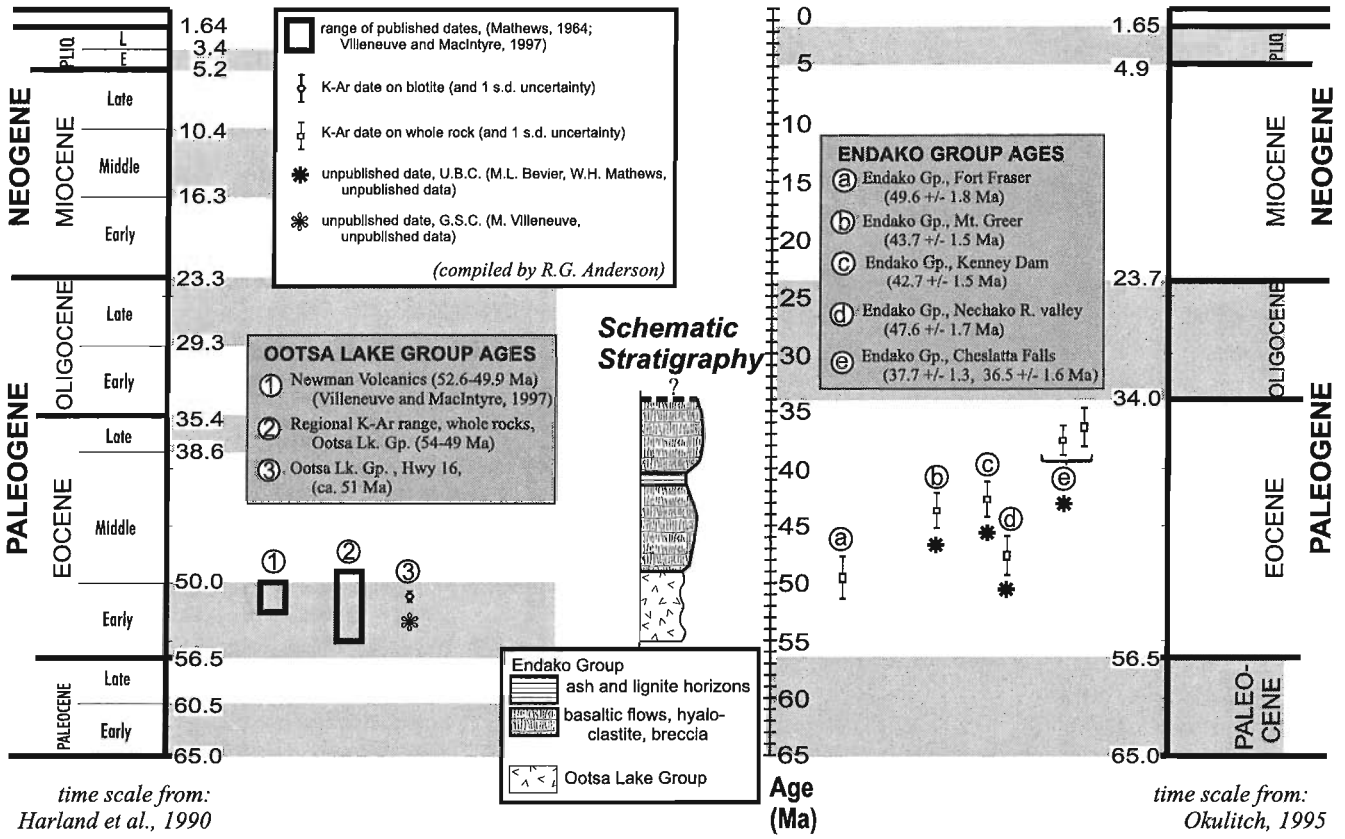

Figure 3. *Schematic time-space summary of Tertiary units in the Fort Fraser-Nechako River area. Comparison of previously determined K-Ar dates for Endako Group rocks with Oligocene-Eocene part of time scale from Harland et al. (1990) and Okulitch (1995, and references therein) shows dates entirely within the Eocene.*

for all hand samples. The database of m.s. and specific gravity measurements for the samples will aid in the interpretation of potential field geophysical data (Struik and McMillan, 1996).

GEOLOGY

Regional geology

The regional geological settings of the four sections studied are given in detail in Struik et al. (1997) for the Nautley River site; in Anderson et al. (1997) and Anderson and Snyder (1998) for the Bungalow Lake and Mount Greer sites; and in Anderson et al. (1998) for the Kenney Dam site. At three of the four sites, the Endako Group basaltic rocks are structurally concordant with and/or rest conformably on felsic volcanic rocks of the Ootsa Lake Group. Northeast-trending block faults (e.g. Bungalow Lake fault) mark the northwestern extent of the main Endako Group outcrops in the Hallett Lake area to the north. To the south, in the Big Bend Creek area, northwest- and northeast-trending faults define an inferred graben within which the Endako Group strata (including that at the Kenney Dam site) are thickest (Fig. 2). In most areas, the Endako Group strata have a gentle, about 20° dip, suggestive of post-Eocene tilting, but are otherwise undeformed.

Nautley River site

The Nautley River section is located on the east side of Fraser Lake approximately 4.5 km north of the Yellowhead Highway (Highway 16; Fig. 1, 2, and 4; base of measured section at UTM E395057, N5937806). It consists of a 70 m thick sequence of basaltic to andesitic volcanic rocks and tuffaceous sediments of the Endako Group directly overlying rhyolite and sedimentary rocks of the Ootsa Lake Group (Fig. 4).

The Ootsa Lake Group consists of white, extensively weathered and clay-altered, poorly indurated, rhyolite tuff containing feldspar and biotite with minor amounts of magnetite, quartz, and glass. The upper 10 m of the rhyolite tuff is covered by mafic volcanic talus (not included in section measured for this study).

The base of the measured section consists of interbedded tuffaceous sand, clay and peat approximately 0.5 m in thickness (Fig. 4). Palynology analysis yielded a likely late

Paleocene to Early Eocene age (White, 1997), indicating correlation with the Ootsa Lake Group in this area. Conformably overlying the peat is a 12 m thick sequence of clastic and reworked pyroclastic material. The lower clastic unit consists of green to tan, weakly-cemented, poorly-sorted, lithic sandstone with pebbly horizons. Overlying the lithic wacke is a 2-2.5 m thick yellow and white tuff unit with rounded pumice fragments and minor grey lithic fragments. The upper layer of sediment is a brown to grey feldspathic lithic sandstone which is weakly crossbedded and contains discontinuous plutonic pebble-bearing horizons. Where exposed, a 15 cm thick, hornfelsed, fine grained sand marks the top of the Ootsa Lake Group and delineates a sharp, undulating contact with the basal Endako Group. No weathering features were observed at the contact.

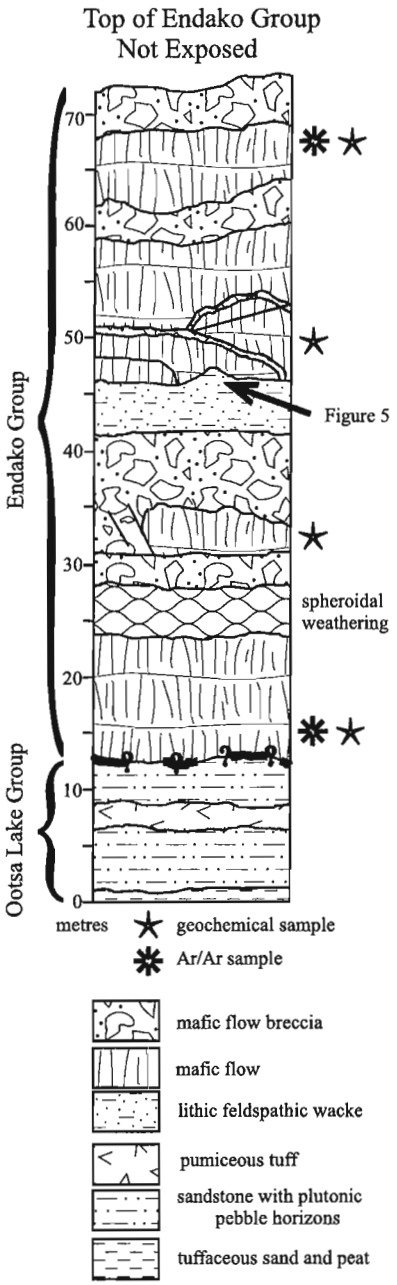

Figure 4. *Schematic section of the Nautley River locality showing sample sites and major lithologies.*

The Endako Group at the Nautley River site consists of 5-20 m thick mafic flows with one 4 m thick section of tuffaceous sediment and numerous thin, discontinuous clastic layers. Individual flows are discontinuous across the exposure and are light to dark brown on the weathered surface and medium grey on fresh surfaces. Microphenocrysts consist of anhedral to subhedral plagioclase crystals and pyroxene altered to chlorite. Olivine is rare in the lower flows but increases in abundance upsection where it comprises a few modal per cent.

Flow bases are characterized by vesiculated zones approximately 15 cm thick. Most vesicles are round and small (1-5 mm in diameter) but some are larger (5-20 mm) and flattened parallel to flow contacts. Explosion breccia representing gas escape structures are commonly found at the base of flows. Basal basalt grades gradually upward into cliff-forming, blocky weathering, massive flows characterized by a few per cent equant vesicles. Oxidized flow tops, averaging one-half of the flow thickness, are red and characterized by abundant, highly vesicular breccia.

Between the second and third flows is a recessive-weathering, grass-covered bench exposing 4-5 m of an orange lithic feldspathic wacke which contains chalky white feldspar and black lithic fragments. A striking soft-sediment deformation/gas escape structure is well exposed between the sediment and the overlying basalt flow (Fig. 5).

Structure and alteration

The Ootsa Lake Group sedimentary rocks at the base of the Nautley section dip 18-20° to the northeast and the overlying mafic flows of the Endako Group are concordant. The lower portion of the measured section (including both Ootsa Lake and Endako rocks) is well jointed with consistent joint orientations.

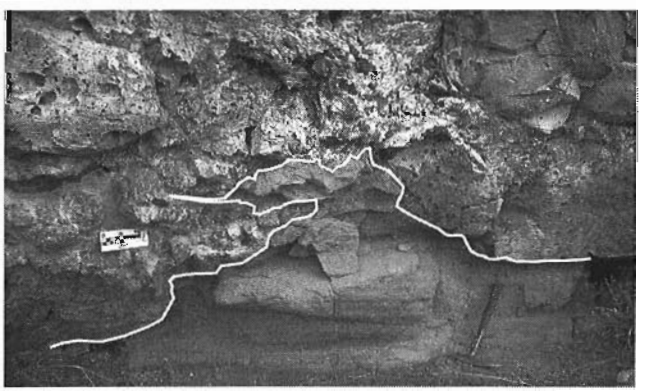

Figure 5. *Photograph of soft sediment squeeze-up and associated gas escape breccia at the Nautley River section. Note pillow forms in lava around the structure.*

Secondary minerals commonly partially fill vesicles and include calcite, chlorite, and a variety of zeolites. Alteration within the flows is generally concentrated around gas escape features where pervasive clay alteration is locally intense. In addition, plagioclase within some flows has oxidized weathering rinds and minor amounts of epidote are present in the upper flows.

Mount Greer site

Mount Greer is one of the higher topographic features in the area. With an elevation of approximately 1250 m at its peak, it stands 500 m above the valley floor (Fig. 1, 2, 6, and 7; base of section at UTM E3980078, N5965513). The south face exposes a lower, white-weathering cliff (Ootsa Lake Group) below a steep exposure of layered dark rock (Endako Group) that dips gently to the east across the mountain (Fig. 6). In addition, plutonic rocks of intermediate composition are exposed on the west flank of Mount Greer and are tentatively correlated with the Brooks Diorite Complex which is more extensive to the south (Wetherup, 1997). Rocks of the Endako and Ootsa Lake groups at Mount Greer were sampled along three transects across a length of approximately 3 km and mapped around the flanks of the mountain (Fig. 7).

The Ootsa Lake Group on the west side of the south face of Mount Greer consists of aphyric to quartz- and alkali feldspar-porphyritic flow-banded rhyolite and rhyolite breccia which locally contain spherulites. On the western flank of Mount Greer, the Ootsa Lake Group includes bedded tuff and biotite- and potassium feldspar-porphyritic dacite.

The Endako Group is characterized by purple to brown, 4-6 m thick mafic and intermediate flows. On the western side, the flows near the base of the section contain plagioclase phenocrysts up to 4 mm long (Fig. 8). The phenocrysts decrease in size and abundance upsection and to the east where many of the flows are aphyric. Pyroxene microphenocrysts and rare olivine were also observed in rocks at Mount Greer.

Figure 6. *View west to the Mount Greer locality. Note conformable contact between white felsic volcanic rocks of Ootsa Lake Group and overlying dark grey Endako Group basaltic flows and breccia. The units are concordant and are tilted 20°.*

Individual flows at Mount Greer show very little internal variation in the amount, size and shape of the vesicles but the thickness and nature of the flow-top breccia is distinctive. The breccia is extremely vesicular and as thick or locally thicker than the associated flow, particularly in the east. The eastern section at Mount Greer exposes many flows with crude columnar jointing and gas escape structures. Flows with curviplanar bases are common in the west.

Numerous dykes of uncertain age were found on Mount Greer. The majority of dykes are mafic and are finely crystalline with plagioclase microphenocrysts and epidote alteration. Dykes of intermediate composition containing plagioclase, potassium feldspar, hornblende, and biotite also occur.

Structure and alteration

At Mount Greer, the entire sequence of volcanic rocks dips 20° or more to the northeast. No consistent orientation was observed in the joint patterns or in dyke orientation.

Alteration of Endako Group rocks at this locality is a result of uniform and extremely pervasive weathering. Chalcedony, calcite, and hisingerite vesicle fillings make up the minor secondary minerals.

Bungalow Lake site

Tertiary volcanic rocks are well exposed on a hill southeast of Bungalow Lake (Fig. 1, 2, and 9; base of section at UTM E389502, N5959737). Located just a few kilometres west of Mount Greer, the rocks are extremely similar. The section consists of a white-weathering cliff (Ootsa Lake Group) below a cliff composed of dark-coloured rock (Endako Group) (Fig. 9). The two near vertical exposures are separated by a recessive weathering, tree covered bench which covers the contact between the units. The entire volcanic section nonconformably overlies intrusive rocks of probable Middle Jurassic age (Anderson and Snyder, 1998).

At the base of the Bungalow Lake section, a 4-5 m thick unit of plagioclase-phyric amygdaloidal basalt is exposed. Translucent chalcedony with lesser fine-grained chlorite vesicle-fillings are abundant. Discontinuous veins of chalcedony up to 4 cm wide are also present. Locally, the basalt exhibits intense clay alteration which imparts a light tan-weathering colour and punky nature. The intensity of clay alteration is not typical in Endako Group rocks in this area and this basalt is thought to be part of the Ootsa Lake Group analogous to a basal basalt unit recognized in the Ootsa Lake Group to the south (Diakow et al., 1997).

Conformably overlying the Ootsa Lake Group basal basalt is a massive rhyolite flow unit 20 m thick. The rhyolite contains a few per cent of quartz, potassium feldspar, and lesser biotite phenocrysts and locally displays planar flow banding. Capping the massive and flow banded rhyolite is an approximately 5 m thick rhyolite breccia with a similar phenocryst assemblage that weathers into distinctive hoodoo structures.

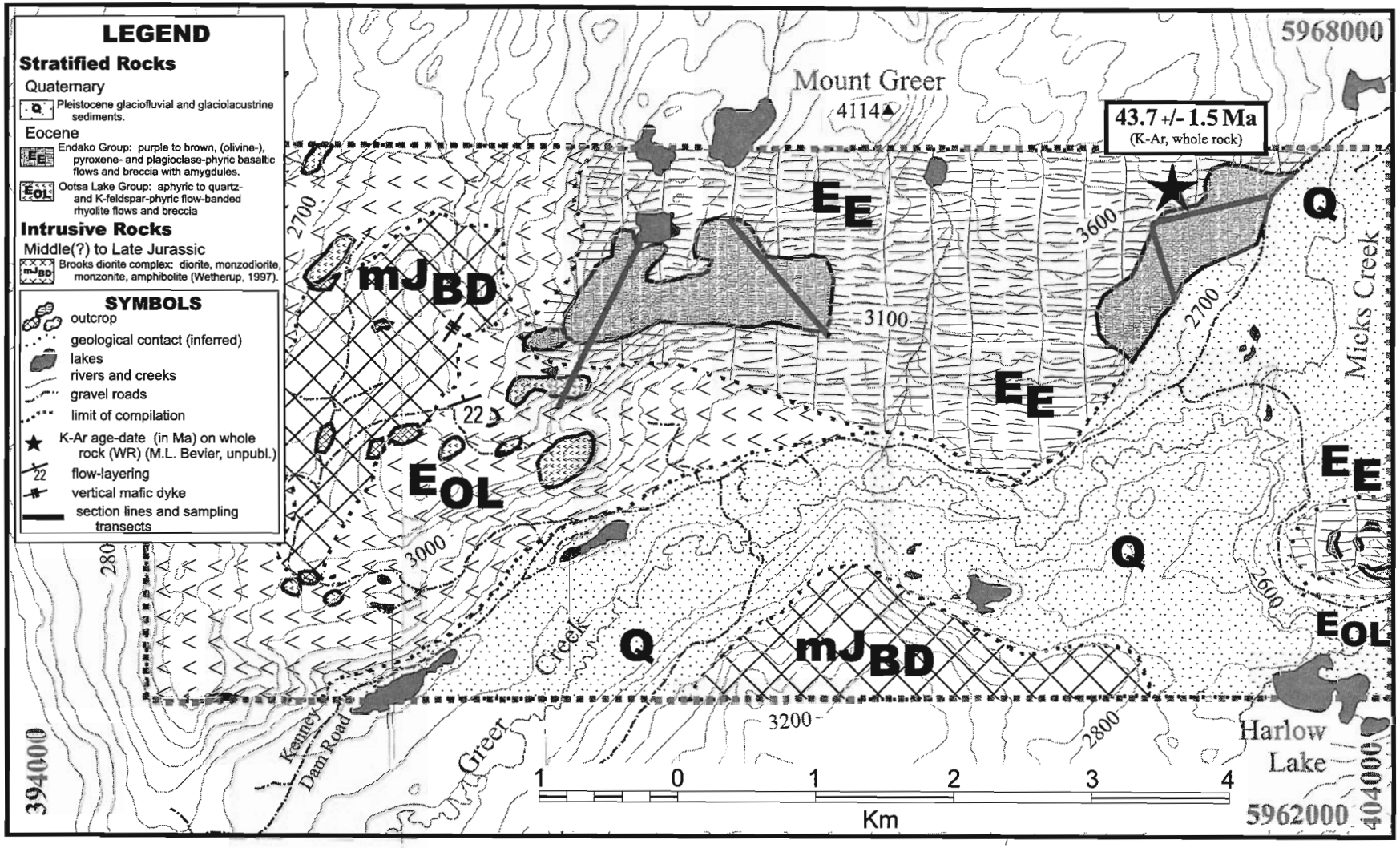

Figure 7. Geological map of the Mount Greer area showing the transects sampled for this study. K-Ar date on whole rock from M.L. Bevier (unpub. data, 1981).

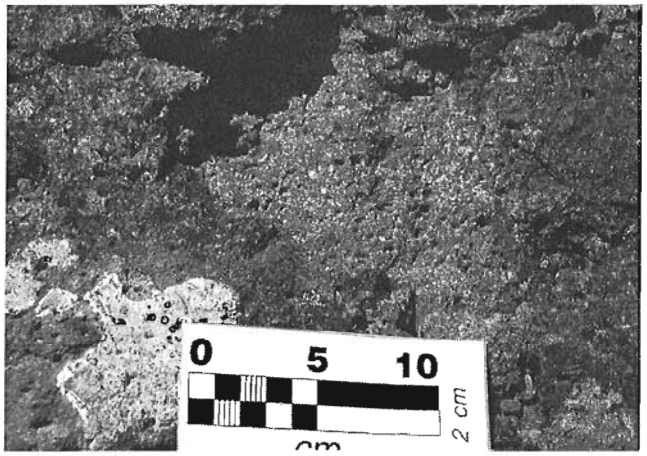

Figure 8. *Photograph of the plagioclase-rich nature of the Mount Greer basalt.*

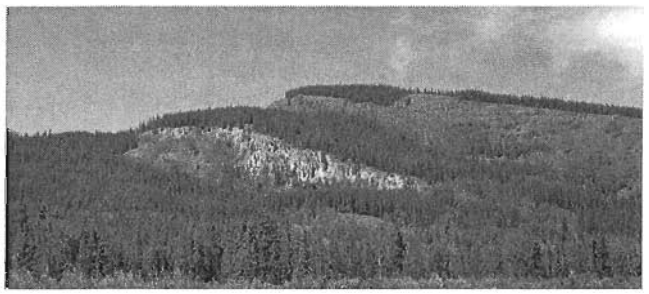

Figure 9. *View west to the Bungalow Lake locality. As at the Mount Greer locality to the northwest, note conformable contact between white felsic volcanic rocks of Ootsa Lake Group and overlying dark grey Endako Group basaltic flow rocks.*

Endako Group mafic rocks are exposed in a one large cliff and discontinuous outcrops along the side of a steep, grass covered slope and are exclusively flows and interbedded flow breccia cut by rare mafic dykes. Plagioclase microphenocrysts, generally not larger than 1-1.5 mm are ubiquitous and one flow contained zoned anhedral to subhedral seriate plagioclase up to 8 mm in size. Rare olivine and pyroxene microphenocrysts are locally observed. The rocks range from massive to vesicular, with common vesicle flattening parallel to flow contacts. Intensely oxidized flow breccia, up to 5 m thick, is well exposed near the top of the section creating fairly continuous red zones.

Structure and alteration

The Tertiary volcanic strata at Bungalow Lake are tilted approximately 20° to the northeast, similar to the sequence at Mount Greer. Structures are rarely observed within the Endako Group, but a small northwest-trending fault occurs in the mafic flows at this locale.

Secondary minerals are restricted to vesicle fillings. A variety of minerals including chalcedony, chlorite, hisingerite, calcite, and an unidentified blue mineral were observed.

Kenney Dam site

The Kenney Dam quarry is located on the northwest side of Knewstubb Lake just southwest of Kenney Dam (Fig. 1, 2, and 10; base of section at UTM E370746, N5937806). It comprises a well-exposed, 95 m cliff of mafic-intermediate volcanic flows and minor hyaloclastite and clastic sediments. The Kenney Dam site is located approximately 100 m above the Nechako River valley, where Endako Group rocks are also nearly continuously exposed. The base of the section in this area is not exposed. Endako Group rocks at the quarry and at the base in the river valley were sampled.

The section consists of consecutively stacked 3-5 m thick flows whose finely crystalline texture imparts a sparkly appearance. The rocks have an orange oxidizing rind on weathered surfaces. Microphenocrysts consist of subhedral, elongate plagioclase up to 3 mm long, and minor pyroxene.

The flow bases are thin (10-30 cm) and only sparsely vesicular. Vesicles are generally round, 1-5 mm in diameter, and evenly distributed throughout. Flow interiors are massive and form blocky-weathering cliffs. The transition from flow interior to top is marked by a gradual increase in vesicle abundance and size range. The larger vesicles are flattened parallel to the flow contacts. Flow tops are 0.5-1 m thick and their porosity provided excellent sites for deposition of secondary minerals. Pillows are well formed in the lower flow at the Kenney Dam quarry and poorly defined pillow features are found in flows higher up in the section. One layer of hyaloclastite breccia, altered to palagonite, was found about halfway up the quarry face on the southwest side of the section. Channels in the lava flows are prominent on the quarry face and some flows have features reminiscent of pahoehoe lava flows. Locally, 1 cm thick discontinuous red feldspathic wacke occurs between the flows.

A well exposed 10-12 m thick, massive lava flow with elongate plagioclase, pyroxene, and minor olivine microphenocrysts is exposed on the floor of the Nechako River valley, at the base of Kenney Dam. A flaggy-weathering, flow-layered mafic unit with microphenocrysts of plagioclase and pyroxene is the lowest accessible exposure in the canyon.

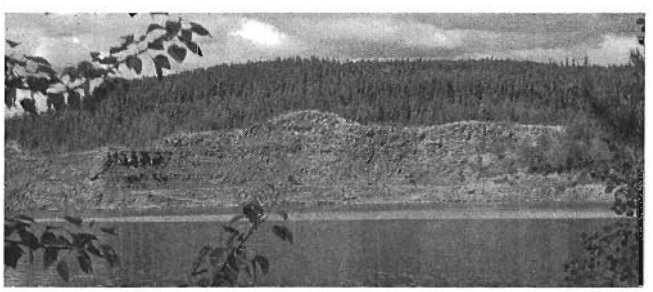

Figure 10. *View west to the Kenney Dam quarry on west side of Knewstubb Lake.*

Structure and alteration

The mafic rocks at Kenney Dam are flat-lying although some individual flows do have a slight northeasterly dip. Joint patterns and orientations are not systematic, and the section is undeformed.

There is an abundance of secondary minerals at the Kenney Dam quarry. Yellow-tan chalcedony, locally with an opaline quality, is the dominant secondary mineral phase and occurs as joint filling, along flow contacts, as a botryoidal hematite-coated vesicle filling, and is abundant in flow top breccia. Locally, 4-6 cm thick chalcedony layers are found within flow tops.

Calcite is found at Kenney Dam as veins and vesicle fillings and, in places, occurs as clear, striated, anhedral crystals. Hematite and chlorite are common vesicle fillings. Zeolites are abundant at the Kenney Dam site and occur as botryoidal, radiating orange spheres and brown-orange rods (0.5-1.5 cm long and 1 mm thick) coated with reflective opaline flakes.

AGE

Unpublished palynology determinations and whole rock K-Ar and Ar-Ar isotopic ages provide constraints on the age of the Endako Group at the localities studied (Fig. 3). Struik et al. (1997) described a unit containing grey and brown organic material at level 17.30-17.42 m in their measured section, that is, at the base of our section at the Nautley River site (Fig. 4). J.M. White at GSC Calgary determined that a sample from that horizon "has a rich palynomorph assemblage ...[whose] age is ...likely late Paleocene to very early Eocene" and no younger than late Eocene (J.M. White, unpub. GSC report 3-JMW-1997, 1997).

Potassium-argon dates for whole rocks from the Ootsa Lake Group in the region range from 54-49 Ma (Fig. 3; dates from Mathews (1964) recalculated by R.L. Armstrong to be consistent with the Steiger and Jäger (1977) decay constants). Biotite from rhyolite tuff which immediately underlies basalt just south of Highway 16, about 4.5 km from the Nautley River section, yielded a $^{40}Ar/^{39}Ar$ date of about 51 Ma (M. Villeneuve, pers. comm., 1997). These are within the range of new $^{40}Ar/^{39}Ar$ dates of 52.6-49.9 Ma for the sub-Endako Group, Newman Volcanics to the north (Villeneuve and MacIntyre, 1997), which are the equivalents to the Ootsa Lake Group in our study area.

Unpublished K-Ar dates for whole rock samples of Endako Group rocks near the measured sections have a range of 48-43 Ma (Fig. 3; M.L. Bevier, unpub. data, 1981) and include samples from Mount Greer (43.7 ± 1.5 Ma), Kenney Dam (42.7 ± 1.5 Ma), and the floor of the Nechako River valley (47.6 ± 1.7 Ma). These dates overlap within uncertainty with the 49.6 ± 1.8 Ma date for the Endako Group east of Fraser Lake in the Fort Fraser map area to the north of the Nechako River area (Mathews, 1989; all uncertainties at 1 standard deviation). The Endako Group dates are younger than dates from the underlying Ootsa Lake Group or equivalents although they overlap within uncertainty at the upper end of Ootsa Lake Group age range.

The dates from Kenney Dam and the Nechako River valley are significantly older than basalt flows at Cheslatta Falls (36.5 ± 1.6 and 37.7 ± 1.3 Ma; W.H. Mathews, unpub. data, 1983) which are upsection from the Kenney Dam flows. The stratigraphically higher and younger flows locally contain olivine, overlie an ash and lignite horizon, (see Anderson et al., 1998) and are Late Eocene or Early Oligocene or younger in age based on flora collections (G. Rouse, unpub. data, 1983). The stratigraphic, fossil, and isotopic age data suggest at least two pulses of Endako basaltic volcanism in the Middle (48-43 Ma) and Late (38-37 Ma) Eocene (Fig. 3), closely followed cessation of the Ootsa Lake Group felsic volcanism in the Middle Eocene.

CONCLUSIONS

The Endako Group in the south-central Fort Fraser and the north-central Nechako River map areas is composed dominantly of amygdaloidal, sparsely porphyritic, intermediate to mafic lava flows with minor hyaloclastite and intercalated tuffaceous sedimentary rocks. These Endako Group rocks overlie various lithologies of the Ootsa Lake Group. The existence and duration of a hiatus between these two compositionally distinct volcanic events is uncertain (Struik et al., 1997) and is the subject of ongoing studies. At the sites where the contact between the Ootsa Lake and Endako groups is best exposed, it appears unweathered and is conformable and structurally concordant. Isotopic age dates from Endako Group rocks are slightly younger than Ootsa Lake Group samples but overlap the younger range of the Ootsa Lake Group within uncertainty.

The Endako Group displays a variety of granularity, ranging from aphyric to plagioclase-, pyroxene-and olivine-phyric. The presence of flow features such as pillow structures, gas escape structures, and hyaloclastite breccia indicate that at least part of the Endako Group was erupted onto a relatively wet substrate or into water. Deposition of clastic material between flows and intensely oxidized and weathered flow tops suggest that volcanism may have been episodic. Eruptive centres have not been documented in the study area.

Future study will focus on geochemical and petrographic characterization of the samples collected and is expected to help clarify the chemical evolution of these rocks. Argon-argon dating underway will further constrain the duration and periodicity of Endako Group volcanism and the hiatus between Ootsa Lake Group and Endako Group magmatism.

ACKNOWLEDGMENTS

We would like to thank Bert Struik for providing logistical support, leadership and a scientific framework for the fieldwork. Discussion and fieldwork with Catherine Hickson proved to be invaluable and her time and energy are greatly appreciated. Field trips led by Larry Diakow and Mary Lou Bevier were critical in the site selection stage of this study. Jonah Resnick, Elspeth Barnes, and Shireen Wearmouth provided excellent assistance during the fieldwork and data

compilation. This study was supported in part by the University of Wisconsin-Eau Claire Office of University Research. Access to geochronological databases from M. Villeneuve (GSC) and J. Mortensen (UBC), and palynological determinations by J.M. White (GSC) are appreciated. Thank you to Nicky Hastings, Elspeth Barnes, Juliana Ferreria, Steve Williams, and Bev Vanlier who helped in the digital preparation of the maps and manuscript. Catherine Hickson's review helped improve the paper and is appreciated.

REFERENCES

Anderson, R.G. and Snyder, L.D.
1998: Jurassic to Tertiary volcanic, sedimentary, and intrusive rocks in the Hallett Lake area, central British Columbia; in Current Research 1998-A; Geological Survey of Canada.

Anderson, R.G., L'Heureux, R., Wetherup. S., and Letwin, L.
1997: Geology of the Hallett Lake map area, central British Columbia: Triassic, Jurassic, Cretaceous, and Eocene? plutonic rocks; in Current Research 1997-A; Geological Survey of Canada, p. 107-116.

Anderson, R.G., Snyder, L.D., Resnick, J., and Barnes, E.
1998: Geology of the Big Bend Creek map area, central British Columbia; in Current Research 1998-A; Geological Survey of Canada.

Armstrong, J.E.
1941: Fort Fraser (east half); Geological Survey of Canada, Map 630A.
1949: Fort St. James map-area, Cassiar and Coast Districts, British Columbia; Geological Survey of Canada, Memoir 252, 210 p.

Armstrong, R.L.
1988: Mesozoic and early Cenozoic magmatic evolution of the Canadian Cordillera; Geological Society of America, Special Paper 218, p. 55-91.

Bellefontaine, K.A., Legun, A., Massey, N., and Desjardins, P.
1995: Digital geological compilation of northeast B.C. - southern half (NTS 83D, E, 93F, G, H, I, J, K, N, O, P); British Columbia Ministry of Energy, Mines and Petroleum Resources, Open File 1995-24.

Bevier, M.L.
1982: Geology and petrogenesis of Mio-Pliocene Chilcotin Group basalts, British Columbia; Ph.D. thesis, University of California at Santa Barbara, Santa Barbara, California, 110 p.
1983a: Implications of chemical and isotopic composition for petrogenesis of Chilcotin Group basalt, British Columbia; Journal of Petrology, v. 24, p. 207-226.
1983b: Regional stratigraphy and age of Chilcotin Group basalts, south-central British Columbia; Canadian Journal of Earth Sciences, v. 20, p. 515-524.

Diakow, L.J., Webster, I.C.L., Richards, T.A., and Tipper, H.W.
1997: Geology of the Fawnie and Nechako Ranges, southern Nechako Plateau, central British Columbia (93F/2,3,6,7); in Interior Plateau Geoscience Project: Summary of Geological, Geochemical and Geophysical Studies, (ed.) L.J. Diakow and J.M. Newell; British Columbia Geological Survey Branch Open File 1996-2 and Geological Survey of Canada, Open File 3448, p. 7-30.

Harland, W.B., Armstrong, R.L., Cox, A.V., Craig, L.E., Smith, A.G., and Smith, D.G.
1990: A Geological Time Scale 1989; Cambridge University Press, 279 p.

Kimura, E.T., Bysouth, G.D., Cyr, J., Buckley, P., Peters, J., Boyce, R., and Nilsson, J.
1980: Geology of parts of southeast Fort Fraser and northern Nechako River map areas, central British Columbia; Placer Dome Incorporated, Internal Report and Maps, Vancouver, British Columbia.

MacIntyre, D.G. and Webster, I.C.L.
1997: Babine Porphyry Belt Project, bedrock geology of the Old Fort Mountain map area (NTS 93M01); in Geological Fieldwork 1996; British Columbia Ministry of Employment and Investment, Paper 1997-1.

Mathews, W.H.
1964: Potassium-argon age determinations of Cenozoic volcanic rocks from British Columbia; Geological Society of America, Bulletin, v. 75, p. 465-468.
1989: Neogene Chilcotin basalts in south-central British Columbia: geology, ages, and geomorphic history; Canadian Journal of Earth Sciences, v. 26, p. 969-982.

Okulitch, A.V.
1995: Geological Time Scale, 1995; Geological Survey of Canada, Open File 3040 (National Earth Science Series, Geological Atlas).

Steiger, R.H.J. and Jäger, E.
1977: Subcommission on Geochronology: convention on the use of decay constants in geo- and cosmochronology; Earth and Planetary Science Letters, v. 36, p. 359-362.

Struik, L.C.
1993: Intersecting intracontinental Tertiary transform fault systems in the North American Cordillera; Canadian Journal of Earth Sciences, v. 30, p. 1262-1274.

Struik, L.C. and MacIntyre, D.
1997: Nechako Plateau NATMAP Project overview, central British Columbia, year two; in Current Research 1997-A; Geological Survey of Canada, p. 57-64.

Struik, L.C. and McMillan, W.J.
1996: Nechako NATMAP Project overview, central British Columbia; in Current Research 1996-A; Geological Survey of Canada, p. 57-62.

Struik, L.C., Whalen, J.B., Letwin, J., and L'Heureux, R.
1997: General geology of southeast Fort Fraser map area, British Columbia; in Current Research 1997-A; Geological Survey of Canada, p. 65-76.

Tipper, H.W.
1963: Nechako River map-area, British Columbia; Geological Survey of Canada, Memoir 324, 59 p.

Villeneuve, M.E. and MacIntyre, D.G.
1997: Laser $^{40}Ar/^{39}Ar$ ages of the Babine Porphyries and Newman Volcanics, Fulton Lake map area, west central British Columbia; in Radiogenic Age and Isotopic Studies: Report 10; Geological Survey of Canada, Current Research 1997-F, p. 131-139.

Wetherup, S.
1997: Geology of the Nulki Hills and surrounding area (NTS 93F/9 and F/16), central British Columbia; in Current Research 1997-A; Geological Survey of Canada, p. 125-132.

Whalen, J.B., Struik, L.C., and Hrudey, M.G.
1998: Bedrock geology of the Endako map area, central British Columbia; in Current Research 1998-A; Geological Survey of Canada.

Williams, S.P.
1997: Geological compilation of the Nechako River (93F) map area, British Columbia; Geological Survey of Canada, Open File 3429, scale 1:250 000.

Geological Survey of Canada Project 950036-04

Re-examination of Late Albian-Cenomanian conglomerate in Churn Creek, Gang Ranch area, southern British Columbia

J.W. Riesterer[1], J. Brian Mahoney[2], and Paul K. Link[1]
GSC Pacific, Vancouver

Riesterer, J.W., Mahoney, J.B., and Link, P.K., 1998: Re-examination of Late Albian-Cenomanian conglomerate in Churn Creek, Gang Ranch area, southern British Columbia; in Current Research 1998-A; Geological Survey of Canada, p. 165-174.

Abstract: Albian-Cenomanian strata are well exposed along Churn Creek at the southern end of the Chilcotin Plateau. Albian amygdaloidal andesite to massive, columnar-jointed basalt occupy the core of a northeast-trending, doubly plunging anticline. Unconformably overlying the volcanic package is a thick (~1100 m) sequence of complexly interfingering Albian-Cenomanian chert, volcanic, and plutonic conglomerate and associated sandstone. Paleocurrent measurements indicate chert detritus was probably derived from the Bridge River terrane to the southwest. Volcanic clasts were derived from a proximal volcanic source along the basin margin. Plutonic clasts were locally derived from a Jurassic-Cretaceous pluton uplifted along a northeast-directed thrust fault in the southwest portion of the study area. Strata in Churn Creek record Albian-Cenomanian contraction, subsidence and coeval volcanism very similar to rocks immediately to the south in the Tyaughton basin. Proposed stratigraphic ties between the two outcrop belts are the subject of ongoing geochemical, isotopic, petrographic, and geochronological studies.

Résumé : Des strates albiennes-cénomaniennes sont bien visibles le long du ruisseau Churn à l'extrémité sud du plateau de Chilcotin. Des andésites amygdaloïdes albiennes passant à des basaltes massifs à structure prismée occupent le noyau d'un anticlinal à double plongement de direction nord-est. Repose en discordance sur ces roches volcaniques une épaisse (~1 100 m) séquence de cherts, de conglomérats volcaniques et plutoniques et de grès associés, interdigités de manière complexe et d'âge albien-cénomanien. Les mesures de paléocourants indiquent que les débris de chert proviennent vraisemblablement du terrane de Bridge River au sud-ouest. Les clastes volcaniques sont issus d'une source volcanique proximale située en bordure du bassin. Les clastes plutoniques proviennent d'un pluton jurassique-crétacé voisin qui a été soulevé le long d'une faille de chevauchement de direction nord-est dans la partie sud-ouest de la région étudiée. Les strates au ruisseau Churn témoignent de contraction, de subsidence et de volcanisme contemporain d'âge albien-cénomanien très semblables à ceux qui caractérisent les roches situées immédiatement au sud dans le bassin de Tyaughton. Des corrélations stratigraphiques proposées entre les deux zones d'affleurement font présentement l'objet d'études géochimiques, isotopiques, pétrographiques et géochronologiques.

[1] Department of Geology, Idaho State University, Pocatello, Idaho 83209
[2] Department of Geology, University of Wisconsin-Eau Claire, Eau Claire, Wisconsin 54702-4004

INTRODUCTION

Albian-Cenomanian conglomerate rich in chert, plutonic, and volcanic clasts and associated sandstone preserved along Churn Creek in south-central British Columbia (Fig. 1) are an important component in the ongoing debate over large-scale terrane translation (Cowan, 1994; Mahoney et al., 1996; Monger and Price, 1996). These conglomeratic strata unconformably overlie Albian volcanic rocks in the core of a northeast-trending anticline. Previous workers have correlated the volcanic rocks with the Albian Spences Bridge Group of the Intermontane superterrane, and the overlying conglomeratic rocks with the Albian-Cenomanian Silverquick conglomerate of the Insular superterrane (Hickson et al., 1991; Mahoney et al., 1992). These correlations are problematic in light of recent paleomagnetic studies which suggest a relative displacement of 1900 km between the Intermontane and Insular superterranes (Irving et al., 1995; Wynne et al., 1995), and therefore these correlations have been questioned (Irving et al., 1996). This investigation was initiated to document the stratigraphy, provenance, and structure of the conglomeratic strata in Churn Creek in order to test previously suggested regional correlations.

Fieldwork in 1997 focused on determining the field relationships between the volcanic and sedimentary units in Churn Creek and characterizing the stratigraphy, lithology, and depositional setting of the conglomeratic strata. Laboratory work in progress includes petrological, isotopic, detrital zircon, and geochemical studies that will be combined with field observations in an effort to determine the provenance and stratigraphic affinity of Albian-Cenomanian sedimentary units and the geochemical character of the Albian volcanic rocks.

GEOLOGICAL SETTING

Churn Creek is a tributary of the Fraser River in the southern Chilcotin Plateau of south-central British Columbia. The study area is bounded to the east by the Fraser fault system and to the southwest by the Yalakom fault system (Fig. 1).

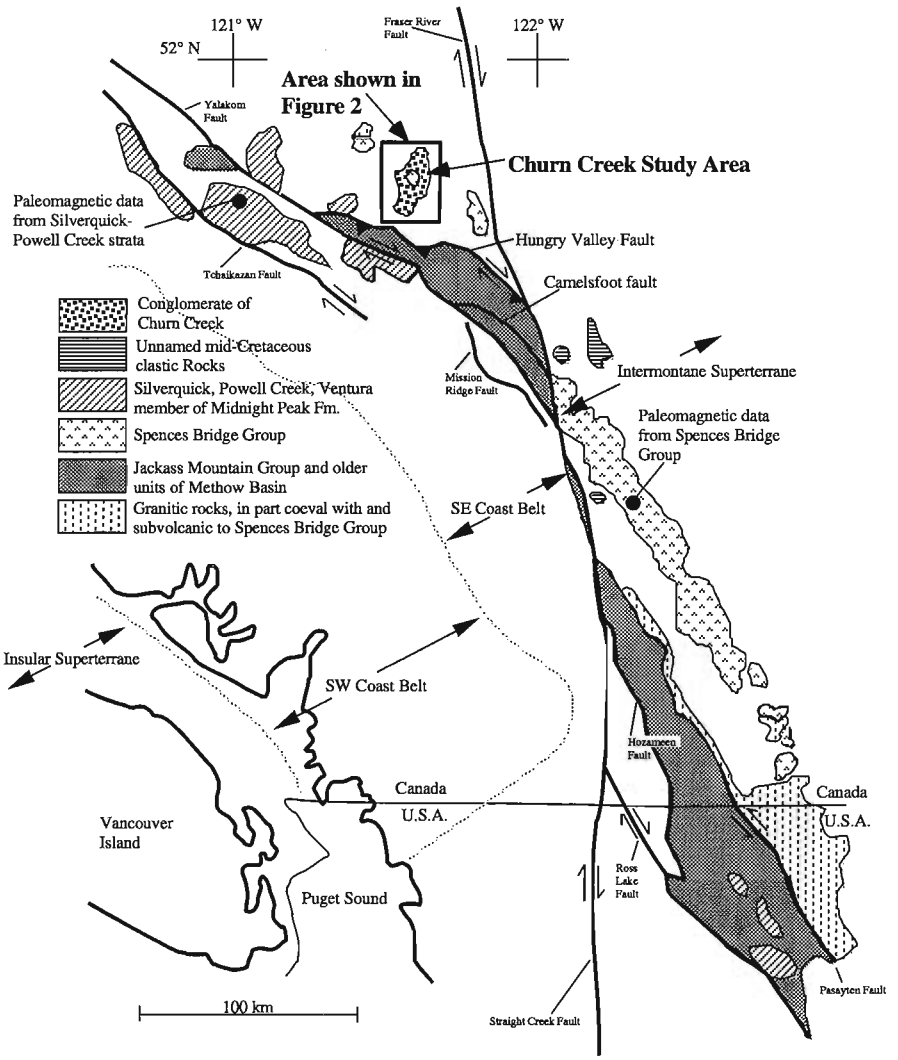

Figure 1.

Generalized geological map of south-central British Columbia, showing the location of the Churn Creek study area, superterrane boundaries, and location of paleomagnetic sampling localities. Modified from Monger and Price (1996).

The oldest rocks in the map area (Fig. 2) are Albian amygdaloidal andesite, basaltic andesite, and basalt (Green, 1990; Hickson et al., 1991). These volcanic rocks are overlain by a thick (>1 km) sequence of complexly interfingering Albian-Cenomanian conglomerate and sandstone. The Upper Cretaceous rocks are overlain by Eocene rhyolite, dacite, and andesite (Hickson et al., 1991). Upper Cretaceous and Eocene rocks are exposed along Churn Creek in an erosional window beneath widespread Miocene and Pliocene Chilcotin plateau basalt. Thick successions of unconsolidated Quaternary glaciofluvial and lacustrine sediments obscure geological relations within the canyon.

PREVIOUS WORK

Previous workers have mapped Cretaceous volcanic and sedimentary rocks along Churn Creek (Tipper, 1978; Green, 1990; Hickson et al., 1991; Hickson, 1992; Mahoney et al., 1992). Albian K-Ar ages for amygdaloidal volcanic rocks exposed in the core of a doubly-plunging anticline along the creek bottom were first reported by Mathews and Rouse (1984), and these rocks were described by Hickson et al. (1991) and Hickson (1992). A thick sequence of Albian-Cenomanian chert, volcanic and plutonic conglomerate and sandstone overlying the Albian volcanic rocks was dated palynologically and described by Hickson et al. (1991). Mahoney et al. (1992) described the stratigraphy and subdivided the conglomeratic strata into three distinct units: a lower chert-rich unit, a middle volcanic-rich unit, and an upper volcanic-and plutonic-rich unit. Chert-rich conglomerate at the base of the succession was interpreted to unconformably overlie Cretaceous volcanic rocks (Hickson et al., 1991; Mahoney et al., 1992). The Cache Creek terrane, located to the north of the study area, was suggested as the likely provenance for chert detritus (Hickson et al., 1991). Volcanic and plutonic conglomerate overlying chert-rich sediments were interpreted to represent both coeval volcanism and intrabasinal uplift in Cenomanian time (Mahoney et al., 1992). Mahoney et al. (1992) correlated the underlying Albian volcanic rocks with the Spences

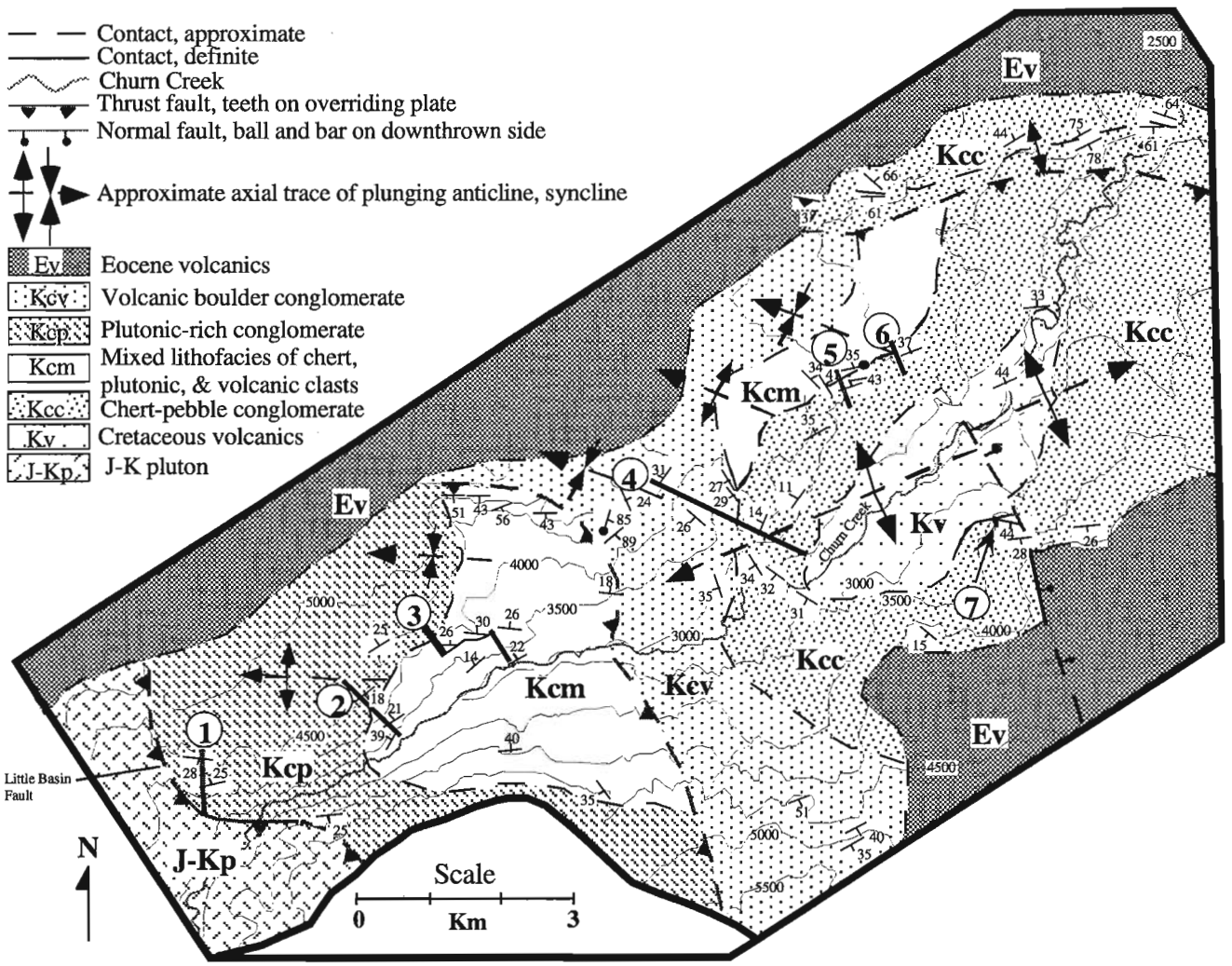

Figure 2. *Geological map of the Churn Creek study area showing location of stratigraphic columns.*

Bridge Group, and the overlying Albian-Cenomanian conglomerate with the Silverquick conglomerate based on similarities in age, lithology, and regional map patterns.

STRATIGRAPHY

Rocks exposed within the study area can be broadly broken into two groups: Albian volcanic rocks (Kv), and Albian-Cenomanian sedimentary rocks (Kc). Due to the level of controversy surrounding the stratigraphic affinity of rocks in the study area, they will be referred to informally in this paper as Cretaceous volcanic rocks and the conglomerate of Churn Creek.

In conjunction with detailed (1:50 000) mapping, six stratigraphic sections were measured in the conglomerate of Churn Creek, with an additional generalized section constructed in an area of limited exposure (Fig. 2, 3).

Cretaceous volcanic unit (Kv)

Andesitic to basaltic volcanic rocks are exposed along Churn Creek in the core of a doubly plunging anticline (Fig. 2). Bedding is very poorly preserved throughout much of the volcanic section, but a conservative estimate suggests a thickness of at least 500 m. A whole rock K-Ar age of 101 ± 3 Ma was obtained from an exposure just northeast of the map area (Mathews and Rouse, 1984).

The lowest portion of the volcanic unit is a highly fractured and altered, grey-weathering, green to brown, amygdaloidal andesite. Overlying and in sharp contact with this member is a dark grey to black, aphanitic, columnar jointed basalt. The basalt appears very fresh on broken surfaces, but is extensively fractured and veined locally. The columnar basalt gradually becomes more rubbly and fractured upsection, and grades into a sequence of highly fractured, moderately altered, medium- to dark-grey, aphanitic and occasionally amygdaloidal, basaltic andesite and andesite. This sequence is locally overlain by a thin (~10 m) layer of red, poorly sorted, matrix supported, volcaniclastic conglomerate/breccia. Clasts are angular to rounded, red, amygdaloidal volcanic rocks up to about 1 m in diameter, averaging 5-10 cm. The composition and character of the uppermost member of the Cretaceous volcanic unit is highly variable, both within and between outcrops. In general, it is moderately fractured and altered, greenish- to brownish-grey, occasionally hornblende- and/or plagioclase-phyric, commonly amygdaloidal andesite.

Conglomerate of Churn Creek

The conglomerate of Churn Creek is divided into four lithofacies mappable on 1:50 000 scale. The lithofacies are defined based on composition and include a chert-rich facies (Kcc), a mixed chert, plutonic- and volcanic-rich facies (Kcm), a plutonic-rich facies (Kcp), and a volcanic-rich facies (Kcv). These facies are complexly interfingered stratigraphically, and have been structurally imbricated during syndepositional contraction. Lithofacies relationships are illustrated in Figures 3 and 5.

Chert-rich lithofacies (Kcc)

Description

The chert-rich lithofacies (Kcc) comprises the basal portion of the Albian-Cenomanian section, and is extensively exposed in the northeastern portion of the map area. The chert-rich lithofacies unconformably overlies Albian volcanic rocks, and is gradationally overlain by the mixed lithofacies of chert, plutonic, and volcanic clasts. The thickest total exposure of unit Kcc occurs in the generalized section (Fig. 3; section 4) where more than 400 m of chert-pebble conglomerate are exposed. The stratigraphically lowest exposures of unit Kcc contain almost 100% chert and sedimentary lithic clasts. The composition changes upsection as an increasing amount of plutonic and, especially, volcanic clasts are incorporated into the conglomerate. The upper contact of unit Kcc is defined as the first redbed interval within the section.

The basal contact of the conglomerate of Churn Creek is exposed in at least two localities within the field area. At these localities, the basal unit Kcc is a thin (<5 m) interval of greenish-grey, laminated, possibly burrowed, commonly fractured mudstone intercalated with fine grained sandstone. This mudstone grades upward into the interbedded chert-lithic sandstone and conglomerate typical of the lithofacies (Fig. 3, section 7). In other localities, poorly exposed volcaniclastic conglomerate, sandstone, and mudstone in the upper portion of the Albian volcanic unit is erosionally scoured by chert-pebble conglomerate.

The chert-rich lithofacies consists of interbedded chert-pebble conglomerate and chert-lithic sandstone. The lithofacies is dominated by light brown, well sorted, clast- to matrix-supported, crudely stratified to massive, chert-pebble conglomerate. Clasts are generally rounded to subrounded varicoloured chert ranging in size from <1 cm to about 8 cm in diameter, with an average size of 2-3 cm. Clasts tend to be of uniform size within individual conglomerate beds or lenses. The matrix is poorly sorted, angular to subangular, medium- to coarse-grained, chert lithic arenite. Sandy intervals within the chert-rich lithofacies are commonly moderately well sorted, subangular to subrounded, medium- to coarse-grained, chert-lithic arenite with chert pebble lags. Channels, trough crossbeds, planar crossbeds, and graded beds are common within this facies. Beds are commonly laterally and vertically discontinuous over a distance of tens of metres, but there is an overall coarsening upward trend within the lithofacies. Rare fine sand to silt intervals containing organic material and plant fragments are preserved locally. Palynomorphs from a siltstone interval near the base of the section yielded a late Albian to Cenomanian age (Hickson et al., 1991).

Paleocurrent measurements from unit Kcc (n=120) trend strongly north to northwest, suggesting a source terrane to the southeast (Fig. 4).

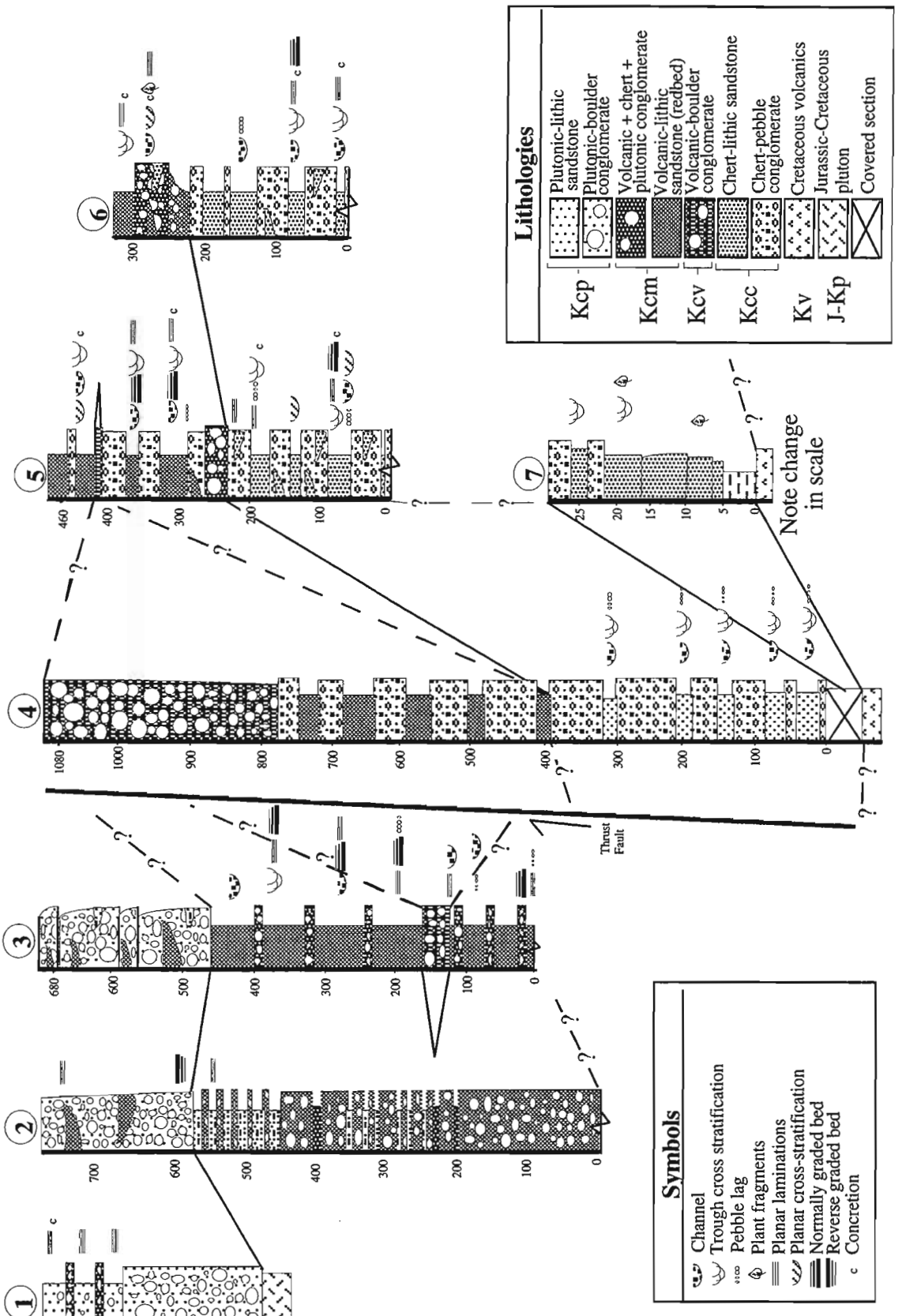

Figure 3. *Stratigraphic columns from the Churn Creek study area. Locations of sections shown in Figure 2. Section 4 is a generalized stratigraphic column, all others are measured sections.*

Depositional environment/source terrane

The predominantly clast-supported nature of the chert-pebble conglomerate, abundance of crossbedded sandstone and conglomerate channels, and the presence of fine grained intervals interpreted as overbank deposits suggests the chert-rich lithofacies was deposited in a braided stream environment. The consistency of north- to northwest-trending paleocurrents (Fig. 4) indicates the source of the chert-rich lithofacies was to the south-southeast. Restoration of motion on the Yalakom and Fraser River fault systems suggests the closest chert-rich source to the south of the study area is the Bridge River terrane. This interpretation contradicts that of Hickson et al. (1991), who suggested derivation of chert detritus from the north. However, the consistency of our paleocurrent data from all stratigraphic levels in the chert-rich lithofacies throughout the study area strongly argues for a southern source of chert detritus (Fig. 4).

Mixed lithofacies of chert, plutonic, and volcanic clasts (Kcm)

Description

The mixed lithofacies of chert, plutonic, and volcanic clasts (Kcm) consists of interbedded lithic sandstone, silty sandstone, and pebble to boulder conglomerate. Conglomerate beds are assigned to the mixed lithofacies where chert comprises less than 50% of the clasts. The mixed lithofacies gradationally overlies the chert-rich lithofacies (Fig. 3, sections 5, 6) across a transition zone that is characterized by a steady increase in the amount of volcanic detritus within the chert-rich lithofacies. This transition zone is locally punctuated by thick beds of purely chert conglomerate. The transition from the chert-rich lithofacies to the mixed lithofacies corresponds to the appearance of fine grained 'redbed' intervals consisting of thin bedded siltstone and fine grained sandstone. The basal contact of unit Kcm is mapped as the lowest redbed interval seen above unit Kcc. Above the transition zone, the mixed lithofacies contains rare thick interbeds of purely volcanic conglomerate, assigned to the volcanic-rich facies (Kcv). Locally, the mixed lithofacies is thin or absent, and the chert-rich lithofacies (Kcc) is directly overlain by the volcanic-rich facies (Kcv).

The thickest exposure of unit Kcm is in the southwestern portion of the map area (Fig. 3, section 2), where it is approximately 580 m thick. Exposures to the northeast are limited, and the upper contact of unit Kcm is not exposed, but a decrease in clast size and bedding thickness suggests that there is a general thinning of unit Kcm from southwest to northeast. The thickest exposure of unit Kcm (Fig. 3, section 2) is dominated by volcanic, and lesser plutonic, boulder conglomerate. Sandstone and silty-sandstone interbeds become more prevalent upsection, suggesting the lithofacies locally records fining-upward successions superimposed on the overall coarsening-upward sequence characteristic of the entire formation.

The mixed lithofacies is dominated by brownish- to greyish-purple, clast- to matrix-supported, poorly sorted, volcanic, plutonic, and chert pebble to boulder conglomerate. Clasts are generally well-rounded, with a maximum clast size of 20 cm, and average clast size of 5-7 cm. Volcanic and plutonic clasts are generally larger than chert clasts, which average approximately 3-4 cm. The matrix is moderately sorted, angular to subangular, biotite- and hornblende-bearing, medium grained sand to granule conglomerate, lithic feldspathic arenite. The conglomerate may be channellized or crudely stratified and/or graded, but few other sedimentary structures are evident.

Sandstone composition varies widely within this lithofacies, but the sandstone is generally greenish- to brownish-grey (occasionally reddish), moderately well sorted, angular, micaceous, medium- to coarse-grained lithic feldspathic arenite. The sandstone is commonly overlain by poorly sorted, thinly laminated, sandy siltstone. The sandy siltstone consists of medium- to coarse-grained quartz, feldspar, and biotite in a reddish, coarse silt to very fine sand matrix. Rare

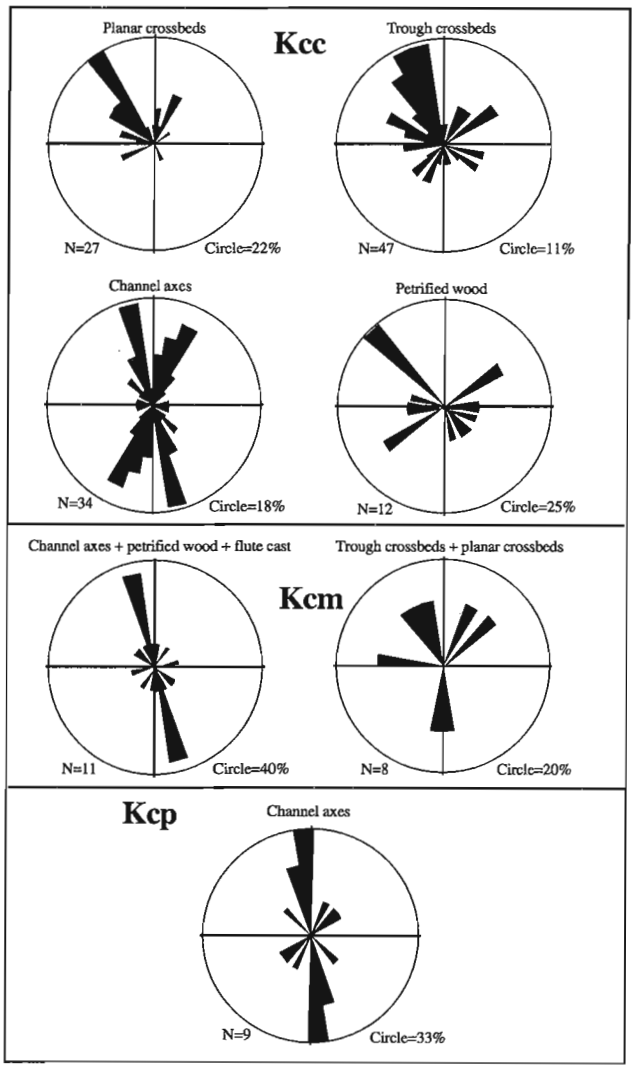

Figure 4. *Summary of paleocurrent measurements from within the conglomerate of Churn Creek.*

thin-bedded tuffaceous sandstone beds are locally present. Pebble lags, conglomerate channels, planar laminations, and graded beds are common; trough crossbeds occur locally.

Paleocurrent measurements within unit Kcm (n=19) are not as definitive as those measured in unit Kcc, but they also suggest north- to northwest-trending paleocurrents (Fig. 4).

Depositional environment/source terrane

The large amount of clast- and matrix-supported conglomerate, the poorly organized nature of the conglomerate, presence of channels, abundance of normal grading, crossbedding, and crude stratification argue for rapid deposition in an area of high relief, probably in an alluvial fan to braided stream environment. The mixed lithofacies is probably the result of mixing of detritus from several sources. Chert clasts within unit Kcm were most likely derived from the same southeastern source as those in unit Kcc. The abundance of volcanic clasts, amount of angular volcanic lithics and plagioclase in associated sandstone, rare tuffaceous beds, and intercalation with the volcanic-rich lithofacies (Kcv) strongly argues for coeval volcanism within or immediately adjacent to the basin. Mahoney et al. (1992) documented syndepositional thrust faulting that uplifted a Jurassic-Cretaceous pluton along the basin margin. Plutonic clasts within the mixed lithofacies were undoubtedly derived from this uplift of plutonic rocks along the Little Basin Fault (Mahoney et al., 1992). An unknown amount of volcanic detritus may have been derived from erosion of volcanic rocks overlying the pluton.

Plutonic-rich lithofacies (Kcp)

Description

The plutonic lithofacies of the conglomerate of Churn Creek consists of interbedded pebble to boulder conglomerate and sandstone. The lower contact is gradational with the underlying mixed lithofacies, and the transition is characterized by a steady increase in the size and prominence of plutonic clasts. However, the absolute abundance of plutonic clasts does not change substantially, and the lower contact is mapped where plutonic clasts become a prominent component of the conglomerate. This contact is easily seen in the field, as the pink plutonic clasts clearly stand out in outcrop. The upper contact of the plutonic lithofacies is the modern erosion surface.

Conglomerate within unit Kcp varies in composition and grain size from southwest to northeast. The largest exposure of unit Kcp occurs immediately adjacent to the Little Basin Fault, where 300 m of unit Kcp are exposed (Fig. 3, section 1). In this locality, unit Kcp is dominated by thick-bedded to massive, structureless, matrix- to clast-supported angular boulder conglomerate. The conglomerate is dominated by diorite clasts (up to 36%) which are up to 1.5 m in diameter. The massive conglomerate is overlain by intercalated buff, matrix-supported, plutonic-rich conglomerate and reddish-purple, clast-supported volcanic and plutonic conglomerate, with minor interbedded sandstone. The matrix-supported plutonic-rich conglomerate is poorly sorted and crudely stratified. Clasts are rounded, commonly widely dispersed (up to 80% matrix in places) but locally concentrated, up to 50 cm in diameter but average about 5 cm, and are almost entirely (~95%) plutonic with no chert. The matrix consists of moderately sorted, angular to subangular, massive to poorly stratified, very coarse sand to granule conglomerate micaceous (biotite) feldspathic arenite. Thin (<10 cm) intervals of green-black, very well sorted, angular to subangular, fine grained, very micaceous (biotite ± chlorite) feldspathic arenite occur within the matrix supported conglomerate. The matrix-supported plutonic conglomerate is intercalated with approximately 10 m thick beds of purple, clast-supported, plutonic and volcanic conglomerate of the mixed lithofacies.

To the northeast of the Little Basin Fault (e.g. Fig. 3, section 3), unit Kcp displays a decrease in maximum clast size and bedding thickness, and an increase in pink quartz monzonite clasts (up to 14%), which reach a maximum diameter of 50 cm. Purely plutonic-rich conglomerate decreases in abundance, and volcanic clast content increases. The conglomerate is clast- to matrix-supported and generally massive, although channellization becomes more common to the northeast. These variations are attributed to progradation of an alluvial fan from southwest to northeast in front of the Little Basin Fault (Mahoney et al., 1992) (Fig. 2, 5).

Sandy interbeds are very rare in the lower portion of unit Kcp in the southwestern portion of the field area (Fig. 2, 3). To the northeast (Fig. 3, section 2, 3), sandy intervals consist of thickly laminated to thinly bedded, poorly sorted, angular to subangular, medium sand to granule conglomerate, feldspathic chert lithic arenite. Planar stratification, graded beds, pebble lags, and channels are common. Sandstone is commonly associated with thinly laminated, moderately- to thickly-bedded, moderately well sorted, poorly lithified, reddish-brown, micaceous siltstone which contains minor quartz grains to 2 mm.

Paleocurrent indicators are relatively rare in the plutonic-rich lithofacies. Limited bidirectional paleocurrent measurements (n=9) collected from within unit Kcp suggest either north- or south-directed paleocurrents (Fig. 4). The decrease in clast size, progressive addition of volcanic material, and changes in bedding characteristics suggest a southwest to northeast transport direction.

Depositional environment/source terrane

Plutonic clasts within unit Kcp are identical to the biotite-rich diorite and pink quartz monzonite that comprises the Little Basin pluton immediately to the southeast. The Little Basin Fault (Mahoney et al., 1992) juxtaposes plutonic rocks in the hanging wall over the plutonic-rich lithofacies in the southwestern corner of the map area. These structural relations, coupled with changes in clast composition and stratigraphic relations to the northeast of the Little Basin Fault indicate syntectonic deposition of unit Kcp, with detritus shed from the rising thrust plate. The overall decrease in clast size within unit Kcp from southwest to northeast and limited paleocurrent data suggest north- to northeast-directed transport. The presence of very coarse angular plutonic-rich conglomerate, crude stratification, lack of sedimentary structures, and

compositional changes away from the proposed source region suggest deposition of unit Kcp on an alluvial fan that prograded into a basin in front of the rising thrust plate.

Volcanic-rich lithofacies (Kcv)

Description

The volcanic lithofacies consists predominantly of thick-bedded to massive, clast-supported volcanic boulder conglomerate. The volcanic lithofacies is areally restricted to the central portion of the study area, and the lithofacies appears to form a lenticular body laterally contiguous with adjacent lithofacies, and perhaps locally capping the entire formation.

The basal contact of the lithofacies is gradational with the chert-rich lithofacies in the central portion of the study area (Fig. 3, section 4). The transition zone is characterized by repeated intercalations of chert pebble conglomerate of unit Kcc with thick beds of the purely volcanic cobble to boulder conglomerate typical of unit Kcv. The contact is mapped at the first appearance of volcanic redbeds below volcanic cobble conglomerate. Above this transition zone, unit Kcv consists of almost 100% volcanic boulder conglomerate. The volcanic lithofacies is locally intercalated with the mixed lithofacies in both the southwestern and northeastern portion of the study area. The top of the volcanic lithofacies is the modern erosion surface.

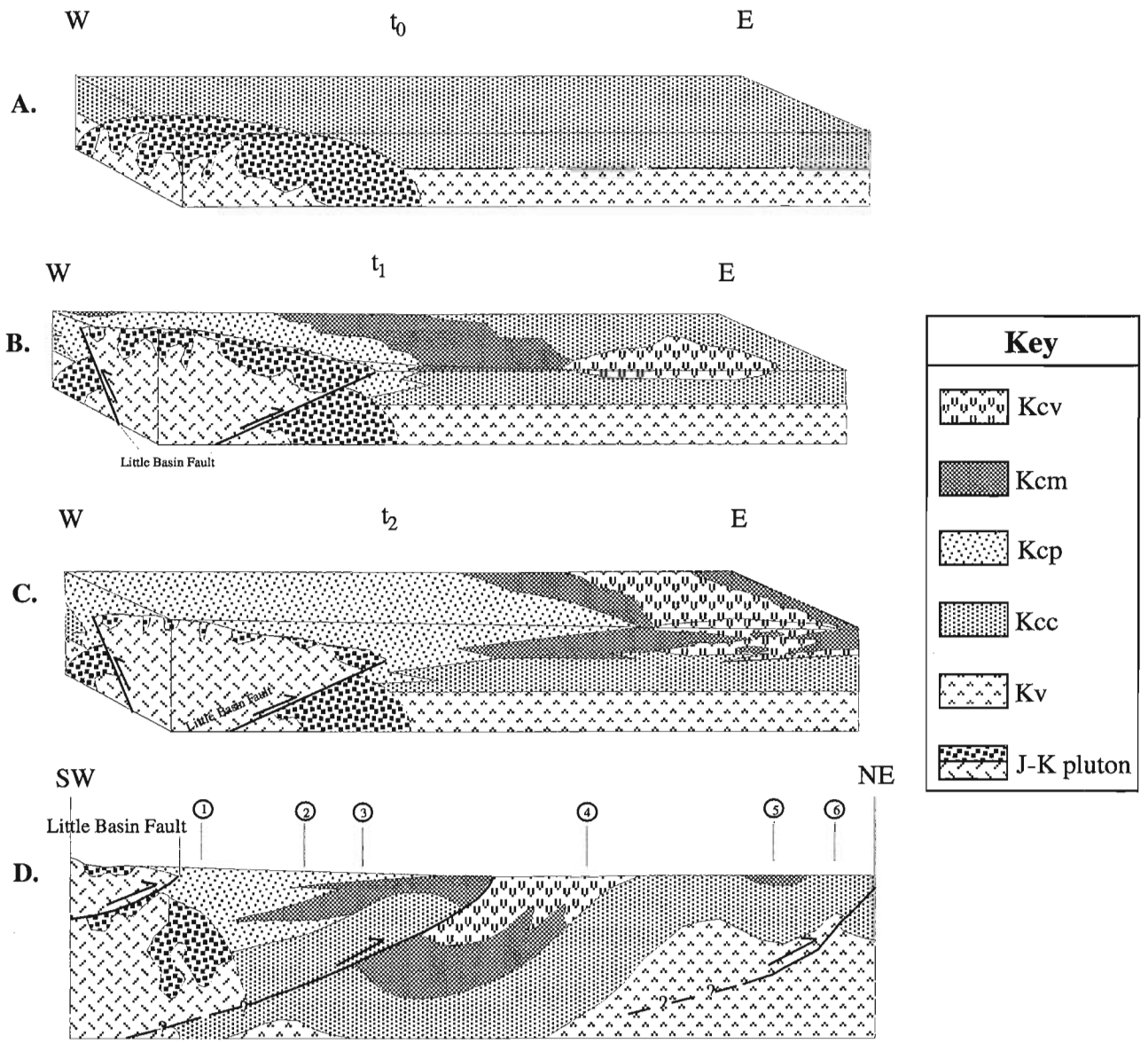

Figure 5A, B, C) *Proposed model of basin evolution in Churn Creek;* ***D)*** *Schematic cross-section of the Churn Creek study area.*

The majority of the volcanic lithofacies consists of very poorly sorted, clast- to matrix-supported, volcanic cobble and boulder conglomerate. Clasts are angular to rounded and almost 100% volcanic. Clasts are dominantly purple plagioclase porphyry with variable amounts of hornblende and pyroxene. The degree of alteration of the clasts varies considerably, and the clasts range from competent purple porphyry to incompetent altered green porphyry. The intermixing of green and purple clasts is a distinctive characteristic of the lithofacies. The matrix consists of poorly sorted, angular to rounded, medium grained sand to granule conglomerate, volcanic lithic arenite to wacke. The lithofacies displays a distinct coarsening upward trend, with clast size increasing from an average clast diameter of about 5-15 cm (maximum 0.5 m) near the base to an average clast size of about 30-40 cm (maximum 1.5 m) in the upper portions of the lithofacies. Redbeds intercalated within the lithofacies are comprised of thinly to moderately bedded (1-15 cm), subangular to rounded, coarse sand to granule conglomerate chert and volcanic lithic arenite. Planar laminations, trough crossbeds, channels, and graded beds are common.

On the south side of Churn Creek, volcanic boulder conglomerate is interbedded with thick and laterally continuous tuffs. These tuffs are green, thickly laminated (3-5 cm) to massive, hornblende, plagioclase, and volcanic lithic lapilli tuffs with lithic clasts locally up to 3 cm in diameter. Lesser amounts of hornblende- and plagioclase-phyric vitric tuffs are intercalated with the lapilli tuff.

Depositional environment/source terrane

The massive nature of unit Kcv conglomerate, its monolithological character, lack of sedimentary structures, and the very coarse grain size within the facies suggest that unit Kcv was deposited on an alluvial fan or volcanic apron immediately adjacent to a proximal volcanic source. Intercalations of unit Kcv with both the chert-rich and mixed lithofacies suggests the volcanic apron locally prograded into a fluvial system. No paleocurrent measurements were obtained from unit Kcv due to the massive nature of most exposures. Volcanic clasts within units Kcv and Kcm are lithologically similar, and they were most likely derived from the same source. Volcanic clasts were collected from each lithofacies for geochemical and isotopic analysis to assist in pinpointing the source of the clasts.

STRUCTURAL OVERVIEW

Northeast-directed contraction

The conglomerate of Churn Creek is deformed by a series of northwest-trending, northeast-vergent folds and northeast-directed thrust faults (Fig. 2). Low amplitude, open folds are present within every lithofacies within the basin. Fold axes are parallel to northeast-directed thrust faults that cut basinal strata. The oldest unit within the basin (Kcc) is deformed to the same degree and in the same style as overlying lithofacies, suggesting that deformation did not begin until after deposition of unit Kcc (post-late Albian time). Contraction is interpreted to be syndepositional in part based on crosscutting relations in the southwestern portion of the study area (Fig. 2, 3). In this area, the plutonic-rich lithofacies nonconformably overlies Jurassic-Cretaceous diorite and quartz monzonite (Mahoney et al., 1992). This sequence is cut by the Little Basin Fault, which juxtaposes identical diorite and quartz monzonite over the lower portion of the plutonic-rich lithofacies. The upper portion of the plutonic-rich lithofacies immediately northeast in the footwall distinctly coarsens upward, and contains clasts derived directly from the adjacent hanging wall. Accumulation of hanging wall-derived detritus in a footwall stratigraphic succession is strong evidence of syndepositional deformation. Contraction probably continued beyond deposition, as all units are deformed by similar northeast-directed structures. Eocene volcanic rocks deposited on top of the Albian-Cenomanian conglomerate are not affected by this deformation, indicating that contraction ceased prior to Eocene time.

Equal-area projections of fold axes in the study area suggest two dominant fold axis orientations; one set trending approximately 300° and one set trending approximately 250°. Folds trending 300° are superimposed on a larger scale, southwest-trending (250°) doubly plunging anticline exposed in the bottom of the Churn Creek canyon. It is unclear if the two fold orientations represent separate periods of deformation or, more likely, spatial and temporal variations in the stress field.

MODEL FOR BASIN EVOLUTION

Integration of stratigraphic and structural data permit construction of a preliminary model of basin evolution (Fig. 5). At t_0, sedimentation is limited to chert pebble conglomerate and chert lithic sandstone derived from the southeast and deposited in a braided stream system. At t_1, northeast-directed contraction was initiated on the Little Basin Fault and associated structures. At approximately the same time, volcanic clasts derived from a proximal source were introduced into the basin. Chert-rich sediments were still being actively deposited. Coeval erosion of multiple source areas resulted in a gradation from the plutonic-rich facies (Kcp) on the southwest through to the mixed facies (Kcm), into the chert-rich facies (Kcc) on the northwest side of the basin. Evidence for simultaneous deposition of a purely chert-rich lithofacies and a plutonic lithofacies is equivocal, but there is no doubt that chert was continually added to the system throughout deposition of the mixed and plutonic lithofacies (Kcm and Kcp). The mixing of sediments derived from plutonic-, volcanic-, and chert-rich sources continued for an extended period of time with the volcanic source gradually becoming dominant. By t_2, motion had ceased on the Little Basin Fault, and the chert-source had been eliminated, possibly as a result of development of a volcanic highland between the chert source and the depositional basin. Deposition of the volcanic lithofacies may have continued beyond cessation of deposition of other lithofacies. Contraction continued through time t_2, as all lithofacies are folded and thrust faulted, but it is unclear if deposition and contraction continued

simultaneously beyond t_2. Figure 5d is a schematic cross-section across the basin immediately prior to deposition of undeformed Eocene volcanic strata.

CONCLUSIONS

Albian-Cenomanian conglomeratic strata exposed along Churn Creek were deposited unconformably on top of Albian andesitic to basaltic volcanic rocks. These strata may be subdivided into four distinct lithofacies, which were derived from at least three separate source terranes. Paleocurrent data argues for a southern source for chert-rich detritus. Plutonic and volcanic detritus were both derived from sources immediately adjacent to the basin margins. Deposition occurred in braided stream and alluvial fan systems within an actively deforming basin influenced by northeast-directed contraction. Northeast-directed contraction controlled sedimentation in the southwestern portion of the basin, and was responsible for formation of low-amplitude folds and thrust faults.

The stratigraphic affinity and terrane designation of units within Churn Creek remain enigmatic at this time. Further investigation will help constrain the stratigraphic affinity of both the Albian volcanic rocks and the Albian-Cenomanian conglomeratic strata.

ACKNOWLEDGMENTS

This study is part of a regional investigation of Albian-Cenomanian conglomeratic strata along the Insular/Intermontane superterrane boundary supported by National Science Foundation grant EAR-9628515 to JBM. Additional support was received from the Idaho State University Graduate Student Research Committee. We would like to thank the Geological Survey of Canada for logistical support and scientific expertise. We thank Jeff Paddock and Tom Danielson for providing superb assistance, patience, and gourmet cooking in the field. Dave Rodgers is thanked for his help in interpreting the structural history of Churn Creek. We are most grateful to Bev Vanlier (GSC) for her editorial assistance. This manuscript was improved by reviews from J.W.H. Monger and J.W. Haggart.

REFERENCES

Cowan, D.S.
1994: Alternative hypotheses for the Mid-Cretaceous paleogeography of the Western Cordillera; GSA Today, v. 4, p. 181-186.

Green, K.C.
1990: Structure, stratigraphy and alteration of Cretaceous and Tertiary strata in the Gang Ranch area, British Columbia; M.Sc. thesis, University of Calgary, Calgary, Alberta, 118 p.

Hickson, C.J.
1992: An update on the Chilcotin-Nechako project and mapping in the Taseko Lakes area, west-central British Columbia; in Current Research, Part A; Geological Survey of Canada, Paper 92-1A, p. 129-135.

Hickson, C.J., Read, P., Mathews, W.H., Hunt, J.A., Johansson, G., and Rouse, G.E.
1991: Revised geological mapping of northeastern Taseko Lakes map area, British Columbia; in Current Research, Part A; Geological Survey of Canada, Paper 91-A, p. 207-217.

Irving, E., Thorkelson, D.J., Wheadon, P.M., and Enkin, R.J.
1995: Paleomagnetism of the Spences Bridge Group and northward displacement of the Intermontane Belt, British Columbia: a second look; Journal of Geophysical Research, v. 100, p. 6057-6071.

Irving, E., Wynne, P.J., Thorkelson, D.J., and Schiarizza, P.
1996: Large (1000 to 4000) northward movements of tectonic domains in the northern Cordillera, 83 to 45 Ma; Journal of Geophysical Research, v. 101, p. 17,901-17,916.

Mahoney, J.B., Hickson, C.J., van der Heyden, P., and Hunt, J.A.
1992: The Late Albian-Early Cenomanian Silverquick conglomerate, Gang Ranch area: evidence for active basin tectonism; in Current Research, Part A; Geological Survey of Canada, Paper 92-1A, p. 249-260.

Mahoney, J.B., Monger, J.W.H., and Hickson, C.J.
1996: Albian-Cenomanian conglomerates along the Intermontane/Insular superterrane boundary, Canadian Cordillera, British Columbia: a critical test for large-scale terrane translation?; in Current Research 1996-A; Geological Survey of Canada, p. 101-109.

Mathews, W.H. and Rouse, G.E.
1984: The Gang Ranch-Big Bar area, south-central British Columbia: stratigraphy, geochronology, and palynology of the Tertiary beds and their relationship to the Fraser Fault; Canadian Journal of Earth Sciences, v. 21, p. 1132-1144.

Monger, J.W.H. and Price, R.A.
1996: Comment on "Paleomagnetism of the Upper Cretaceous strata of Mount Tatlow: Evidence for 3000 km of northward displacement of the eastern Coast Superterrane, British Columbia" by P.J. Wynne et al., and on "Paleomagnetism of the Spences Bridge Group and northward displacement of the Intermontane Superterrane, British Columbia: A second look" by Irving et al; Journal of Geophysical Research, v. 101, p. 13,793-13,799.

Tipper, H.W.
1978: Taseko Lakes (92-0) map-area; Geological Survey of Canada, Open File 534.

Wynne, P.J., Irving, E., Maxson, J.A., and Kleinsphen, K.L.
1995: Paleomagnetism of the Upper Cretaceous strata of Mount Tatlow: evidence for 3000 km of northward displacement of the eastern Coast Belt, British Columbia; Journal of Geophysical Research, v. 100, p. 6073-6091.

Geological Survey of Canada Project 890039

A re-evaluation of the geology adjacent to Shuswap Lake, Vernon map area, British Columbia

N.M. Slemko[1] and R.I. Thompson
GSC Pacific, Vancouver

Slemko, N.M. and Thompson, R.I., 1998: A re-evaluation of the geology adjacent to Shuswap Lake, Vernon map area, British Columbia; in Current Research 1998-A; Geological Survey of Canada, p. 175-179.

Abstract: Near Shuswap Lake, British Columbia, hanging-wall rocks of the Eagle River Fault consist of two distinctive lithostratigraphic assemblages, a locally upright succession of Silver Creek, Sicamous, and Eagle Bay formations overlain by higher grade pelitic schist, marble, and quartzite termed the 'Queest Mountain assemblage.' The contact between the assemblages is sharp, planar, north-dipping, and interpreted as a contraction fault consistent with the juxtaposition of higher metamorphic grade rocks onto lower grade ones. The metamorphic history of the area is polyphase and the structural history is complex. The Queest Mountain assemblage was previously considered correlative with the Eagle Bay Formation, an interpretation no longer tenable.

A large intrusion of granite to granodiorite, previously correlated with the Devonian Mount Fowler Batholith, cuts the metasedimentary rocks and crosses the contraction fault without offset. It postdates high-grade metamorphic mineral development in the hanging wall of the contraction fault.

Résumé : À proximité du lac Shuswap, en Colombie-Britannique, les roches du compartiment supérieur de la Faille d'Eagle River consistent en deux assemblages lithostratigraphiques distinctifs, soit une succession localement verticale de roches des formations de Silver Creek, de Sicamous et d'Eagle Bay, que recouvre l'«assemblage de Queest Mountain», composé de schiste pélitique, de marbre et de quartzite plus intensément métamorphisés. Le contact entre ces assemblages est net et planaire et plonge vers le nord; il est interprété comme une faille de contraction, ce qui est compatible avec la juxtaposition de roches plus métamorphisées sur des roches moins métamorphisées. L'histoire métamorphique de la région est polyphasée et l'histoire structurale est complexe. On considérait jusqu'à présent qu'il y avait corrélation entre l'assemblage de Queest Mountain et la Formation d'Eagle Bay, mais cette interprétation n'est plus défendable.

Une grande intrusion de granite passant à de la granodiorite, antérieurement corrélée avec le batholite dévonien de Mount Fowler, recoupe les roches métasédimentaires et la faille de contraction sans rejet. Elle est postérieure à la formation de minéraux de fort métamorphisme dans le compartiment supérieur de la faille de contraction.

[1] Department of Earth and Atmospheric Sciences, University of Alberta, #1 - 26 Earth Sciences Building, Edmonton, Alberta T6G 2E3

INTRODUCTION

Geological mapping in the Shuswap Lake region began with Dawson (1899) and Daly (1915). Jones (1959) published a comprehensive map and report of the Vernon map area at 4 mile = 1 inch scale that was followed by more detailed stratigraphic and structural studies by a number of workers (Campbell and Okulitch, 1973; Okulitch, 1974, 1975, 1989; Okulitch and Cameron, 1976). Field results reported here build on mapping by Johnson (1990), who documented the Eagle River Fault, a down-to-the-west Eocene extensional structure. Recent work by Thompson and Daughtry (1997) indicated the potential for reinterpretation of previous work.

The Shuswap Lake area is part of the Omineca Belt, a morphogeological division of the Cordillera containing both pericratonic and displaced terranes (Gabrielse et al., 1991). This study, which took place in northeastern Vernon map area (82 L) (Fig. 1), focuses on stratigraphic, structural, and metamorphic relations between Proterozoic schist and gneiss (Silver Creek Formation of Jones, 1959) of miogeoclinal affinity and Paleozoic carbonate and volcanic strata (Sicamous and Eagle Bay formations of Jones, 1959) of eugeoclinal affinity.

Fieldwork in the summer of 1997 extended from the town of Sicamous north to Cinnemousun Narrows, on Shuswap Lake (Fig. 2), and focused on rocks in the hanging wall of the Eagle River Fault. The purpose of this study was to elucidate the relationship between miogeoclinal and eugeoclinal strata, to determine the relationship between rocks on the east and west sides of the lake, to investigate the internal stratigraphy of the Silver Creek, Sicamous, and Eagle Bay formations, and to establish the structural and metamorphic history of the region. Evidence for pre-Devonian metamorphism and deformation is presented.

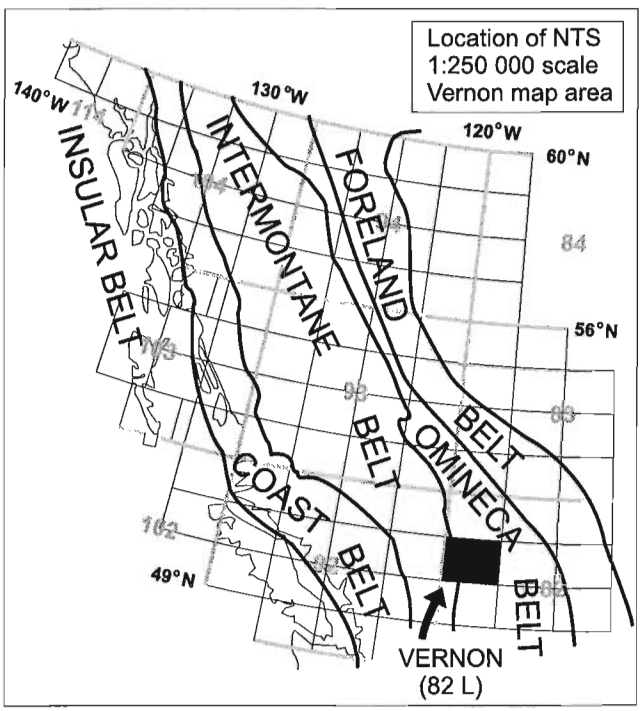

Figure 1. *Location of the Vernon map area on the NTS 1:250 000 scale map grid and within the tectonic belts of the Canadian Cordillera.*

STRATIGRAPHY AND METAMORPHISM

Queest Mountain assemblage

In the northeast part of the area mapped is an assemblage of high metamorphic-grade carbonate and calc-silicate schist, garnetiferous feldspar-quartz-mica schist, and quartzite. Minor amphibole- and feldspar-rich rocks of possible volcanic affinity are also present. The carbonates and calc-silicates are typically grey or buff coloured on weathered surfaces and white on fresh surfaces; they form a layer approximately 1 km thick. The calc-silicate schist contains calcite, quartz, feldspar, diopside, grossular, amphibole, and epidote. The garnetiferous feldspar-quartz-mica schists are white to pink, locally contain almandine and hornblende or sillimanite, and host partial melt in places. These features are diagnostic of amphibolite-facies metamorphism, higher grade than the greenschist-facies Eagle Bay Formation to the south. The contact between the Queest Mountain assemblage and Eagle Bay Formation is sharp and planar. Previously (Okulitch, 1974; Johnson, 1990), the Queest Mountain assemblage rocks had been mapped as part of the Eagle Bay Formation, however, on the basis of protolith composition and metamorphic grade, the former have a much closer affinity with older (Neoproterozoic) quartz- and feldspar-rich assemblages such as the Silver Creek Formation. Although further work is required to determine the exact regional stratigraphic affinity of the high-grade rocks, for the purpose of this report we call them the Queest Mountain assemblage.

Silver Creek Formation

The miogeoclinal Neoproterozoic Silver Creek Formation is well exposed along the Trans-Canada Highway west of Sicamous, and along the northern shore of Salmon Arm. The Silver Creek Formation is composed mainly of biotite-muscovite-quartz schist, with minor calcareous mica schist. These rocks are pale brown on weathered surfaces and off white to pale brown on fresh surfaces. The Silver Creek Formation is intruded by numerous pegmatite and aplite sills and dykes, which prompted Daly (1915) to term it the 'sill--sediment complex.' The Sicamous-Silver Creek contact exposed along the Trans-Canada Highway is a mixed gradation of biotite-muscovite-quartz schist and fine-grained marble, and is inferred to be depositional. In the area mapped, the Silver Creek Formation does not contain any high-grade metamorphic minerals, and is at greenschist grade, as are the overlying Sicamous and Eagle Bay formations. Regionally, rocks mapped as Silver Creek Formation (Okulitch, 1974; Thompson and Daughtry, 1997) are at garnet-sillimanite grade. Therefore, there must be a change in metamorphic grade within rocks mapped as Silver Creek Formation. This change could be a metamorphic gradient, an unconformity, or

a fault. If it is an unconformity or a fault, it is unlikely that both the low-grade and high-grade rocks termed 'Silver Creek Formation' are equivalent.

Sicamous Formation

The Silver Creek Formation is overlain by the Lower (?) Paleozoic Sicamous Formation. The Sicamous Formation is well exposed along the Trans-Canada Highway west of Sicamous, along the shore of Shuswap Lake on the north side of Old Town Bay, and along the west shore of Shuswap Lake north of Canoe Point. This eugeoclinal succession is a fine- to medium-grained metamorphosed carbonaceous limestone, with a distinctive black and white layering in outcrop. The Sicamous-Eagle Bay contact interdigitates near Old Town Bay.

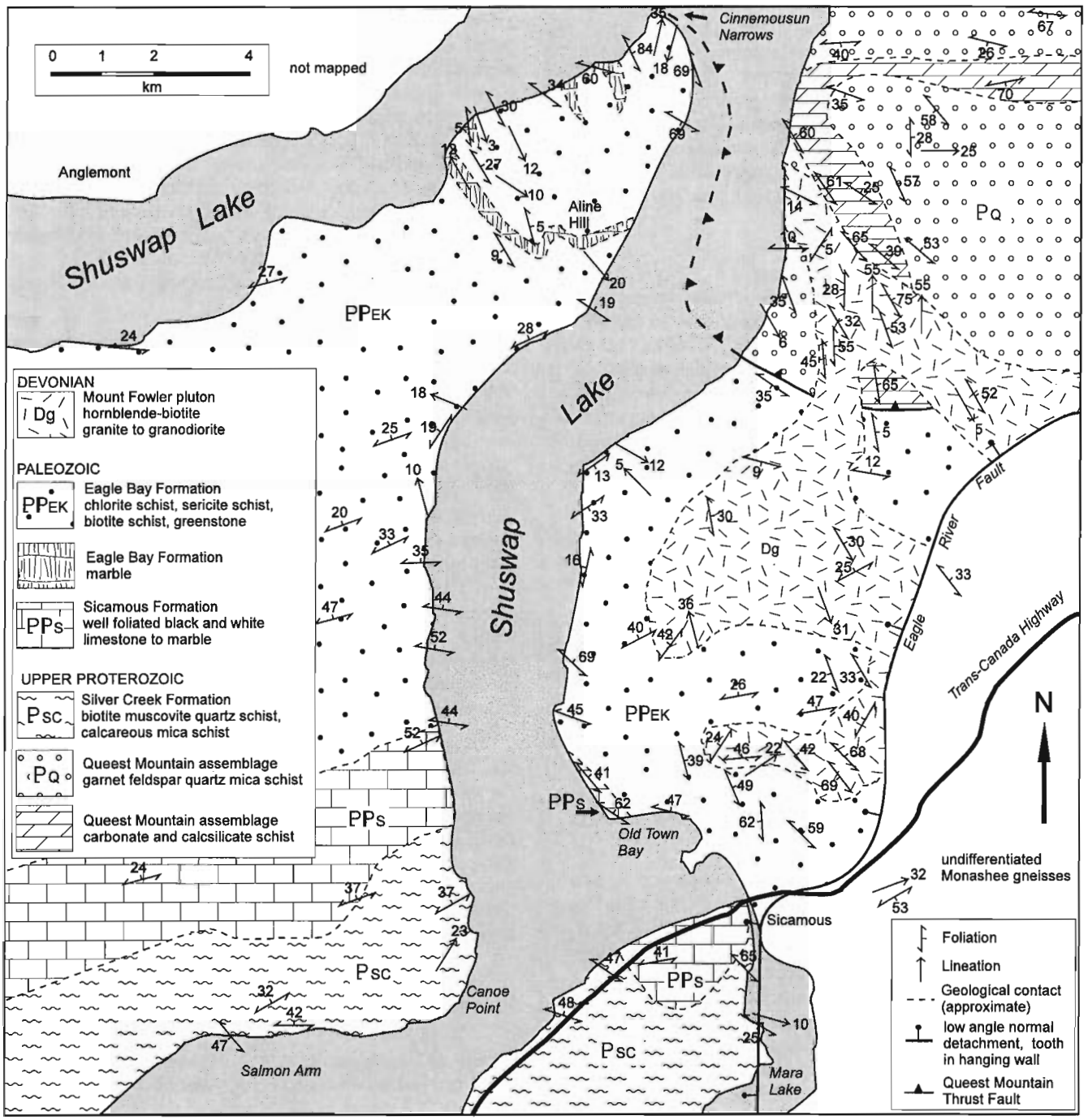

Figure 2. *Geological map of the Shuswap Lake area north of Sicamous.*

Eagle Bay Formation

The Lower (?) Paleozoic Eagle Bay Formation consists of volcanic and clastic strata of eugeoclinal aspect that, along with the Sicamous, are inferred to be deposited at the outer margin of the North American craton (Thompson and Daughtry, 1997). This formation is well exposed near Aline Hill and to the north of Old Town Bay (Fig. 1). The Eagle Bay Formation contains fine-grained chlorite schist, chlorite-sericite schist, biotite-muscovite schist, and volcanic greenstone. Most rock types are typically dark green or grey, both on fresh and weathered surfaces. Garnet or amphibole is a minor local constituent; pyrite is locally abundant. One or more streaked, white to black, marble marker horizons, typically 100 m to 200 m thick, are present. Significant lateral variations in apparent metamorphic grade occur over distances of 1 to 2 km, from lower greenschist-grade chlorite schist to upper greenschist-facies biotite-muscovite schist. Textural relationships of the chlorite suggest that these variations result from irregular or patchy retrogression.

Unit Dg

A large intrusion of biotite-hornblende, equigranular to megacrystic granite to granodiorite, correlated by Okulitch (1975) with the Devonian Mount Fowler Batholith, cuts the Eagle Bay Formation and the Queest Mountain assemblage north of Sicamous. This unit is light brown on weathered surfaces and black and white on fresh surfaces. It is resistant and often forms blocky cliffs. Strain within the granodiorite is heterogeneous, varying from none to penetrative. Strain fabrics within the country rocks, principally schistosity and folded schistosity, are cut by the granodiorite. Hornblende and biotite in Unit Dg have been retrogressed to chlorite grade. Geochronological work is in progress to establish the crystallization and metamorphic ages of this unit.

STRUCTURE

Folding

The mica-rich metasedimentary rocks are well foliated, whereas the marbles are largely massive as a result of the lack of micaceous minerals. Mineral lineation, locally present in schist, has no apparent preferred orientation, based on a sample of 24 locations.

Only one foliation is observed, with one exception near Aline Hill, where two are present. The main foliation is a fine schistosity to phyllitic cleavage, S_1. Near Aline Hill, the S_1 foliation is folded into upright mesoscopic folds with wavelengths less than 1 m and amplitudes less than 0.5 m. A weak cleavage, S_2, is axial planar to these folds. Transposed bedding is also preserved in this outcrop, and is approximately parallel to the S_1 foliation. The single foliation observed at other locations, S_1, is parallel or subparallel to major lithologic contacts.

From the strike variation and dip reversals seen at map scale, the S_1 foliation is inferred to be folded into large (approximately 10 km wavelength), open upright folds. Fold axes trend broadly west-northwest, and appear to plunge shallowly. Data are insufficient to accurately locate the axial traces of these folds. The folds may be contemporaneous with the S_2 foliation near Aline Hill, but did not give rise to a pervasive axial foliation. The folding event likely records principal compression in a northeast-southwest orientation.

Queest Mountain contraction fault

There is a sharp change in metamorphic grade where the lower grade Eagle Bay Formation is mapped against higher grade Queest Mountain assemblage strata approximately 5 km north of Old Town Bay. The contact separates amphibolite-grade quartzite, micaceous quartzite, and marble from greenschist-grade chloritic phyllite (Fig. 2); the contact is sharp, planar, west-northwest striking, and moderately north-northeast-dipping. Present field data do not constrain the dip of the fault. The sharp change in metamorphic grade is likely caused by a fault, which we interpret as a pre-Devonian contraction structure placing the higher grade (and older?) Queest Mountain assemblage above the Eagle Bay. Mapping near Aline Hill demonstrates that the contraction fault bends abruptly northward and passes up Shuswap Lake and through Cinnemousun Narrows.

The Queest Mountain contraction fault resulted from northeast compression. Its strike is parallel to the axial traces of the large open folds on the east side of Shuswap Lake, suggesting that the fault and folds may be kinematically related.

Unit Dg

The schistosities in Unit Dg and host rocks are generally discordant. This suggests that Dg has not undergone the same early deformation as the country rock. Dg foliation is not axial planar to the large-scale open folds, and is variable in orientation and intensity. The schistosity may result from a weak deformation postdating S_1 foliation in the host rocks. It is not pervasive, and its orientation was controlled in part by the attitude of contacts. The event producing it could have intensified or transposed the foliation in host rocks.

Unit Dg is mapped across the Queest Mountain contraction fault with no map-scale offset (Fig. 2). The intrusion of Dg postdates metamorphic mineral growth and early fabric development in the Queest Mountain assemblage, because the Queest Mountain assemblage has been metamorphosed to a higher grade than Dg and its fabric has been cut by Dg. If the pluton correlates with the Devonian Mount Fowler suite (Okulitch et al., 1975), a record of pre-Devonian deformation is preserved.

FUTURE WORK

Geochronological work on Dg will allow for the refinement of the age and regional affinity of this unit. Future fieldwork will focus on mapping the location of the Queest Mountain contraction fault to the northwest, and examining high-grade Monashee gneisses in the footwall of the Eagle River Fault to help determine the regional stratigraphic affinity of the

Queest Mountain assemblage. The internal stratigraphy and metamorphism of the Silver Creek Formation will be mapped to the west and north to study the nature and location of the change from high metamorphic grade to low grade.

CONCLUSIONS

The miogeoclinal Neoproterozoic Silver Creek Formation appears within the map area to be in stratigraphic contact with eugeoclinal Lower (?) Paleozoic Sicamous and Eagle Bay formations; there is no change in metamorphic grade at the Silver Creek-Sicamous contact. However, elsewhere the Silver Creek reaches much higher grades, implying either a lateral change in metamorphic grade within the Silver Creek or non-equivalence of strata assigned to the formation locally to strata elsewhere.

Lithological differences between rocks on the east and west sides of Shuswap Lake, as well as metamorphic contrasts north of the town of Sicamous, have led to the recognition of the Queest Mountain assemblage in rocks previously mapped as Eagle Bay Formation. The Queest Mountain contraction fault dips north-northeast, verges south-southwest, and juxtaposes the high-grade Queest Mountain assemblage against the lower grade Eagle Bay Formation.

The Queest Mountain contraction fault is cut by granitoid rocks regionally correlated with the Devonian Mount Fowler Batholith. If this correlation is correct, the fault itself, as well as the metamorphism and deformation evidenced in the rocks it juxtaposes, are of pre-Devonian age.

REFERENCES

Campbell, R.B. and Okulitch, A.V.
1973: Stratigraphy and structure of the Mount Ida Group, Vernon (82 L), Adams Lake (82 M W1/2), and Bonaparte (92 P) map-areas; in Report of Activities, Part A: April to October 1972; Geological Survey of Canada, Paper 73-1, p. 21-23.

Daly, R.A.
1915: A geological reconnaissance between Golden and Kamloops B.C., along the Canadian Pacific Railway; Geological Survey of Canada, Memoir 68, 260 p.

Dawson, G.M.
1899: Shuswap Sheet; Geological Survey of Canada, Map 604.

Gabrielse, H., Monger, J.W.H., Wheeler, J.O., and Yorath, C.J.
1991: Part A. Morphogeological belts, tectonic assemblages, and terranes; in Chapter 2 of Geology of the Cordilleran Orogen in Canada, (ed.) H. Gabrielse and C.J. Yorath; Geological Survey of Canada, Geology of Canada, no. 4 (also Geological Society of America, Geology of North America, v. G-2.), p. 15-28.

Johnson, B.J.
1990: Geology adjacent to the western margin of the Shuswap Metamorphic Complex; Province of British Columbia Ministry of Energy, Mines and Petroleum Resources, Open File 1990-90, 15 p.

Jones, A.G.
1959: Vernon map-area, B.C.; Geological Survey of Canada, Memoir 296, 186 p.

Okulitch, A.V.
1974: Stratigraphy and structure of the Mount Ida Group, Vernon (82 L), Seymour Arm (82 M), Bonaparte Lake (9 2P) and Kettle River (82 E) map-areas, British Columbia; in Report of Activities: Part A, April to October 1973; Geological Survey of Canada, Paper 74-1, Part A, p. 25-30.
1975: Stratigraphy and structure of the western margin of the Shuswap Metamorphic Complex, Vernon (82 L) and Seymour Arm (82 M) map-areas, British Columbia; in Report of Activities: Part A, April to October 1974; Geological Survey of Canada, Paper 75-1, Part A, p. 27-30.
1989: Revised stratigraphy and structure in the Thompson-Shuswap-Okanagan map area, southern British Columbia; in Current Research, Part A; Geological Survey of Canada, Paper 89-1A, p. 51-60.

Okulitch, A.V. and Cameron, B.E.B.
1976: Stratigraphic revisions of the Nicola, Cache Creek, and Mount Ida Groups, based on conodont collections from the western margin of the Shuswap Metamorphic Complex, south-central British Columbia; Canadian Journal of Earth Sciences, v. 13, p. 44-53.

Okulitch, A.V., Wanless, R.K., and Loveridge, W.D.
1975: Devonian plutonism in south-central British Columbia; Canadian Journal of Earth Sciences, v. 12, p. 1760-1769.

Thompson, R.I. and Daughtry, K.L.
1997: Anatomy of the Neoproterozoic - Palaeozoic continental margin, Vernon map area, British Columbia; in Current Research 1997-A; Geological Survey of Canada, p. 145-150.

Geological Survey of Canada Project 930036

Stratigraphic linkages across Vernon map area, British Columbia

Robert I. Thompson and Kenneth L. Daughtry[1]
GSC Pacific, Vancouver

Thompson, R.I. and Daughtry, K.L., 1998: Stratigraphic linkages across Vernon map area, British Columbia; in Current Research 1998-A; Geological Survey of Canada, p. 181-187.

Abstract: Jones' (1959) stratigraphic legend can be amended in the following ways: 1) map unit 13 is Triassic age and overlies map unit 15; 2) map unit 14 contains two volcanic successions, one of Permian age that underlies unit 15, and one of Triassic age that overlies unit 13.

Time-stratigraphic correlation between Tsalkom-Sicamous-Eagle Bay formations; the Chapperon Group; and an amphibolitic schist-marble-quartzite map unit is indicated. These assemblages were metamorphosed and deformed prior to deposition of Permian strata.

Permian strata consist of two primary lithotypes – volcanic rocks and limestone. The limestone is discontinuous, occurring as local build-ups within a mosaic of volcanic rocks.

Triassic strata consist of argillite, carbonaceous limestone, and volcanic rocks. They link the Slocan Formation on the east with the Nicola Formation on the west.

Alteration halos associated with mafic and ultramafic intrusions into Triassic argillite may represent mineral exploration targets.

Résumé : La légende stratigraphique de Jones (1959) peut être modifiée des manières suivantes : 1) l'unité cartographique 13 est d'âge triasique et recouvre l'unité cartographique 15; 2) l'unité cartographique 14 comporte deux successions volcaniques, une d'âge permien qui est sous-jacente à l'unité 15 et une d'âge triasique qui recouvre l'unité 13.

Les corrélations chronostratigraphiques entre les formations de Tsalkom-Sicamous-Eagle Bay, le Groupe de Chapperon et une unité cartographique de schiste amphibolitique-marbre-quartzite sont indiquées. Ces assemblages ont été métamorphisés et déformés avant le dépôt des strates permiennes.

Les strates permiennes comportent deux lithotypes principaux, soit des roches volcaniques et du calcaire. Le calcaire est discontinu, se rencontrant sous forme de monticules locaux dans une mosaïque de roches volcaniques.

Les strates triasiques comportent de l'argilite, du calcaire carbonacé et des roches volcaniques. Elles relient la Formation de Slocan à l'est et la Formation de Nicola à l'ouest.

Les auréoles d'altération liées aux intrusions mafiques et ultramafiques dans l'argilite triasique pourraient constituer des cibles d'exploration minérale.

[1] Discovery Consultants, P.O. Box 933, Vernon, British Columbia V1T 6M8

INTRODUCTION

Fieldwork in 1997 focused on the northwestern quadrant of Vernon map area (NTS 82L)from Glenemma northwest to Charcoal Creek, and from Falkland west to Westwold; time was also spent in the headwaters of the Salmon River at the western margin of the map area; and a brief reconnaissance was undertaken in the vicinity of Mount Todd located at the northwestern extreme of the map area (Fig. 1). The purpose of this work was threefold: 1) to map out Paleozoic and Mesozoic stratigraphic units in the Falkland-Glenemma area to better refine our understanding of the stratigraphic succession there; 2) to lay some of the groundwork for stratigraphic correlation between this area, Vernon to the southeast, and the Adams Lake-Mount Cahilty area to the northwest; and 3) to test the hypothesis that the Chapperon Group of Jones (1959), which is exposed along the western margin the Vernon map area is, in fact, a part of the Tsalkom-Sicamous-Eagle Bay assemblage established by Jones (1959) in the Shuswap Lakes part of Vernon map area.

This work builds on recent quality mapping completed by Read (1996) between Falkland and Chase.

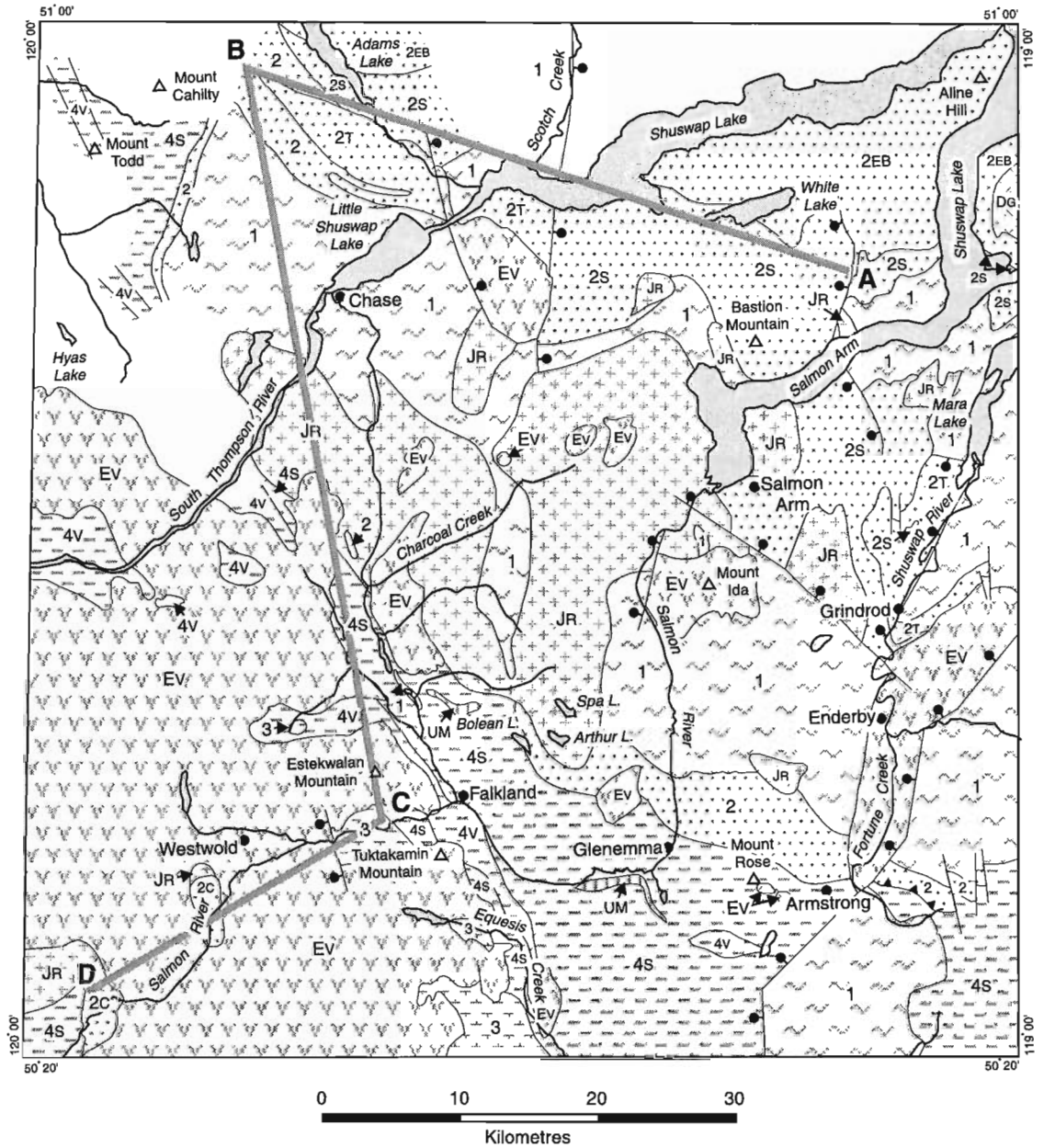

Figure 1. *Generalized geological map for the northwest quadrant of Vernon map area accompanied by a legend illustrating major stratigraphic subdivisions and correlations.*

SUMMARY OF STRATIGRAPHIC RELATIONS

In a previous article we (Thompson and Daughtry, 1997) made the case for separating rocks in the Vernon map area into two fundamental divisions, an Eocambrian and older, shallow water clastic succession having miogeoclinal affinities, and a Cambrian and younger succession of deeper water shales, volcanic rocks, and local carbonate buildups having eugeoclinal affinities. The change from miogeoclinal clastic facies to finer grained, carbonaceous eugeoclinal facies reflects the breakup of Rhodinia: separation of East Antarctica-Australia from Laurentia (Dalziel, 1991). Rift-related grits, pelites, and quartzites derived from Laurentian shield areas and local basement highs, dominated pre-breakup strata; after breakup, the "bottom dropped out" from beneath the outer continental margin and access to shield-derived clastic sediment was cut off by a broad carbonate platform and shelf that fringed the shallow-water part of the continental margin. Applying local stratigraphic terms that relate specifically to Vernon map area, the Silver Creek Formation (Jones, 1959) represents pre-breakup, Eocambrian and older strata; the Tsalkom, Sicamous and Eagle Bay formations (Jones, 1959) represent post-breakup strata.

Mapping within the post-breakup assemblage showed significant lateral changes in lithofacies (Thompson and Daughtry, 1997); specifically, the Tsalkom Formation volcanic succession and the Sicamous Formation limestone succession change character in a northwestward direction to become a dominantly carbonaceous shale, now metamorphosed to greenschist facies (Fig. 2); growth faults, active at the time of deposition, influenced the style of lithofacies change. We speculated that the shale lithofacies of the Tsalkom and Sicamous formations might be traced from the Mount Cahilty area in the northwesternmost part of Vernon map area southwest to Vernon, along a belt of carbonaceous argillite and volcanic rocks mapped by Jones (1959, his map units 13 and 14).

Results from 1997 fieldwork, presented below, when combined with excellent mapping by Read (1996) show that most stratified rocks between Mount Cahilty and Vernon are Triassic age. In places, they overlie Permian strata (Fig. 2), elsewhere, they overlie a distinctive and laterally persistent lithostratigraphic assemblage consisting of chloritized biotite schist, amphibolitic schist, recrystallized limestone, and quartzite and quartz pebble conglomerate (Fig. 1 and 2). This latter assemblage overlies micaceous quartzite and pelite belonging to the Silver Creek Formation, placing it in the same relative stratigraphic position as the Tsalkom-Sicamous-Eagle Bay assemblage.

Along the upper reaches of the Salmon River, adjacent to the western border of Vernon map area, Triassic strata rest unconformably on metamorphosed volcanic and siliciclastic rocks named the Chapperon Group by

Legend for Figure 1

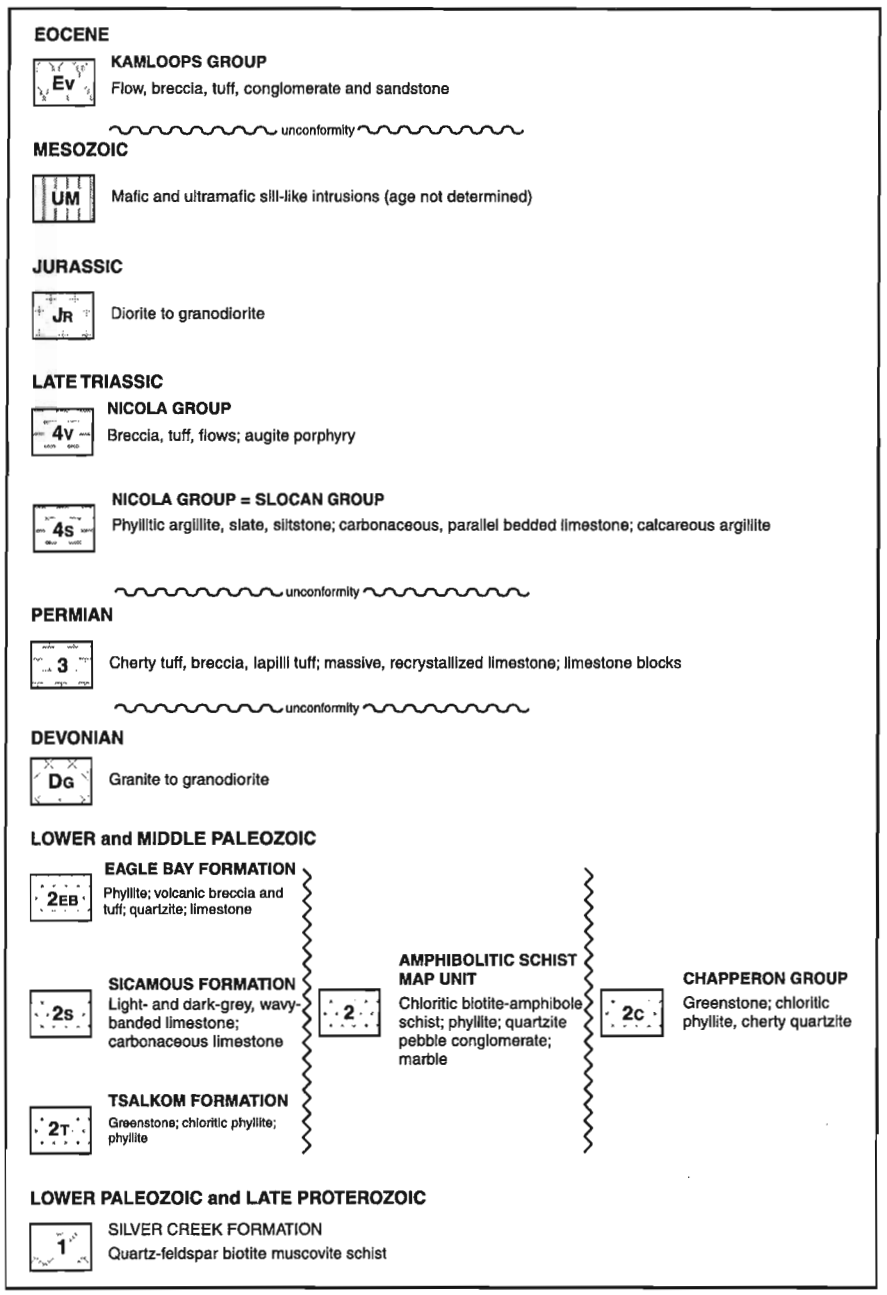

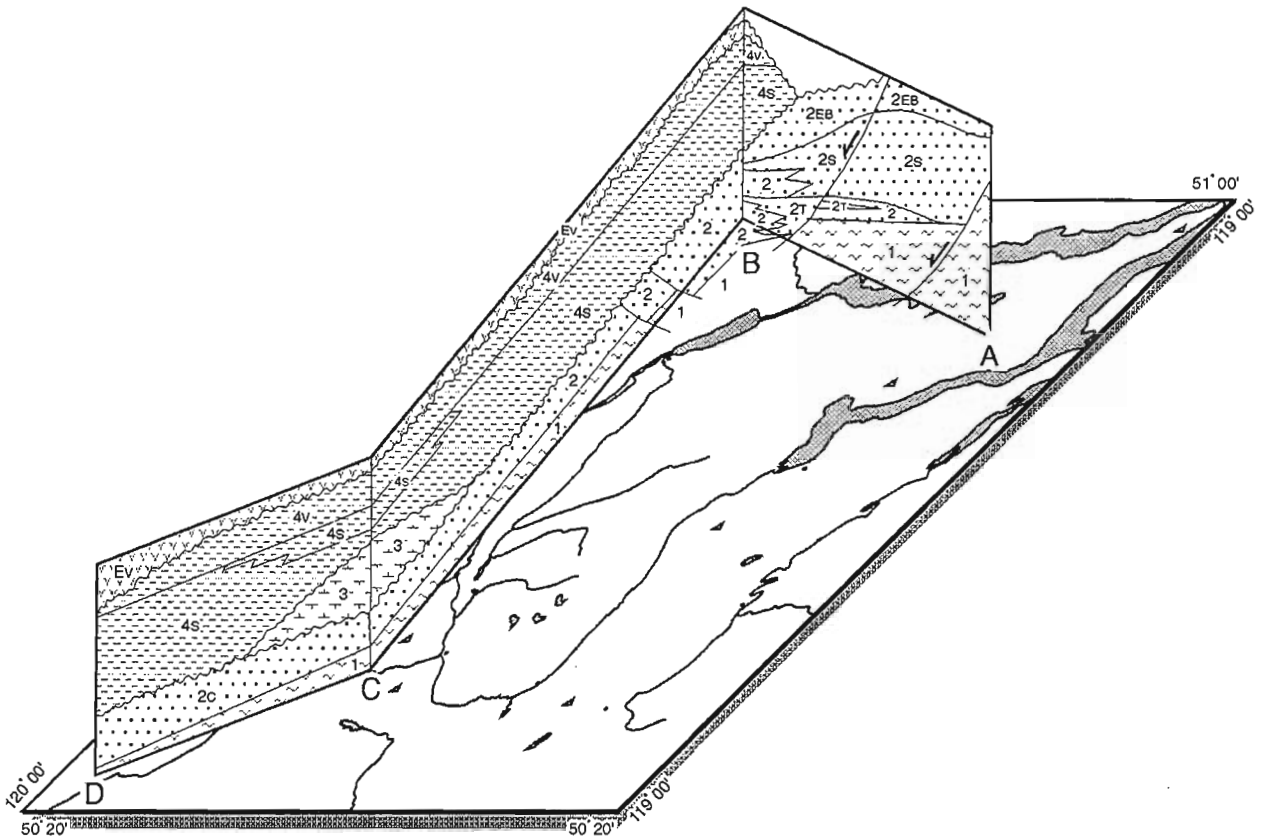

Figure 2. *Generalized stratigraphic fence diagram across the northwest quadrant of Vernon map area illustrating lateral stratigraphic correlations; refer to legend, Figure 1, for description of rock units.*

Jones (1959; Read and Okulitch, 1977). He remarked on the lithological similarity between the Chapperon Group and the Eagle Bay Formation, and implied a time stratigraphic correlation on his geology map legend. We agree with this correlation on lithostratigraphic grounds and suggest a change in stratigraphic nomenclature making the Chapperon Group part of the Tsalkom-Sicamous-Eagle Bay assemblage.

Given the stratigraphic context summarized above, much of what Jones (1959) mapped as "Carboniferous(?) And Permian Cache Creek Group", his map units numbered 13, 14 and 15, can be amended in the following ways: 1) his map unit 13 is, for the most part, Late Triassic; 2) part of his map unit 14 is also Late Triassic, overlies unit 13, and represents the eastward continuation of Nicola volcanic lithofacies mapped in adjacent Ashcroft map area (Monger and McMillan, 1989); other volcanic rocks included in map unit 14 are Permian and underlie or are interbedded with limestone belonging to his map unit 15; 3) his map unit 15 is Permian and underlies his map unit 13. These changes are reflected in Figure 1 showing the distribution of Paleozoic and Mesozoic strata based on recent mapping by the authors and by Read (1996), and in Figure 2, an interpretative fence diagram showing lateral relations of one stratigraphic facies to another.

In a broader context, field studies in 1997 confirm that stratigraphic position combined with lithological similarity suggest a correlation between the Tsalkom-Sicamous-Eagle Bay assemblage, the Chapperon Group, and the amphibolitic schist-marble-quartzite assemblage mapped between Vernon and Mount Cahilty (Fig. 1, 2). The younger Permian succession occurs as erosional remnants beneath a Triassic unconformity; local carbonate buildups suggest a shallow water origin. The succession of Triassic shales, fine grained turbidites, and parallel-bedded argillaceous limestones is relatively thick and was probably deposited into relatively deep water.

More detailed stratigraphic descriptions follow.

STRATIGRAPHY

Chapperon Group as Tsalkom-Sicamous-Eagle Bay formations equivalent

Massive, phyllitic greenstone containing bleached lenses and pods rich in quartz and feldspar, is a dominant and characteristic lithology in the Chapperon Group. These rocks form major cliffs along the headwaters of the Salmon River Valley (Fig. 1, 2) and exhibit a general appearance that is characteristic of the massive, chloritic greenstone packages within the

Tsalkom and Eagle Bay formations. Both successions share common attributes including metamorphic grade, nature and style of internal deformation, outcrop appearance, and composition.

Internal variations in lithology support correlation of Chapperon Group strata with the Tsalkom and or Eagle Bay formations. For example, the Chapperon Group contains chloritic talc-bearing phyllite; black, carbonaceous, cherty argillite; fine, siliceous rocks that may be recrystallized quartzite or metamorphosed acid volcanic rock; massive, grey-green-weathering, metasiltstone; homogenous, waxy-green, phyllitic, metamudstone containing irregular light-grey weathering siliceous lenses and blebs; cherty quartzites; and micaceous and slightly calcareous fine crystalline quartzite containing nondescript dark cherty interbeds. All of these lithologies are typical of the Tsalkom and Eagle Bay formations yet atypical of the younger Permian and Triassic successions.

Okulitch (1973) correlated the Chapperon Group with the Kobau Formation and speculated on a Carboniferous age for both. We suggest the Chapperon Group belongs, instead, to the Tsalkom-Sicamous-Eagle Bay assemblage and that it was overlain unconformably by Permian strata which were later stripped by erosion prior to deposition of Late Triassic shales. We entertain the possibility that the Kobau Group also correlates with the Tsalkom-Sicamous-Eagle Bay formations (Fig. 2).

"Amphibolitic schist-marble-quartzite map unit" as Tsalkom-Sicamous-Eagle Bay formations equivalent

A stratigraphic succession, distinguished by the association amphibolitic schist-marble-quartzite and quartzite pebble conglomerate, has been traced westward from north of Silver Star Mountain across the North Okanagan Valley to Glenemma (Thompson and Daughtry, 1994, 1996, 1997); this past field season the succession was mapped from Glenemma to Bolean Lake where it is truncated by a Jurassic pluton (Fig. 1 and 2). It is a convenient, if somewhat cryptic, marker succession separating Silver Creek schists from Triassic argillite and slate. So far, strata of Permian age have not been observed overlying it. Thickness is estimated at about 100-400 m.

Internal stratigraphic relationships vary and may, in part, reflect structural disruption. We reported on stratigraphic details from near Armstrong (Thompson and Daughtry, 1994); but one of the most interesting exposures discovered more recently occurs four kilometres east-southeast of Arthur Lake (Fig. 1). Here, the succession consists, in ascending order, of sheared, two-mica granite; stretched-pebble conglomerate; black, fine-crystalline, hornblende biotite schist; grey and white streaked marble; and bladed actinolite schist. Hornblende biotite schist is the dominant lithology. These rocks have a penetrative schistosity defined by the parallel alignment of micaceous minerals. The conglomerate is polymictic and includes stretched granite pebbles that contain little in the way of internal deformation, confirmation that the granite and overlying units were deformed after deposition of the conglomerate. Farther north, between Salmon Arm and Mount Cahilty, we argued that the contact between the Silver Creek and overlying Tsalkom and Sicamous formations was gradational with little or no evidence of a significant hiatus. Here, relations between the two-mica granite and the overlying pebble conglomerate suggests an erosional unconformity separates the two rock units. Since the granite intrudes the Silver Creek Formation, there must have been a period of uplift and erosion of Silver Creek rocks prior to deposition of the conglomerate.

The amphibolitic schist-marble-quartzite succession was recognized near Armstrong by Jones (1959) and by Okulitch (1979) both of whom correlated it with the Tsalkom Formation. We support this correlation but expand it to include the Sicamous and Eagle Bay formations as well (Fig. 2).

Permian succession

The Permian stratigraphic succession, where we've observed it in the Falkland and Pinaus Lake areas, consists of volcanic and volcaniclastic rocks, thin, discontinuous recrystallized limestone lenses, and lesser amounts of fine siliciclastic strata (Fig. 1, 2). These strata are not present along the belt of amphibolitic schist-marble-quartzite, and they are not observed overlying the belt of Chapperon Group rocks near the headwaters of the Salmon River.

Near Westwold, at least two mappable lenses of recrystallized limestone, light grey and void of internal features, occur within a succession dominated by light green-weathering, cherty volcaniclastic rocks. The limestone successions are on the order of 50 m thick, have an exposed lateral extent of about 1 km, and have mixed gradational contacts with enveloping volcaniclastic rocks. The volcaniclastic rocks are, for the most part aphanitic metamorphosed flows and or tuffs; they are fine grained to cherty and composed of feldspar in a green, amorphous matrix. Presence of small (a few metres in diameter) pods or blocks of limestone within the volcanic succession suggests they are part of a slope deposit derived from the eroded edges of local carbonate patch reefs.

East of Westwold, the upper contact with Triassic argillite and slate appears gradational; volcanic tuff and breccia containing blocks (possibly displaced) of limestone are overlain by calcareous and noncalcareous metamudstone. There is no obvious evidence of an erosional or angular unconformity separating the two successions. We interpret the contact as a disconformity. This observation is important when estimating the time of Paleozoic deformation and metamorphism. Read and Okulitch (1977) postulate a pre-Late Triassic orogenic event, discussed below; we suggest the exposures near Westwold constrain the timing of this event to pre-Permian.

Triassic succession

Rocks of Triassic age can be subdivided into the following three mappable rock units in ascending order (Read, 1996): carbonaceous argillite, slate and siltstone; black, argillaceous, parallel-bedded limestone with argillaceous partings

and interbeds; and volcanic breccia, tuff, and flows (Fig. 1, 2). All rocks are metamorphosed to greenschist facies, argillaceous components are cleaved, and sedimentary textures are poorly preserved. The limestone map unit has the most limited distribution, confined primarily to the Equesis Valley drainage and the eastern slopes of Estekwalan and Tuktakamin mountains.

The argillite-slate-siltstone succession weathers dark grey-brown to black and consists of metamorphosed shale, mudstone, and siltstone. The coarser grained beds show evidence of grading; they generally have sharp bases and little in the way of internal layering save occasional parallel laminae; low-angle cross-stratification was observed in two localities. These beds are interpreted as distal turbidites. Beds of volcanic detritus (tuff or redeposited tuff) a few centimetres to a metre or so in thickness are common near the top of the unit; their sharp basal contacts and lack of internal sedimentary features suggest they were deposited as sediment gravity flows.

Facing directions confirm map patterns that show this to be the oldest of the Triassic map units.

The overlying limestone map unit consists of planar, thin- to medium-bedded, carbonaceous, fine crystalline limestone interbedded with calcareous argillite. Similar limestones have been mapped by Okulitch (1979) near the town of Lumby (east of Vernon) and on the south flank of Vernon Hill (Thompson and Daughtry, 1994). Microfossil collections reported by Read (1996) confirm a Late Triassic age, consistent with ages reported by Okulitch and Cameron (1976) and by Thompson and Daughtry (1996). This succession is interpreted to be of relatively deep water origin, and map patterns suggest it grades laterally into and out of the argillite-slate-siltstone succession.

Volcanic rocks of this map unit consist of volcanic breccia and finer grained varieties thought to represent tuff and lapilli tuff; Read (1996) reported both crystal and crystal-lithic tuff. The basal part of the unit typically contains tabular argillite clasts derived from the underlying map unit. Augite porphyry is present as units up to one or two metres thick but the proportion of this rock type is difficult to estimate; in the South Thompson Valley, south of Pritchard, Read (1996, p. 7) reported "a thick sequence of the characteristic augite porphyry andesite and basalt flows and tuff-breccia of the Nicola Group...".

Triassic strata in Vernon map area are a stratigraphic bridge between the Nicola Group on the west and the Slocan and Rossland groups on the east. The strata we have described are linked physically with the eastern sedimentary and volcanic facies of the Nicola Group in adjacent Ashcroft map area (NTS 92I; Monger and McMillan, 1989); and the older fine grained clastic part of the succession can be traced discontinuously eastward from the town of Vernon to Upper Arrow Lake (Okulitch, 1979; Read, 1979) where phyllite, siltstone, and minor volcanic breccia are mapped as Late Triassic Slocan Group. Here, a succeeding volcanic succession consisting of porphyritic augite basalt flows, breccia, and tuff is Lower Jurassic age and mapped as part of the Rossland Group (Read, 1979). Both the Slocan and Rossland groups extend an additional 60 km farther east in adjacent Lardeau map area (NTS 82K; Read and Wheeler, 1976).

Correlation of the Nicola Group with the Slocan and Rossland groups is not new (e.g. Monger et al., 1992); the stratigraphic revisions we suggest in western Vernon map area support this interpretation. In other words, the Nicola, Slocan, and Rossland groups comprise a single, physically linked basinal assemblage that extends from Kamloops Lake on the west to Kootenay Lake on the east, a breadth of 300 km. However we disagree with the notion that this Triassic basin assemblage together with its stratigraphic underpinnings of Permian (and ?Carboniferous) strata is allochthonous with respect to underlying "North American" strata (Thompson and Daughtry, 1996).

Possible evidence for Late Triassic extension

In at least two localities, mafic and ultramafic intrusions occur within the argillite-slate-siltstone map unit. These intrusions are sill-like, they are accompanied by alteration halos, and may represent laccoliths derived from deep in the crust during late Triassic extension accompanying basin formation – an interpretation having significant implications for mineral potential of adjacent Triassic strata. This interpretation is consistent with a back-arc setting.

STRUCTURE AND THE SUB-TRIASSIC UNCONFORMITY

An angular unconformity separates Triassic rocks from underlying Chapperon Group rocks along the headwaters of the Salmon River (Preto, 1964; Read and Okulitch, 1977). According to Read and Okulitch (1977) the unconformity truncates foliation and bedding within the Chapperon Group and is overlain by conglomerate containing variably oriented clasts of foliated Chapperon Group rocks. We were unable to confirm the truncated bedding relationship, however we agree there is a well developed basal conglomerate containing randomly oriented clasts of the underlying succession; we also agree that the intensity of deformation, mainly as cleavage, is more penetrative in the older Chapperon rocks.

Deformation within the Triassic succession is variable, depending on lithology. Black argillite and feldspathic grit beds show little in the way of internal deformation whereas limestone conglomerate preserves evidence of layer parallel shear; limestone clasts show evidence of flattening and elongation, and matrix flow patterns around clasts are preserved.

Read and Okulitch (1977) assumed low-grade metamorphism and deformation in Permian-Triassic time, based largely on a presumed Mississippian age for the Chapperon Group. As discussed above, we suggest the Chapperon Group predates Permian deposition and was metamorphosed and deformed prior to the Permian. Our best guess would be Late Devonian, coincident with emplacement of Devonian plutons (Okulitch, 1985; Slemko and Thompson, 1998).

CONCLUSIONS

We suggest a time-stratigraphic correlation between Tsalkom-Sicamous-Eagle Bay formations; the Chapperon Group; and the amphibolitic schist-marble-quartzite map unit. We submit that these rocks were metamorphosed and deformed prior to deposition of Permian strata.

Permian strata consist of two primary lithotypes – volcanic rocks and limestone. The limestone is discontinuous, occurring as local build-ups within a volcanic mosaic. These strata are preserved in a narrow belt interpreted as an erosional remnant.

Triassic strata consist, in ascending order, of carbonaceous argillite-slate-siltstone; carbonaceous, parallel bedded limestone; and volcanic flows and clastic rocks. These strata are a physical link between the Slocan and Rossland groups on the east and the Nicola Group on the west.

Mafic and ultramafic intrusions into Triassic argillite are associated with alteration halos and may represent targets for mineral exploration.

ACKNOWLEDGMENTS

We thank Murray Journeay for a helpful critical review, Richard Franklin for drafting the figures, and Bev Vanlier for final processing of the manuscript.

REFERENCES

Dalziel, I.W.D.
1991: Pacific margins of Laurentia and East Antarctica-Australia as a conjugate rift pair: evidence and implications for an Eocambrian supercontinent; Geology, v. 19, p. 598-601.

Jones, A.G.
1959: Vernon map-area, British Columbia; Geological Survey of Canada, Memoir 296, 186 p.

Monger, J.W.H. and McMillan, W.J.
1989: Geology, Ashcroft, British Columbia; Geological Survey of Canada, Map 42-1989, sheet 1, scale 1:250 000.

Monger, J.W.H., Wheeler, J.O., Tipper, H.W., Gabrielse, H., Harms, T., Struik, L.C., Campbell, R.B., Dodds, C.J., Gehrels, G.E., and O'Brien, J.
1992: Part B. Cordilleran terranes; in Upper Devonian to Middle Jurassic assemblages, Chapter 8 of Geology of the Cordilleran Orogen in Canada, (ed.) H. Gabrielse and C.J. Yorath; Geological Survey of Canada, Geology of Canada, no. 4, p. 281-327 (also Geological Society of America, The Geology of North America, v. G-2).

Okulitch, A.V.
1973: Age and correlation of the Kobau Group, Mount Kogau, British Columbia; Canadian Journal of Earth Sciences, v. 10, p. 1508-1518.
1979: Lithology, stratigraphy, structure and mineral occurrences of the Thompson-Shuswap-Okanagan area, British Columbia; Geological Survey of Canada, Open File 637.
1985: Paleozoic plutonism in southeastern British Columbia; Canadian Journal of Earth Sciences, v. 22, p. 1409-1424.

Okulitch, A.V. and Cameron, B.E.B.
1976: Stratigraphic revisions of the Nicola, Cache Creek, and Mount Ida groups, based on conodont collections for the western margin of the Shuswap Metamorphic Complex, south-central British Columbia; Canadian Journal of Earth Sciences, v. 13, p. 44-53.

Preto, V.A.
1964: Structural relationships between the Shuswap Terrane and the Cache Cree Group in Southern British Columbia; M.Sc. thesis, University of British Columbia, Vancouver, British Columbia.

Read, P.B.
1979: Geology and mineral deposits, eastern part of Vernon east-half map-area; Geological Survey of Canada, Open File Map 658.
1996: Kamloops to Vernon: Tertiary stratigraphy and structure, industrial mineral and precious metal potentials, Kamloops, Nicola and Vernon mining divisions; British Columbia Geological Survey, Assessment Report, 2 vol.

Read, P.B. and Okulitch, A.V.
1977: The Triassic unconformity of south-central British Columbia; Canadian Journal of Earth Sciences, v. 14, p. 606-638.

Read, P.B. and Wheeler, J.O.
1976: Geology, Lardeau west-half, British Columbia; Geological Survey of Canada, Open File 432.

Slemko, N. and Thompson, R.I.
1998: A re-evaluation of the geology adjacent to Shuswap Lake, Vernon map area, British Columbia; in Current Research 1998-A; Geological Survey of Canada.

Thompson, R.I. and Daughtry, K.L.
1994: A new regional mapping project in Vernon map area, British Columbia; in Current Research 1994-A; Geological Survey of Canada, p. 117-122.
1996: New stratigraphic and tectonic interpretations, north Okanagan Valley, British Columbia; in Current Research 1996-A; Geological Survey of Canada, p. 135-141.
1997: Anatomy of the Neoproterozoic-Paleozoic continental margin, Vernon map area, British Columbia; in Current Research 1997-A; Geological Survey of Canada, p. 145-150.

Geological Survey of Canada Project 930036

The Kalamalka Lake metamorphic assemblage, tectonic infrastructure in the Vernon map area, British Columbia

Philippe Erdmer[1], Robert I. Thompson, and Kenneth L. Daughtry[2]
GSC Pacific, Vancouver

Erdmer, P., Thompson, R.I., and Daughtry, K.L., 1998: The Kalamalka Lake metamorphic assemblage, tectonic infrastructure in the Vernon map area, British Columbia; in Current Research 1998-A; Geological Survey of Canada, p. 189-194.

Abstract: The oldest metamorphic rocks along Kalamalka Lake are heterogeneous paragneiss units several kilometres thick. Migmatitic biotite-sillimanite schist, calc-silicate and marble, and amphibolite, greenstone, and gneissic rocks are intruded by foliated granite to granodiorite of inferred Middle Jurassic age. Mineral assemblages in pelite indicate peak metamorphic temperatures near 650°C and minimum pressures of 4 kb. The paragneiss sequence is also cut by leucocratic granite of inferred Jurassic age, by folded pegmatite dykes and sills, and by massive alkali-feldspar porphyry dykes of inferred Eocene (Coryell) age. A shallow west-dipping zone of ductile mylonitic fabrics, several hundred metres thick and more than 20 km along strike, overprints the metamorphic rocks. It records stretching along west-northwest shallowly plunging axes in present orientation. Coarse synkinematic sillimanite and amphibolite-grade mineral assemblages in other rock types are characteristic of this shear zone and of the Eagle River detachment in northern Vernon map area.

Résumé : Les plus anciennes roches métamorphiques en bordure du lac Kalamalka sont des unités de paragneiss hétérogènes de plusieurs kilomètres d'épaisseur. Des schistes à biotite-sillimanite migmatitiques, des roches calco-silicatées et des marbres, ainsi que des amphibolites, des roches vertes et des roches gneissiques sont injectés par des granites ou granodiorites foliés datant probablement du Jurassique moyen. Les associations de minéraux des pélites indiquent des températures métamorphiques maximales de près de 650 °C et des pressions minimales de 4 kb. La séquence de paragneiss est également recoupée par un granite leucocrate d'âge vraisemblablement jurassique, par des dykes et filons-couches pegmatitiques plissés et par des dykes massifs de porphyres à feldspaths alcalins d'âge éocene (Coryell) supposé. Une zone peu profonde à pendage ouest de fabriques mylonitiques ductiles, de plusieurs centaines de mètres d'épaisseur et s'étendant sur plus de 20 km parallèlement à la direction, surimprime les roches métamorphiques. Elle matérialise un étirement le long d'axes ouest-nord-ouest à faible pendage selon l'orientation actuelle. Des sillimanites syncinématiques à grain grossier et des associations de minéraux du faciès des amphibolites dans d'autres lithotypes caractérisent cette zone de cisaillement ainsi que le décollement d'Eagle River dans le nord de la région cartographique de Vernon.

[1] Department of Earth and Atmospheric Sciences, University of Alberta, Edmonton, Alberta T6G 2E3
[2] Discovery Consultants, P.O. Box 933, Vernon, British Columbia V1T 6M8

INTRODUCTION

Little is known about the tectonic affinity and evolution of large areas of undifferentiated gneiss and schist in the south-central Vernon map area (NTS 82L). The rocks were originally mapped as "Monashee Group" by Jones (1959) and are shown in part as undivided metamorphic rocks and in part as Eagle Bay assemblage on the Tectonic Assemblage Map (Wheeler and McFeely, 1992). The rocks constitute tectonic basement as they are continuous with the similar Neoproterozoic-Paleozoic high-grade metamorphic infrastructure to the east. Their North American margin affinity and their stratigraphic continuity with overlying rocks previously thought to be exotic with respect to the ancient margin make it critical to understand their detailed evolution. The metamorphic rocks display ductile strain fabrics inferred by previous workers to be of Jurassic or Cretaceous age. Some rocks host ductile extensional strain fabrics similar to Eocene fabrics in the Okanagan Valley fault zone to the south and the Eagle River fault zone to the north.

Reconnaissance for the Vernon mapping project identified an area of nearly continuous exposure of high-grade rocks along 20 km of the east shore of Kalamalka Lake, and mapping at 1:20 000 scale was conducted in 1997 (Fig. 1). The objectives were to elucidate the structural and metamorphic evolution before and during Mesozoic tectonism, by examining mineral assemblages and strain fabrics in the rocks, testing their correlation with other regional high-grade assemblages, and establishing the extent and structural geometry of the high strain zone(s) affecting them. Preliminary results reported here show that regional metamorphism and schistosity development in a range of supracrustal rocks predated the emplacement of a leucocratic hornblende-biotite granodiorite of presumed Middle Jurassic age, that these rocks display Middle Mesozoic or younger ductile extensional strain fabrics, and that they are cut by undeformed dykes of the Coryell suite.

STATE OF KNOWLEDGE AND TECTONIC AFFINITY

The rocks along Kalamalka Lake were initially grouped with granitoid gneiss, augen gneiss, mica-sillimanite-garnet schist, quartzite, marble, hornblende gneiss, and slate phyllite forming Unit 1 (Monashee Group) of Jones (1959), which occupies more than 50% of Jones' one inch to four mile scale Vernon map. They are shown as undifferentiated gneiss of the Shuswap Complex in the compilation by Okulitch (1979), and were described as a biotite/hornblende-feldspar-quartz schist assemblage by Thompson and Daughtry (1994), who, together with Jones (1959), recognized at least one marker unit of calcareous quartzite to siliceous marble near Cosens Bay.

Although the rocks are distinguished on the Tectonic Assemblage Map (Wheeler and McFeely, 1992) from amphibolite-grade rocks assigned to the Eagle Bay Formation and extending northward for several tens of kilometres to the northern boundary of the Vernon map area (approximately from the city of Vernon to the Trans-Canada Highway), the similarity of lithological assemblages, metamorphic grade, and penetrative strain fabrics strongly suggest that they form part of a single tectonic and stratigraphic unit (Thompson and Daughtry, 1994).

GEOLOGY ALONG KALAMALKA LAKE

Metamorphic units

Biotite-sillimanite schist assemblage

Medium- to coarse-grained biotite pelite is the main rock type. Coarse sillimanite visible in hand sample is present in most outcrops and garnet occurs in many. Layers of quartzofeldspathic migmatite a few centimetres thick are common, and are aligned in the schistosity. Fine-grained schist layers have a salt-and-pepper, black-and-white appearance, while coarse-grained ones display an irregular wavy schistosity defined by biotite horizons. Other rock types include semipelite, quartz-rich schist, quartz-muscovite schist, quartzite, calc-silicate, and minor hornblende-biotite schist, amphibolite, and amphibole-quartzofeldspathic schist. These generally form layers a few metres thick in the biotite schist and contacts are sharp. Discordant coarse-grained granite-pegmatite or aplite veins cut schistosity and lithological layering at varied angles, and range in thickness from less than one metre to several tens of metres. Most are folded, with fold shapes ranging from open to isoclinal.

The unit is interpreted to be a metamorphosed fine-grained clastic succession dominated by shale and siltstone. The inferred protolith of these metamorphic rocks resembles the older Neoproterozoic to Early Paleozoic miogeoclinal assemblage that extends across most of the Vernon map area (see Thompson and Daughtry, 1997).

Calc-silicate, marble, and calcareous quartzite

Medium- to coarse-grained diopside-grossular-amphibole-quartz-calcite calc-silicate, marble, quartzitic marble, and calcareous quartzite are included in this unit on Figure 1. They occur in relatively resistant, compositionally uniform layers ranging from a few tens of metres to over 100 m thick. One of these layers has a strike length of at least 5 km, extending southeast from Kalamalka Lake Provincial Park (north shore of Cosens Bay, on Fig. 1), and was previously noted as a marker by Jones (1959) and Thompson and Daughtry (1994). This marker is similar to others recognized regionally by Jones (1959), some of which can be traced as single layers uninterrupted for 20 km, and others linked discontinuously for up to 40 km along strike.

A sample of calc-silicate to calcareous quartzite from the marker north of Cosens Bay has yielded preliminary U-Pb ages of 101 Ma for zircon and 78 to 73 Ma for titanite (R. Friedman, pers. comm., 1997). These are thought to date a protracted metamorphic event; however, the ages are younger, by 50 Ma, than a crosscutting granitoid sill (see below).

Contacts with adjacent rock types of the biotite schist assemblage are sharp and foliation-parallel. They are interpreted as transposed stratigraphic contacts. The unit is inferred to have protoliths ranging from siliceous to argillaceous calcareous rocks of miogeoclinal affinity.

Amphibolite, greenstone, and mafic schist

This heterogeneous map unit includes a range of rock types containing various proportions of hornblende and plagioclase. Rock types include medium- to coarse-grained amphibolite, hornblende-biotite-plagioclase schist and gneiss, plagiogneiss, and massive to well layered hornblende-epidote greenstone and gneiss. Garnet porphyroblasts and (or) quartz occur in many places within the mafic rocks. Retrograde chlorite and epidote are locally prominent. Contacts between rock types are gradational, and transitional rock compositions occur. Thin, locally disrupted layers of biotite schist or semipelite are found in a few outcrops.

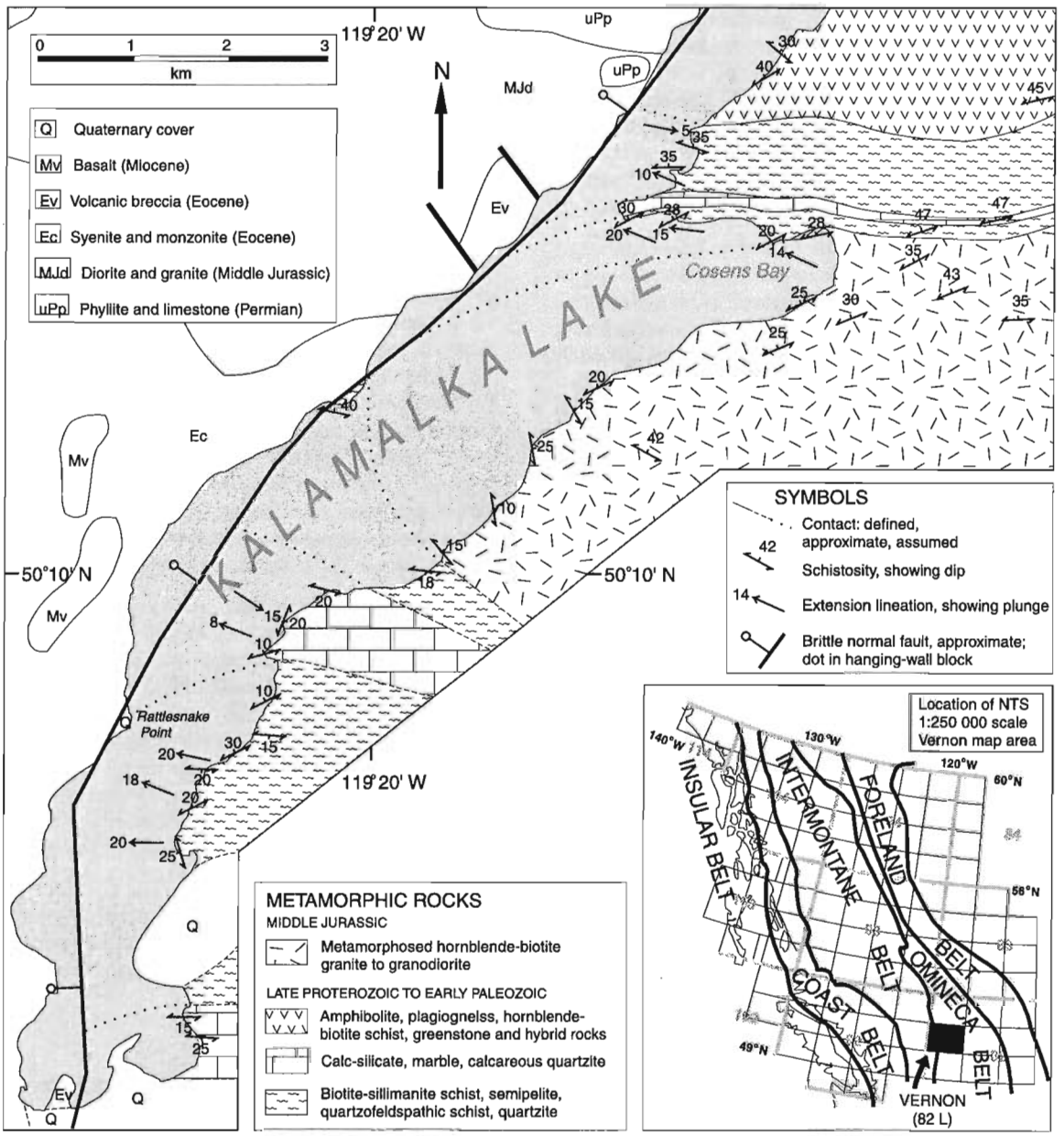

Figure 1. *Distribution of metamorphic rocks along Kalamalka Lake and location of the Vernon map area on the NTS 1:250 000 scale map grid and within the tectonic belts of the Canadian Cordillera. Geology on the west side of Kalamalka Lake is summarized from previous mapping for the Vernon Project.*

The hornblende-bearing rocks are interpreted to be a transposed mafic to intermediate metavolcanic assemblage whose protolith was compositionally heterogeneous. The rocks forming this map unit are inferred to be in primary contact with the biotite schist unit.

Granite and granodiorite

Texturally homogeneous medium- to coarse-grained, locally megacrystic, metamorphosed hornblende-biotite granodiorite, diorite, and granite form a large intrusion exposed along the east shore of Kalamalka Lake and at higher elevations inland to the east (Fig. 1), and named here the Cosens Bay pluton. The unit is mesocratic to leucocratic, and locally includes tonalite. Horizons of metagranodiorite a few metres to a few tens of metres thick are interlayered with sillimanite schist along the north shore of Cosens Bay. The number and thickness of these layers decrease gradually away from the contact. They are interpreted to be former dykes or sills of the main pluton that were rotated parallel to the host-rock schistosity during later strain.

The Cosens Bay pluton is a distinctive unit that lithologically resembles bodies of the Devonian Mt. Fowler suite to the north (see Okulitch et al., 1979), as well as bodies of Jurasic granodiorite mapped west and south of Kalamalka Lake, and Jurassic orthogneiss reported to the east by Okulitch (1979). A sill of megacrystic granodiorite cutting biotite schist, exposed in the parking lot at the gate to Kalamalka Lake Provincial Park a few hundred metres northeast of Cosens Bay, has yielded a preliminary U-Pb zircon date of 153.9 ± 1.2 Ma (R. Friedman, pers. comm., 1997). The sill is interpreted to be an apophyse of the Cosens Bay pluton, which supports a provisional correlation with the regional Nelson plutonic suite of Middle Jurassic age. A sample of the main phase of the Cosens Bay pluton is being processed for U-Pb dating.

Minor intrusive rocks

Granite and granite pegmatite

At at least two locations along the lakeshore, weakly foliated, leucocratic, fine- to medium-grained grey biotite granite to aplite forms dykes or small stocks a few metres to a few tens of metres across that cut the biotite schist. These intrusions have a distinctive blocky weathering appearance. On the basis of compositional similarity, they are correlated with a granite pluton that straddles the Okanagan Valley south of Kalamalka Lake and has yielded dates near 164 Ma (R. Friedman, pers. comm., 1997). A sample of one of the stocks is being processed for U-Pb dating.

The paragneiss units (biotite schist, marble and calc-silicate, and hornblende-bearing rocks) are cut by abundant granite pegmatite veins, dykes, and sills ranging in thickness from less than one metre to several tens of metres. The granite intrusions are dominantly muscovite-bearing, and locally host almandine. They occur as planar crosscutting bodies, folded layers, or layers parallel to the main schistosity. They may represent S-type intrusions resulting from the melting of deeper continental rocks, or simply locally derived melts produced during metamorphism and remobilized during deformation. Their age is inferred to range from Mesozoic to Early Cenozoic.

Alkali-feldspar porphyry dykes

On the north side of Cosens Bay, dykes of pink- to buff-weathering fine-grained alkali-feldspar biotite porphyry a few metres wide cut the biotite schist. The rock is fresh and massive, and compositionally similar to a porphyritic quartz monzonite pluton found a few kilometres to the west across Kalamalka Lake, which is part of the Coryell suite and has yielded a U-Pb zircon age of 50.1 ± 0.3 Ma (R. Friedman, pers. comm., 1997). The dykes are correlated with the Coryell intrusions and inferred to be of Eocene age. A sample is being processed for U-Pb dating.

Metamorphic conditions

The migmatitic biotite-sillimanite schist assemblage, the calc-silicate unit, and the amphibolitic unit are regionally metamorphosed rocks characterized by coarse-grained, equigranular texture, well developed metamorphic porphyroblasts, and only minor local chlorite-grade retrogression. From the local interleaving of rock types and the continuity of the carbonate markers, the paragneiss units are inferred to have been metamorphosed together as a sequence. From porphyroblast and matrix characteristics, such as large, strain-free sillimanite crystals defining schistosity, only moderate draping of biotite- or hornblende-defined schistosity around garnet, and local equilibrium triple junction textures in various mineral aggregates, metamorphism was synkinematic with respect to the main tectonic fabrics.

When plotted on a petrogenetic grid, the occurrence of muscovite and quartz together with sillimanite and K-feldspar, in pelite that also contains partial melt, records minimum metamorphic temperatures of about 650°C and minimum pressures near 4 kb, corresponding to a depth of burial of at least 13 km. Mineral assemblages and petrogenetic relations indicate equilibration in the high-temperature region of the amphibolite metamorphic facies. While less constrained in P-T space, mineral assemblages in calc-silicate and amphibolite are compatible with the minimum conditions indicated by pelite, i.e. close to the "second sillimanite" isograd.

Static retrogression to chlorite-epidote mineral assemblages, recording a greenschist-facies overprint, is evident locally in a number of units; its regional extent is unclear.

Structure

The schistose metamorphic rocks are overprinted by a ductile shear zone characterized by strong linear fabrics. The biotite schist, calc-silicate, and amphibolitic units are well foliated. Local compositional banding parallel to the schistosity likely represents transposed layering. None of the metaclastic units preserve depositional structures. Schistosity and compositional layering are truncated by the Cosens Bay

metagranodiorite. A schistosity is developed in the latter unit, recording another phase of fabric development; this is not a magmatic foliation, as it occurs together with a stretching lineation. The fine-grained grey granite intrusions cut schist and display weak to moderate internal schistosity.

Abundant mesoscopic folds of the schistosity are visible in outcrop. These range from open waves of continuous layers to detached and tightly appressed isoclinal hinges most commonly from one to several metres in amplitude. The axes of open folds are variously oriented. The axes of isoclinal folds are gently plunging to subhorizontal in the main planar fabric, suggesting that hinges have been passively rotated into alignment with an axis of later stretching recorded by the orientation of a pervasive lineation (see below). The existence of macroscopic (regional) folds of the schistosity is suggested by the spread of orientations along Kalamalka Lake noted by Jones (1959). We observed dip reversals and moderate strike variability of schistosity over distances of up to several hundred metres along the lakeshore (Fig. 1), which outline large-amplitude long-wavelength moderate folds affecting the paragneiss and metagranodiorite units.

A strong extension lineation defined by quartz or quartzofeldspathic rodding, drawn-out and segmented porphyroclasts, and mineral lineation, is present in most, but not all, outcrops of paragneiss and affects the margins of the Cosens Bay pluton along the lakeshore. It is accompanied by mylonitic fabric characterized by grain-size reduction in quartz mosaic aggregates, granulation of feldspars, moderate undulose extinction of mineral grains, preferred shape fabric and preferred crystallographic fabric orientation, porphyroclast differentiation from matrix, C-S fabric and numerous other indicators of non-coaxial ductile strain such as delta and sigma porphyroclasts, shear bands, back-rotated boudins, and asymmetrical tiling of "domino" grains. Extensional ductile duplexes on a scale of a few tens of centimetres to several metres are exposed in vertical outcrop faces at high angle to the northeast elongation of the lake. Cataclasis, while clearly resulting in grain-size reduction, did not greatly outpace recrystallization, showing that most of the strain was imposed at depths below the brittle-ductile transition. There are few, if any, seams of dark, fine-grained comminuted material, and only rare irregularly fractured matrix grains or porphyroclasts; these brittle structures could result from later deformation or locally higher strain rates under ambient ductile conditions. Coarse sillimanite in pelite is synkinematic with respect to the strain fabrics, for example showing crystal alignment in C-S planes and only slight undulose extinction. No chlorite-grade brecciation or other evidence of widespread brittle strain characterize the rocks. The entire east shore of the lake sems to be part of a single mylonite zone; the few outcrops where mesoscopic mylonitic fabrics were not seen are interpreted as domains resulting from local strain partitioning.

The stretching lineation trends dominantly west-northwest with gentle plunge (10° to 20°). Abundant shear-sense indicators in both outcrop and thin section record consistent hanging-wall-down motion in present orientation, i.e. top-down-to-the-west-northwest along low-angle surfaces. The motion was not down dip in the present attitude of foliation.

On the basis of the distribution of mylonitic fabrics and the consistent orientation and asymmetry of the extensional lineation, we infer that a regional-scale ductile shear zone is exposed along the present topographic surface at lake level. The geometry of the trace of the lakeshore and the occurrence of metamorphic rocks on the west side of the lake (Fig. 1) suggest a minimum thickness of several hundred metres for the shear zone.

An outcrop of friable, brecciated, and fractured mylonitic quartz-rich gneiss with thin dark gouge seams and brittle cataclasite zones occurs along the railway tracks in Kekuli Bay Provincial Park on the west side of Kalamalka Lake, approximately 4.5 km northeast of Rattlesnake Point (Fig. 1). It is interpreted to be the locus of a steep down-to-the west, northeast-striking normal fault that juxtaposes the metamorphic rocks against Upper Paleozoic to Eocene rocks to the west. Eocene volcanic rocks occur less than 30 m away from the fault zone. An outcrop of mylonitic quartz-rich schist on the lakeshore a few tens of metres east of the railway track shows only weak overprinting by brittle cataclasis. Farther south along Kalamalka Lake, rocks of the Coryell suite are cut by similar steep zones of brittle cataclasis.

IMPLICATIONS FOR REGIONAL EVOLUTION

The truncation of an amphibolite-grade metamorphic fabric by the Cosens Bay pluton records regional deformation during or before the Middle Mesozoic. The evidence of Jurassic magmatism, and subsequent deformation that may be linked in part to that magmatism, records orogeny of Late Mesozoic or younger age. The significantly lower metamorphic grade of Permian phyllite and limestone occurring on the west side of Kalamalka Lake a few hundred metres away from the rocks described here (Fig. 1; see Thompson and Daughtry, 1994) implies differential regional uplift of up to 10 km by the Late Paleozoic. The Coryell dykes cutting the metamorphic rocks constrain the end of penetrative fabric development, and possibly of significant tectonic activity, to Eocene or earlier time.

The synkinematic growth of coarse sillimanite in a regional west-northwest-dipping shear zone along Kalamalka Lake is also characteristic of the Eagle River detachment zone (Johnson, 1990) where it is exposed a few kilometres northeast of Sicamous in the northern part of the Vernon map area (see report by Slemko and Thompson, 1998). There, as along Kalamalka Lake, no chlorite-grade retrogression or brittle cataclasis are recognized, and the presence of sillimanite records a minimum temperature of 500°C during deformation and metamorphism. This suggests that the thickness of the hanging wall was greater than the thickness of Eocene (Kamloops) volcanic strata and that the shear zone(s) are mid-crustal structures. On Silver Star Mountain,

approximately 20 km north of the area in Figure 1, rocks that would form the hanging wall to the north along strike are high-grade undeformed (noncataclastic) metamorphic rocks.

Thompson and Daughtry (1994, 1996) presented some of the chronological, stratigraphic, and structural reasons why it is difficult to interpret the North Okanagan Valley as the locus of a shallow west-dipping detachment with tens of kilometres of down-to-the-west motion. Their data support the existence of steeply dipping, domino-style normal faults with displacements of a few kilometres at most. Although they recognized the presence of ductile cataclastic zone(s) similar to the one described here, they offered no geometric, kinematic, or temporal data to explain how detachments and the steeper-dipping domino-style faults might relate. Their resistance to the detachment model centred on the lack of evidence for a shallow-dipping surface or zone separating low-grade suprastructure (e.g. Permian and Triassic carbonate and siliciclastic rocks) from high-grade infrastructure. Not only can the suprastructure be mapped across the North Okanagan Valley, but schists belonging to the infrastructure are exposed on the valley's west flank, where they are cut by an undeformed Jurassic pluton that extends more than 15 km across strike from supposed hanging-wall plate into supposed footwall plate.

If the detachment is contained wholly within the high-grade infrastructure of schists, as seems to be the case along the east side of Kalamalka Lake, then the steep-dipping fault that follows the western margin of the lake is a post-detachment structure placing suprastructure down on the west at a high angle against infrastructure. This explains the near-juxtaposition of ductile cataclastic zone(s) within the high-grade rocks against brittly deformed low-grade strata of Permian and Triassic age. Farther south, where the Jurassic pluton bridges the Okanagan Valley and supposedly cuts the detachment, the search for a shallow, west-dipping detachment zone should focus deeper within the infrastructure, well to the east of the valley. The Jurassic pluton may itself be truncated by a detachment fault.

Central to this project is careful and detailed mapping of detachment zone(s) to ascertain whether, and how, they cut up-section or down-section along strike. For example, a short distance to the south near Kelowna, a shallow west-dipping detachment fault is mapped at the base of Eocene volcanic and sedimentary rocks (Tempelman-Kluit and Parkinson, 1986; Bardoux and Mareschal, 1994); does this detachment link with the one we have recognized at Kalamalka Lake? The answer has important implications with respect to current interpretations of the Okanagan Valley-Eagle River detachment fault and, at a more regional scale, the geometry, magnitude, and timing of crustal extension in the Omineca Belt

REFERENCES

Bardoux, M. and Mareschal, J.-C.
1994: Extension in south-central British Columbia: mechanical and thermal controls; Tectonophysics, v. 238, p. 451-470.

Johnson, B.J.
1990: Geology adjacent to the western margin of the Shuswap Metamorphic Complex; Province of British Columbia, Ministry of Energy, Mines and Petroleum Resources, Open File 1990-30, 15 p.

Jones, A.G.
1959: Vernon map-area, British Columbia; Geological Survey of Canada, Memoir 296, 186 p.

Okulitch, A.V.
1979: Lithology, stratigraphy, structure and mineral occurrences of the Thompson-Shuswap-Okanagan area, British Columbia; Geological Survey of Canada, Open File 637.

Okulitch, A.V., Wanless, R.K., and Loveridge, W.D.
1979: Devonian plutonism in south-central British Columbia; Canadian Journal of Earth Sciences, v. 12, p. 1760-1769.

Slemko, N.M. and Thompson, R.I.
1998: A re-evaluation of the geology adjacent to Shuswap Lake, Vernon map area, British Columbia; in Current Research 1998-A; Geological Survey of Canada.

Tempelman-Kluit, D.J. and Parkinson, D.L.
1986: Extension across the Eocene Okanagan crustal shear in southern British Columbia; Geology, v. 14, p. 318-321.

Thompson, R.I. and Daughtry, K.L.
1994: A new regional mapping project in Vernon map area, British Columbia; in Current Research 1994-A; Geological Survey of Canada, p. 117-122.
1996: New stratigraphic and tectonic interpretations, north Okanagan Valley, British Columbia; in Current Research 1996-A; Geological Survey of Canada, p. 132-141.
1997: Anatomy of the Neoproterozoic-Paleozoic continental margin, Vernon map area, British Columbia; in Current Research 1997-A; Geological Survey of Canada, p. 145-150.

Wheeler, J.O. and McFeely, P.
1992: Tectonic assemblage map of the Canadian Cordillera and adjacent parts of the United States; Geological Survey of Canada, Map 1212A, scale 1:2 000 000.

Geological Survey of Canada Project 930036

Neogene structural elements of northern Cascadia, British Columbia

J. Murray Journeay and Joost van Ulden[1]
GSC Pacific, Vancouver

Journeay, J.M. and van Ulden, J., 1998: Neogene structural elements of northern Cascadia, British Columbia; in Current Research 1998-A; Geological Survey of Canada, p. 195-206.

Abstract: Brittle structures in the Coast Mountain region of northern Cascadia record a history of inhomogeneous deformation that may shed light on the Neogene crustal response to oblique subduction and dextral transcurrent faulting along the Cordilleran plate margin of western North America. Structures in the intra-arc and backarc regions record an older Paleogene history of dextral transpression, and a Neogene history of orogen-parallel compression that likely reflects distributed Pacific/North American plate motions, and the effects of mechanical buttressing at the leading edge of the southern Cascadia forearc. Structures in the northern Cascadia forearc record effects of both orogen-normal and orogen-parallel compression, likely associated with oblique subduction of the Juan de Fuca plate. The pattern and history of strain partitioning provide an important framework for natural hazards assessment, and for exploration of natural resources that may be localized, in part, by brittle faulting and fluid migration in the upper crust.

Résumé : Des structures cassantes dans la région de la chaîne Côtière de la Cascadie du nord témoignent de déformations inhomogènes pouvant jeter la lumière sur la réponse de la croûte néogène à la subduction oblique et au jeu de failles de coulissage dextres le long de la limite de plaque cordillérienne de l'ouest de l'Amérique du Nord. Les structures dans les régions de l'arc interne et de l'arrière-arc témoignent d'une histoire paléogène plus ancienne de transpression dextre et d'une histoire néogène de compression parallèle à l'orogène reflétant vraisemblablement les mouvements répartis des plaques pacifique/nord-américaine ainsi que les effets de l'arc-boutement mécanique le long de la marge frontale de l'avant-arc de la Cascadie du sud. Les structures dans l'avant-arc de la Cascadie du nord enregistrent les effets de la compression à la fois normale et parallèle à l'orogène, liée vraisemblablement à la subduction oblique de la plaque Juan de Fuca. La configuration et l'historique de la répartition des contraintes fournissent un cadre utile pour l'évaluation des risques naturels et pour l'exploration des ressources naturelles dont la localisation est en partie tributaire des mouvements de failles cassantes et de la migration des fluides dans la croûte supérieure.

[1] Geomatics Program, British Columbia Institute of Technology, 3700 Willingdon Avenue, Burnaby, British Columbia V5G 3H2

INTRODUCTION

Geophysical measurements and modelling of the active Cascadia subduction zone (Hyndman et al., 1990, 1996; Wang et al., 1995; Wang, 1996) have shed considerable light on the mechanical and physical processes of oblique underplating along the continental margin of western North America. Yet, we know comparatively little about how continental lithosphere in the upper plate of the subduction complex responds to these dynamic forces over geological time frames of 10-20 Ma. The pattern and history of strain partitioning along the continental margin, and more specifically, the question of whether upper crustal deformation is homogeneously distributed across a broad network of faults with small displacements or concentrated along a few discrete zones of large displacement, remain largely enigmatic.

Understanding the pattern and history of strain partitioning in northern Cascadia has important implications, both for mitigating natural hazards associated with earthquake and landslide activity in the region, parts of which are densely populated, and for the exploration of natural resources, such as epithermal vein deposits and geothermal springs, which are localized along upper crustal zones of brittle faulting and channelled fluid flow. In this paper, we present new data on the orientation and timing of brittle structures in the southern Coast Mountains, and a working hypothesis for interpreting the pattern and history of strain partitioning in the Canadian segment of the northern Cascadia continental margin.

REGIONAL SETTING

The Neogene arc of northern Cascadia (Souther and Yorath, 1991) includes both an older belt of Oligocene and Miocene plutons and erosional remnants of associated volcanic rocks (Pemberton Volcanic Belt), which extend northwestward from Washington to the Queen Charlotte Islands, and a younger belt of en échelon, Plio-Pleistocene volcanic centres (Garibaldi Volcanic Belt), which extend north-northwestward from Howe Sound to the Meager Mountain region, where the two belts intersect (Fig. 1, 2). The change in orientation of the Pemberton and Garibaldi arc segments is coeval with a shift in Pacific plate motion at 5 Ma (see Engebretson et al., 1985), and likely reflects corresponding adjustments to both the Juan de Fuca Ridge system (10-15° clockwise rotation) and the northern Cascadia subduction zone margin. The active part of the Cascadia arc, which extends more than 1200 km southward through Washington, Oregon to northern California, is situated 280-300 km inboard from the Cascadia trench, and is interpreted to have formed by partial melting and thermal upwelling above the subducted Juan de Fuca plate.

The backarc region of northern Cascadia extends more than 200 km inboard from the axis of the Neogene arc (Fig. 1), and includes both localized fault-bounded basins of lacustrine and fluvial-deltaic sedimentary rocks, and overlying plateau basalts of the Chilcotin Group (Bevier, 1983; Souther and Yorath, 1991). Chilcotin Group lavas are coeval with arc volcanics of both the Pemberton and Garibaldi volcanic belts, and are interpreted to be the remnants of a formally extensive backarc volcanic field. Post-Miocene uplift of the Coast Mountains resulted in eastward tilting and erosion of this backarc volcanic field (Parrish, 1983; Mathews, 1989), leaving behind only a few isolated remnants of plateau lavas west of the Fraser and Yalakom faults (Fig. 2).

The Cascadia forearc extends eastward from the Juan de Fuca trench to the Garibaldi volcanic front, and includes Neogene continental margin assemblages of the Cascadia accretionary complex and exhumed pre-Tertiary crystalline rocks of Vancouver Island and the Western Coast Mountains (Fig. 1). The record of Neogene deformation is best preserved in the continental margin forearc succession, where shallow northeast-dipping thrust faults and associated folds of upper Tertiary sedimentary and low-grade metamorphic rocks record a protracted history of margin-normal shortening, imbrication, and uplift associated with northeastward underthrusting of the Juan de Fuca plate (Riddihough and Hyndman, 1991). Southwestward tilting of Miocene and younger erosion surfaces in the Western Coast Mountains, together with patterns of uplift and cooling indicated by

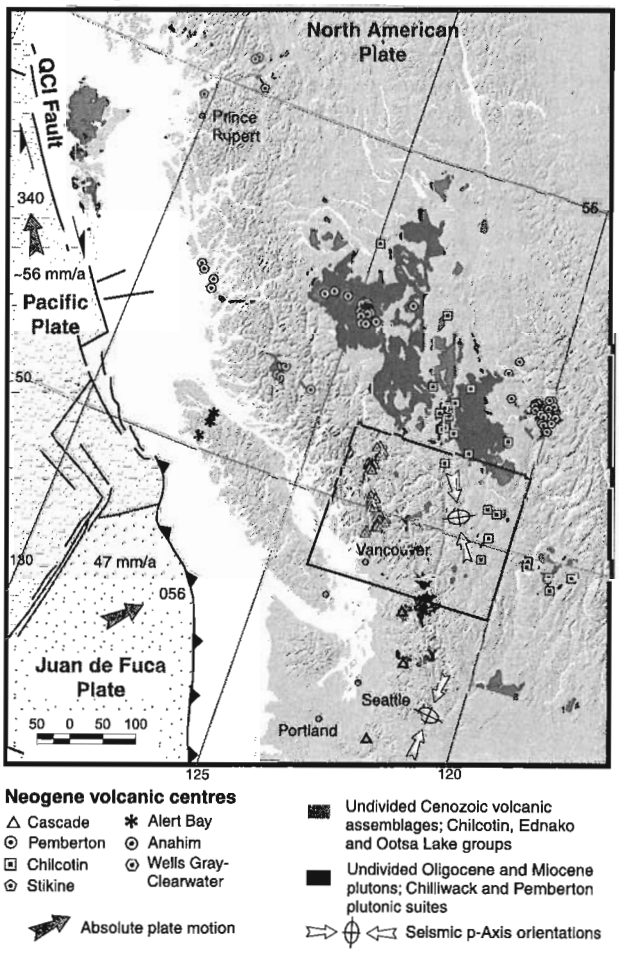

Figure 1. *Neogene framework of northern Cascadia showing distribution of forearc, intra-arc and backarc features of the continental margin.*

regional apatite fission track studies (Parrish, 1983; Currie and Grist, 1996), record a significant component (2-3 km) of Pliocene and Recent (5-0 Ma) uplift in the eastern Cascadia forearc. The cause of this uplift, whether by thermal expansion along the Cascadia arc (Parrish, 1983) and/or by incremental displacement along discrete fault structures, remains uncertain.

Due to the limited exposure of Neogene assemblages in the southern Coast Mountains, and the erosion of surface features during Pleistocene glaciation, we know comparatively little about the pattern and history of Late Cenozoic deformation in the arc and backarc regions of northern Cascadia. Documented examples of Neogene deformation include: 1) displacement along a system of northwest- and northeast-trending, oblique-normal faults in the Coast and northern

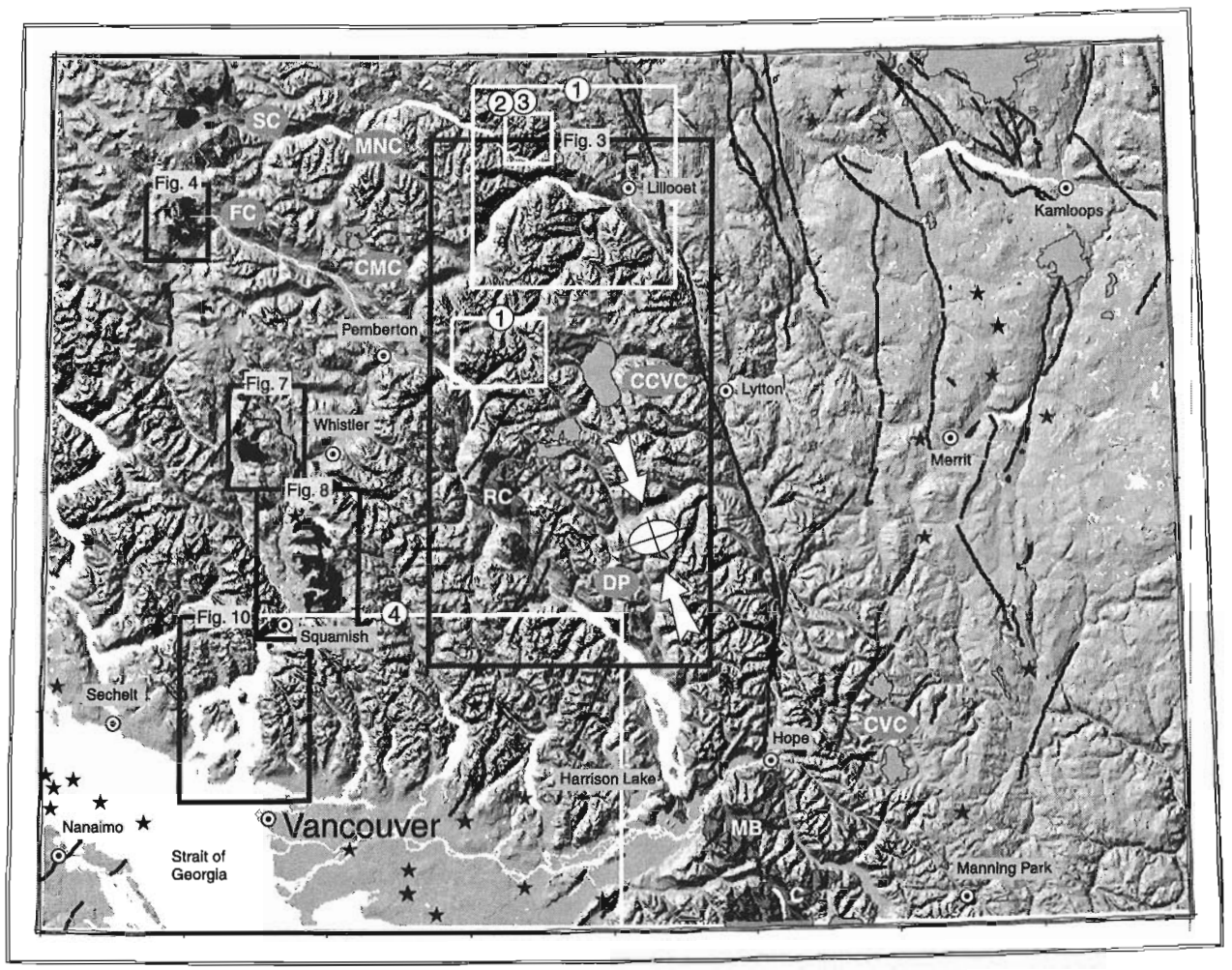

Figure 2. *Digital elevation model of southern Coast Mountain study area showing distribution of Neogene assemblages and fault structures that are presumed to have been active during Neogene deformation.*

Cascade Mountains (Berman and Armstrong, 1980; Journeay and Csontos, 1989; Monger and Journeay, 1994; Mustard and Rouse, 1994); 2) brittle fracturing and tilting of post-Miocene volcanic and sedimentary successions along splays of the Fraser, Pasayten, and Yalakom fault systems (Mathews, 1989); and 3) reactivation of en échelon north- and northeast-trending brittle normal faults in the Interior Plateau region of the Cascadia backarc (Monger, 1989).

Responding to this gap in our understanding of Neogene deformation, B.C. Hydro initiated a comprehensive paleoseismic study of the Cascadia backarc region, with the purpose of characterizing geological hazards of known brittle faults, and identifying seismic risks of potential fault structures near major hydroelectric installations and support facilities (Psutka, 1995). The study, which involved a combination of remote sensing/air photo interpretation and reconnaissance field mapping, identified seventeen potentially significant fault structures that may record evidence of postglacial displacement.

In this study we expand the scope of the B.C. Hydro paleoseismic initiative, and build on the results of previous GSC bedrock mapping programs of Roddick and Hutchison (1971-1975), Monger (1985-1996), and Journeay (1989-1996) in an effort to establish a regional framework for evaluating the Neogene tectonic history of northern Cascadia. Preliminary results indicate that Neogene brittle structures are more widespread than previously suspected and record a multi-stage history of inhomogeneous deformation that likely reflects a process of strain partitioning across the northern Cascadia continental margin.

ARC-BACKARC TRANSITION

The arc-backarc transition zone of the southern Coast Mountains extends eastward from the Harrison Lake-Lillooet River valley to the Fraser Canyon (Fig. 2). Neogene volcanic assemblages in this region include the Crevasse Crag (24 Ma), Anderson Lake, Chipmunk Mountain (26 Ma) and Mount Noel (19 Ma) complexes (Roddick and Hutchison, 1973; Woodsworth, 1977; Coish and Journeay, 1992), erosional remnants of Miocene volcanic flows and flow breccias that were erupted onto the northeastern flank of the Pemberton arc. Volcanic centres in the Crevasse Crag and Mount Noel complexes are aligned in a northeast direction, and are locally intercalated with coarse-grained fluvial sandstone and imbricated channel conglomerate. They are interpreted to have been erupted into a system of northeast-trending paleovalleys that have since been uplifted and incised by younger drainage networks of the eastern Coast Mountains.

Brittle structures believed to have been active during this stage of arc and backarc volcanism are represented by a system of reactivated northeast-trending oblique-normal faults along the Lillooet River valley (Journeay and Csontos, 1989), and by a system of northwest-trending dextral strike-slip faults, the most prominent of which include reactivated portions of the Harrison Lake, Owl Creek, and Marshall Creek faults (Journeay and Csontos, 1989; Journeay and Northcote, 1992). Both sets of fault structures record an older Paleogene history of dextral strike-slip displacement and margin-parallel (NW) extension, and are interpreted to have formed in a transpressional forearc setting (Journeay and Csontos, 1989), during oblique underthrusting of the Farallon plate and accretion of the Pacific Rim and Crescent terranes along the outboard margin of Wrangellia (Hyndman et al., 1990). Following collision, underplating and westward progradation of the accretionary complex in Oligocene time, the locus of arc magmatism in the eastern Coast Mountains shifted westward to a position along the axis of the Pemberton Volcanic Belt. As a result, structures that had initially formed in a forearc setting were reactivated and continued to accommodate episodic Neogene crustal movements in an intra-arc and backarc setting.

The association of Paleogene faults with intrusive breccias and eruptive centres of the Crevasse Crag complex (24 Ma) suggests that these structures may have acted as structural conduits for the effusion of volcanic material, and likely controlled the geometry of drainage basins into which the volcanic rocks accumulated. Geochemical signatures of basaltic andesites near the base of the Crevasse Crag Complex, and the northeast elongation of epizonal plutons along the axis of the Pemberton Belt (e.g., Doctors' Point pluton) are consistent with this interpretation (Coish and Journeay, 1992). Other documented examples of reactivated Neogene brittle structures in the arc-backarc region include syndepositional fault-bounded basins of the Miocene (21 Ma) Coquihalla Volcanic Complex (Berman and Armstrong, 1980), tilted and deformed Pliocene lavas along the northern extension of the Fraser Fault (Mathews, 1989), and dextral strike-slip displacements of Holocene sediments along the trace of the Hell Creek Fault (Psutka, 1995).

While it is clear that Neogene deformation in the Cascadia backarc was accommodated in part by reactivation of older Paleogene structures, new data presented in this study indicate that active brittle deformation (e.g., coulomb-type failure) also occurred throughout the Neogene. Measurements of over 300 structures reveal well defined sets of brittle faults, fractures, and extensional dykes that are inclined with respect to older Paleogene structures (compare Fig. 3a, d, e). Mafic dykes, presumed to be of Neogene age, display a strong preferred orientation to the north-northwest (340°-350°), while brittle faults and fractures define strong north (360°) and northwest (320°-330°) trends (Fig. 3b, c, respectively). The apparent conjugate relationship of brittle fault/fracture sets, together with extensional dykes that align with the acute bisectrix of these structures, suggest that they likely formed in response to margin parallel, north-northwest (~340-350) compression, with associated extension directed nearly perpendicular (070-080) to the axis of the Pemberton Volcanic Belt. Although kinematic data are sparse for the region, documented cases of dextral strike-slip along the northwest-trending fault set, and sinistral or normal oblique slip along the north-trending fault set, are consistent with a history of margin-normal shortening.

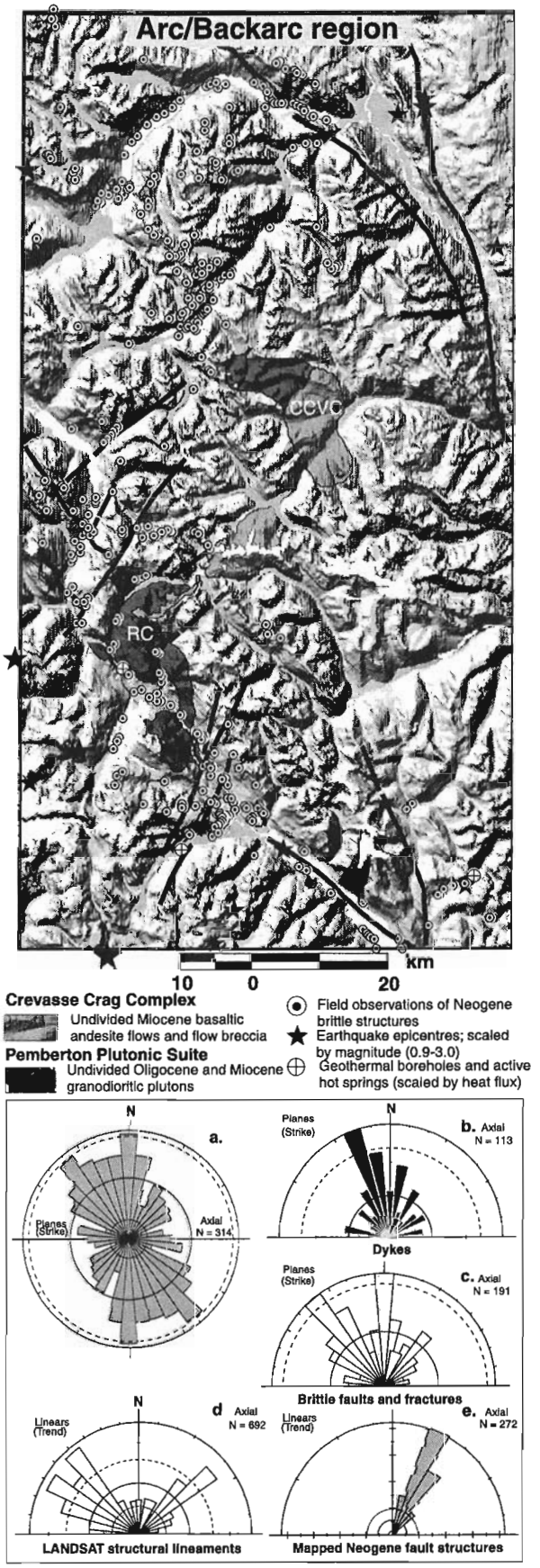

Figure 3. *Digital elevation model of study area in northern Cascadia backarc and synoptic histograms of observed brittle structures.*

INTRA-ARC

The record of Neogene deformation in the Cascadia intra-arc is similar to that documented in the backarc region, and includes both the reactivation of older northeast-trending Paleogene structures, and the development of coulomb-type brittle faults and related fractures, that locally outlast eruption of Garibaldi Group volcanics in the Plio-Pleistocene segment of the arc.

Pemberton Volcanic Belt

The intrusive core of the Pemberton Volcanic Belt is represented by a chain of Oligocene and Miocene epizonal plutons that extend northwestward through the Cascade and southern Coast Mountains (Fig. 2; Souther and Yorath, 1991). From south to north, these include the Silver Creek Stock (35 Ma), the Chilliwack Batholith (29-26 Ma), the Mount Barr Batholith (21-16 Ma), the Harrison Lake Pluton (24-19 Ma), Doctor's Point Pluton (24 Ma), Rogers' Creek Pluton (16 Ma), Fall Creek Pluton (9-10 Ma), and the Salal Creek Pluton (8 Ma). Many of these plutons are elongate to the northeast or northwest and appear to have been structurally emplaced along older Paleogene fault structures.

Rogers' Creek Pluton is an elongate, north-northwest-trending body of granodiorite and tonalite with a distinctive sigmoidal shape defined by north-northeast-trending apophyses at both its north and south ends. Its core is defined by a north-northwest-trending tabular sheet of coarse-grained granodiorite, which becomes increasingly more miarolitic along strike to the north, and at its northeast-trending termination along Rogers Creek, where it intrudes older Miocene lavas of the Crevasse Crag Complex in what is interpreted to be a north-northeast-trending fault-bounded graben (Fig. 3).

The Fall Creek (10-9 Ma) and Salal Creek (8 Ma) plutons are elongate to the northwest and northeast, respectively, and are aligned with steep Bouger gravity gradients that flank a prominent gravity low in the Bridge River "highlands" of the central Coast Mountains (Fig. 2). Gravity profiles across these steep gradients are nearly symmetrical, suggesting possible fault offsets of underlying crystalline rocks, an interpretation that is consistent with documented occurrences of northeast-trending silicic dykes and shear zones in the Salal Creek Pluton, which are interpreted to have formed "along a northeasterly-trending axis of uplift that was active during emplacement and crystallization of the pluton," (Stephens, 1972, as reported by Souther and Yorath, 1991).

Collectively, these observations suggest that components of both margin-normal and margin-parallel extension were active along the axis of the Pemberton Volcanic Belt throughout the Miocene. Crustal extension was accommodated in part by reactivation of north-northeast- and northwest-trending Paleogene faults, and by displacements along north- and northwest-trending Neogene structures. The pattern of orthogonal extension suggests that the north-northwest-trending component of margin-parallel shortening, as recorded by brittle structures in the Cascadia backarc region (Fig. 3), was likely balanced by a vertical component of uplift

associated with thermal expansion and/or pluton emplacement along the axis of the arc. This interpretation is corroborated by zircon and apatite fission track studies (Parrish, 1983), which record episodic uplift of ~0.1 km/Ma in Late Oligocene and Miocene time (30-10 Ma), followed by accelerated uplift of 0.6 km/Ma along the axis of the arc in Miocene to Recent time (10-0 Ma).

Garibaldi Volcanic Belt

The Garibaldi Volcanic Belt (Mathews, 1958; Souther, 1977) is made up of three en échelon, north-trending volcanic centres, often referred to in the literature as the northern, central, and southern segments of the northern Cascadia arc. The volcanic stratigraphy and eruptive histories of these volcanic centres are well documented and summarized by Green et al. (1988) and Souther and Yorath (1991). In this paper, we concentrate primarily on the geometry and timing of basement structures that may have localized these eruptive centres, and the implications of these structures for Neogene crustal deformation in this part of the Cascadia arc.

Northern segment

The northern segment of the Garibaldi Volcanic Belt includes north-trending hypabyssal intrusions and overlapping volcanic successions of the Meager Mountain complex, and erosional remnants of coeval volcanic flows preserved in the Bridge River "highlands" to the northeast. Both suites of volcanic rock are constructed in part on previously uplifted and dissected epizonal Miocene plutons of the Pemberton Volcanic Belt (Fall Creek and Salal Creek plutons; see Fig. 2). Meager Mountain complex (Fig. 4) is a composite Pleistocene-Holocene volcano comprising an early eruptive phase, which produced rhyodacite and associated pyroclastic rock (2.2-1.9 Ma), followed by two episodic phases involving the intrusion of hypabyssal plutons and the eruption of associated porphyritic flows (1.9-015 Ma and 0.15-0.1 Ma), and a final explosive phase involving the eruption of scoriaceous lava, tephra, and ash layers, the youngest of which are dated at 2490 years BP (Green et al., 1988).

Structural measurements of 231 brittle structures involving intermediate eruptive phases of the Meager Mountain complex (1.9-0.15 Ma) and underlying plutonic and metamorphic basement rocks of the Western Coast Belt reveal a pattern of deformation that resembles that documented in older Miocene rocks of the Pemberton Volcanic Belt. Mafic dykes, presumed to be part of the Meager Mountain complex, record a wide spectrum of orientations (Fig. 4b), suggesting a pattern of plane strain likely associated with vertical uplift centred beneath the volcanic complex. Hypabyssal intrusions and relic hydrothermal vent complexes young to the north and appear to be structurally localized along distinct north-northwest-trending (~340°) zones that reflect a regional component of margin-parallel compression.

Brittle faults and associated fracture sets, marked by narrow (0.5-1 m) zones of brecciation, clay gouge and hydrothermal alteration (Fig. 5, 6), show strong preferred orientations to the north (005°) and northwest (340°) in the

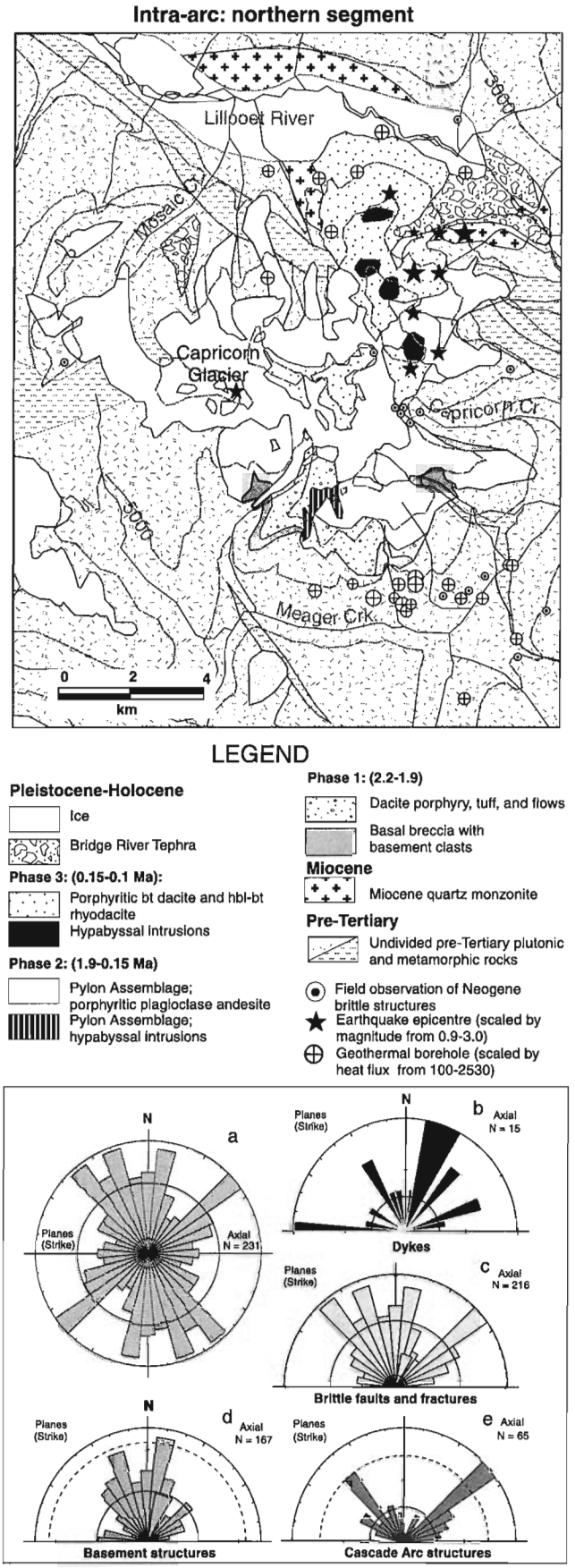

Figure 4. *Simplified geological map of the northern segment of the Garibaldi Volcanic Belt and synoptic histograms of observed brittle structures.*

basement complex, and to the northwest (320°) and northeast (050°) in overlying Pleistocene volcanic rocks of the Meager Mountain complex (Fig. 4d, e, respectively). Available kinematic data, including conjugate shear fractures, extension veins, and offset mafic dykes in the basement complex, record sinistral strike-slip and normal dip-slip displacements along north- and northwest-trending faults, respectively, suggesting a history of margin-parallel compression, similar to that documented in the backarc region. Brittle fault sets in the overlying Pleistocene volcanics record mainly normal dip-slip displacement and are aligned with regional northeast- and northwest-trending Paleogene structures that localize Miocene epizonal plutons of the adjacent Pemberton Volcanic Belt (Fall Creek and Salal Creek plutons). They are interpreted to have formed by reactivation of underlying basement structures during rapid Pleistocene-Recent uplift along the axis of the Garibaldi Volcanic Belt.

Central segment

The central segment of the Garibaldi Volcanic Belt is defined by a north-northwest-trending chain of eight distinct volcanic centres situated along Mount Fee, Mount Cayley, and adjacent parts of the Powder Mountain Range, and by basaltic flows localized along the upper Squamish and Callaghan creek drainages (Fig. 7). Volcanic complexes range in age from 3.8 to 0.25 Ma and record an episodic history of hypabyssal intrusion, and eruption of compositionally heterogeneous flows and associated pyroclastic rocks (see Green et al., 1988 for details).

Figure 5. *View southeastward along trace of fracture zone in volcanic breccia of Meager Mountain Complex (foreground) and of underlying brittle faults of the basement complex (in distance).*

Figure 6. *Brittle fault marked by zone of intense fracturing, clay gouge, and hydrothermal alteration, cutting 1.0-0.5 Ma volcanic flows of the Meager Mountain Complex.*

Field relationships documented by Souther and Yorath (1991) indicate that eruption of these volcanic centres is likely to have been localized along sets of en échelon north- and northwest-trending fault zones. Brittle faults are locally marked by networks of hydrothermally altered fractures and associated geothermal springs (Mount Cayley complex), and by metre-wide dilatant zones of intense brecciation (Mount Fee complex) along which intrusive rhyodacite is quenched to thin selvages (40-50 cm) of granular porphyritic glass.

Independent measurements of 420 structures define a prominent north-northwest-trending pattern of high-angle brittle faulting and related fracturing, involving both plutonic rocks of the underlying basement complex and Plio-Pleistocene volcanic rocks of the overlying Garibaldi Group (Fig. 7a-e). Available kinematic data, mainly conjugate shear

fractures and offset mafic dykes, record a history of right-lateral oblique and normal dip-slip displacement along north-northwest-trending (330°-340°) faults, and normal dip-slip displacement along north-northeast-trending (350°-010°) faults.

The preferred orientations of mafic dykes (Fig. 7b) and the kinematics of associated brittle shear zones provide further evidence that eruptive centres in this part of the Garibaldi Volcanic Belt were structurally controlled along a system of brittle faults that likely accommodated a significant component of margin-parallel compression. The alignment of brittle structures in both plutonic basement and volcanic cover and the offset of mafic dykes, presumed to be feeder pipes to overlying volcanic rocks of the Garibaldi Group, suggest that margin-parallel compression along this segment of the Cascadia arc was active through the Pliocene and into the Pleistocene.

Southern segment

The southern segment of the Garibaldi Volcanic Belt (Mathews, 1958) comprises a chain of four composite volcanic centres and associated late glacial basaltic flows that extend northwestward through Garibaldi Provincial Park, between the Mamquam and Cheakamus rivers (Fig. 8). Major volcanic phases are represented by a preglacial succession of interleaved andesitic breccia, lahar and overlying columnar basalt, believed to have been erupted into a series of prominent north- and northeast-trending paleotopographic valleys (Mathews, 1958); overlapping successions of Pelean tuff breccia, dacite flows, and associated pyroclastic rocks that were erupted beneath and onto regionally extensive Pleistocene icesheets; and a series of late glacial valley basalts that were channelled in river drainages developed along the flanks of the exhumed volcanic complex (see Green et al., 1988, for details).

Neogene structures in this segment of the Garibaldi Volcanic Belt record a pattern of deformation similar to that documented in the north and central segments of the Cascadia arc (Fig. 8a). North-northwest-trending fault zones, marked in basement rocks by 1-2 m zones of brecciation, clay gouge, and associated hydrothermal alteration, seem to have acted as conduits for the intrusion of mafic dykes (Fig. 9) and for the effusion of pyroclastic volcanic material in vent regions located along upper Ring Creek valley, and on Gargoyle Peak. The orientation of these structures reflects a history of margin-parallel compression. Evidence for Pleistocene reactivation of these fault systems include dextral offsets of mafic dykes across both northwest-trending (~330°) and east-trending (095°) fault splays at the head of Ring Creek, and the local development of north-trending (010°) breccia and gouge zones in Holocene flows of the Ring Creek Complex. Preferential development of orthogonal northeast-trending (050°) and northwest-trending (300°) fracture sets in volcanic rocks of the Garibaldi Group (Fig. 8e) suggests reactivation of older Paleogene structures.

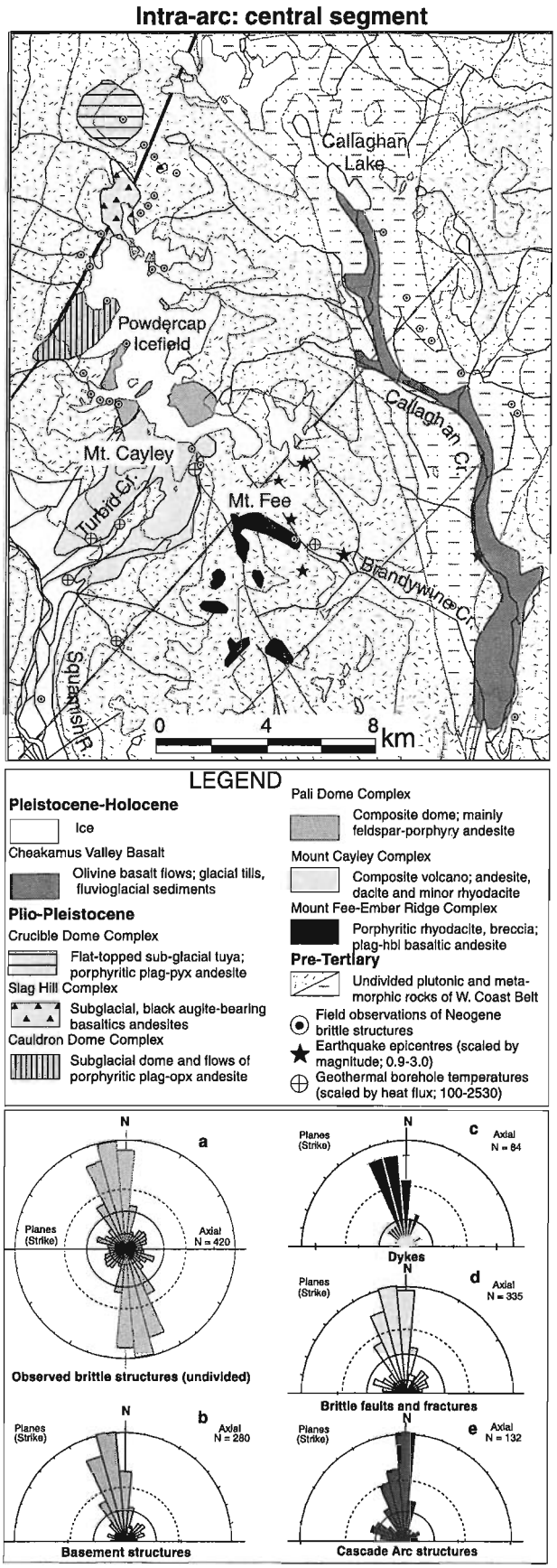

Figure 7. *Simplified geological map of the central segment of the Garibaldi Volcanic Belt and synoptic histograms of observed brittle structures.*

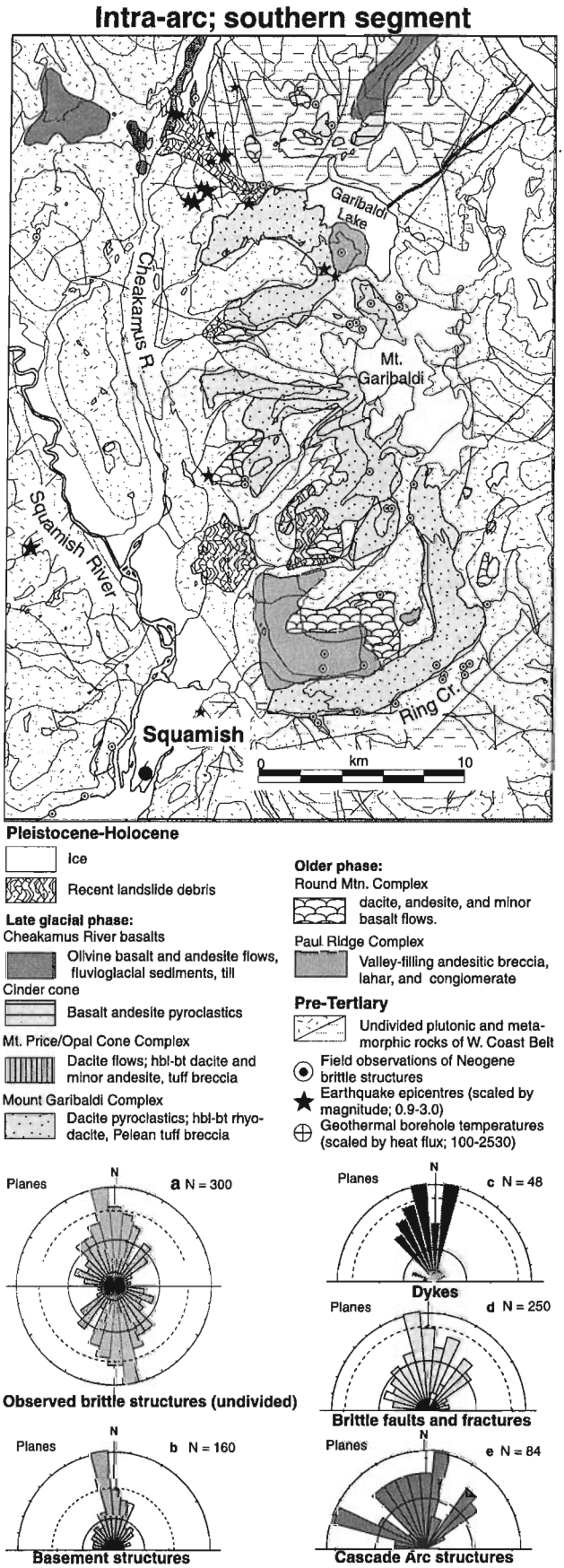

Figure 8. *Simplified geological map of the southern segment of the Garibaldi Volcanic Belt and synoptic histograms of observed brittle structures.*

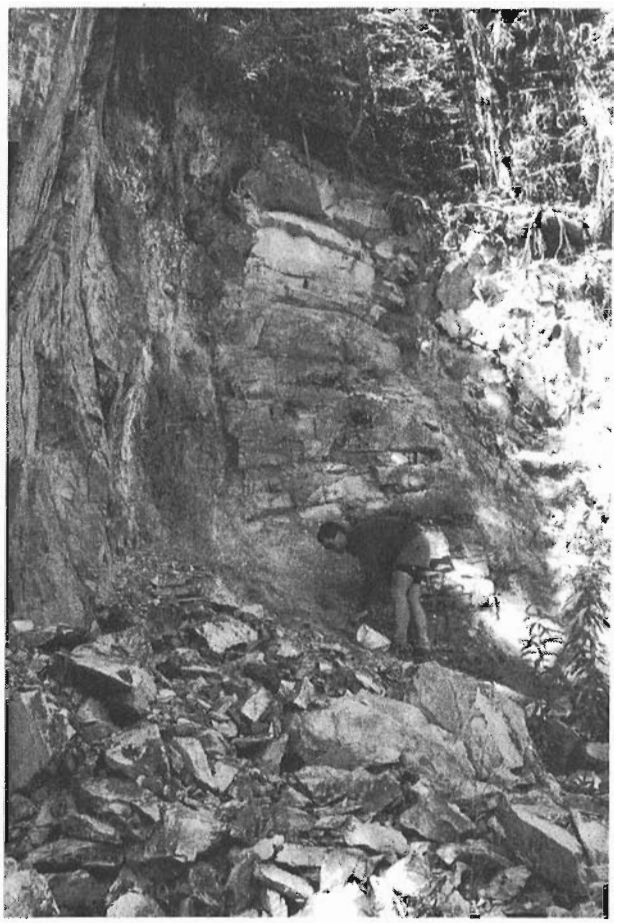

Figure 9. *North-trending brittle fault zone in basement complex, cut by mafic dyke presumed to be a feeder to overlying Garibaldi Group volcanic rocks (dating in progress).*

FRONTAL ARC

Analysis of Neogene structures in the frontal arc region of northern Cascadia was limited to reconnaissance mapping along the coastline of Howe Sound, where older basement rocks of the western Coast Belt record a complex, but distinct history of brittle deformation (Fig. 10). Digital elevation models and airphoto interpretations of the Howe Sound region and adjacent parts of the southern Coast Mountains (English, 1996) delineate prominent sets of north-northeast-trending (~020°), northeast-trending (050°), northwest-trending (320°), and west-northwest-trending (~280°) lineaments that are interpreted to be structurally controlled. Measurement of more than 500 brittle structures along the shore of Howe sound (Fig. 10a, b, c) confirms that many of these lineament trends are represented in the field by narrow zones of brittle faulting and associated fracturing. Faults are typically 0.25-0.5 m wide and are marked by concentrated zones of intense fracturing, brecciation, and local development of clay gouge.

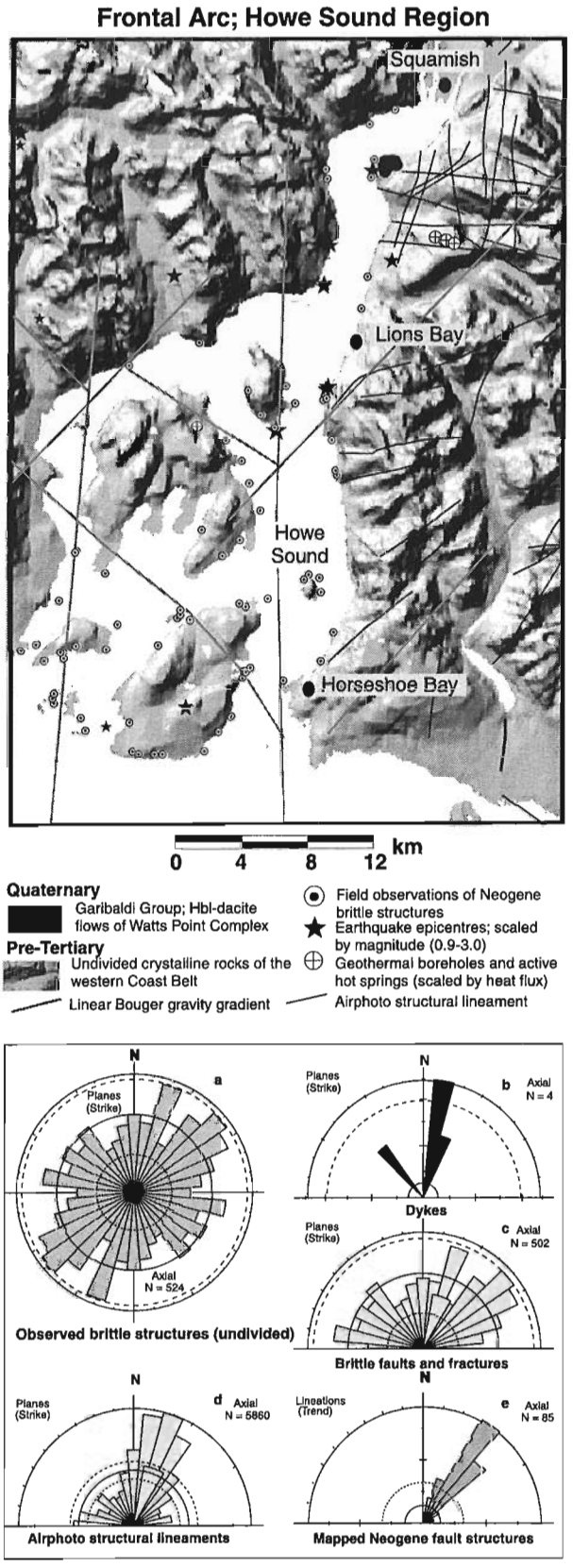

Figure 10. *Digital elevation of the Cascadia forearc in the Howe Sound region and synoptic histograms of observed brittle structures.*

Dominant structures are aligned with north-northeast-, northeast-, and northwest-trending Paleogene faults, which are interpreted to have formed initially by margin-normal compression in a forearc setting, prior to the westward shift in arc magmatism in late Eocene/Early Oligocene time. Kinematic indicators, although well developed along many of the Howe Sound fault structures, do not record a consistent sense of displacement from region to region, suggesting a complex, multistage history of faulting and reactivation. Although the interpretation of these structures remains uncertain, it is clear that Neogene patterns of margin-parallel compression, which dominate the intra-arc and backarc regions, represent a smaller component of overall crustal strain in this part of the Cascadia forearc.

WORKING HYPOTHESIS

A working hypothesis for the evolution of Neogene structures in northern Cascadia is summarized in Figure 11. Our interpretation is based in part on plate reconstruction models of Engebretson et al. (1985), which predict orthogonal subduction of the Juan de Fuca plate along the western margin of North America throughout the Late Paleogene and Neogene, and on the observations of Jarrard (1986) and Fitch (1972), which demonstrate that orthogonal subduction of relatively young oceanic crust is likely to result in mechanical decoupling of the overriding plate, with the margin-normal

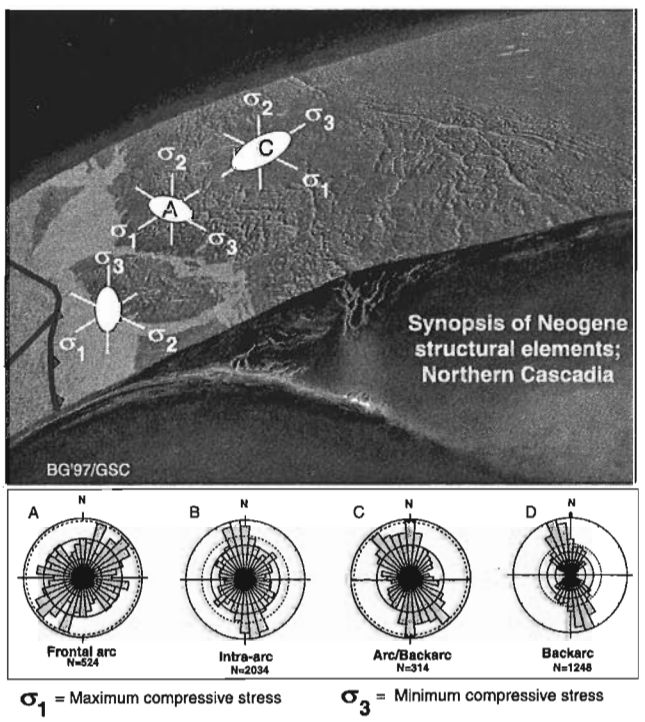

Figure 11. *Summary histograms of observed brittle structures and proposed working hypothesis for Neogene deformation in northern Cascadia.*

component of displacement concentrated in the forearc, and the margin-parallel component of displacement concentrated in the arc and backarc regions.

We interpret the pattern of margin-parallel compression in the arc and backarc regions of the southern Coast Mountains to be a consequence of mechanical buttressing at the leading edge of the Oregon Coast Range block, a decoupled forearc sliver of the southern Cascadia subduction zone which has undergone northward translation and clockwise rotation since Late Miocene time (<20 Ma; Walcott, 1993). This interpretation is consistent with predictions of incremental stress variation along the Cascadia margin, as modeled by Wang (1996), and with measured margin-parallel compressive stress deduced from earthquake first-motion studies (Wang et al., 1995).

The nature of Neogene deformation in the forearc region is less clear, but likely reflects a component of margin-normal shortening associated with northeastward underthrusting of the Juan de Fuca plate. In the Cascadia accretionary complex, where the intermediate compressive stress axis is presumed to have been horizontal throughout the Neogene, shortening is accommodated by imbrication along low-angle thrust faults. In the eastern forearc and frontal arc regions, where intermediate compressive stress is vertical, shortening is accommodated by displacements along integrated systems of strike-slip and margin-normal extension faults. The implication is that Neogene deformation is inhomogeneously distributed across the northern Cascadia margin, possibly due to mechanical decoupling and dextral strike-slip faulting along the western flank of the Pemberton and Garibaldi volcanic belts, where elevated heat flow associated with thermal upwelling and pluton emplacement in the arc resulted in substantial weakening of the crustal lithosphere.

ACKNOWLEDGMENTS

Many of the ideas expressed in this paper have evolved through discussions with colleagues Jim Monger and Kelin Wang of the GSC Pacific Division, and with John Psutka, who contributed information compiled as part of the B.C. Hydro Paleoseismic Initiative. We thank Tom Bell and fellow rangers of Garibaldi Park for arranging boat access to the Sentinal Bay research station, and Pemberton Helicopters for their help in coordinating air support during a busy fire season. Processing of LANDSAT remote sensing and airphoto lineament data were made possible through AML programs written by Stephen Williams of the GSC Vancouver office. We thank Jim Monger for critical review of the manuscript.

REFERENCES

Berman, R.G. and Armstrong, R.L.
1980: Geology of the Coquihalla complex, southwestern British Columbia; Canadian Journal of Earth Sciences, v. 17, p. 985-995.

Bevier, M.L.
1983: Regional stratigraphy and age of Chilcotin Group basalts, south-central British Columbia; Canadian Journal of Earth Sciences, v. 20, p. 515-524.

Campbell, K.V.
1994: Paleoseismic study of Bridge River area, report no. 1, Preliminary results of remote sensing investigation, Southwestern British Columbia, NTS 92I, J, and O; unpublished report by ERSI-Earthsat Resource Surveys, Inc. to B.C. Hydro, 5 May 1994.

Clague, J.J. and Evans, S.G.
1994: The Crevasse Crag volcanic complex, southwestern British Columbia: Structural controls on the geochemistry of arc magmas; in Current Research 1994-A; Geological Survey of Canada, p. 193-200.

Coish, R.A. and Journeay, J.M.
1992: The Crevasse Crag volcanic complex, southwestern British Columbia: Structural controls on the geochemistry of arc magmas; in Current Research, Part A; Geological Survey of Canada, Paper 92-1A, p. 95-103.

Currie, L.D. and Grist, A.M.
1996: Diachronous low-temperature Paleogene cooling of the Alberni Inlet area, southern Vancouver Island, B.C.: evidence from apatite fission track analyses; in Current Research 1996-A; Geological Survey of Canada Paper, p. 119-128.

Engebretson, D.C., Cox, A., and Gordon, R.G.
1985: Relative motions between oceanic and continental plates in the Pacific basin; Geological Society of America Special Paper, v. 206, 59 p.

English, R.
1996: Lineament analysis of the southwestern Coast Mountains; MSc. thesis, University of British Columbia, Vancouver, British Columbia.

Fitch, T.J.
1972: Plate convergence, transcurrent faults, and internal deformation adjacent to southeast Asia and the western Pacific; Journal of Geophysical Research, v. 77, p. 4432-4460.

Green, N.L., Armstrong, R.L., Harakal, R.L., Souther, J.G., and Read, P.B.
1988: Eruptive history and K-Ar geochronology of the late Cenozoic Garibaldi volcanic belt, southwestern British Columbia; Geological Society of America Bulletin, v. 100, p. 563-579.

Hyndman, R.D., Rogers G., Dragert, H., Wang, K., Clague, J.J., Adams, J., and Bobrowsky, P.T.
1996: Giant earthquakes beneath Canada's west coast; Geoscience Canada, v. 23, p. 63-72.

Hyndman, R.D., Yorath, C.J., Clowes, R.M., and Davis, E.E.
1990: The northern Cascadia subduction zone at Vancouver Island: seismic structure and tectonic history; Canadian Journal of Earth Sciences, v. 27, p. 313-329.

Jarrard, R.D.
1986: Relations among subduction parameters; Reviews of Geophysics, v. 24, p. 217-284.

Journeay, J.M. and Csontos, L.
1989: Preliminary report on the structural setting along the southeast flank of the Coast Belt, British Columbia; in Current Research, Part A; Geological Survey of Canada, Paper 89-1A, p. 177-187.

Journeay, J.M. and Northcote, B.R.
1992: Tectonic assemblages of the eastern Coast Belt, southwest British Columbia; in Current Research, Part A; Geological Survey of Canada, Paper 92-1A, p. 215-224.

Mathews, W.H.
1958: Geology of the Mount Garibaldi map-area, southwestern British Columbia, Canada: Part 1, Igneous and metamorphic rocks; Part 2, Geomorphology and Quaternary volcanic rocks; Geological Society of America Bulletin, v. 69, p. 161-198.
1989: Neogene Chilcotin basalts in south-central British Columbia: geology, ages, and geomorphic history; Canadian Journal of Earth Sciences, v. 26, p. 969-982.

Monger, J.W.H.
1989: Geology of Hope and Ashcroft map areas, B.C.; Geological Survey of Canada, Map 41-1989 and 42-1989 (scale 1:250 000).

Monger, J.W.H. and Journeay, J.M.
1994: Guide to the geology and tectonic evolution of the southern Coast Belt; Geological Survey of Canada, Open File 2940, 77 p.

Mustard, P.S. and Rouse, G.E.
1994: Stratigraphy and evolution of Tertiary Georgia Basin and subjacent Upper Cretaceous sedimentary rocks, southwestern British Columbia and northwestern Washington State; in Geology and Geological Hazards of the Vancouver Region, Southwestern British Columbia, (ed.) J.W.H. Monger; Geological Survey of Canada, Bulletin 481, p. 97-169.

Parrish, R.R.
1983: Cenozoic thermal evolution and tectonics of the Coast Range of British Columbia: 1. Fission track dating, apparent uplift rates and patterns of uplift; Tectonics, v. 2, p. 601-631.

Psutka, J.F.
1995: Paleoseismic study of the Bridge River area, southwestern British Columbia; B.C. Hydro Maintenance, Engineering and Projects Report, v. MEP40.

Riddihough, R.R. and Hyndman, R.D.
1991: Modern plate tectonic regime of the continental margin of western Canada, Chapter 13; in Geology of the North American Orogen in Canada, H. Gabrielse and C.J. Yorath (ed.); Geological Survey of Canada, Geology of Canada, no. 4, p. 435-455 (also Geological Society of America, The Geology of North America, v. G-2).

Roddick, J.A. and Hutchison, W.W.
1973: Pemberton east-half; Geological Survey of Canada, Map 13-1973.

Souther, J.G.
1977: Volcanism and tectonic environments in the Canadian Cordillera - a second look; in Volcanic Regimes in Canada, (ed.) W.R.A. Barager et al.; Geological Association of Canada Special Paper, v. 16, p. 3-24.

Souther, J.G. and Yorath, C.J.
1991: Neogene assemblages, Chapter 11; in Geology of the Cordilleran Orogen in Canada, H. Gabrielse and C.J. Yorath (ed.); Geological Survey of Canada, Geology of Canada, no. 4, p. 373-410 (also Geological Society of America, The Geology of North America, v. G-2).

Walcott, R.I.
1993: Neogene tectonics and kinematics of western North America; Tectonics, v. 12, p. 326-333.

Wang, K.
1996: Simplified analysis of horizontal stresses in a buttressed forearc sliver at an oblique subduction zone; Geophysical Research Letters, v. 23, no. 16, p. 2021-2024.

Wang, K., Mulder, T., Rogers, G.C., and Hyndman, R.D.
1995: Case for very low coupling stress on the Cascadia subduction fault; Journal of Geophysical Research, v. 100, p. 907-918.

Woodsworth, G.J.
1977: Pemberton (92J) map area, British Columbia; Geological Survey of Canada, Open File 482.

Geological Survey of Canada Project 930036

New geophysical data from the Yahk map area, southeastern British Columbia – part of the East Kootenay multiparameter geophysical survey

C. Lowe[1], D.A. Brown[2], M.E. Best[3], R. Woodfill[4], and C. Kennedy[4]
GSC Pacific, Vancouver

Lowe, C., Brown, D.A., Best, M.E., Woodfill, R., and Kennedy, C., 1998: New geophysical data from the Yahk map area, southeastern British Columbia – part of the East Kootenay multiparameter geophysical survey; in Current Research 1998-A; Geological Survey of Canada, p. 207-216.

Abstract: High-resolution electromagnetic, aeromagnetic, and gamma-ray spectrometric data were recently acquired in a 500 km^2 area in the Yahk map area (82F/1), southeastern British Columbia. An initial analysis of these data, coupled with brief ground follow-up investigations, has led to the identification of previously unmapped Moyie sills, and shown that the orientation of an inferred fault in the Russell Creek area is more north-trending than previously thought. There are relatively few non-cultural finite electrical conductors identified in the Yahk area. In addition, the lower Creston Formation is very magnetic here and faults are commonly associated with linear zones of steep magnetic gradient. Surficial sediments infilling some of the major drainages are conductive and magnetic and may have placer potential.

Résumé : Des données électromagnétiques, aéromagnétiques et spectrométriques gamma à haute résolution ont été acquises récemment dans une région de 500 km^2 dans la région cartographique de Yahk (82F/1), dans le sud-est de la Colombie-Britannique. Une analyse initiale de ces données couplée à de brèves recherches de suivi sur le terrain a débouché sur l'identification de filons-couches de Moyie jusqu'ici non cartographiés et a démontré qu'une faille dont l'existence est inférée dans la région du ruisseau Russell a une direction plus vers le nord qu'on ne le croyait antérieurement. Il existe relativement peu de conducteurs électriques finis non anthropiques qui aient été identifiés dans la région de Yahk. En outre, la partie inférieure de la formation de Creston est ici très magnétique et les failles sont en général associées à des zones linéaires de fort gradient magnétique. Les sédiments superficiels remplissant certains des principaux bassins hydrographiques sont conducteurs et magnétiques et recèlent peut-être un potentiel placérien.

[1] GSC Pacific, Natural Resources Canada, P.O. Box 6000, 9860 West Saanich Road, Sidney, British Columbia V8L 4B2
[2] British Columbia Geological Survey Branch, Ministry of Employment and Investment, 1810 Blanshard Street, Victoria, British Columbia V8W 9N3
[3] Bemex Consulting International, 5288 Cordova Bay Road, Victoria, British Columbia V8Y 2L4
[4] Abitibi Mining Corporation, Cranbrook Field Office, 3380 Wilks Road, P.O. Box 215 Main Station, Cranbrook, British Columbia V1C 4H7

INTRODUCTION

Data acquisition of the East Kootenay multiparameter geophysical survey was completed in 1996 when high-resolution aeromagnetic, radiometric, and electromagnetic data were acquired in the Yahk survey area. This 500 km^2 area lies just north of the international border with the U.S.A., extending from 5 km east of Creston to 5 km east of Yahk in southeastern British Columbia (Fig. 1, area 3).

As part of the same survey, similar data were previously acquired in the St. Mary and Findlay areas to the north of Yahk (British Columbia Ministry of Employment and Investment, 1996). Lowe et al. (1997a) describe how the data in these areas augment our understanding of the regional geology, and Brown et al. (1997) discuss how the geophysical signatures associated with known mineral occurrences provide useful guides for future mineral exploration in the Purcell Supergroup.

Data acquisition in all three survey areas was funded by the Government of British Columbia and co-ordinated by the Geological Survey of Canada. Flight lines were east-trending, spaced approximately 400 m apart, and flown at a mean terrain clearance of 60 m. The geophysical tools utilized were identical in all survey areas and are described in Lowe et al. (1997a).

Here we describe the Yahk data set, emphasizing those areas where the geophysical responses are anomalous. We evaluate their utility for geological mapping and mineral exploration. While much of our evaluation is based on correlations observed among the geophysical parameters, follow-up ground investigations were required for rock property measurements and constraining anomaly sources. This article serves as an interpretation guide to the 1:50 000 scale Open File images of the data (British Columbia Ministry of Employment and Investment, 1996) and the reader is advised to refer to the published images to accurately locate features discussed in this text. A Landsat image (Kung et al., 1997) covering this region is useful for interpretation of the radiometric data.

GEOLOGICAL SETTING

The Yahk survey area is underlain entirely by the Purcell Supergroup, a thick succession of siliciclastic and subordinate carbonate rocks that accumulated in a pericratonic basin during the middle Proterozoic (Fig. 1). The supergroup is preserved in an area extending from southeastern British Columbia to eastern Washington, Idaho, and western Montana. In British Columbia, the succession is at least 12 km thick and exposed in a broad, gently north-plunging, structural culmination, the Purcell Anticlinorium. The Aldridge Formation, the basal part of the supergroup, hosts the Sullivan sedimentary exhalative (Sedex) lead-zinc deposit. The Aldridge Formation is more than 3500 m thick and was deposited in deep water as turbidites. It contains distinctive laminated siltstone marker units (laminates), is intruded by numerous metagabbros (the 'Moyie Intrusions'), and has disseminated pyrrhotite throughout.

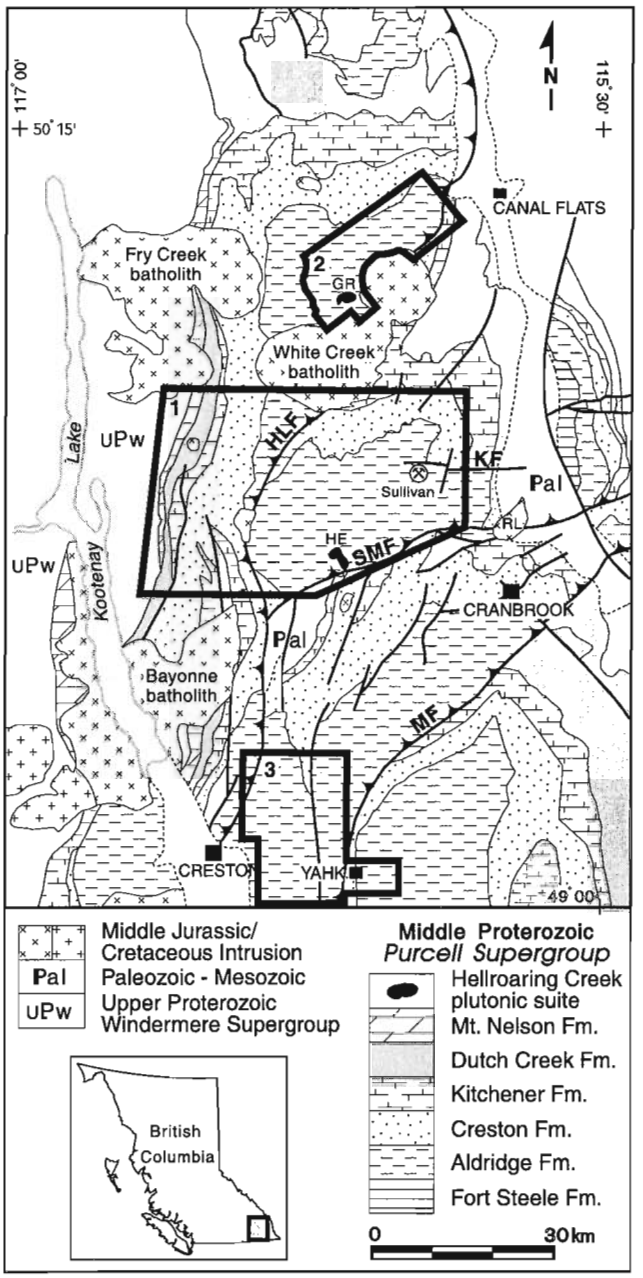

Figure 1. *Regional geological setting of the Purcell Supergroup (modified from Höy et al., 1995). The locations of the three survey areas constituting the East Kootenay multiparameter geophysical survey are outlined: 1, Findlay area; 2, St. Mary River area; 3, Yahk area. Abbreviations are as follows: GR, Greenland Creek stock; HE, Hellroaring Creek stock; HLF, Hall Lake fault; KF, Kimberley Fault; MF, Moyie fault; RL, Reade Lake pluton; SMF, St. Mary fault.*

The Creston Formation, which gradationally overlies the Aldridge Formation, is composed of quartz wackes, siltstones, and argillites. It contains at least three stratabound copper-silver deposits (Troy, Montanore, and Rock Creek). It is about 2300 m thick and in the Yahk survey area is best exposed in the footwall of the Moyie Fault and on the west side of the Carroll Fault (Fig. 2). The overlying Kitchener Formation, which includes the lowermost significant carbonate accumulation in the Purcell succession, is also exposed in the footwall of the Moyie Fault.

The Moyie Intrusions are dominantly sills, but include rare dykes. They are fine- to medium-grained, massive hornblende (± pyroxene) metagabbro to hornblende quartz diorite and hornblendite. They vary from less than 10 m to more than 300 m thick.

MINERAL OCCURRENCES

Forty-three mineral occurrences are recorded in the provincial Minfile data base for the Yahk map sheet (Fig. 2). With the exception of two fireclay occurrences (88, 98) in Quaternary and Recent glaciofluvial deposits, all other recorded occurrences are hosted in the lower and middle Aldridge Formation and/or in Moyie Intrusions. There has been minor lead and silver production from mineralized quartz veins in the Delaware, Leadville, and Blackmore mines. The Iron Range fault zone hosts sixteen occurrences of hematite-magnetite breccia mineralization (Stinson and Brown, 1995). Sha (082FSE104) is the only known Sedex occurrence; nonetheless, Sedex deposits remain the primary exploration target. The lower-middle Aldridge contact, the stratigraphic

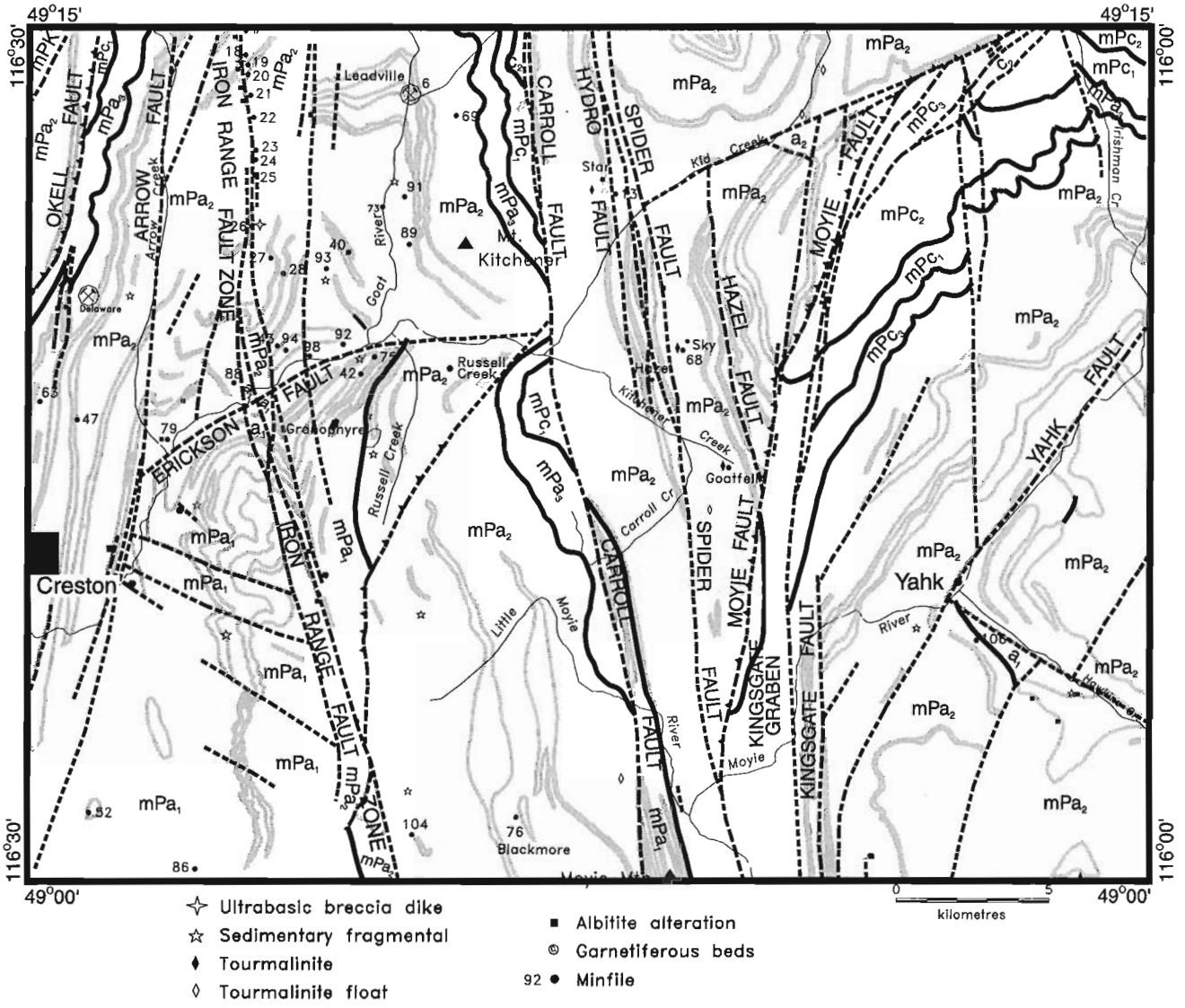

Figure 2. *Detailed geology of the Yahk survey area (modified from Brown et al., 1995) showing the location of selected mineral occurrences. Abbreviations are as follows: mPa1/a1, lower Aldridge Formation; mPa2/a2, middle Aldridge Formation; mPa3/a3, upper Aldridge Formation; mPc1/c1, lower Creston Formation; mPc2/c2, middle Creston Formation; mPK, Kitchener Formation. Moyie Intrusions are outlined in grey.*

position of the Sullivan deposit, is exposed or inferred in the cores of the Moyie and Goat River anticlines, and in uplifted fault panels in the centre of the survey area.

CLAIM STAKING

Following announcement of the survey on July 19, 1995, there were 6369 hectares of new claims staked in the Yahk map area, more than twice that of the seven previous years. The new claims were concentrated in three regions: along, and to the east of, the northern portion of the Iron Range Fault where isolated diatremes are exposed; south and east of Mount Thompson where intraformational conglomeratic units (fragmentals) occur within a faulted package of lower and middle Aldridge rocks; and over a sill-rich package of middle Aldridge rocks in the Hawkins Creek area (Fig. 2). Sedex deposits are the primary targets in the latter two areas. The new geophysics data were released on March 20th, 1997, and by July 1997 more than 15 288 hectares of new claims had been staked over magnetic anomalies in the Hawkins Creek area, in a 3.0 - 6.0 km wide, north-trending corridor west of Carroll Fault where radiometric, electromagnetic, and magnetic anomalies are observed, and over magnetic anomalies in the Kid Creek region.

PHYSICAL PROPERTY MEASUREMENTS

In order to calibrate the airborne geophysical responses, outcrop measurements of magnetic susceptibility and gamma-ray spectrometry were conducted during 1996 and 1997. In addition, hand-sized samples were collected for laboratory analyzes (Table 1). The Koenigsberger ratio (ratio of induced to remanent magnetization) was measured on 55 rock samples from the three survey areas. With the exception of the middle Aldridge Formation, which had a mean Koenigsberger ratio of 4.11 (12 samples), all other units had ratios which were significantly less than one, obviating in these cases the need to consider remanence when interpreting and modelling magnetic anomaly data.

In general, siliciclastic rocks of the Aldridge Formation have low magnetic susceptibility values, whereas the metagabbroic Moyie Intrusions typically have high susceptibility values (Table 1). However, there are exceptions to this generalization. High susceptibility values have been measured in a few localities in the Aldridge Formation where it is faulted and/or contains stringers and blocks of magnetite. A spectacular example of this occurs along the trace of the Iron Range fault zone where susceptibility values up to 402 x 10^{-3} SI have been measured on some hematite-magnetite breccias. The measurements in Table 1 indicate that the upper Aldridge Formation has a somewhat lower mean magnetic susceptibility than the lower or middle Aldridge Formation.

Table 1. Magnetic susceptibility and radioelement concentrations of major rock units in Yahk survey area. Numbers in brackets are the observed range.

	Magnetic susceptibility (10^{-3} SI)		Mean radioelement concentrations			
Rock Unit	Mean	#	K%	eU	eTh	#
Creston Formation	15.20 (0.00 - 108.40)	33	2.1 (0.5 - 3.2)	2.9 (1.9 - 4.2)	11.3 (9.2 - 12.8)	5
Moyie Intrusions (MI)	6.84 (0.00 - 160.00)	70	1.1 (0.7 - 2.2)	1.31 (0.2 - 2.3)	4.59 (2.2 - 9.0)	8
MI in mPa1	2.03 (0.13 - 8.42)	23				
MI in mPa2	5.81 (0.13 - 45.24)	24				
Aldridge Formation	0.78 (0.00 - 7.50)	130	3.3 (1.1 - 6.2)	3.8 (1.0 - 5.5)	13.7 (7.4 - 21.6)	18
upper	0.42 (0.00 - 0.88)	5	3.2 (2.8 - 3.6)	3.0 (2.8 - 3.2)	17.3 (15.7 - 18.9)	2
middle	0.86 (0.00 - 7.50)	62	2.8 (1.5 - 3.8)	3.3 (1.0 - 4.5)	11.6 (6.1 - 13.7)	4
lower	0.82 (0.00 - 3.77)	63	3.4 (1.1 - 6.2)	4.2 (2.3 - 5.5)	12.4 (7.4 - 18.8)	9
Tourmalinites	0.21 (0.11 - 0.3)	2	1.85 (1.1 - 2.6)	3.0 (2.3 - 3.7)	10.4 (7.4 - 13.4)	2
Marker laminates	0.46 (0.0 - 1.01)	6	1.1	2.3	7.4	1
Magnetite breccias and stringers	42.12 (3.0 - 402.12)	19	0.4	3.9	12.8	1
Fragmental rocks	0.63 (0.15 - 2.0)	11	3.8 (2.9 - 4.2)	4.8 (3.3 - 5.6)	14.8 (7.8 - 18.7)	7

The observed ranges and mean susceptibility values of the laminates, fragmentals, and rocks partially to wholly replaced with tourmaline (tourmalinites) which are associated with mineralization at many known Sedex occurrences are lower than their Aldridge host rocks, but not so much that they may be uniquely distinguished. However, Moyie Intrusions, which are intimately associated with more than 65% of known mineral occurrences in the survey areas have a mean magnetic susceptibility which is more than six times higher than that of the Aldridge Formation which they intrude. Indeed, where these intrusions are dissected by faults or shear zones, or where they are proximal to younger granitic stocks and plutons, their measured magnetic susceptibilities may be as much as 160 times greater (Table 1). These observations suggest that much of their magnetism is a secondary phenomenon related to thermal and/or hydrothermal alteration. In a few field localities where Moyie Intrusions were jointed, anisotropy of magnetic susceptibility was observed: susceptibility values were an order of magnitude larger on joint surfaces oriented parallel to the intrusive margin relative to orthogonal joint surfaces.

Although the mean magnetic susceptibility value of the Creston Formation is almost 15 times higher than that of the Aldridge, most units in the formation have susceptibility values which are only 2-4 times higher. However, measured susceptibility values of a green arenaceous unit which contains magnetite porphyroblasts in the middle Creston are up to 126 times higher those of the Aldridge Formation. This unit is well exposed in the Kingsgate Graben of the Yahk survey area.

Mean radioelement (K%, eU, and eTh) concentrations are about three times lower in Moyie Intrusions relative to the Aldridge Formation (Table 1). Fragmental rocks in the Aldridge Formation do not have distinctive radioelement concentrations, although tourmalinites and magnetite-bearing breccias and stringers are relatively depleted in potassium (note however, that few measurements were conducted on these latter units). The Creston Formation is depleted in both potassium and uranium relative to the Aldridge Formation and this depletion may be used as a mapping guide.

REGIONAL CHARACTERISTICS OF GEOPHYSICAL DATA

Electromagnetics

Electromagnetic data in the Yahk survey area (Fig. 3) have several features in common with those of the St. Mary and Findlay areas to the north (Fig. 1): the observed resistivity range for each coil frequency pair is comparable in all three areas suggesting little change in the overall conductivity of sediments within the basin (one notable exception is reported below); the Aldridge and Creston formations are characterized by generally high electrical resistivities (typically >3000 Ω·m), although resistivities observed over most Moyie Intrusions are usually higher yet (typically >5000 Ω·m). Wet, clay-rich surficial material infilling channels along most of the major drainages correspond with significantly lower resistivities (commonly <100 Ω·m). In contrast with the previous two surveys, relatively few, non-cultural, finite conductors are recognized in the Yahk data set. Consequently, if massive sulphides or other good electrical conductors are present in this region they must lie at depths in excess of ~80 m, that is, deeper than the estimated maximum penetration of the 900 Hz coaxial coil pair. The presence of disseminated sulphides at any depth is not, however, precluded by the absence of strong conductors.

Of the non-cultural finite conductors identified, most are quite weak (<50 S) and are associated with clay-rich surficial material along the Goat River, Kitchener Creek, and Hawkins Creek valleys, as well as to the east of the Kingsgate Graben. However, several narrow bedrock conductors (up to 40S) are identified in the upper part of the middle Aldridge to the west of the Carroll Fault. These conductors lie within a north-northwest-trending zone of high conductivity (Fig. 3). Field investigations identified a thick package of black, graphite-bearing mudstones in the upper part of the middle Aldridge Formation as the likely source of the high conductivities. However, relatively few Moyie Intrusions are mapped in the upper portion of the middle Aldridge and this too results in higher apparent conductivities. The mudstones and the associated zone of high conductivity persists along strike through the entire Yahk survey area. In some cases the finite conductors within the mudstone unit are aligned across a number of adjacent flight lines, for example, those located near the Leadville Mine. Disseminated mineralization or clay-rich alteration products developed in shear zones are possible explanations of these aligned conductors, and for this reason they warrant investigation by explorationists.

It is interesting to note that apparent conductivities in the Goat River valley near the western limit of the survey area (i.e. proximal to the Lucky Minfile occurrence) are higher on the 7200 Hz than on the 56 Khz coplanar coil pair. This indicates that the conductive source most probably lies beneath the uppermost surficial cover. Throughout the East Kootenays gold-bearing, magnetite- and pyrrhotite-rich placers are present at the bedrock-surficial contact along several of the major drainages including St. Mary River (Lowe et al., 1997b), Hellroaring Creek, and Perry Creek. Although the conductivity increase could be due to a buried clay layer, elevated magnetic anomaly values (see below), suggest buried pyrrhotite and/or magnetite placers are a more likely source of the high conductivities in this area. Any association with placer gold is yet to be determined.

Moderate (up to 100 Ω·m, 56 KHz coplanar coil pair) apparent conductivities are observed in a region largely underlain by Moyie Intrusions east of the Yahk Fault to the north of Hawkins Creek (Fig. 3). Although comparison with apparent conductivity data observed using the 7200 Hz coplanar coil suggests that the source of the conductivities lies largely in the uppermost few metres, this sill package is magnetically and radiometrically anomalous also.

Interestingly, there is no conductivity anomaly associated with mineralization in the Iron Range Fault. Although several finite conductors are mapped along, or proximal to, the trace of the fault, most are extremely weak (<5 S) and are cultural

in origin. Stinson and Brown (1995) observed that with the exception of the northern part of Iron Range Mountain where up to 3-4% pyrite occurs in the hematite-magnetite breccias elsewhere throughout the fault zone, sulphide minerals are rare. Nonetheless the absence of an electromagnetic response is intriguing since fine-grained fault gouge constitutes the matrix of several large breccia bodies mapped around Iron Range Mountain.

Magnetics

With rare exception, there is excellent correlation between the observed aeromagnetic anomaly data (Fig. 4), the measured magnetic susceptibility values (Table 1), and the mapped geology (Fig. 2). As was the case in the Findlay and St. Mary areas, siliciclastic rocks of the Aldridge Formation typically have low magnetic susceptibility values and correspondingly low magnetic anomaly values. Exceptions occur in the Iron Range Fault zone, in the Hawkins Creek area, and in a north-trending, oval-shaped zone west of Carroll Fault where high magnetic anomaly values are observed.

The most intense magnetic feature in the survey area is a north-trending linear belt of intense magnetic anomalies (up to 1130 nT) which extends along the mapped trace of Iron Range Fault zone (Fig. 4). The width of this anomalous belt varies from ~2.5 km at the international border, to less than 1 km in the Goat River valley, to ~4 km in the northern survey area where the mapped fault zone attains maximum width. Geologically, the fault is a north-trending, steeply dipping, structure characterized by strong albite and sericite alteration and locally by iron oxide mineralization. Field studies confirm that the primary magnetic sources are the zones of iron-oxide mineralization, which are composed of massive lenses of hematite and magnetite (0.3 - 5 m wide), surrounded by

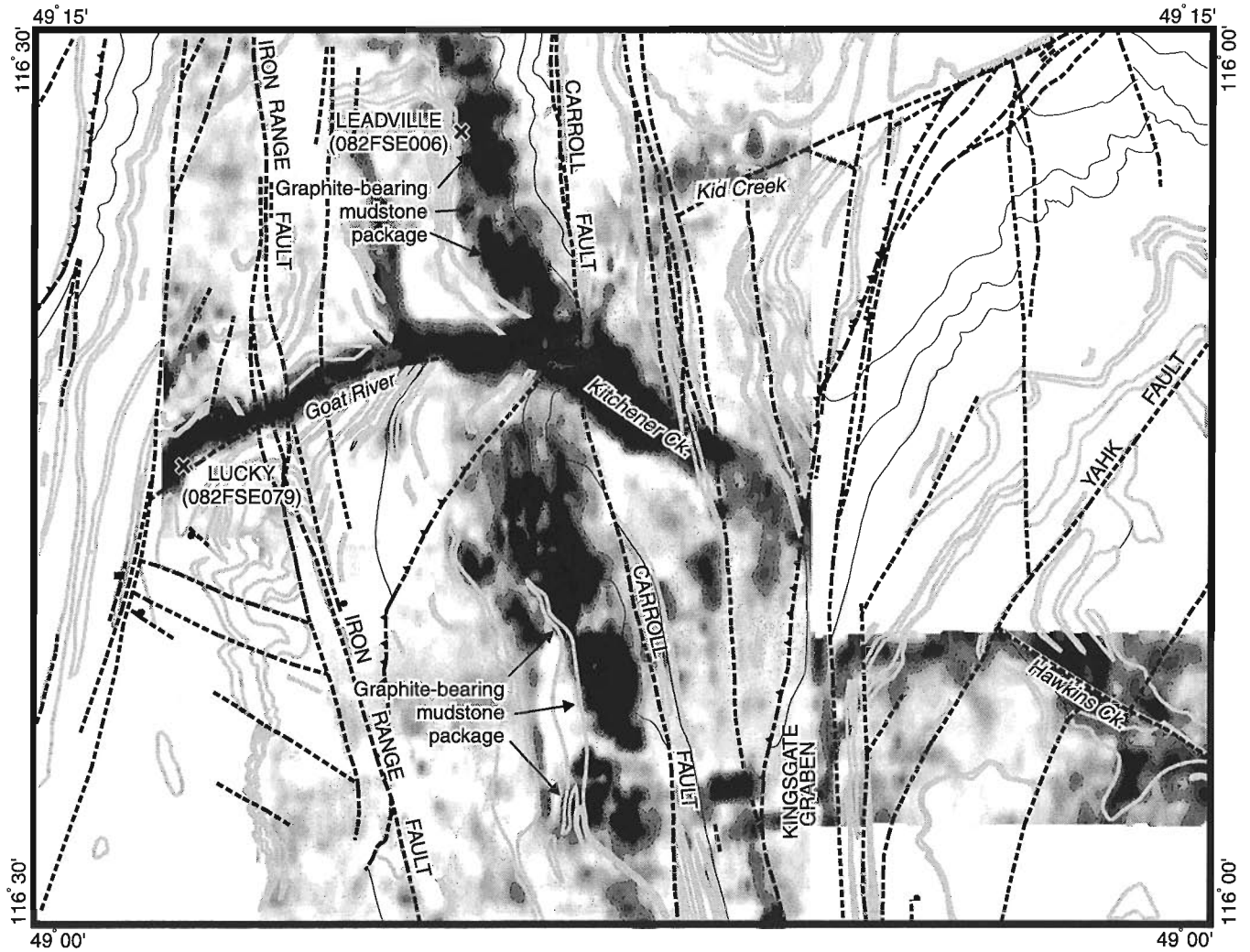

Figure 3. *Apparent conductivity map for the Yahk survey area computed from 7200 Hz coplanar coil data. Light shades are regions of low apparent conductivities and dark shades are regions of high apparent conductivity. See text for a description of the annotated features.*

zones of hematite-rich breccias which grade outwards to wider, less-brecciated zones. Original magnetite abundances in the lenses and breccias ranged from 5 to 30%, most is pseudomorphed by hematite, although commonly cores of magnetite remain (Stinson and Brown, 1995). The highest magnetic susceptibility values in the entire East Kootenay survey area were measured in these lenses (>400 x 10^{-3} SI, Table 1). Peaks in magnetic intensity which do not directly correspond with these iron-oxide zones may be indicative of buried mineralization, although elevated anomaly values are also associated with the disseminated magnetite in the fault zone, as well as with altered Moyie Intrusions in and adjacent to the fault zone.

Several subsidiary faults are mapped and/or inferred within the Iron Range fault zone (Fig. 2), although many are not identified on the aeromagnetic data. However, a ground magnetometer survey conducted ~6 km northwest of Mount Thompson identified two distinct magnetic peaks within the anomaly that defines the fault zone (Fig. 4 inset). One of these peaks correlates directly with the mapped fault trace, the other is thought to delineate the surface trace of an unexposed inferred fault segment. Ground magnetic data may therefore help locate mineralized zones along subsidiary faults.

A broad zone of moderately high magnetic anomaly values (>100 nT) occurs in the Hawkins Creek area (Fig. 4). High-resolution industry data (Abitibi Mining Corp., pers comm., 1997) shows this magnetic anomaly persists at least 4 km farther to the north beyond the bounds of the Yahk survey, such that it is elongated to the northeast, and approximately 10 km long by 6 km wide. Bedrock in the anomalous region comprises thinly-bedded quartz wacke, siltstone, and quartzofeldspathic wacke beds of the lower and middle

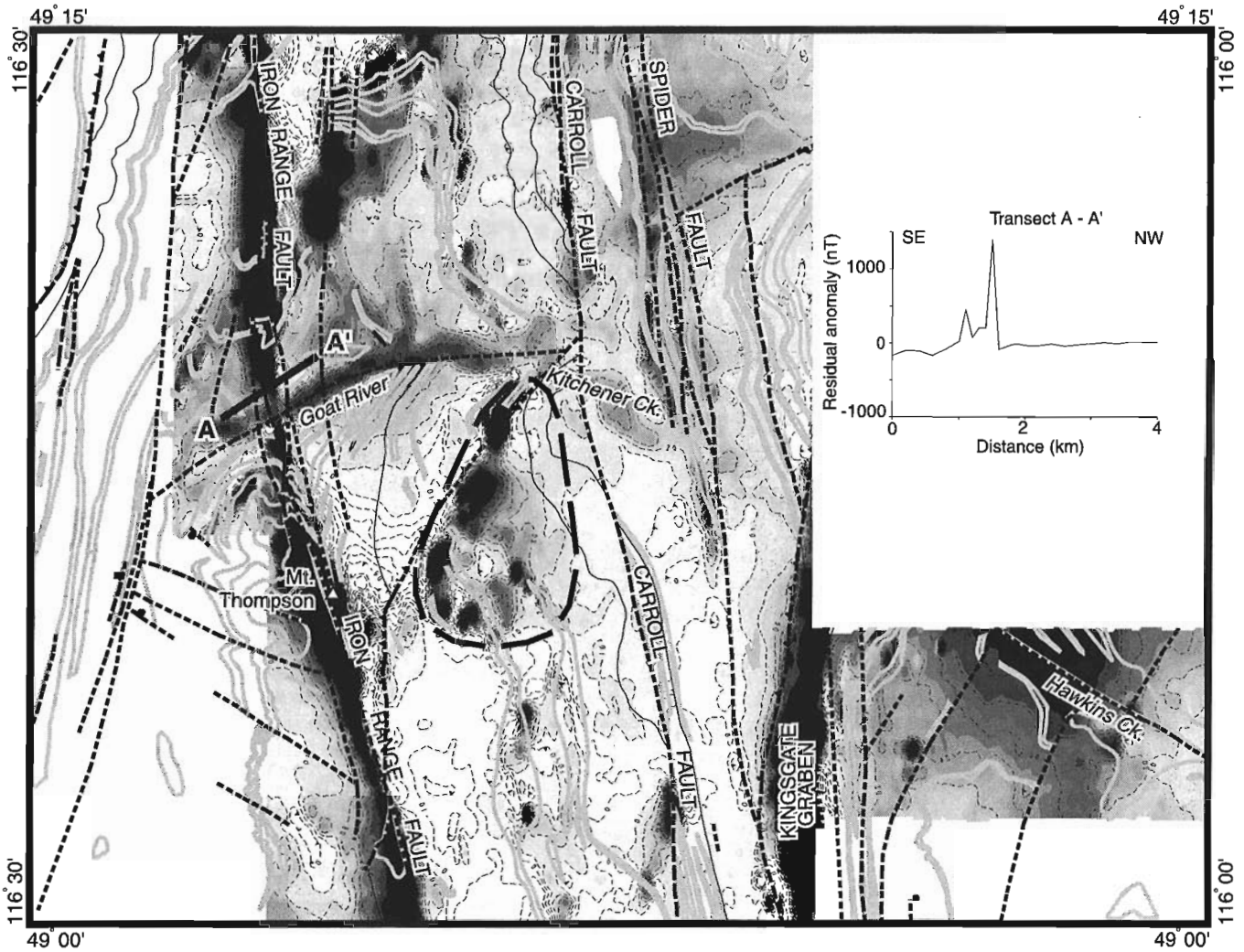

Figure 4. *Magnetic anomaly map for the Yahk survey area. Low magnetic anomaly values are shown in light shades and high magnetic anomaly values in dark shades. Anomalies were computed at an elevation of 1640 m using the 1996 International Geomagnetic Reference Field. See text for a description of the annotated features. Inset shows ground magnetic anomaly data for the traverse A-A' across the Iron Range Fault. The peak on the right corresponds with the mapped surface trace of the fault, and that on the left with the inferred surface trace of a subsidiary fault.*

Aldridge Formation (Brown et al., 1994). North of Hawkins Creek and east of the Yahk Fault, these rocks have been intruded by several Moyie sills (Fig. 2). Susceptibility measurements conducted on sedimentary rocks in the magnetically anomalous area are consistent with those measured in Aldridge siliciclastic rocks elsewhere in the basin. The magnetic susceptibilities of the sill package are unusual in that they vary very little along strike and nowhere are they greater than 7.5 x 10^{-3} SI. The low susceptibility values of the outcropping rocks require the source of the magnetic anomaly to lie at some depth in the crust (note: no corresponding anomaly is recognized in the gamma-ray spectrometry or electromagnetic data sets). The magnetic anomaly is not disrupted or truncated by the Yahk or other northeast-trending faults mapped in this region. This suggests either limited offset across the faults, or that they are listric and flatten at depths shallower than the upper surface of the magnetic source.

Within the middle Aldridge Formation to the west of the Carroll Fault, variations in magnetic intensity on the order of 200 nT are common and several elongate northeast- and northwest-trending anomalies are recognized within a larger sub-oval anomalous region (thick dashed line in Fig. 4). Some of the small anomalies within this region are clearly associated with mapped sills. Ground follow-up studies identified two unmapped sills as the source of others. The western boundary of the larger sub-oval anomaly is marked by steep gradients and is most likely the locus of the inferred northwest-trending fault in this area.

Unlike other parts of the basin, the lower Creston Formation exposed in the Yahk survey area corresponds with anomaly values as high as those mapped in regions which are underlain by the middle Creston Formation (typically 50-250 nT, Fig. 4). The lower Creston Formation typically comprises fine-grained argillites, and in the Yahk map area, contains disseminated and stringer magnetite. The restriction of magnetite to the lower Creston Formation in this part of the basin potentially reflects an original facies difference. The source of the elevated magnetic values in the Middle Creston is magnetite porphyroblasts in a green arenaceous sandstone horizon (Lowe et al., 1997a).

Many mapped and/or inferred faults in the Yahk survey area are commonly associated with linear zones of steep magnetic gradient, for example, the Carroll, Moyie, Spider, and Iron Range faults. In contrast, faults which cut similar Purcell Supergroup stratigraphy farther north in the St. Mary and Findlay areas have little magnetic expression. The sources of the magnetic responses in the Yahk map area include the massive and disseminated magnetite-hematite breccias and veins, as well as, the sheared and altered Moyie Intrusions present in the fault planes. These features are best developed along the Iron Range and Spider faults. Smaller and relatively fewer magnetite-hematite breccias are observed along other faults. The source of iron in the breccias is thought to be the iron-bearing altered mafic minerals in the gabbros. The predominance of these breccias in the Yahk area reflects, perhaps, differences in fluid conditions during faulting.

A distinct magnetic anomaly, which is discordant with the mapped geology, is observed along the valleys of the Goat River and Kitchener Creek (Fig. 5). This anomaly is similar but more intense than one observed along the St. Mary River Valley (Fig. 1, area 2). Lowe et al. (1997b) showed the latter anomaly was most likely related to magnetite/pyrrhotite-rich placers at the bedrock-surficial contact. The anomaly in the Goat River may have a similar origin and follow-up investigations should be conducted to test this theory and to determine if there is any association with placer gold.

Gamma-ray spectrometry

Gamma-ray spectrometry provides geochemical information on the top few tens of centimetres of the Earth's surface. As with any near-surface geochemical method, such as water, soil, or biogeochemistry, interpretation requires an understanding of the nature of any surficial materials present (tills, outwash, fluvial, or lacustrine deposits) and their relationship to the underlying bedrock.

Potassium (K), uranium (U), and thorium (Th) are present in variable amounts in all rocks and derived materials. The corresponding radioelement signatures (K, eU-equivalent uranium, eTh-equivalent thorium) determined from the gamma-ray spectrometric survey, are used to characterize and map the distribution of various lithologies. Where the normal distribution of these elements is modified by a mineralizing process, the resulting radioelement anomaly provides direct exploration guidance. In general, radioelement patterns complement magnetic data, as they are elevated in non- to weakly magnetic, evolved felsic rocks and relatively low in less evolved, more magnetic, mafic units.

Although less rugged than the St. Mary and Findlay areas, topography in the Yahk region also has a significant influence on the total radioactivity measured. In general, south- and west-facing slopes are drier, less vegetated, and have greater exposures of bedrock and talus than north- or east-facing slopes, and consequently yield higher radioelement concentrations which are closer to local bedrock values. To extract geologically significant information, radiometric data are therefore best examined in conjunction with Landsat images, aerial photographs, or other terrain data. Topographic effects are also minimized by using the radioelement ratios (eU/eTh, eU/K, and eTh/K). Regionally, a number of distinct radioelement patterns and anomalies are recognized in the new data.

Outcropping Moyie Intrusions are recognized by low concentrations of all three radioelements (Fig. 5), but are best delineated by their very low uranium concentrations (Table 1). This correlation offers assistance for improved sill mapping, and is important for exploration as more than 65% of known mineral occurrences are intimately associated with Moyie Intrusions. An exception to this general rule is the package of Moyie sills which outcrops east of the Yahk Fault and north of Hawkins Creek. This sill package is characterized by moderate radioelement concentrations and is electromagnetically and magnetically anomalous.

In the western part of the survey area, a series of elevated eTh/K ratio anomalies (low potassium concentrations) defines a north-trending belt corresponding with the trace of the Iron Range fault zone. In this case, the airborne pattern reflects the presence of albitite and albite-rich (that is, potassium-poor) breccias in the fault zone proper and regions of extensive albitic alteration in and adjacent to the fault zone (Stinson and Brown, 1995). The most intense anomalies correspond with regions where albitic alteration is most intense, for example, Iron Range Mountain, in and adjacent to Mount Thompson, and west of the Sha Sedex occurrence (Fig. 5).

West of the Carroll Fault, high potassium concentrations demarcate a thick package of north-northwest-trending black mudstones in the upper part of the middle Aldridge Formation. This graphite-bearing mudstone package is also conductive and well imaged in the electromagnetic data (Fig. 3). There are no known mineral occurrences hosted in this package.

Several discrete eTh/K lows are identified in the Yahk survey data. Brown et al. (1997) showed that farther to the north, in the Sullivan - North Star corridor, similar lows correspond with regions of well-developed sericitic alteration in the sub-vertical root zone of the Sullivan orebody. Sercitic alteration is a characteristic feature of many known Sedex deposits in the East Kootenays including the Sha occurrence (Fig. 4). Consequently, the eTh/K lows in the Yahk area warrant investigation by explorationists, especially where they occur in association with other Sedex features such as fragmental rocks, tourmalinites, and manganese-rich garnets.

Unconsolidated deposits along the major drainages, such as Goat River, Hawkins Creek, and Kitchener Creek produce elevated eTh/K ratio and low potassium concentrations patterns (Fig. 5). This signature is characteristic of fluvial deposits, reflecting in part, elevated levels of stable thorium-bearing minerals associated with heavy mineral concentrations. However, water, swamps, and wet surficial materials absorb gamma rays thereby reducing the measured radioelement concentrations. The lowest measured potassium

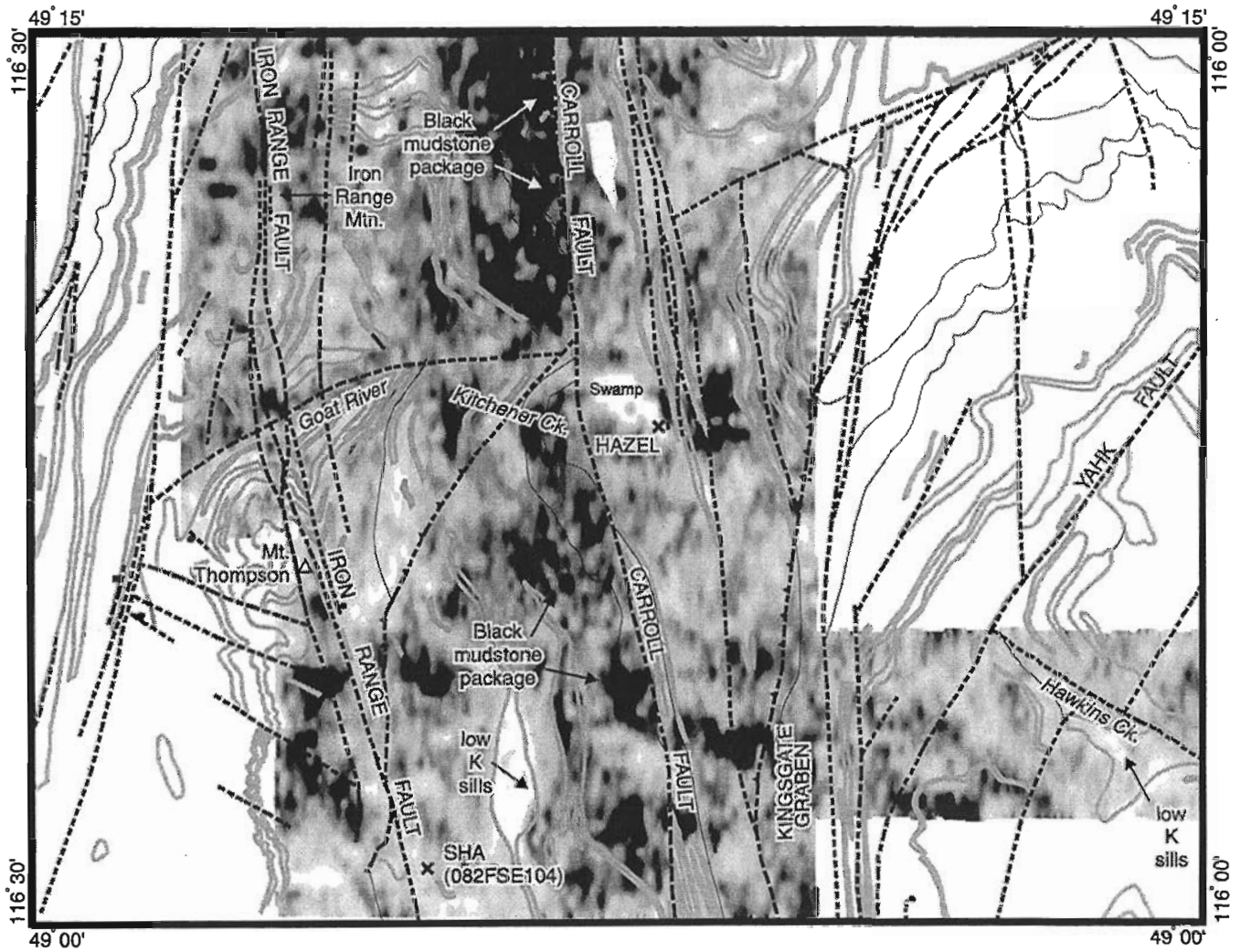

Figure 5. Potassium concentration map for the Yahk survey area. Low concentrations are shown in light shades and high concentrations in dark shades. See text for a description of the annotated features.

concentrations correspond with a large swamp located approximately 1 km west of the Hazel mineral occurrence in Kitchener Creek valley (Fig. 5). Radioelement data consequently offer limited exploration and geological assistance in wet and vegetated areas such as these.

CONCLUSIONS

Analyses of the high-resolution geophysical data acquired in the Yahk map area coupled with ground-truth studies provide important new guides for mineral explorationists. In particular, the paucity of non-cultural finite conductors recognized in the electromagnetic data set indicates that if massive sulphides or other good electrical conductors are present in this region they must lie at depths in excess of 80 m. Consequently, 'deeper-probing' geophysical tools such as gravity, magnetic, or seismic surveys will be required to accurately locate any such deposits. Known gold placers in the East Kootenays have high concentrations of magnetite and pyrrhotite. Buried pyrrhotite and/or magnetite placers could explain the elevated magnetic anomaly values and high electrical conductivities associated with the deep surficial cover in the western part of the Goat River valley. Ground investigations are warranted in this region to assess this interpretation and determine any possible association with placer gold. Similarly, eTh/K lows, especially those which occur in association with laminates, metamorphic tourmaline, or fragmental rocks, should be targeted for detailed Sedex exploration.

The new airborne data and ground truth investigations provide new insights into the geology of the region. Previously unmapped Moyie sills have been identified south of Erickson fault in the Russell Creek area. Here, magnetic data suggest the orientation of an inferred fault is more north-trending than previously mapped. West of the Carroll Fault electromagnetic and gamma-ray spectrometric data demarcate a stratabound package of black, graphite-bearing mudstones which is not recognized in either the Findlay or St. Mary survey areas. Also in the Yahk survey area faults are commonly associated with linear zones of steep magnetic gradient due in part to magnetite-hematite breccias and altered Moyie sills along fault planes. Structural control on mineralization and a clear association with Moyie Intrusions is well documented for many of the known mineral occurrences in the Purcell basin. For all of these reasons the new data warrant careful consideration by the exploration industry.

ACKNOWLEDGMENTS

We thank R. Shives (GSC Ottawa) for conducting the spectrographic measurements reported in this paper. P. Klewchuk (Abitibi Mining Corp.) and S. Coombes (Kennecott Canada Exploration Inc.) freely shared their geological knowledge of the area. Staff at the British Columbia Mineral Titles Branch, Cranbrook provided information on staking activity. R. Franklin drafted the figures. T. Hamilton (GSC Pacific) critically reviewed this manuscript and suggested many improvements.

REFERENCES

British Columbia Ministry of Employment and Investment
1996: East Kootenay Geophysical Survey - Yahk area, British Columbia, NTS 82 F/1; British Columbia Ministry of Employment and Investment, Open File 1996-23.

Brown, D.A., Bradford, J.A., Melville, D.M., Legun, A.S., and Anderson, D.
1994: Geology and mineral deposits of Purcell Supergroup in Yahk map area, southeastern British Columbia (82 F/1); in Geological Fieldwork 1994; British Columbia Ministry of Energy, Mines and Petroleum Resources, Paper 1994-1, p. 129-151.

Brown, D.A., Bradford, J.A., Melville, D.M., and Stinson, P.
1995: Geology of the Yahk map area, southeastern British Columbia (82 F/1); British Columbia Ministry of Energy, Mines and Petroleum Resources, Open File 1995-14, scale 1:50 000.

Brown, D. A., Lowe, C., Shives, R.B.K. and Best, M.E.
1997: The East Kootenay multiparameter geophysical survey, southeastern British Columbia (82 F, G, K) - Sullivan-North Star Area; in Geological Fieldwork 1996, British Columbia Ministry of Employment and Investment, Paper 1996-1, p. 3-15.

Höy, T., Price, R.A., Legun, A., Grant, B., and Brown, D.A.
1995: Purcell Supergroup, southeastern British Columbia; British Columbia Ministry of Energy, Mines and Petroleum Resources, Geoscience Map 1995-1, scale 1:250 000.

Kung, R., Brown, D.A., Lowe, C. and Rencz
1997: Geology and Landsat imagery of the Yahk map area, southeastern British Columbia, NTS 82 F/1; Geological Survey of Canada, Open File 3430.

Lowe, C., Brown, D.A., Best, M.E., and Shives, R.B.K.
1997a: East Kootenay multiparameter geophysical survey, southeastern British Columbia: regional synthesis; in Current Research 1997-A, Geological Survey of Canada, p. 167-176.
1997b: The East Kootenay multiparameter geophysical survey, southeastern British Columbia; 14th Annual Cordilleran Geology and Exploration Roundup, Vancouver, British Columbia, p. 6-7.

Reesor, J.E.
1981: Grassy Mountain, Kootenay Land District, British Columbia (82 F/8); Geological Survey of Canada, Open File 820.

Stinson, P. and Brown, D.A.
1995: Iron Range deposits, southeastern British Columbia (82 F/1); in Geological Fieldwork 1994, (ed) Grant B., and Newell, J.M.; British Columbia Ministry of Energy, Mines and Petroleum Resources, Paper 1995-1, p. 127-134.

Geological Survey of Canada Project 910027

Geological evidence for past large earthquakes in southwest British Columbia

J.J. Clague, P.T. Bobrowsky[1], I. Hutchinson[2], and R.W. Mathewes[3]
Terrain Sciences Division, Vancouver

Clague, J.J., Bobrowsky, P.T., Hutchinson, I., and Mathewes, R.W., 1998: Geological evidence for past large earthquakes in southwest British Columbia; in Current Research 1998-A; Geological Survey of Canada, p. 217-224.

Abstract: Large earthquakes have left evidence of land-level change, tsunamis, and strong shaking in coastal sediments in southwest British Columbia. Sudden lowering of the land during earthquakes accounts for buried tidal marsh and forest soils on Vancouver Island and near Vancouver. Some sand layers in peaty and muddy marsh sediments on western Vancouver Island were deposited by tsunamis triggered by Pacific earthquakes. Liquefaction features, including dykes and blows of mainly sandy sediments, provide direct evidence for ground shaking, but have been documented thus far only on the Fraser River delta south of Vancouver. Much of the evidence for subsidence, tsunamis, and shaking is attributed to great earthquakes at the boundary between the North America and Juan de Fuca plates, but some of the evidence probably results from one or more earthquakes within the crust of North America. In addition, some tsunami deposits on Vancouver Island are products of great earthquakes in Alaska.

Résumé : De forts tremblements de terre ont laissé des traces de changements du niveau du sol, de tsunamis et de forts ébranlements dans les sédiments côtiers de la partie sud-ouest de la Colombie-Britannique. Les abaissements soudains du terrain lors des tremblements de terre sont à l'origine de l'enfouissement de marais littoraux et de sols forestiers sur l'île de Vancouver et près de Vancouver. Dans la partie ouest de l'île de Vancouver, certaines couches de sable dans des sédiments de marécages tourbeux et boueux sont des dépôts de tsunamis déclenchés par des tremblements de terre dans le Pacifique. Des formes dues à la liquéfaction, notamment des dykes et des cratères de sédiments essentiellement sableux, fournissent des témoignages directs d'ébranlements du sol, mais n'ont jusqu'ici été décrites que dans le delta du Fraser, au sud de Vancouver. Les formes observées découlant de phénomènes de subsidence, de tsunamis et d'ébranlements sont pour la plupart imputables à de forts tremblements de terre dont l'épicentre se trouve à la limite entre la plaque nord-américaine et la plaque Juan de Fuca; cependant, certaines d'entre elles résultent probablement d'un ou plusieurs tremblements de terre au sein de la croûte de l'Amérique du Nord. Par ailleurs, certains dépôts de tsunamis sur l'île de Vancouver sont le produit de forts tremblements de terre en Alaska.

[1] British Columbia Geological Survey Branch, P.O. Box 9320, Stn. Provincial Government, Victoria, British Columbia V8W 9N3
[2] Department of Geography, Simon Fraser University, Burnaby, British Columbia V5A 1S6
[3] Department of Biological Sciences, Simon Fraser University, Burnaby, British Columbia V5A 1S6

INTRODUCTION

In the late 1980s, we began to search for geological evidence of large prehistoric earthquakes in southwest British Columbia in order to provide a better understanding of seismic risk in this highly populated region. This search has been productive — to date, evidence for past earthquakes has been found and documented at nearly 30 sites on Vancouver Island and adjacent mainland British Columbia (Clague, 1996). The work has demonstrated that very large earthquakes, much larger than any of the short period for which we have instrumental records, have affected the region in the recent geological past. The work has further provided important indications as to the likely effects of the next large earthquake in southwest British Columbia.

Three main types of geological evidence for past earthquakes have been found in southwest British Columbia: buried marsh and forest soils, tsunami deposits, and sand dykes and blows (Clague et al., 1995; Clague, 1996). Much of the evidence has been attributed to great (moment magnitude 8 or larger) plate-boundary earthquakes (i.e. earthquakes that ruptured the boundary between the subducting Juan de Fuca plate and overriding North America plate beneath the Pacific Ocean; Cascadia subduction zone in Fig. 1). Some of the features, however, are probably the result of large earthquakes within the crust of North America (Clague, 1996).

In this paper, we catalogue sites in southwest British Columbia where paleoseismic evidence has been found. Similar evidence is widespread in other parts of Cascadia (Washington, Oregon, and northern California) but is not discussed in this paper due to lack of space (see Atwater et al., 1995, for a general regional review and a comprehensive list of references).

SUDDEN LAND-LEVEL CHANGE

Buried wetland soils resulting from episodic sudden subsidence (Fig. 2a) have been identified at tidal marshes at Tofino, Ucluelet, Bamfield, and Port Renfrew on the west coast of Vancouver Island, near Victoria on southern Vancouver Island, and at Serpentine River south of Vancouver (Fig. 3, Table 1). The buried soils are abruptly overlain by intertidal muds. Well preserved stems and leaves of herbaceous marsh plants rooted in some of the soils are covered by the muds (Clague and Bobrowsky, 1994a), suggesting that submergence was sudden rather than slow, as would occur if the sea gradually rose in relation to the land. Rapid submergence is also indicated by abrupt changes in fossil plant and animal assemblages across contacts between soils and overlying muddy sediments (Guilbault et al., 1995, 1996; Peterson et al., 1997). The buried soils formed in high marsh and forest margin environments, whereas overlying muds are low marsh and tidal flat deposits.

Buried wetland soils on western Vancouver Island are no more than several hundred years old (Clague and Bobrowsky, 1994b; Nelson et al., 1995) and were probably produced by coseismic subsidence during the last great plate-boundary earthquake in Cascadia in A.D. 1700 (Satake et al., 1996). No buried soils of this or any other age have yet been found in tidal marshes on northern Vancouver Island (Benson, 1996; Benson et al., 1997), suggesting that the Cascadia subduction zone may not rupture this far north. Likewise, no buried soils just a few hundred years old have been found at study sites in the Victoria and Vancouver areas. This is consistent with geophysical evidence that the zone of coseismic subsidence during plate-boundary earthquakes in Cascadia does not extend far eastward of the west coast of Vancouver Island (Hyndman and Wang, 1993, 1995; Dragert et al., 1994).

Amounts of coseismic subsidence during the A.D. 1700 earthquake have been estimated by comparing fossils extracted from buried wetland soils and overlying tidal muds with living intertidal plants and animals at the same sites. Subsidence near Tofino, estimated in this manner, was 0.5-1 m (Guilbault et al., 1995, 1996). Less subsidence likely occurred at most of the other sites where the A.D. 1700 buried soil has been found.

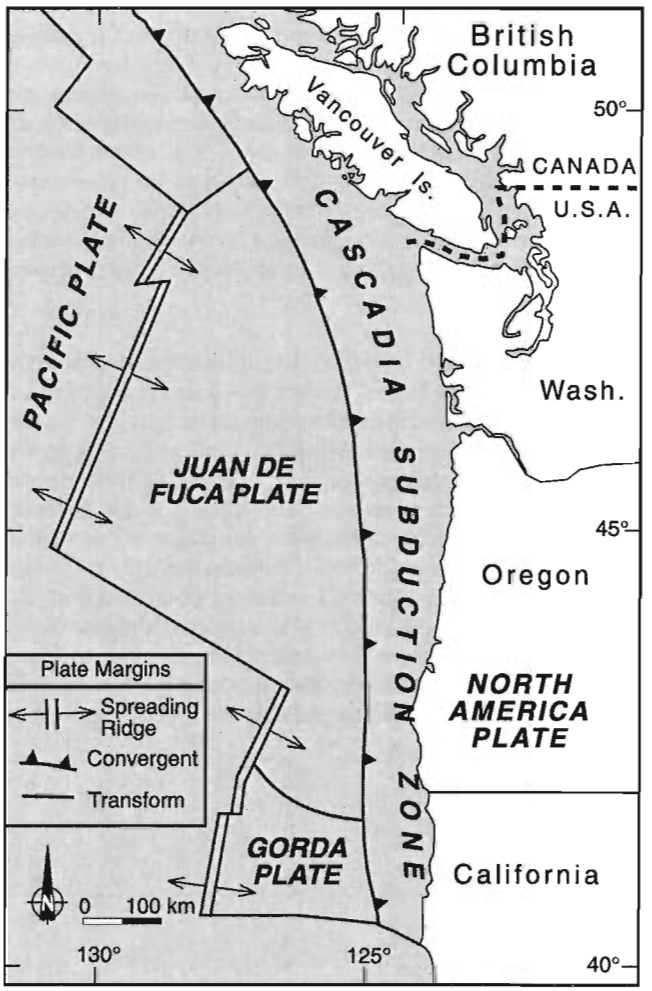

Figure 1. *Map of southwest British Columbia showing the location of the Cascadia subduction zone.*

Older buried soils, dating to about 1700-1900 and 3400 years ago, occur at several sites on southern Vancouver Island and at Serpentine River on the mainland (Mathewes and Clague, 1994; Clague, 1997). Mathewes and Clague (1994) attributed subsidence and burial during the younger of these two events to a large crustal earthquake in south-coastal British Columbia. Radiocarbon dating suggests that this earthquake occurred at about the same time as a plate-boundary earthquake off the coast of North America (Clague et al., 1997). The source of the older earthquake is uncertain; Mathewes and Clague (1994) presented evidence for subsidence about 3400 years ago at their study sites on Vancouver Island, but suggested that the land rose slightly on the adjacent mainland. The inferred pattern of crustal deformation during this event resembles that of a plate-boundary earthquake, but it could also result from a large crustal earthquake.

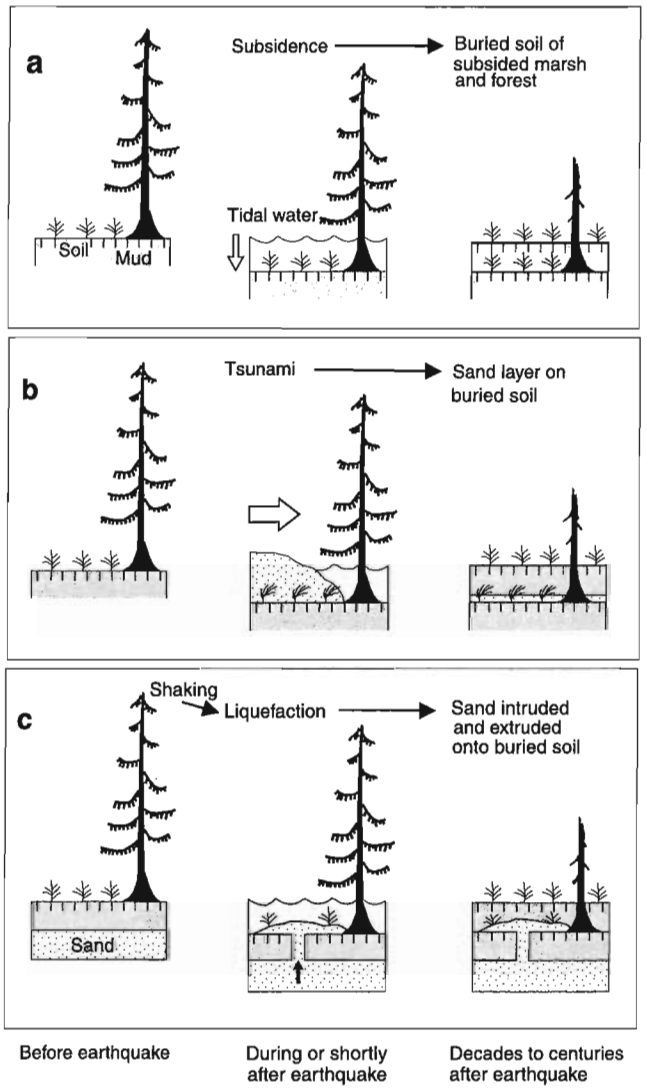

Figure 2. *Simplified diagrams showing origins of coastal geological evidence for plate-boundary earthquakes in Cascadia (modified from Atwater et al., 1995, Fig. 3, with permission from the Earthquake Engineering Research Institute).* ***a)*** *A marsh subsides into the intertidal zone during an earthquake and is buried by mud.* ***b)*** *A tsunami deposits sand on a coseismically subsided surface.* ***c)*** *Liquefied sand moves upward through cohesive sediment and spills onto a coseismically subsided surface. Tsunamis and liquefaction can also occur without attendant land-level change; in such instances, tsunami deposits, sand dykes, and sand blows are not associated with buried soils.*

TSUNAMIS

Marshes

Thin sheets of sand, gravel, and silt found in peat and mud deposits beneath tidal marshes on western Vancouver Island are interpreted to be tsunami deposits, based on their setting and physical characteristics (Fig. 3, Table 1; Clague and Bobrowsky, 1994b; Benson, 1996; Benson et al., 1997). The deposits are, in places, distant from streams, become thinner and rise in a landward direction, and may contain marine microfossils; these characteristics argue for an offshore rather than fluvial source. Similar coarse sediments have been deposited by tsunamis following historical large earthquakes (Wright and Mella, 1963; Bourgeois and Reinhart, 1989; Minoura and Nakaya, 1991; Minoura et al., 1994).

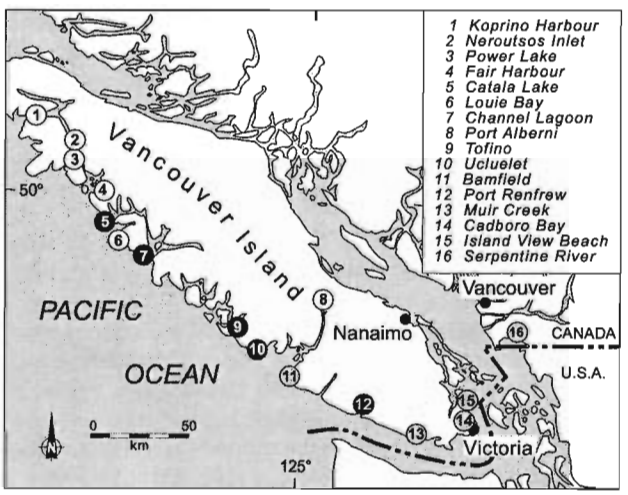

Figure 3. *Marshes in southwest British Columbia where evidence has been found for coseismic land-level change and/or tsunamis (Table 1). Sites with evidence for tsunamis only are shown as open circles; sites with evidence for coseismic land-level change only are indicated by circles with gray infill; sites with evidence for both tsunamis and coseismic land-level change are indicated by circles with black infill.*

Table 1. Marshes examined for evidence of land-level change and tsunamis.

Site (location, Fig. 3)	Location	Coseismic subsidence[1]	Tsunami deposits			Reference
			AD1964	AD1700	Older	
Koprino Harbour (1)	50°30'N, 127°50'W		X	X		Benson et al. (1997)
Neroutsos Inlet (2)	50°20'N, 127°26'W		X	X		Benson et al. (1997)
Power Lake (3)	50°11'N, 127°29'W		X	X		unpublished
Fair Harbour (4)	50°03'N, 127°06'W		X	X		Benson et al. (1997)
Catala Lake (5)	49°50'N, 127°03'W	minor?		X	X	Clague et al. (in press a)
Louie Bay (6)	49°44'N, 126°57'W		X?	X		unpublished
Channel Lagoon (7)	49°36'N, 126°39'W	minor?			X?	unpublished
Port Alberni (8)	49°15'N, 124°50'W		X	X	X	Clague and Bobrowsky (1994a, b), Clague et al. (1994)
Tofino (9)	49°07'N, 125°52'W	X	X	X	X	Clague and Bobrowsky (1994a, b)
Ucluelet (10)	48°57'N, 125°34'W	X	X	X	X	Clague and Bobrowsky (1994a, b)
Bamfield (11)	48°49'N, 125°09'W	X?				unpublished
Port Renfrew (12)	48°35'N, 124°25'W	minor		X		unpublished
Muir Creek (13)	48°23'N, 123°52'W	X				Mathewes and Clague (1994)
Cadboro Bay (14)	48°28'N, 123°18'W	minor				Mathewes and Clague (1994)
Island View Beach (15)	48°35'N, 123°22'W	minor				Mathewes and Clague (1994)
Serpentine River (16)	50°20'N, 127°26'W	X				Mathewes and Clague (1994)

[1]Coseismic subsidence: Muir Creek - ca. 3400-year-old earthquake; Cadboro Bay, Island View Beach, and Serpentine River - ca. 1700-1900-year-old earthquake; all other sites - A.D. 300 earthquake.

In open coastal settings, the deposits of rare large storms are commonly difficult to discriminate from tsunami deposits. Dawson et al. (1988, 1991), however, suggested that tsunami waves typically spread sediment widely above the upper limit of tides, whereas storm waves are less likely to move sediment far inland. Sediment containing marine fossils at elevations well above the reach of storms is likely a tsunami deposit (Nelson et al., 1996). Storm deposits are unlikely to be found far inland from the coast in protected tidal inlets because as water levels rise, current velocities in channels drop below values required to transport enough sand to form widespread sheets (Bourgeois and Reinhart, 1989; Peterson and Darienzo, 1996). Also, some sand sheets on Vancouver Island consist of two or more beds, suggestive of deposition by successive tsunami waves (Benson, 1996; Benson et al., 1997) rather than a storm surge.

Some tsunami sands at Tofino and Ucluelet on west-central Vancouver Island rest directly on the soil of the inferred A.D. 1700 plate-boundary earthquake. The presence in these sands of delicate stems and leaves of herbaceous plants rooted in the underlying soil argues that sand deposition coincided with subsidence (Clague and Bobrowsky, 1994a, b). The association of sand deposition and subsidence points to a common cause: an earthquake that caused the coast to subside while generating a tsunami offshore (Fig. 2b).

Sand of the A.D. 1700 tsunami is also present beneath tidal marshes on northern Vancouver Island, but it does not rest on a soil at these sites. This observation suggests that northern Vancouver Island did not subside significantly during at least the most recent Cascadia plate-boundary earthquake.

Other tsunami deposits have been found at marshes on western Vancouver Island. A near-surface sheet of sand or silt found at many tidal marshes was deposited by the tsunami of the great Alaska earthquake in 1964 (Clague et al., 1994; Benson, 1996; Benson et al., 1997). A 500- to 800-year-old sheet of sand and gravel at Tofino and Port Alberni may be a deposit of the tsunami of the penultimate great plate-boundary earthquake in Alaska which is of similar age (Clague and Bobrowsky, 1994b; Mann and Crowell, 1996). Many other, older sands, encountered during drilling at Port Alberni, may also be tsunami deposits, although their sources are uncertain. These earlier tsunamis may be responsible for repeated abandonment of coastal villages by native peoples, which is suggested by gaps in the archaeological record (Hutchinson and McMillan, 1997).

No tsunami deposits have yet been found along the shores of southern Vancouver Island or the Strait of Georgia. North Pacific tsunamis lose much energy during their passage into the Strait of Georgia and may be too small to produce significant run-ups there.

Lakes

Tsunami deposits have been found in low-lying lakes and tidal inlets on the west coast of Vancouver Island (Fig. 4, Table 2; Hutchinson et al., 1997; Clague et al., in press a). Tsunamis entered the lakes by surging up outlet streams. Sediments deposited by the tsunamis are much coarser than the organic-rich silty and clayey lake sediments that are typically deposited in lakes and tidal inlets, and they commonly contain abundant plant detritus that can be radiocarbon dated.

Heights, and therefore sizes, of tsunamis can be estimated by comparing sequences of sand layers from two or more lakes at different elevations within the same area. Sources of the tsunamis, however, cannot be determined from the lake sediments alone; rather, lacustrine stratigraphies must be compared with other records of past earthquakes or tsunamis, for example, intertidal sediments in nearby marshes.

Tsunami deposits of the A.D. 1700 plate-boundary earthquake have been found so far only in lakes a short distance (<200 m) from the present shoreline and less than 4 m above

mean sea level (<2 m above the upper limit of tides). This tsunami apparently was not large enough to carry sediment into higher lakes farther from the shore. It must be pointed out, however, that most of the lakes that have been studied are situated on the open outer coast. Tsunami waves in such areas are likely to be smaller than those at the heads of shallow bays and inlets that indent the west coast of Vancouver Island (Dunbar et al., 1989, 1991; Hebenstreit and Murty, 1989; Ng et al., 1990, 1991; Whitmore, 1993). Ng et al. (1991), for example, suggested on the basis of numerical modelling that tsunami waves may amplify by a factor of up to three in bays and inlets on Vancouver Island.

Older tsunami deposits have been found at three lakes on western Vancouver Island. Two of the lakes (Catala and Deserted) are less than 1 m above the tidal limit, thus the presence of older deposits is not surprising. The third lake (Kanim), however, is about 4 m above the tidal limit, beyond the reach of the A.D. 1700 tsunami. The presence of a ca. 2700-year-old tsunami sand in this lake can be explained by progressive, gradual uplift of western Vancouver Island (Clague et al., 1982; Friele and Hutchinson, 1993). Kanim Lake was a lagoon during the mid-Holocene, but has risen and become increasingly separated from the sea over time (Hutchinson et al., 1997). With continued uplift, the lake has passed through the zone of possible tsunami inundation and now is beyond reach of even the largest tsunami that might strike Vancouver Island.

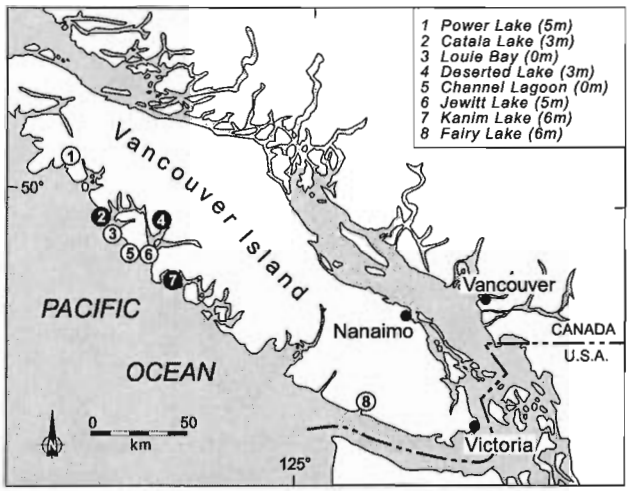

Figure 4. *Lakes on Vancouver Island that have been cored for tsunami deposits (Table 2). Lakes containing tsunami deposits are indicated by filled circles.*

SHAKING

Liquefaction occurred at many sites on eastern Vancouver Island and on nearby smaller islands during a magnitude-7.2 earthquake in 1946 (Fig. 5; Rogers, 1980). Nearly all of the occurrences were along the coast within 100 km of the epicentre.

Sand dykes, sills, and blows found at 12 sites on the Fraser River delta and Serpentine River flats near Vancouver were produced by shaking during one or more prehistoric earthquakes (Fig. 2c, 6; Table 3; Clague et al., 1992, 1997; Naesgaard et al., 1992; Mathewes and Clague, 1994). The features are less than 4000 years old; all of them are possibly about 1700 years old, which is the age of well dated dykes and blows at one site (Clague et al., 1997). Although earthquakes as small as magnitude 5 can liquefy sediments (Ambraseys, 1988), the number, size, and extent of the dykes, sills, and blows in the Vancouver area argue for one or more much larger earthquakes. This inference is supported by evidence for coincident liquefaction and sudden subsidence 1700-1900 years ago at Serpentine River (Mathewes and Clague, 1994), because only a large (magnitude >6.5) earthquake can cause significant land-level change over a large area. As mentioned previously, this earthquake was probably centered in the North America plate and may have occurred at about the same time as an offshore plate-boundary event.

Earthquake shaking can also trigger landslides and subaqueous mass movements (Shilts and Clague, 1992). For example, the 1946 Vancouver Island earthquake triggered hundreds of landslides (Fig. 5), although only one was large (Mathews, 1979; Evans, 1989). The largest historical landslides in British Columbia, however, have been triggered by nonseismic processes (e.g., excessive rainfall, freeze-thaw activity, debuttressing of mountain slopes due to glacier

Table 2. Lakes and tidal inlets that have been cored for tsunami deposits.

Site (location, Fig. 4)	Location	Elevation[1] (m)	Area (km²)	Distance[2] (km)	Tsunami deposits		Reference
					AD1700	Older	
Power Lake (1)	50°12'N, 127°29'W	ca. 5	0.6	0.7			unpublished
Catala Lake (2)	49°50'N, 127°03'W	ca. 3	0.1	0.5	X	X	Clague et al. (in press a)
Louie Bay (3)	49°44'N, 126°56'W	0	0.4	0.5			unpublished
Deserted Lake (4)	49°46'N, 126°30'W	3	0.5	0.5	X	X	unpublished
Channel Lagoon (5)	49°36'N, 126°40'W	0	0.2	0.6			unpublished
Jewitt Lake (6)	49°36'N, 126°38'W	ca. 5	0.4	0.1			unpublished
Kanim Lake (7)	49°24'N, 126°20'W	6	1.2	0.7		X	Hutchinson et al. (1997)
Fairy Lake (8)	48°35'N, 124°21'W	ca. 6	0.4	5			unpublished

[1]Datum is mean sea level; subtract approximately 2 m for elevation above high-tide level.
[2]Approximate distance of lake outlet from seashore.

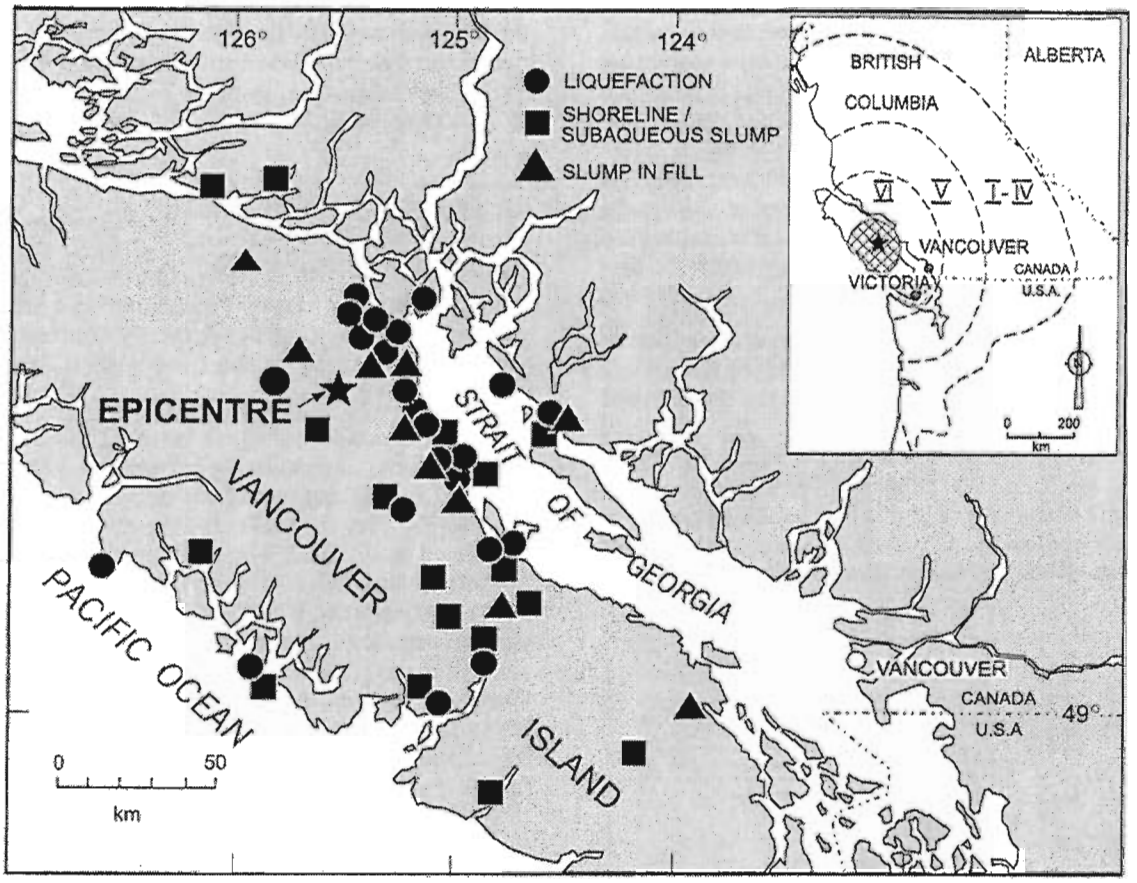

Figure 5. *Known sites of soil failure during the 1946 Vancouver Island earthquake (M = 7.2). The inset is an isoseismal (modified Mercalli Intensity) map; liquefaction occurred in areas of intensity VI and greater (modified from Rogers, 1980, Figs. 1, 2).*

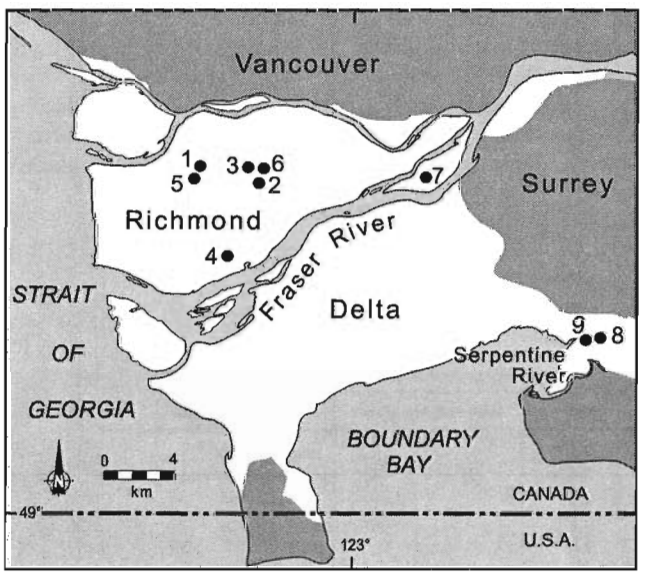

Figure 6. *Sites near Vancouver where evidence has been found for seismic liquefaction (Table 3).*

downwasting); thus it is extremely difficult to identify those prehistoric landslides that were caused by earthquakes (Clague and Shilts, 1993).

Sediment gravity-flow deposits intercalated with varved marine muds in Saanich Inlet, a fiord on southern Vancouver Island, have been attributed to earthquakes (Bobrowsky and Clague, 1990; Blais, 1995; Blais-Stevens et al., 1997). A study of Saanich Inlet sediments in piston cores suggests that sediment gravity flows have occurred, on average, once every 100 years over the past 1500 years, which is consistent with the average recurrence of moderate and large earthquakes on southern Vancouver Island (Blais-Stevens et al., 1997). The sediment record probably includes small, local earthquakes as well as much larger, more distant events. Varved marine sediments in other inlets on the west coast are an untapped resource for more precisely dating prehistoric earthquakes in the region.

Table 3. Sites with evidence for seismic liquefaction.

Site (location, Fig. 6)	Location	Type of evidence	Age (a)[1]	Reference
1	49°10.5'N, 123°07.5'W[2]	dykes, sills, blows	<3900	Clague et al. (1992)
2	49°09.9'N, 123°05.1'W[3]	dykes, sills	<2700	Clague et al. (1992)
3	49°10.7'N, 123°05.8'W[4]	dykes, sills		Clague et al. (1992)
4	49°07.9'N, 123°05.9'W[5]	dykes, blows	<4500	Clague et al. (1992)
5	49°09.9'N, 123°08.0'W[6]	dyke		Clague et al. (1992)
6	49°10.8'N, 123°04.9'W[7]	dykes		Clague et al. (in press b)
7	49°09.8'N, 122°57.1'W[8]	dykes, sills, blows	ca. 1700	Clague et al. (1997)
8	49°05.3'N, 122°49.3'W[9]	dykes	<2300	Mathewes and Clague (1994)
9	49°05.3'N, 122°50.4'W[10]	dykes	<2000	Mathewes and Clague (1994)

[1]Age in calendar years BP.
[2]Kwantlen College, near intersection of Lansdowne Road and Kwantlen Street, Richmond.
[3]Highway 99, south of Westminster Highway, Richmond.
[4]Highway 99, north of Highway 91, Richmond.
[5]Near intersection of Steveston Highway and Shell Road, Richmond.
[6]Anderson Road, east of No. 3 Road, Richmond.
[7]Highway 91, between No. 5 Road and Jacombs Road, Richmond.
[8]Annacis Island sewerage treatment facility, near intersection of Derwent Way and Eaton Place, Delta.
[9]Serpentine River, west of Highway 99A, Surrey.
[10]Serpentine River, just east of Highway 99, Surrey.

ACKNOWLEDGMENT

We thank John Adams for a helpful review of a draft of the paper.

REFERENCES

Ambraseys, N.N.
1988: Engineering seismology; Earthquake Engineering and Structural Dynamics, v. 17, p. 1-105.

Atwater, B.F., Nelson, A.R., Clague, J.J., Carver, G.A., Yamaguchi, D.K., Bobrowsky, P.T., Bourgeois, J., Darienzo, M.E., Grant, W.C., Hemphill-Haley, E., Kelsey, H.M., Jacoby, G.C., Nishenko, S.P., Palmer, S.P., Peterson, C.D., and Reinhart, M.A.
1995: Summary of coastal geologic evidence for past great earthquakes at the Cascadia subduction zone; Earthquake Spectra, v. 11, p. 1-18.

Benson, B.E.
1996: The stratigraphy and neotectonic significance of tsunami deposits beneath tidal marshes on Vancouver Island, British Columbia; M.Sc. thesis, University of British Columbia, Vancouver, B.C., 112 p.

Benson, B.E., Grimm, K.A., and Clague, J.J.
1997: Tsunami deposits beneath tidal marshes on northwestern Vancouver Island, British Columbia; Quaternary Research, v. 48, p. 192-204.

Blais, A.
1995: Foraminiferal biofacies and Holocene sediments from Saanich Inlet, British Columbia: implications for environmental and neotectonic research; Ph.D. thesis, Carleton University, Ottawa, Ontario, 280 p.

Blais-Stevens, A., Clague, J.J., Bobrowsky, P.T., and Patterson, R.T.
1997: Late Holocene sedimentation in Saanich Inlet, British Columbia, and its paleoseismic implications; Canadian Journal of Earth Sciences, v. 34, p. 1345-1357.

Bobrowsky, P.T. and Clague, J.J.
1990: Holocene sediments from Saanich Inlet, British Columbia, and their neotectonic implications; in Current Research, Part E; Geological Survey of Canada, Paper 90-1E, p. 251-256.

Bourgeois, J. and Reinhart, M.A.
1989: Onshore erosion and deposition by the 1960 tsunami of the Rio Lingue estuary, south-central Chile [abstract]; Eos (Transactions of the American Geophysical Union), v. 70, p. 1331.

Clague, J.J.
1996: Paleoseismology and seismic hazards, southwestern British Columbia; Geological Survey of Canada, Bulletin 494, 88 p.
1997: Earthquake hazard in the Greater Vancouver area; in Environmental Geology of Urban Areas, (ed.) N. Eyles; Geological Association of Canada, GEOtext3, p. 423-437.

Clague, J.J. and Bobrowsky, P.T.
1994a: Evidence for a large earthquake and tsunami 100-400 years ago on western Vancouver Island, British Columbia; Quaternary Research, v. 41, p. 176-184.
1994b: Tsunami deposits beneath tidal marshes on Vancouver Island, British Columbia; Geological Society of America Bulletin, v. 106, p. 1293-1303.

Clague, J.J. and Shilts, W.W.
1993: Two landslide-dammed lakes in the Cascade Mountains, southwestern British Columbia; in Current Research, Part E; Geological Survey of Canada, Paper 93-1E, p. 47-54.

Clague, J.J., Bobrowsky, P.T., and Hamilton, T.S.
1994: A sand sheet deposited by the 1964 Alaska tsunami at Port Alberni, British Columbia; Estuarine, Coastal and Shelf Science, v. 38, p. 413-421.

Clague, J.J., Bobrowsky, P.T., and Hyndman, R.D.
1995: The threat of a great earthquake in southwestern British Columbia; BC Professional Engineer, v. 46, no. 9, p. 4-8.

Clague, J., Harper, J.R., Hebda, R.J., and Howes, D.E.
1982: Late Quaternary sea levels and crustal movements, coastal British Columbia; Canadian Journal of Earth Sciences, v. 19, p. 597-618.

Clague, J.J., Hutchinson, I., Mathewes, R.W., and Patterson, R.T.
in press a: Evidence for late Holocene tsunamis at Catala Lake, British Columbia; Journal of Coastal Research.

Clague, J.J., Naesgaard, E., and Mathewes, R.W.
in press b: Geological evidence for prehistoric earthquakes; in Geology and Natural Hazards of the Fraser River Delta, British Columbia, (ed.) J.J. Clague, J.L. Luternauer, and D.C. Mosher; Geological Survey of Canada, Bulletin 525.

Clague, J.J., Naesgaard, E., and Nelson, A.R.
1997: Age and significance of earthquake-induced liquefaction near Vancouver, British Columbia, Canada; Canadian Geotechnical Journal, v. 34, p. 53-62.

Clague, J.J., Naesgaard, E., and Sy, A.
1992: Liquefaction features on the Fraser delta: evidence for prehistoric earthquakes?; Canadian Journal of Earth Sciences, v. 29, p. 1734-1745.

Dawson, A.G., Foster, I.D.L., Shi, S., Smith, D.E., and Long, D.
1991: The identification of tsunami deposits in coastal sediment sequences; Science of Tsunami Hazards, v. 9, p. 73-82.

Dawson, A.G., Long, D., and Smith, D.E.
1988: The Storegga slides: evidence from eastern Scotland for a possible tsunami; Marine Geology, v. 82, p. 271-276.

Dragert, H., Hyndman, R.D., Rogers, G.C., and Wang, K.
1994: Current deformation and the width of the seismogenic zone of the northern Cascadia subduction thrust; Journal of Geophysical Research, v. 99, p. 653-668.

Dunbar, D., LeBlond, P.H., and Murty, T.S.
1989: Maximum tsunami amplitudes and associated currents on the coast of British Columbia; Science of Tsunami Hazards, v. 7, p. 3-44.
1991: Evaluation of tsunami amplitudes for the Pacific coast of Canada; Progress in Oceanography, v. 26, p. 115-177.

Evans, S.G.
1989: The 1946 Mount Colonel Foster rock avalanche and associated displacement wave, Vancouver Island, British Columbia; Canadian Geotechnical Journal, v. 26, p. 447-452.

Friele, P.A. and Hutchinson, I.
1993: Holocene sea-level change on the central west coast of Vancouver Island, British Columbia; Canadian Journal of Earth Sciences, v. 30, p. 832-840.

Guilbault, J.-P., Clague, J.J., and Lapointe, M.
1995: Amount of subsidence during a late Holocene earthquake — evidence from fossil tidal marsh foraminifera at Vancouver Island, west coast of Canada; Palaeogeography, Palaeoclimatology, Palaeoecology, v. 118, p. 49-71.
1996: Foraminiferal evidence for the amount of coseismic subsidence during a late Holocene earthquake on Vancouver Island, west coast of Canada; Quaternary Science Reviews, v. 15, p. 913-937.

Hebenstreit, G.T. and Murty, T.S.
1989: Tsunami amplitudes from local earthquakes in the Pacific Northwest region of North America; Part 1: the outer coast; Marine Geodesy, v. 13, p. 101-146.

Hutchinson, I. and McMillan, A.D.
1997: Archaeological evidence for village abandonment associated with late Holocene earthquakes at the northern Cascadia subduction zone; Quaternary Research, v. 48, p. 79-87.

Hutchinson, I., Clague, J.J., and Mathewes, R.W.
1997: Reconstructing the tsunami record on an emerging coast: a case study of Kanim Lake, Vancouver Island, British Columbia; Journal of Coastal Research, v. 13, p. 545-553.

Hyndman, R.D. and Wang, K.
1993: Tectonic constraints on the zone of major thrust earthquake failure: the Cascadia subduction zone; Journal of Geophysical Research, v. 98, p. 2039-2060.
1995: The rupture zone of Cascadia great earthquakes from current deformation and the thermal regime; Journal of Geophysical Research, v. 100, p. 22,133-22,154.

Mann, D.H. and Crowell, A.L.
1996: A large earthquake occurring 700-800 years ago in Aialik Bay, southern coastal Alaska; Canadian Journal of Earth Sciences, v. 33, p. 117-126.

Mathewes, R.W. and Clague, J.J.
1994: Detection of large prehistoric earthquakes in the Pacific Northwest by microfossil analysis; Science, v. 264, p. 688-691.

Mathews, W.H.
1979: Landslides of central Vancouver Island and the 1946 earthquake; Bulletin of the Seismological Society of America, v. 69, p. 445-450.

Minoura, K. and Nakaya, S.
1991: Traces of tsunami preserved in inter-tidal lacustrine and marsh deposits: some examples from northeast Japan; Journal of Geology, v. 99, p. 265-287.

Minoura, K., Nakaya, S., and Uchida, M.
1994: Tsunami deposits in a lacustrine sequence of the Sanriku coast, northeast Japan; Sedimentary Geology, v. 89, p. 25-31.

Naesgaard, E., Sy, A., and Clague, J.J.
1992: Liquefaction sand dykes at Kwantlen College, Richmond, B.C.; in Geotechnique and Natural Hazards; BiTech Publishers, Vancouver, British Columbia, p. 159-166.

Nelson, A.R., Atwater, B.F., Bobrowsky, P.T., Bradley, L.-A., Clague, J.J., Carver, G.A., Darienzo, M.E., Grant, W.C., Krueger, H.W., Sparks, R, Stafford, T.W., Jr., and Stuiver, M.
1995: Radiocarbon evidence for extensive plate-boundary rupture about 300 years ago at the Cascadia subduction zone; Nature, v. 378, p. 371-374.

Nelson, A.R., Shennan, I., and Long, A.J.
1996: Identifying coseismic subsidence in tidal-wetland stratigraphic sequences at the Cascadia subduction zone of western North America; Journal of Geophysical Research, v. 101, p. 6115-6135.

Ng, M. K.-F., LeBlond, P.H., and Murty, T.S.
1990: Numerical simulation of tsunami amplitudes on the coast of British Columbia due to local earthquakes; Science of Tsunami Hazards, v. 8, p. 97-127.
1991: Simulation of tsunamis from great earthquakes on the Cascadia subduction zone; Science, v. 250, p. 1248-1251.

Peterson, C.D. and Darienzo, M.E.
1996: Discrimination of climatic, oceanic and tectonic mechanisms of cyclic marsh burial; in Assessing Earthquake Hazards and Reducing Risk in the Pacific Northwest, (eds.) A.M. Rogers, T.J. Walsh, W.J. Kockelman, and G.R. Priest; U.S. Geological Survey, Professional Paper 1560, p. 115-146.

Peterson, C.D., Barnett, E.T., Briggs, G.G., Carver, G.A., Clague, J.J., and Darienzo, M.E.
1997: Estimates of coastal subsidence from great earthquakes in the Cascadia subduction zone, Vancouver Island, B.C., Washington, Oregon, and northernmost California; Oregon Department of Geology and Mineral Industries, Open-File Report 0-97-5.

Rogers, G.C.
1980: A documentation of soil failure during the British Columbia earthquake of 23 June, 1946; Canadian Geotechnical Journal, v. 17, p. 122-127.

Satake, K., Shimazaki, K., Tsuji, Y., and Ueda, K.
1996: Time and size of a giant earthquake in Cascadia inferred from Japanese tsunami records of January 1700; Nature, v. 378, p. 246-249.

Shilts, W.W. and Clague, J.J.
1992: Documentation of earthquake-induced disturbance of lake sediments using subbottom acoustic profiling; Canadian Journal of Earth Sciences, v. 29, p. 1018-1042.

Whitmore, P.M.
1993: Expected tsunami amplitudes and currents along the North American coast for Cascadia subduction zone earthquakes; Natural Hazards, v. 8, p. 59-73.

Wright, C. and Mella, A.
1963: Modifications of the soil pattern of south-central Chile resulting from seismic and associated phenomena during the period May to August 1960; Bulletin of the Seismological Society of America, v. 53, p. 1367-1402.

Geological Survey of Canada Project 950029-03

Evidence of catastrophic rock avalanche potential and past failures, east face of Mount Livingstone and Windsor Ridge, Alberta[1]

Lionel E. Jackson and Daniel Lebel[2]
Terrain Sciences Division, Vancouver

Jackson, L.E. and Lebel, D., 1998: Evidence of catastrophic rock avalanche potential and past failures, east face of Mount Livingstone and Windsor Ridge, Alberta; in Current Research 1998-A; Geological Survey of Canada, p. 225-231.

Abstract: Extensive rockslides and the potential for catastrophic rock avalanches were discovered in two areas of the Rocky Mountains: 1) an extensive fissure system was noted near the summit of Mount Livingstone at the northern end of the Livingstone Range, and 2) a postglacial rockslide complex was mapped and investigated near Windsor Ridge, northwest of Waterton Lakes National Park in the headwaters of the east fork of Castle River and Mill Creek. Active fractures and the geological setting observed at this locality suggest that the area is prone to rockslides and possibly catastrophic rock avalanches. This report describes these features and identifies the possible hazards that they represent. Monitoring of these failures and proactive measures to identify similar situations elsewhere in nearby areas of the Rocky Mountains are suggested.

Résumé : On a reconnu de vastes éboulements et des sites où pourraient se produire des avalanches de pierres catastrophiques dans deux régions dans les Rocheuses : 1) un vaste réseau de fissures a été reconnu près du sommet du mont Livingstone, à l'extrémité nord de la chaîne Livingstone, et 2) un complexe d'éboulement postglaciaire a été cartographié et étudié près de la crête Windsor, au nord-ouest du parc national des Lacs-Waterton, dans le cours supérieur du bras est de la rivière Castle et du ruisseau Mill. La présence de ces fractures actives et le contexte géologique de l'endroit portent à croire que la région est propice à des éboulements et possiblement à des avalanches de pierres catastrophiques. Le présent rapport a pour objets de décrire ces éléments et de reconnaître les risques éventuels qu'ils posent. Des mesures de surveillance et des mesures proactives pour reconnaître des situations semblables dans les régions voisines des Rocheuses sont proposées.

[1] Contribution to the Eastern Cordillera NATMAP Project
[2] Institute of Sedimentary and Petroleum Geology, 3303-33rd Street N.W., Calgary, Alberta T2L 2A7

INTRODUCTION

Landslides and landslide activity have been systematically mapped in the Alberta Foothills and contiguous areas of the Rocky Mountains and Interior Plains as a part of the Eastern Cordillera NATMAP Project, over the period 1993-1997 (Jackson, 1995). During the 1996 field season, extensive rockslides and the potential for catastrophic rock avalanches were noted, including an extensive fissure system immediately south of the 2423 m summit of Mount Livingstone at the northern end of the Livingstone Range, and an extensive and active rockslide complex in the Windsor Ridge area northwest of Waterton Lakes National Park. This report describes these features and identifies the possible hazards that they and incipient failures represent. In addition, monitoring and proactive measures are suggested to identify similar problems elsewhere in the Rocky Mountains.

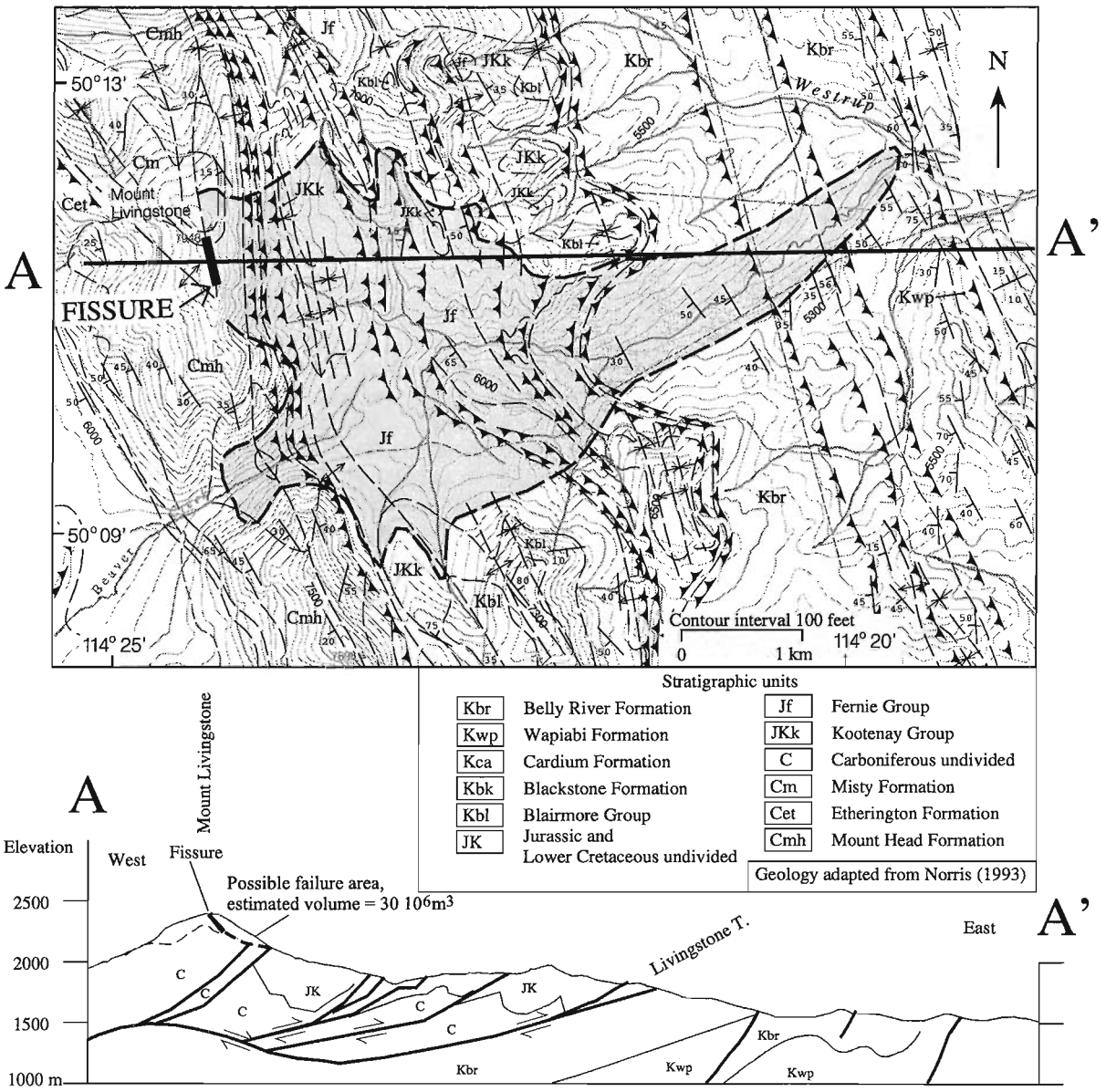

Figure 1. *Structural and stratigraphic setting of summit fissure on Mount Livingstone (map with geological cross-section through Mount Livingstone generalized from Norris, 1993). The Mount Livingstone ridge exposes inclined, massive carbonate rock units of the Rundle Group (Mount Head Formation [Cmh]) in fold cores, a setting very similar to that of Turtle Mountain, site of the Frank Slide. Strongly folded and faulted coal-bearing Mesozoic clastic rocks, riding the Livingstone thrust fault, are exposed in the lower slopes. The shaded area could be in danger in the event of a major rock avalanche from the east face of Mount Livingstone.*

FISSURES ON MOUNT LIVINGSTONE

The east face of Mount Livingstone (50°8.5'N, 114°24'W; Langford Creek map area, NTS 82J/1, Norris, 1993) has a relief of about 600 m above the floor of the south fork of Westrup Creek. It is composed of a thrust sheet of Mississippian Rundle Group limestone and dolostone, which overlies complexly folded and thrust-faulted Mesozoic sandstone, shale, and coal (Fig. 1). It shares similar structural and stratigraphic architecture with Turtle Mountain, site of the Frank Slide (Cruden and Krahn, 1973), as does much of the Livingstone Range. The fissure system (Fig. 1, 2) was recognized in August 1996 during a helicopter traverse of known rock avalanches in the area. It is about 100 m in length and ranges from less that 5 m to about 10 m in width. Only a few minutes were spent inspecting this feature on the ground. Breaks in the rock are fresh in appearance and the thin and patchy alpine soil that covers parts of the summit area has apparently subsided into the fissure system.

ROCK AVALANCHE HAZARD

In the absence of more detailed investigation of this feature, prudence dictates that it should be regarded as an incipient failure of the east face of Mount Livingstone. Such a failure would produce a highly mobile and fast moving rock avalanche with speeds of many tens of metres per second. Large rock avalanches (10^6 m^3) can climb and overtop hills and be destructive (Mollard, 1977; Plafker and Erikson, 1978; Melosh, 1987; Jackson and Isobe, 1990). The Frank Slide was such an event (Daly et al., 1912). Although voluminous literature exists about these events, the paths and limits of such events cannot be accurately predicted. The shaded area on Figure 1 is that which could be affected by such a failure. It includes most of the basin of the south fork of Westrup Creek and the headwaters of Beaver Creek. Its delineation is based on the assumption that a rock avalanche from Mount Livingstone would travel up to ten times the initial fall distance of 600 m in a linear direction and run up 30 per cent of the fall distance on opposite or adjacent valley sides within a few kilometres of the failure. These assumptions are reasonable and conservative based on the behaviour of similar failures elsewhere (Eisbacher, 1979; Eisbacher and Clague, 1984, p. 49-50). The actual behaviour of a failure would depend upon the volume and geometry of the failure and other factors that might influence mobility such as whether the region was snow covered at the time of failure.

Windsor Ridge rockslide complex

Field mapping and digital photogrammetry have permitted the delineation of five major and several minor rockslides that together cover over 13 km^2 in the headwaters of the east fork of Castle River and Mill Creek (Fig. 3; D. Lebel, work in progress, 1997), near Windsor Ridge. The rockslide complex is situated in the eastern part of the southern portion of the Bow-Crow Forest Reserve, overlapping the Beaver Mines and Sage Creek map areas (82G/08 and 82G/01). All these rockslides occur on dip slopes. Dip slopes are commonly associated with large landslides in the Canadian Rocky Mountains. In the Windsor Ridge area, the slopes are west-dipping and underlain by west-dipping strata (Fig. 4a, b). In the case of the Windsor Ridge slide complex, the rock units exposed in the upper elevations of Windsor Ridge are particularly prone to sliding because of their heterogeneity.

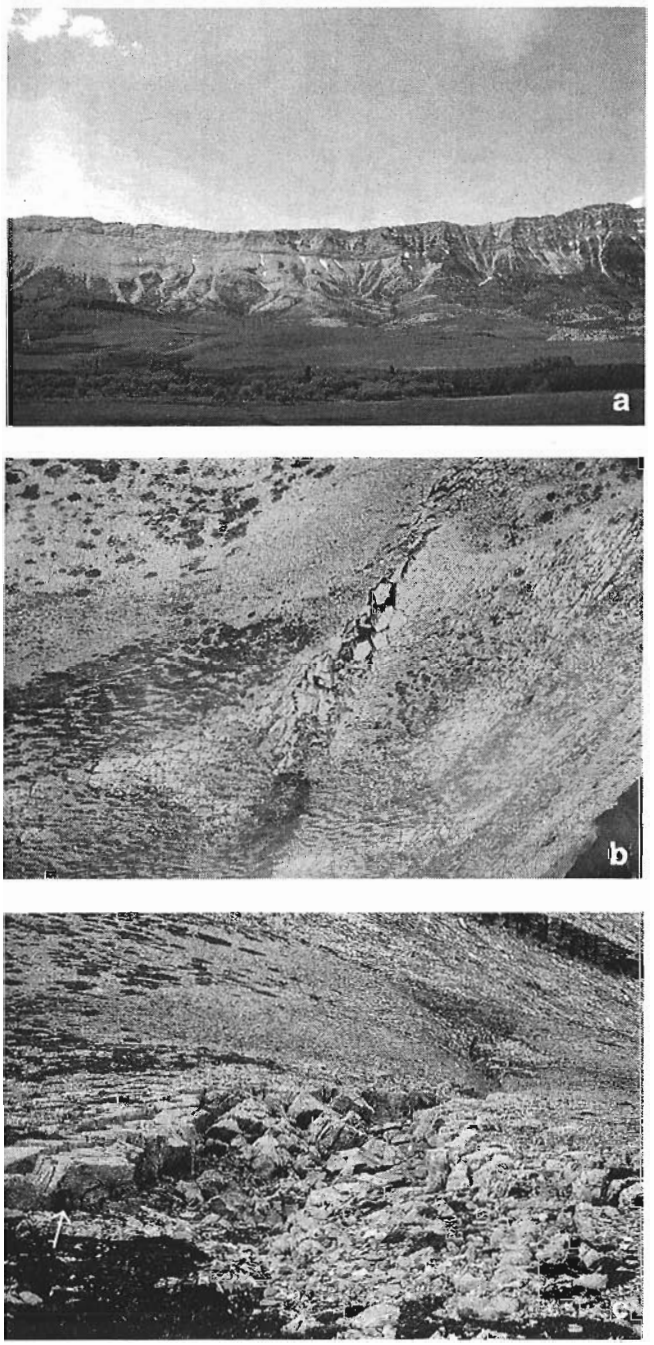

Figure 2. a) *Panoramic view of Livingstone Range, looking west.* ***b)*** *Aerial view of Mount Livingstone area, looking south along fissure.* ***c)*** *View to the north from the south end of the fissure. Total width of fracturing in this area is about 5 m. The arrow points to a 20 cm tall notebook.*

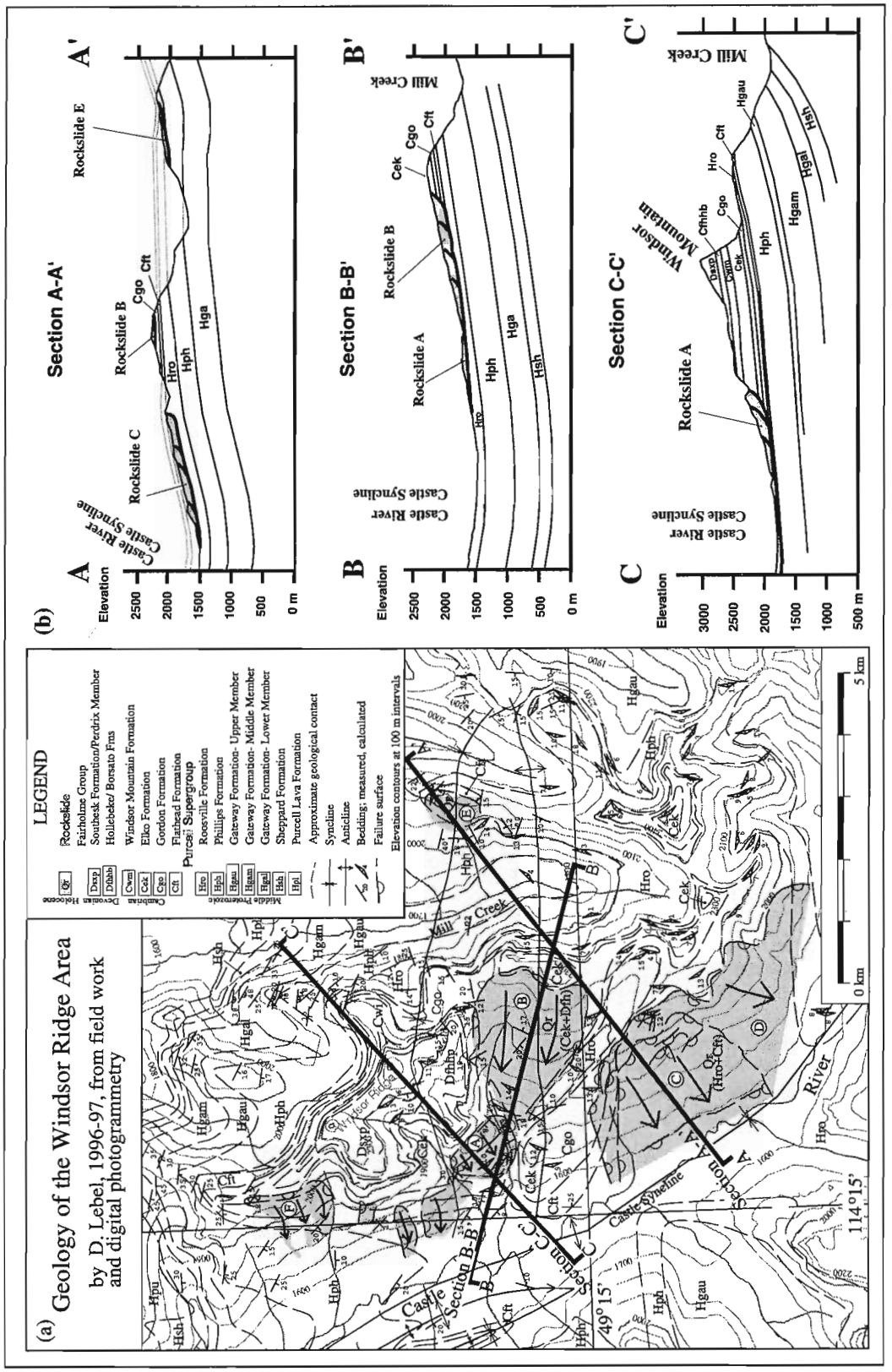

Figure 3. *Structural and stratigraphic setting of Windsor Ridge [(**a**) map and (**b**) geological cross-sections with no vertical exaggeration]. Large rockslides that were investigated are denoted A to E.*

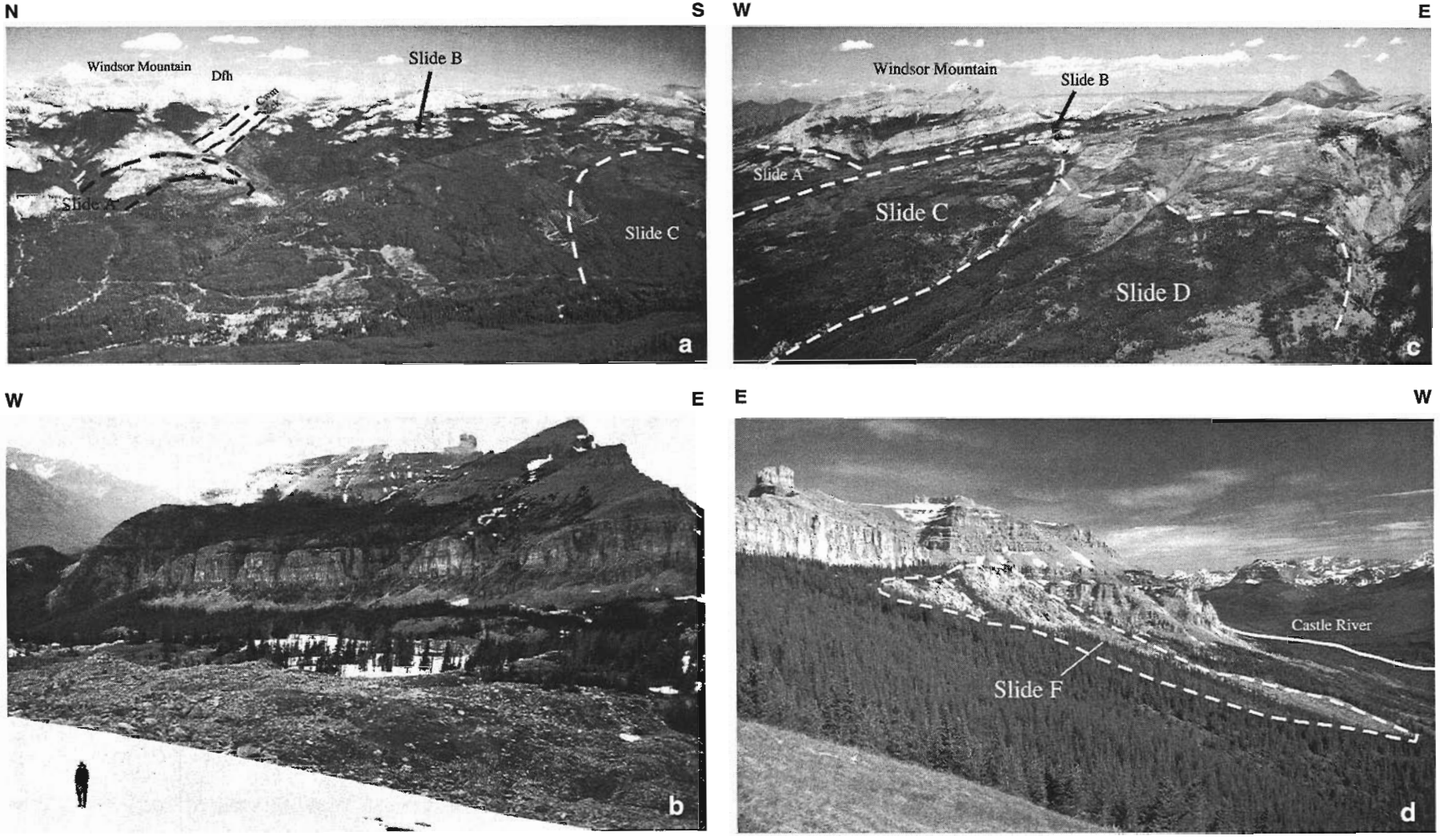

Figure 4. *(**a**) Oblique airphoto of rockslides A, B, and C, looking eastward. (**b**) View of rockslide B from its summit. Blocks reach several hundred metres in size. (**c**) Oblique airphoto of rockslides C and D, looking north. (**d**) Windsor Ridge, rockslide F and other smaller rockslides, looking south up the Castle River valley.*

Cross-sections (Fig. 3b) show that most of the rockslides are underlain by and are presumably failing along weak shaly or slaty horizons (Cambrian Gordon Formation [Cgo] and Middle Proterozoic Roosville Formation [Hro]). At Windsor Ridge, these weak units are overlain by strong, resistant carbonate rock and quartzite units that form towering cliffs, including the Flathead [Cft], Elko [Cek], and Windsor Mountain [Cwm] formations, and the Fairholme Group [Dfh]. All rockslides near Windsor Ridge have occurred in these four stratigraphic units (Fig. 3, 4) and have considerable relief. For example, the toe-to-crown difference in elevation is approximately 750 m for rockslide A and about 600 m for rockslide B.

Rockslides C and D are largely dip-slope failures within the Roosville and Flathead formations alone without overlying resistant units (cross-section A-A', Fig. 3). Rockslide C seems to be active. Networks of large fissures occur along its northwestern crown. These fissures are several hundred metres long, up to a metre wide, and of unknown depth. They are fresh, judging from the angularity, the unweathered surfaces of the broken rock along their walls, and the collapse of pedological soil and vegetation into them. Cross-section A-A' (Fig. 3) suggests that the basal detachment horizon of rockslide C is along bedding planes within the Roosville Formation. Little displacement has apparently taken place so far in rockslide D, which has the potential to grow as it expands headward into the adjacent upland.

ROCKSLIDES, ROCK AVALANCHES, AND LANDSLIDE DAM POTENTIAL

The rockslides in the Windsor Ridge area are of particular concern because of their potential to form landslide dams along the east fork of Castle River. Rockslides A, C, and D have the greatest potential to form dams. Such dams are commonly unstable. Consequently, a landslide-dammed lake could imperil settlements and public works downstream. The stability of Windsor Ridge itself is also of concern. The ridge rises approximately 1000 m above the Castle River and is underlain by the weak Gordon and Roosville formations, which dip about 10° towards the Castle River valley (cross-section C-C', Fig. 3). Mountain-sized blocks of massive Paleozoic carbonate rocks have broken off the Windsor Ridge massif at rockslide A and at other slide sites to the north. The potential for massive rotational or toppling failures or rock avalanches on the scale of the Frank Slide exists, enhanced by north- and northeast-trending fracture systems (Fig. 5). Rockslide B covers over 3 km² and contains the remains of a large carbonate ridge that used to be the southern extension of Windsor Ridge. Fissures in its crown area also seem fresh. Further headward growth of rockslide B may eventually destabilize the west and east margins of Windsor Ridge, which towers 600 m above Mill Creek. Another rockslide (E) observed on the east side of the Mill Creek valley also seems to be active but apparently does not present problems beyond its immediate location.

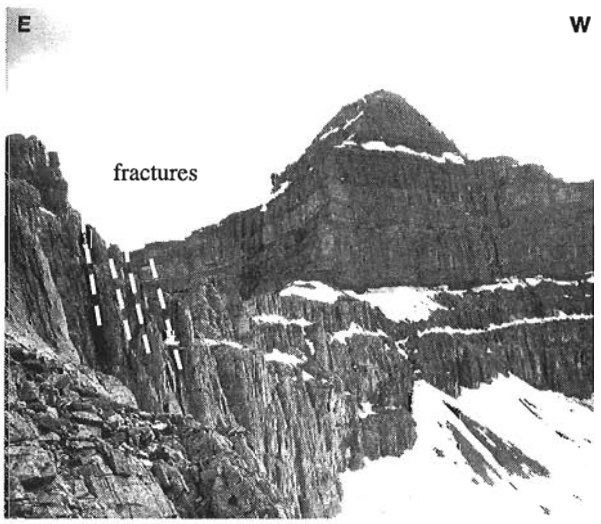

Figure 5. *Northeast-trending vertical fracture system cutting through dolostone units (Elko and Windsor Mountain formations) at Windsor Ridge; photo taken from the northeast promontory of Windsor Ridge, looking south.*

SUGGESTED MONITORING AND PROACTIVE MEASURES

A detailed slope stability study and monitoring program for the fissure system and adjacent areas of Mount Livingstone and the rockslide complexes at Windsor Ridge have been recommended to Alberta provincial authorities. The monitoring program will measure the rates of landslide movement, the expansion of landslides into the adjacent uplands, and the growth rate of incipient failures.

Surficial geology mapping carried out by the Geological Survey of Canada has found evidence of many rock avalanches along the Livingstone Range (Jackson, 1995, in press; Jackson and Leboe, in press). Consequently, an additional recommendation was made for a high-resolution aerial photography survey of the Livingstone Range in order to detect the presence of other fissure systems that could signal incipient failure. Although the area below Mount Livingstone is largely within the Forest Reserve and uninhabited, other areas along the Livingstone Range are populated. Furthermore, major gas pipelines and power transmission lines run parallel to the east side of the Livingstone Range. The rock avalanche hazard to these works has not been investigated. Detailed investigation of all the failures described in the Windsor Ridge area was also recommended, including a monitoring program to measure rockslide movement rates and changes in movement rates over time as well as fissures within the unfailed parts of Windsor Ridge.

Until more detailed evaluations are made, casual land users should be made aware of the potential hazards of these failures, and settlements and public works should be discouraged in both areas.

REFERENCES

Cruden, D.M. and Krahn, J.
1973: A reexamination of the geology of the Frank Slide; Canadian Geotechnical Journal, v. 10, p. 581-591.

Daly, R.A., Miller, W.G., and Rice, R.S.
1912: Report to the commission appointed to investigate Turtle Mountain, Frank, Alberta; Geological Survey of Canada, Memoir 27, 34 p.

Eisbacher, G.H.
1979: Cliff collapse and rock avalanches (sturzstroms) in the Mackenzie Mountains, northwestern Canada; Canadian Geotechnical Journal, v. 16, p. 309-334.

Eisbacher, G.H. and Clague, J.J.
1984: Destructive mass movements in high mountains: hazard and management; Geological Survey of Canada, Paper 84-16.

Jackson, L.E. Jr.
1995: Quaternary geology and terrain inventory, Eastern Cordillera NATMAP project. Report 1: Regional landslide characterization; in Current Research 1995-A; Geological Survey of Canada, p. 159-166.
in press: Landslide activity and landscape evolution, Rocky Mountains and foothills, southwestern, Alberta, Canada; Reviews in Engineering Geology, Geological Society of America.

Jackson, L.E. Jr. and Isobe, J.S.
1990: Rock avalanches in the Pelly Mountains, Yukon Territory; in Current Research, Part E; Geological Survey of Canada, Paper 90-1E, p. 263-269.

Jackson, L.E. Jr. and Leboe, E.R.
in press: Surficial geology, Blairmore, Alberta (82G/9); Geological Survey of Canada, A-series map (scale 1:50 000).

Melosh, H.J.
1987: Mechanics of large rock avalanches; in Debris Flows/Avalanches: Process, Recognition, and Mitigation, (ed.) J.E. Costa and G.F. Wieczorek; Geological Society of America, Reviews in Engineering Geology, v. VII, p. 41-49.

Mollard, J.D.
1977: Regional landslide types in Canada; in Landslides: Reviews in Engineering Geology III, (ed.) D.R. Coates; Geological Society of America, p. 29-56.

Norris, D.K.
1993: Geology and structure cross-sections, Langford Creek (west half), Alberta; Geological Survey of Canada, Map 1837A (scale 1:50 000).

Plafker, G. and Erikson, G.E.
1978: Nevados Huascaran avalanches, Peru; in Rockslides and Avalanches, 1, (ed.) B. Voight; Amsterdam, Elsevier Scientific Publishing Company, p. 277-314.

Geological Survey of Canada Projects 930006 and 930043

Interior Plains and Arctic Canada

Plaines intérieures et région arctique du Canada

An analysis of the thermal field to determine constraints on gas hydrate stability in Yukon Territory and western Northwest Territories

S.L. Smith[1]
Terrain Sciences Division

Smith, S.L., 1998: An analysis of the thermal field to determine constraints on gas hydrate stability in Yukon Territory and western Northwest Territories; in Current Research 1998-B; Geological Survey of Canada, p. 235-241.

Abstract: Stability conditions for the existence of gas hydrate have been analyzed for the Yukon and western Northwest Territories south of the Mackenzie Delta region. Structure I methane hydrate is stable only in the northern portion of the study area. Petrophysical evidence suggests that gas hydrate may exist over a more extensive area. Conditions for methane-propane hydrate and methane hydrogen sulphide hydrate stability were found to exist over a large part of the region. An analysis of gas composition in the region suggests that gas hydrates composed of heavier hydrocarbons or hydrogen sulphide may be present. Results of the analysis also indicate the possible existence of gas hydrates within 100 m of the ground surface.

Résumé : Les conditions de stabilité pour l'existence d'hydrates de gaz ont été analysées dans la partie du Yukon et des Territoires du Nord-Ouest qui se trouve au sud de la région du delta du Mackenzie. L'hydrate de méthane de structure I n'est stable que dans le nord de la région étudiée. Les données pétrophysiques suggèrent la possibilité que les hydrates de gaz soient présents sur une plus grande superficie. On a constaté qu'une bonne partie de la région est propice à la stabilité des hydrates de méthane-propane et des hydrates de méthane et de sulfure d'hydrogène. Une analyse de la composition du gaz dans la région laisse supposer l'existence d'hydrates de gaz composés d'hydrocarbures plus lourds ou de sulfure d'hydrogène. Les résultats de l'analyse indiquent en outre que des hydrates de gaz sont peut-être présents à moins de 100 m de profondeur.

[1] Consulting geoscientist, 2-775 Trojan Ave., Ottawa, Ontario K1K 2P6

INTRODUCTION

Natural gas hydrates are a class of solids consisting of gas molecules such as methane enclosed in the cage-like structure of water molecules (Davidson, 1973). They represent a significant source of greenhouse gas (methane) that may be released into the atmosphere as gas hydrates decompose in response to climate warming. They also present a hazard to drilling and conventional oil and gas production. Ground stability may also be affected if gas hydrates decompose and this must be considered when planning development in permafrost regions. An assessment of the conditions for stability of gas hydrates is therefore necessary in order to determine the environmental hazard to oil and gas development and the effect that changing climatic conditions may have on the methane balance between the atmosphere and the lithosphere.

Temperature and pressure are the main factors determining gas hydrate stability and thus the presence of gas hydrate. Other factors such as optimal geological conditions (supply of gas and water) and gas chemistry are also important (Lewin and Associates, 1983; Sloan, 1990). Suitable conditions for the existence of gas hydrate are present in the Yukon and western Northwest Territories (south of 68°N between 115° and 141°W) south of the Mackenzie Delta region. An analysis of geophysical data from industry exploration wells (Hardy Associates (1978) Ltd., 1984) suggests that natural gas hydrate occurs in this region. Recently, the evidence for the presence of gas hydrates has been assembled in database form (Smith and Judge, 1993). In this paper, the thermal conditions and gas chemistry for gas hydrate stability are assessed for the Yukon and western Northwest Territories, the area shown in Figure 1. The results are compared to the distribution of gas hydrates determined from geophysical data. This extends the regional surveys previously reported for the Beaufort/Mackenzie area (Judge and Majorowicz, 1992).

CONDITIONS FOR STABILITY OF GAS HYDRATES

Gas hydrate stability is dependent on temperature and pressure. The form of the temperature-pressure relationship is also dependent on gas composition as illustrated in Figure 2. In the study area, methane accounts for most of the gas in gas hydrates (Sanderson, 1971), but other gases may occur in significant amounts. The phase diagram used to describe conditions for methane (structure I) hydrate stability shown in Figure 2 can be found in Collett et al. (1988) and Lewin and Associates (1983).

The thickness of the gas hydrate stability zone may be determined by comparing the ground temperature for a given location and the gas hydrate stability curve as illustrated in Figure 2. The maximum depth of the gas hydrate stability zone is determined by calculating the depth of the intersection of the gas hydrate stability curve and the ground temperature profile.

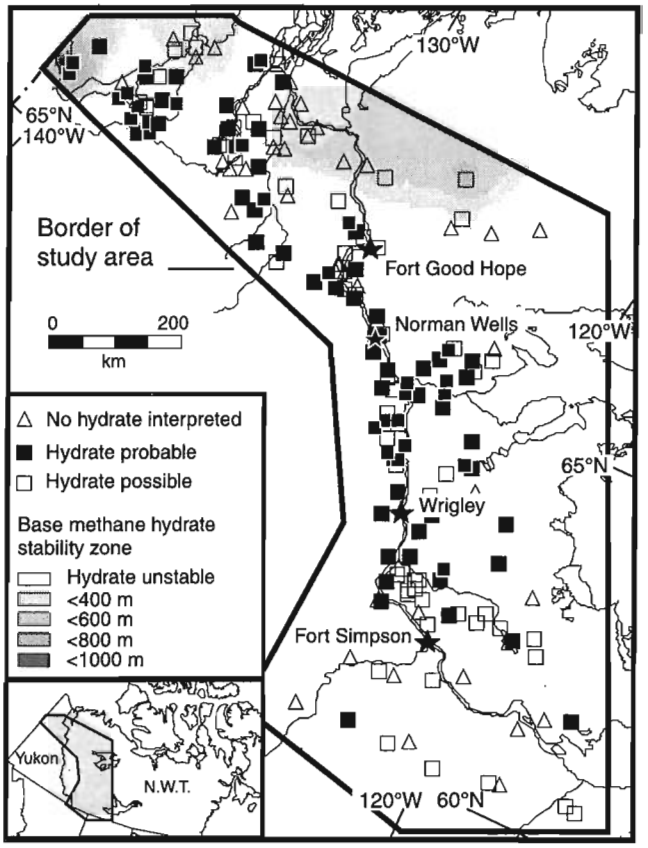

Figure 1. *Estimated base of structure I methane hydrate stability zone in the study area and distribution of natural gas hydrate as interpreted from geophysical well logs.*

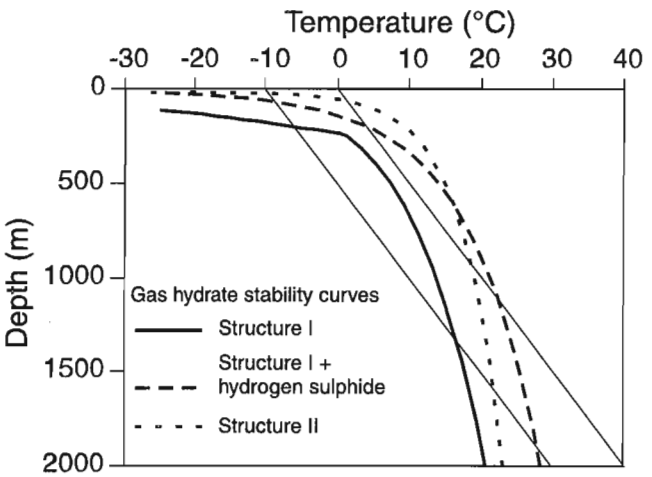

Figure 2. *Theoretical temperature profiles (20K/km) superimposed on gas hydrate stability curves for (1) structure I methane hydrate; (2) structure I gas hydrate with a gas composition of 93 per cent methane and 7 per cent hydrogen sulphide; (3) structure II gas hydrate with a gas composition of 96.5 per cent methane and 3.5 per cent propane. The area to the left of the gas hydrate stability curve represents conditions for gas hydrate stability.*

ANALYSIS OF GROUND TEMPERATURE DATA

Industry exploratory wells are the primary source of ground temperature data for this analysis. Bottom-hole and drill-stem-test temperature data were available for depths up to 4 km (Geotech Engineering Ltd., 1984) for many of the 220 wells considered in the study area (Fig. 1). Additional temperature data for some wells were available from precise (±0.01°C) measurements made in the upper few hundred metres by the Geological Survey of Canada (Taylor and Judge, 1974, 1975; Judge et al., 1979, 1981; Taylor et al., 1982). Reliable determinations from geophysical well logs of the depth to the base of ice-bearing permafrost and therefore the approximate depth of the -1°C isotherm are available for some wells (Hardy Associates (1978) Ltd., 1984). Additional information on the base of permafrost (depth to 0°C isotherm) is available for several sites in the study area and is summarized in the update of the database by Young and Judge (1986).

The bottom-hole data generally do not represent true formation temperatures because circulation of mud in the well during drilling disturbs the temperature in the surrounding rock. However, if successive temperature measurements are made at the same depth at different times following the cessation of fluid circulation and if the circulation time is known, the Horner plot method can be used (see Majorowicz et al., 1988; Judge and Majorowicz, 1992) to estimate the equilibrium formation temperature. Drill-stem-test data were also available to provide further information on the formation temperature. Drill stem tests record temperature over a depth interval as a function of time in an isolated section of the well, but they must be used with care as drilling mud or gas can distort the temperatures from true formation values (Geotech Engineering Ltd., 1984). Corrected bottom-hole and drill-stem-test data were compiled for the study area and were analyzed for each well.

Temperatures derived from corrected bottom-hole and drill-stem-test data and the temperature at the permafrost base were plotted as a function of depth for each well, and the thermal gradient was determined. A linear temperature gradient was established between the deep-borehole data and the temperature at the permafrost base using linear regression as a first-order approximation (see Judge and Majorowicz, 1992). Additional information on geothermal gradient in the study area is provided by the analysis of deep-temperature data by Majorowicz et al. (1988).

Thermal gradients in the study area vary from 20 to 60 K/km. A northwestward decline in the thermal gradient is suggested by the data. Majorowicz et al. (1988) suggest that variations in heat flow are related to hydrodynamic conditions. Areas of low thermal gradient may correspond to areas of high hydraulic head and high topographic elevation, since groundwater recharge and downward movement of fluid occur in such areas (Majorowicz and Jessop, 1981). Thus, convective heat transfer is more important than conduction. Areas of high thermal gradient correspond to lower hydraulic head and lower topographic elevation. In the study area, a general decrease in thermal gradient and heat flow occurs westward from the Canadian Shield into the Cordilleran fold belt possibly as convective heat transfer becomes more important (Majorowicz et al., 1988) The hydrodynamic effect, however, becomes less important north of 65°N because continuous permafrost inhibits large-scale fluid recharge, motion, and discharge.

The study area covers many climatic zones and ground surface temperatures vary from 0°C in the south to -10°C in the north. The variability in surface climate and geothermal gradient results in a significant variation in the thickness of both permafrost and the gas hydrate stability zone. This is illustrated in Figure 2, which shows the typical thermal regimes present in the study area. The thickness of the gas hydrate stability zone would be greater in areas of low surface temperature and small thermal gradient, such as in the northwest part of the study area. In areas of higher surface temperature or where thermal gradients are steep, the stability zone may be thin or nonexistent, as would be the case in the southeastern part of the study area.

GAS HYDRATE STABILITY CONDITIONS IN THE STUDY AREA

The maximum depth of the gas hydrate stability zone was determined for each well by calculating the depth of the intersection of the methane hydrate (structure I gas hydrate) stability curve and the temperature profile (Fig. 2). The error associated with the calculation of the base of the gas hydrate stability zone due to difficulties in determining thermal gradients from the well data is ±200 m.

The average depth to the base of the methane hydrate stability zone in wells for which methane hydrate is stable is 430 m (standard deviation = 138 m). Methane hydrate is unstable over a large (89 per cent) part of the study area (Fig. 1) where permafrost is generally thin. Conditions for methane hydrate stability are present in the northern portion of the study area. A general northwestard increase in the thickness of the methane hydrate stability zone corresponds to a general decrease in the geothermal gradient and increase in permafrost thickness. At its maximum thickness, the methane hydrate stability zone extends to a depth of about 830 m.

GEOPHYSICAL EVIDENCE OF GAS HYDRATES

Petrophysical data for 220 exploratory oil and gas wells in the study area have been examined for the presence or absence of gas hydrates (Hardy Associates (1978) Ltd., 1984). The petrophysical characteristics of gas hydrate intervals include high resistivity, especially on the deep induction logs, very low sonic velocity with cycle skipping, high acoustic velocity on the more deeply penetrating crystal cable log, low density, high neutron porosity, and an enlarged borehole diameter on the caliper log. When available, mud gas logs can be used to confirm gas hydrate picks. The detection of gas hydrates can

be ambiguous at times since the well-log responses in a well drilled with chilled mud are not the same as those drilled with warm mud when the hydrated sediments in the bore walls are partly thawed. Thus, factors other than gas hydrate can exhibit similar physical responses on geophysical logs. Gas hydrates within permafrost are difficult to identify because the petrophysical response exhibited by ice-bearing permafrost is similar to that of gas hydrates. Often, mud gas logs provide the only confirmation of the presence of gas hydrate. Thus, the thermal predictions of the gas-hydrate-prone zone must be used to constrain the well-log interpretation.

Hardy Associates (1978) Ltd. (1984) identified intervals interpreted to contain gas hydrates in 173 of the 220 wells. A reliability factor ranging from '1' (probable gas hydrate) to '3' (possible gas hydrate) was assigned to each pick. The presence of gas hydrate has been interpreted as probable in 82 wells and as possible in 91 wells. Figure 1 shows the location of wells in which gas hydrate could be present. The average top and bottom of the probable gas-hydrate-bearing zone is 380 m (standard deviation = 292) and 900 m (standard deviation = 543) respectively. Gas hydrate has been detected with good reliability at depths as great as 2000 m and as shallow as 15 m (Hardy Associates (1978) Ltd., 1984). Gas hydrates are generally detected at greater depth in the northwestern part of the study area.

DISCUSSION

Comparison of predicted and detected gas hydrate distribution

The interpreted distribution of gas hydrates is compared to methane hydrate stability conditions in Figure 1. In some cases, no gas hydrate has been detected in areas where temperature data indicate that methane hydrate would be stable. This is not unexpected since the predicted methane hydrate stability zone represents the zone in which structure I methane hydrate would be stable provided all other conditions for gas hydrate formation are met including the presence of sufficient methane. The existence of methane hydrate and the actual depth at which it would be found depend on the availability of gas and water and the geological environment, which influences the location of hydrocarbon reservoirs and traps. It seems that in some areas, these conditions for gas hydrate formation are not met. The interpreted occurrence of gas hydrate in 159 wells outside the predicted methane hydrate stability zone presents more of a challenge.

The detection of gas hydrates can be ambiguous and misinterpretations may have occurred in some cases. Gas chemistry is another important factor to consider. Gas containing propane and heavier gases forms a structure II gas hydrate that is stable at higher temperatures and lower pressures than structure I methane hydrate. Holder et al. (1983) suggest that structure II gas hydrate will form whenever small (0.1 percent) amounts of propane are present. Sanderson (1971) reports that gas hydrate in the study area can contain propane and other heavier gases such as butane, which form structure II gas hydrate. Figure 2 shows the stability curve for structure II gas hydrate composed of 96.5 per cent methane and 3.5 per cent propane, based on experimental data from Lewin and Associates (1983). Gas hydrate containing propane may be stable at temperatures at which methane hydrate would be unstable. In cases where methane hydrate is stable (Fig. 2), the base of the gas hydrate stability zone predicted for the methane-propane hydrate is approximately 300 m deeper than that for methane hydrate. The difference between the two stability zones increases as temperature gradients decrease. Thus, the presence of heavier hydrocarbons will significantly influence the thickness and areal extent of the gas hydrate stability zone.

To examine the effect that heavier hydrocarbons such as propane may have on gas hydrate distribution, the base of the methane-propane hydrate stability zone was determined (using the curve shown in Figure 2) for each well for which suitable temperature data were available. The results are shown in Figure 3. The average depth of the base of the methane-propane hydrate stability zone is 560 m (standard deviation = 244 m) and is deeper than the 430±138 m determined for methane alone. Methane-propane hydrate is stable

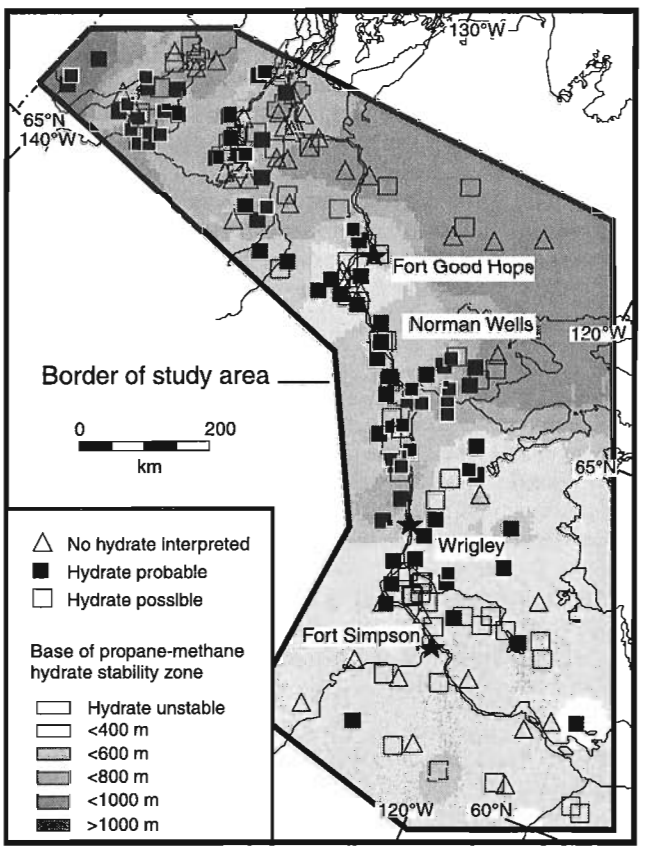

Figure 3. *Estimated base of the stability zone for a structure II gas hydrate with a gas composition of 96.5 per cent methane and 3.5 per cent propane. The distribution of natural gas hydrates as interpreted from well logs is also shown.*

over most of the study area, and most of the gas hydrate detected is found within the methane-propane hydrate stability zone (Fig. 3).

Other gases such as hydrogen sulphide may further enhance the stability of structure I methane hydrate. Hydrogen sulphide has been reported in logs for an Arctic Red well (66.8°N, 133.9°W) and in the upper 300 m in the Hay River area (60.8°N, 116.7°W). Figure 2 presents the stability curve for a structure I gas hydrate consisting of 93 per cent methane and 7 per cent hydrogen sulphide (data from Sloan 1990). The addition of hydrogen sulphide results in a shift of the stability curve (Fig. 2) to the right of the methane curve. The base of the methane-hydrogen sulphide stability zone was determined for each well for which suitable temperature data were available (Fig. 4). The average depth to the base of the methane-hydrogen sulphide hydrate stability zone is 730 m (standard deviation = 258 m). Methane-hydrogen sulphide hydrate is stable over a considerable portion of the study area, especially north of 65°N. Not all the gas hydrate present is necessarily of this type, but gas composition may well play a role in determining the thickness of the stability zone.

Gas composition within the Northwest Territories and Yukon area

Sanderson (1971) reports that gas hydrate in the Norman Wells area can contain propane and other heavier gases such as butane that form structure II gas hydrate. Gas analyses of the Imperial Formation, for example, show that gas is composed of 94 to 96.5 per cent methane and 1.2 to 1.5 per cent propane. An analysis of gas in the Kee Scarp reservoir in the Norman Wells area shows that methane accounts for 44 to 74 per cent of the total gas composition and propane, 6 to 20 per cent. Sanderson (1971) presents specific gravities of gas believed incorporated in gas hydrates in the study area. Most of the sites considered were north of 64°N. In most of the area, wet or slightly wet gas with gravity values greater than 0.6 are found (see Fig. 5). Wet gas contains methane and heavier hydrocarbons and is often associated with oil (Tissot and Welte, 1984). The only area in which dry gas of a lower gravity value was found is in the northwest corner of the study area. Over most of the area, natural gas is found with a gravity value higher than that of pure methane, and gas hydrate formed from it will be stable over a greater depth interval than that for structure I gas hydrate (Sloan, 1990).

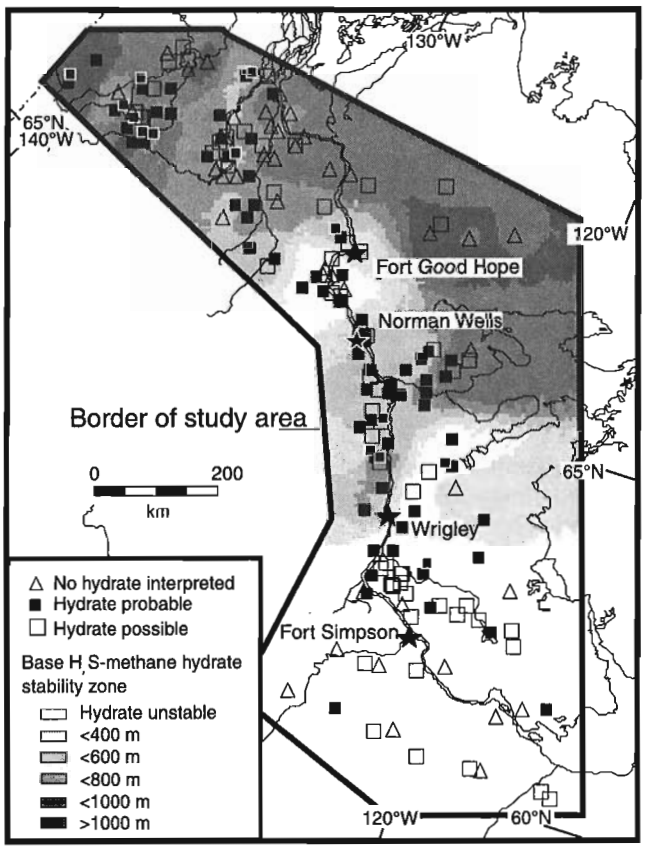

Figure 4. *Estimated base of the stability zone for a structure I gas hydrate with a gas composition of 93 per cent methane and 7 per cent hydrogen sulphide. The distribution of natural gas hydrates as interpreted from well logs is also shown.*

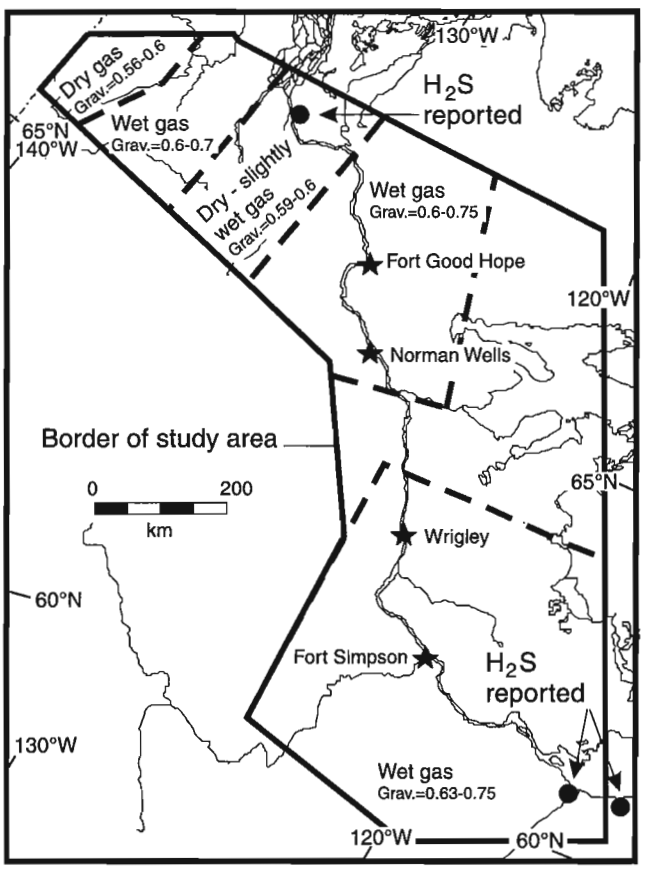

Figure 5. *Characteristics of gas believed to be incorporated in gas hydrates in the study area (data from Sanderson, 1971). Grav. refers to specific gravity.*

The highest gravity values are found between 60° and 67°N and 124 and 131°W. Source rocks in this region are marginally mature to mature and within the main zone of oil generation (Snowdon et al., 1987). Wet gas containing a significant amount of gases heavier than methane would be produced (Tissot and Welte, 1984). As maturation increases to the northwest (Snowdon et al., 1987; Feinstein et al., 1988a, b, 1989), cracking of oil producing mostly methane results in lower gas gravity. The hydrogen sulphide content of gas may also increase to the northwest as cracking of Type II kerogen and oil occurs (Tissot and Welte, 1984). Hydrogen sulphide gas has been reported in Arctic Red well logs (location shown in Figure 5).

Dry gas is found in the northwest corner of the study area (Sanderson, 1971). Devonian source rocks are thermally overmature between 65 and 67°N and 135 and 141°W (Dougherty and Uyeno, 1989). Degradation of organic matter in this area generates mostly dry gas consisting of methane (Link and Bustin, 1989).

South of 64°N, maturity ranges from immature in the eastern part of the study area to overmature west of 122°W (Feinstein et al., 1988b, 1989). In a large portion of this area (central part), source rocks are within the zone of oil generation and wet gas containing methane and heavier hydrocarbons would be expected to occur. Dry methane gas of biogenic origin may be found in gas hydrate in the eastern part of the study area. Dry methane gas produced by thermal cracking would likely be found in the western part of the study area.

Sulphide deposits occur south of Great Slave Lake and have been reported in logs for Hay River and Pine Point (location shown in Figure 5). Shallow gas blows and hydrogen sulphide gas have been reported in the upper 280 m in this area.

Carbon dioxide may also enhance methane hydrate stability. Sanderson (1971) reports that CO_2 may account for 0.6 to 0.9 per cent of the gas composition of gas hydrates in the Norman Wells area.

Gas chemistry and therefore the size of the gas hydrate stability zone and the composition of gas hydrates present will reflect these variations in maturity and organic matter type.

Occurrence of shallow gas hydrate

The upper limit of the methane hydrate stability zone is approximately 200 m for the Northwest Territories/Yukon study area. The high slope of the upper section of the stability curve means that the top of the stability zone is not very temperature dependent (Fig. 2). Figure 2 shows that the upper limit of the gas hydrate stability zone for both the propane-methane mixture and the hydrogen sulphide-methane mixture is at a shallower depth than for methane hydrate. This suggests that gas hydrates containing these gases could be present within 200 m of the surface. For example, at a temperature of 0°C, a structure II gas hydrate containing propane and methane would be stable at a depth of 35 m (Fig. 2). It is also important to note that experimental results (Lewin and Associates, 1983; Sloan, 1990) indicate that propane and hydrogen sulphide hydrates are stable near the earth's surface at temperatures of about -20°C. The depth of the upper limit of the propane-methane hydrate stability zone is about 100 m in the southern part of the study area and decreases to less than 20 m in the northern part. Gas hydrate has been interpreted with fair to good reliability to occur (Hardy Associates (1978) Ltd., 1984) in 10 wells at depths less than 100 m (Fig. 6) and has been detected at depths as shallow as 15 m. The shallowest occurrences (above 50 m) of gas hydrate are between 65.5 and 67.6°N and 131.8 and 137.8°W. The well logs for these 10 wells have been reviewed and, although the log responses could be interpreted as gas hydrate, ice-bearing permafrost also could be responsible for the responses in this zone (upper 100 m). Mud gas logs are not available for these wells. It is therefore impossible to distinguish between gas hydrate and ice-bearing permafrost at shallow depths.

The possible presence of gas hydrate in the upper 100 m becomes important when considering the impact of short-term global warming in these areas (Nisbet, 1989). Under existing warming scenarios, significant ground warming and permafrost degradation could occur over the next 50 to 100 years. Shallow gas hydrates would likely become unstable and decompose in response to warming. The surface temperature is assumed to vary exponentially with time in response to an exponential buildup of greenhouse gas (MacDonald, 1990). Assuming an increase in surface temperature of 2°C per century (MacDonald, 1990), significant increases in temperature may occur in the upper part of the methane-propane and methane-hydrogen sulphide hydrate stability zones in less than 100 years. Up to 1 m of these stability zones may erode over a period of 50 years. It takes approximately 100 years for the temperature increase to reach the top of the methane-hydrate stability zone. Under longer warming periods of thousands of years, the remainder of the gas hydrate column becomes vulnerable. Significant amounts of gas hydrate may become unstable over periods of only several hundreds of years, however, where temperature gradients are large and ground temperatures are close to that required for gas hydrate stability.

Shallow gas hydrates are also a potential hazard during drilling. The possible existence of shallow gas hydrates needs to be considered during seismic and geotechnical investigation and mining exploration as well as hydrocarbon exploration.

CONCLUSIONS

Given the permafrost depths and the geothermal gradients in the area, structure I methane hydrate would only be stable over a limited area and generally above a depth of 800 m. For methane gas to be stored as gas hydrate over a greater area and at the greater depths suggested by the petrophysical evidence, it must coexist with heavier hydrocarbon gases such as propane as structure II gas hydrate or with gases such as hydrogen sulphide, both of which would increase the thickness and areal extent of the gas hydrate stability zone. For gas hydrate to be present over a large part of this area, it must be in a form other than structure I methane hydrate.

Knowledge of gas chemistry is also important in estimating the amount of methane stored as gas hydrate. The increased thickness of the gas hydrate stability zone associated with structure II gas hydrate or significant hydrogen sulphide in structure I gas hydrate may increase the overall methane storage by 30 per cent.

Structure II gas hydrate or methane-hydrogen sulphide hydrate is stable at shallower depths than structure I methane hydrate and may occur within 100 m of the ground surface. Therefore, gas chemistry must also be considered when assessing drilling hazard or when estimating the amount of methane that may be released from gas hydrates during climate warming.

ACKNOWLEDGMENTS

This project was funded by the Panel on Energy Research and Development. This analysis depended heavily on high-quality measurements made during exploratory drilling in northern Canada, and the dedication of numerous oil industry, logging company, and government regulatory personnel is acknowledged. R. Palmiere of the National Energy Board provided well logs and drilling reports. Support provided by A. Judge while the author was a visiting scientist at the Geological Survey of Canada is greatly appreciated. The author also wishes to thank Scott Dallimore for much helpful advice.

REFERENCES

Collett, T.S., Bird, K.J., Kvenvolden, K.A., and Magoon, L.B.
1988: Geologic interrelations relative to gas hydrates within the North Slope of Alaska; U.S. Geological Survey, Open File 88-389, 150 p.

Davidson, D.W.
1973: Clathrate hydrates; in Water: A Comprehensive Treatise, (ed.) F. Franks; Plenum Press New York, v. 1, p. 115-234.

Dougherty, B.J. and Uyeno, T.T.
1989: A conodont based thermal maturation study of some Lower and Middle Devonian rocks, northwestern District of Mackenzie and Yukon Territory; Geological Survey of Canada, Paper 89-1G, p. 37-42

Feinstein, S., Brooks, P.W., Fowler, M.G., Snowdon, L.R., and Williams, G.K.
1988a: Families of oils and source rocks in the central Mackenzie Corridor: A geochemical oil-oil and oil-source rock correlation; Canadian Society of Petroleum Geologists, Memoir, v. 15, p. 543-552.

Feinstein, S., Brooks, P.W., Gentzis, T., Goodarzi, F., Snowdon, L.R., and Williams, G.K.
1988b: Thermal maturity in the Mackenzie Corridor, Northwest and Yukon Territories, Canada; Geological Survey of Canada, Open File 1944, 80 p.

Feinstein, S., Goodarzi, F., Gentzis, T., Snowdon, L.R., and Williams, G.K.
1989: Preliminary organic maturation studies of Horn River strata in the Tathlina High area, Northwest Territories; Geological Survey of Canada, Paper 89-1G, p. 43-50.

Geotech Engineering Ltd.
1984: Subsurface temperature data from Arctic wells; Energy, Mines, and Resources Canada, Earth Physics Branch, Open File 83-11.

Hardy Associates (1978) Ltd.
1984: A study of well logs in the Western Northwest Territories and Yukon to outline permafrost thickness and/or gas hydrate occurrence; Energy, Mines, and Resources Canada, Earth Physics Branch, Open File 84-27, 290 p.

Holder, G.D., Angert, P.F., and Pereira, V.
1983: Implications of gas hydrates associated with gas reserves; in Natural Gas Hydrates, (ed.) J.L. Cox; Butterworth Publication, p. 91-114.

Judge, A.S. and Majorowicz, J.A.
1992: Geothermal conditions for gas hydrate stability in the Beaufort-Mackenzie Area: The global change aspect; Global and Planetary Change, v. 6, p. 251-263.

Judge, A.S., Taylor, A.E., and Burgess, M.
1979: Canadian geothermal data collection - northern wells 1977-78; Energy, Mines, and Resources Canada, Earth Physics Branch, Geothermal Series, no. 11, 188 p.

Judge, A.S., Taylor, A.E., Burgess, M., and Allen, V.S.
1981: Canadian geothermal data collection - northern wells 1978-1980; Energy, Mines, and Resources Canada, Earth Physics Branch, Geothermal Series, no. 12, 190 p.

Lewin and Associates
1983: Handbook of gas hydrate properties and occurrence; Report for U.S. Department of Energy, Office of Fossil Energy, contract No. DE-AC 21-82-MC19239, Morgantown, West Virginia.

Link, C.M. and Bustin, R.M.
1989: Organic maturation and thermal history of Phanerozoic strata in Northern Yukon and Northwestern District of Mackenzie; Bulletin of Canadian Petroleum Geology, v. 37, p. 266-292.

MacDonald, G.J.
1990: Role of methane clathrates in past and future climates; Climatic Change, v.16, p. 247-281.

Majorowicz, J.A. and Jessop, A.M.
1981: Regional heat flow patterns in the Western Canadian sedimentary basin; Tectonophysics, v. 74, p. 209-238.

Majorowicz, J.A., Jones, F.W., and Jessop, A.M.
1988: Preliminary geothermics of the sedimentary basins in the Yukon and Northwest Territories (60°N–70°N) – Estimates from petroleum bottom-hole temperature data; Bulletin of Canadian Petroleum Geology, v. 36, p. 39-51.

Nisbet, E.G.
1989: Some northern sources of atmospheric methane: production, history, and future implications; Canadian Journal of Earth Science, v. 26, p.1603-1611.

Sanderson, W.J.
1971: Permafrost and solid gas hydrates in the Norman Wells Field, NWT; Imperial Oil Ltd. Northern Exploration Department. Edmonton, Alta. Report. no. IPRNWT-3MG-71.

Sloan, E.D.
1990: Clathrate Hydrates of Natural Gases; Marcel Dekker, New York, 641 p.

Smith, S.L. and Judge, A.S.
1993: Gas hydrate database for Canadian Arctic and selected East Coast wells; Geological Survey of Canada, Open File 2746, 120 p.

Snowdon, L.R., Brooks, P.W., Williams, G.K, and Goodarzi, F.
1987: Correlation of the Canol formation source rock with oil from Norman Wells; Organic Geochemistry, v. 11, p. 529-548.

Taylor, A.E. and Judge, A.S.
1974: Canadian geothermal data collection - northern wells 1955 to February 1974; Energy, Mines, and Resources Canada, Earth Physics Branch, Geothermal Series, no. 1, 171 p.
1975: Canadian geothermal data collection - northern wells 1974; Energy, Mines, and Resources Canada, Earth Physics Branch, Geothermal Series, no. 3, 127 p.

Taylor, A.E., Burgess, M., Judge, A.S., and Allen, V.S.
1982: Canadian geothermal data collection - northern wells 1981; Energy, Mines, and Resources Canada, Earth Physics Branch, Geothermal Series, no. 13, 153 p.

Tissot, B.P. and Welte, D.H.
1984: Petroleum Formation and Occurrence; Berlin, Springer Verlag, 699 p.

Young, S.E. and Judge, A.S.
1986: Canadian permafrost distribution and thickness data collection: a discussion; Proceedings of National Student Conference on Northern Studies, (ed.) W.P. Adams and P.G. Johnson, p. 223-228.

Geological Survey of Canada Project 970017

AUTHOR INDEX

NOTE TO CONTRIBUTORS

Submissions to the Discussion section of Current Research are welcome from both the staff of the Geological Survey of Canada and from the public. Discussions are limited to six double-spaced typewritten pages (about 1500 words) and are subject to review by the Managing Editor. Discussions are restricted to the scientific content of Geological Survey reports. General discussions concerning sector or government policy will not be accepted. All manuscripts must be computer word-processed on an IBM compatible system and must be submitted with a diskette using WordPerfect. Illustrations will be accepted only if, in the opinion of the editor, they are considered essential. In any case no redrafting will be undertaken and reproducible copy must accompany the original submissions. Discussion is limited to recent reports (not more than two years old) and may be in either English or French. Every effort is made to include both Discussion and Reply in the same issue. Current Research is published in January and July. Submissions should be sent to the Managing Editor, Geological Survey of Canada, 601 Booth Street, Ottawa K1A 0E8.

AVIS AUX AUTEURS D'ARTICLES

Nous encourageons tant le personnel de la Commission géologique que le grand public à nous faire parvenir des articles destinés à la section discussion de la publication Recherches en cours. Le texte doit comprendre au plus six pages dactylographiées à double interligne (environ 1500 mots), texte qui peut faire l'objet d'un réexamen par la rédactrice en chef administrative. Les discussions doivent se limiter au contenu scientifique des rapports de la Commission géologique. Les discussions générales sur le Secteur ou les politiques gouvernementales ne seront pas acceptées. Le texte doit être soumis à un traitement de texte informatisé par un système IBM compatible et enregistré sur disquette WordPerfect. Les illustrations ne seront acceptées que dans la mesure où, selon l'opinion du rédacteur, elles seront considérées comme essentielles. Aucune retouche ne sera faite aux illustrations et dans tous les cas, une copie qui puisse être reproduite doit accompagner le texte original. Les discussions en français ou en anglais doivent se limiter aux rapports récents (au plus de deux ans). On s'efforcera de faire coïncider les articles destinés aux rubriques discussions et réponses dans le même numéro. La publication Recherches en cours paraît en janvier et en juillet. Les articles doivent être envoyés à la rédactrice en chef administrative, Commission géologique du Canada, 601, rue Booth, Ottawa K1A 0E8.

Geological Survey of Canada Current Research, is released twice a year, in January and July. The four parts published in January 1998 (Current Research 1998-A to D) are listed below.

Recherches en cours, une publication de la Commission géologique du Canada, est publiée deux fois par année, en janvier et en juillet. Les quatre parties publiées en janvier 1998 (Recherches en cours 1998-A à D) sont énumérées ci-dessous.

Part A:	Cordillera and Pacific Margin
Partie A:	Cordillére et marge du Pacifique
Part B:	Interior Plains and Arctic Canada
Partie B:	Plaines intérieures et région arctique du Canada
Part C:	Canadian Shield
Partie C:	Bouclier canadien
Part D:	Eastern Canada and national and general programs
Partie D:	Est du Canada et programmes nationaux et généraux